PROCEEDINGS OF THE 22ND INTERNATIONAL MINING CONGRESS OF TURKEY

MAY-11-13, 2011 / ANKARA-TURKEY

EDITORS

Nuray DEMİREL Ömer ERDEM Mustafa ERKAYAOĞLU

UCTEA

THE CHAMBER OF MINING ENGINEERS OF TURKEY

IMCET 2011 / ANKARA / TURKEY / MAY 11-13

PROCEEDINGS OF THE 22nd INTERNATIONAL MINING CONGRESS AND EXHIBITION OF TURKEY

EDITORS

Nuray Demirel
Ömer Erdem
Mustafa Erkayaoğlu

PROCEEDINGS OF THE 22nd INTERNATIONAL MINING CONGRESS AND EXHIBITION OF TURKEY

MAY 11-13, 2011
ANKARA

Edited By,

Asst.Prof. Nuray DEMİREL
Ömer ERDEM
Mustafa ERKAYAOĞLU

UCTEA
THE CHAMBER OF MINING ENGINEERS OF TURKEY

This Congress is supported by TÜBİTAK (The Scientific and Technological Research Council of Turkey

ISBN : 978-605-01-0103-4

Published by : KORZA YAYINCILIK
BASIM SAN. VE TİC. LTD. ŞTİ.
Büyük San. 1. Cadde 95/1 İskitler-Ankara
Phone : 0.312 342 22 08 • Fax: 0.312 341 14 27
www.korzabasim.com.tr

Adress : TMMOB Maden Mühendisleri Odası
Selanik Cad. 19/4 Kızılay-ANKARA
Phone : 0312 425 10 80 Fax: 0312 417 52 90
: www.maden.org.tr
: maden@maden.org.tr

Member of Boards of the Chamber

President	:	Mehmet TORUN
II. President	:	Niyazi KARADENİZ
Secretary	:	Nahit ARI
Treasurer	:	İbrahim YILMAZOĞLU
	:	Necmi ERGİN
	:	Cemalettin SAĞTEKİN
	:	H. Can DOĞAN

Executive Committee of the Congress

President	:	Prof. Dr. Tevfik GÜYAGÜLER
Secretary	:	İlker ERTEM
Members	:	Asst.Prof. Nuray DEMİREL
	:	Nahit ARI
	:	Niyazi KARADENİZ
	:	Dr. Bülent TOKA
	:	Ömer ERDEM
	:	Mustafa ERKAYAOĞLU
	:	Esin PEKPAK

Scientific Committee

Dr.	Najdat Aziz	Dr.	Halit Ziya Kuyumcu
Dr.	Ernest Baafi	Prof.Dr.	Uğur Özbey
Dr.	Jani Bakallbashi	Em. Prof.Dr.	Levent Özdemir
	Tomo Benovic	Dr.	George N.Panagiotou
Dr.	Raimondo Ciccu	Prof.Dr.	Hasan Sevim
Dr.	Doru Cioclea	Prof.Dr.	Raj Singhai
Prof.Dr.	Kadri Dağdelen	Dr.	Tzolo Voutov
Dr.	Katerina Demnerova	Dr.	Slobodan Vujic
Dr.	Carsten Drebensted	Dr.	Tuncel Yegülalp
Prof.Dr.	Şevket Durucan	Prof.Dr.	Stojan Zdravev
Prof.Dr.	Samuel Frimpong	Dr.	Nuri Ali Akçin
	Emanouel Frogoudakis	Dr.	Mesut Anıl
Dr.	Miodrag Gomilanovic	Dr.	Ergin Arıoğlu
Dr.	Güner Gürtunca	Dr.	Ali İhsan Arol
	Marjan Hudej	Dr.	Ümit Atalay

Dr. Yusuf Aydın
Dr. İrfan Bayraktar
Dr. H. Aydın Bilgin
Dr. Nuh Bilgin
Dr. Naci Bölükbaşı
Dr. Mehmet Canbazoğlu
Dr. Atilla Ceylanoğlu
Dr. İlknur Cöcen
Dr. Neş'e Çelebi
Dr. Ahmet Demirci
Dr. Nuray Demirel
Dr. Halim Demirel
Dr. Vedat Didari
Dr. H. Şebnem Düzgün
Dr. İ. Göktay Ediz
Dr. Zafir Ekmekçi
Dr. Kaan Eraslan
Dr. Şinasi Eskikaya
Dr. Hasan Gerçek
Dr. İsmail Girgin
Dr. M.kemal Gökay
Dr. Nilgün Güleç
Dr. Oğuz Gündoğdu
Dr. Lütfullah Gündüz
Dr. Cenk Güray
Dr. Özcan Gürsoy
Dr. Tevfik Güyagüler
Dr. Cahit Hiçyılmaz
Dr. Mehmet Ali Hindistan
Dr. Çetin Hoşten
Dr. Fikri Kahraman
Dr. Celal Karpuz
Dr. Mehmet Kayadelen
Dr. Mevlüt Kemal

Dr. Ayhan Kesimal
Dr. Adnan Konuk
Dr. Halil Köse
Dr. Seyfi Külaksız
Dr. Orhan Kural
Dr. Yadigar V. Müftüoğlu
Dr. Ahmet Hakan Onur
Dr. Güner Önce
Dr. Gülhan Özbayoğlu
Dr. Hüseyin Özdağ
Dr. Metin Özdoğan
Dr. Abdurrahim Özgenoğlu
Dr. Şafak G. Özkan
Dr. Mesut Öztürk
Dr. Hasan Öztürk
Dr. Günhan Paşamehmetoğlu
Dr. M.Saim Saraç
Dr. Cem Saraç
Dr. Cem Şensöğüt
Dr. Nejat Tamzok
Dr. A.Erhan Tercan
Dr. Bülent Toka
Dr. Levent Tutluoğlu
Veli Ünal
Dr. Bahtiyar Ünver
Ömer Ünver
Dr. Mahir Vardar
Dr. Ercüment Yalçın
Yük.Mad.Müh. Ömer Yenel
Yük.Mad.Müh. Levent Yener
Yük.Mad.Müh. Fehmi Yıldırım
Yük.Mad.Müh. Necati Yıldız
Dr. A. Ekrem Yüce

PREFACE

The 22nd International Mining Congress and Exhibition of Turkey (IMCET 2011), organized by the Chamber of Mining Engineers of Turkey, was held from 11 to 13 May, 2011, in Ankara, Turkey. The main objective of the congress was to promote scientific information exchange, to share experiences, and to discuss innovations related to the mining industry for the participants.

Among the 350 participants from 10 countries we welcomed, 17 representatives from government institutions and engineering firms; 50 participants from 23 national and 18 international universities contributed to the congress.

The technical program included 81 oral and 20 poster presentations about advanced techniques, technological developments, and the best practices in the areas of surface and underground mining, mineral processing, mineral economy, mine ventilation, and safety. There were also four plenary presentations given by distinguished keynote lecturers. In addition a panel about "occupational safety and health in mining activities" was arranged in the framework of the congress.

With your participation we hope that IMCET will continue to be an exceptional opportunity to share with colleagues and learn about new technologies and industrial practices in mining industry.

We would like to thank everyone who contributed their time and energy to the organization of this meeting. We would especially like to thank:

The authors for their papers and presentations and also for their willingness to travel to Ankara to share their experiences,

The technical reviewers for dedicating their time in the evaluation of each paper to ensure the quality of this proceeding book,

The technical session chairs for their work in preparing a well-rounded and an interesting program, and

The sponsors for their generous support.

Thanks are extended to the Organizing Committee, the Executive Board, and the Scientific Committee members for their time and effort to make IMCET 2011 a true success.

Finally, we thank all of you, the participants, who have made this inspiring exchange of knowledge and ideas possible with your enthusiasm and motivation.

Prof. Dr. Tevfik GÜYAGÜLER

Congress Chairman

Mehmet TORUN

President of the Chamber of Mining Engineers of Turkey

The volume of proceeding was sponsored by DEMİR EXPORT CO.

CONTENTS

MINING ECONOMY **1**

Aspects on the Macedonian Mine Industry through exploitation of the metallic ores in the Mines of Bucim and Sasa.,

Dambov R., Petroska M., Nikolov N., Prohorov M. *3*

The Affective Factors Analysis on Exploration of Gourchopan Copper Deposit Using GIS Technique.,

Mehdipour A., Abrishamifar S.A., Ranjbar H.H., Mehdipour F. 13

Application of structure models in planning the development of EPIS production sectors.,

Maksimović S., Miljanović I. 21

Risks in optimization of consumables supplies in mining.,

Vujic S., Bosevski S., Miljanovic I., Petrovski A., Milutinovic A., Cebasek V., Gajic G. 29

RESERVE ESTIMATION **35**

Concurrent optimization of mine block sequencing and cut-off grades.,

Kumral M. 37

A New Production Scheduling Approach Considering Mill Requirements.,

Kumral M. 41

Robustness In Mine Planning Problem: Trade-Off Between Optimality And Feasibility.,

Kumral M. 47

Reserve and Grade Characterisitics of the Feldspar Deposit Using Geostatistical Methods.,

Yünsel T. Y., Ersoy A. 55

Assessment of Uncertainty in Grade-Tonnage Curves of a Multivariate Lateritic Bauxite Deposit Through Min/Max. Autocorrelation Factor Transformation,

Kizil M.S., Erten O. 67

An Application of Risk-Based Mine Planning Methods for a Copper Porphyry Deposit-Case Study.,

Heidari S. M., Saydam S. 79

Evaluating the risk of critical infrastructures by fuzzy inference system.,

Chamzini A. Y., Alidoosti A., Nejad J. H., Basiri M. H. 87

Coal supply derived from EPS supplementary mining facilities in order to respond to Serbian increasing energy demand in next decade.,

Popović N., Jakovljević M. 95

ROCK MECHANICS **103**

Influence of the Rock Microhardness on the Cut Depth in Abrasive Waterjet Cutting.,

Karakurt İ, Aydın G., Aydıner K. 105

A Study on the use of Taguchi Aproach in Abrasive Waterjet Machining of the Granite.,

Aydın G., Karakurt İ, Aydıner K. 111

Partition of Plastic / Elastic Energy in Mine Blasts.,

Aldas G.G.U., Ecevitoglu B., Kaypak B., Can A., Toprak B., E. Babayiğit, İ. Erguder, Kaçan M 117

TBM selection based on geotechnical risk assessment.,

Ghasempour N., Ejtemaei M. 127

Application of Modified Kuz-Ram Fragmentation Model by Gheibie et al. at the Sungun Copper Mine.,

Gheibie S., Duzgun Başkan S. H. *137*

Comparison of RMR and SRC classification systems for determination of support requirements in Ghazvin-Rasht railway tunnel, Iran.,

Entezari A., A. Farhadian, Mirzaei H. *143*

The Introduction of Uk Rock Bolting Technology Into Coal Mines Around the World.,

Daws G., Oxley A., Woodward N. *151*

Development of Cuttability Abacuses in Diamond Wire Cutting Method on Limestone Sample.,

Özçelik Y., Kanbir E. S. 161

MINING METHODS **171**

Use of Pyrotechnical Method in Bench Planes Recultivation at the Limestone Open Pit, Krivelj.,

Lekovski R., Mikić M., Pantović R. *173*

Influencing the energetic efficiency of clay minerals open pit mines by corrections in technology processes real time.,

Vujic S., Kasas K., Miljanovic I., Petrovski A., Kermeci Z., Popov K., Milutinovic A. *181*

Ground Surface Deformation as Effect of Longwall Mining of the Coal Seam No. 3 of the Livezeni Mine.,

Onica I., Cozma E., Marica D. *189*

Development of an underground coal mine project in Turkey using a 3D-modelling program.,

Förster I. *191*

Formation of geoinformation system of the coal mine with underground coal exploitation.,

Milutinovic A., Miljanovic I., Petrovski A., Pejovic M., Beljic P., Gajic G., Cebasek V. *209*

MINERAL PROCESSING **217**

Investigation of lead extraction process from galena concentrates by full factorial design.,

Ay N., Nasymov G. *219*

Ultra fine grinding of calcite powder in a stirred media mill: Effect of parameters on product size distribution.,

Toraman O.Y. 227

The Effects of Ball Filling and Ball Diameter on Breakage Kinetics of Barite Mineral.,

Deniz V. 233

The Investigation of Upgrading Possibility of Çorum-Alaca Chromites by Magnetic Separation.,

Bentli İ., Yıldırım Ç. 243

The Effect of Heap Height and Particle Size on the Copper Recovery and Acid Consumption.,

Hashemzadeh M. 249

Back-calculation of mechanical parameters of shell and balls materials from DEM simulations.,

Arabzadeh B., Farzanegan A., Hasanzadeh V. 257

Estimation of Soil Water Characteristic Curve through Weighted Residual Approximations.,

Shakiba-Nia K., Abdi M. *263*

Determination of the Parameters of Leaching Sulfuric Acid of Nickel Ores Low-Grade.,

Sadi F. H. Boukhemikem Z. 277

Copper Cementation With Zinc Powder From Zinc Sulfate Solution.,

Moradkhani D., Aghajanloo A., Sedaghat B., Abdollahzadeh A.A., ... 283

Design and Manufacturing of Laboratory Jameson Flotation Cell.,

Moradkhani D., Khoda Karamia M., Sedaghat B. 289

Determination of the optimum conditions for the separation of cobalt and manganese using by N-N reagent.,

Moradkhani D., Ataei E., Sedaghat B., Behnian D. 295

Factors affecting leaching behavior of copper oxide ore of Chodarchaei Mine.,

Moradkhani D., Sedaghat B. 301

Optimization of Lead Flotation of Anguran Low Grade Sample by DX7 Software.,

Moradkhani D., Rajaie M., Sedaghat B. 307

Zinc Leaching Optimization from Tajkooh Shaking Table Residue.,

Moradkhani D., Kamran Haghighi H., Sedaghat B. 313

Comparison the performance of Dissolved Nitrogen Predispersed Solvent Extraction and conventional SX methods in synthetic dilute and dense copper solutions.,

Koleinia S. M. J., Mohammadi M. R. T., Abdollahya M. 319

Evaluation the influence of performance mode Dissolved Nitrogen Predispersed Solvent Extraction method on selectivity of copper solvent extraction.,

Mohammad S.,Koleinia J., Mohammadi M. R. T., Abdollahya M. 331

Optimization of grinding circuit of Ardabil cement plant by BMCS software.,

Ardia E. G., Farzanegan A., Valianc A. 343

Flotation of Green Phosphate Sample of Esfordi Phosphate Mine.,

Dehghani M., Ostovar A., Noaparast M., Shafaei Z 349

Iron Removal from Mehran Fireclay Sample by Dry Magnetic Separation.,

Ostovar A., Dehghani M., Noaparast M., Shafaei Z. 355

Ash and Sulphur Rejection from Coal by Using Waste Motor Oil.,

Yavuz M., Uslu T. 361

Grain Size Distribution Properties of Chromite Particles in Polished Sections of Sieve Fractions.,

Taşdemir A. Özdağ H. Önal G. 367

OCCUPATIONAL HEALTH AND SAFETY **375**

Application of Technical and Economic Analysis in Refuge and Self Breathing Apparatus Design.,

Vahed A. T., Bahrami A., Demirel N. 377

Towards Benchmarking of Safety Performance in the Mining Sector.,

Genc B., Hermanus M. 385

Application of OHSAS 18000 to Bigadiç Boron Work to Improve Existent Working Conditions.,

Gökçek S.,Güyagüler T. 397

MINING AND ENVIRONMENT **407**

Comparison of CO_2 Emission related to Off-highway Trucks and Belt Conveyors in an Open Pit Coal Mine.,

Erkayaoğlu M., Demirel N. 409

Potential of CO2 Sequestration in abandoned coal mines in Australia.,

Jalili P., Jordan L. P., Saydam S., Cinar Y. 417

Modern Possibilities for Observing Land Surfaces and Constructions in order to Reduce Subsidence Damages.,

Octavian H. 425

Use of Remote Sensing in Determining the Environmental Effects of Open Pit Mining and Monitoring the Recultivation Process.,

Uça Avcı Z. D., Kahraman M., Özelkan E. 437

MINING ECONOMY

Aspects on the Macedonian Mine Industry through exploitation of the metallic ores in the Mines of Bučim and Sasa

Prof. Dr. Risto Dambov,
Dr.Sci.,University"Goce Delcev", Institute of Mining, Stip, R. Macedonia
Marija Petroska,
Macedonian association for mining (MAR), Economic Chamber of Macedonia
Nikolajco Nikolov,
MAR President, Mine Bučim, Radovis, R. Macedonia,
Maxim Prohorov,
MAR, Mine Sasa, M. Kamenica , R. Macedonia

ABSTRACT In this paper work are given some aspect of the exploitation of metallic ores and production of the colored metals from poly-metallic ores resulted from their processing and enriching in some of the more important Mines in the Republic of Macedonia.

We present the two biggest mines for production and processing of lead – zinc ores (Sasa) and copper ore (Bučim) in the view of the existing Mines, the assessment of the present state of art and produced capacities and results in the recent few years.

In short, we have set up the parallel of the existing legislation in the Republic of Macedonia which regulates this activity and development tendencies in mining in the view of the new investments, efficient and economical production, concession and other compensations.

Define the new findings and verification of the geological reserves, reconstruction and expansion of the present production capacities, opening or extension of the new exploitation fields and reveres, ecological aspect at mine exploitation, etc.

1 INTRODUCTION

Geographical position of Macedonia and geological conditions, caused to form the formations of many different rocks masses ranges with the presence of a large number of useful mineral resources.

Although relatively with small area Republic Macedonia is rich with a lot of different mineral resources metal ores, non metals, rare minerals, dimension stone blocks for the architecture, energy raw materials (coal) and other raw materials that make Macedonian mining industry.

More significant research works to define the larger ore reserves to which were initiated and carried out in the middle of the XIX Century. Since then today is made lot of numerous geological researches, mining research activities to a smaller extent and be established the new mineral fields with economic significance.

All of these activities contribute to create conditions for development of mining industry as an important segment in the overall economy of the Republic of Macedonia.

1.1 Brief review of mining in Macedonia

As a result of the quality of ores and quantitative contents of mineral resources in existing mines, and their technological–technical condition, the same mines in the transition period (after 1990) are not under gone significant changes.

Existing mines of non - ferrous metals (copper, lead, zinc, etc.) after the transformation of the capital and social changes, in the period after 1990, especially after 2000year, went up reactivated, to set up to high levels in terms of management, technical equipment, the level of geologic explorations the organization of work as well and stable standard of the workers.

Also there are lot of different types of travertine, granite blocks and slabs, and semi – precious stones of onyx which are characterized by their characteristic cappuccino colors.

Existing mines of nonmetallic mineral resources are also significant potential for the development of this economic branch.

These raw materials are almost with various entities throughout the territory of Macedonia and a large number of different quantitative and qualitative characteristics.

They represents a potential raw materials for the development of small quarries, small businesses for processing and shaping, which is have already been proven and in previous decades. With relatively small investments, limited resources and rapid turnover of the capital for several years, in these existing facilities are established stable low capacity, high quality raw materials and teams succeed for management and appearances on local and world market.

Especially here invoked the large number of low capacity for receiving and processing (large number of fractions with granulation from several microns up to several centimeters) of different types of limestone, igneous rocks of technical stone, and especially set as acquiring queries and processing of decorative white marble, with high quality with trade mark.

2 SOME PARAMETERS FOR MINING PRODUCTION

In the past two - three years the export of mineral resources has a high share in the total exports of RM from about 35% - 40%.

These percentages expressed in cash throu gh 1.100.000 dollars. For the same period the imports of this branch will move to over 800 million dollars and the percentage share of around 20%.

According to the latest parameters and tendencies which are expressed in the last three four years there is tremendous interest in the concessions, particularly in the area of non-metallic mineral resources and in recent times, with interest from several world companies have come in more attractive concessions for detailed geological research for metallic ores such as the copper, gold, lead, zinc, ferronickel, etc.

Table 1. Production of some ores of the active mines for copper, lead, zinc, and ferronickel

Products	Unit measures	2007	2008	2009	I -IV-2010 (≈2010)
Copper ore	t	4109464	4239500	3766500	1407500
Concentrates of copper	t	33467	38337	35430	12761(39000)
Lead Concentrates	t	48702	67401	63227	19624 (60000)
Zinc concentrates	t	61913	77473	77296	23654 (72000)
Ferronickel	t	15321	15026	12000	4531(13500)

* Source: State Statistical Office of the RM

In the previous period (the last two-three years) and according to the set priorities of the Government, is awarded through public tender more than 300 new sites under concession for research and exploitation of a large number of different mineral resources.

In Table 1 are presented the results of production of some mineral resources of the active mines for copper, lead, zinc, and ferronickel.

As it is seen from Table 1 the production of metal ores in recent years is constantly increasing. Exception can be said for the year 2009 decreasing for all metals shown in the table because the world economic crisis is reflected in the direct production and sales due to reduced purchasing of large companies and major consumers, the drop in prices of metals on world markets.

We can see that in just the first quarter of 2010 the production will go up for certain parameters, and will exceed production in the previous year.

In Table 2 are given the parameters of the production of some non-metallic mineral raw material that represent an important segment of the mining. Although these mineral resources do not have an important financial share in the overall mining industry and there are still important from the aspect of working labor, appropriate participation in the export performance of RM with direct products, or indirectly through the semi finished or finished products obtained in other industries.

This part in getting the finished products for purposes and general consumption (pharmacy, getting on the cement, porcelain, plastic mass, isolations materials, asphalt, etc.) can not affect the ordinary figures and all sorts of their would be unrealistic because the these products are taking part and other components.

3 LEGISLATION

Geological research of any type and volume, the mining of mineral raw materials, supervision and control as well technical inspections are regulated by the Law on mineral resources. (Official Gazette of RM no. 24/07, 88/08, 52/09)

According to this Low which so far has a few changes and supplements in the last year of the regulated manner of obtaining the concession for detailed geological research, mining permit, concession fees, necessary technical documentation for all permits related to this activity, as well as penal provisions prescribed by this Low.

As part of this paper to briefly give the method of obtaining the concession for exploration and exploitation. The procedure for a new concession of detailed geological research starts with getting a license for geological research, which in turn is achieved by applying the published public tender conducted by the authority in charge of this activity in the Ministry of Economy.

At this public auction stand out (publish) a number of concessions - new locations of raw materials of general interest such as: all kinds of metallic non metallic materials and resources, groundwater, thermo mineral waters and others.

All these concessions are public in the year general program adopted by the government after a request for research by interested domestic and foreign legal entities.

After the conclusion of a concession contract for detailed geological research, entity has the opportunity of two to four years (depending on the type of mineral raw materials) to perform geological surveys and preparation of report for mining reserves on the particular areas, a major mining project for exploitation, elaborate on the impact of environmental and other documents required by this law to obtain permission for the exploitation of mineral resources.

The granted concession for detailed geological surveys are paid one-time charge which offered the concession granted to the public tender, while the exploitation of mineral raw material is paid an annual fee according to the space occupied by mining activities and compensation for the exploitation of mineral raw material obtained by annual amounts and type of the mineral resource in the percentage that ranges from 0,5 to 1,5%.

Table 2. Production of typical materials for civil engineering and non-metallic products

Products	Unit measures	2007	2008	2009	I-IV- 2010
Marble and travertine, cut into blocks	m^3	19.925	22.857	24.100	8.789
Marble panel (slabs)	m^2	395.365	389.532	301.654	/
Gypsum	t	255.500	242.400	154.654	39.788
Limestone	t	848.498	827.100	694.968	148.243
Dolomite	t	96.723	75.855	78.523	17.000
Silicate sand	t	151.019	131.712	112.106	19.019
Sand for civil eng.	t	45.774	63.295	49.009	/
Crushing and broken stones	t	69.216	56.445	108.724	28.036
Bentonite	t	22.509	13.689	9.033	77
Volcanic tuffs	t	80.910	103.476	113.064	17.472
Quartzite	t	12.599	21.083	1.135	/
Sodium feldspar	t	32.814	28.920	19.377	4.327

* Source: State Statistical Office of the RM

4 BRIEF DESCRIPTION OF IMPORTANT METALLIC ORE MINES

This section will present two mines with their main parameters and certainly most important for the mining industry in Macedonia. The purpose of this item is given by numbers and technology of obtaining the basic features of these mines in order to obtain an impression of technical technological level, management attitude towards work, the results achieved in recent years, the prospective development of them, improving the conditions for facilities etc.

4.1 Mine for copper ore "Buchim" - Radovis

Mine's location in south-eastern part of Macedonia near the town of Radovis and only 3km away from the highway Strumica-Radovis-Stip. Mine copper ore "Buchim" is working more than 30 years.

After unsuccessful transformation of capital into bankruptcy the mine was buys from the company Solvej published an international tender in 2005 year. Since the company established by the management team worked successfully for 5 years to meet the foreseen production capacity and doubled the capacity of waste.

The existence of this mine and successful work had great importance for the city and in general for RM. This is the only mine in Macedonia for the copper ore from which gets a quality copper – clear metal, and a certain quantity of gold and silver.

Quantities of waste rock and ore in the last 5 (five) years the options presented in the Figure 1.

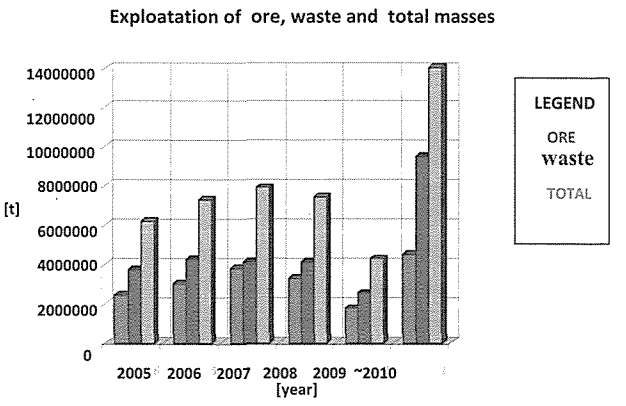

Figure 1. Production of ore and waste for period of 6 years

4.1.1 Technological process

The open pit is exploited copper ore containing copper, which despite small percentage of gold and silver. The quality of ore varies depending of ore body, copper mineralization and recent years have been exploited by average ore content of 0,235% Cu, 0,22 g/t Au and 0,72 g/t Ag.

According to these values this mine is classified in the group of poorest mines for copper in the world.

The exploitation is carried out on the lot of slopes and working more ore bodies, as follows: RT Čukar I and II, RT Central ore body, RT "Northeast" and RT Vršnik (new).

Year capacity of copper ores is more than 4.000.000tons, with the possibility of increasing the same because there are real possibilities and potentials. Capacity realized in the last year (2010) on the total weight of distracted from the open pit mine is about 15 million tons.

Exploitation is carried out in the open type of surface height-depth type of slopes with height of 15 meters. Drilling is performed with powerful drilling machines with a diameter of 250 mm of drilling. In an average week are done after 3 to 4 blasting series to ensure sufficient quantities of ore mass or waste.

Charging system is mechanized with Slurry and AN-FO type of explosives. Initiation is done by initiating Nonel system which provides quality blasting, safety at work and increasing cost per ton blasted mass.

Figure 2. Part of open pit „Bucim"

In this open pit mining has been done the biggest blasting series on the Balkans (1989) by applying 143 tons of explosives laid in 375 drill holes is obtained when the masses distracted from more than 800,000 tons.

Loading of blasted mass is done with electric and diesel excavators where the buckets are with a volume of 8 to 11,5 m^3. Excavators are from world famous companies P&H, O&K, and are successfully operating since the beginning of mine with made the necessary repairs.

The transport is done with the dumper trucks of different types (Caterpillar, Wabco, Terex) with a payload of 100 to 130 tons. With these trucks to be transferred the blasted ore to primarily crushing which is the capacity of 1000 t/h.

The same can accommodate size of a piece of max. 1 m^3.

After the primary crushing the pieces with a size up to 203 mm are transportation through the storage of an open line with capacity of 800.000 t.

From there by adding ~ the ore and is worn on the secondary, tertiary crushing continue to the mills (two number) to be have the granulation (0,074 mm) for appropriate flotation process.

After flotation and three level purification is obtained copper concentrate with a content of moisture from 7 - 8%, copper by 21% and gold 10 -15 g / t. This concentrate is transported to a smelter in Serbia and Bulgaria, from where it gets pure copper, gold and silver.

4.1.2 Development Perspective

In further period of operation in the Bucim mine are exploration of the adjacent ore bodies for their definition and classification of mineral reserves. During this year are expected beginning of the exploitation of the new ore body Vrsnik, where are defined ore reserves of over 10 million tons.

This ore, which the majority is oxide would be particularly manufacturing with technological Plants within the limits of the mine itself. Underway is the preparation of technical documentation for these previous mentioned plans and the only preparation of technical documentation and new agreements to obtain new concessions for geological exploitation of copper ore in the wider environment of the mine.

From the ecological aspect of the mine Buchim is given appropriate attention that show and the specific activities of this field.

Tailing dump from flotation process is under reclamation process and its is constantly under the existing project for reclamation with the trees and grass. Last year built is also a filter station for collecting the unclear water and catchments water from widest region of the mine in which part of this water will be used as technical and part will be already clear in the existing river for the biological minimum.

4.2 Mine for lead - zinc ore "Sasa" - Mac. Kamenica

The mine is placed in SI part of RM, 8 km from the city. The mine is situated in elevation from 800 to 1600 meters.

According rendered geological explorations and persistent in depth which are carried out continuously be ascertained ore reserves that are classified in the appropriate categories.

The main ore reserves were limited in scope zone between the level XIII and XIVb. Based on the indications for the emergence of new ore reserves at the depth, and in correlation with the existing concession agreement for detailed geological research approaches to the realization of program for detailed geological research in the Zone between level XIVb and zone "Kozja reka" and a level of 830 to the zone "Golema reka."

This zone presents a natural continuation of the ore bodies by the deep which can be seen from the vertical cross-section given in Figure 3.

On the basis of established, quantitative and qualitative parameters of mining reserves is defined technology for mining operations dynamics of preparation and production, and values of the ore.

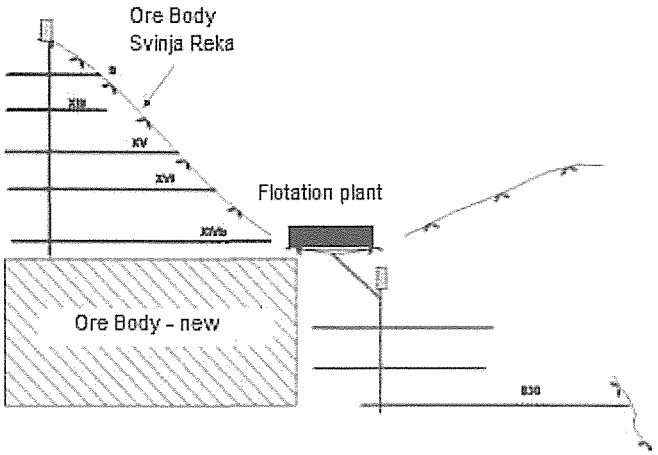

Figure 3. Vertical cross section of exploring area with objects for opening and development

4.2.1 Description of technology for exploitation, and development of the ore

Based on the results obtained from geological surveys and detailed analysis of possible ways of opening, development and excavation of ore zone between the horizons XIVb and 830, defined a way for basic mining and joined to the preparation of technical documentation level of additional mining project.

Given the past positive experiences with modified excavation methods they planned to apply for the excavation in this ore zone.

According to the technical characteristics of the method, ore zone is divided into 6 blocks with height of about 80 m and 300 m wide, for two of each horizon.

The main system for ventilation is diagonal with two main fans (Korfmman) for separately ventilation where are used most modern systems of fans (Zitrone) and flexible pipelines.

The realization of this production will be adequate done with preparation, which includes construction of service blocks ramps, hallways, ventilation objects , and ore / waste finch.

According to the operational plans of the mine, and on the basis of the available ore reserves the ability of the applied methods and technologies of exploitation is defined.

Mining dynamics of individual blocks for the entire period of exploitation for the next 15 years.

For the exploitation used most modern equipment for drilling (Atlas Copco - Bommer 281, Simba), freight transport machine Atlas Copco Wagner LHD STD 3.5, mining trucks Atlas Copco MT2000 as a whole series of service and auxiliary machinery (for anchoring Boltec, installation of shotcrete - Putzmeister, transport of raw materials with MINKA etc. All equipment is modernized, by applying with diesel engines.

The method of exploitation in the zone "Golema reka" is a method of keeping the grill and method of the backfill of excavated area with flotation tailings. The transport of the ore to the plant for primary crushing is done with export transport tape. After secondary and tertiary crushing the ore is done to smelting in two separate stages.

Flotation is a process of selective flotation on the main lead and zinc minerals. Flotation is obtained from two separate concentrates on the lead with over 73% of lead and zinc concentrate with over 50% with humidity of about 6 - 6,5%. The organization of the work is supported by appropriate systems for telecommunications and monitoring throughout the pits. For all workers will be provided with most modern equipment and personal protective equipment, as well as ongoing training. Sasa mine works with great success with annual capacity of 850 000 tons of lead - zinc ore, which is obtained from more zone and level. The quality varies according to ore level and zone - horizon of the average amounts, for A - Reserve Pb = 5.06%, Zn = 4.33%.

In the exploitation phase mine disposes over 10 million tons of ore reserves of A and B categories and with over 80 million tons of potential reserves, which in future should be done with surface deep drilling .

Besides the systemic organization of the technological process, all processes in Sasa mine be systematized and are prescribed according standard procedures and guidelines, in accordance with quality standards ISO 9001-2000, which was obtained in 2008 from the renowned Institute for Quality of Slovenia.

- ***Perspective***

The perspectives for the development of this mine is great. These is done permanent investigative drilling developments in spaces with be done and detailed the ore bodies.

At the same time performing at the surface investigative drilling developments with a plan for research for a longer period.

To prepare technical documentation for obtaining a new concession for research as well as documentation for the expansion of the existing concessions.

According with NVP and long-term plan are planned investments in all technological phase of over 30 million.

5 CONCLUSION

According to all the knowledge and perspective that are projected from expert in this field, it is emphasized that mineral resources in Macedonia as well as in the whole world, will be a basic ranged human potential for the development of the overall economy of a country.

Respective mining companies, government and ministries should be done for these tendencies to be achievable in the further period. The perspectives for the development of this activity in Macedonia as well in the world, directly depend on the activities undertaken in the sphere of legislation, prepared by laws - regulations and the appropriate documents (Tariffs) for regulation the basic duties, taxes and fees.

With the introduction of incentive measures, appropriate interest rate policy of the commercial banks and similarity of the legal provisions for new concessions and appropriate the technical documentation of mining only part of the measures should be taken in this important economic activity.

With the growth of prices on world markets for metals, greater demand in world terms, in the future will be created better conditions for the already existing mines and will give incentives for investment activities of domestic companies and even before the entry of foreign capital in the most active capabilities for their promotion of technological process, obtaining concessions for geological researches and opening of new mines.

REFERENCES :

Journal "Macedonian mining and geology", N^0 8/2008, 10/2008, 11/2008, 12/2009, 15/2009, SRGIM, ISSN 1409-8288, Skopje,

Journal "Minno delo i geologija", No.9/2006, "Zemja 93", ISSN 0861–5713, Sofija, R. Bulgarija

Data base from Republic Statistical Office of the R. Macedonia, Skopje, R. Macedonia

Technical documentation from Bucim – mine, (period 2005 – 2010)

Technical documentation from Sasa – mine, (period 2005 – 2010)

The Affective Factors Analysis on Exploration of Gourchopan Copper Deposit Using GIS

Ali Mehdipour, S. Amir Abrishamifar
I. A. University of Tehran, Tehran, Iran.

Hojjatollah Ranjbar
University of Bahonar, Kerman, Iran.

Fatemeh Mehdipour

ABSTRACT The study on affective factors to appear an ore deposit and its exploration operations is one of the important steps and procedure for any poly-metallic deposit exploration. By considering the affective factors, the obtained results guarantee the maximum efficiency for finding the ore deposit limits and preventing the capital lost of the exploration operations.

The geographical information systems "GIS" can be applied for geographical data management. The main scope of the paper is related to applying GIS for integration of affective factors of Gourchopan copper deposit exploration by usage both Boolean logic and index overlaying methods. The results show that by usage the GIS technique, determination of the ore deposit limits is more reliable. Additionally, by considering the weight factor in index overlaying method, the defined model gives better results than Boolean method for exploration maps. Choosing the accurate weight for the factors is one of important criterion in this method.

1 INTRODUCTION

Mineral resource quantitative prediction and assessment is one of the steps of mineral resource exploration based on multi-information (geology, physical geography, geochemistry, and remote sensing), synthetic technology, and metallogenic theory (Cheng & et al 2007). On the basis of the distribution of deposits and the multi-information of regional geology, geophysics, geochemistry, and remote sensing, mineral resource prediction is used not only to summarize the regional geology setting and the regional metallogenic theory, but also to establish regional exploration models (Xiao & Zhang 2007). The key to mineral resource prediction is to build deposit prediction modeling and delineate mineral prospects based on the metallogenic theory, mineralized condition, and mathematical method. At present, geologists generally use the GIS technology to extract mineralized multi-information and make region-mine-potential predictions with suitability modeling.

In general, finding potential areas is one of geographic information systems' capabilities and producing prioritized mineral potential maps is a method that GIS uses to predetermined exploration regions. Most of the GIS applied techniques to provide potential maps can be divided into three main steps: In the first step, all the required data are collected into "GIS" database. This phase includes identifying desired data sources, gathering data, digitizing their pictures to the computer, organizing and

interpreting some of the initial data. Next, classification, analysis and data processing in order to provide appropriate patterns related mineralization model, takes place. In the last step, all prepared data layers are integrated to produce final suitability map. The most important point about performing mentioned routine is using appropriate data integration method in order to lead decision makers to tangible and reliable results (Bonham-Carter 1994).

2 STUDY AREA DESCRIPTION

2.1 Geography And Geomorphology

This study was carried out in northeast part of Sarcheshmeh copper mine at Kerman state in southeast of Iran named Gourchopan region. This cold and mountainous region is located between longitudes of 55 ° 45′, 56 ° 00′ and latitudes of 30 ° 00′, 30 ° 15′. Gourchopan has been formed by igneous rocks with sedimentary rocks. Figure1 shows location and geologic structure map of the study area.

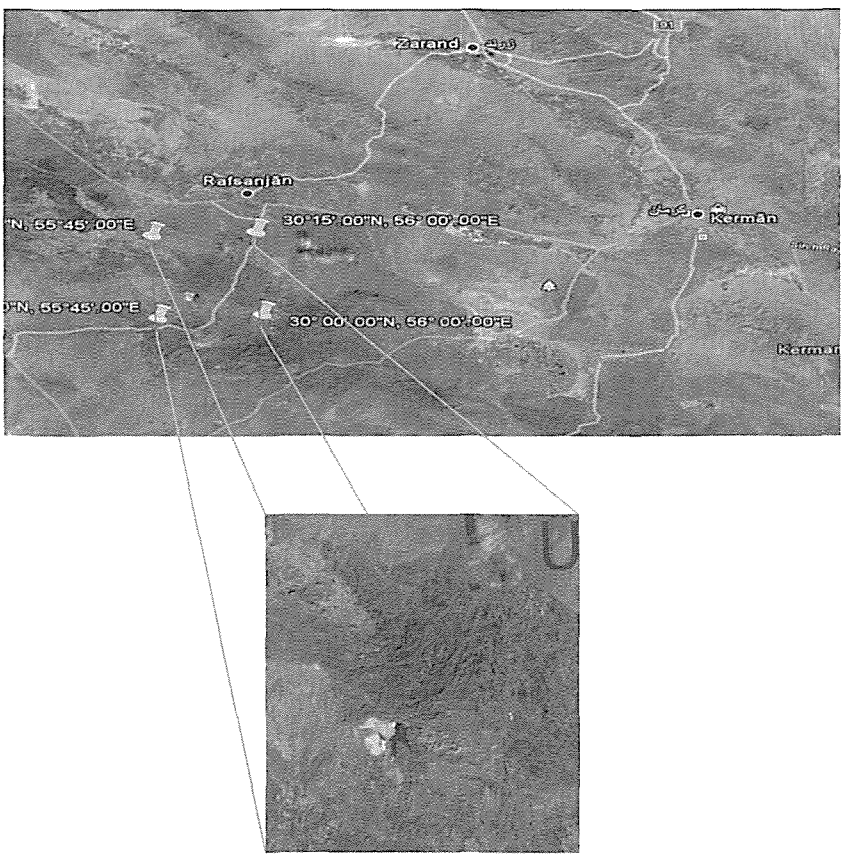

Figure1. Location and geologic structure map of Gourchopan area.

2.2 Geology

The study area has a variety of lithologies. The oldest reported rocks in the area which belong to the Eocene period include sedimentary rocks (carbonate and sandstone) and volcanic rocks such as agglomerate, andesite, trachyte and albite. Sub-volcanic dacite masses in the northwest and north parts of the study area were exposed.

Neogene sandstones in the middle area have lied on the volcanic rocks discordantly. Quaternary sedimentary rocks have occupied large part of our area. Gourchopan was active from the viewpoint of structural geology and existing faults has northeast-southwest directions. Some others directed in northwest-southeast.

Figure 2 is shown Geological map of Gourchopan which is produced by GIS.

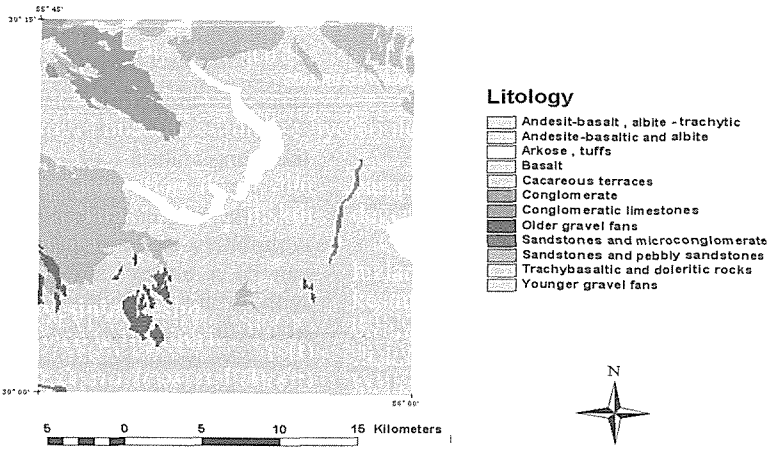

Figure2. Geological map of Gourchopan produced by GIS

3 GIS MODEL TO INTEGRATE EXPLORATION DATA

3.1 Required Data Layers

According to main characteristics of copper deposits, the useful data layers for mapping potential areas are as followings:

1- Basaltic intrusion.

2- Existence of dykes and faults around the intrusion, which can be tectonic expression of that part of the region.

3- Geophysical data such as radiometric and magnetic data which is helpful in recognition of copper potential areas.

3.1.1 Geological map

Large part of the region has been formed by volcanic rocks such as agglomerate, andesite, andesite, trachyt albite. These rocks can be a good guide to explore porphyry deposits, especially porphyry copper deposits.

3.1.2 Faults and fractures

Because they generally have higher permeability, faults and fractures have always been considered of great importance in porphyry systems (Hanano 2000). Surface indicators of the presence of main faults and high-density fracture zones have in fact proved useful in the past when

seeking areas of secondary permeability (Prol-Ledesma, 2000).

3.1.3 Geophysical data

Geophysical data that is used in this project includes an air bone geo-magnetic map and three air bone radiometry maps at 1:50000 scale produced by Atomic Energy Organization of Iran from north part of Sarcheshme in 1978. The process of data collection has been carried out using two methods including radiometric and magnetic surveys. Each method has been briefly explained as below:

3.1.3.1 Radiometric method

After 1944 that the airplane was used for first time to find the uranium during, radiometric method has been developed widely. Due to the use of aircraft in progress, this method is one of the fastest methods. Required data is harvested by a multi-channel spectrometer. Gamma-ray spectrometer is a device that separates gamma rays resulting from decay of potassium, uranium and thorium to identify the source. It contains four or five valves to measure the amount of potassium, uranium and thorium in different objects. This work (separation of mentioned elements' gamma ray) is done using the spectrum emission which is unique for each element.

3.1.3.2 Magnetic Measurement

This method has been established on the basis of presence of significant magnetic minerals like magnetite and Pyrrhotite. According to use of aircraft, it is one of the appropriate and fast ways for initial explorations. Because porphyry deposits especially copper porphyry deposits have low susceptibility, magnetic method is effective for their exploration. Sampling devices used in this method measure the magnetic field of the earth in nT unit.

Measurements conditions for this research were:

1-Flight line interval is 500 meters.
2-Flying azimuth is 41 degrees.
3-Sampling was done by the rate of one sample per second.
4-Maximum speed of airplane was 70 meters per second.
5-Minimum speed of airplane was 46 meters per second.

3.2 Map Integration Methods

In this study all required data layers has been integrated by following methods:

3.2.1 Boolean integration model

Boolean modeling involves the logical combination of binary maps resulting from the application of conditional binary operators.

As the purpose of creating such a map to completely exclude the unsuitable areas, it can be a binary map, in which the areas with limiting condition (not suitable) are given the value of zero and the allowed (suitable) areas are given the value of one. These maps are overlaid using the Boolean Operation, where input maps can be integrated by using logical operators such as AND, OR, XOR and NOT (Bonham Carter 1991).

In spite of simple structure, calculation and performance of Boolean integration method, absence of weighting process causes decision makers not be able to define suitability classes. So, all suitable places determined by Boolean model, have similar level of suitability and cannot be prioritized.

3.2.2 Index Overlay integration model

Index Overlay is a GIS operation whereby the layers with a common area are joined on the basis of their occupation of space (Clarke 1999). The overlay function creates composite maps by combining diverse data sets. Each class of map is given a different score, allowing for a more flexible weighting system. Score tables and the map weights can be adjusted to reflect the

judgment of an expert in the domain of the application under consideration.

Factor maps are integrated using following Equation:

$$S=\frac{\sum W_i S_{ij}}{\sum W_i}$$

Where:

W_i= weight of ith factor map

S_{ij}= ith spatial class weight of jth factor map

S= the spatial unit value in output map(Ebadi & et al 2004)

3.3 Execution

In this section, we describe regular steps that identify the optimum model for cupper potential areas as shown through following flowchart (fig.3).

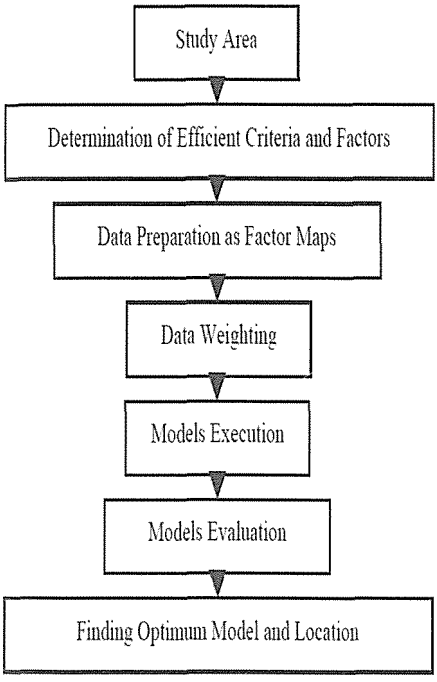

Figure3. Integration models execution and evaluation steps.

3.3.1 Data preparation

Since all acquired data was paper based, they had to be digitized in order to be used as input maps. Afterwards, these maps exported from CAD format into GIS environment as shp files. Finally, some GIS ready methods including determination of projection system and datum, conversion vector layers to raster and producing distance map carried out on shp files that input layers got ready to be integrated according their weights to find suitable places.

3.3.2 Boolean execution

We used statistical operations on data layers to get the most desirable areas of mass deposit. To lead this, mean(X) and standard deviation(S) of each radiometry maps was calculated and map algebra was evaluated to find pixel values more than X+S which is shown in table1.

Integration of radiometry, magnetic and geology maps by Boolean method the final suitability map was produced as shown in figure4.

3.3.1 Index Overlay execution

This model was executed in two steps including data weighting and data integrating.

3.3.1.1 Data Weighting

Determination of correct weight for effective factors is the most important step while performing index overlay method. The weight of each factor map indicates amount of its value as comparing with the other factor maps. Correct weights can help finding convenient location for cupper potential area. Table 2 shows weights and suitability class number of each factor and weight of each suitability class according to expert knowledge.

Table1. Mean and Standard deviation data for radiometry and magnetic maps

Element	Range	Mean(X)	Standard deviation (S)	X+S
Uranium	0.5-7	3.5	2.45	5.95
Thorium	0-38	19	11.8	30.8
Potassium	0.5-4	2.25	1.23	3.48
Magnetic	-1000-900	-50	590	540

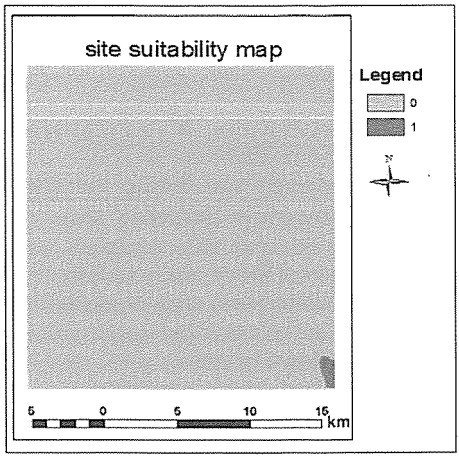

Figure4. Desirable area map to exploration copper deposit by Boolean model

3.3.1.2 Data Integration

In this step all determined weights applied into factor maps and suitability classes that leaded us to produce weighted maps. Finally, these maps has been integrated using index overlay formula and formed final site suitability map which is shown in Figure5. In final map, value associated for each pixel demonstrates the amount of pixel's copper potential.

4 CONCLUSIONS

The main propose of this paper was evaluation of applying GIS technique for cupper resource prediction by integrating affective factors in copper deposit exploration. The results illustrate the successful implementation of a GIS technology for determination of mineral potential areas.

Additionally, by considering the weighting process in index overlay method, the defined model gives prioritized results as numerical values between 0 and 1. This characteristic causes index overlay method to be more reliable than Boolean method. Choosing the accurate weight for the factors is an important criterion about index overlay method which directly impacts final suitable areas. So, data weighting task required to be done with adequate studies about effect of each factor on potential areas.

Table2. The value and factors related to weight classes

Evidence layer	Layer type	Weight	Number of class	Factor class	Weight of class
Lithology layer	Polygon	0.95	3	On mass	1
				0-1000(m)	0.8
				1000-2000(m)	0.6
Fault layer	Polyline	0.9	3	On fault	1
				0-500(m)	0.8
				500-1000(m)	0.6
Magnetic layer	Polyline	0.85	3	-1000--500(nT)	0.95
				-500-0(nT)	0.85
				0-500(nT)	0.8
Potassium layer	Polyline	0.8	3	3-4(%)	0.9
				2-3(%)	0.7
				0.5-2(%)	0.5
Thorium layer	Polyline	0.75	2	30-38(ppm)	0.9
				15-30(ppm)	0.7
Dyke layer	Polyline	0.7	3	On dyke	1
				0-500(m)	0.8
				500-1000(m)	0.9
Uranium layer	Polyline	0.65	2	5-7(ppm)	0.9
				2-5(ppm)	0.7

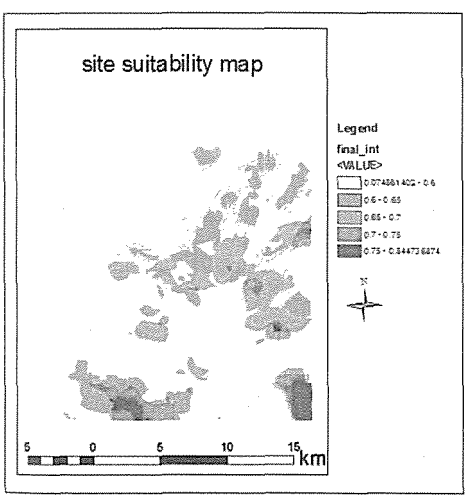

Figure5. Desirable area map to exploration copper deposit by index overlay model

REFERENCES

Bonham-Carter, G.F., 1991. *Integration of geoscientific data using GIS,* Longman, Essex, pp. 171–184.

Bonham-Carter, G.F., 1994. Geographical Information Systems for Geoscientists: Modeling with GIS. *Computer Methods in the Geosciences,* 13, 398p.

Bonham-Carter, G.F., Agterberg, F.P., Wright, D.F., 1988. Integration of geological data sets for gold exploration in Nova Scotia. *Photogrammetric Engineering and Remote Sensing,* 54, pp.1585–1592.

Noorollahi, Y., Itoi R., Fujii H., Tanaka T., 2008, GIS integration model for geothermal exploration and well siting, *Geothermics*, 37, pp.107–131.

Cheng Q. M., Chen Z. J., 2007, Application of fuzzy weights of evidence method in mineral resource assessment for gold in Zhenyuan district, Yunnan Province, China. Earth Science

Journal of *China University of Geosience*, 32, pp.175-184.

Clarke, K.C., 1999, *Getting Getting StartedWith Geographic Information Systems*, second ed. Prentice Hall, Upper Saddle River, NJ, USA, 338p.

Ebadi H., Shad R., Valadanzoej M. J., Vafaeinezhad A., 2004, Evaluation of Indexing Overlay, Fuzzy Logic and Genetic Algorithm Methods for Industrial Estates Site Selection in GIS Environment, *ISPRS*, Istanbul, Turkey.

Gongwen, W., Jianping, C., 2008, Mineral Resource Prediction and Assessment of Copper Multi-mineral Deposit Based on GIS Technology in the North of Sanjiang Region, China, *EARTH SCIENCE FRONTIERS,* 15, pp.27–32.

Hanano, M., 2000. Two different roles of fractures in geothermal development. In: Proceedings of the *World Geothermal Congress,* Kyushu–Tohoku, Japan, 28 May–10 June, pp.2597-2602.

Prol-Ledesma, R.M., 2000. Evaluation of the reconnaissance results in geothermal exploration using GIS. *Geothermics,* 29, pp.83–103.

Xiao K Y, Zhang X H, Li J C., 2007, Quantitative assessment method for national important mineral resources prognosis. *Earth Science Frontiers*, 14, pp.20–26

Application of structure models in planning the development of EPIS production sectors

S. Maksimovic
Electric power industry of Serbia, Head office for Energy Production, Belgrade, Serbia

Igor Miljanovic, Aleksandar Petrovski, Milena Josipovic Pejovic
Faculty of Mining and Geology, University of Belgrade, Serbia

ABSTRACT For the modern business circumstances, enforced by the intensification of restructuration of the thermoenergy sector of the Electric Power Industry of Serbia, a demand for the overall planning and management over the complex business systems is endorsed. The application of structure models, the intersector models is one of the confirmed and reliable ways that, regrettably haven't so far find their place in this area of business. This paper is aiming to put focus to some of the positive effects of the application of such model.

1 INTRODUCTION

The experts made the assessment that the current financial and economy crisis can become even deeper and with even more negative consequences in comparison with the crisis that was going on during the 30's. The response to the crisis must be sought and reached at all business levels and sectors, even in the coal sector. The sooner the analysis of the crisis consequences occurs, the bigger are the chances that it is prevented or at least its consequences diminished.

The coal sector, as the most important part of the material production holds the great production multiplier. The importance of coal sector for the business and the overall development is a consequence of the diverse influence to the development of all the others business branches, and even to the non-production related activities in a certain way.

Together with the stronger breakthroughs of science and technology, the material costs are lowering down, and the work productivity increases significantly. This branch of industry provides job to a vast number of employees, leading to the increase of the living standard. In other words, it becomes the essential factor of the overall development of society and economy. Significant portion of the coal sector development was held by the competition, and its role did not change even today.

The development of the coal sector has never and nowhere happened in the environment of free competition, independently of the economy policy carriers. The carriers of the economy policy have always treated coal sector as an area of the material production whose development should be consciously directed and manage it in parallel with the free competition.

However, with the even faster coal sector development, certain disturbances and crisis occurred, influencing the increase of the economy policy carrier influence, their role grew stronger, and the field of planning and management and the instruments of management became wider, with time.

For coal sector management, a huge number of diverse information is necessary: on resources, physical scope and the value of industrial production, new technologies, working staff. The information is produced, collected, processed and stored by numerous institutions (scientific institutes, faculties, industrial companies, statistical institutes, chambers, banks, stock markets, etc.).

With the increase in size of managed object – very fast and out of any proportion the cognitive, mathematical, algorithmic, information, ..., complications and difficulties in rational determination of appropriate decisions are rising as well.

All attempts made so far shows that the structure models can provide for a far more realistic overview of mutually very complex dependencies and influences within and outside of the coal sector.

2 GENERAL ASSUMPTIONS OF THE STRUCTURE MODELS (SM) OF BUSINESS ASSOCIATIONS (BA)

In order to accomplish the mutual comparison of the structural tables (ST) for the level of business organizations, and with the data of the future STs, a unique methodology in their development should be applied. In the STs of business organizations it is necessary to dissect the mutual relations between the productive activities. The next thing to do is to dissect the existing business activities into smaller units. Having in mind that certain business activities and their sub-activities are displaced spatially into various regions, it is necessary to determine the appropriate transport costs and the market costs, which is a very complex task.

Certification of harmonization between the productive and non-productive units within the BA, and the relationship between the all productive and non-productive units with all the other organizational units of other BA and organizations appearing either as raw materials, or as the buyers of the final products is an extremely complex task because these relations are commonly, as a rule in modern business, very complex.

Table 1. Basic structure table of the business association TP OP "Kostolac" (planned for the year 2007.) in thousands RSD

Sector	Drmno	Cirikovac	TP OP Kostolac A	TP OP Kostolac B	Total	Final consumption	SUM
Drmno	2,500	0	568,400	4,753,500	5,324,400	537,780	5,862,180
Cirikovac	0	640	704,800	0	705,440	527,300*	1,232,740
TP OP "Kostolac A"	0	47,300	37,100	0	84,400	2,115,700	2,200,100
TP OP "Kostolac B"	153,100	0	0	102,000	255,100	9,140,980	9,396,080
Total	155,600	47,940	1,310,300	4,855,500	6,369,340	12,321,760	18,691,100
Overall material costs (OMC)	**2,145,000**	**265,550**	**1,470,550**	**5,161,900**	**9,043,000**		
Amortization (AM)	1,221,100	105,940	125,000	2,132,300	3,584,340		
Net profit (NP)	613,800	387,600	275,000	266,180	1,542,580		
Production excess (PE)	1,882,280	473,650	329,550	1,835,700	4,521,180		
Societal product (SP)	**3,717,180**	**967,190**	**729,550**	**4,234,180**	**9,648,100**		
Production (P)	5,862,180	1,232,740	2,200,100	9,396,080	18,691,100		
Decrease of stocks (Z)	-	-	-	-	-		
Import by origin (I)	-	-	-	-	-		
Available resources (AR)	**5.862.180**	**1.232.740**	**2.200.100**	**9.396.080**	**18.691.100**		

The simplified processes of the economy system are also the significant shortcoming of the structure model, articulated in particular through the introduction of two basic assumptions:

a) The production units of the Business Association are the separated technological entities where the production process is accomplished in a particular way;

b) The quantity of all types of production costs of any production unit (PU) is a linear dependency on the production level of the production unit.

The Business Association comprises of several production unit (x_1, x_2, ..., x_n) each separately representing a certain homogenous entity regarding the operational technology, i.e. the production activity.

3 STRUCTURE TABLE CONTENTS OF THE BA TP OP "KOSTOLAC"

Business association TP OP (Thermal Power Plant Open Pit Mine) "Kostolac" is disassembled into four production sectors: open pit mines OP Drmno, OP Cirikovac and thermal power plants TP OP A and TP OP B. The planned values for the 2007, are presented in thousands of RSD in the intersector table (Table 1).

3.1 Technical coefficients (production norms) for the BA TP OP "Kostolac"

Based on the table 1, technical coefficients or the production norms were calculated. They represented the direct production dependency between the each pair of production sectors in completing their activities within the BA TP OP "Kostolac".

Technical coefficients were not separated in this paper by their origin into technical coefficients of domestic or imported origin, having in mind that the product of domestic origin is processed in the reproductive system.

The technical coefficient matrix of the BA TP OP "Kostolac" has the following form:

$$A[a_{ij}] = \begin{vmatrix} 0.00043 & 0 & 0.25835 & 0.50590 \\ 0 & 0.00052 & 0.32035 & 0 \\ 0 & 0.03837 & 0.01686 & 0 \\ 0.02612 & 0 & 0 & 0.01086 \end{vmatrix}$$

3.2 Technical coefficients of the BA TP OP "Kostolac" realization

Based on the table 1, the technical coefficients of realization were calculated, and presented as a matrix of the technical coefficients realization

$$A[b_{ij}] = \begin{vmatrix} 0.00043 & 0 & 0.09696 & 0.81088 \\ 0 & 0.00052 & 0.57173 & 0 \\ 0 & 0.02150 & 0.01686 & 0 \\ 0.01629 & 0 & 0 & 0.01086 \end{vmatrix}$$

3.3 The inverse matrices of the BA TP OP "Kostolac" technical coefficients

Based on the matrix of direct technical coefficients (a_{ij}), an inverse matrix of technical coefficients was calculated.

Inverse matrix elements are interpreted only by columns. For example, if the production at the OP Drmno is to be ensured for the purpose exclusively to the final consumption at a value of 100 RSD, it is necessary that the production value within that sector reaches 101.4 RSD, and in the TP OP B sector 2.7 RSD. The conditioned increase in production for 1.4 RSD above the necessary for the final consumption at the Drmno sector, together with the induced increase in production in the TP OP B sector

for 2.7 RSD should only provide for the functioning of the reproductive process that would only result in the production of OP Drmno sector at a value of 100 RSD for the final consumption.

$$[I\text{-}A]^{-1} = \begin{vmatrix} 1.014 & 0.010 & 0.270 & 0.519 \\ 0 & 1.013 & 0.330 & 0 \\ 0 & 0.040 & 1.030 & 0 \\ 0.027 & 0 & 0.007 & 1.025 \end{vmatrix}$$

By adding the elements of the inverse matrix by columns, values of $(I\text{-}A)^{-1}$ = [1.041 1.063 1.637 1.544] were obtained. The element 1.041 shows that the BA TP OP "Kostolac" should accomplish the planned production in 2007 at the value of 104.1 RSD in order to enable the activity to the Drmno sector in coal production aimed solely to the final consumption with the value of 100 RSD.

4 EXAMINING THE CONCORDANCE STRUCTURE OF THE BA TP OP "KOSTOLAC"

The basic structure table of the BA TP OP "Kostolac" for the year 2007, the matrices of the technical and inverse coefficients, realization coefficients, inverse realization coefficients and their parallel review, the society product coefficients are providing wider possibilities for testing the structure of the concordance of thermoenergy complex, meaning to review the position of each production unit (sector) in BA in whole.

The detailed analysis of the technical coefficient matrix and the matrix of inverse coefficients provides wider possibilities in testing the structure of concordance of the Business Association Kostolac. Besides, if the overall scope of production for a certain production sector, for example the Drmno sector, for the external realization (Y) is known in advance, then the following relation is obtained by matrix multipliers (the elements of the technical coefficient matrix):

$X_1 = 1.014 \cdot 537.780 + 0.010 \cdot 527.300 + 0.270 \cdot 2.115.700 + 0.519 \cdot 9.140.980 = 5.862.180$ (thousands RSD)

Table 2. Parallel review of technical coefficients and the inverse matrix coefficients for the existing sectors

Sectors	Drmno		Cirikovac		TPOP-A		TPOP-B	
	a_{ij}	$(I-A)^{-1}$	a_{ij}	$(I-A)^{-1}$	a_{ij}	$(I-A)^{-1}$	a_{ij}	$(I-A)^{-1}$
Drmno	0.00043	1.014	0	0.010	0.25835	0.270	0.50590	0.519
Cirikovac	0	0	0.00052	1.013	0.32035	0.330	00	0
TPOP-A	0	0	0.03837	0.040	0.01686	1.030	00	0
TPOP-B	0.02612	0.027	0	0	0	0.007	0.01086	1.025
Total:	0.02655	1.041	0.03889	1.063	0.59556	1.637	0.51676	1.544

Table 2, for example, shows that, if the sector production of the Drmno sector (intended for external realization) is to be increased by 100 RSD, it is necessary to increase the overall production of the Drmno sector by 101.4 RSD, Cirikovac by 1.0 RSD, TP OP A by 27.0 RSD and TP OP B by 51.9 RSD, or, overall by 181.3 RSD, so that the concordant proportion of the production structure for this BA is ensured.

Table 3 presents in parallel the values of the overall production vector value (X) and external realization (Y), both for the existing and for the planned condition. The multipliers are notably efficient as a simple tool for determining the necessary overall production of the production sectors necessary to ensure

the increased external realization. By further disaggregation of the external realization vector (Y) to the real consumers of the coal produced to OP Drmno and Cirikovac, as well as the disaggregation of the external costs vector (D) to the elements of costs by material type, services, etc., different analysis are possible as well as quantification of certain effects occurring due to external and internal factors for the particular production sector and the BA in general.

Table 3. Parallel review of the overall production vector values (X) and the overall external realization (Y) for the existing and the planned condition (thousands RSD)

Sector title	Current condition		Planned condition	
	External realization title	Overall production value	Leveled value of the external realization	Expected overall production
	[Y]	[X]	[Y']	[X']
Drmno	446,171	6,672,102	537,780	5,862,180
Cirikovac	0	541,224	527,300*	1,232,740
TP OP-A	2,925,857	3,014,997	2,115,700	2,200,100
TP OP-B	8,600,939	8,878,460	9,140,980	9,396,080
Total, %	Y=11,972,967 %=100.00	X=19,106,783 %=100.00	Y'=12,321,760 %=102.91	X'=18,691,100 %=97.83

* transferred from external realization in Drmno

Planned distribution of resources for the OP-PA Cirikovac should provide for the basic reproduction. The additional 527.3000.000 RSD was to be ensured, 336.170.000 RSD taken from the position of accumulation at the OP Drmno, and the additional 191.130.100 RSD by increasing the final consumption through production and sales of coal as the consumer goods. At the end of the business year 2007, OP Cirikovac had a drop in coal production by 194,000 tons, amounting to 181.770.000 RSD. Table 3 presents the increase in overall realized material costs (OMC) by 376.658.000 RSD in relation to planning and gross product by 173.000.000 RSD for the purpose of increase of production (IP).

The difference in the business income and the business expenses, for the year 2007, was 1,077,000 million RSD, which had predominantly reflected on the business results of the OP Drmno. The management was supposed to intervene even before 2007 in the matter of the constant increase of expenses at the OP Cirikovac, occurring with the introduction of the open pit to the closure process (conservation), and radicalize the restructuring regarding the working staff and further utilization of the available equipment. Unfortunately, this hasn't happened even in 2008, which burdened the business at the BA TP OP "Kostolac" even more.

5 TESTING THE INTEGRITY DEGREE OF THE BA TP OP "KOSTOLAC"

Table 4 presents the fitting of production sectors within the BA TP OP "Kostolac" into a certain integration entity, as well as the justification of such integration, taking into account the matrix of technical coefficients (a_{ij}) and realization coefficients (b_{ij}), or the arithmetic mean value of the sum of all coefficients for the sector k.

Table 4. Parallel review of $\sum_{i=1}^{n} a_{ij}$, $\sum_{j=1}^{n} b_{ij}$ and $\left(\sum_{i=1}^{n} a_{ij} + \sum_{j=1}^{n} b_{ij}\right)/2$ for the sectors named by the values of the named parameters

Sector title	$\sum_{i=1}^{n} a_{ij}$	Sector title	$\sum_{j=1}^{n} b_{ij}$	Sector title	$\left(\sum_{i=1}^{n} a_{ij} + \sum_{j=1}^{n} b_{ij}\right)/2$
TP OP-A	0,59556	Drmno	0,90827	Drmno	0,46741
TP OP-B	0,51676	Cirikovac	0,57225	TP OP-A	0,31136
Cirikovac	0,03889	TP OP-B	0,03836	Cirikovac	0,30557
Drmno	0,02655	TP OP-A	0.02715	TP OP-B	0,27756

For example, the value of the sum of mean arithmetic value of technical coefficients and realization coefficients ranges from 0.28 (for the TP OP-B sector) to 0.47 (for the Drmno sector), pointing to the different degrees of integration of the listed production sectors. Having in mind that the difference is not distinct, this problem can be exceeded through certain remodeling of the organization model.

6 CONCLUSION

The results of the application of structure models in mining are a subject of a small number of papers. Even this small number shows the possibility of the real overview of mutual and very complex dependencies and influences within the Business Association.

Originated from the tables obtained are the numerous, wide and important findings concerning the: direct and recurrent production subsystems connections, bidirectional dependencies of the system and the environment, i.e. the nature and the intensity of the production system (or the systems in their value structure) dependencies, the proportions and the structure of the final consumption, i.e. the external realization, the way and the degree of their influence of its changes to the system production, the structure of certain costs category and the value of production accomplished, etc.

There are no obstacles in applying the certain models of the structure analysis in the coal sector, public enterprises, business associations and the smaller organization units.

REFERENCES

Vujic S., Miljanovic I., Maksimović S., Milutinović A., Benović T., Hudej M., Dimitrijević B., Čebašek V., Gajić G., Optimal dynamic management of exploitation life of the mining machinery: Models With Undefined Interval *Journal of Mining Science*, Vol. 46, No. 4, July-August 2010, (pp. 425-430).

Stanojevic R., (1998), *Intersector models*, Institute of Economy Belgrade, Belgrade (in Serbian).

Popović S., Nešić V., Petrović J., (1977), An application of the input-output analysis in the complex organization of the associated labor for the example of Mining and Energy Industry Combine "Kolubara", *SYM-OP-IS 77*, Herceg Novi, (pp. 439-460), (in Serbian).

Petric J., Popovic S., Nesic V., (1981), An application of the intersector analysis model for the natural parameters of the associated labor, *Director*, No. 4, Belgrade. (in Serbian).

Popovic S., Nesic V., Petric J., (1977), Prijmena input-output analiza u složenoj organiazciji udruženog rada na primeru REIK "Kolubara", SIM-OP-IS 77, Herceg Novi, pp. 19-21.

Maksimovic S. (2009), An application of the intersector analysis in the business associations of the thermoenergy sector of the Electric Power Industry of Serbia, *Elektroprivreda*, No. 1, Belgrade, (pp. 85-92), (in Serbian).

Maksimovic S., Milinović Z., Miljanović I., Boševski S., Hudej M., Benović T., Application of Input-Output analysis in corporate enterprises of the Electric Power Industry of Serbia Thermal Power Sector, *3rd Balkan Mining Congress*, 01-03.10.2009., Izmir, Turkey, (pp. 491-498).

Maksimovic S., Miljanovic I., et al., (2010), The sensitivity of production in certain production sectors of the Business Association of TP OP "Kostolac" to the changes in technical coefficients, *Mining 2010.*, Tara, (pp. 85-92), (in Serbian).

Petrović S.,(1986), Construction and informational contents of the business associations production system Input-Output table, *Yearbook of the*

Faculty of Economy in Kragujevac, Kragujevac, (pp. 301-323), (in Serbian).

BA TP OP "Kostolac", (2007), *Business report, 2007.* (in Serbian).

Maksimovic S., Milinovic Z., et al., (2009), An application of the Input-Output analysis in enterprises of the thermoenergy sector of the EPIS, *SYM-OP-IS 2009*, (pp. 587-590), (in Serbian).

Maksimović S., Miljanović I., Changing influence into technological matrix on some production sectors in Kolubara and TENT economic association units, *IX International scientific opencast mining conference, Vrnjačka Banja,* 20-23.10. 2010., (pp. 130 - 142), (in Serbian).

Risks in optimization of consumables supplies in mining

Slobodan Vujic[1], Stefko Bosevski[2], Igor Miljanovic[1], Aleksandar Petrovski[1], Aleksandar Milutinovic[1], Vladimir Cebasek[1], Grozdana Gajic[3], Milena J. Pejovic[1]

[1] *Faculty of Mining and Geology, University of Belgrade, Serbia*
Tel. +381 11 3238564, Fax. +381 11 3347934, e-mail: vujic@rgf.bg.ac.rs
[2] *Rudproekt, Skopje, Republic of Macedonia*
[3] *Faculty of Forestry, University of Belgrade, Serbia*

ABSTRACT This paper, is analysing the problem of consumables stock supplies (energetic resources, lubricating oils, explosives and explosive means, flotation agents, tires, spare parts, etc.) at mines, and reviewing the practical concerns on the stock supply theory on the example of the open pit mine "Zelenikovec".

1 INTRODUCTION

In order for an objective review of the problem of consumables supplies in mining, test experimental researches at the real mining object were conducted.

Starting from the basic condition that for the research on the object of analysis and testing, there must be reliable information regarding consumption of consumables during a longer period of time (Bosevski, 2010), it is assessed that the limestone open pit mine "Zelenikovec" near Skopje, Macedonia, provides an excellent basis for experimental testing. In completing the analysis, previous findings from the study researches in the subject area, realized at the Department of Applied Computing and System Engineering of the Faculty of Mining and Geology, University of Belgrade, were used.

According to the economical parameters, "Zelenikovec" limestone open pit mine is operating successfully during the last 10 years (Bosevski, 2010). This is at the same time the period suitable for the subject test – experimental analysis. The average annual production for these 10 years is 83,200 (t). The open pit is producing these fractions: for concrete 0–4 (mm), 4-8 (mm), 8-16 (mm) and 16-32 (mm) and fractions for the tampon layer 0-32 (mm) and 0-60 (mm).

In experiments, the data on the consumption of diesel fuel, motor and hydraulic oil, explosive and nonel (the initial explosive mean) were used, being the most significant in the structure of production costs at the "Zelenikovec" open pit mine. These materials account for more than 80 (%) of the overall material costs.

Since the consumption and supplies of material resources at the open pit mine are a production function, the initial step of the analysis was related to the trends of production for the ten-year period. Figure 1 shows production of limestone at the open pit from 2000 to 2009. The production held an upward trend, in general (dashed line on the figure 1), with the significant drop in 2001 to 50.000 (t) due to military operations, and in 2008 and 2009, due to negative influence of the world economy crisis. The highest production achieved was 100,000 (t) of limestone in 2007.

It is typical for this type of production at the open pit mines, and also for this open pit mine, that it is susceptible to weather conditions (Vujic et al., 1993, Vujic et al., 1994). This is the reason for selecting grouping by trimester (quarter) in data

classification, in relation to the seasons: winter, springtime, summer and autumn. Avoiding being strict in calendar determination of the seasons, the winter period for the purpose of this analysis encompass January through March, springtime April through June, summer: July through September, and autumn: October through December.

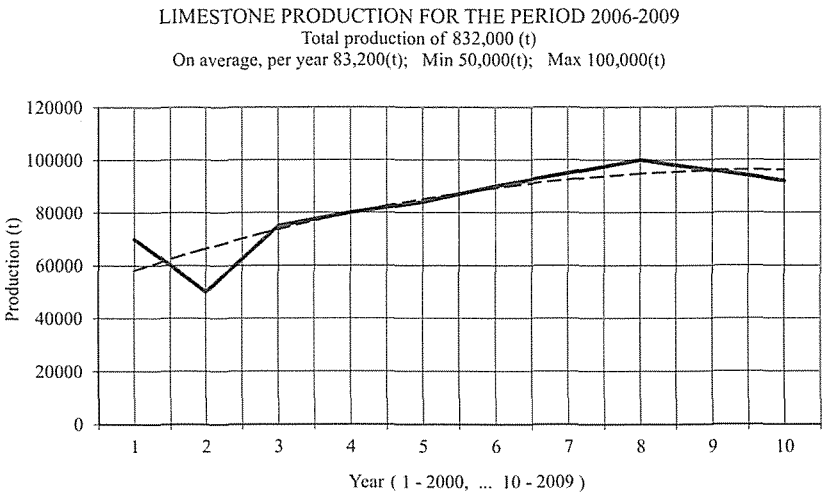

Figure 1. Limestone production trend at the "Zelenikovec" open pit mine

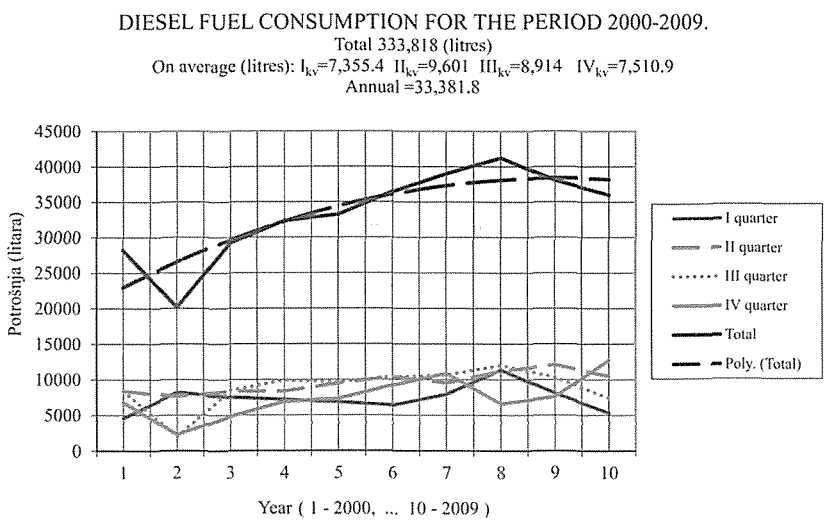

Figure 2. The overall and quarterly consumption of the diesel fuel at the "Zelenikovec" open pit mine

2 EXPERIMENTAL RESEARCH

Aiming to determine the trend in overall and quarterly consumption of diesel fuel, motor and hydraulic oil, explosive and the nonel, a regression analysis was completed, by using the APR01 software. Since trend analysis is common knowledge, it will not be discussed in particularities here. The following trends were discovered in the analysis:

Consumable: Regression function:	Correlation coefficient:
Diesel fuel (*litres*) $p_t = 3{,}839.58 + 4{,}538.82 \cdot k_v - 912.17 \cdot k_v^2$	$K_k = 0.96$
Motor oil (*litres*) $p_t = 166.90 + 255.48 \cdot k_v - 50.80 \cdot k_v^2$	$K_k = 0.99$
Hydraulic oil (litres) $p_t = 65.15 + 76.99 \cdot k_v - 15.45 \cdot k_v^2$	$K_k = 0.96$
Explosive (*kilos*) $p_t = 1{,}270.91 + 2{,}957.57 \cdot k_v - 645.398 \cdot k_v^2$	$K_k = 0.98$
Nonel-explosive mean (*pieces*) $p_t = 7.45 + 75.77 \cdot k_v - 12.65 \cdot k_v^2$	$K_k = 0.99$

Where: p_t – consumption; k_v - quarter (1, 2, 3, 4)

It can be noted that all the function of regression are second degree polynoms, with high functional values of correlation coefficients between 0.96 and 0.99. The mutual equivalence of the regression functions confirms the reliability and validity of data on consumption of resources observed at the "Zelenikovec" open pit mine, and at the same time shows that there is an immediate connection between the limestone production dynamics and material resources consumption.

The results obtained by the mathematical-statistical and regression analysis served as the input for calculations by quarters of optimal supplies of the analysed consumables. The analysis used a general stochastic model of the supply theory.

Due to the inflation, economic circumstances, and the impossibility for correlation of the storage costs and urgent purchase for the ten years period observed, the absolute currency values for the costs of storage of the resource unit (C1) and the costs of the subsequent (urgent) purchase of a unit of the resource (C2), were not taken into account, instead the relative ones were used. In this way, a realistic ratio of these two categories of costs (Stanojevic, 2004, Stanojevic, 1995) that hold an immediate influence on the calculation outcome, i.e. the optimal solution of the supplies was established.

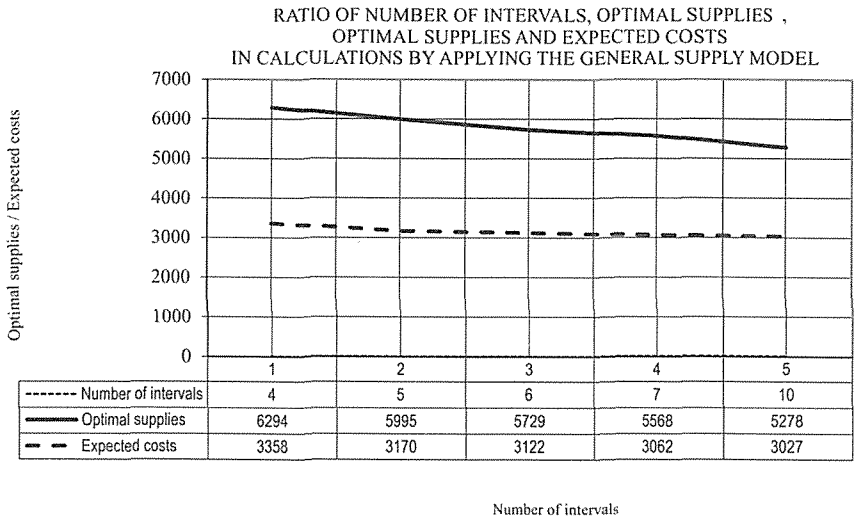

Figure 3. Influence of interval numbers to the optimal supplies and expected costs in calculations of the general supply model

By noting the importance of the interval number in the calculation process to the determination of the optimal solution, and aiming to test this hypothesis and to determine the degree of influence of the number of intervals to the optimal supplies, the calculation of optimal supplies of diesel fuel for the 1st quarter was reproduced for the following number of intervals: 4, 5, 6, 7 and 10, shown in Table 1. Calculation results have confirmed the thesis that by increasing the number of intervals, optimal supplies decrease. For example, for the diesel fuel in the 1st quarter, ranging from 6,293.75 litres for 4 intervals to 5,277.50 litres for 10 intervals, or by 19.3 (%).

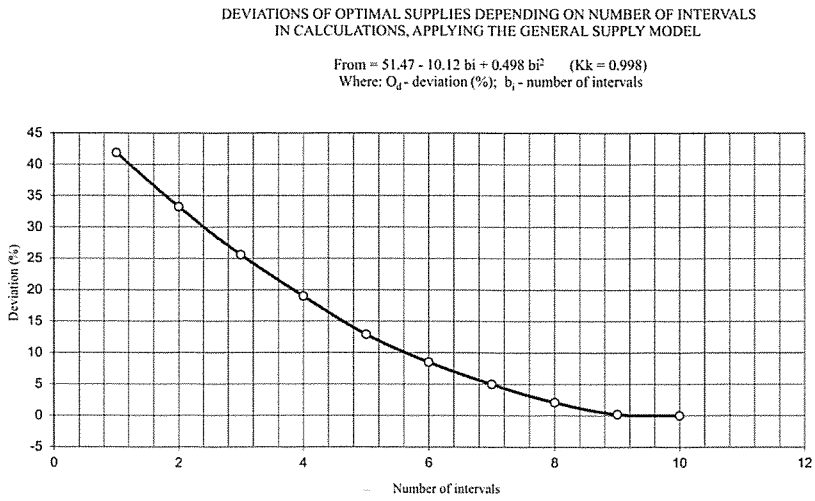

Figure 4. Influence of interval numbers to the optimal supplies deviations in calculations of the general supply model

Table 1. Optimal supplies of diesel fuel

u	*x*	*p(x)*	*p(x)/x*	$\sum_{x=u+1}^{\infty}[p(x)/x]$	$(u+1/2)\sum_{x=u+1}^{\infty}[p(x)/x]$	$\sum p(x)$	*F(x)*
I QUARTER, 4 intervals							
4,600.00	4,600.00	0.20	0.00004	0.00011	0.528	0.200	0.728
6,293.75	6,293.75	0.50	0.00008	0.00004	0.223	0.700	0.923
7,987.50	7,987.50	0.20	0.00003	0.00001	0.083	0.900	0.983
9,681.25	9,681.25	0.10	0.00001	0.00000	0.000	1.000	1.000
For C1/C2=1/3 to *C1/C2*=1/7, *Optimal supplies of diesel fuel:* **6,293.75** *(litres), Expected costs* **3,358.223** *(c.u.)*							
I QUARTER, 5 intervals							
4,600.00	4,600.00	0.20	0.00004	0.00012	0.529	0.200	0.729
5,955.00	5,955.00	0.30	0.00005	0.00006	0.385	0.500	0.885
7,310.00	7,310.00	0.40	0.00005	0.00001	0.073	0.900	0.973
8,665.00	8,665.00	0.00	0.00000	0.00001	0.086	0.900	0.986
10,020.00	10,020.00	0.10	0.00001	0.00000	0.000	1.000	1.000
For C1/C2=1/3 *to C1/C2*=3/8, *Optimal supplies of diesel fuel:* **5,955.00** *(litres), Expected costs* **3,169.508** *(c.u.)*							
I QUARTER, 6 intervals							
4,600.00	4,600.00	0.20	0.00004	0.00011	0.522	0.200	0.722
5,729.17	5,729.17	0.20	0.00003	0.00008	0.450	0.400	0.850
6,858.33	6,858.33	0.30	0.00004	0.00003	0.239	0.700	0.939
7,987.50	7,987.50	0.20	0.00003	0.00001	0.078	0.900	0.978
9,116.67	9,116.67	0.00	0.00000	0.00001	0.089	0.900	0.989
10,245.83	10,245.83	0.10	0.00001	0.00000	0.000	1.000	1.000
For C1/C2=1/3 to *C1/C2*=3/6, *Optimal supplies of diesel fuel:* **5,729.17** *(litres), Expected costs* **3,121.622** *(c.u.)*							
I QUARTER, 7 intervals							

u	x	$p(x)$	$p(x)/x$	$\sum_{x=u+1}^{\infty}[p(x)/x]$	$(u+1/2)\sum_{x=u+1}^{\infty}[p(x)/x]$	$\sum p(x)$	$F(x)$
4,600.00	4,600.00	0.20	0.00004	0.00011	0.513	0.200	0.713
5,567.86	5,567.86	0.10	0.00002	0.00009	0.521	0.300	0.821
6,535.71	6,535.71	0.20	0.00003	0.00006	0.411	0.500	0.911
7,503.57	7,503.57	0.40	0.00005	0.00001	0.072	0.900	0.972
8,471.43	8,471.43	0.00	0.00000	0.00001	0.081	0.900	0.981
9,439.29	9,439.29	0.00	0.00000	0.00001	0.091	0.900	0.991
10,407.14	10,407.14	0.10	0.00001	0.00000	0.000	1.000	1.000
For C1/C2=1/3 *to C1/C2*=2/5, *Optimal supplies of diesel fuel:* **5,567.86** *(litres), Expected costs* **3,061.691** *(c.u.)*							
I QUARTER, 10 intervals							
4,600.00	4,600.00	0.10	0.00002	0.00013	0.587	0.100	0.687
5,277.50	5,277.50	0.10	0.00002	0.00011	0.574	0.200	0.774
5,955.00	5,955.00	0.10	0.00002	0.00009	0.547	0.300	0.847
6,632.50	6,632.50	0.20	0.00003	0.00006	0.410	0.500	0.910
7,310.00	7,310.00	0.20	0.00003	0.00003	0.251	0.700	0.951
7,987.50	7,987.50	0.20	0.00003	0.00001	0.075	0.900	0.975
8,665.00	8,665.00	0.00	0.00000	0.00001	0.081	0.900	0.981
9,342.50	9,342.50	0.00	0.00000	0.00001	0.087	0.900	0.987
10,020.00	10,020.00	0.00	0.00000	0.00001	0.094	0.900	0.994
10,697.50	10,697.50	0.10	0.00001	0.00000	0.000	1.000	1.000
For C1/C2=1/3 *to C1/C2*=2/3, *Optimal supplies of diesel fuel:* **5,277.50** *(litres), Expected costs* **3,027.194** *(c.u.)*							
II QUARTER, 10 intervals							
7,650.00	7,650.00	0.10	0.00001	0.00010	0.731	0.100	0.831
8,092.10	8,092.10	0.30	0.00004	0.00006	0.474	0.400	0.874
8,534.20	8,534.20	0.00	0.00000	0.00006	0.500	0.400	0.900
8,976.30	8,976.30	0.00	0.00000	0.00006	0.525	0.400	0.925
9,418.40	9,418.40	0.20	0.00002	0.00004	0.351	0.600	0.951
9,860.50	9,860.50	0.00	0.00000	0.00004	0.368	0.600	0.968
10,302.60	10,302.60	0.20	0.00002	0.00002	0.184	0.800	0.984
10,744.70	10,744.70	0.00	0.00000	0.00002	0.192	0.800	0.992
11,186.80	11,186.80	0.20	0.00002	0.00000	0.000	1.000	1.000
11,628.90	11,628.90	0.00	0.00000	0.00000	0.000	1.000	1.000
For C1/C2=1/5 *to C1/C2*=5/7, *Optimal supplies of diesel fuel:* **8,092.10** *(litres), Expected costs* **4,315.30** *(c.u.)*							
III QUARTER, 10 intervals							
1,964.00	1,964.00	0.10	0.00005	0.00010	0.198	0.100	0.298
2,969.00	2,969.00	0.00	0.00000	0.00010	0.299	0.100	0.399
3,974.00	3,974.00	0.00	0.00000	0.00010	0.400	0.100	0.500
4,979.00	4,979.00	0.00	0.00000	0.00010	0.501	0.100	0.601
5,984.00	5,984.00	0.00	0.00000	0.00010	0.602	0.100	0.702
6,989.00	6,989.00	0.10	0.00001	0.00009	0.603	0.200	0.803
7,994.00	7,994.00	0.20	0.00003	0.00006	0.490	0.400	0.890
8,999.00	8,999.00	0.20	0.00002	0.00004	0.352	0.600	0.952
10,004.00	10,004.00	0.30	0.00003	0.00001	0.091	0.900	0.991
11,009.00	11,009.00	0.10	0.00001	0.00000	0.000	1.000	1.000
For C1/C2=1/2 *to C1/C2*=2/2, *Optimal supplies of diesel fuel:* **5,984.00** *(litres), Expected costs* **3,333.31** *(c.u.)*							
IV QUARTER, 10 intervals							
7,435.00	7,435.00	0.11	0.00001	0.00090	0.683	0.111	0.794
7,892.90	7,892.90	0.00	0.00000	0.00090	0.725	0.111	0.837
8,350.80	8,350.80	0.22	0.00003	0.00070	0.545	0.333	0.879
8,808.70	8,808.70	0.00	0.00000	0.00070	0.575	0.333	0.909
9,266.60	9,266.60	0.11	0.00001	0.00050	0.494	0.444	0.938
9,724.50	9,724.50	0.11	0.00001	0.00040	0.407	0.555	0.963
10,182.40	10,182.40	0.22	0.00002	0.00020	0.204	0.778	0.982
10,640.30	10,640.30	0.11	0.00001	0.00010	0.102	0.889	0.991
11,098.20	11,098.20	0.00	0.00000	0.00010	0.107	0.889	0.996
11,556.10	11,556.10	0.11	0.00001	0.00000	0.000	1.000	1.000
For C1/C2=1/4 *to C1/C2*=4/5, *Optimal supplies of diesel fuel:* **7,892.90** *(litres), Expected costs* **4,104.45** *(c.u.)*							

3 IMPORTANT CONCLUSIONS

The range of experimental research enabled the reliable analysis and an assessment of the application of supply theory in solving the real problems of this type in mining. Experimental research and results obtained completely confirm the application of the general stochastic model of supplies, and confirms the assumptions on wider possibilities of its application in mining.

Two manipulative-operational positions with significant influence to the determination of optimal supplies were noted. The first position is related to the phase of mathematical-statistical preparation of the input data. In calculating probabilities of material resources consumptions, highly important are the sizes of ranges, or intervals, i.e. the number of intervals in the period observed.

Bigger intervals lead the mathematical-modelling mechanism in the condition of complete insensibility. These are situations with high concentration of data in one or two classes, which can lead even to senseless situations in the final calculations of optimal supplies. This problem can be classified into the group of the known "artillery problem" of objective bifurcation.

Figure 3 shows the ratio of the number of intervals, i.e. the range (width) of the interval and the values of optimal solutions, or expected costs of supply storage and urgent purchase. It can be noted that, by increasing the number of intervals, and decreasing the width of the interval belt, the values calculated for supplies decrease (Figure 3). Figure 4 shows the graphical representation of the influence of number of intervals to the deviations of optimal supplies in calculations of the general stochastic model of supplies.

The deviations range from 19.3 (%) for 4 intervals, to 0 (%) for 10 intervals, and they are determined by the correlation function.

$$o_d = 51.47 - 10.12 \cdot b_i - 0.498 \cdot b_i^2$$

for $K_k = 0.998$

Where: o_d – deviation (%);
b_i – number of intervals.

The findings show that the intervals number determining the width of the interval belt with satisfaction ranges from 8 to 10.

The second important notion is the mechanism of influence of the storage costs and urgent purchase to the optimal solution. The punctuality of calculations for optimal solutions does not depend on the absolute currency values of these two categories of costs, but of their ratio. This is of particular importance from the aspect of practical application of the general supplies model, because in the environment of economic instability (present for a longer time in our country), costs expressed in currency unit can be extremely fluid. However, when the C1 to C2 ratio is set realistically, the currency type and monetary conditions have no influence on the optimal solution.

REFERENCES

Bosevski S., (2010), *Dynamic models of management of supplies of production and consumption in mining of non-metallic mineral resources,* Faculty of Mining and Geology, Belgrade, Doctoral thesis (in Serbian).

Vujic S., Zdravev S., Petrovski A., (1994), Optimization of material resources supplies at the Bucim open pit mine, *2nd International conference on opencast mining*, Vrnjacka Banja, (in Serbian).

Vujić S., Zdravev S., (1993), *Management of supplies of material resources at mines, Operations research Symposium, SYMOPIS 93*, Beograd, (in Serbian).

Stanojević R., (1995), *Optimization of supplies in serial production*, Institute of Economy, (in Serbian).

Stanojević R., (1970), *Introduction to operations research*, Institute of industrial economics, Belgrade, (in Serbian)

Stanojević R., (2004), *Dynamic programming,* Institute of Economy, Belgrade (in Serbian).

RESERVE ESTIMATION

Concurrent Optimization of Mine Block Sequencing and Cut-off Grades

M.Kumral
Department of Mining Engineering, Inonu University, 44280 Malatya - Turkey

ABSTRACT Mine block sequencing, ore-waste discrimination and determination of production rates are main sub-problems of mine production scheduling. The objective is to maximize net present value under access and capacity constraints. The problems are currently solved in a sequential way: First, production rates and corresponding costs are initiated. Using this cost structure, a cut-off schedule is determined. Finally, the block sequencing is executed for marginal cut-off grades and pre-defined production rates. This process is repeated until maximum net present value (NPV) is found. However, these problems should be solved simultaneously instead of iterative procedure because production rates and cut-offs cannot be known without block sequencing. In this paper, ore-waste discrimination and block sequencing are optimized concurrently through mixed integer programming (MIP) model. This procedure also considers relationship between capacities and accessibility. To observe the performance of new model, a case study is implemented. An increase in NPV is observed.

1 INTRODUCTION

Open pit mines are represented by a block model, which discriminates the entire orebody. Block sizes are governed by the equipment size, geology, data spacing and the selected blasting pattern. A grade/quality value is estimated/simulated for each block using a kriging/geostatistical simulation technique. Block monetary values are then calculated on the basis of block grades estimated/simulated. These values are used as an input in mine production scheduling, which creates a strategic blueprint to make a decision whether mining proceeds or not. In other words, mine production scheduling may be seen as a guide to exploit mine and assist making other operational decisions such as equipment selection and allocation.

Mine production planning is one of the most challenging areas in the design, planning and scheduling of mining ventures. As the rule of thumb, the solution approaches to mine production planning can be categorized into two mainstreams. In the first approach, a schedule is generated on the basis of nested pits through an ultimate pit limit (UPL) algorithm based on a maximum weigh closure algorithm by parameterization of commodity price. The nested pits are then grouped in a manner that pushbacks are obtained. Depending upon orebody size, the pushbacks are used a schedule or further processed that the sequencing is implemented for the blocks within each pusback (Lerchs and Grosmann, 1965). This approach was developed in 60's and has had some modifications (Zhao and Kim, 1992, Hochbaum and Chen, 2000 and Hochbaum, 2001). The approach suits very well to the problem size and complexity problems. This methodology is currently an industry standard and used by many commercial softwares. However, the spectacular growing

in computer and software technologies led to mixed integer programming (MIP) as the second solution approach to the problem (Gershon, 1983, Knowles, 1999, Menabde *et. al.*, 2004). In the MIP, UPL is inevitable outcome of the extraction sequencing. The MIP becomes the competitor of UPL - nested pits - pushback design – sequencing approach in recent years. It is well-known phenomenon that using a marginal cut-off grade is undervalued ore resources (Lane, 1988, Dagdelen, 1992, Cetin and Dowd, 2002, Asad, 2007 and Rendu, 2008). To overcome this problem, some authors developed a cut-off grade schedule through incorporation of opportunity cost in such a way as to generate high cut-offs to marginal cut-off at the end of planning periods (Lane, 1964 and Dagdelen and Asad, 2007). Although this heuristic approach increases NPV, this is still away from optimality and poses different problems such as the calculation of opportunity cost.

2 PROPOSED MODEL

In this model, decision variable is not only extraction period but also block destination. In other words, ore – waste discrimination is made by optimization process.

$$Max \quad f(x) = \sum_{i=1}^{T} \sum_{j=1}^{N} \sum_{d=1}^{D} V_{ijd} * x_{ijd} \tag{1}$$

$$V_{ijd}(1) = \begin{pmatrix} [(\text{price} - \text{sales costs}) * \text{recovery} * \\ \text{ore tonnage of block j} * \\ \text{grade of block j}] - \\ [(\text{mining cost} + \text{mineral proc.cost}) * \\ \text{tonnage of block j}] \end{pmatrix} * (1+n)^{-i} \tag{2}$$

$$V_{ijd}(0) = -(\text{mining cost} * \text{tonnage of block j}) * (1+n)^{-i} \tag{3}$$

Subject to

- Access constraint

$$\sum_{i=1}^{T} \sum_{d=1}^{D} x_{lid} \geq \sum_{i=1}^{T} \sum_{d=1}^{D} x_{jid} \quad \forall j \; blocks \; overlying \; block \; l \tag{4}$$

- Destination capacity constraint

$$\sum_{j=1}^{N} f_j x_{ijd} - Upp_d \leq 0 \quad i = 1,...,T \quad and \quad d = 1,...,D \tag{5}$$

$$\sum_{j=1}^{N} f_j x_{ijd} - Low_d \geq 0 \quad i = 1,...,T \quad and \quad d = 1,...,D \tag{6}$$

- Process control constraint

$$\sum_{j=1}^{N} c_j x_{ijd} \leq H_{du} \sum_{j=1}^{N} x_{ijd} \quad i = 1,...,T \quad and \quad d = 1,...,D \tag{7}$$

$$\sum_{j=1}^{N} c_j x_{ijd} \geq H_{lu} \sum_{j=1}^{N} x_{ijd} \quad i = 1,...,T \quad and \quad d = 1,...,D \tag{8}$$

- Block conservation constraint

$$\sum_{i=1}^{T} \sum_{d=1}^{D} x_{ijd} \leq 1 \quad j = 1,...,N \tag{9}$$

- Binary constraint

$$x_{ijd} \in \{0,1\} \quad i = 1,...,T, \; j = 1,...,N \quad and \quad d = 1,...,D \tag{10}$$

where N is the number of blocks, T is the number of periods, D is the number of destinations that should be at least two (waste dump and one processing destination), V_{ijd} is net present value of block j in period i if it is sent to destination d, x_{ijd} is binary variable (if block j is sent to destination d in period i, the variable is 1. Otherwise, it is zero) and f_j is the tonnage of block j, n is the discount rate, A is the processing capacity, C is the mining capacity, H_u and H_l are the lower and upper limits on grade and c_j is the grade of block j. Bear in mind that sequential Gaussian simulation was used to simulate orebody. Sequential indicator simulation cannot be used because this technique requires cut-offs to calculate ore and waste quantities in the blocks. However, the proposed technique does not use any cut-off grade.

3 CASE STUDY

A case study is conducted to observe the performance of the technique proposed. Using a gold drill-hole data, orebody has been simulated 50 times using sequential Gaussian simulation. Average grade of each block are computed. Block economic values were calculated for each possible destination. All other parameters used in the optimization models are given in Table 1.

Table 1. Input parameters

Number of blocks	43*40*15 (25800 in total)
Block size	5*5*5 m (Easting * Northing * Depth)
Block weight	500 tonnes
Number of periods	4
Mining cost	4 $/tonne
Processing cost	27 $/tonne
Recovery	0.8%
Price	30 $/g
Mining capacity	0 – 3000000
Processing capacity	1500000 –2500000
Grade requirement in processing	1 – 30 g/tonne

Using ZIMPL/IBM's CPLEX optimization engine, a schedule were generated. Some computational outputs are given in Table 2.

Table 2. Some computational results.

Number of variables	206400
Number of constraints	488315
Running time (in seconds)	94453.23

The problem was solved in 26.2 hours. In Table 3, NPV to be generated is given.

Table 3. Net present value generated regarding periods

Period 1	976 109 018
Period 2	778 649 372
Period 3	161 541 217
Period 4	121 993 265
Total (NPV in $ totals)	2 038 292 873

Table 4 summarizes the schedule on the basis the number of blocks to be extracted in periods.

Some cross-sections of schedule obtained are given in Figure 1.

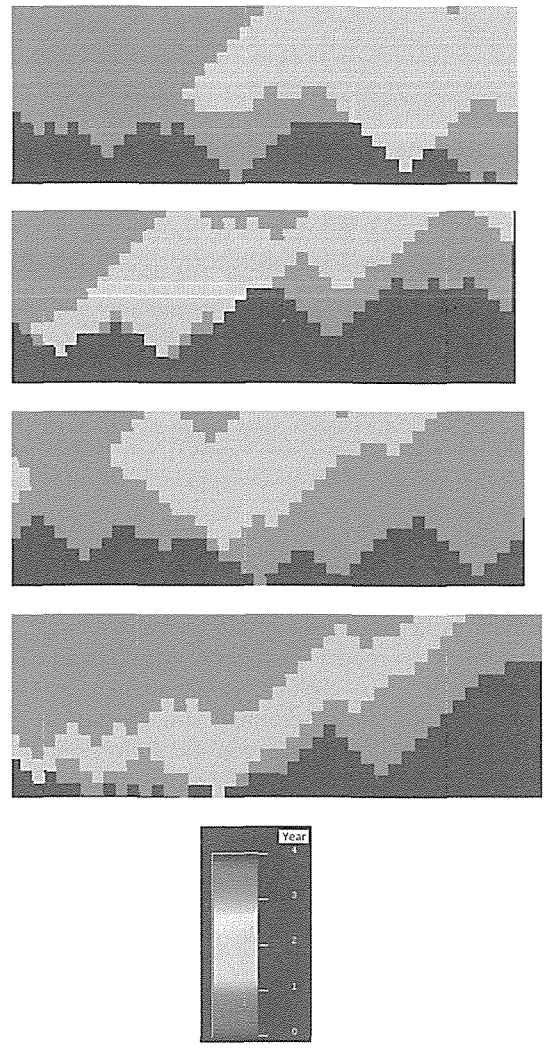

Figure 1. Some cross-sections from the schedule

Table 4. A summary of numbers of blocks to be extracted in each period

Period	Number of waste blocks	Number of processing blocks
1	4556	4132
2	3587	3909
3	1668	3256
4	1485	3207
Total	11296	14504

Table 5 gives the details of average grades generated in each period.

Table 5. A summary of average grades of ore material to be extracted in each period

Period	Average grade (g/tonne)
1	23.13
2	21.53
3	6.88
4	6.01

4 CONCLUSIONS

This paper attempts to solve mine planning problem a model based on MIP. In the approach, the block sequencing and destinations are determined simultaneously. The proposed approach considers possibility of extra profit through the incorporation of determination of block destination instead of the use of marginal cut-off grade. The model, which does not use pre-defined material classification, has more flexibility because some low grade material may be assessed as ore (*vice versa*) to reach more valuable region under capacity constraints. In other words, the reconciliation between accessibility and capacity constrains can be ensured by using more alternatives. Future research should be focused on incorporating truck allocation and dispatching problem into mine production planning.

5 REFERENCES

Asad, M.W.A., (2007). Optimum cut-off grade policy for open pit mining operations through net present value algorithm considering metal price and cost escalation, *Engineering Computations*, 24: 723 – 736

Cetin, E., Dowd, P.A., (2002). The use of genetic algorithms for multiple cutoff grade optimization, *Proceedings of the 30th International Symposium on Application of Computers & Operations Research in the Mineral Industry*, Ed: Bandopadhyay, pp.769-769.

Dagdelen K., (1992). Cut-off Grade Optimization, *Proceedings of the 23rd International Symposium on Application of Computers & Operations Research in the Mineral Industry*, pp.157-165.

Dagdelen, K., and Asad, M.W.A., (1997). Multi-mineral cutoff grade optimization with option to stockpile, SME Annual Meeting, Preprint No. 97186.

Gershon, M.E., (1983). Optimal mine production scheduling: evaluation of large scale mathematical programming approaches, *International Journal of Mining Engineering*, Vol. 1, pp. 315-329.

Hochbaum, D.S. and Chen, A., (2000). Performance analysis and best implementation of old and new algorithms for the open-pit mining problem, *Operations Research*, 48: 894-914.

Hochbaum, D.S., (2001). A New-old algorithm for minimum-cut and maximum-flow in closure graphs, *Networks: An International Journal*, 37: 171-193.

Knowles, T. W., (1999). Optimization models for mine planning, *Computers & Industrial Engineering*, 37: 469-472.

Lane, K.F., (1964). Choosing the optimum cutoff grade, *Colorado School of Mines Quarterly*, 59: 811-29.

Lane, K.F., (1988). The economic definition of ore, Mining Journal Book Ltd., London

Lerchs, H and Grosmann, I.F., (1965). Optimum design of open-pit mines, *CIM Transactions*, 58: 47-54.

Menabde, M., Froyland, G., Stone, P., and Yeates, G., (2004). Mining Schedule Optimisation for Conditionally Simulated Orebodies, *Proceedings of Orebody Modelling and Strategic Mine Planning - Uncertainty and Risk Management*, pp. 357-342, Perth.

Rendu, J.M., (2008). An introduction to cut-off grade estimation, Society for Mining Metallurgy & Exploration Publication.

Zhao, Y. and Kim, A., (1992). A New Optimum Pit Limit Design Algorithm, *Proceedings of 23. APCOM Symposium*, In: Ramani RV (ed), pp. 500-506

A New Production Scheduling Approach Considering Mill Requirements

M.Kumral
Department of Mining Engineering, Inonu University, 44280 Malatya - Turkey

ABSTRACT Geo-metallurgical variables control the performances of mining and mineral processing operations. As the fluctuations of geo-metallurgical variables increases, mine production scheduling will be difficult procedure. In conventional approach, the objective is to maximize net present value (NPV) of project. This objective generates descending order of average grade mean. This imposes additional problems on recoveries and throughput in the mill. The problem may be, to some extent, controlled by blending constraint in traditional approach. The blending constraint keeps average grade within upper and lower limits. If there is a very narrow range between upper and lower limits, the average grade of production in each period will be similar. However, the inclusion of this constraint will substantially increase computational time. Therefore, a new model is proposed to tackle with the problem such that computational time is reduced. The idea behind this model is to extract more homogenous metal quantity in the periods instead of maximization of NPV. In new model, the objective function is expressed as a maximin (maximize the minimum) problem. In the case where there is correlation between grade and geo-metallurgical variables, this model generates reasonably good results.

1 INTRODUCTION

The economic values of blocks are only a function of grade in the current practice. In fact, this treatment of mining and processing costs does not reflect the reality. Given that the grade is treated as a particular realization of a random function, the same approach should be extended to other variables affecting orebody characterization. These variables are called geo-metallurgical variables. This paper focuses on incorporating the influence of these variables into mine production scheduling procedure. The fluctuations in geo-metallurgical variables lead to three consequences:

1. Mining and processing costs of each block will vary depending upon material properties for the required recovery and throughput. For example, in addition to grade, the rock properties such as strength, porosity or water content are heterogeneous at orebody. Therefore, fragmentation and processing costs cannot be fixed in practice. As material and process properties vary, mining and processing costs will also change.
2. If one insists on using the fixed costs, the recoveries and throughput will vary. This is not acceptable due to quality reasons. One way to solve the fluctuation problem of geo-metallurgical variables is to establish a bed-blending operation (Gy, 1981; Dowd, 1989; Robinson, 2004; Kumral, 2006). In some industries consumed raw materials such as glass, cement, fertilizer and coal-fired electricity generation, bed-blending is an inevitable operation. In metallic raw materials, bed-blending can be also required to control the amount of variation within acceptable limits. For example, it was reported in some recent applications in metallic ores (Robinson, 2004). However, if

the mine-mill operation does not contain adequate bed-blending, mine production scheduling should be integrated with mineral processing requirements.

3. Another consequence of varying costs of block extraction is on ore-waste discrimination. In the traditional approach, the discrimination is implemented on the basis of a cut-off grade, which is calculated as follows:

$$g_i = \frac{process\,\text{cost} + \frac{n(NPV)_i}{A} + \frac{f_i}{A}}{(price - sales\,\text{cost})\,\text{recovery}} \qquad (1)$$

where g_i is the cut-off grade at period i, $n(NPV)_i$ is the net present value of future cash flows from year i to the end of mine life, $\frac{n(NPV)_i}{A}$ is the opportunity cost at period i, f_i is annual fixed cost, and A is the processing capacity. The cut-off grade changes with time because the opportunity cost is a function of time. Given that processing cost and recovery change in space under consideration of geo-metallurgical variables, the cut-off grade does not only change in time but also in space. When geo-metallurgical variables are incorporated into the calculation of cut-off grade, it is impossible to use a cut-off only varying in periods.

2 CONVENTIONAL APPROACH

The traditional mine production scheduling problem is formulated as follows:

$$Max \quad f(x) = \sum_{i=1}^{T} \sum_{j=1}^{N} V_{ij}(m) * x_{ij} \qquad (1)$$

$$m = \begin{cases} 1 & if\ the\ grade\ of\ block\ j \geq cut-off_i \\ 0 & otherwise \end{cases} \qquad (2)$$

$$V_{ij}(1) = \left(\begin{array}{l} [(\text{price - sales costs}) * \text{recovery} * \\ \text{ore tonnage of block j} * \\ \text{grade of block j}] - \\ [(\text{mining cost + mineral proc.cost}) \\ * \text{tonnage of block j}] \end{array} \right) * (1+n)^{-i} \qquad (3)$$

$$V_{ij}(0) = -(mining\ cost * tonnage\ of\ block\ j) * (1+n)^{-i} \qquad (4)$$

Subject to

$$\sum_{i=1}^{T} x_{li} \geq \sum_{i=1}^{T} x_{ji} \quad \forall j \text{ blocks overlying block } l \qquad (5)$$

$$\sum_{j=1}^{N} (d_j + v_j) x_{ij} - C \leq 0 \quad i = 1,\ldots,T \qquad (6)$$

$$\sum_{j=1}^{N} d_j x_{ij} - A \leq 0 \quad i = 1,\ldots,T \qquad (7)$$

$$\sum_{j=1}^{N} c_j\, x_{ij}\, d_j \leq H_u \quad i = 1,\ldots,T \qquad (8)$$

$$\sum_{j=1}^{N} c_j\, x_{ij}\, d_j \geq H_l \quad i = 1,\ldots,T \qquad (9)$$

$$\sum_{i=1}^{T} x_{ij} \leq 1 \quad j = 1,\ldots,N \qquad (10)$$

$$x_{ij} \in \{0,1\} \quad i = 1,\ldots,T,\ j = 1,\ldots,N \qquad (11)$$

where V_{ij} is the present value of block j in period i, N is the number of blocks, T is the number of periods, n is the discount rate, d_j is the ore mass in block j, A is the processing capacity, v_j is the waste mass in block j and C is the mining capacity, H_u and H_l are the lower and upper limits on grade and c_j is the grade of block j.

2 MAXIMIZATION OF MINIMUM NPV

Depending upon market requirement and mill features, the blending constraint is used to maintain the average grade of extraction in each time period. This constraint may tackle geo-metallurgical considerations implicitly. Under the assumption that there is a correlation between grade and geo-metallurgical variables, the constraint may serve to ensure more homogenous

production in terms of geo-metallurgical variables. However, the inclusion of this constraint will substantially increase computational time. The objective function forces more valuable blocks to earlier periods. However, the blending constraint keeps average grade within upper and lower limits. If there is a very narrow range between upper and lower limits, the average grade of production in each period will be similar. This observation motivates to use different approaches in such a way as to generate more uniform production among periods.

In this section, a maximin (maximize the minimum) objective function is proposed to spread the metal allocation more evenly in periods instead of decreasing order. The model is given as:

$$max\ f(x) = min\left\{\sum_{j=1}^{N} B_j x_{ij} \qquad i = 1,\ldots,T\right\} \tag{12}$$

Where B_j is the metal quantity of block j. The objective is to maximize the metal quantity in the period that is extracted minimum metal quantity. That is, it is the best of the worst possible outcome. The objective function given in Equation 12 is a non-linear problem. However, the constraints are still linear. By an appropriate modification of the non-linear form, the objective function can be formulated as an equivalent linear objective function. The transformation procedures can be found in (Kaplan, 1974). The modification is fulfilled by introducing a new variable, h, which is objective function value and maximize h subject to a system of linear constraints keeping h no more than any term of the minimum. Applying this modification to maximin version of mine production scheduling produce a linear model:

$$max \quad h \tag{13}$$

Subject to

$$h \le \sum_{j=1}^{N} B_j x_{ij} \qquad i = 1,\ldots,T \tag{14}$$

$$\sum_{i=1}^{T} x_{ki} \ge \sum_{i=1}^{T} x_{ji} \quad \forall j\ blocks\ overlying\ block\ k \tag{15}$$

$$\sum_{j=1}^{N} (d_j + v_j) x_{ij} - C \le 0 \quad i = 1,\ldots,T \tag{16}$$

$$\sum_{j=1}^{N} d_j x_{ij} - A \le 0 \quad i = 1,\ldots,T \tag{17}$$

$$\sum_{i=1}^{T} x_{ij} \le 1 \quad j = 1,\ldots,N \tag{18}$$

$$x_{ijk} \in \{1\}\ i = 1,\ldots,T,\ j = 1,\ldots,N \tag{19}$$

New variable h is the only term of the objective function, which makes the objective linear.

3 CASE STUDY

In order to demonstrate the models recommended, a case study is conducted. The samples cut from orebody are assayed for the grade of valuable material. Mining and processing costs of each sample are calculated by experimentation. Depending upon drilling, blasting, hauling and transportation costs, a mining cost is calculated for each sample location using regression model. Similarly, a processing cost of each sample is calculated for the required recovery. The processing cost consists of crushing, grinding, classification and flotation costs. Since there is a non-linear relation between grade and recovery, low grade blocks above cut-off grade may not reach the required recovery. In this case, the highest possible processing cost corresponding to the highest possible cut-off grade is assigned to the sample. A 3D block model is then created. Using sequential simulation, a grade is assigned to each block. Cost values of each block are generated from regression models. These blocks are submitted to the models developed. The model provides an opportunity to consider geo-metallurgical variables by a deterministic model. The objective is to maximize the profit of the period generating the minimum profit. The parameter file used is given in Table 1.

Table 1. Parameter file

The number of total periods (Years)	8
Number of simulations	3
Number of processing cost scenarios	3
Number of price scenarios	3
Block tonnage	500 tonnes
Discount rate (%)	15
Maximum processing rate (tons)	350 blocks
Maximum mining rate (tons)	700 blocks
Recovery	0.90

This indicates breaking away from the traditional paradigm based on maximization of NPV of the project. In the traditional approach, the NPVs of periods are in descending order because the valuable blocks are forced to early periods. Although the traditional approach maximizes the NPV of the project, it imposes different problems from a mineral processing point of view. If there was a linear relation between grade and other geo-metallurgical variables, the material extracted in each period would have different characteristics. The fluctuations in material characteristics among periods lead to additional costs in mineral processing. That is, a sophisticated bed-blending operation or multiple production faces can be required. Therefore, more even extraction among periods can be preferred.

The same block model is used to perform the maximin model. In order to make a comparison, the traditional deterministic model based on the expected grade and cost values is also performed. In Tables 2, the results generated from maximin model is given. The maximin model does not use NPVs for block. However, in order to make a meaningful comparison with the traditional model, the revenue values obtained from the maximin model was converted to NPV terms.

The traditional model may yield higher NPV. However, if the result generated from the traditional approach is implemented in practice, some additional costs may arise because of unrealistic assumptions of mineral processing costs. There will be also recovery and throughput problems. In the maximin model, average grade of material extracted in each period is more uniform in comparison to that of the conventional approach (Figure 1).

Table 2. The schedule by maximum model

Period	NPV ($)	The total number of blocks	The number of ore blocks	Average Grade
1	46579750	700	295	11.7
2	36142900	700	279	9.6
3	27759400	700	254	8.1
4	28778650	700	277	7.7
5	17537200	700	197	6.6
6	17836900	692	228	5.8
7	16759600	688	218	5.7
8	14537500	632	196	5.5
Total	205931900			

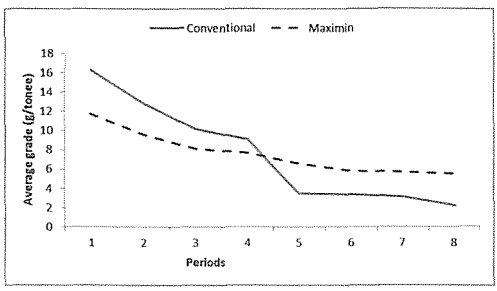

Figure 1. Evolution of averge grades of periods of conventional and maximin models

4 CONCLUSIONS

Given that mine production scheduling aims to obtain maximum utility from the process, the fluctuations in geo-metallurgical variables should be incorporated into the scheduling process to avoid deviating from unrealistic assumptions and coefficients values. Since rock properties change in each process stage, the recovery and throughput characteristics cannot be inferred from *in-situ* properties. The model is a maximin model to generate more even results. A maximin model can especially be useful in the production scheduling of raw materials entailing strict grade requirements. The maximization of net present value of the project can give the best utility if one

considers the process until ore deliverance to mill. Decreasing order of cash flows means decreasing metal quantity in each period. This may be indicator of change in geo-metallurgical characteristics in such a way as to cause more costly mineral processing stages. No matter how equipment properties are considered as controllable variable, there are also uncontrollable issues such as failures and breakdowns the equipment properties.

5 REFERENCES

Dowd PA (1989). The design of a rock homogenising stockpile, *Mineral Processing in the UK*, IMM, London, pp 63-82.

Gy PM (1981). A New theory of bed-blending derived from the theory of sampling –development and full - scale experimental check. *International Journal of Mineral Processing* 8: 201-238.

Kaplan S (1974). Applications of programs with maximin objective functions to problems of optimal resources allocations, *Operations Research* 22(4): 802-807.

Kumral M (2006). Bed blending design incorporating multiple regression model and genetic algorithms. *Journal of the Southern African Institute of Mining and Metallurgy* 106: 229-236.

Robinson GK (2004). How much would a blending stockpile reduce variation? *Chemometrics and Intelligent Laboratory Systems* 74(1): 121-133.

Robustness in Mine Planning Problem: Trade-off between Optimality and Feasibility

M.Kumral
Department of Mining Engineering, Inonu University, 44280 Malatya - Turkey

ABSTRACT Mine production scheduling under uncertainty is one of main challenges in mining ventures. Since the values of coefficients in the optimization procedure are obtained in medium of sparse data, sampling and assaying errors, and unknown future events, the implementations based on the deterministic models may lead to destructive consequences to the mining company. In this paper, a robust stochastic optimization (RSO) approach is used to deal with mine production scheduling in a manner that the solution is insensitive to changes in input data. The model was demonstrated on a case study. It was observed that RSO could be executed to solve mine production scheduling problem under an uncertain environment efficiently.

1 INTRODUCTION

Many mine production scheduling approaches do not consider uncertainty emanated from future. This forces planner/scheduler to reconstruct the operation on the basis of new information, namely reactive optimization. This may not simple due to integration of different information and difficulties in learning of new information. Therefore, robust solution can be required such that the solution is insensitive to input data. As the heterogeneity of variables throughout orebody increases, the scheduling will be very complicated task. Grades and financial data used in the mine production scheduling are based on simulation and/or estimation generated from sparse data and unknown future events affected by commodity prices, extraction costs and discount rare. Therefore, the scheduling process involves a significant degree of uncertainty. In order to deal with grade and financial uncertainties, various stochastic approaches can be recommended. For example, probabilistic programming (change-constrained programming, Kataoka's model) has a potential to solve the problem. However, it is difficult to formulate the problem in a linear form. To express the problem MIP form, it is required a series of critical assumptions such as normality distribution and block independency of block economic values. Another approach may be the stochastic programming with recourse. The formulation of the problem in the stochastic programming with recourse may not be possible because it is hard to divide the problem into the stages, which entail to take a corrective action after a random event. This paper extends the MIP model of deterministic mine production scheduling problem into stochastic arena through robust stochastic programming.

2 DETERMINISTIC MINE PRODUCTION SCHEDULING

The notations used in the problem formulation are given as: T is the number of periods, N is the number of blocks, V_{ij} is present value of block j in period i, n is discount rate, d_j is the ore mass in block j, A is the processing capacity, T^k is the period under consideration, v_j is waste mass in block j and C is the mining capacity.

$$Max \sum_{i=1}^{T} \sum_{j=1}^{N} V_{ij}(m) * x_{ij} \quad (1)$$

$$m = \begin{cases} 1 & \text{if the grade of block } j \geq cut-off_i \\ 0 & \text{otherwise} \end{cases} \quad (2)$$

$$V_{ij}(1) = \begin{pmatrix} [(price - sales\ costs) * recovery * \\ ore\ tonnage\ of\ block\ j * \\ grade\ of\ block\ j] - \\ [(mining\ cost + mineral\ proc.\ cost) * \\ tonnage\ of\ block\ j] \end{pmatrix} * (1+n)^{-i} \quad (3)$$

$$V_{ij}(0) = -(mining\ cost * tonnage\ of\ block\ j) * (1+n)^{-i} \quad (4)$$

$$x_{ij} = \begin{cases} 1 & \text{if the block is produced in period } i \\ 0 & \text{otherwise} \end{cases} \quad (5)$$

Subject to

$$\sum_{i=1}^{T^k} x_{ki} \geq \sum_{i=1}^{T^k} x_{ji} \quad \forall j\ blocks\ overlying\ block\ k \quad (6)$$

$$\sum_{j=1}^{N} (d_j + v_j) x_{ij} - C \leq 0 \quad i = 1,\ldots,T \quad (7)$$

$$\sum_{j=1}^{N} d_j x_{ij} - A \leq 0 \quad i = 1,\ldots,T \quad (8)$$

$$\sum_{i=1}^{T} x_{ij} \leq 1 \quad j = 1,\ldots,N \quad (9)$$

Block economic values are the function of many uncertain variables in mine production scheduling. Financial parameters such as price, costs and discount rate depend upon a series of unknown future events and are modeled by stochastic processes. On the other hand, the block grades are generated by conditional simulation from sparse drillhole data exposing sampling and assaying errors. Using the realizations of these uncertain variables, probable scenarios are generated. Each scenario will yield different NPV and the production rates of mining and processing. The investor may encounter totally different financial figure than the expected and/or, overcapacity or idle capacity problems. Deterministic mine production approaches do not consider data uncertainties. The implementations based on deterministic solutions may lead to significant NPV losses/awards and/or capacity utilization problems. In other words, when data values are different from nominal (expected) values, some constraints may be violated and solution may not be any longer optimal (Sim, 2004). The generation of many equally probable simulations and the probabilities of financial parameters give an opportunity to produce scenarios, $s \in \Omega = \{1, 2, 3, \ldots, S\}$, and take into account the stochastic optimization approaches in mine production scheduling in order to generate a robust solution.

3 ROBUST STOCHASTIC OPTIMIZATION

Data uncertainties may lead to quality, optimality and feasibility problems when deterministic models are used. Therefore, it is required to generate a solution, which is immune to data uncertainty. In other words, the solution should be robust (Bertsimas and Sim, 2004). Mulvey *et. al.* (1995) developed a stochastic model called RSO so as to capture randomness of uncertain parameters. Aim of RSO is not only to

maximize/minimize the objective function but also to obtain a robust solution. In other words, RSO attempts to generate a solution, which is insensitive to different realizations of input data.

The method consists of the addition of two essential parts into the deterministic objective function. The first, a variability measure is incorporated to create mean-variance trade-off form. The variance is the most used parameter in RSO to reduce variability of the performance vector of scenarios. The variability measure is expressed in terms of fluctuations of block economic values from the expected value. The second, the deviations from capacities are allowed under a cost in goal programming form. Deviations from pre-specified mining and processing capacities are allowed under a cost. The measurement of robustness can be defined in two parts: Solution robustness in terms of optimality if an optimal solution is "close" to optimal for any scenario $s \in \Omega$ and model robustness in terms of feasibility if an optimal solution is "almost" feasible for any scenario $s \in \Omega$. The RSO seeks a balance between solution and model robustness.

Let $\|o\|$ show the norm of o. The norm can be any parameter such as the variance or the absolute value. However, the choice of norm will affect the solution performance. S is total number of scenarios, p_s is the probability of scenario s. In this research, block grades, ore price, mining and processing costs are used to produce the probabilities. λ is the weight to measure risk trade-off between the expected NPV and the scenarios, w_i and ψ_i are penalty weights arising from deviations of mining and processing capacities for period i, respectively. Robust mine production scheduling can be formulated as:

$$Max \sum_{s=1}^{S} p_s \sum_{i=1}^{T} \sum_{j=1}^{N} V_{sij}(m) * x_{ij} - \lambda \sum_{s=1}^{S} p_s \left\| \sum_{i=1}^{T} \sum_{j=1}^{N} V_{sij}(m) * x_{ij} - \left(\sum_{s=1}^{S} p_s \sum_{i=1}^{T} \sum_{j=1}^{N} V_{sij}(m) * x_{ij} \right) \right\| - \sum_{s=1}^{S} p_s \sum_{i=1}^{T} w_i \left\| \sum_{j=1}^{N} (d_{sj} + v_{sj}) x_{ij} - C \right\| - \sum_{s=1}^{S} p_s \sum_{i=1}^{T} \psi_i \left\| \sum_{j=1}^{N} d_{sj} x_{ij} - A \right\| \quad (10)$$

Subject to

$$\sum_{i=1}^{T^k} x_{ki} \geq \sum_{i=1}^{T^k} x_{ji} \quad \forall j \text{ blocks overlying block } k \quad (11)$$

$$\sum_{i=1}^{T} x_{ij} \leq 1 \quad j = 1,\ldots, N \quad (12)$$

$$x_{ij} \in \{0,1\} \; i = 1,\ldots,T \quad and \quad j = 1,\ldots,N \quad (13)$$

$$\lambda, w_i \; and \; \psi_i \geq 0 \quad i = 1,\ldots, T \quad (14)$$

The first term of the objective function is the expected NPV of the venture. The second term is the cost of the risk measure of NPV. If NPVs of scenarios have wild fluctuations, the value of this term will increase. The following part of objective function given in Eq. 10 refers to robust stochastic optimization model with solution robustness:

$$Max \sum_{s=1}^{S} p_s \sum_{i=1}^{T} \sum_{j=1}^{N} V_{sij}(m) * x_{ij} - \lambda \sum_{s=1}^{S} p_s \left\| \sum_{i=1}^{T} \sum_{j=1}^{N} V_{sij}(m) * x_{ij} - \left(\sum_{s=1}^{S} p_s \sum_{i=1}^{T} \sum_{j=1}^{N} V_{sij}(m) * x_{ij} \right) \right\| \quad (15)$$

The third term is the cost of deviation between mining capacity and production rate. Finally, the fourth term is the cost of deviation between processing capacity and production rate. The following part of objective function given in Eq. 10 refers to robust stochastic optimization model with model robustness:

$$Max \sum_{s=1}^{S} p_s \sum_{i=1}^{T} \sum_{j=1}^{N} V_{sij}(m) * x_{ij} - \sum_{s=1}^{S} p_s \sum_{i=1}^{T} w_i \left\| \sum_{j=1}^{N} (d_{sj} + v_{sj}) x_{ij} - C \right\| - \sum_{s=1}^{S} p_s \sum_{i=1}^{T} \psi_i \left\| \sum_{j=1}^{N} d_{sj} x_{ij} - A \right\| \quad (16)$$

Let θ_s^+ and θ_s^- denote the violation for the expected value for scenario s, δ_{si}^+ and δ_{si}^- represent the violation of the mining capacity for scenario s in period i, ρ_{si}^+ and ρ_{si}^- represent the violation of the processing capacity for scenario s in period i. Another strategy is proposed in goal programming form:

$$Max \sum_{s=1}^{S} p_s \sum_{i=1}^{T} \sum_{j=1}^{N} V_{sij}(m) * x_{ij} - \lambda \sum_{s=1}^{S} p_s (\theta_s^+ + \theta_s^-) - \sum_{s=1}^{S} p_s \sum_{i=1}^{T} (v_i^+ \delta_{si}^+ + w_i^- \delta_{si}^-) - \sum_{s=1}^{S} p_s \sum_{i=1}^{T} (\psi_i^+ \rho_{si}^+ + \psi_i^- \rho_{si}^-) \quad (17)$$

subject to

$$\sum_{i=1}^{T} \sum_{j=1}^{N} V_{sij}(m) * x_{ij} - \left(\sum_{s=1}^{S} p_s \sum_{i=1}^{T} \sum_{j=1}^{N} V_{sij}(m) * x_{ij} \right) = \theta_s^+ - \theta_s^- \quad s = 1,\ldots,S \quad (18)$$

$$\sum_{j=1}^{N} (d_{sj} + v_{sj}) x_{ij} - C = \delta_{si}^+ - \delta_{si}^- \quad i = 1,\ldots,T \text{ and } s = 1,\ldots,S \quad (19)$$

$$\sum_{j=1}^{N} d_{sj} x_{ij} - A = \rho_{si}^+ - \rho_{si}^- \quad i = 1,\ldots,T \text{ and } s = 1,\ldots,S \quad (20)$$

$$\sum_{i=1}^{T^k} x_{ki} \geq \sum_{i=1}^{T^k} x_{ji} \quad \forall j \text{ blocks overlying block } k \quad (21)$$

$$\sum_{i=1}^{T} x_{ij} \leq 1 \quad j = 1,\ldots,N \quad (22)$$

$$x_{ij} \in \{0,1\} \quad i = 1,\ldots,T \quad \text{and} \quad j = 1,\ldots,N \quad (23)$$

$$\lambda, w_i \text{ and } \psi_i \geq 0 \quad i = 1,\ldots T \quad (24)$$

Since the computational complexity of the problem is high, it is necessary to find computational efficiently equivalent. The model defined above can be solved by the initiation of artificial variables into Eq. 18-20. Two phases or big-M approaches may be used to tackle with this issue (Rardin, 1998). Using big-M approach, the following model is obtained:

$$Max \sum_{s=1}^{S} p_s \sum_{i=1}^{T} \sum_{j=1}^{N} V_{sij}(m) * x_{ij} - \lambda \sum_{s=1}^{S} p_s (\theta_s^+ + \theta_s^-) - \sum_{s=1}^{S} p_s \sum_{i=1}^{T} (v_{si}^+ \delta_{si}^+ + w_{si}^- \delta_{si}^-) \sum_{s=1}^{S} p_s \sum_{i=1}^{T} (\psi_{si}^+ \rho_{si}^+ + \psi_{si}^- \rho_{si}^-) K \sum_{s=1}^{S} \left(\alpha_s + \sum_{i=1}^{T} \beta_{si} + \chi_{si} \right) \quad (25)$$

subject to

$$\sum_{i=1}^{T} \sum_{j=1}^{N} V_{sij}(m) * x_{ij} - \left(\sum_{s=1}^{S} p_s \sum_{i=1}^{T} \sum_{j=1}^{N} V_{sij}(m) * x_{ij} \right) = \theta_s^+ - \theta_s^- - \alpha_s \quad s = 1,\ldots,S \quad (26)$$

$$\sum_{j=1}^{N} (d_{sj} + v_{sj}) x_{ij} - C = \delta_{si}^+ - \delta_{si}^- - \beta_{si} \quad i = 1,\ldots,T \text{ and } s = 1,\ldots,S \quad (27)$$

$$\sum_{j=1}^{N} d_{sj} x_{ij} - A = \rho_{si}^+ - \rho_{si}^- - \chi_{si} \quad i = 1,\ldots,T \text{ and } s = 1,\ldots,S \quad (28)$$

$$\sum_{i=1}^{T} x_{ki} \geq \sum_{i=1}^{T} x_{ji} \quad \forall j \text{ blocks overlying block } k \quad (29)$$

$$\sum_{i=1}^{T} x_{ij} \leq 1 \quad j = 1,\ldots,N \quad (30)$$

$$x_{ij} \in \{0,1\} \quad i = 1,\ldots,T \quad \text{and} \quad j = 1,\ldots,N \quad (31)$$

$$\lambda, w_i, \psi_i, \alpha_s, \beta_{si} \text{ and } \chi_{si} \geq 0 \quad i = 1,\ldots,T \quad s = 1,\ldots,S \quad (32)$$

where α, β and χ are artificial variables and K is a large positive number.

To summarize, in this section, the generalized RSO optimization model is defined firstly. This is a non-linear problem. Afterward, using different risk profile, the problem has been linearized. However, problem size is still large. Therefore, computationally efficiently equivalent has been derived finally.

4 MODEL

In order to tackle with size issue of the problem, a further improvement was fulfilled

on the basis of a theorem developed by (Li, 1996) as follows:

$$Min \quad P = |f(x) - g|$$

subject to

$$X \in F \tag{33}$$

Where F is a feasible set and $f(x) - g = \zeta^+ - \zeta^-$. It can be linearized as follows:

$$Min \quad P' = f(x) - g + 2\zeta \tag{34}$$

subject to

$$g - f(x) - \zeta \le 0, \zeta \ge 0, X \in F \tag{35}$$

The theorem can be proved in the following way:

If $f(x) - g \ge 0$, ξ is then forced to zero in the optimal solution. In this case, $P = P'$. In other case, if $f(x) - g < 0$, ξ is then forced to $\xi = g - f(x)$. In this case, $P' = g - f(x) = P$.

Same theorem can be extended to the weighted goal programming problem, which is:

$$Min \quad P = w^+\zeta^+ - w^-\zeta^-$$

subject to

$$X \in F \tag{36}$$

Where F is a feasible set and $g(x) - Y = w^+\zeta^+ - w^-\zeta^-$. It can be linearized as follows:

$$Min \quad P' = w^+(g(x) - Y + \zeta) - w^-\zeta^-$$

subject to

$$-g(x) + Y - \zeta \le 0, \zeta \ge 0, X \in F \tag{37}$$

On the basis of these theorems, the problem is formulated as follows:

$$\begin{aligned} Max & \sum_{s=1}^{S} p_s \sum_{i=1}^{T} \sum_{j=1}^{N} V_{sij}(m) * x_{ij} - \\ & \lambda \sum_{s=1}^{S} p_s \left[\sum_{i=1}^{T} \sum_{j=1}^{N} V_{sij}(m) * x_{ij} - \left(\sum_{s=1}^{S} p_s \sum_{i=1}^{T} \sum_{j=1}^{N} V_{sij}(m) * x_{ij} \right) + 2\theta_s \right] \\ & - \sum_{s=1}^{S} p_s \sum_{i=1}^{T} w_i^+ \left[\left(\sum_{j=1}^{N} (d_{sj} + v_{sj}) x_{ij} - C + \delta_{si} \right) + w_i^- \delta_{si} \right] \\ & - \sum_{s=1}^{S} p_s \sum_{i=1}^{T} \psi_i^+ \left[\left(\sum_{j=1}^{N} d_{sj} x_{ij} - C + \rho_{si} \right) + \psi_i^- \rho_{si} \right] \end{aligned} \tag{38}$$

subject to

$$\sum_{i=1}^{T} \sum_{j=1}^{N} V_{sij}(m) * x_{ij} - \left(\sum_{s=1}^{S} p_s \sum_{i=1}^{T} \sum_{j=1}^{N} V_{sij}(m) * x_{ij} \right) - \theta_s \le 0 \quad s = 1,...,S \tag{39}$$

$$-\sum_{j=1}^{N} (d_{sj} + v_{sj}) x_{ij} + C - \delta_{si} \le 0 \quad i = 1,...,T \text{ and } s = 1,...,S \tag{40}$$

$$-\sum_{j=1}^{N} d_{sj} x_{ij} + A - \rho_{si} \le 0 \quad i = 1,...,T \text{ and } s = 1,...,S \tag{41}$$

$$\sum_{i=1}^{T^k} x_{ki} \ge \sum_{i=1}^{T^k} x_{ji} \quad \forall j \text{ blocks overlying block } k \tag{42}$$

$$\sum_{i=1}^{T} x_{ij} \le 1 \quad j = 1,...,N \tag{43}$$

$$x_{ij} \in \{0,1\} \quad i = 1,...,T \quad and \quad j = 1,...,N \tag{44}$$

$$\lambda, w, \psi, \alpha, \beta \text{ and } \chi \ge 0 \quad i = 1,...,T \tag{45}$$

5 CASE STUDY

A case study is conducted on an orebody to demonstrate the merits of model developed. Block grades, price, mining and processing costs are treated as uncertain parameters. In order to deal with grade uncertainty, five realizations are generated using conditional simulation. Thus, block grades and quantities

of ore and waste material of each block are generated. Since commodity prices fluctuate wildly in the markets depending upon a series of political and economic factors, it is very difficult to predict future prices based on historical data. As far as the mining and processing costs are concerned, the geo-metallurgical characteristics, proximity to mineral processing design and presence of deleterious elements affect these costs. Mining cost is a function of drillability and fragmentation in blasting. Processing cost is affected by the recovery, throughput, grindability, liberation and existence of unwanted materials.

Please note that as price and processing cost change, cut-off grade also changes. The model matrix is generated by ZIMPL. The model is then solved by CPLEX optimization engine. A cross-section of production schedule generated for a weights configuration is given in Figure 3. For early periods, the penalty values will be larger relatively in order to force the extraction to have less deviation in early periods. This leads to the solution robustness in decreasing order because the mine can be re-scheduled later as more information is obtained. However, this causes an increase NPV in late periods. This means the decreasing effect of discount rate, which is used to force the valuable blocks to earlier periods.

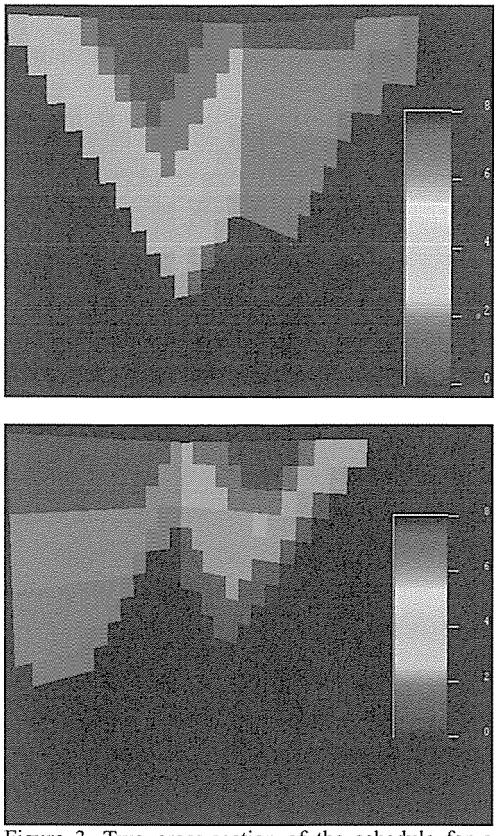

Figure 3. Two cross-section of the schedule for a weights configuration for eight periods

6 CONCLUSIONS

Mine production scheduling emerges as one of key procedures to improve efficiency and profitability of the venture. In current practice, the variables based on the expected values derived from sparse data and unknown future events are used. However, as the realizations of uncertain variables fluctuate, vital problems may takes place on the profitability and capacity utilization.

In this paper, a RSO approach is used to obtain a solution to insensitive to different realizations. The approach incorporates a variability measure indicating effect on NPV of uncertainty and allowing infeasibilities under a cost. These incorporations make problem multi-objective optimization problem. The first objective is to maximize NPV of the venture such a way as to force less variable blocks to earlier periods and the second one is to minimize deviations in the capacities. The problem is solved by weighting method, which reflects a trade-off risk perception of investor. The case study showed that the approach could be used in mine production scheduling problem in an efficient way. As the number of scenarios increases, the implementation can be

prohibitively difficult. Therefore, future researches should concentrate on reducing the problem size.

7 REFERENCES

Bertsimas, D. & Sim, M., 2004. The price of robustness. *Operations Research*, 52(1), 35-53.

Mulvey J.M., Vanderbei, R.J. and Zenios, S.A., 1995. Robust optimization of large-scale systems. *Operations Research*, 43(2), 264-281.

Rardin R., 1998. *Optimization in operations research*, USA, Prentice-Hall, 919 p.

Sim, M., 2004. *Robust Optimization*, PhD Thesis, Massachusetts Institute of Technology, 171 p.

Reserve and Grade Characteristics of the Feldspar Deposits Using Geostatistical Methods

Tayfun Yusuf YÜNSEL, Adem ERSOY
Department of Mining Engineering, Çukurova University, Adana, Turkey

ABSTRACT This study addresses a case study on grade and reserve characteristics of feldspar deposit in Sarpdere region (Çine-Aydın-Turkey). The study has been carried out using both conventional statistics and geostatistical methods. Directional, omnidirectional and vertical experimental semivariograms of the variables such as Na_2O, SiO_2 and Al_2O_3 showed that neither geometric nor zonal anisotropy exists in the data. The variogram models have been tested by cross validation analysis. Grade and tonnage curves and total tonnage estimation in the particular grade intervals were determined using the ordinary kriging results of the variables in order to make successful mining operation and future planning.

1 INTRODUCTION

The base of the development for a country is up to its natural resources. The economic evaluation of the natural resources depends on the accuracy of reserve estimation which is very useful in making decisions about opening up new mines, or in planning future investments for operating mines. Resource estimation and grade control are the basis for successful mining operation. Both overestimation and underestimation of ore reserve can have severe consequences for mine planning. Underestimations may result in a potentially feasible operation being disposed of when it could actually develop into a profitable mine. The more likely consequence is an under designed plant overestimation may lead to construction of a mine where no profitable ore body exists. More commonly, lifespan of the mine operation is shorter than it was anticipated.

Reserve and grade characteristics are the most commonly used variables in the geostatistical evaluation of mineral deposit. The reserve and grade distribution in an ore deposit are controlled and influenced by various geological processes. When a model of these distributions is constructed, it is extremely important to consider the relationship between geology and geostatistics. There are many studies which have been made to emphasize the relationship between geology and the geostatistics (e.g. Rendu, 1984; Dowd, 1986; Clark, 1979 and 1993; Clark and Harper, 2000; Glacken and Snowden, 2001). However, these studies have been carried out to use detailed geologic information. As geologic information is inadequate, it is difficult to establish such a relationship. In such cases, geostatistical tools (variogram and simulation) may be useful. It should be emphasized that there is limited geological information and available for this study.

The traditional methods such as polygon, triangular prism, trapezoid, isopac maps, geological section and block techniques do not allow a determination of reliability of the calculations. The error is high and its actual value cannot be determined. Geostatistical techniques do not only give estimations in any points but also make it possible to find

weighting coefficients for a given mining block and also data configuration that minimises the error or to obtain their associated variance.

This paper aims to assess the spatial structure on the distributions of grade and reserve for the feldspar deposits, in which limited information on geological process of the feldspar deposit characteristics is available. The spatial structure, grade and tonnage estimation were determined by variogram and ordinary kriging using core samples from the drill holes.

2 THE FELDSPAR DEPOSIT AND THE DATA

The feldspar deposit is located in Sarpdere area and 20 km West of the Karpuzlu village in Çine, Aydın, Turkey). The location map of the study area is given Figure 1.

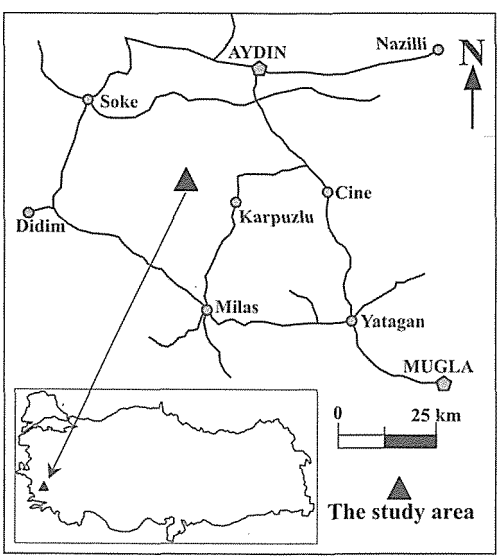

Figure 1. Location map of the study area.

The area is formed on Menderes Massif, where metamorphic rocks are exposed. The feldspar deposit occurs in augen gnesis, quartzite, garnet-mica schists and metagranite rocks. These formations are related to Precambrian age. Metamorphic facies range from green schists and amphibolite facies to eclogite and granulite facies. Menderes Massif consists of high-grade metamorphic core (mainly gneiss, migmatite, amphibolite), and low grade metamorphic cover rocks (mainly schist and marbles). Even though the complex history of metamorphism in the Menderes Massif is still debated, five phases of metamorphism are identified (Bozkurt, 2004).

The main mineralization of the deposit is albite (Na-feldspar) which is produced. The albite is commonly associated with gangue minerals such as mica (muscovite and biotite) which affects the quality of the production. Thus, the existence of such minerals in the area takes a significant role to determine their distribution. In the deposit, the open pit mining method has been employed for the production which is carried out through a valley due to the nature of the deposit.

Main production scheme is given in Figure 2. The produced material is transported to the bulk location in the plant. Then, the material is crushed and grinded for granulometric distribution. The grinded material is classified depending on granulometric distribution and its chemical content. The classified material is sold without mineral processing treatment. The produced feldspar is mainly used in glass and ceramic industries.

The data consists of core samples obtained from 31 drill holes, the locations of which are shown in Figure 3. The exploration boreholes intersected with the feldspar were logged. These logs include the thickness of the intersection, chemical contents of the feldspar and coordinates of the drill holes. Chemical analysis was carried out in order to determine the concentrations of the following compounds: SiO_2, Al_2O_3, CaO, MgO, K_2O, Na_2O, Fe_2O_3 and TiO_2. However, the study was made for Na_2O, SiO_2 and Al_2O_3

Alterations, definition of rock types, faults, fault directions and slopes and other geological properties have not been determined during core drilling.

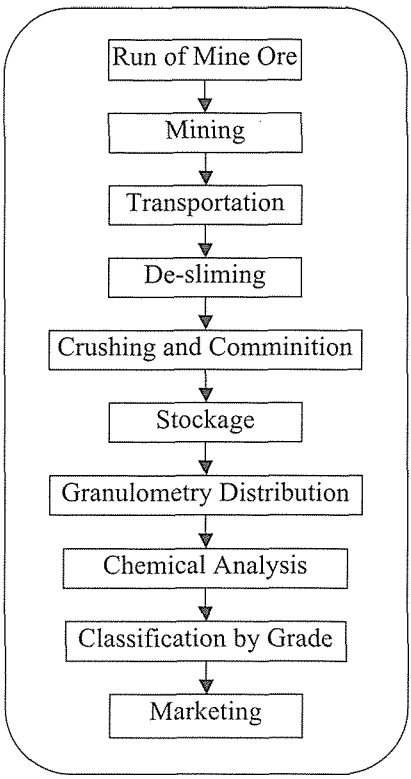

Figure 2. Production flowsheet of feldspar deposit.

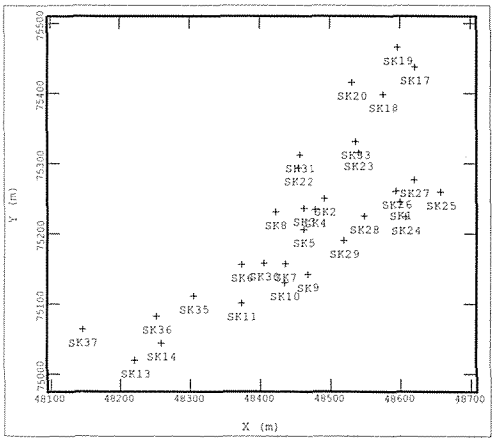

Figure 3. Drillhole locations in the study area.

The feldspar quality depends on these compounds. Thus, as quality variables the deposit content in each of the compounds Na_2O, Al_2O_3, SiO_2, K_2O, and TiO_2 given that these vary greatly depending on the part of the deposit where the sample is obtained. The CaO, MgO, Fe_2O_3 and Al_2O_3 values do not vary greatly in the deposit and remain within the admissible market values for applications in the glass and ceramics industries due to treatment in the laboratory. The quality classification of the feldspar according to the chemical content of the compounds is presented in Table 1.

Table 1. Quality classification of the products.

	Compound Content			
Product Code	Na_2O	SiO_2	K_2O	TiO_2
Ultrawhite–75	10.71	69.08	0.30	0.10
Superwhite–75	10.90	68.78	0.13	0.15
Extra–CG75	10.60	69.63	0.14	0.25
Standard–CG75	9.65	70.00	0.17	0.35
Extra–GQ	11.04	67.41	0.14	0.30
Standard–GQ	10.87	67.98	0.14	0.28

3 GEOSTATISTICS

Geostatistical methods are useful for site assessment, characterisation and monitoring situations where data are collected spatially. These methods are particularly suited to cases where spatial dependence structure and the maps of reserve parameters or other variables are needed. Geostatistics, known as the theory of regionalised variables (Kitanidis, 1999), is a term associated with a number of techniques used to analyse and predict values of variables distributed in a space and/or time. The approach preferred in a geostatistical study is to apply an iterative three-step approach involving:

- Exploratory data analysis,
- Structural analysis (variogram model),
- Making predictions (kriging estimation and/or simulations).

There are several types of the variogram models. However, in the study, Gaussian, spherical and exponential variogram models were used due to the data fitting to these

models. These models are very convenient for the characterisation of ore deposits.

Kriging is a form of weighted average estimator which are assigned on the basis of the model fitted to function such as the variogram. The most frequently used form of kriging is ordinary kriging which was applied to this study. Ordinary kriging derives a weighted block grade estimate from the grades within a defined search ellipse using the semivariogram to calculate the weights for the best linear unbiased estimate.

4 RESULTS AND DISCUSSIONS

Mainly commercial (Isatis, 2006) or public domain software packages was used for the data assessment and interpretation of reserve and grade characteristics in the study area. An advanced professional mining requires a software aided design for the operational phase. The kriging methodology implemented in the latest release of the geostatistical software, ISATIS, offers enhanced capabilities for reserve and grade estimation. This has been successfully applied to the estimation of ore deposits. The results from the analyses were included as exploratory data, the spatial structure, cross validation, calculating the grade-tonnage distributions.

4.1 Exploratory Data Analysis

There are 31 well bore locations to be included in the analyses. The regularisation is an essential phase of a study using 3D data, especially in the mining industry, although the principle is much more general. 2 m composites of the raw data over ore exploration level were considered 417 composite values of the data were obtained. All geostatistical analyses were carried out on the composite data. The summary statistics of the data set over 417 sample composites are shown in Table 2. It is a good idea to check the effect of the regularisation on the statistics for each variable. We would expect the mean to remain unchanged, but the variance to decrease. There are a slight skewness and curtosis for the each variable (Table 2).

Table 2. Summary statistics after the composition of the raw data.

VARIABLE	Na_2O	SiO_2	Al_2O_3
Number of S.	417	417	417
Minimum	3.64	66.12	12.50
Maximum	11.99	78.32	21.70
Mean	9.15	71.03	17.37
Median	9.96	69.92	17.98
Std. Dev.	1.92	3.24	2.15
Variance	3.67	10.47	4.62
Coef. Var.	0.21	0.05	0.12
Skewness	-1.09	0.71	-0.60
Kurtosis	3.13	2.10	2.32

Histograms of the data for each variable are presented in Figure 4a, b and c. The histograms show that the variables were reasonably close to Gaussian distribution. The measures of the central tendency such as mean and median values are close to each other (Table 2). This also supports to the Gaussian distribution. However, the presence of a few outliers affects the distribution. Consequently, the data distributions provide that statistical assumption for the geostatistical analysis is obtained.

4.2 Variogram Analysis

The variogram is used in various procedures of resource and reserve evaluation. The variogram in the study is used to quantify the geological factors that affect the accuracy of estimates. The semivariogram analyses have been carried out directly on the composite data obtained. Both directional (for the directions of 0°, 45°, 90° and 135° respectively) and omnidirectional experimental semi-variograms of compounds Na_2O, SiO_2 and Al_2O_3 were performed separately and studied carefully. Directional experimental semivariogram graphs of the compounds revealed neither severe geometric nor strong zonal anisotropy, and sill values fluctuated more or less around sample variances. The directional variograms were not presented here.

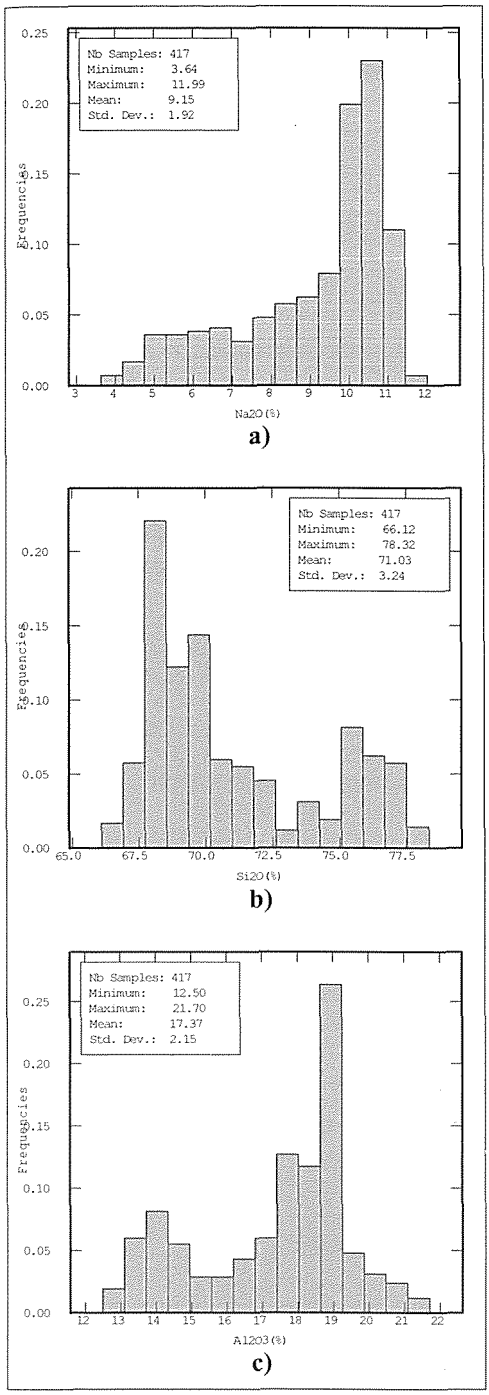

Figure 4. Histograms of the variables. **a)** Na_2O, **b)** SiO_2, **c)** Al_2O_3.

Thus, horizontal and vertical variograms of the compounds are shown in Figure 5a-c. The parameters of the variogram structures are presented in Table 3. In the variogram graphs, the pointed continuous lines and bold continuous lines represent the experimental and theoretical variograms respectively. Visual examination of experimental variograms suggested that theoretical Gaussian, spherical and exponential models are reasonable in agreement with the data. The variogram graphs mostly exhibit clear spatial structures. It is important to be stressed that the sill value of the theoretical models of each variable were found almost close to the variance of the variable (Table 3, Figure 5a-c). The diagonal distance in the study area is about 780 m. Approximately 350-400 m distance for the horizontal variogram analysis is optimum. Consequently, semivariogram analysis findings revealed that sampling design is consistent, that distances between samples are enough to determine spatial dependence structure model.

4.3 Cross Validation Test

The cross validation is a procedure which checks the compatibility between a set of data and their structural model. This procedure consists of in considering each data point in turn, removing it temporarily from the data set and using its neighbouring information to predict (by a kriging procedure) the value of the variable at its location and using the model previously fitted. The estimation is compared true value to produce the estimation error, standardised by the standard deviation of estimation. The neighbourhood concept tells the system which data points, located close enough to the target, will be used during the estimation. The neighbourhood was chosen so that the mean of the standardised estimation error and variance are close to 0 and 1 respectively.

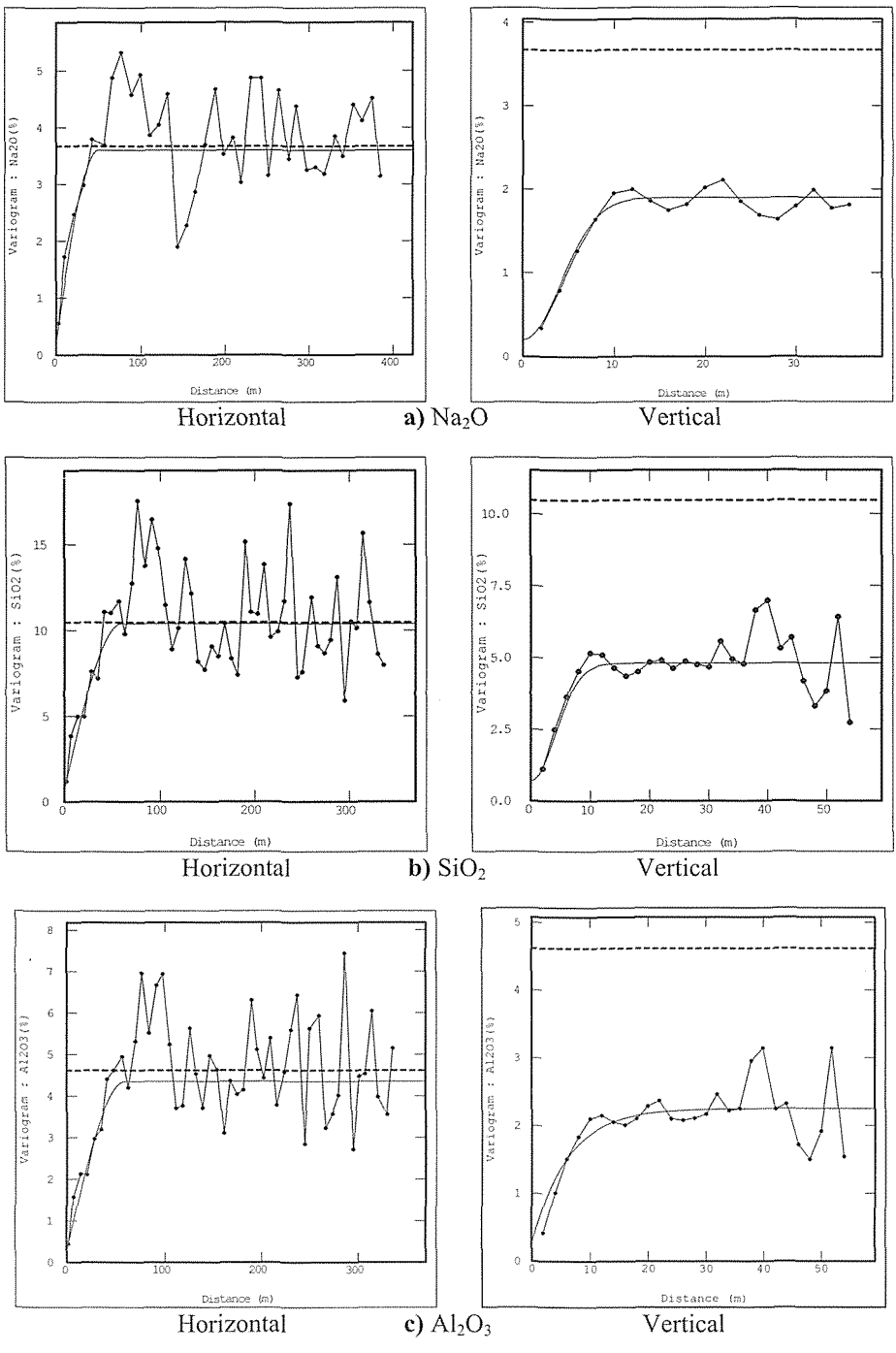

Figure 5. Horizontal and vertical variograms of the variables: **a)** Na_2O, **b)** SiO_2, **c)** Al_2O_3.

Table 3. Variogram parameters of the compounds.

Variogram parameters	Na_2O		SiO_2		Al_2O_3	
Type	Horizontal	Vertical	Horizontal	Vertical	Horizontal	Vertical
Model	Spherical	Gaussian	Spherical	Gaussian	Spherical	Exponential
Lag distance (m)	11	2	7	2	7	2
Number of lags	36	19	49	28	49	28
Range (m)	50	10	60	10	60	18
Sill	3.4	1.7	9.7	4.1	4.1	2
Nugget effect	0.2		0.7		0.25	
Optimum points to use	4		6		12	

Mean of the standardized squared error (MSSE) and mean error (ME) of the Gaussian, spherical and exponential models produced the most favourable results indicating that search strategy, neighbourhood parameters, model and model parameters etc. used in estimation are appropriate. Furthermore, ME of the variogram models proved that the unbiassedness condition of the kriging algorithm worked properly. Thus, these models were chosen for the variables (Figures 5a, b, c; Table 3). Cross validation of the models were graphically given in Figure 6-8 for the variables Na_2O, SiO_2 and Al_2O_3 respectively. The tabulated results of the cross validation test are presented in Table 4. Each model reasonably satisfies the global unbiasedness condition, where distribution of errors is centered on a zero mean. The spread errors and the correlation coefficient of the known values against the kriged estimates were used to determine an adequate search strategy. On this basis, a search radius and the use of the nearest points for each variable were selected as an optimal model.

Table 4. Cross validation results of the experimental variogram models.

Compounds	Standardized mean	Standardized variance
Na_2O	0.01115	0.99092
SiO_2	-0.00110	1.00320
Al_2O_3	0.01934	0.99003

A sample was considered as an outlier as soon as its standardised estimation error (SEE) is larger than a given threshold (Isatis, 2006) in absolute value. Outliers were depicted on the basemap (a), scatter diagram of the observed data versus the estimated value (b) and scatter diagram of the estimated value versus SEE (d) in Figures 6-8. Outliers of the variables did not follow a particular pattern. Scatter plots of the observed data versus the estimated value with conditional expectation line (the 45° diagonal line) of the Figure 6b-8b show slightly conditional bias and little high variability. There is very strong correlation between true and estimated values. Correlation coefficients between the true (experimental) and the estimated values for Na_2O, SiO_2 and Al_2O_3 are 0.90, 0.94 and 0.91 respectively. This indicates to accuracy and reliability of the variogram models. Consequently, the cross validation graphs of estimation value versus SEE proved that the controversy in estimation is within the acceptable limits, excluding the outliers (bold dots) (Figure 6d-8d). Histograms of SEE for all the variables (Figure 6c-8c) were in good agreement with the findings of cross validation analyses mentioned above. In theory, it is expected that the mean of the estimation and standard deviation or variance equal to 0 and 1 respectively. The cross validation results showed that the estimation is reasonably acceptable (Table 4).

4.4 Grade/Tonnage Estimation

The objective of geostatistical estimation for ore deposit evaluation is to provide a continuous representation of grade variation that accounts for structural, lithological and mineralogical discontinuities. The block size of 10x10x5m was used for the variables. The grid design characteristics of the study area are given in Table 5.

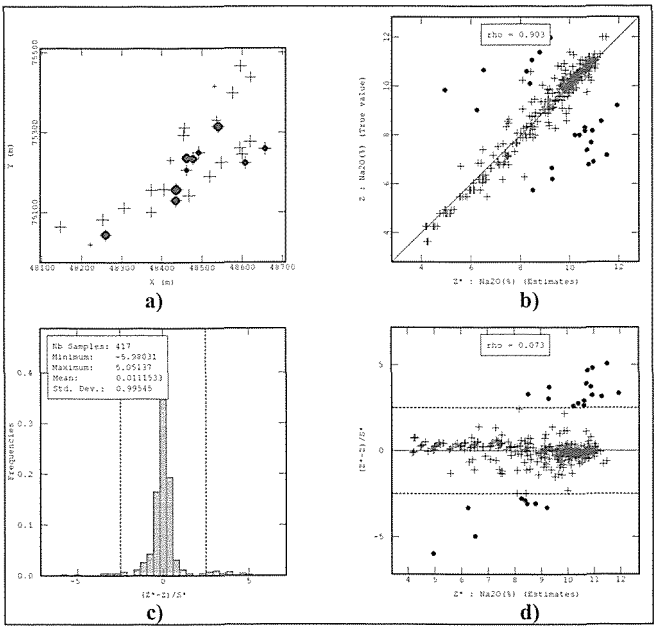

Figure 6. Cross validation results of the Na_2O: **a)** Basemap, **b)** The scatter diagram of observed data (Z) vs. estimated values (Z*), **c)** Histogram of the standardized estimation errors (SSE), **d)** Scatter diagram of SEE vs. Z*.

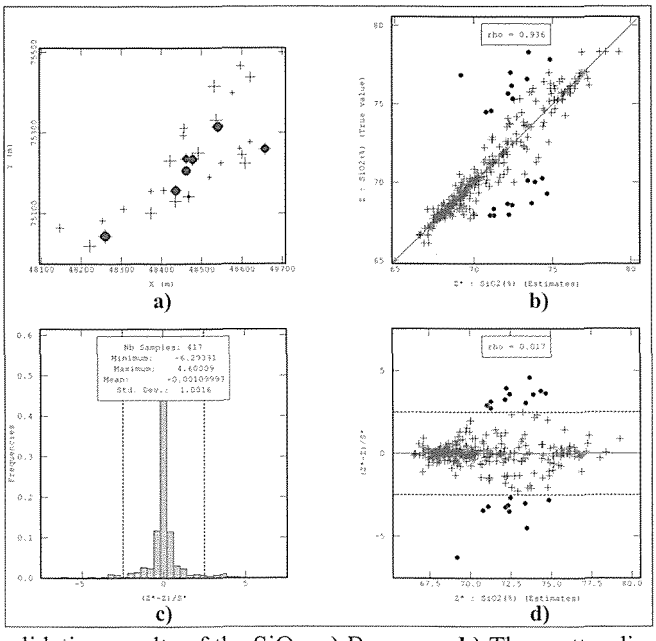

Figure 7. Cross validation results of the SiO_2: **a)** Basemap, **b)** The scatter diagram of observed data (Z) vs. estimated values (Z*), **c)** Histogram of the standardized estimation errors (SSE), **d)** Scatter diagram of SEE vs. Z*.

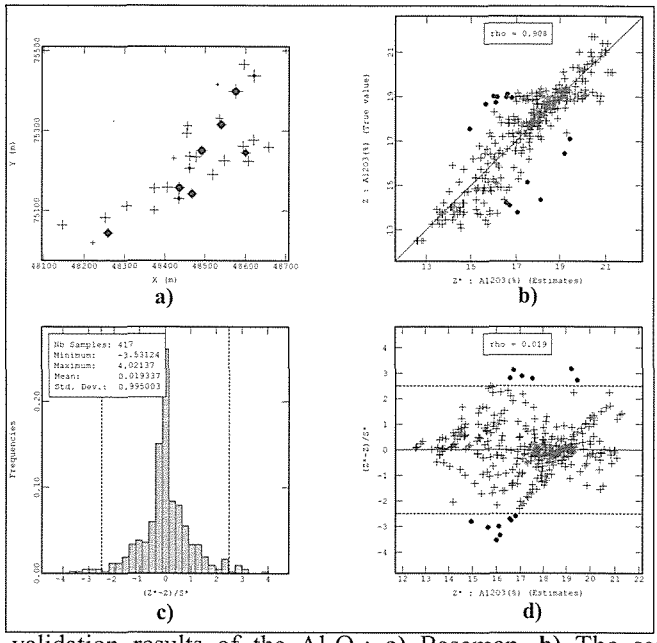

Figure 8. Cross validation results of the Al_2O_3: **a)** Basemap, **b)** The scatter diagram of observed data (Z) vs. estimated values (Z*), **c)** Histogram of the standardized estimation errors (SSE), **d)** Scatter diagram of SEE vs. Z*.

Table 5. Grid design of the study area for kriging.

	X	Y	Z
Origin	48100	75000	300
Mesh	10	10	5
Nodes Number	60	55	50

The grade-tonnage curves and tonnage estimations were obtained using ordinary kriging results of the variables. The total tonnage above cut off grade is calculated using the following equations [1, 2].

$$T = (\sum T_i) * V_b * d \qquad [1]$$

Where,

$\sum T_i$ = Total tonnage of 1 block in percentage,

V_b= Volume in m^3 of 1 block,

d = Density (ton/m^3).

Mean grade above cut off is calculated using the following equation,

$$M = \frac{1}{n} \sum m_i \qquad [2]$$

Where;

m_i = Mean grade unit,

n = Number of samples

Figure 9 shows cut off grade of the variables versus their tonnage. The tonnages of the variables for a particular cut off grade interval are presented in Tables 6-8. Consequently, these results can be basis of production design, successfully mining operation and future planning of the feldspar deposit.

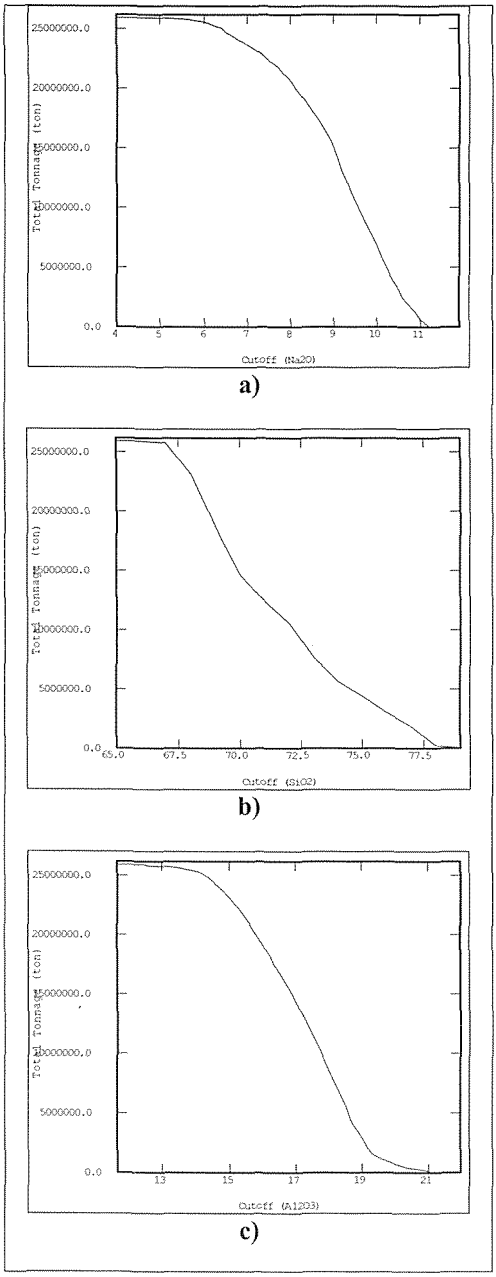

Figure 9. Grade and total tonnage curves for the variables: **a)** Na_2O, **b)** SiO_2, **c)** Al_2O_3.

Table 6. Tonnages with different cut off grade intervals for the Na_20.

Cut Off	Total Tonnage	Mean Grade
4	25914200	9.04
5	25886900	9.05
6	25555400	9.09
7	23614500	9.30
8	20580300	9.55
9	15061800	9.93
10	6745700	10.50
11	686400	11.11

Table 7. Tonnages with different cut off grade intervals for the SiO2.

Cut Off	**Total Tonnage**	**Mean Grade**
65	25914200	71.42
67	25779000	71.44
69	18595200	72.69
71	12420200	74.15
73	7681700	75.45
75	4440800	76.55
77	1856400	77.24
79	23400	79.76
81	2600	81.15

Table 8. Tonnages with different cut off grade intervals for the Al_2O_3.

Cut Off	**Total Tonnage**	**Mean Grade**
11	25914200	17.13
12	25911600	17.13
13	25758200	17.16
14	25339600	17.22
15	23108800	17.47
16	19230900	17.87
17	14393600	18.32
18	8593000	18.87
19	3036800	19.60
20	718900	20.54

5 CONCLUSIONS

Geostatistics provides a set of tools and techniques for addressing the problem of evaluation of mineral deposit. Variograms can be used to characterize the spatial variability of grade and reserve geostatistical simulations can be helpful in interpreting the results obtained from variogram analysis under inadequate geologic information.

The study carried out with the data set showed the benefits of joint use both conventional statistics and geostatistical methods in the assessment of data interpretation, sampling strategy and estimation of values at unsampled areas to determine grade and reserve characteristics. Sufficient, good quality data and exploratory analysis of the data are essential in order to produce good estimates for the study area.

The saleable feldspar was characterised in terms of the factors that determine its market value, namely, its content in Na_2O, SiO_2 and Al_2O_3.

Anisotropy was not detected in the three dimensional experimental semivariograms of the compounds Na_2O, SiO_2 and Al_2O_3. Omnidirectional vertical and horizontal experimental variogram of each compound was found the most representative among the fitted to Gaussian, spherical and exponential models. Variogram analysis revealed that the sampling is consistent, and the distance between samples are enough to determine spatial structure model. The experimental variograms showed a clear spatial structure. These models have been tested by cross validation analysis which proved that the models with their parameters and kriging search parameters are representative for the area under the study.

The grade and tonnage curve for the all variables have been constructed. The tonnages of the variables for particular grade intervals have also been calculated. These are the basis for successful mining operation and future planning of the feldspar deposits.

REFERENCES

Bozkurt, E, 2004. Granitoid rocks of the Southern Menderes Massif (southwest Turkey): field evidence for Tertiary magmatism in an extensional shear zone, *International Journal of Earth Sciences*, 93, pp.52-71.

Clark, I., 1979. Practical Geostatistics, *Elsevier Science Publications*, London.

Clark, I., 1993. Practical Reserve Estimation in a Shear-Hosted Golded Deposit, Zimbabwe. *International Mining Geology Conference, Kalgoorlie WA*, pp. 157-160.

Clark, I. and Harper, W.V., 2000. Practical Geostatistics 2000. *Greyden Press, Columbus*, 116 p.

Dowd, P.A., 1986. Variogram Modelling and Interpretation: Two Examples, *Leeds University Mining Association Journal,* pp. 87-100.

Glacken, I. and Snowden, D.V., 2001. Mineral Resource Estimation in Mineral Resource and Ore Reserve Estimation, *The AusIMM Guide to Good Practise. Ed. A.C. Edwards*, pp. 189-198.

Isatis Software, 2006, Geovariances and Ecole Des Mines De Paris, France.

Kitanidis, P.K., 1999. Introduction to Geostatistics: Applications in Hydrogeology, *Cambridge University Press, Cambridge, UK*, 249 p.

Rendu, J.M., 1984. Interactive graphics for semivariogram modeling, *Mining Engineering*, 36, No: 9, pp.1332-1340.

Assessment of Uncertainty in Grade-Tonnage Curves of a Multivariate Lateritic Bauxite Deposit through Min/Max Autocorrelation Factor Transformation

O. Erten, M. S. Kizil, B. B. Beamish
The University of Queensland, School of Mechanical and Mining Engineering, Brisbane, Australia

L. McAndrew
RioTinto Alcan Brisbane, Australia

ABSTRACT Assessing uncertainty in grade-tonnage curves is rather crucial in resource estimation, as these curves provide information on how much ore within the deposit is above/below a given cut-off grade value. Conditional simulation algorithms can provide robust quantification of the ore production by generating multiple realisations of the ore deposits. However, when the ore deposit is characterised by multiple variables that are spatially correlated, these attributes need to be jointly simulated in order to preserve the spatial correlation. The application of co-simulation algorithms to the grade attributes requires large co-kriging matrices to be solved, making the whole process computationally inefficient and impractical. The minimum/maximum autocorrelation factor (MAF) transformation, however, offers a solution to the simulation of the multivariate deposits by transforming the original attributes into non-correlated orthogonal factors which can then be simulated independently, while preserving the spatial correlation among the attributes. This paper discusses the joint simulation of Al_2O_3, SiO_2, Fe_2O_3, and TiO_2 variables of a lateritic bauxite deposit through the MAF transformation and the results of the grade-tonnage curves for each realisation to express the uncertainty.

1 INTRODUCTION

Geostatistical simulation algorithms are used to model the spatial variability of attributes and quantify the uncertainty associated with geology through a certain amount of realisations. From the perspective of mining economics, simulation algorithms are also very critical in terms of expressing the financial risk involved in mining of a particular ore. Whether a mine would be feasible or not depends heavily on the knowledge of the average grade of the ore that is above the pre-determined threshold grade value. Therefore, it is imperative that the financial assessment of mining of a particular ore be based on the generation of possible grade/tonnage curves that the actual deposit could have. This can only be achieved by conditional simulation.

Application of the conditional simulation algorithms to one attribute is rather straightforward and computationally efficient, as there is no need for the cross-variograms which require the linear model of coregionalisation. However, most deposits are represented by more than one variable each of which should be accounted for in the geological model. For instance, bauxite, nickel laterite and iron ore deposits are characterised by the content of several variables. Alumina (Al_2O_3) is a critical variable for lateritic bauxite deposits but when the downstream processes are considered, silica (SiO_2) is also a crucial variable as any increase in the silica content of the ore will increase the processing cost. Therefore, the geological model should express the joint variation of all the attributes

that are spatially correlated within the deposit. This can be achieved through the use of conditional simulation algorithms that take into account all attributes of interest. Different joint simulation approaches have been proposed by several researchers. Chiles & Delfiner (1999) proposed a method that is based on the model of linear coregionalisation and conditioning of simulated variables. Myers (1988) developed a joint simulation method that uses the conditional univariate Lower-Upper (LU) decomposition. Verly (1993) proposed a joint simulation technique that is based on sequential Gaussian simulation. However, one drawback of these approaches is that the joint simulation of the attributes of interest using traditional co-simulation algorithms requires large co-kriging matrices to be solved at each node, and modelling cross-variograms might also sometimes be very tedious, making the whole process computationally inefficient and impractical.

Principal component analysis (PCA) is an alternative to the traditional co-simulation algorithms, which provides a practical solution for the simulation of the multivariable deposits. In multivariate data analysis, the PCA is used to reduce the dimensionality of the multivariate dataset while preserving the relevant information about the underlying phenomenon Davis (2002). The PCA basically transforms the correlated variables into non-correlated factors which can be simulated independently while maintaining the joint spatial variation among the variables. The PCA approach was used to de-correlate the attributes Davis & Greenes (1983); David (1988); Goovaerts (1993). The major drawback of this method is that PCA de-correlates variables at a lag distance of zero and it requires assumptions on the type of coregionalisation Wackernagel, et al. (1989).

Unlike the PCA, The minimum/maximum autocorrelation factor (MAF) transformation spatially orthogonalises the attributes into non-correlated factors for all lags with an assumption that the variogram model of the related variables follows a linear model of coregionalisation with at most two structures. It was first developed by Switzer & Green (1984). The MAF approach was first used to simulate the multivariate spatial dataset by Desbarats & Dimitrakopoulos (2000). Joint simulation of the attributes with the MAF approach is performed on the transformed data values of each variable independently. The simulated variables are then back-transformed to the normal score values and original data values subsequently. The MAF approach proved to be an effective and efficient method for joint simulation of multivariate data sets Desbarats & Dimitrakopoulos (2000); Boucher (2003); Dimitrakopoulos & Fonseca (2003); Boucher & Dimitrakopoulos (2007).

This paper presents the joint simulation of the multivariate lateritic bauxite deposit through the use of the MAF approach. Firstly, the variables are transformed to their normal scores. Secondly, the transformation matrix that transforms the normal scores to the non-correlated factors is derived. Thirdly, the variography is performed for each factor and then each factor is simulated independently using a sequential Gaussian simulation algorithm. Simulated variables are then validated and back-transformed to the simulated normal scores and original data values subsequently. Lastly, the grade/tonnage curve of each generated realisation is plotted to express the associated uncertainty.

2 WEIPA BAUXITE MINE

Weipa bauxite mine, which is one of the largest lateritic open-cut bauxite mines in the world, is located on the west coast of Cape York Peninsula in northern Queensland. The mine consists of two major mining areas called Andoom and Weipa located in the north-west and south-east respectively in the map of mining lease. Rio Tinto has been supplying bauxite from Weipa to the alumina refineries mainly Comalco alumina refinery which is located at Gladstone in the state of Queensland.

Bauxite ore at Weipa is formed as a result of in-situ weathering of the rocks up to 20-30 metres deep Evans (1975). The Weipa and

Andoom mining areas overlay Cretaceous marine sediments of the Palaeogene Bulimba Formation and Rolling Downs Group respectively. Rolling Downs Sediments belong to Cretaceous period and are expected to be 50 to 100 million years old whereas Bulimba formation belong to the tertiary period and are expected to be 50 million years old. The Andoom bauxite has lower silica content than the Weipa bauxite. The thickness of the bauxite ore ranges from 3 to 12 metres across the mine. The bauxite ore within the lateritic profile overlies a ferricrete section rich in silica and underlies the redsoil section. The main bauxite ore zone contains bauxite pisolites with varying alumina and silica grades.

One of mine sites of the Andoom mining area is selected for this study. The selected area is approximately 1500 metres long by 2900 metres wide, and it is covered by 699 vertical exploration boreholes, representing 10,041 0.25-metre long composites of alumina (Al_2O_3), silica (SiO_2), iron (Fe_2O_3) and titanium (TiO_2). Drilling density is on a regular grid of 76.2 metres by 76.2 metres, with the exception of culturally protected areas, as shown in Figure 1. As the bauxite ore with high alumina (Al_2O_3) content is the key product, the data of the lateritic profile representing only the pisolitic bauxite ore section are restricted by top and bottom wireframes in the Datamine mine planning software package Datamine (2005).

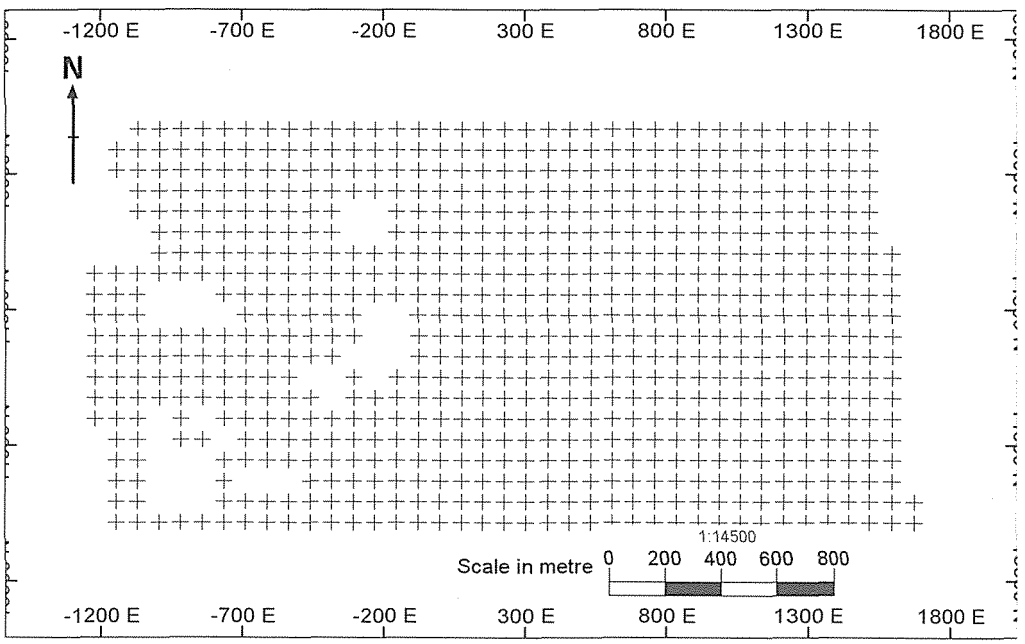

Figure 1. Plan view of the exploration borehole locations

After extraction of the pisolitic bauxite section, the resulting number of sample data used for simulation was 6736.

3 METHODOLOGY

3.1 Exploratory Data Analysis

The first task in any geostatistical study starts with an exploratory data analysis, which includes the computation of univariate, bivariate, multivariate statistics, histograms, regression plots, etc. In this

study, only the univariate statistics of the variables are calculated as the major aim is to perform the joint simulation of the variables to quantify the uncertainty involved in grade/tonnage curves. Univariate statistics of each variable of interest is contained in Table 1.

Table 1. Univariate statistics of the variables

	Mean	Min.	Max.	Variance	Std. dev.	Interq. range	Coeff. of var.	Coeff. of skew.
Al_2O_3 (%)	50.68	21.40	60.89	18.02	4.25	4.82	0.08	-1.37
SiO_2 (%)	6.37	1.18	40.30	26.55	5.15	2.96	0.81	3.17
Fe_2O_3 (%)	16.45	4.34	44.70	26.09	5.11	7.19	0.31	0.45
TiO_2 (%)	2.56	0.92	3.56	0.123	0.35	0.41	0.14	-0.72

It is inferred from the variances given in Table 1 that SiO_2 is the variable that varies most compared with other attributes. The Q-Q plots, which are not presented here, indicate the distributions of Fe_2O_3 and TiO_2 are very close to a theoretical normal distribution. The coefficients of skewness of Fe_2O_3 and TiO_2 are also close to zero which confirms that the distributions of Fe_2O_3 and TiO_2 are rather close to normal. It is noted that SiO_2 is highly positively skewed, which needs to be taken into account during the simulation process. Al_2O_3 is, on the other hand, slightly negatively skewed. The coefficient of variation is also important in that it gives an idea about the presence of the possible erratic values and outliers in the data set. As a rule of thumb, if the coefficient of variation is greater than one, one should be cautious about the presence of erratic or outlier values in the data set Isaaks & Srivastava (1989). The coefficients of variation of all variables in the data set of interest are less than one. The distribution of the values of each variable is also illustrated in the histograms presented in Figure 2.

3.2 Topography Unfolding

Implementation of the geostatistical algorithms to the data set requires the calculation of the distance between each sample and the point to be estimated. In geostatistical applications, the distance between paired samples is measured in a Cartesian XYZ coordinate system in which all distances exhibit straight lines.

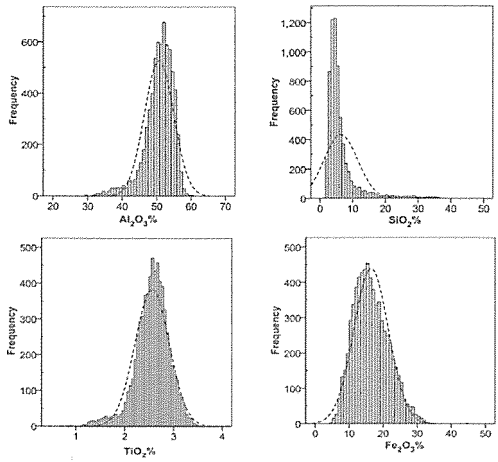

Figure 2. Histograms of the variables

However, in reality, the distance between paired samples may not necessarily exhibit a straight line if a deposit is of undulating or faulted topography. If the presence of corrugation in the topography is not taken into account, the computed variogram may not be robust enough to show true spatial continuity of a variable. Therefore, if a geological deposit exhibits a folded structure, it should be corrected before the spatial continuity is quantified by a variogram model. The unfolding method enables the sample coordinates to be transformed into an unfolded system where the variography and

estimation are performed. Once the estimation is performed for each node within the unfolded model, the transformed coordinates can then be back-transformed to the original space. Performing grade estimations in folded deposits have been dealt with by several researchers Wellmer & Giroux (1980); Dowd et al. (1989); Murphy et al. (2004); Audet & Ross (2005); Carew (2005); Glass & Cornah (2006). The topography of the selected mine site is unfolded using the unfolding tool in ISATIS geostatistical software package Isatis (2009). The unfolded and re-folded models of the selected mine site are presented in Figure 3.

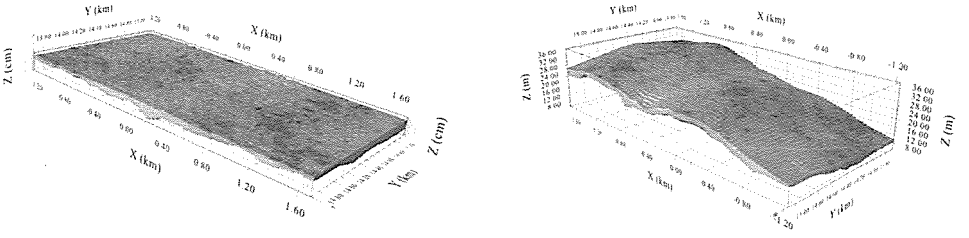

Figure 3. Left: unfolded topography and right: re-folded topography

3.3 Minimum/Maximum Autocorrelation Factor Transformation

Consider a stationary and ergodic non-Gaussian vector random function (RF) $\mathbf{Z}(u) = \{Z^1(u),...,Z^K(u)\}$ with K representing the number of attributes of a natural phenomenon measured at point support. $\mathbf{Z}(u)$ has zero mean and is represented by a two-structure linear model of coregionalisation. The MAF transformation for joint simulation of multivariable deposits proceeds as follows:

First step: Normalising the variables

Normal score transformation of the variables is first performed to decrease the influence of the outliers. The normal scores are calculated as shown in Equation 1.

$$\mathbf{Y}(u) = \{Y^1(u),...,Y^K(u)\} = \{\phi_1(Z^1(u)),...,\phi_p(Z^K(u))\} \quad (1)$$

where; $\mathbf{Y}(u)$ is the matrix of the normal scores of each variable, ϕ is the anamorphosis function, $Z^1(u)$ is the datum of the variable. The matrix of $\mathbf{Y}(u)$ is assumed to be multi-Gaussian.

Second step: The MAF transformation

The transformation of the normal scores of the original data values to non-correlated factors can be written as shown in Equation 2.

$$\mathbf{M}(u) = \mathbf{A}^T\mathbf{Y}(u) \quad (2)$$

$\mathbf{M}(u)$ is the linear combination of the multi Gaussian vector RF $\mathbf{Y}(u)$ with a set of weights given by the orthogonalisation coefficient matrix $\mathbf{A}$. This coefficient matrix is calculated as presented in Equation 3.

$$2\Gamma_Y(h)\mathbf{B}^{-1} = \mathbf{A}^T\Lambda\mathbf{A} \quad (3)$$

The variance/covariance matrix of normal scores at lag zero is presented in Equation 4.

$$\mathbf{B} = \mathrm{cov}[\mathbf{Y}(u), \mathbf{Y}(u)] \quad (4)$$

where; $\mathbf{B}$ is the variance /covariance matrix of $\mathbf{Y}(u)$ at lag zero.

The variance/covariance matrix of normal scores at lag h is presented in Equation 5.

$$2\Gamma_Y(h) = \mathrm{cov}[\mathbf{Y}(u) - \mathbf{Y}(u+h), \mathbf{Y}(u) - \mathbf{Y}(u+h)] \quad (5)$$

where; $\Gamma_\gamma(h)$ is the variogram matrix at lag h

Derivation of the coefficient matrix **A** is equivalent to performing two successive PCA decompositions Desbarats & Dimitrakopoulos (2000). Al_2O_3, SiO_2, TiO_2 and Fe_2O_3 variables are first transformed into their normal scores through the use of the ISATIS geostatistical software package. The normal scores of each variable are then used as inputs for the MAF tool in ISATIS. The variance/covariance matrix of the Gaussian variables at lag zero is calculated as follows:

$$\mathbf{B} = \begin{bmatrix} 1.000 & -0.5196 & -0.6359 & 0.8430 \\ -0.5196 & 1.000 & 0.0332 & -0.6251 \\ -0.6359 & 0.0332 & 1.000 & -0.4840 \\ 0.8430 & -0.6251 & -0.4840 & 1.000 \end{bmatrix}$$

The variance/covariance matrix of the Gaussian variables at lag 76.2 metres is calculated as follows:

$$\Gamma_\gamma(h) = \begin{bmatrix} 1.1257 & -0.3554 & -0.9061 & 0.8064 \\ -0.3554 & 1.4790 & -0.3366 & -0.6664 \\ -0.9061 & -0.3366 & 1.6387 & -0.5156 \\ 0.8064 & -0.6664 & -0.5156 & 1.0993 \end{bmatrix}$$

The coefficient matrix **A** is then calculated:

$$\mathbf{A} = \begin{bmatrix} 0.9149 & -0.8296 & -1.3464 & -1.1816 \\ 0.1049 & -1.0386 & 0.7544 & -0.6161 \\ 0.4746 & -1.2879 & -0.3744 & 0.3062 \\ 0.4196 & -0.3116 & 1.7630 & 0.8841 \end{bmatrix}$$

The multiplication of the matrix **A** by the data matrix $\mathbf{Y}(u)$ yields orthogonal non-correlated factors of the variables which can be simulated independently, while preserving the spatial correlation. The de-correlation between factors is assessed through the computation of the cross-variograms presented in Figure 4. As it is clear from the cross-variograms, de-correlation of the factors at all lags is rather satisfactory.

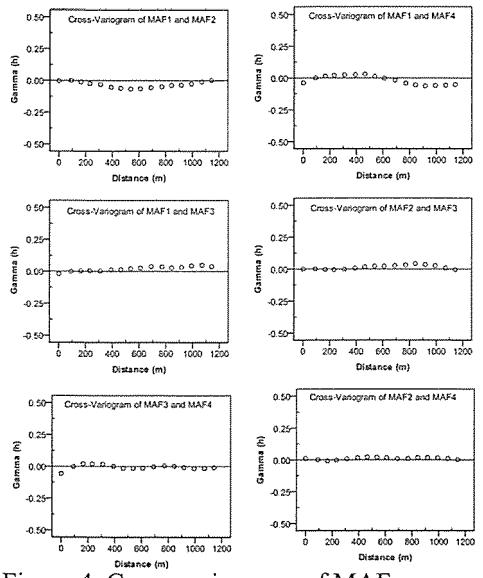

Figure 4. Cross-variograms of MAFs

3.4 Variography of the MAF

An experimental variogram of each MAF is computed according to the anisotropy directions detected through the variogram maps. Except MAF-3, all other MAFs exhibit geometric anisotropy. The experimental variogram of each MAF is fitted with a linear model of regionalisation. Experimental directional variograms and the fitted models are presented in Figure 5.

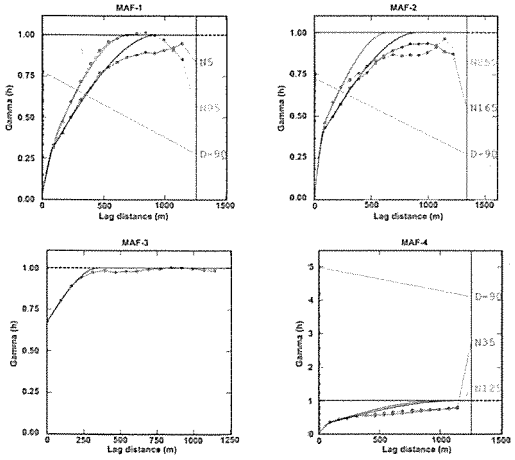

Figure 5. Experimental variograms of MAFs

3.5 Simulations of the MAFs

A sequential Gaussian simulation algorithm is used to simulate each MAF independently. Simulations are performed on a grid of 36,382 nodes within the selected mine site. Twenty realisations are generated for each MAF. Fifth realisation of each variable is presented in Figure 6. It is noted that each realisation is generated using unfolded data set and then re-folded back to the original data space.

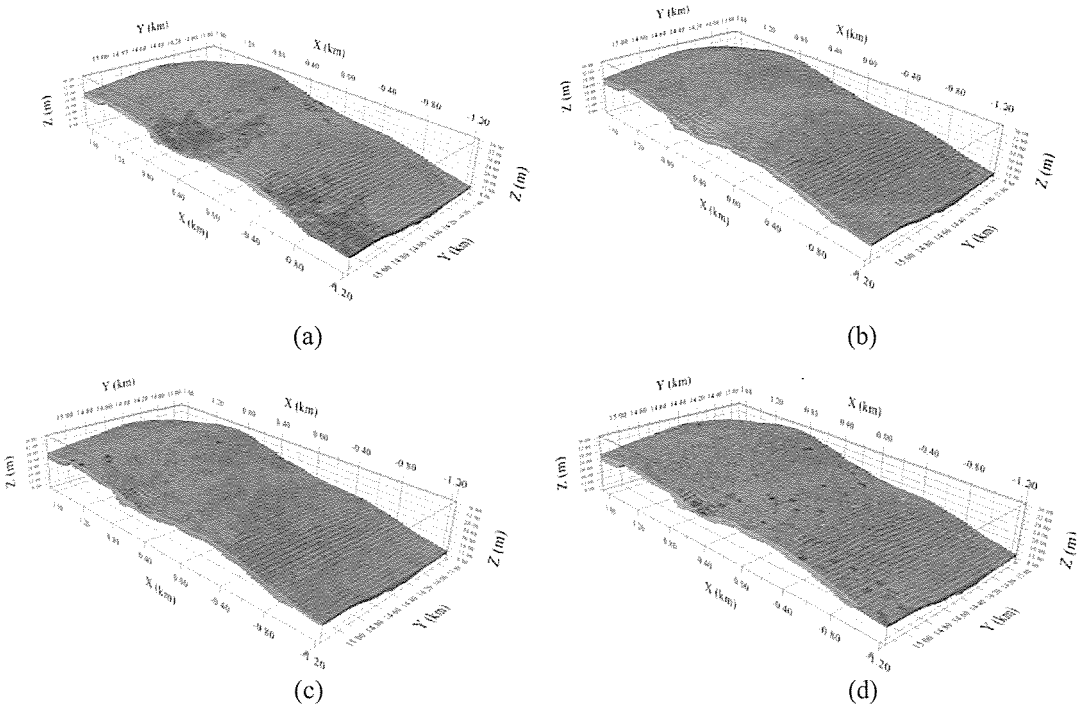

Figure 6. Fifth realisation of each variable (a): Al_2O_3, (b): SiO_2, (c) Fe_2O_3, (d): TiO_2

3.6 Back-transformation of MAF

After generating the simulated realisations for each MAF, the simulated values are back-transformed to the original values. The multiplication of the simulated values of each MAF by the inverse matrix of A yields the values in the original data space. The inverse matrix of the matrix A is as follows:

$$A^{-1} = \begin{bmatrix} 0.9122 & -0.6169 & -0.3068 & 0.8955 \\ 0.2664 & -0.4555 & -0.6440 & 0.2616 \\ -0.0141 & 0.3395 & -0.3463 & 0.3376 \\ -0.3109 & -0.5447 & 0.6092 & 0.1250 \end{bmatrix}$$

3.7 Validation of the simulation Realisations

The generated realisations are validated by comparing the histograms of simulated variables with the histograms of the original variables. As it is seen from Figure 7, the histograms of the fifth, tenth and fifteenth realisations of each variable have the distribution which is rather close to the original distribution of the variables given in Figure 2. It can be inferred that the sequential Gaussian simulation algorithm perfectly reproduced the spatial variability of each variable of interest.

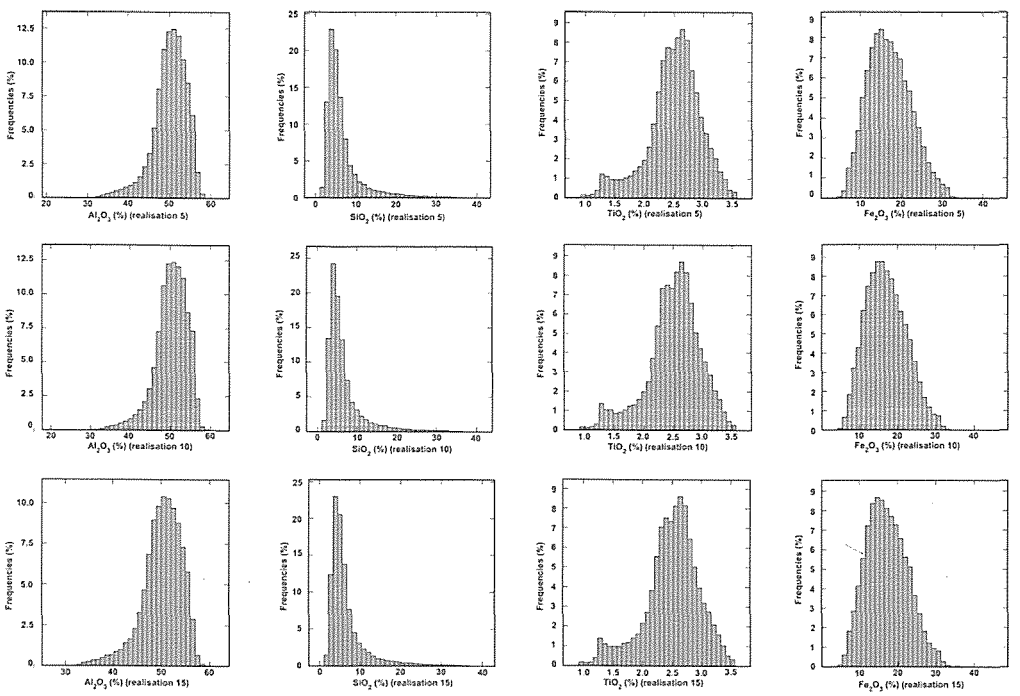

Figure 7. Histograms of the three different realisations of each variable

4 RESULTS AND DISCUSSIONS

As the selected mine site is a multivariate lateritic bauxite deposit, the content of each attribute within the excavated ore is of critical importance in terms of the downstream processes. In this study, Al_2O_3 and SiO_2 are the attributes that characterise the quality of the excavated bauxite ore. The grade/tonnage curves of these variables can provide information on how the tonnage percentage of these variables is changing within the bauxite ore being sent to the refinery. After performing the joint simulation of the variables of interest, the grade/tonnage curve for each individual realisation is plotted to determine the tonnage variation of these variables. As the quantity of Al_2O_3 and SiO_2 within the excavated ore is of concern, the grade/tonnage curves are plotted for 20 realisations of Al_2O_3 and SiO_2 as presented in Figures 8 and 9 respectively. As it is seen from Figure 8 the variation in Al_2O_3 tonnage according to the cut-off grade, which is 54% of Al_2O_3, ranges from 16.4% to 17.2%. This result indicates the fact that how much ore above a given cut-off (54%) could change. It is inferred from the grade/tonnage curve that the tonnage change for Al_2O_3 would be 0.8%. As for the SiO_2, it is important to find out how much ore is below the given SiO_2 cut-off value (4.7%). As it is seen from Figure 9, The SiO_2 tonnage would change about 0.95% among the realisations. As far as the mean grade of Al_2O_3 and SiO_2 is concerned, the grade seems to be quite stable for several cut-off values for both variables.

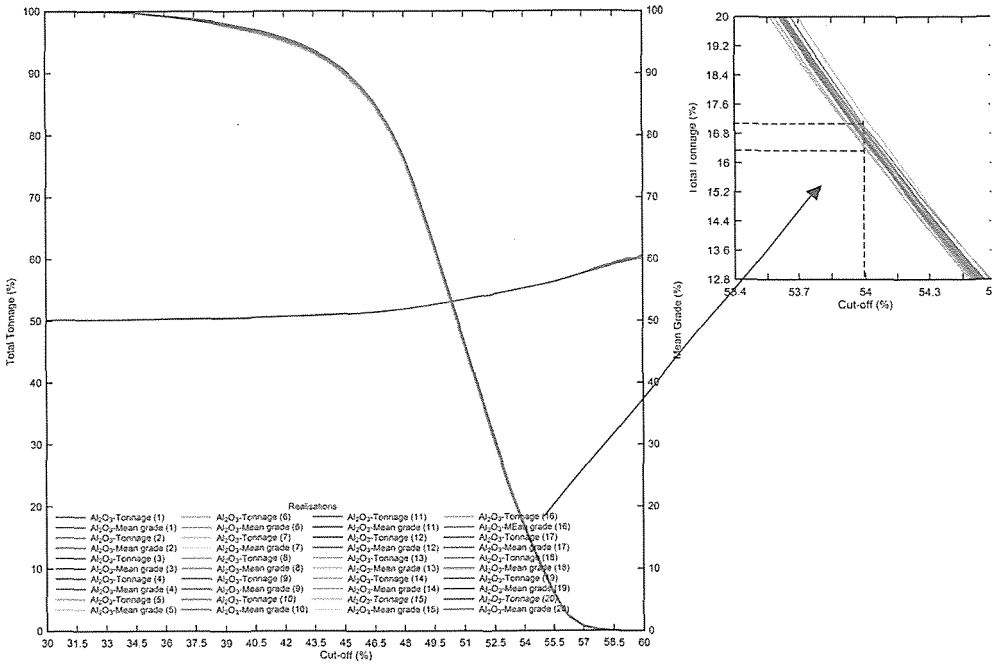

Figure 8.Grade/tonnage curves of the simulated realisations of Al_2O_3

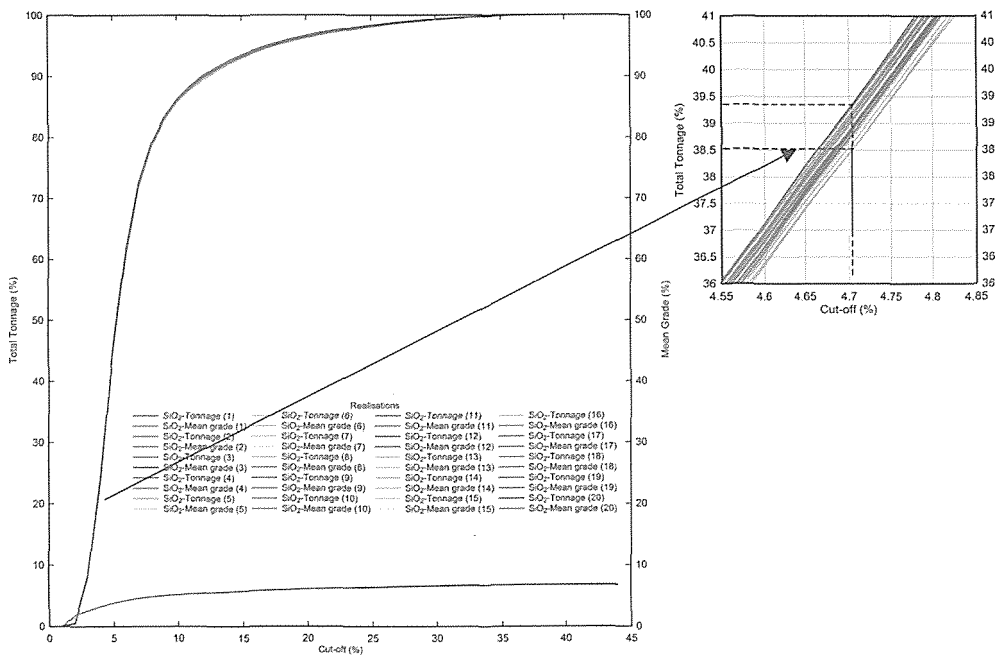

Figure 9. Grade/tonnage curves of the simulated realisations of SiO_2

5 CONCLUSIONS

Joint simulation of the multivariate deposits has been a challenging work with the traditional co-simulation algorithms. The major drawback of the use of these algorithms is the size of the variance/covariance matrix of the spatially correlated variables, which increases the computation time of the simulation significantly. If the variables are de-correlated and simulated independently, the computation time can be reduced, which allows multivariate deposits to be simulated in an easy way.

Minimum/maximum autocorrelation factor (MAF) is a transformation method which enables spatially correlated multiple variables to be de-correlated, which can then be simulated independently avoiding the solving process of the big sized matrices.

In this paper, MAF transformation was used to de-correlate the variables of a lateritic bauxite deposit at Weipa in Australia. The selected deposit is characterised by four major variables including Al_2O_3, SiO_2, Fe_2O_3, and TiO_2. In the scope of this study, these variables are first transformed into their normal scores to reduce the erratic values and outliers within the data set. Secondly, the normal scores of each variable are transformed into their orthogonal factors which avoided the computation of the cross-variograms between the variables of interest. Experimental variograms are then computed for each MAF and fitted with a theoretical model. The sequential Gaussian algorithm was performed on each MAF based on the model obtained from the variograms. Twenty realisations were generated for each MAF and the simulated MAF was back-transformed to the normal scores of the variables using the inverse matrix of the transformation matrix derived earlier. Another transformation was performed to transform the normal scores to the values in the data space. Lastly, the grade/tonnage curves were plotted for Al_2O_3 and SiO_2 to determine how different the tonnage of the variables would be within the excavated ore. It is inferred from the grade tonnage curves that the variables of Al_2O_3 and SiO_2 exhibit very less variation.

6 REFERENCES

Audet, M. and Ross, A. F., 2005. Koniambo Lateritic Ni-Co Deposits, New Caledonia-A Case Study from Geological Modelling to Mineral Resource Classification *Proceedings of Orebody Modelling and Strategic Mine Planning, Uncertainty and Risk Management* R. Dimitrakopolous and S. Ramazan. Perth, WA, Australia, pp. 215-224.

Boucher, A., 2003. *Conditional joint simulation of random fields on block support.* Department of Earth Sciences. Brisbane, The University of Queensland. MPhil thesis, 137 p..

Boucher, A. and Dimitrakopoulos, R., 2007. A New Efficient Joint Simulation Framework and Application in a Multivariate Deposit. *Orebody Modelling and Strategic Mine Planning.* Spectrum Series Volume 14, pp. 319-328.

Carew, T. J., 2005. Unfolding-Getting the Geometry Right. *APCOM Application of Computers and Operations Research in the Mineral Industry.* S. Dessureault, R. Ganguli, V. Kecojevic and J. G. Dwyer. Tucson, Arizona, USA, pp. 103-110.

Chiles, P. J. and Delfiner, P., 1999. *Geostatistics Modelling Spatial Uncertainty.* New York, John Wiley&Sons, 695 p.

Datamine, 2005. *Introductory geoloogy training manual studio 3.* Somerset, The United Kingdom, 318 p.

David, M., 1988. *Handbook of Applied Advanced Geostatistical Ore Reserve Estimation.* Amsterdam, Elsevier, 364 p..

Davis, J. C., 2002. *Statistics and Data Analysis in Geology.* New York, Chichester, Brisbane, Toronto, Singapore, Wiley, 638 p.

Davis, M. V. and Greenes, K. A., 1983. *Estimation using spatially distributed multivariate data: an example with coal quality.* Mathematical Geology 15(2), pp. 287-300.

Desbarats, A. J. and Dimitrakopoulos, R., 2000. *Geostatistical simulation of regionalised pore-sized dostributions using min/max autocorrelation factors.* Mathematical Geology 32(9), pp. 919-942

Dimitrakopoulos, R. and Fonseca, M. B., 2003. *Assessing risk i ngrade-tonnage curves in a complex copper deposit, northern Brazil, based on an efficient joint simulation of multiple correlated variables.* APCOM/SAIMM, pp. 373-382

Dowd, P. A., Johnstone, S. A. W., and Bower, J, 1989. *The application of structurally controlled geostatistics to the Hilton Orebodies, Mt Isa, Australia.* 21st Application of Computers and Operations Research in the Mineral (APCOM) Industry. A. Weiss. Colorado, USA, pp. 275-285.

Evans, H. J., 1975. *Weipa bauxite deposit, Queensland.* Economic Geology of Australia and Papua New Guinea, Australasian Institute of Mining and Metallurgy. Monograph 5, pp. 959-963.

Glass, H. J. and Cornah, A. J., 2006. *Unfolding the Luce Deposit to improve variograms.* 6th International Mining Geology Conference. Darwin, Northern Territory, Australia, pp. 217-224.

Goovaerts, P., 1993. *Spatial orthogonality of the principal components computed from coregionalised variables.* Mathematical Geology 25(3), pp. 281-302.

Isaaks, E. H. and Srivastava, R. H., 1989. *An Introduction to Applied Geostatistics.* New York, Oxford University Press, 561 p.

Isatis, 2009. *Beginner's guide* Avon Cedex, France, Isatis, 150 p.

Murphy, M., Bloom, L., Mueller, U. A., 2004. *Using unfolding to obtain improved estimates in the Murrin Murrin Nickel-Cobalt Laterite Deposit in Western Australia.* Geostatistics Banff, Quantitative Geology and Geostatistics, Springer.

Myers, D. E., 1988. *Vector Conditional Simulation.* Geostatistics. Avignon, Kluwer Academic Publishers, pp. 283-292.

Switzer, P. and Green, A. A., 1984. *Min/max autocorrelation factors for multivariate spatial imagery.* Technical Report No 6, Department of Statistics, Stanford University.

Verly, G. W., 1993. *Sequential Gaussian Cosimulation.* Geostatistics. A. Soares. Dordrecht, Kluwer Academic Publisher, pp. 543-554.

Wackernagel, H., Y. Petitgas, and Touffait, Y., 1989. *Overview of methods for coregionalisation analysis.* Geostatistics, Kluwer Academic Publishers: Dordretcht, pp. 409-420.

Wellmer, F. W. and Giroux, G. H., 1980. *Statistical and geostatistical methods applied to the exploration work of the Nanisivk Zn-Pb mine, Baffin Island, Canada.* Mathematical Geology 12, pp. 321-337.

An Application of Risk-Based Mine Planning Methods for a Copper Porphyry Deposit-Case Study

S. Mehrdad Heidari
The School of Mining Engineering, The University of New South Wales, Sydney, NSW, Australia

Serkan Saydam
The School of Mining Engineering, The University of New South Wales, Sydney, NSW, Australia

ABSTRACT: Impact of any kind of geological uncertainty, especially grade on orebody modeling, is a critical problem in optimisation of open pits. In the intervening years, several researches have addressed the issue with applying conditional simulation techniques to assess the grade risk. This paper presents an application of two approaches, Maximum Upside / Minimum Downside, and Risk Rated Pits for four key project performance indicators; net present value, revenue, amount of ore and metal content. A copper porphyry deposit, which has a typical medium-high grade, has been designed by these approaches. In this paper, we discussed about applications, advantages and limitations of these approaches to optimise of open pit mines.

1 INTRODUCTION

Major sources of financial risk of designing a mine include various uncertainties such as geological, future commodity prices, demand levels and even engineering judgment (Reza Sayadi et al, 2010). The latter risks are in some sense easier to account quantitatively for when assessing project risks, as the prices and demands are small values in practice, which can be modelled as time series in different ways. Geological uncertainty is much more difficult to model, as there are complicated spatial considerations, which not present in prices or demand levels.

Current state-of-the-art approaches, to assess grade uncertainty on optimisation in mine planning, utilise conditional simulation techniques of the geological resource (Dimitrakopoulos, 1998). A conditional simulation is a randomly sampled outcome of commodity grades in mine reserve. The "conditional" descriptor refers to the fact that each simulation should be geologically realistic, in the sense that second order grade statistics, defined for example by a variogram, are respected. In principle, other forms of conditioning may be applied to each simulation to guarantee geological accuracy. One of the most common practical methods of producing realisations is Sequential Gaussian Simulation (SGS) (Deutsh.C.V et al, 1998). By producing many conditional simulations of a single geological reserve, a naive, but instructive, assessment of financial risk due to geological uncertainty would be to evaluate a putative mine exploitation plan against each conditional simulation, thus obtaining a spread of financial outcomes in terms of net present value (NPV) for example. The spread of financial outcomes of several competing mine plans can be assessed in this way. In addition to the above risk assessment technique, which will be

explained further in Sections 3 and 4, an application of a recent practical mine optimisation method - "A Maximum Upside / Minimum Downside Approach" (R. Dimitrakopoulos et al, 2007) also presented in this paper in Section 5. The following notes should be considered in this study:

Note 1: Only four parameters (NPV, revenue, amount of ore and metal content) were quantified in grade uncertainty in mine designs, although there are several project performance indicators such as internal rate of return (IRR), metal production, any sort of operating costs and so on.

Note 2: In order to assess grade uncertainty, in this study, NPV4 Scheduler software is used. This software has powerful options to handle the risk analysis especially for Risk Rated k-Pits option (discussed further in Section 4).

2 APPLICATION AT A COPPER PORPHYRY DEPOSIT

The mineralisation is hosted in quartz-monzonite porphyry (QMP), which undergone several phases of hydrothermal alteration common in porphyry systems. The economic mineralisation appears as small veins and disseminated grains primarily in the QMP. No preferred orientation in this mineralisation has been observed, although it is considered parallel to the dykes and main faults. Mineralized zones (domains) have been classified by the degree of leaching and supergene enrichment of the original hypogene sulphide primary and high-grade economic mineralization occurred within the supergene zone. This conforms that this mineralisation is a classical porphyry copper style model, but in a small scale. A single estimation domain is focused where 48 Mt of measured and indicated geological resources. Within the supergene domain, the copper grades determined for a set of 414 six-meter composites from the drill holes. The mean copper grade and the standard deviation of it are 0.75% and 0.353, respectively. The block model has 2,805 blocks with 25×25×12.5 (x, y and z direction) sizes.

Experimental variogram maps were calculated using composite samples for the total copper grades and its normal scores. The variogram sets are calculated in x, y and z orthogonal directions. One stage spherical models were used to model the experimental variograms. The variogram results revealed that the model has a high nugget effect, which confirms high small-scale variations over the supergene zone. Based on this, it is assumed that a high-grade variation is expected in the realisations.

3 IMPACT OF GRADE UNCERTAINTY ON PIT OPTIMISATION

In order to assess the possible range of financial outcome of mine designs, 24 realizations are generated by using conditional sequential Gaussian simulation.

The techno-economic parameters which shown in Table 1 are used to optimize throughout this paper.

Table 1. Mine design parameters

Parameters	Value	Unit
Mining cost	1.25	$/tonnes
Processing cost	20.0	$/tonnes
Other costs	450.0	$/tonnes
Mine production	2,500,000	tonnes/years
Pit slope	38.0	degree
Copper recovery	85.0	%
Discount rate	16.0	%
Copper price	5,000	$/ton

By applying Lerchs & Grossmann (LG) algorithm and stepping the copper price through a series of values, 50 optimal pit alternatives (nested pits) are created inside of the each initial optimal pits.

Figure 1 illustrates the variations of NPVs of 24 optimizations for 50 nested pits. The same graphs can be drawn for the other project indicators, but to make a better sense of how they vary we just show , in Table 2, the statistical parameters of the project indicators probability distributions (such as minimum, mean, maximum, standard deviation (Std.) and coefficient of variation).

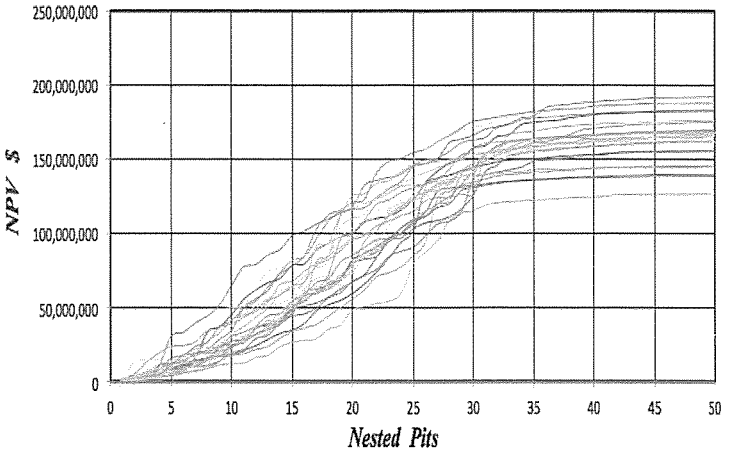

Figure 1. NPV of 24 optimizations based on 50 nested pits

Table 2. Statistical parameters of project indicators distributions

	Unit	Minimum	Average	Maximum	Std.	CV.
NPV	$	126,495,299	164,346,598	192,400,858	17,096,027	10.40%
Revenue	$	1,150,605,630	1,241,982,892	1,332,918,314	54,530,129	4.39%
Metal content	tonnes	291,987	313,886	338,253	13,269	4.23%
Ore tonnage	tonnes	33,292,188	36,628,057	40,321,875	1,807,579	4.93%

The coefficient of variation (CV) of the probability distribution of project indicators is a useful parameter to compare the degree of variation, which can be used to assess the grade uncertainty risk for the project. As can been seen in Table 2, the CVs are not high for all mentioned indicators. Therefore, it may not be a risky project as a rough judgment.

As seen in Figure 1 for all cases, the pits number 50 has the highest NPV, although there are some fluctuations on their final NPVs. By looking at the NPVs of the nested pits, one can be seen that after pit number 35, the NPVs are not much improved by increasing the mine size , and the curves are almost flat. Thus, this pit may be considered as optimum final pit in terms of NPV. However, as the mine is small compared to normal copper porphyry mines, the pit number 50 is considered as final pit to have higher minable deposit.

4 FINDING A PIT WITH AN ACCEPTABLE RISK

For each optimal pit (from Section 3), there may be blocks in the optimal pits that are included in all 24 optimal pits. Other blocks may be included in 23 optimal pits, 22 optimal pits, and so on. Obviously, some of the blocks will not be included in any optimal pits at all. Considering the pit shell (k-Pit) that consists of all blocks included in at least k ultimate pits, where k is an optimal pit between 1 and 24, the block will definitely be inside of k-1 pit, if it is in k-pit. It means k-pits are nested which are ranked by the grade uncertainty. The risk rating of a k-pit can be quantified by the following formula (NPV scheduler, Tutorial).

$$S = (100 \times k) / N$$

where N is the number of the optimal pits

In this case, we will have pit shells with 100%, 95.83% confidence and so on, if

k=24, 23 and so on. It means, these pit shells are defined by these blocks which occur in at least 100% or 95.83% and so on of all 24 optimal pits.

Before selecting an appropriate risk rated pit, the ultimate pits have to be generated for any k-pit (from 1 to 24) by following the same practical mining constraints and financial parameters. Table 3 shows the results of the optimizations just for the first 5 risk rate pits.

The decision about the appropriate risk factor regarding to the project performance indicators, can be made by any criteria, which may be important for mine designers. For instance, pit 2 (95.83% confident) could be selected to get more NPV than the average of NPV shown in Table 2.

The next step is the same as conventional methods, which is applying optimization and pushback designs on pit 2. Before coming to conclude about this section, following explanation about the pushback designs have to be considered.

The philosophy of nested pit generation is to realize the greatest amount of grade can be mined as early as possible to get the highest NPV. In pushback generation phase, if the number of pushbacks is theoretically increased (up to nested pits) NPV meets higher value. However, practically, there will not be sufficient access space between two pushbacks or minimum mining operating space at mines. Therefore the number of pushbacks is limited, and NPV would be lower than the optimized pit.

In this case, three pushbacks have been used to get the optimum solution. As can be seen in Table 4, the final optimized NPV is around 148 M$, which is less than the given average NPV in Table 2 (164 M$).

Table 3. The optimized 5 first risk rated pits

Risk Rate Pits	Rock tonnes	Revenue $	NPV $	Ore tonnes	Metal content tonnes
Pit 1 (100 % safe)	38,539,302	767,282,773	160,420,896	20,556,250	194,712
Pit 2 (95.83% safe)	44,430,860	887,398,031	170,981,830	24,165,625	225,194
Pit 3 (91.67% safe)	48,290,479	963,667,322	175,824,537	26,623,438	244,548
Pit 4 (87.50% safe)	51,178,425	1,017,986,030	179,034,234	28,359,376	258,333
Pit 5 (83.33% safe)	57,785,982	1,099,569,682	182,162,308	30,989,064	279,036

Table 4. The indicators of optimized pit 2 (95.83% Safe) based on 3 pushbacks

Pushback No.	Rock tonnes	Revenue $	NPV $	Ore tonnes	Metal content tonnes
1	14,312,512	304,269,834	93,337,748	6,978,125	77,214
2	17,772,235	258,725,629	29,762,314	7,528,125	65,656
3	12,346,113	324,402,568	24,996,583	9,659,375	82,323
Total	44,430,860	887,398,031	148,096,645	24,165,625	225,194

5 MAXIMUM UPSIDE / MINIMUM DOWNSIDE APPROACH

Regarding to different generated realizations from a model, the upside potential can be defined, if an individual mine design is able to achieve a better value for a desired project indicator than what is expected, and vice versa for down side risk. The target of this

approach is finding just one design (among the other pit designs) that can minimize risk of loses while maximize the chance of getting higher value of project performance indicators in a set of generated realizations. The approach can be explained through the following steps (R. Dimitrakopoulos et al, 2007):

1- Generating N realizations of a geological block model and applying conventional mine design in order to optimize each realization. As a result of this step, N different optimal pits with corresponding pushbacks are made.
2- Applying each optimized design on the other (N-1) realisations to calculate the mine indicators, and then ignoring the designs that cannot satisfy the defined criteria for the indicators.
3- Selecting a single design that can capture the maximum upside / while is able to get the minimum downside.

For this section the project indicator is just NPV, as there is no significant variation in the rest of indicators.

5.1.1 Capturing maximum upside / minimum downside based on final pits OES

In order to evaluating the effect of mine design (pushbacks design) on the results, the conventional optimization and mine design are investigated individually.

It should be noted that all the various stages of optimization and mine planning can be represented by Optimal Extraction Sequences (OES).In this study, OES is used instead of using the pit shells.

The optimal extraction sequences can be derived by using the LG algorithm for each realization grades. As a consequence, the output extraction sequences are optimal just regarding to its model but not for the other optimizations.

By applying the each extraction sequences of optimal pit on all 23 realizations, 24 NPVs can be calculated, for each realization (shown in Figure 2). As can be seen, maximum upside (i.e. upside potential) and minimum downside (i.e. down side risk) for 24 pit designs for the ore body are comparable.

For making any decision about accepting or discarding the mine plans, a based point has to be defined regarding to the project criteria. For instance, if the minimum acceptable NPV for the project is 90 M$, there is no significant downside risk in mine plans. Therefore capturing the maximums' upside (as a reward) will be a target, while the project may be risky, if minimum acceptable NPV is 140 M$.

5.1.2 Capturing maximum upside / minimum downside based on pushbacks OES

Figure 3 shows the impact of applying 24 pushbacks extraction sequences on NPVs of each optimization.

The difference between Figure 2 and 3 comes from impact of practical mining constraints on the result of NPVs. In all cases, the NPVs in Figure 3 are lower than Figure 2. If the minimum acceptable NPV is around 110 M$, Figure 3 shows that design pit number 8 has the minimum downside risk (with at least 105 M$).This is significantly higher than the other minimum downsides. It means just the pushback design 8 guarantees getting at least 105 M$ for any grade variation inside the set of generated realizations. It is very close to the minimum acceptable NPV - 110 M$. On the other side, although designs 9, 20 and 23 have higher upside potential to get higher NPV than the design 8, they have higher downside risk. Therefore, the design 6 can be selected as the best practical mine designs.

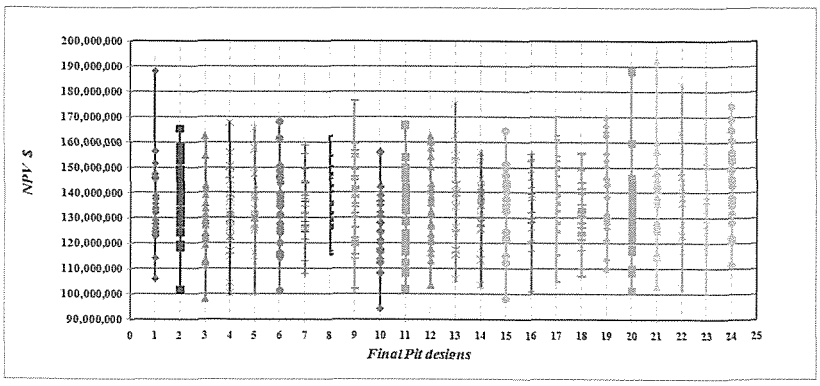

Figure 2. Comparison between NPV outcomes and 24 different final pit designs

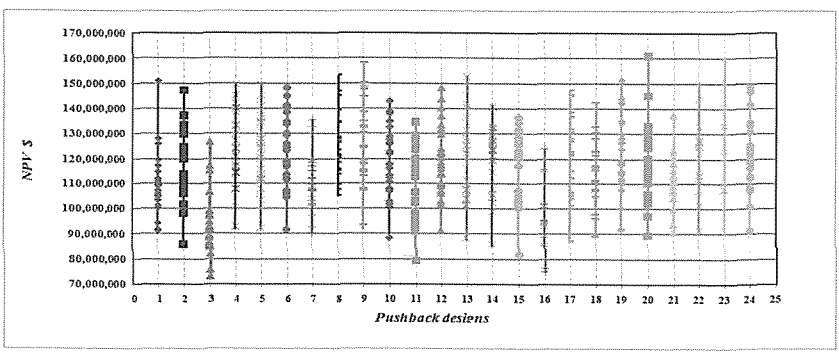

Figure 3. Comparison between NPV outcomes and 24 different pushback designs

6 CONCLUSIONS

Optimization and mine planning regarding to stochastic approach have significant different from conventional method in the point of results. Stochastic approach , have different results depends on methods and the risk factor while conventional doesn't. Therefore, knowledge about the principle of stochastic methods which is used ,and their advantages, disadvantages and limitation is essential.

Risk rate pits method, the main advantage of this approach is to provide quickly a series of pit shells with different level of confidence. As consequence of that fact, before any further design, we know how much risk (about any project performance indicators) is taken on the design .But the main issue, as can be seen in Table 3, this approach sacrifices the NPV, revenue and ore tonnage to get a highest confidence. Therefore, in some cases, this approach cannot really find the high confidence pit shells which have enough reserve to be mined.

Maximum upside/ minimum downside method, it is a powerful approach for dealing with risk and getting a best practical design for all possible grade fluctuation which is in a set of realizations, but suffers from following issues.

1- The method highly depends on N selected realisations for mine designs, thus, there is no guarantee that realisation N+1 (or N+i) does not give the better result.

2- In some cases, even for one criterion, finding a design that can significantly minimise risk of loses and maximises the chance of getting higher value, is not always possible.
3- While realizations can be relatively easily generated, a detailed mine planning of each realization is time consuming (R. Dimitrakopoulos et al, 2007).
4- The traditional optimizers are not able to handle more than one criterion at same time. It means the approach cannot provide the best solution over the mine life (R. Dimitrakopoulos et al, 2007).

REFERENCES

Dimitrakopoulos R. 1998. Condition simulation algorithm for modeling orebody uncertainty in open pit optimisation. *International of surface mining,* Reclamation *and Environment,* 12:173-178.

Deutsh.C.V and Journel. A.G. 1998. GSLIB *Geostatistical Software Library and user's guide.* Oxford University Press, New York, NY, USA.

R. Dimitrakopoulos, L. Martinez, and S. Ramazan 2007.Maximum Upside / Minimum Downside approach to the traditional optimization of open pit mine design. *Journal of Mining Science* Vol. 43, No .

Reza Sayadi, S. M. Heidari, S. Saydam 2010.Study of key factors in geometrical and grade modelling of copper porphyry deposits. *International Journal of Mining and Mineral Engineering* Vol. 2, No.1 pp. 59 - 77.

NPV scheduler Software,2011.Version 4.19, Tutorial, *Datamine company.*

Evaluating the Risk of Critical Infrastructures Using Fuzzy Inference System

Abdolreza Yazdani-Chamzini
Ms of Mining Engineering, Tarbiat Modares University, Tehran, Iran

Ali Alidoosti
Ms of Mechanic Engineering, Maleke Ashtar University of Technology, Tehran, Iran

Zhila Hosseini Nejad
Ms in Reconstruction after Disaster, School of Architecture and Urban Planning, Shahid Beheshti University, Colleague of Maleke Ashtar University of Technology, Tehran, Iran

Mohammad Hossein Basiri
Professor Assistant of Mining Department, Faculty of Science and Engineering, Tarbiat Modares University, Tehran, Iran

ABSTRACT Critical infrastructures are the most important part of a country. Therefore governments always seek the solutions to prevent or at least reduce the vulnerability of this infrastructure to minimize the risk. There is a variety of methods to evaluate and classify risk. Fuzzy set is one of the best methods to categorize and evaluate risks, because this method is able to make into account the uncertainty of risk in modeling. In this article, fuzzy inference system is applied to evaluate and assess the value of risk in critical infrastructures. This research will show the high accuracy and efficiency of this technique to assess the risk of critical infrastructure.

1 INTRODUCTION

Nowadays security is one the most important purposes of countries. Therefore governments approve large amount of budget for necessary critical infrastructures to achieve the goal of country stability and resistant development.

The National Strategy adopted the definition of "critical infrastructure" in P.L. 107-56, providing the following list of specific infrastructure sectors (and its assets) falling under that definition which sectors include (Security & Preparedness, 2010): (i) agriculture and food production, (ii) banking and finance, (iii) chemical production, (iv) critical manufacturing, (v) communications, (vi) emergency services, (vii) energy, (viii) government facilities, (ix) information technology, (x) nuclear energy and facilities, (xi) postal shipping, (xii) public health and healthcare, (xiii) transportation and logistics services, (xiv) water and wastewater treatment, and key resources include: (xv) defense industrial base, (xvi) commercial facilities, (xvii) dams, and (xviii) National monuments and icons in governmental and private sectors.

Depending on the importance of critical infrastructures in political, economical, social and cultural aspects, governments are always seeking for new methods to provide a complete security and risk reduction for these facilities and their operations.
Researchers have proposed several qualitative and quantitative techniques for analyzing risks such as Leontief-based

models (Haimes & Jiang, 2001), Markov chains (Asavathiratham et al, 2001) hierarchical holographic modeling (HHM) (Ezell et al, 2000; Haimes, 2004), Preliminary hazard analysis (PHA) (Fullwood & Hall, 1988), Hazard and operability study (HAZOP) (Sutton, 1992), Failure mode and effects analysis (FMEA) (Yuan, 1985; Pinna et al, 2008), and so on. These methods are often used to understand what would happen based on the likelihood and consequences of a mistake.

In order to understand the behavior of critical infrastructures, it is necessary to accurately model and quantify their interdependencies (Rinaldi et al, 2001). On the other hand, with regard to high efficiency of fuzzy set on modeling uncertainty, we employed fuzzy set in order to model the risk of critical infrastructures.

2 FUZZY RISK

Fuzzy set theory provides a simple way to reason with vague, ambiguous, and imprecise input or knowledge (Kahraman, 2008). Unlike crisp (or ordinary) sets, fuzzy sets have no sharp or precise boundaries (Aydin, 2004). In crisp logic, every statement is true or false; i.e., it has a truth value 1 or 0. In contrast, fuzzy sets have more flexible membership requirements that allow for partial membership in a set. Everything is a matter of degree, and exact reasoning is viewed as a limiting case of approximate reasoning (Kahraman, 2008). The ability of fuzzy set theory to deal effectively with the uncertainties encompassing vagueness and fuzziness, and variables that are defined linguistically or qualitatively (Fleming et al, 2007) caused this method by different researchers be used.

Markowski, Mannan (2009) used Fuzzy logic for piping risk assessment. This paper explores the application of the fuzzy logic for risk assessment of major hazards connected with transportation of flammable substances in long pipelines. As a basis for risk assessment, the framework of the fuzzy Layer of Protection Analysis (fLOPA) was used. fLOPA presents a new approach to risk assessment based on two assumptions: 1. different effects of the layer of protection functions on particular elements of the risks (frequency and severity of consequence), and 2. the application of fuzzy logic system (FLS) composed of three elements: fuzzification, inference process and defuzzification.

Elsayed (2009) developed Fuzzy inference system for the risk assessment of liquefied natural gas carriers during loading/offloading at terminals. Zhao et al (2006) used fuzzy for risk assessment of the network security. Their applied method was combines AHP method and fuzzy logical method.

Davidson et al (2006) proposed fuzzy risk assessment tool for microbial hazards in food systems. Chen (2001) presented a new algorithm to evaluate the rate of aggregative risk in software development using fuzzy set theory under the fuzzy group decision making environment. Zeng et al (2007) developed an application of a fuzzy based decision making methodology to construction project risk assessment. They stated the application of fuzzy reasoning techniques provides an effective tool to handle the uncertainties and subjectivities arising in the construction process.

3 FUZZY INFERENCE SYSTEM

Fuzzy inference is the process of formulating the mapping from a given input to an output using fuzzy logic (see Figure 1). There are various types of inference system. Mamdani-type inference and Sugeno-type systems have most application. Mamdani-type inference expects the output membership functions to be fuzzy sets. After the aggregation process, there is a fuzzy set for each output variable that needs defuzzification. In general, Sugeno-type systems can be used to model any inference system in which the output membership functions are either linear or constant (www.mathworks.com).

Following steps are necessary for successful application of modelling through a general fuzzy system:

3.1 Fuzzify Inputs

The first step is to take the inputs and determine the degree to which they belong to each of the appropriate fuzzy sets via membership functions. The inputs are always a crisp numerical value limited to the universe of discourse of the input variable. Fuzzification of the input and output variables carry out by considering appropriate linguistic subsets such as high, medium, low, heavy, light, hot, warm, big, small.

3.2 Construction of rules base

Construction of rules based on expert knowledge and/or the basis of available literature. The rules relate the combined linguistic subsets of input variables to the convenient linguistic output subset (Ross, 1995). Any fuzzy rule includes statements of "IF . . . THEN. . ." with two parts. The first part that starts with IF and ends before the THEN is referred to as the predicate (premise, antecedent) which combines in a harmonious manner the subsets of input variables. Consequent part comes after "THEN" which includes the convenient fuzzy subset of the output based on the premise part. This implies that there is a set of rules which is valid for a specific portion of the inputs variation domain. The input subsets within the premise part are combined most often with the logical "and" conjunction whereas the rules are combined with logical "or".

3.3 Apply Implication Method

The implication part of a fuzzy system is defined as the shaping of the consequent part based on the premise (antecedent) part and the inputs are fuzzy subsets.

3.4 Aggregate All Outputs

Because decisions are based on the testing of all of the rules in a FIS, the rules must be combined in some manner in order to make a decision. Aggregation is the process by which the fuzzy sets that represent the outputs of each rule are combined into a single fuzzy set. Aggregation only occurs once for each output variable, just prior to the fifth and final step, defuzzification (www.mathworks.com). The input of the aggregation process is the list of truncated output functions returned by the implication process for each rule. The output of the aggregation process is one fuzzy set for each output variable.

3.5 Defuzzify

Defuzzification is one of the most important subjects in fuzzy math. The result appears as a fuzzy subset and therefore, it is necessary to defuzzify the output for obtaining a crisp value that would be required by the administrators or engineers. Perhaps the most popular defuzzification method is the centroid calculation, which returns the center of area under the curve. There are five built-in methods supported (www.mathworks.com): centroid, bisector, middle of maximum (the average of the maximum value of the output set), largest of maximum, and smallest of maximum.

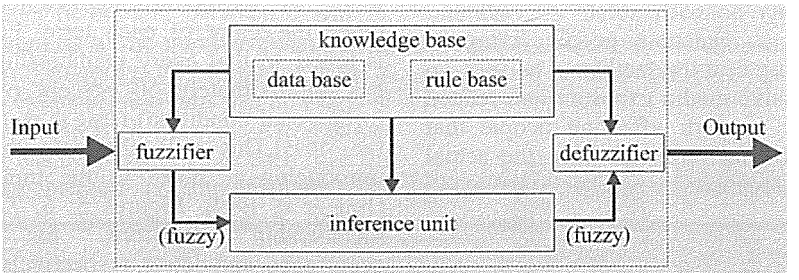

Figure 1. Structure of fuzzy system

4 FUZZY INFERENCE SYSTEM DESIGN

In here, by experts' opinion, structure of fuzzy inference system is made. Expert judgments are normally the primary sources of information in typical engineering risk analysis methods, and can be collected through more or less formalized methods (interviews, surveys, workshops etc.) (Holmgren, 2007). Based on experts' opinion 3 agents as affective factors are selected that is comprised as:

4.1 Likelihood

Reliable estimates of the likelihood of an event for non-random processes should be based on a history of similar events that have occurred under similar conditions.

4.2 Consequences

The severity of the consequences of a security event at a facility is generally expressed in terms of the degree of injury or damage that would result if there were a successful attack. Malevolent acts may involve effects that are more severe than expected with accidental risk. Some examples of relevant consequences can include:

- Injuries to the public or to workers.
- Environmental damage.
- Direct and indirect financial losses to the company and to suppliers and associated businesses.
- Disruption to the national economy, regional, or local operations and economy.
- Loss of reputation or business viability.
- Need to evacuate people living or working near the facility.
- Excessive media exposure and related public concern affecting people that may be far removed from the actual event location.

4.3 Vulnerability

Vulnerability is any weakness that can be exploited by an adversary to gain unauthorized access and subsequent destruction or theft of an asset. Vulnerabilities can result from, but are not limited to, weaknesses in current management practices, physical security, or operational security practices.
the inputs and output divided to 5 different fuzzy linguistic sets as very Low (VL), Low (L), Medium (M), High (H), and Very High (VH). Membership function of likelihood as sample is shown in Figure 2. With regard to Figure 2, fuzzy numbers, in this paper, are Gaussian fuzzy number. It is chosen because the Gaussian kernel function exhibits properties that are mathematically and computationally tractable (Masters, 1993; Masters, 1995). The Gaussian kernel function is also a continuously differentiable function, and has the advantage of being smooth and nonzero at all points (Xie, 2003). Because of its smoothness and concise notation, the Gaussian membership function is a popular method for specifying fuzzy sets (Jang, 2005). Besides, past experiences have indicated that it is a suitable choice in many applications, and has been a reliable performer (Masters, 1993; Masters, 1995). The Gaussian membership function can be represented by:

$$Gaussion(x;c,\sigma) = e^{-\frac{1}{2}(\frac{x-c}{\sigma})^2} \quad (1)$$

Where c and σ are center and width of the membership function, respectively. For each input, c is fixed to "1" for the first linguistic term; "10" for the last linguistic term and for others the center of each term. Parameter σ is tuned so that every membership function has approximately 50 percent overlapping (orthogonal condition) (Jang et al, 1997; Lin & Lee, 1995).This will eliminate the risk of introducing a "hole" in the input domain (Jang et al, 1997). Figures 5, 6, 7 show the membership functions for severity, occurrence, and detect, respectively.

The input of likelihood is the interval between 0 and 100, the inputs of vulnerability and consequences are the interval between 0 and 1. The output is a fuzzy degree of membership in the qualifying linguistic set (always the interval between 0 and 1).

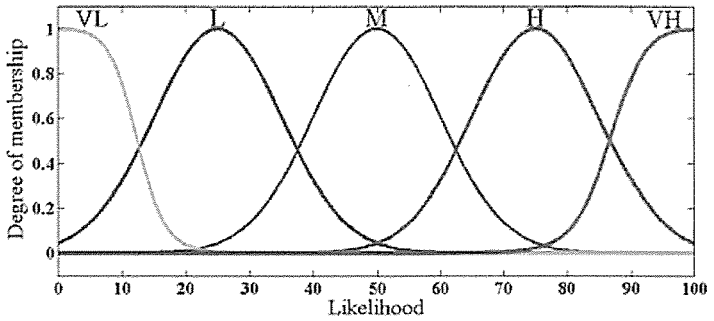

Figure 2. Membership function of likelihood

This example is built on 125 rules, and each of the rules depends on resolving the inputs into a number of different fuzzy linguistic sets: likelihood is M, vulnerability is H, and consequences is H, risk is H, and so on. Before the rules can be evaluated, the inputs must be fuzzified according to each of these linguistic sets. After the inputs are fuzzified, the degree to which each part of the antecedent is satisfied for each rule. If the antecedent of a given rule has more than one part, the fuzzy operator is applied to obtain one number that represents the result of the antecedent for that rule. This number is then applied to the output function. The input to the fuzzy operator is two or more membership values from fuzzified input variables. The output is a single truth value.

Before applying the implication method, you must determine the rule's weight. Every rule has a *weight* (a number between 0 and 1), which is applied to the number given by the antecedent. Generally, this weight is 1 (as it is for this example) and thus has no effect at all on the implication process. After proper weighting has been assigned to each rule, the implication method is implemented. The consequent is reshaped using a function associated with the antecedent (a single number). The input for the implication process is a single number given by the antecedent, and the output is a fuzzy set. Implication is implemented for each rule. Two built-in methods are supported, and they are the same functions that are used by the AND method: *min* (minimum), which truncates the output fuzzy set, and *prod* (product), which scales the output fuzzy set.

As long as the aggregation method is commutative (which it always should be), then the order in which the rules are executed is unimportant.

The input for the defuzzification process is a fuzzy set (the aggregate output fuzzy set) and the output is a single number. As much as fuzziness helps the rule evaluation during the intermediate steps, the final desired output for each variable is generally a single number. Defuzzification procedure is frequently achieved through centroid method as applied in this paper.

$$FD = \frac{\sum \mu \cdot D}{\sum \mu} = \frac{\mu_U . D_U + \mu_{LH} . D_{LH} + \cdots}{\mu_U + \mu_{LH} + \cdots} \quad (2)$$

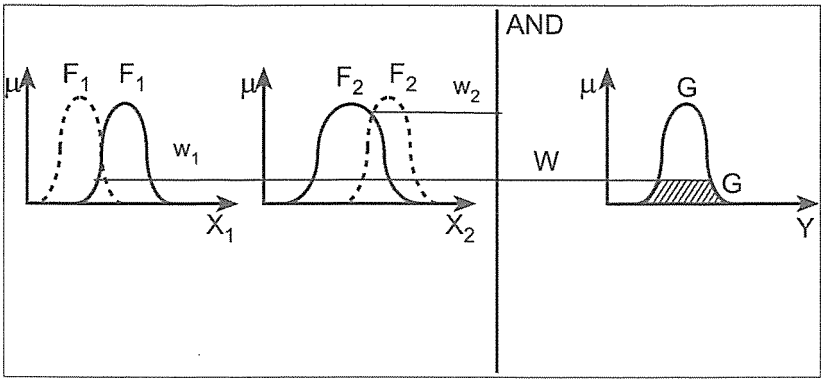

Figure 3. Gaussian membership function

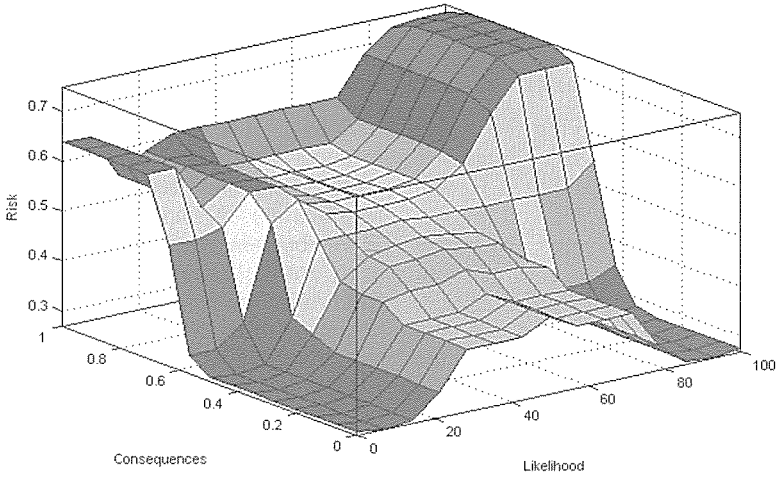

Figure 4. The Effects of likelihood and consequences on risk

Sensitive analysis related to risk with regard to alterations of likelihood and consequences is shown in Figure 4. As in Figure 4 is indicated when likelihood and consequences ascend as result of them risk increase. Then, for validation of presented model, 5 cases are tested. The result is represented in Table 1.

Table 1: model validation

Case	Likelihood	Consequences	Vulnerability	Risk	Linguistic
1	*24*	*0.45*	*0.3*	*0.29*	*Relatively Low*
2	*26*	*0.7*	*0.4*	*0.52*	*Medium*
3	*70*	*0.75*	*0.55*	*0.64*	*Relatively High*
4	*76.5*	*0.55*	*0.58*	*0.7*	*High*
5	*10*	*0.25*	*0.14*	*0.25*	*Low*

4 CONCLUSION

Critical infrastructures play central role of a country so that governments always search solutions for reducing or preventing risks related to this sector. There are a variety of methods for evaluating risk. Fuzzy set is one of the best methods in this field because this method make into account uncertainty on modeling. In this paper, fuzzy set is employed in order to evaluate and classify the risk of critical infrastructures. The results of this research demonstrate the designed fuzzy model has high efficiency for this purpose.

REFERENCES

Asavathiratham, S., Lesieutre, B., & Verghese, G., (2001). "The inuence model". *IEEE Control Systems* 21(6), pp. 52-64.

Aydin, A., (2004). "Fuzzy set approaches to classification of rock masses". *Engineering Geology* 74, pp. 227–245.

Chen, Sh-M., (2001). Fuzzy group decision making for evaluating the rate of aggregative risk in software development, *Fuzzy Sets and Systems* 118, 75-88.

Davidson, V. J., Ryks, J., Fazil, A., (2006). Fuzzy risk assessment tool for microbial hazards in food systems, *Fuzzy Sets and Systems* 157, 1201 – 1210.

Ezell, B., Farr, J., & Wiese, T., (2000). "Infrastructure risk analysis model", *Journal of Infrastructure Systems* 6(3), pp. 114-117.

Elsayed, T., (2009). Fuzzy inference system for the risk assessment of liquefied natural gas carriers during loading/offloading at terminals, *Applied Ocean Research* 31, 179-185.

Fleming, G., Merwe, M. V. D., McFerren, G., (2007). Fuzzy expert systems and GIS for cholera health risk prediction in southern Africa. *Environmental Modelling & Software* 22, pp. 442-448.

Fullwood, R.R., and Hall, R.E. (1988). Probabilistic risk assessment in the nuclear power industry, 1st Ed. *Pergamon Press.*

Haimes, Y., (2004). "Risk Modeling, Assessment and Management", *Wiley-Interscience*, Hoboken, New Jersey.

Haimes, Y., & Jiang, P., (2001). "Leontief-based model of risk in complex interconnected Infrastructures". *Journal of Infrastructure Systems* 7(1), pp. 1-12.

Holmgren, Å. J., (2007). A Framework for Vulnerability Assessment of Electric Power Systems. Critical Infrastructure Reliability and Vulnerability, *Springer-Verlag Berlin Heidelberg*, Chapter 3.

Jang, J.S.R. (2005), Fuzzy Logic Tool Box 2.2.2March, *MathWorks*.

Jang, J.S.R., Sun, C.T. and Mizutani, E. (1997), Neural-Fuzzy and soft Computing, *Prentice-Hall*, Englewood Cliffs, NJ.

Kahraman, C., (2008). "Multi-criteria decision making methods and fuzzy sets", *Springer*, Vol. 16, pp. 1-18.

Lin, C.T. and Lee, C.S.G. (1995), Neural Fuzzy Systems: A Neuro-Fuzzy Synergism to Intelligent Systems, *Prentice-Hall*, Englewood Cliffs, NJ.

Markowski, A. S., Mannan, M. S., (2009). Fuzzy logic for piping risk assessment (pfLOPA), *Journal of Loss Prevention in the Process Industries* 22, 921–927

Masters, T. (1993), Practical Neural Network Recipes in C ++, *Academic Press*, San Diego, CA.

Masters, T. (1995), Advanced Algorithms for Neural Networks: A C ++ Sourcebook, *Wiley*, New York, NY.

Pinna, T., Caporali, R., Tesini, A., (2008). Failure Mode and Effect Analysis for remote handling transfer systems of ITER, *Fusion Engineering and Design* 83, 1710–1714.

Rinaldi, S., Peerenboom, J. & Kelly, T., (2001). Identifying, understanding and analyzing critical infrastructure interdependencies, *IEEE Control Systems* 21(6), pp. 11-25.

Security, H., & Preparedness, E., (2010). "Critical Infrastructure". *Taylor and Francis Group*, Second Edition, Chapter 1.

Ross, J. T. (1995). "Fuzzy logic with engineering applications". *New York: McGraw-Hill Inc,* p. 593.

Sutton, I.S. (1992). Process reliability and risk management, 1st Ed. *Van Nostrand Reinhold.*

www.mathworks.com

Xie, M. (2003), Fundamentals of Robotics: Linking Perception to Action, *World Scientific Publishing Co Ltd*, London.

Yuan, J., (1985). A Strategy to Establish a Reliability Model with Dependent Components through FMEA, *Reliability Engineering* 11, 37-45.

Zeng, J., Nigel, M., Smith, J., (2007). An Application of a fuzzy based decision making methodology to construction project risk assessment, *International Journal of Project Management* 25, 589–600.

Zhao, D-M., WANG, J-H., MA, J. F., (2006). Fuzzy risk assessment of the network security, *Proceedings of the Fifth International Conference on Machine Learning and Cybernetics*, Dalian, 13-16 August 2006, 4400-4405.

Coal supply in next decade derived from EPS supplementary open cast mining facilities

Milan Jakovljevic
Nenad Popovic
Electric Power Industry of Serbia,Head Office for Energy Production, Belgrade, Serbia

ABSTRACT The Republic of Serbia has only limited indigenous energy resources and lignite makes a substational contribution to the country's energy supply. Lignite obtained from mines with surface mining remains one of the main supports for power generation within the long term development plans of EPS (Electric Power Industry of Serbia). Up to the year 2020, according to the accepted Energy Development Strategy it has foreseen important investments to output increasing at the Mining Basins and Economic Association TPPs-OPMs Kolubara and Kostolac. Modernisation and upgrading of the existing open pit mines and opening of the a new and expansion of current deposits are preconditions for increasing of power generation from existing and new thermo capacities planed by EPS to be constracted. The opencast operation use modern mining equipment, including bucket-wheel excavaters, belt conveyors, and spreaders with an average capacity of 4000-6000 cbm/h. This technology allows continuous extraction and thereby ensures a steady flow of the fuel to the power stations.

In Kolubara basin in 2010, have been produced 29.7 and in Kostolac 7.5 million tons of coal what in total is 37.2 million tons of coal.

1. MINING AND ENERGY DEVELOPMENT STRATEGY

In 2010,a total of 37.8 million tons of coal were produced at open-cast coal mines in Serbia operated by EPS (Kolubara and Kostolac basins). This coal was used to generate 69% of all electricity generated by EPS. This, combined with the generation from thermal power plants in Kosovo and Metohija,accounts for 73% of total electricity generation in the teritory of the Republic of Serbia.

Coal produced in the corporate enterprise Mining Basin Kolubara enabled generation of 46.2% of the total electricity generated in EPS thermal power plants,while the coal from TPPs-OCMs Kostolac provided for 14.4% of this generation (for the past ten years-since 1999, Electric Power Industry of Serbia has not operated its facilities in Kosovo and Metohija and detailed data on the operation of these coal mines are not available).

Of the total lignite output in mines operated by EPS, Kolubara basin accounted for 77.2%, and Kostolac basin for 22.8% in 2010.

According to the previously accepted Energy Development Strategy, within the MB Kolubara is planned extending of Field D and Tamnava West Field and opening of mines Field E, C and Radljevo.

According to the mentioned Energy Development Strategy, in the TPPs-OPMs KOSTOLAC is scheduled development and capacity extension at the mine Drmno overtaking entire coal production, after the operation at mines Cirikovac and Klenovnik were finished in 2009. At the moment coal

mining in Mining Basin Kolubara took place at four open-cast mines: Field B, Field D, Veliki Crljeni and Tamnava-West Field. They supplied TPP Kolubara, TPPs Nikola Tesla A and B and TPPs Morava with coal.

In TPPs-OCMs Kostolac, the mine Drmno is in operation and supply TPPs Kostolac A and B with coal.

Coal production was proceded by appertaining overburden removal. Ratio of excaveted overburden and coal is 2.19 m^3/t in Mining Basin Kolubara and 4.00 m^3/t in TPPs-OCMs Kostolac.

Additional development is impossible without area resettlements within the MB Kolubara, which can be obstacle for futher development of the mine advance directions. Land acquisition at the area of Vreoci settlement is condition for expansion of the existing and opening of new open pit mines in the MB Kolubara. If this is going to be in delay, saused circumstances could be far-reaching concerning providing of safe electric energy in Serbia.

DIAGRAM OF EPS OPEN CAST MINES

KOLUBARA BASIN

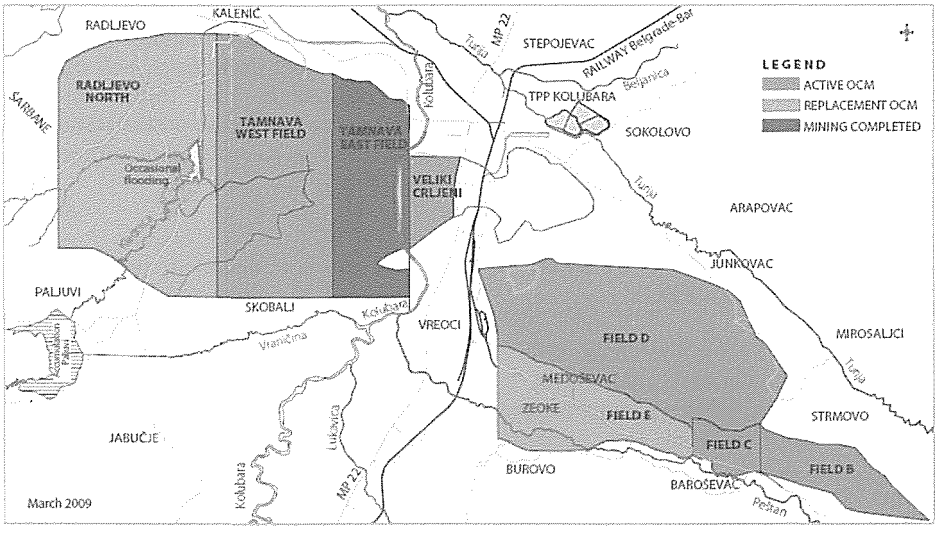

Figure 1. Kolubara Basin open-cast coal mines and supplementary fields

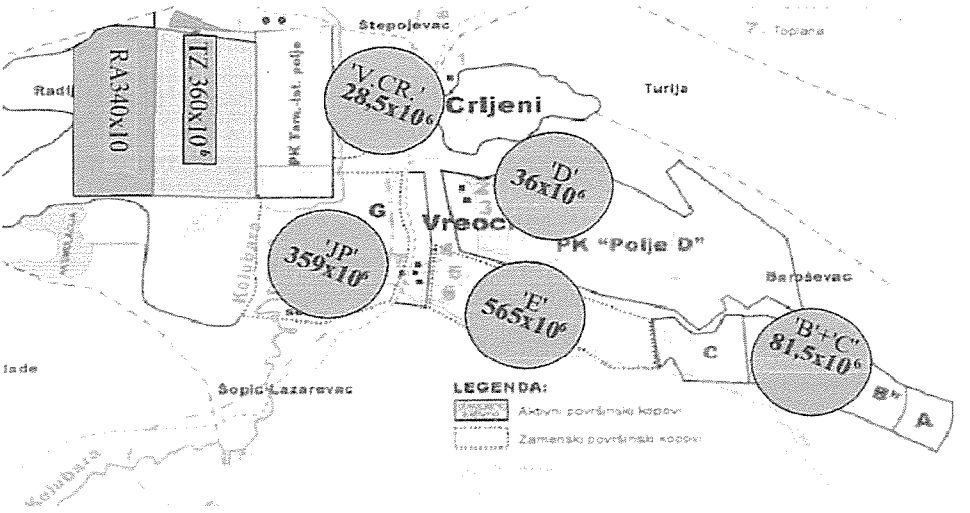

Figure 2: Lignite field reserves in Kolubara Basin

The new open-cast coal mine in MB Kolubara – Veliki Crljani started operation in the last quarter of 2009. High-quality coal at this open-cast mine should ensure the quality required for the operation of thermal power plants as well as the mining of lower-quality parts of the coal deposit, which could not be utilisated without blending coal.

Owing to years-long problems with the relocation of the community of Vreoci and inability to mine-out the coal resources, overburden removal and mining of the coal seam top at Field E,adjacent to Field D, was started. Coal mining started towards the end of 2009. The output from this should overcome the problem arising as a result of delay in the relocation of Vreoci. As regards the land expropriation process, there were problems in all EPS open-cast mines,which resulted in underperformance in overburden removal in comparison with the realistic possibilities.

Overburden removal in 2009 was marked by land expropriation problems,low bearing capacity of the soil and difficulties in the operation of the eastern dump site of field D. In this zone,excavation is conducted with four of the six available excavator-conveyor-stacker (ECS) systems,in order to provide prerequisites for the opening of the future open-cast mine Field E, which will be the largest and depest open-cast mine in EPS.

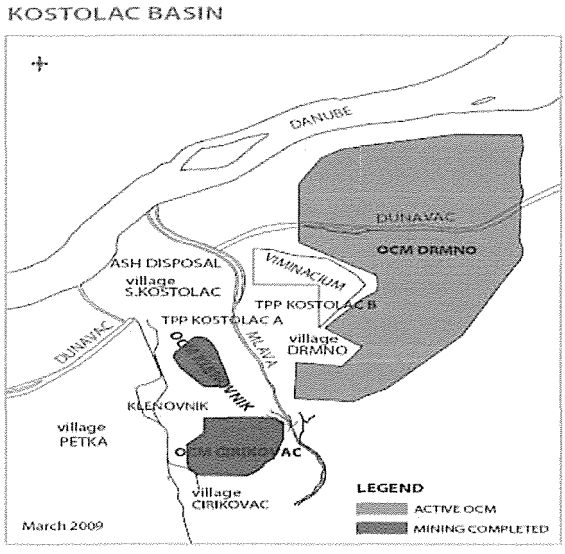

Figure 3.Kostolac coal basin

In the first half of 2009, operation of the Cirikovac open–cast mine was stopped. Most of equipment from this mine was transported to the Drmno mine and placed in service following rehabilitation. The remaining equipment will also be rehabilitated and put to use in the production process at this open-cast mine.

Expert Council by EPS has accepted Long-term Development Strategy for the Kostolac coal basin by preparing mine Drnmo for output of 12 million tons annualy. The first step is in the increasing of the production to 9 million tons of coal annualy and in 2009 started a new overburden system, which provide preconditions for larger coal production.

Figure 4.Coal production in EPS

BUILT CAPACITIES OF OPEN-CAST MINES

million

	t	m³
Kolubara	31.0	65.0
Field B	2.0	4.0
Field D	12.0	33.0
Tamnava – West Field	12.0	22.0
Veliki Crljeni	5.0	6.0

million

	t	m³
Kostolac	8.5	37.0
Drmno	8.5	37.0

Figure 5.Built capacities

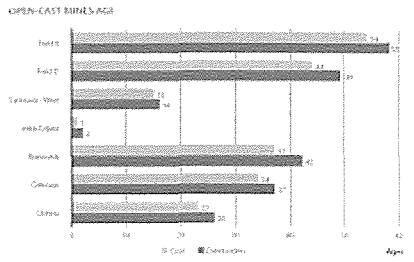

Figure 6.Open-cast mines age

2. POTENTIAL COAL SUPPLIERS AND PREDICTIONS

Strategic and Development Plan of Electric Power Industry of Serbia anticipate the construction of new thermal power plant capacities requiring the provision of necessary coal amounts.In order to maintain fuel supply to existing TPP capacities and to ensure the supply for the new TPP capacities the mining company needs to open up new lignite fields at Radljevo and/or Southfields deposits.

The main issue is to improve resource utilisation and search for possibilities to maximize lignite extraction,to examine different mine development scenarios, consider lignite quality fluctations over lifetime of new mines and finaly investigate different output scenarios and operational costs.

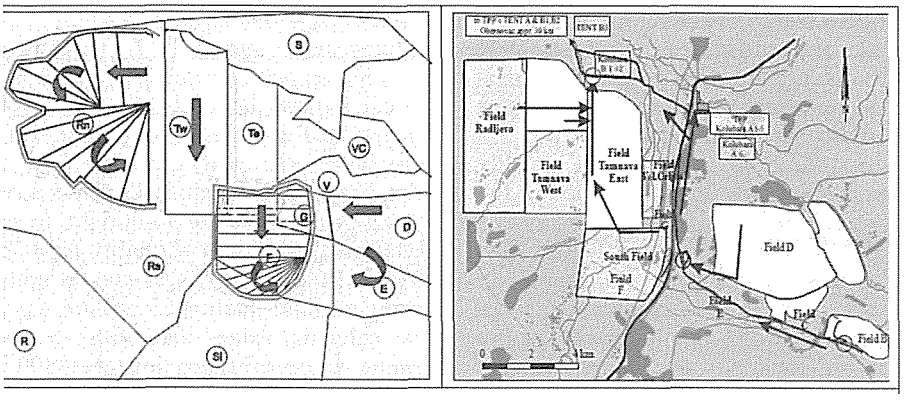

Figure 7. Kolubara lignite basin and supplementary fields position

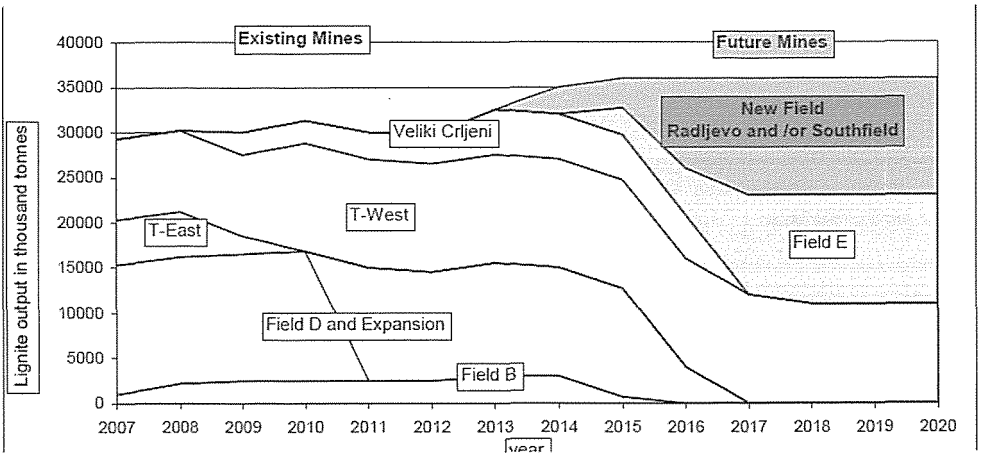

Figure 8. Supplementary mines and forecast of coal outputs in Kolubara Basin

Natural condition of Sauthfield and Radljevo differ significantly.

Southfield is a compact but more than 250 m deep deposit consisting of three mine-able lignite seams. Lignite quality of floor seam is very good and quality generaly deteriorates from North to South.

Results of floor seam coal quality exploration show low heating values in the range from 2700Kj/kg up to 12700 Kj/kg.

The Radljevo lignite deposit ia less than 100 m deep and compared to Southfield shallow and less compact.It is characterises by the appearance of 6 lignite seams. Quality fluctation in Radljevo are larger than in Southfield and determined heating values range from 2500/3000 kJ/kg to 8500 Kj/kg.

Southfield showes higher regular reserves and higher heating value of coal on the average but higher stripping ratio.

Expectation during the first of Southfield development is that coal qulity will be good since coal will be extracted from G Field. For the Radljevo field the forecast indicates reasonable coal qulity over the first 2/3 of mine lifetime. In the mid of exploatation it is even higher than in the Southfield. In the last sectors the average coal quality drops below 6500 MJ/t. The aim is to ensure minimum average lignite quality 55 million tonnes of low calorific value coal with an average heating value of approximately 5300 MJ/t. Practicly this means that Radljevo mine output during the last decade of operation will split into supply of regular coal with sufficient heating value as well as low calorific value coal.

3. COAL MASS CALCULATION AND COAL QUALITY COMPARISON

Considering the depletion of the coal reserves in the mines Field D and Field B towards fuel demand of existing and planned new power capacities, a future annual deficit of approximately 13 million tonnes of coal will be covered by opening up the new Radljevo and/or Southfield mines.

Southfield requires less overburden removal in the initial years. Few years later output capacity constrains will accur during the transfer from sub-field G into sub-field F where the coal seam is strongly dippng downwards into southern directions. The expected maximal output capacity of Southfield can be achived only rather late after 10 years of operation when mine reached the 250 m deep bottom seam and the lower benches are establish.

Radljevo mine can rich a continuous and stable annual output of 13 mt rather fast within three years from opening up coal.Radljevo mine can maintain the 13 million t/a output level over the full lifetime without capacity constrains.

Resettlement and relocation measures are inevitable in both fields. While settlement is concetratedon the eastern deposit area in the southfield, it is spread over the entire field in Radljevo.

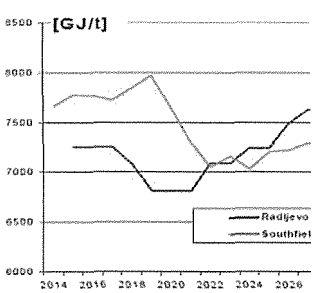

Figure 9. Development of average coal heating value

Summarizing the options between the Radljevo or Southfield, conclusion will be that Radljevo mine shall get clear preferences for development or contrary the Southfield is not recommended to be opened up next as far as the Radljevo field can be development before.

According to the Energy Development Strategy for MB Kolubara is necessery at east part of basin to provide at least 17 million tons of lignite. Following on the coal production at from Field B to Field C it will be fullfil coal production supplementation of shortage Field D, which are on the end.

As supplementary coal production capacity for Field D is predicted the new open-cast coal mine – Field E, which will be operational during the 2011. But as far as the new capacity reach full capacity range,the coal from Field C need to be excaveted. Serious coal production shortage at Field D is caused by as follows reasons:cementary at Vreoci village which need to be get arounded for the purpose of normal production enlargement toward village, therefore the lignite reserves are decreased by 40 millions tons. The second reason: increasing coal demand for the purpose of combustion in the TPP Nikola Tesla which units has been improved since 2001 in order to produce more energy.

This was the reason for coal production increasing at Field D due to the excavation lifetime of Field D is significaly shortouted.

Coal production transition to area of the Field C is geologicaly and technologicaly continuance with active Field B,but disturbed with the eastern part of Field D dumping zone.Increasing coal output for Field B/C is from 2 to 5 million tons annualy.

4. CONCLUSION

Strategic and Development plans of Electric Power Industry of Serbia anticipate the construction of new thermal power plant capacities requiring the provision of necessary coal amounts. Additionaly issues which needed to be analysed and definaded more specifically is the question of fuel supply to these new capacities as preconditions for finding the strategic partners in the construction of new power capacities.

In order to satisfy these preconditions it is necessary to improve resource utilisation and search for possibilities to increase lignite extraction,assesment different mine development scenarios, consider lignite quality fluctuation over lifetime of new mines. In the same time is important to analyse the geological situation and develop a workable digital models allowing detailed forecast of each year coal quality for the supplemented open-cast mines.

Future coal supply to existing and new TPP caoacity can be ensured by opening up of one new mine with maximum capacity of 13 millions tonnes annualy instead of parallel opening up of two new mines with lower capacity.

The Radljevo Field will get priority for development. Compared with Southfield it requires lower total investments and requires lower operating costs.

Planed lignite production expansion activities should be futher direct toward possible long-term coal supply to all TPP and optimum mix of operation of existing and new coal producing capacities in terms of required quantities, qualities at lowest possible cost. It shall consider the development and expansion of each of the existing mines,changes of overburden ratio, changes of lignite quality, investment requirements for existing mines, resettlement and mine closure coast in the Kolubara basin. Future coal supply from RB Kolubara to existing and new TPP will likely be a mix of coal from different mines.

Accepted Long-term Development Strategy for the Kostolac coal basin by preparing mine Drmno for output of 12 million tons annualy. The first step is in the increasing of the production to 9 million tons of coal annualy and in 2009 started a new overburden system, which provided preconditions for larger coal production. In that way it will be satisfied preconditions for construction additional 350 MW of a new thermo capacity. With output of 12 millions tons of lignite and during predicted lifetime, it is necessary to provide about 440 million tons of coal.

Long term Development plan of EPS anticipate the strategy that the lignite further remains main energy resource for power generation in Serbia in next decades.

REFERENCES

(2005) "Preliminary project and Feasibility Study of coal excavation of Field C",
Electric Power Industry of Serbia, Belgrade.
(2006) "Preliminaru project and Feasibility Study of opening and excavation of Field E",
Electric Power Industry of Serbia, Belgrade.
(2006) "Main Mining project of coal production to the nine million tons of lignite at open cast mine Drmno in TPPs Kostolac",
Electric Power Industry of Serbia,Belgrade.
(2008) "Study on the Selection of limitation and opening of opencast mines South Field and Radljevo with comparative overview of coal mining for the selection of priority coal supplier of CHP Kolubara B",
University of Belgrade, Faculty of Mining and Geology, Belgrade; Vattenfall Europe Mining AG, Belgrade,Cottbus.
(2009) Annual Report,
Electric Power Industry of Serbia, Belgrade.

ROCK MECHANICS

Influence of the Rock Microhardness on the Cutting Performance of AWJ

Izzet Karakurt, Gokhan Aydın, Kerim Aydıner
Karadeniz Technical University, Department of Mining Engineering, Trabzon-TURKEY

ABSTRACT: As well known, the granite includes various hard and brittle minerals with different behaviors. Therefore, the resistance of the granite to any mechanical breakdown depends on the several factors including microhardness of each mineral. The present paper aims at presenting the preliminary results of an experimental study investigating the influence of the microhardness of the rock, one of the lesser known variables involved in the cutting process, on the cutting performance of abrasive waterjet (AWJ). In this respect, pre-dimensioned granite samples having different properties were cut by an AWJ for various process (control) parameters. As a result of the study, a consistent relationship between the cut depth, cutting wear zone, kerf angle and the microhardness was found.

1 INTRODUCTION

Material cutting using abrasive waterjet (AWJ) has gained attention, increasingly used and rapidly spread in many industrial applications in all over the world. In this cutting process, a thin, high velocity waterjet accelerates abrasive particles that are directed through an abrasive waterjet nozzle at the material to be cut (Kovacevic, 1993; Aydin et al., 2010a). In the technique; the material is cut by erosion and the rate of material removal, surface finish and tolerances of the cut-edge depend critically on numerous variables including material properties.

Numerous studies of AWJ in different materials have been conducted to determine both the influence of process parameters and the material properties on cutting performance. Among them, Shanmugam and Masood (2009) investigated the kerf characteristics of layered composites cut by AWJ in terms of the kerf angle. They suggested that a combination of process parameters is required to minimize the kerf angle. A new model was developed to predict the cut depth of alumina ceramics in AWJ. Then an experimental study was carried out to verify the data obtained through developed model (Wang, 2009). It was found that the developed model can give adequate predictions of this cutting performance measure with about 1% average error. Vijay (1991) conducted an experimental study to investigate the drilling and slotting of hard rock samples by abrasive, plain and cavitating waterjets for different mining applications. He found that the hard rocks or rock formations require very high pressure and hydraulic power for drilling and slotting. Influence of some properties of granite on waterjet performance was studied by Agus et al. (1993). They concluded that the mineral composition is important for heterogeneous materials whereas in the case of mono-mineral rocks, the porosity plays the most important role. Karakurt et al. (2009), investigated the effect of traverse speed on cutting performance of AWJ in different rocks. They concluded that increasing of traverse speed decreases the cut depths of the rocks. In addition, it was observed that the surface roughness of the rocks tested

deteriorates with an increase in traverse speed. More recently, major process parameters statistically affecting the cut depth of the granite were determined using experimental design method (Aydin et al., 2010b). It was determined that the traverse speed and the abrasive size are the most significant process factors on the cut depth of the granites tested. Effect of the process parameters on the kerf width of the granites was investigated by Karakurt et al. (2010). It was stated that kerf widths were strictly affected by the standoff distance, followed by the traverse speed.

In this study, an experimental study was carried out to find out a relation between the rock microhardness and cutting performance of AWJ in terms of the cut depth, cutting wear zone and kerf angle of the granites.

2 EXPERIMENTAL STUDY

2.1 Material and Method

In the experiments, pre-dimensioned nine granite samples of 3 cm thickness, 20 cm length and 10 cm width were cut by a KMT international waterjet cutter driven a "Model SL-V 50 HP" intensifier pumping system with operating pressure of up to 380 MPa. The motion of the nozzle is controlled by a computer as shown in Fig. 1. The granite samples were similar in mineral compositions, but diverse in microhardness. Abrasive type used in the study is garnet and it chemically consists of 36 % FeO, 33 % SiO_2, 20 % Al_2O_3, 4 % MgO, 3 % TiO_2, 2 % CaO and 2 % MnO_2. Additionally, some properties of the samples are given in Table 1. In the present study, five machining parameters were considered as control factors as given in Table 2. The parameters and levels were selected based on the literature review of some studies that had been documented on AWJ machining on rock and/or rocklike materials. All machining procedures were done using a single-pass cutting. Some of the machining parameters including impact angle (90°), nozzle diameter and length of the nozzle were kept constant during the experiments.

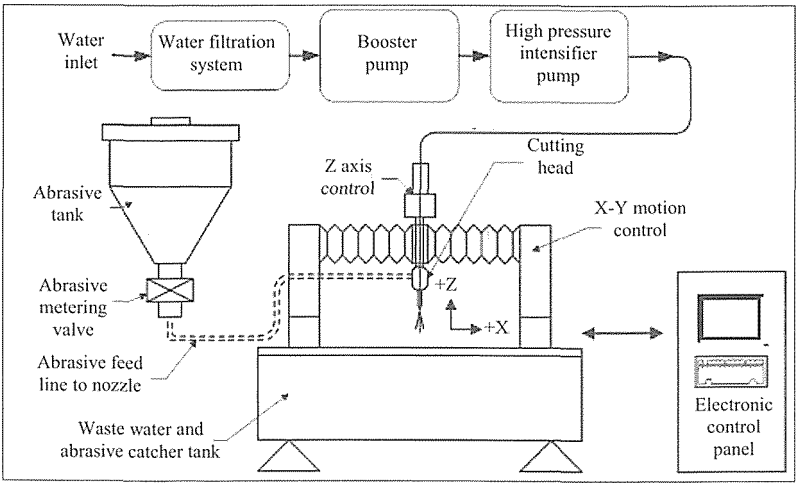

Fig.1. Schematic illustration of the experimental set-up (adapted from Duflou et al., 2001).

Additionally, named as also the kerf wall inclination, the kerf angle for each cut is determined from the equation (1) (Wang and Guo, 2003).

$$\theta = \tan^{-1}\left(\frac{W_{top} - W_{bottom}}{H}\right) \quad (1)$$

where; W_{top} and W_{bottom} are the top and the bottom kerf widths respectively and H, the distance from the top kerf to where the cut depth is measured. In this study, four readings for top and bottom kerf widths on each specimen were respectively taken and the average was taken as the final reading for the calculation of kerf angle through equation (1). Furthermore, for measuring the cut depths and cutting wear zones of the samples, four measurements for each specimen on each cut were carried out and the average was taken as the final reading for the output parameters.

Table 1. Some properties of the samples

Granite	Microhardness (Vickers)	Mineralogical composition (%)				
		Alkali feldspar	Quartz	Plagioclase	Biotite	Others
Rosa Minho	530.3	54	29	10	5	2
Baltic Brown	505.6	57	21	15	3	4
Carmen Red	516	47	37	10	5	1
Giresun Vizon	540	52	14	24	4	6
Aksaray Yaylak	545	26	22	40	7	5
Azul Platino	535	57	25	10	6	2
Balaban Green	570.8	52	23	13	8	4
Multicolor Red	556	51	36	5	6	2
Bergama Grey	544.8	52	23	13	8	4

Table 2. Machining factors and their levels considered for the experimentation

Factors	Units	Levels
Traverse speed	mm/min	100
Abrasive flow rate	g/min	150
Standoff distance	mm	2
Water pressure	MPa	200
Abrasive size	mesh	80

3 RESULTS AND DISCUSSION

In this paper, the influence of the rock microhardness was evaluated on the basis of the cut depth, cutting wear zone and kerf angle of the granites. In this respect, the correlations between rock microhardness and cut depth, cutting wear zone and kerf angle were presented and discussed. The main results of the experiments were given in Table 3.

Based on the results of the study, it was observed that higher cut depths were unexpectedly obtained in the granites having high microhardness. This significant, but reversely occurred phenomenon was also depicted in Fig. 1. It is known the fact that the granite includes various hard and brittle minerals with different material behaviors. Therefore, the resistance of the granite to any mechanical breakdown depends on the several factors including microhardness of each mineral as well. The microhardness is a measure of a crystalline structure's resistance to mechanical breakdown, which reflects the strength of atomic bond within the crystallographic lattice of a specific mineral. It is also the resistance to indentation under a steadily applied stress. And, the granite is gradually cut by micro abrasive grits in microscopic range, responding to material micro-resistibility described by micro-hardness. It means that less micro-hardness distribution can improve machining efficiency. This also means that it is difficult to machine granite including high-hardness mineral and various different minerals. However, the micro fractures, grain boundaries, mineral cleavages and twinning planes also have effects on the microhardness of the granites as well as their behavior to cutting since the microstructure of a rock is known to influence its characteristics. On the other hand; when the grain size of a granitic rock decreases, the microhardness of it increases together with the increasing of weaknesses available inside the individual minerals. In other words,

these weaknesses may control the direction in which failure of rock occurs and they may act in favour of getting deeper cut depths in the granites having high microhardness as is in the present paper. The similar correlation with the cut depth-microhardness was obtained between microhardness and cutting wear zone of the granites tested (Fig.2). But, the power of the correlation ($r^2 = 0.46$) is as not significant as the power of the correlation in Fig.1.

Table 3. The results of the experiments

Granite	Cut depth (mm)	Cutting wear zone (mm)	Kerf angle (degree)
Rosa Minho	20.45	9.92	11.80
Baltic Brown	19.52	9.73	12.87
Carmen Red	19.56	10.13	10.22
Giresun Vizon	23.31	12.25	7.38
Aksaray Yaylak	21.43	11.89	8.21
Azul Platino	23.33	13.30	6.05
Balaban Green	23.75	13.21	6.24
Multicolor Red	24.63	16.17	6.63
Bergama Grey	25.09	16.49	5.24

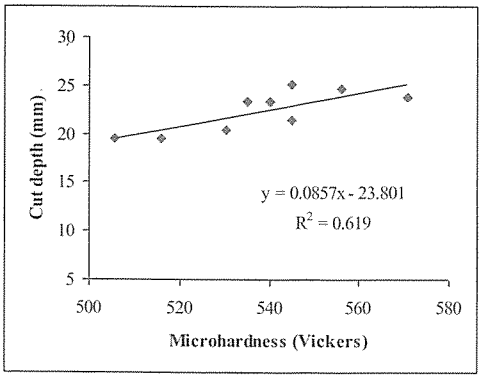

Fig.1. The correlation between microhardness and cut depth of the granites tested

Kerf angle, an important cutting performance measure, is a special and undesirable geometrical feature inherent to abrasive waterjet machining. It reflects the inclination of the kerf wall from the top surface to the bottom of the kerf.

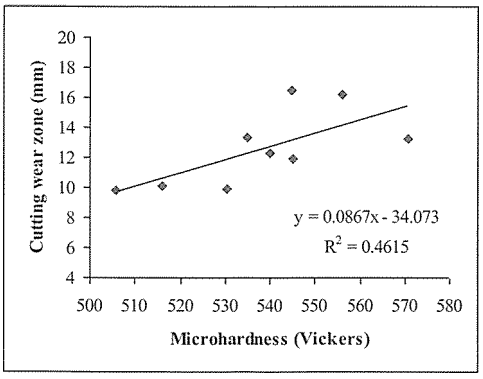

Fig.2. The correlation between microhardness and cutting wear zone of the granites tested

The results of study in terms of the kerf angle showed that small kerf angle was occurred in the granites having high microhardness (Table 1-3). The correlation between microhardness and kerf angle of the granites tested is also an evident of this phenomenon as shown in Fig.3.

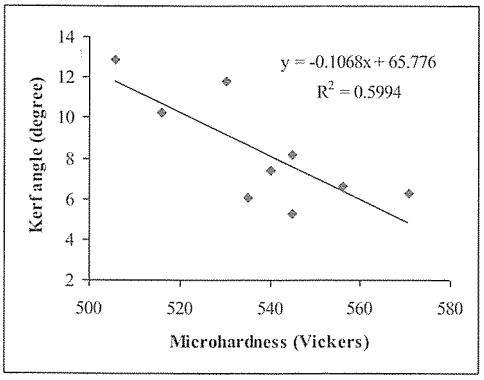

Fig.3. The correlation between the microhardness and kerf angle of the granites tested.

Obtaining the small kerf angles in the granites having high microhardness may be attributed to the amount of minerals and their grain boundaries located through cutting line and/or per unit area. That is; in fine-grained granites, which have high microhardness there are much more minerals or grains and grain boundaries through cutting line and/or per unit area and the abrasive waterjet has to penetrate more minerals/grains and grain boundaries. This would lead to less differences between kerf widths in both up and bottom. Thus, small kerf angles may be obtained in the granites having high microhardness values as found in the current study.

4 CONCLUSIONS

The main conclusions from this experimental study can be summarized as below:

i. Higher cut depths were obtained in the granites which have high microhardness. Similar trend was observed for the cutting wear zone of the granites.
ii. Bigger kerf angles were occurred in the granites having low microhardness values.
iii. The resistance of the granite to any mechanical breakdown depends on the several factors including microhardness of each mineral. Therefore, the microhardness values of granites should be taken into consideration in machining and/or processing of these kinds of rocks.

ACKNOWLEGDEMENTS

The authors would like to express their sincere thanks and appreciation for the financial support to TÜBİTAK (The Scientific and Technological Research Council of Turkey) (Project No 108M370).

REFERENCES

Agus, M., Bortolussi, A., Ciccu, R., Kim, W.M., Manca, P.P., 1993. The influence of rock properties on waterjet performance. In proceedings of 7th. American Water jet Conference, pp. 427-442, Seattle, Washington, U.S.A.

Aydın, G., Karakurt, İ., Aydıner, K., 2010a. Assessment of the surface quality of the granite cut by abrasive waterjet. Technology, Karabük University, 13(1), 41-49.

Aydın, G., Karakurt, İ., Aydıner, K., 2010b. Determination of major process parameters affecting the cut depths of granite in abrasive waterjet cutting, The 20th. International Conference on Water Jetting, pp. 477-483., Graz, Austria.

Duflou, J.R., Kruth, J.P., Bohez, E.L., 2001. Contour cutting of pre-formed parts with abrasive waterjet using 3-axis nozzle control, Journal of Materials Processing Technology 115(1), 38-43.

Karakurt, İ., Aydın, G., Aydıner, K., 2009. Investigation of traverse speed effect on cutting performance in abrasive waterjet cutting system. The 21st International Mining Congress and Exhibition of Turkey, pp. 347-354., Antalya-Turkey.

Karakurt, İ., Aydın, G., Aydıner, K., 2010. Effect of process parameters on the kerf widths in abrasive waterjet cutting. The 10th International Multidisciplinary Scientific Geo-Conference&EXPO (SGEM 2010), Vol. 1, pp. 415-421., Varna, Bulgaria.

Kovacevic, R., 1993. Surface texture in abrasive waterjet cutting, Journal of Manufacturing Systems 12(1), 32-46.

Shanmugam, K.D., Masood, H.S., 2009. An investigation on kerf characteristics in abrasive waterjet cutting of layered composites, Journal of Materials Processing Technology 209, 3887–3893.

Vijay, MM., 1991. Comparison of the performance of high-speed abrasive-entrained, cavitating and plain waterjets for selective Mining applications. In proceedings of the 6th American Waterjet Conference, pp. 195-212., Louis, Missouri, U.S.A.

Wang, J., Guo, D.M., 2003. The cutting performance in multipass abrasive waterjet machining of industrial ceramics. Journal of Materials Processing Technology. 133, 371–377.

Wang, J., 2009. A new model for predicting the depth of cut in abrasive waterjet contouring of alumina ceramics. Journal of Materials Processing Technology 209(5), 2314-2320.

A Study on the Use of Taguchi Approach in AWJ Machining of the Granite

Gokhan Aydın, Izzet Karakurt, Kerim Aydıner

Karadeniz Technical University, Department of Mining Engineering, Trabzon-TURKEY

ABSTRACT: Among the experimental designs, Taguchi approach facilitates the studies of interaction of a large number of variables spanned by factors and their settings with a small number of experimental runs leading to considerable economy in time and cost for the process. The intent and objective of this study were to apply of Taguchi approach for conducting the experiments and to determine the significant parameters in machining of granites by an abrasive waterjet. Five factors, one at two levels and the other at four levels were selected and a standard orthogonal array layout of $L_{16}(4^4*2^1)$ performed. The experimental results were analyzed in terms of the cut depths to extract independently the main effects of the factors; the analysis of variance technique was then applied to determine which factors were statistically significant.

1 INTRODUCTION

Abrasive waterjet (AWJ) machining process is one of the non-traditional machining processes that have been used extensively in various industry related applications. The basic principles of AWJ machining were reviewed in details by Summers (1984). This technology is less sensitive to material properties as it does not cause chatter, has no thermal effects, impose minimal stresses on the workpiece, and has high machining versatility and high flexibility in particular for machining and/or processing of dimension stones (Karakurt and Aydıner, 2007; Azmir and Ahsan, 2008).

The use of granite as building material is dramatically increasing in all over the world. This is mainly due to the excellent properties of the granites, such as resistance to environmental influences, its hardness and aesthetic properties (Yılmaz et al., 2009). Nevertheless, the actual stone diffusion such as marble and granite may be further increased partially due to the intrinsic difficulty of machining these kinds of materials. In fact the inclusion of seaweed and fossils in a matrix of calcite crystals has pointed out the limits of the traditional diamond removal manufacturing processes. Further requirements are the reduction of discards with a subsequent decreased impact on environment, the improvement of worker conditions and the safety (Carrino et al., 2001). Due to the mentioned reasons, there is an increasing demand in the sector for the machining and/or processing of granite in order to improve the productivity and reduce costs. Among the innovative processes, abrasive waterjet can meet the required standards for machining/processing and/or manufacturing of rocks; more specifically dimension stone (e.g. granite).

AWJ cutting process parameters can be categorized as follows: hydraulic, abrasive, mixing and cutting parameters. Figure 1 shows the various input parameters influencing the output parameters in AWJ cutting. On the other hand, the performance of AWJ cutting is often evaluated in terms of cut depth, kerf structure, surface topography and material removal rate.

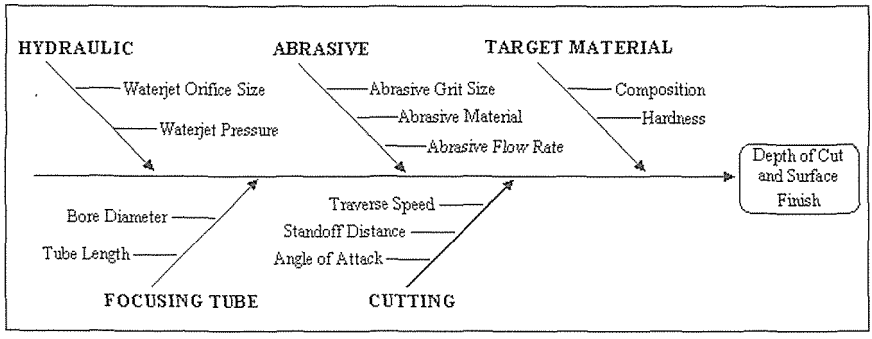

Fig.1. Process parameters influencing the AWJ cutting process (Jegaraj and Babu, 2007)

In this study, machining of granite was tested using the design of experiment (DOE) method. DOE was based on the Taguchi's standard orthogonal arrays. The results were evaluated in terms of the obtained cut depths and analysis of variance (ANOVA) was applied to determine which factors were statistically significant on the machining process.

2 EXPERIMENTAL STUDY

2.1. Material and Method

In the experiments, a pre-dimensioned granite sample of 30 mm thickness, 200 mm length and 100 mm width was cut by an abrasive waterjet which is schematically illustrated in Fig.2, for evaluating the machinability in terms of the cut depth. The main properties of the sample are given in Table 1. Abrasive type used in the study is garnet and it consists of chemically 36 % FeO, 33 % SiO_2, 20 % Al_2O_3, 4 % MgO, 3 % TiO_2, 2 % CaO and 2 % MnO_2.

Design of experiments (DOE) is the process of planning the experiments considering the process parameters at different levels. Experimental design using Taguchi's method provides a simple, efficient and systematic approach for an optimal design of experiments to assess the performance, quality and cost (Aydin et al., 2010). Statistically designed experiments are conducted more efficiently as they consider multiple factors simultaneously and they can detect important interactions with minimum number of experiments unlike traditional experimentation which considers only one factor at a time while keeping the other parameters constant.

Table 1. Main properties of the sample used for the experimentation

Features		Rosa Minho
Physical and mechanical	Grain size (mm)	13.16
	Water absorption (%)	0.30
	Specific bulk density (KN/m^3)	27.2
	Uniaxial compressive strength (MPa)	110
	Flexural strength (MPa)	15.3
Mineralogical composition (%)	Alkali feldspar	54
	Quartz	29
	Plagioclase	10
	Biotite	5
	Other	2

In this work, four factors varied at four levels and one factor varied at two levels were considered. Based on the Taguchi's standard orthogonal arrays, the process parameters and their levels used for this study are shown in Table 2. An orthogonal array of $L_{16}(4^4*2^1)$ was found to be appropriate. A total of 16 runs were tested in this experimental investigation.

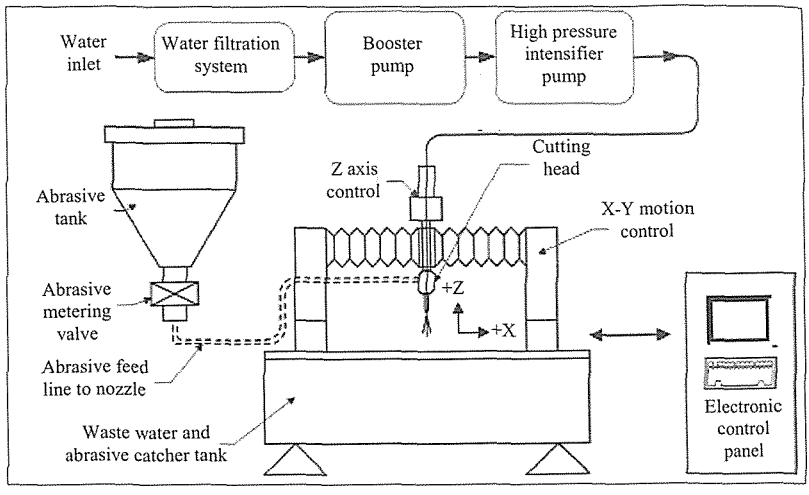

Fig.2. Schematic illustration of the experimental set-up (adapted from Duflou et al., 2001).

In the Taguchi method, the signal to noise (S/N) ratio is expressed as a log transformation of the mean squared deviation as the measure for analysis of experimental results (Azmir et al., 2009). It is named as loss function and the S/N ratio shows the deviations between the experimental value and the desired value. Usually, there are three S/N ratios available, depending on the type of characteristics. One is the lower-the better, other is the higher-the better, and the last is the nominal-the better. In abrasive waterjet cutting, the higher cut depth is an indication of better performance. Therefore, the higher-the better was selected for cut depth of the granite. The S/N ratios for each type of characteristics can be calculated as follow;

The higher-the better:

$$\text{S/N ratio} = -10\log\left(\frac{1}{n}\sum_{i=1}^{n}\frac{1}{y_i^2}\right)$$

The nominal-the better:

$$\text{S/N ratio} = 10\log\left(\frac{\bar{y}}{s_y^2}\right)$$

The lower-the better:

$$\text{S/N ratio} = -10\log\left(\frac{1}{n}\sum_{i=1}^{n}y_i^2\right)$$

where $\bar{y}$ is the average of the observed data, s_y^2 is the variance of y, n is the number of observation, and y is the observed data. Regardless of the category of the performance characteristics, the greater S/N ratio means the better performance characteristics. Therefore, the optimal level of the process parameters is the level with the highest S/N ratio (Hasçalık and Çaydaş, 2008).

3 RESULTS AND DISCUSSION

The experimental layout and results for cut depth and corresponding S/N ratios by the higher-the better are given in Table 3. The optimum condition represents the combination of machining parameter levels that is expected to produce the best performance.

Table 2. Factors and their levels considered for the experiments

Symbol	Machining Parameters	Units	Level 1	Level 2	Level 3	Level 4
T	Traverse speed	mm/min	100	150	200	250
M	Abrasive flow rate	gr/min	150	200	250	300
D	Standoff distance	mm	2	4	6	8
P	Water pressure	MPa	200	250	300	350
S	Abrasive size	mesh	80	120		

The average S/N ratio for each factor level shows the possible effects of the various factors on the quality characteristics of cut depth of the granite. In Taguchi analysis, the greater S/N ratio means the better performance characteristics. Therefore, based on the average S/N ratio for each factor level shown in Fig.3, the optimal machining performance for the cut depth was achieved at the first level for the traverse speed (100 mm/min), the third level for the abrasive flow rate and water pressure and coarse-grained abrasive size. Although the best performance for the cut depth was obtained at the third level of the abrasive flow rate, it can be concluded that this control factor did not have a discernible effect on the cut depth. Similarly, the control factor standoff distance did not affect the cut depth of the granite tested as observed from the main effects plot depicted in Fig.3. On the other hand; as a result, the optimum parametric combination for the cut depth of the granite is T1, M3, P3 and coarse-grained abrasive. The standoff distance was excluded, since it does not have discernible effect on the cut depth.

In the analysis of variance (ANOVA), *F* ratio was used to determine the significant process factors on the cut depth of the granite sample. An F ratio is calculated from the experimental results and then compared to the critical value. If the F ratio calculated is larger than the F critical value, it is an indication that the statistical test is significant at the confidence level selected.

Table 3. Experimental layout and results for $L_{16}(4^4 * 2^1)$ orthogonal array including S/N ratios

Experiment number	Factors					Response (results)	S/N ratios
	T	M	D	P			
1	1	1	1	1	1	24.77	27.88
2	1	2	2	2	1	29.66	29.44
3	1	3	3	3	2	26.14	28.35
4	1	4	4	4	2	25.53	28.14
5	2	1	2	3	2	18.62	25.39
6	2	2	1	4	2	20.16	26.09
7	2	3	4	1	1	25.08	27.98
8	2	4	3	2	1	29.65	29.44
9	3	1	3	4	1	11.31	21.07
10	3	2	4	3	1	21.89	26.80
11	3	3	1	2	2	15.11	23.58
12	3	4	2	1	2	15.67	23.90
13	4	1	4	2	2	12.18	21.71
14	4	2	3	1	2	13.04	22.30
15	4	3	2	4	1	18.71	25.44
16	4	4	1	3	1	19.67	25.87

If not, it indicates that the statistical test is not significant at the confidence level. In addition, larger F ratio value indicates that there is a big considerable on the performance characteristic due to the variation of the process parameters (Azmir and Ahsan, 2008; Azmir et al., 2007).

In this work, analysis of variance was carried out for the confidence level of 95 %. Table 4 shows the result of ANOVA for machining outputs, respectively. It was found that the factors traverse speed (T) and abrasive size (S) was the most significant factor influencing the assessment of the cut depth of the Rosa Minho. It was also found that the control factors M (abrasive flow rate), D (standoff distance) and P (water pressure) failed the test of significance confidence level and were considered to be insignificant for the cut depth of the granite.

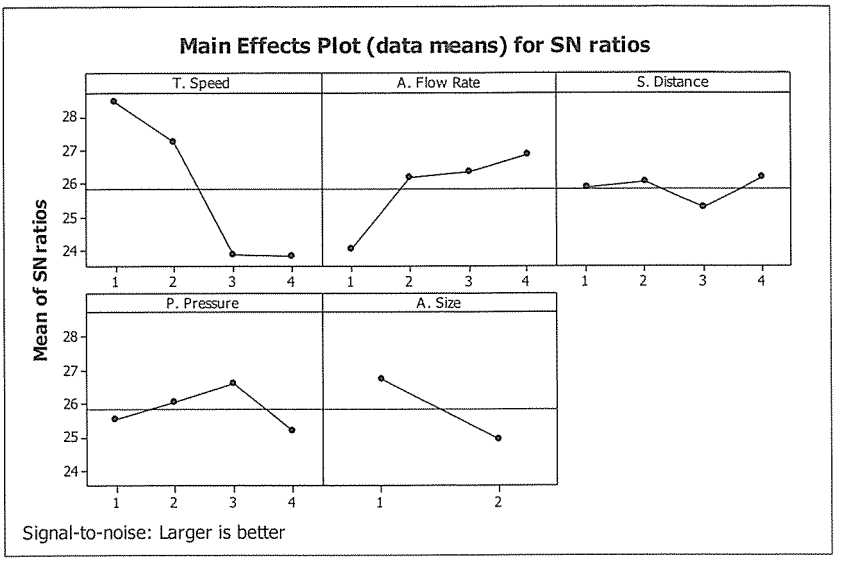

Fig.3. Main effects plot (data means) for S/N ratios for the granite tested (produced through MINITAB statistical software)

The last column of the above table indicates the percentage of each factor contribution (%) on the total variation, thus exhibiting the degree of influence on the result (Şahin, 2009). It is important to observe the contribution-values in the table. From the analysis in Table 4, the factor T (61.71 %) showed a high significant effect on the cut depth. It was followed by abrasive size (12.01 %).

Table 4. Results of analysis of variance (ANOVA) for the cut depth of the granite

Granite	Source	Degree of freedom	Sum of squares	Mean square	F ratio	Cont. rate (%)
Rosa Minho	T	3	67.10	22.36	13,10	61.71
	M	3	18.73	6.24	3.66	17.23
	D	3	1.79	0.59	0.35	1.65
	P	3	4.64	1.54	0.91	4.27
	S	1	13.06	13.06	7.65	12.01
	Error	2	3.41	1.70		3.14
	Total	15	108.73			100

4 CONCLUSIONS

In this study, the machinability of a granite by an abrasive waterjet was tested on the basis of Taguchi's experimental design philosophy. Depending on the experimental results, following conclusions were drawn from the study.

i. Based on the S/N ratios, it can be concluded that the traverse speed and abrasive size, more specifically the first level of traverse speed and coarse-grained abrasive, were two of important control factors on the cut depth of the granite.
ii. As a result of the ANOVA, the traverse speed and abrasive size were statistically found to be the most significant control factors on the results.
iii. The optimal machining parameters for higher cut depth were found as T1, M3, P3 and coarse-abrasive size. The standoff distance was excluded since it has not discernible effect on the cut depth of the granite.

ACKNOWLEGDEMENTS

The authors would like to express their sincere thanks and appreciation for the financial support to TÜBİTAK (The Scientific and Technological Research Council of Turkey) (Project No 108M370).

REFERENCES

Aydın, G., Karakurt, İ., Aydıner, K., 2010, Determination of Major Process Parameters Affecting the Cut Depths of Granite in Abrasive Waterjet Cutting, The 20th. International Conference on Water Jetting, Graz, Austria, pp. 477-483.

Azmir, A.M., Ahsan, K.A., Rahmah, A., 2009. Effect of abrasive waterjet machining Parameters on aramid fibre reinforced plastics composite. Int. Journal of Mater. Forming 2, 37-44.

Azmir, A.M., Ahsan, K.A., 2008. Investigation on glass/epoxy composite surfaces machined by abrasive water jet machining. Journal of Materials Processing Technology 198, 122–128.

Azmir, M.A., Ahsan, A.K., Rahmah, A., 2007. Investigation on abrasive waterjet machining of Kevlar reinforced phenolic composite using Taguchi approach. The International Conference on Mechanical Engineering. pp. 1-6., Dhaka-Bangladesh.

Carrino, L., Polini, W., Turchetta, S., Monno, M., 2001. AWJ to machine free form profiles in natural stone. The 11th. American Waterjet Conference, pp. 309-327., Minneapolis-Minnesota, U.S.A.

Duflou, J.R., Kruth, J.P., Bohez, E.L., 2001. Contour cutting of pre-formed parts with abrasive waterjet using 3-axis nozzle control, Journal of Materials Processing Technology 115(1), 38-43.

Hasçalık, A., Çaydaş, U., 2008. Optimization of turning parameters for surface roughness and tool life based on the Taguchi method, Int. Journal of Manufacturing Technology 38, 896-903.

Jegaraj J.J.R., Babu N.R., 2007. A soft computing approach for controlling the quality of cut with abrasive waterjet cutting system experiencing orifice and focusing tube wear. Journal of Materials Processing Technology 185, 217-227.

Karakurt, İ., Aydıner, K., 2007. Rock cutting performances of abrasive waterjet cutting systems, The 20th International Mining Congress and Exhibition of Turkey, pp. 127–134., Ankara-Turkey.

Summers, A.D., 1984. Waterjetting Technology, published by E&FN Spon, an imprint of Chapman&Hall, London SE1 8HN.

Şahin Y., 2009. Comparison of tool life between ceramic and cubic boron nitride (CBN) cutting tools when machining hardened steels. Journal of Materials Processing Technology 209, 3478–3489.

Yılmaz, G.N., Karaca, Z., Goktan, R.M., Akal, C., 2009. Relative brittleness characterization of some selected granitic building stones: Influence of mineral grain size. Construction and Building Materials, 23, 370-375.

Partition of Plastic/Elastic Energy in Mine Blasts

G.G.U. Aldaş
Ankara Üniversitesi Mühendislik Fakültesi, Jeofizik Mühendisliği, Ankara

B. Ecevitoğlu
Ankara Üniversitesi Mühendislik Fakültesi, Jeofizik Mühendisliği, Ankara

B. Kaypak
Ankara Üniversitesi Mühendislik Fakültesi, Jeofizik Mühendisliği, Ankara

A. Can
MTA, Deniz Araştırmaları Koordinatörlüğü, Ankara

B. Toprak
JEOIT, Ankara Üniversitesi Teknopark, Ankara

E. Babayiğit
TKİ Genel Müdürlüğü, Ankara

İ. Erguder
TKİ Genel Müdürlüğü, Ankara

M. Kaçan
TKİ, YLİ, Milas

ABSTRACT The amount of energy spent in mine blasts to just demolish the rocks is not clearly known. In this work, we propose a technique to obtain the plastic to elastic energy ratio, directly available from the seismic field data. We developed a novel approach to define the plasticity and elasticity of the rocks. In other words, we can determine the plastic energy used for fragmentation of the rock and elastic energy spent as vibration, air blast, etc. We extracted the input wavelet from the real data. We convolved (linear-process) this wavelet with the time series containing time-delayed spikes corresponding to each blast in the group, to obtain a synthetic time-series representing the linear behavior, hence the elasticity. The plasticity, on the other hand, is represented by the actual field data. The energy may simply be defined by the sum of the squares of the amplitudes in a time series. Therefore, the ratio of the energies related to the plasticity and elasticity provides the partition of the energy in a mine blast. The ratio so obtained is deduced from the seismic signals. Therefore, this ratio is a measure of the elasticity. The plasticity, on the other hand, is considered as the complementary of the elasticity. A field example of the plastic / elastic ratio (P/E ratio) values is given and the results are discussed.

1 INTRODUCTION

Rock blasting is considered to be the most economical method for rock excavation either on surface or underground. Explosives are the primary source of energy for rock breaking in the mining, quarrying and construction industries. The work into which the energy is converted transforms rock into a distribution of fragments and displaces them so that they can be conveniently loaded and hauled for further comminition and processing. Although the energetic qualification of explosives is not particularly high (any fuel/oxygen mixture used in the power industry delivers more energy per unit mass than do explosives), they are compact

sources, which are able to deliver their energy in an autonomous form at a very fast rate. This results in reaction products at high pressure that can perform mechanical work in deforming and breaking the material in their vicinity. This is what makes explosives useful and, in many cases, irreplaceable for rock excavation. This fast energy delivery, in the form of a large amount of reaction products at high pressure and high temperature, is inseparable of a number of transformations other than the desired fragmentation and throw, such as the seismic wave into the rock. In other words, although the primary objective of rock blasting is fragmentation, the explosive energy is not fully utilized for this purpose. Therefore, how much energy was spent during a blast for rock fragmentation is one of the challenges that interest researchers nowadays (Spathis 1999, Sanchidrian and Lopez 2003).

In this study, we propose a different technique to obtain the plastic-to-elastic energy ratio, directly available from the seismic field data. It is known that, in delayed-blast techniques widely used in mining, subsequent blasts in a group interact among themselves. In such case, the seismic signal of a group blast will differ from the some of the signals of the participating blasts when they were exploded individually. The reason of this difference is the failure of the superposition principle of the linear behavior. In order to overcome the problem of differences between signals of individual blast-holes, we extracted the input wavelet from the real data, instead of using one-signature hole's signal. We convolved (linear-process) this wavelet with the time series containing time-delayed spikes corresponding to each blast in the group, to obtain a synthetic time-series representing the linear behavior, hence the elasticity. The plasticity, on the other hand, is represented by the actual field data. The energy may simply be defined by the sum of the squares of the amplitudes in a time series. Therefore, the ratio of the energies related to the plasticity and elasticity, provides the partition of the energy in a mine blast. The ratio so obtained is deduced from the seismic signals. Therefore, this ratio is a measure of the elasticity. The plasticity, on the other hand, is considered as the complementary of the elasticity.

2 FORMULATION OF NON-LINEAR BEHAVIOR OF BLASTING PROCESS

In order to determine the plastic to elastic energy ratios of blasting process, one should first define the linear and non-linear behavior of blasting. Like many researchers, Aldas and Ecevitoğlu (2008) dealed with minimization of blast-induced ground vibrations. The crucial point of this methodology is the use of "Pilot-Blast Signal", which embraces the seismic properties of all complex geology between the blast and target locations, to model the "Group-Blast Signal". The aim was to minimize the "Group-Blast Signal" by using appropriate delay elements. The main assumption of this methodology was "Linear-Behavior" of blasting process. Every blast in the "Group-Blast" is assumed to be the same as "Pilot-Blast". Therefore, "Superposition Principle" was valid (Bullen 1963, Oppenheim and Schafer 1975, Karu 2002).

This principle is applicable when the vibrations are measured at a certain distance (far-field) from blast-location. However, it loses its validity at the blasting point and within near-field. Blasting produces large strains in the surrounding medium, which, in turn, implies a non-linear response of the material. It is, therefore, questionable to use a linear superposition scheme at the near-field researches like determination of plastic to elastic energy ratio of blasting process.

The classical approach for non-linearity determination in seismic and seismology is using spectral ratio of seismic signals belonging to same source but different station and depth levels. This ratio removes both the source-dependent effects and common-path effects of signals. The remaining from the spectral ratio is the picture and physical properties of the field between related stations (Shearer 1999).

In this work, mathematical formulation of above mentioned classical approach is interpreted by a different point of view, at first. Knowing that both Pilot-Blast Signal and Group-Blast Signals follow the same route from blast-location and record station (target), spectral ratio of Group and Pilot-Blast Signal was taken at first. This ratio was then transformed back to the time domain. Therefore, all the effects related to the geologic-path, time-delays and convolution effects, resulting in seismic signal stretch were removed. The remaining from this spectral ratio was Non-Linear Behavior of Group Blast. The signal, named as Non-Linear Behavior Response Signal *h(t)*, is the equivalent of "Source-Time Function" in seismology. However, it is a fact that, in delayed-blast techniques widely used in mining, subsequent blasts in a group interact among themselves. In such case, the seismic signal of a group blast will differ from the some of the signals of the participating blasts when they were exploded individually. The reason of this difference is the failure of the superposition principle of the linear behavior. Therefore, we appreciate that our pilot-signal cannot represent all individual blast-hole signals in a group. For this reason, we extracted the input wavelet (instead of using pilot-blast signal) from the real data. The following part gives this mathematical formulations and relating explanations.

Mathematical Formulation

Symbols used in Equations (1) to (14) are given below:

$*$	: Convolution operator
$\otimes$	: Correlation operator
e	: Exponential operator
ln	: Natural logarithm operator
$\sum$	: Summation operator
$\mathcal{F}^{-1}$	: Forward Fourier transform
$\mathcal{F}^{+1}$	: Inverse Fourier transform
$\mathcal{H}$	: Hilbert transform
i	: Imaginary ($\sqrt{-1}$)
t	: Time
ω	: Angular frequency
$g(t)$	: Group signal in time domain
$G(\omega)$	: Group signal in frequency domain
$f(t)$	: Input signal in time domain
$F(\omega)$	: Input signal in frequency domain
$h(t)$	: Deconvolved group signal in time domain
$H(\omega)$	: Deconvolved group signal in frequency domain
$a(t)$	: Autocorrelation of group signal in time domain
$A(\omega)$	: Autocorrelation of group signal in frequency domain
$\lvert A(\omega)\rvert$	: Amplitude spectrum of the autocorrelation of group signal
$\lvert F(\omega)\rvert$	: Amplitude spectrum of input signal
$\phi(\omega)$	: Phase spectrum of input signal
h_i	: Linear behavior blast coefficients (frequency independent)
$H_i(\omega)$	:Non-linear behavior blast coefficients (frequency dependent)
Δt_i	: Time delays related to blast coefficients
f	: Discrete input signal in time domain
g	: Discrete group signal in time domain
u	: Discrete elastic group signal in time domain
E	: Elastic energy percent
P	: Plastic energy percent

Seismic signal measured from a group blast, *g(t)*, may be considered as the convolution of the input signal *f(t)* with the deconvolved signal, *h(t)* (Formula (1)). The autocorrelation *a(t)* of the group signal *g(t)* is given by Formula (2). Their related Fourier transforms are given in Formula (3). The deconvolved signal *h(t)* may be computed from Formulae (4), (5), and (6). The analytic presentations of linear elastic behavior and non-linear plastic behavior are given in Formula (7) and (8), respectively. The amplitude spectrum $|F(\omega)|$, and the phase spectrum $\Phi(\omega)$ (as defined in Formula (9)) of the input signal *f(t)* are computed from Formulae (10) and (11), respectively (References). The inverse Fourier transform

in Formula (12) provides the required input signal *f(t)* (or its discrete form *f*).

Ideally, if the group blast, *g(t)*, is purely elastic (linear behavior), then whole energy is spent to seismic wave propagation. In this case, the blast coefficients are frequency independent, consisting of sequence of spikes, h_1, h_2, h_3, ..., as many as the number of individual blasts in the group, and spike amplitudes being proportional to the charges of individual blasts. When individual blasts are identical, their corresponding spikes assume unit amplitudes, separated by preset time-delays, Δt_1, Δt_2, Δt_3, ..., related to individual blasts (Formula (7)).

On the other hand, if the group blast is plastic (non-linear behavior), then portion of the energy is spent to the fragmentation of rocks. In such case, blast coefficients are function of frequency, consisting of non-spiky, overlapping sequences, $H_1(\omega)$, $H_2(\omega)$, $H_3(\omega)$, ..., where it would be difficult to discriminate individual blasts within the group, due to the interactions among individual blasts, and overlaps of their generated seismic signals (Formula (8)).

Once the discrete form of the input signal, *f*, is computed from Formula (12), it can be convolved with the frequency independent linear behavior blast coefficients, h_1, h_2, h_3, ..., (Formula (7)) to yield the discrete elastic group signal, *u*, (Formula (13)). Comparison of the discrete group signal, *g*, (measured field seismic data) to the discrete elastic group signal, *u*, (computed seismic data) yields the Elastic, (*E*), and Plastic, (*P*), energy percents as given in Formula (14).

$$g(t) = f(t) * h(t) \tag{1}$$

$$a(t) = g(t) \otimes g(t) \tag{2}$$

$$g(t) \xrightarrow{\mathcal{F}^{-1}} G(\omega) \quad ; \quad f(t) \xrightarrow{\mathcal{F}^{-1}} F(\omega) \tag{3-}$$

a) $h(t) \xrightarrow{\mathcal{F}^{-1}} H(\omega) \;\; a(t) \xrightarrow{\mathcal{F}^{-1}} A(\omega)$ (3-

b)

$$G(\omega) = F(\omega)\, H(\omega) \tag{4}$$

$$H(\omega) = \frac{G(\omega)}{F(\omega)} \tag{5}$$

$$H(\omega) \xrightarrow{\mathcal{F}^{+1}} h(t) \tag{6}$$

$$G(\omega) = F(\omega)\left(h_1 e^{-i\omega\Delta t_1} + h_2 e^{-i\omega\Delta t_2} + h_3 e^{-i\omega\Delta t_3} + \cdots \right) \tag{7}$$

$$G(\omega) = F(\omega)[H_1(\omega) e^{-i\omega\Delta t_1} + H_2(\omega) e^{-i\omega\Delta t_2} + H_3(\omega) e^{-i\omega\Delta t_3} + \cdots]$$

$$F(\omega) = |F(\omega)| e^{i\phi(\omega)} \tag{8}$$

$$\tag{9}$$

$$|F(\omega)| = \sqrt{|A(\omega)|} \tag{10}$$

$$\phi(\omega) = \Im\left[\ln |F(\omega)| \right] \tag{11}$$

$$F(\omega) \xrightarrow{\mathcal{F}^{+1}} f(t) \tag{12}$$

$$u = f * (h_1, 0, 0, 0, \cdots, h_2, 0, 0, 0, \cdots, h_3, 0, 0, 0, \cdots) \tag{13}$$

$$E = 100 \times \frac{\sum g^2}{\sum u^2} \quad ; \quad P = 100 - E \tag{14}$$

3 ILLUSTRATION OF NON-LINEAR BEHAVIOR

Determination and analysis of non-linear behavior of blast phenomena is necessary to effectively evaluate the partition of P/E energy ratio. Thus, one can optimize the blast parameters to achieve successful blasting operation (in terms of good fragmentation and easy loading of broken material) and to restrict the influence of vibration on nearby settlements.

In this study, I illustrate the formulation of non-linear behavior of blasting operation. The field work of the study was carried out at Turkish Coal Enterprise's (TKI's) open pit coal mine's, at Eskihisar, Yatağan and Muğla, Turkey.

In the studied area the population is very dispersed. There are three small city near the mine, i.e.,Yesilbağcılar, Turgut and Eskihisar. This situation forces the mining company to take extreme precautions when they are designing blasts so that the blast effects, which are mainly vibration and aerial waves, do not disturb their surrounding neighbours. In this work, the aim was to find the partition of P/E energy ratio of a typical blast to determine the amount of vibration given to nearby settlement.

The blast parameters are given in Table 1. The Blasting induced ground vibration was measured by four seismographs, having three component geophone and 1 Hz geophone frequency.

Graphics depicting the measured group signal, $g(t)$, its related deconvolved signal, $h(t)$, and the frequency independent linear behavior blast coefficients h_1, h_2, h_3, ... (spikes of unit amplitude, located at 0 ms, 50 ms, and 150 ms preset time-delays) are shown in Figure (1).

Table 1. Blast parameters

Date of the blasting operation	01.06.2009
Blast type	Overburden blast
Drill hole diameter	165 mm
Bench height	20 m
Explosive type	ANFO (Ammonium Nitrate + Fuel-Oil), primer dynamite
Charge amount	100 kg ANFO + 0.5 kg primer dynamite per drill hole
Initiation system	Detonating cord+ delay relay
Number of blast hole in the group	3
Delay time per blast hole	0ms, 50ms, 150ms
Instrument used for vibration measurement	Instantel Minimate Plus-1 Hz geophone frequency

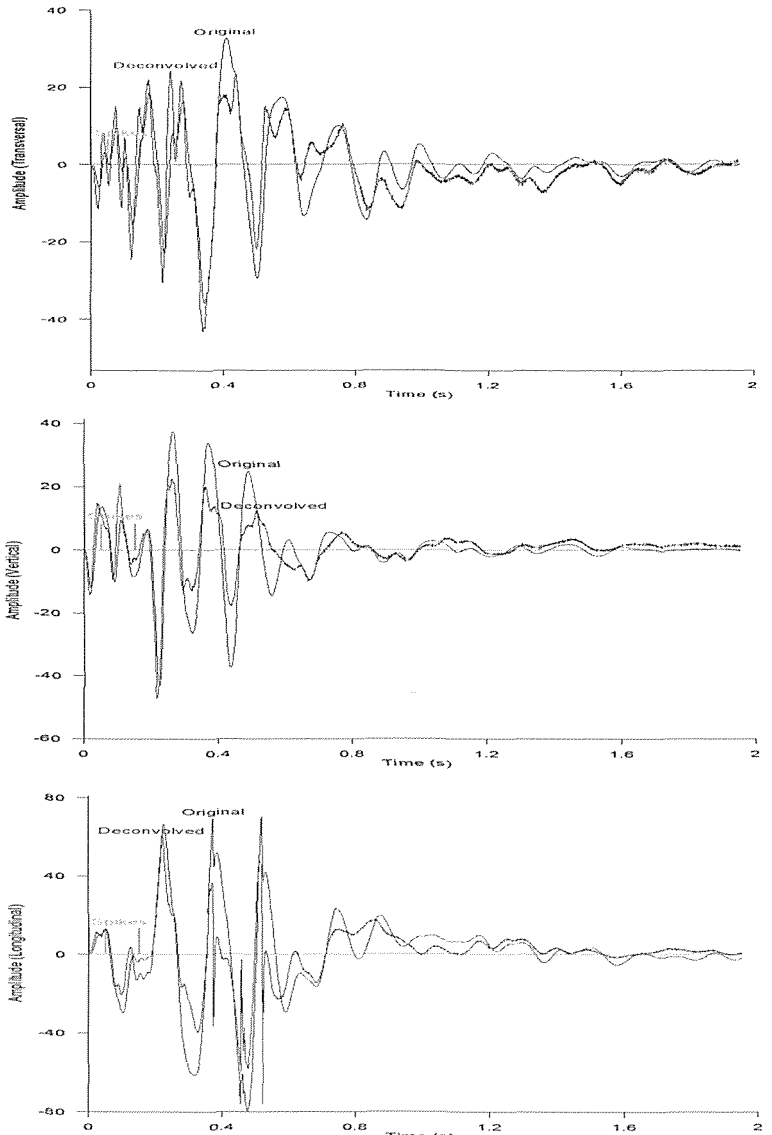

Figure 1. Group, *g(t)*, and deconvolved, *h(t)*, signals corresponding to transversal, vertical and longitudinal components. Spikes are located at 0 ms, 50 ms, and 150 ms.

Earth's natural convolution operator smoothens the seismic signal and obscures the details. The deconvolution operator (an inverse filter in frequency domain, Formula (5) recovers the details barely visible in the measured field data. Deconvolution operation, however, does not constitute the purpose of this study. Instead, we aim to obtain the input signal, *f(t)*, hidden in the group signal *g(t)* (measured field seismic data). To extract the input signal, *f(t)*, from

the group signal, $g(t)$, the following two important assumptions are made:
(i) Any event that follows the initial impulse of the blast (such as subsequent blasts in the group, their interactions, secondary seismic sources caused by additional cracks, fissures, slides, rock-ejects, gas-exhausts, etc.) is random in nature. This assumption permits the prediction of the amplitude spectrum $|F(\omega)|$ of the input signal (Formula (10)) from the autocorrelation of the group signal $a(t)$ (Figure 2) (Mesko 1984, Kanasewich 1981).

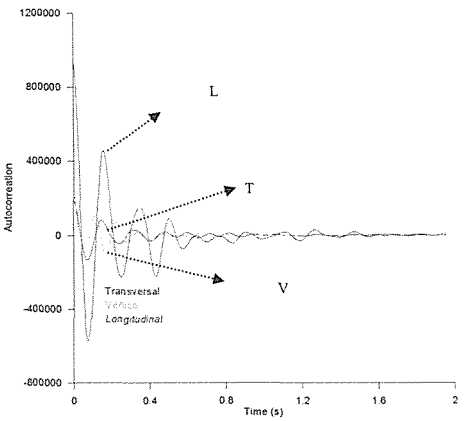

Figure 2. Autocorrelation of the group signal, $a(t)$, corresponding to transversal (T), vertical (V) and longitudinal (L) components.

(ii) Once the amplitude spectrum $|F(\omega)|$ of the input signal is known, its phase spectrum $\emptyset(\omega)$, possessing minimum-phase properties, is obtained from Formula (11) (Mesko 1984, Kanasewich 1981, Oppenheim and Schafer 1975).

Based on the above considerations; the input signal $f(t)$, its amplitude spectrum $|F(\omega)|$, and its phase spectrum $\emptyset(\omega)$ are depicted in Figure (3).

If the group blast is perfectly elastic, i.e. there exist no interactions among individual blasts within the group, and each blast consists of a simple impulse (no secondary seismic sources caused by additional cracks, fissures, slides, rock-ejects, gas-exhausts, etc.); then individual blasts within the group may be represented by spikes of unit amplitudes (assuming individual blasts within the group are identical), spaced in time with respect to their preset time-delays (Figure 4).

Under these circumstances, the convolution (Formula 13) of the discrete input signal f with the frequency independent linear behavior blast coefficients h_1, h_2, h_3, ... yields the discrete elastic group signal u (Figure 4).

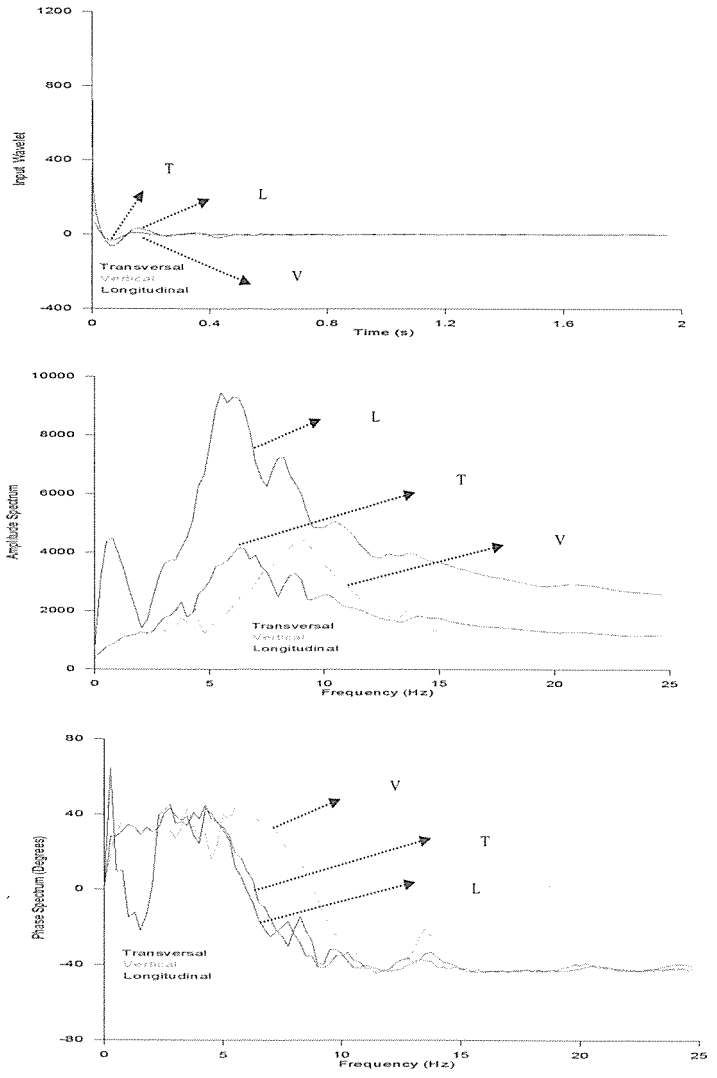

Figure 3. Input signal, *f(t),* and its corresponding amplitude, $|F(\omega)|$, and phase, $\emptyset(\omega)$, spectra.

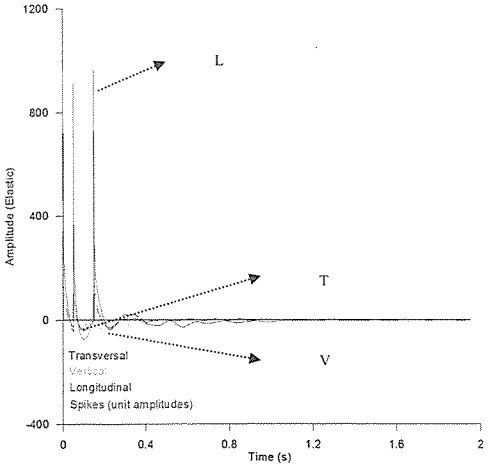

Figure 4. Discrete elastic group signal u corresponding to transversal, vertical and longitudinal components. Spikes are located at 0 ms, 50 ms, and 150 ms.

4 COMPUTATION OF ELASTIC/PLASTIC ENERGY PERCENT

Once the discrete group signal g obtained from field measurements, and the discrete elastic group signal u obtained from computations are known, then the elastic energy percent E, and plastic energy percent P can be calculated from Formula (14) (see Table 2).

Table 2. Calculation of elastic (E) and plastic (P) energy percents corresponding to transversal, vertical and longitudinal components.

	Σg^2	Σu^2	E	P	$E+P$
Trans	185548	1077901	17.21	82.79	100
Vert	212646	1212674	17.54	82.46	100
Long	925382	5490197	16.86	83.14	100

5 DISCUSSION AND CONLUSION

The type of explosives (dynamite, ANFO, emulsion etc.), blast pattern, the properties of the rocks (massive or fragmented rocks, and their water content), explosive/rock interaction, and workmanship in drill-hole preparation play an important role in the P and E distribution. Therefore, it is advised to conduct some experiments to build a P and E standard pertinent to the work area.

Use of *identical blasts* (explosive type and amount, hole-depth and diameter, stemming, etc.) within a group is an accepted consensus in mining. This is the reason why the frequency independent linear behavior blast coefficients h_1, h_2, h_3, ... are assumed as spikes of unit amplitude. In practice, however, due to the difficulties faced in the field (such as water invasion of the holes) *identical blasts* concept (unit amplitude assumption) may not be achieved. Under these circumstances, the P and E computations may not be reliable. P and E computations performed in seam-blasts may be misleading due to the presence of channel waves within the coal layers.

In mine blasts and seismic source considerations, the percent of energy spent for rock fragmentation (plastic behavior), and the percent of energy spent for seismic wave propagation (elastic behavior) constitute an important issue in blast and seismic source performances. From the

viewpoint of miners, the former (plastic behavior) is preferable, and from the viewpoint of geophysicists, the latter is favored. In this paper, we described a technique to quantitatively determine the blast performance in terms of elastic energy percent *E*, and plastic energy percent *P*. It is proved that the group seismic signal measured in the field is sufficient to compute *E* and *P*.

REFERENCES

Aldas, G.G.U. and Ecevitoğlu, B., 2008. Waveform analysis in mitigation of blast-vibration. *Journal of Applied Geophysics* 66: 25-30.

Bullen, K.E., 1963. *Introduction to the Theory of Seismology*. Cambridge University Press, p.381.

Kanasewich, E.R., 1981. *Time sequence Analysis in Geophysics*. The University of Alberta Press, p.370.

Karu, Z. Z., 2002. *Signals and Systems Made Ridiculously Simple*. ZiZi Press, p.124.

Mesko, A., 1984. *Digital Filter Applications in Geophysical Exploration for Oil*. John Wiley&Sons, New York, total 636 p.

Oppenheim, A.V. and Schafer, R.W., 1975. *Digital Signal Processing*. Prentice Hall, p.585.

Sanchidrian, J.A. and Lo´pez, L.M., 2003. Calculation of the explosives useful work-comparison with cylinder test data. In: *2nd World Conference on Explosives and Blasting Technique Technique*. Prague. 10–12 September, Balkema, Netherlands, p.65-78.

Shearer, P.M., 1999. *Introduction to Seismology*. Cambridge University Press, p.260.

Spathis, A.T., 1999. On the energy efficiency of blasting. In: *6th International Symposium on Rock Fragmentation by Blasting*, Johannesburg, 8–12 August, The South African Institute of Mining and Metallurgy, South Africa, p.186-195.

TBM Selection of Golab Water Transfer Tunnel Based on Geotechnical Risk Assessment

Nader Ghasempour, Majid Ejtemaee
Fater institute, Tehran, Iran

ABSTRACT The Tunnel Boring Machine (TBM) can excavate tunnel at rates unrivalled by other mining methods. However, the rock mass will present the tunnel team with one or more problematic geotechnical conditions that can have significant negative impact(s) on TBM performance. This paper is to discuss rock TBM selection based on geotechnical risk assessment. Based on the newly recommended approach, the most suitable TBM is one that has the minimum risk level either before or after hazards mitigation measures. To be able to check the performance of this approach in practice, selection of machine for Gholab water transfer tunnel has been evaluated. A double shielded TBM was proposed for the tunnel based on the newly proposed method. A double shield TBM was selected because of its continuous operation and more flexibility when encountering difficult ground conditions.

1 INTRODUCTION

Recent years have shown an extraordinary development of underground structures. Tunnels are constructed under many types of geological conditions varying from hard rock to very soft sedimentary layers. It must be said that the problems encountered in hard rock are quantitatively of reduced importance when compared with those occurring in soils or soft rock.

Procedures commonly taken for tunneling are excavation, ground support, mucking and lining. Variety of construction methods have been developed for tunneling such as cut and cover, drill and blast, submerged tube, push or pulling box, and by the use of tunnel boring machine (TBM). TBM excavation represents a big investment in an unflexible but potentially very fast method of excavating and supporting a rock tunnel. When difficult ground conditions are encountered without warning, time schedule and practical consequences TBM driven tunnel are far suitable than a drill and blast tunnel. Difficult ground conditions includes tunneling through fault zones with water bearing gouge, high volume of groundwater inflow, karstic cavities, gassy formations, sticky grounds, unstable and running or blocky grounds, hard and abrasive rocks, squeezing phenomenon and swelling rocks with potential for high convergence in tunnel adverse geological conditions lead to long downtime and consequently low machine utilization in addition to costs imposed onto the project. Although these conditions could be unavoidable, their related consequences may be mitigated by conducting appropriate site investigation in design phase to know the ground conditions along the tunnel alignment and select the tunneling method and machinery to cope with the anticipated conditions.

2 GEOTECHNICAL RISK ASSESSMENT FOR TBM SELECTION

Most accidents and other associated problems occur during construction of

geotechnical structures, and are very often related to uncertainties in side ground conditions. Therefore, it becomes essential to develop risk analysis systems and to avoid its occurrence. Appropriate TBM selection in tunnel excavation plays an important role in project success from the safety, time and economical points of view. Although a certain degree of geotechnical risk is expectable for each TBM, selection of an appropriate one decreases the risk as minimum as possible.

Table 1. Comparison of three rock TBM's

Open TBM	Single shielded TBM	Double shielded TBM
Advantages		
Easy operation	Wide range of application	Wide range of application (good to fair rock)
Applicability in hard rock	Safety	Safety
High excavation rate	Precast, segmental, lining, instalation	Support system flexibility
Support system flexibility	Slower than the double shielded TBM	Simultaneous installation of final support system
Less construction cost	Working in falling ground	Working in falling ground
Less investment cost	Less likely to get stuck	Controlling water inflow with closed shield
Disadvantage		
Grippers inability in unstable rock mass	Cannot reach high performances in hard rock and are sensitive to squeezing ground and face instabilities	High investment cost
Support installation in weak rock masses	Drive in weak ground	Complex operation
Too sensitive to poor rock condition	Need of precast lining	Need of cleaning the telescopic joint
	High investment cost	Possibility of TBM jamming in highly convergent ground
	Complex operation	Are still sensitive to squeezing ground and to face instabilities
	Need of segment plant	

The practically infinite number of combinations of rock, soil and environmental conditions which may be encountered during tunnel excavation has determined a great difference in the types and characteristics of the available TBM's. There are many different schemes for the classification of tunneling machines. As a general classification scheme, TBMs can be divided into two main groups consisting of hard rock and soft ground TBMs. Rock TBMs were divided into unshielded TBM (i.e. Open TBM) and single and double shield TBMs. Comparison of three types of rock TBMs are illustrated in Table 1 based on their advantages and disadvantages.

Various methods for TBM selection have been proposed and discussed up to now. Several countries such as Japan, Norway, Italy and France have proposed different guidelines and recommendations for TBM selection based on geological and geotechnical conditions. These guidelines published by AITES/ITA entitled "Recommendations and Guidelines for Tunnel Boring Machines (TBMs)" (AITES-ITA Working Group No. 14, 2000). However, these standards provide some general guidelines for selection of tunnelling techniques and were rather optional. Almost none of these guidelines have been used as a universal method for TBM selection. Decision making process which can provide a rational procedure for selection of the most appropriate TBM based on consistency with existing conditions requires a decision analysis. A new approach developed for TBM selection using a decision tree. The proposed approach for selecting the most appropriate TBM mainly include geotechnical hazards considerations and involves integrating the following essential elements:

1. Collecting available geological and geotechnical data of the tunnel alignment.
2. Determination of similar geological units along tunnel alignment.
3. Geotechnical and geomechanical characterization and quantitative description of uncertainties associated with each unit using probabilistic procedures.
4. Definition and determination an acceptable risk vulnerability index for geotechnical hazards.

5. Geotechnical hazards assessment which could be possibly encountered during tunneling operation.

6. Establishing a framework for selecting the optimum excavation method using the decision tree technique.

7. Determination of the most appropriate TBM on the basis of a detailed decision analysis with the aim of minimizing geotechnical risk.

Table 2. Main geotechnical hazards and their common mitigation measures

Geotechnical hazards	Mitigation measures
Borability (hardness, abrasivity)	Use of larger discs Use of resistant steel (with costs consideration) Applying higher torque Provision of easier access to cutterhead Use of cutterheads with back-loaded disc cutters
Walls instability (often encountered by open TBM)	Use of support systems such as steel arches, shotcrete installed behind cutterhead Pretreatment by injection holes Tunnel lining with precast concrete segments Use of shielded TBMs
Face instability	The voids filled with resin foams and the collapsed material in front of the face consolidated with chemical grout mix In the most critical sections A pattern of fiberglass pipes were executed through specific holes in the rear shield of the TBM in order to stabilise the crown of the tunnel (blocky ground) Use of shotcrete (for soft and raveling ground) Creating artificial face Using grill bars in cutterhead
Karstic voids	Drilling drainage holes Filling the karstic voids Forepoling
Fault zones	Probe drilling Ground improvement Segmental lining Freezing Drilling drainage holes (high water pressure present) Use of shielded TBMs
Squeezing	Over cutting Use of lubricator such as bentonite, grease Prevention of machine break downs Increasing thrust of longitudinal jacks
Water inflow	Probe drilling Drainage Pre-injection Freezing Use of shielded TBMs

Geotechnical hazards are often appeared because of insufficient geological–geotechnical studies and can cause serious and even catastrophic consequences during tunneling operation. Even though a definite degree of geotechnical hazard is expectable using any kind of TBM, selecting the appropriate one will decrease it as minimum as possible. Main geotechnical hazards (including rock hardness and abrasivity, tunnel face and walls instability, karstic voids, fault zones and squeezing behavior) and common mitigation measures are illustrated in Table 2.

As a general rule, the likelihood of occurrence and consequence can be divided into arbitrary levels. Here, in order to get more precise results, the five-level of each one was used. The rating of likelihood and consequence is presented in Tables 3 and 4.

Table 3. Rating of likelihood of hazards occurrence.

Likelihood	Rating	Description
Importable	1	vent is extremely unlikely to occur once
Remote	2	Event is unlikely to occur once
Portable	3	Event is likely to occur at least once
Expected	4	Event is likely to occur more than once but infrequently
Frequent	5	Event is likely to occur frequently

Table 4. Rating of consequence of hazards occurrence

Consequence	Rating	Description
Negligible	1	Event does not cause delay or damage
Moderate	2	Event causes minor damage and/or delay up to 2 days
Serious	3	Event causes repairable damage and/or delays up to 1 week
Critical	4	Event causes significant repairable damage and/or delays between 1 and 2 weeks
Catastrophic	5	Event causes irreparable damage and/or delays greater than 2 weeks

Combining the likelihood rating and the consequence rating results in a risk index of between 1 and 25 for any given risk are presented in Table 5.

Decision tree is an efficient ones among other decision aids which help decision maker select an alternative or more through various alternatives based on specific criteria.

Selection of tunnelling machines can be performed based on different criteria such as costs and time scheduling. The specific decision tree proposed for geotechnical risk mitigation based selection of rock TBM is illustrated in Fig. 1.

Table 5. Risk index for any given risk

Risk level	Index	Description
Low	1-4	Risk is tolerable without any mitigation
Medium	5-9	Risk is moderately tolerable. Mitigation may be needed
High	10-15	Risk is at the border of tolerability. Mitigation should be identified and implemented to reduce risk
Very high	16-25	Risk is intolerable. Mitigation that reduces risk must be implemented

At first on the basis of criteria such as tunnel geometry, environmental constraints, design constraints (i.e. time and cost of construction) and geomechanical–geotechnical parameters one of three excavation method including drilling and blasting, mechanized tunnelling using partial face excavation machines and full face excavation machines is selected. Having found full face tunnelling machine as appropriate excavation alternative, one of the hard rock or soft ground TBM is selected based on ground conditions (i.e. being soft or hard rock) along tunnel alignment. The most important effective criteria for selection of one of the three rock TBMs in decision tree include:

– geotechnical hazards,
– capability of mitigation measures in reducing the geotechnical risk and
– accepting or rejecting the final geotechnical risk according to acceptable vulnerability index.

Generally speaking, the most reliable machines are the simple ones as they have the least amount of equipment that can break down. So, in decision tree one should choose route 1 including Open TBM, if this machine is not appropriate, then route 2 and finally 3. However, being appropriate or not, depends on evaluation of each machine's excavation capabilities (i.e. acceptance or rejection of risk) encountering geotechnical hazards. With each TBM reaches a geotechnical hazard, two states may be appeared, the condition is such that machine either can easily pass it or cannot (low or high risk). If machine can pass it (Yes) one should go to another hazard. But, if machine cannot pass it or may hardly pass it (No) (i.e. the risk level is not acceptable), one should select mitigation measures (in Table 2). After testing mitigation measures two states may appears including either acceptable or not acceptable risk level. If risk level is acceptable (Yes) one can go to another hazard. But, if it is not acceptable (No) one should search another excavation technique. As an example, if an open TBM is to be encountering a section with highly hard and abrasive rock, one should apply mitigation measures such as choosing larger disc cutters with resistant steel to overcome the high risk. If this cannot cause machine pass it, conventional tunnelling method including drilling and blasting will be selected.

3 GOLAB WATER TRANSFER TUNNEL

The long of the first lot of Golab water transfer tunnel is10129 m which is one of the longest water transfer project in Iran. This tunnel is being excavated by a 4.58 m diameter full face telescopic shield TBM in rock. The tunnel passes through several formations with rock mass conditions varies from weak to good, with RMR ranging from 40 to 76 (in Met-Sch and Ig-Di formations, respectively). Based on the field engineering geological investigations the main lithological units consist of schist, granite and diorite. The maximum depth of tunnel is 212 m. The groundwater level varies from 97 to 423 m above the tunnel crown. The typical geological and geotechnical conditions of the project are illustrated in Fig. 2 with the longitudinal profile of lot 1.

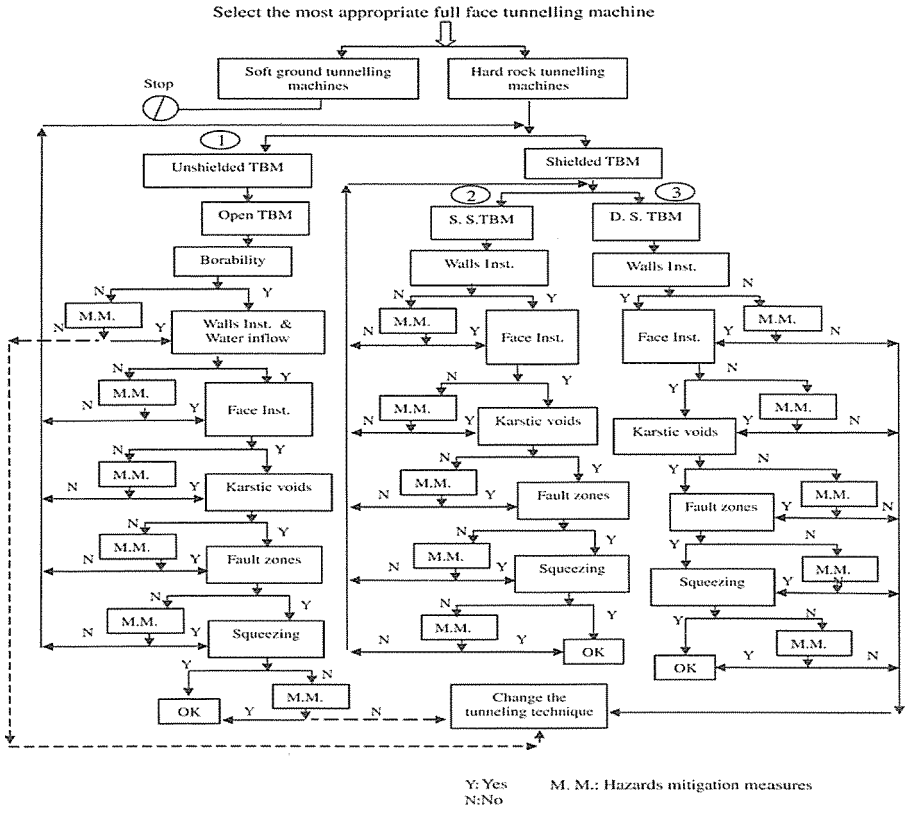

Figure 1. Decision tree for selecting the most appropriate rock TBM

3.1 Selection of tunneling method for Golab tunnel

According to time scheduling of Golab water transfer project, excavation rate based on geological condition varies from 1 to 7 m/h. It is obvious that achievement of this rate by conventional excavation method seems impossible. On the other hand, this tunnel is a water transfer one, so application of a TBM with a circular shape is preferable.

Selection of TBM for Golab Tunnel was performed based on a detailed decision analysis. Three following factors must be provided during the decision making process:

1. Minimum geotechnical problems (acceptable risk level).
2. Acceptable reliability.
3. Project duration correspond to the scheduling.

Selection of the most appropriate TBM for Golab tunnel was performed based on proposed decision tree in Fig. 1. Finally a mechanized TBM tunnelling because of its high advance rates in comparison with drilling and blasting and partial face tunnelling machines was selected after feasibility and technical studies. According to International Society for Rock Mechanics, soft ground and hard rock are material with compressive strength 5–50 and 50–100 MPa, respectively. Tunnel alignment passes through hard rock layers. So, selection of a rock TBM is found suitable. Based on developed method, applicability of three rock TBMs compared when encountering geotechnical hazards in difficult ground conditions and finally the most appropriate

TBM is selected based on minimizing risk level. Geotechnical risk levels for application of three rock TBMs including open, single and double shield TBM in Golab tunnel is presented in Table 6.

An open TBM is cheaper and easier to drive and less likely to get stuck in comparison with other rock TBMs. So, applicability of this machine is firstly evaluated based on developed approach.

3.1.1 Borability (rock hardness and abrasivity)

Rock hardness and abrasivity are the most important parameter which should be considered when using a TBM in difficult ground conditions. The abrasiveness of the rock directly affects the costs of tunneling. This effect, which can only be determined within limits, arises as a result of the increased cutter changing time and occasional interruptions of tunneling to exchange wearing parts such as scrapers or buckets.

Presence of granite in Gr.Gmet formation which is a highly abrasive material and, when broken down into the conditioned paste in the working chamber of a TBM, it becomes a very effective grinding paste. This keeps abrasiveness high can be a major problem in Golab tunnel where cutter wear necessitated frequent replacement of cutters.

Considering high and medium abrasive minerals content in sections of Golab tunnel may impede using a shielded TBM. Geotechnical risk index for using a shielded TBM in such conditions is medium according to Table 6, so applying risk mitigation measures presented in Table 2 in these sections may be required.

3.1.2 Tunnel walls instability and water inflow

Water circulation depends on primary permeability, related to the original rock porosity and by a secondary permeability generated by brittle deformation. Primary permeability can be generally considered very low in crystalline rocks, while secondary permeability related to fracturing may be responsible for severe water inflow.

The hydrogeological risks related to unexpected heavy water inflow and drainage of surface resources represents, together with the occurrence of unexpected geological and geomechanical conditions, one of the most challenging and troublesome aspects related to tunneling.

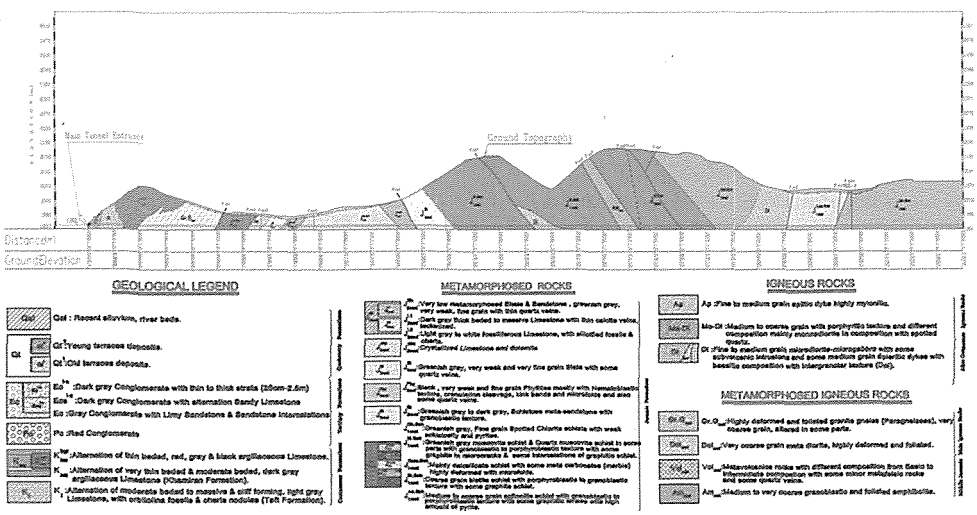

Figure 2- Longitudinal geological profile of Golab tunnel (lot 2)

With the presence of schist layers and igneous rocks, walls and roof instabilities is expected. On the other hand, the jointed rock masses in other strong rock formations may cause structural instabilities. The presence of groundwater in formations (especially in J^{St}_{2met}) with high permeability may worsen the situations. The presence of water in crushed zones in the vicinity of fault zones also cause running ground occurrence. The gripping system in open TBM limits its application in such unstable conditions. Geotechnical risk originated from ground water by using open TBM is very high. The use of a shielded TBM to provide continuous tunnel walls support, therefore is inevitable at least for 20% of tunnel alignment. These reasons on one hand and low acceptable risk from the project owner on the other hand, make the decision makers consider a shielded TBM. This raises the question as to whether a double or single shield should be used.

Table 6. Geotechnical risk indices for using three rock TBMs.

No.	Geotechnical hazards	Occurrence likehood	Open TBM		SS TBM		DS TBM	
			Cons.	Risk	Cons.	Risk	Cons.	Risk
1	Hard and abrasive	4	2	8	2	8	2	8
2	Tunnel walls instability and water inflow	5	5	25	2	10	1	5
3	Tunnel face instability	4	5	20	2	8	2	8
4	Karstic voids	4	5	20	3	12	3	12
5	Fault zones	5	5	25	3	15	3	15
6	squeezing	4	1	4	2	8	2	8

Cons.: consequence, SS TBM: single shielded TBM and DS TBM: double shielded TBM.

3.1.3 Face instability

Based on tunnel face stability analysis, encountering this phenomenon in schist and also in blocky ground is expectable. If this instability appeared, using fiberglass rock bolts can be helpful. Using shotcrete in soft and raveling ground is applicable. Pre-treatment inside the shield before encountering unstable face is an effective way to overcome such difficult areas. To avoid problems in mucking system resulted from large falling blocks, using grill bars in cutterhead openings is required.

As presented in Table 6 geotechnical risk resulted from face instabilities for application of shielded TBM is medium (however at the border of acceptability). Application of risk mitigation measures for face instabilities, the shielded TBM can pass through this hazard.

3.1.4 Karstic voids

Rock TBMs are very prone to misalignment when working in faces of mixed ground or when they encounter karstic cavities.

The combination of soft and hard ground provokes a deviation of the machine towards the soft side and, when this is in the lower part of the section, the machine can progressively sink until the advance must be stopped in order to realign the machine. When long shields are used the machine works as a cantilever fixed at its rear end, with a marked trend to sink at the cutterhead.

This problem is more important in mechanized tunnels than in conventional ones, as the machine considerably limits the possibilities of probing ahead of the excavation as well as the restricting space for ground treatment. Drill and blast methods appear to be more flexible in dealing with karstic cavities.

Approximately 80% of the tunnel alignment is consisted of schist and its components. On the other hand, almost whole tunnel is below the underground water table.

Encountering karstic terrane therefore, is expectable along the tunnel alignment. The risk resulted from this phenomenon is high for shielded TBMs. So, application of mitigation measures such as drainage holes, filling the karstic voids and forepoling is required. This application makes shielded TBMs pass through the karsts without any considerable problem.

3.1.5 Fault zones

A fault zone destroys much of the familiar tangential stress arch, and tunnel stability problems often arise as a result. High pressure inflow and falls of clay and rock blocks are other factors. Another problem in fault zones is the grippers, and maybe also the shield i.e. delayed treatment of rock that actually requires pre-treatment.

Based on early geological investigations, 11 main faults have been distinguished throughout the tunnel. So, it is frequent the likelihood of encountering the fault. The estimated width of these faults is between 3 and 30 m. These fault zones are very weak, crushed rock, intense water inflow and unstable sections. Consequently, the risk of encountering fault zones are high for shielded TBMs as presented in Table 6. Based on stability analyses in falling crushed zones, TBM driving in these zones seems possible if a shielded TBM is used. Use of double-shield TBM can solve minor stability problems without encountering significant delays, but when significant fault zones are intersected, the double-shield may actually represent a hindrance to rapid recovery, as pre-treatment of the ground ahead is hindered by the long shields.

3.1.6 Squeezing

Tunnel convergence was one of the biggest concerns in the project design phase since the large tunnel diameter and the presence of argillite rock formations under high cover. Ground squeezing behavior should be well evaluated when using a shielded TBM. A single shield TBM because of its shorter shield in comparison with a double one has advantages in this situation. On the other hand a double shield TBM because of its continuous operation in excavation and segment installation has more advantages. So the exposed time is shorter in this machine.

In three sections (F.m4, F.m5 and F.m6) of Golab tunnel alignment which occurred in fault crushed zones with highly thick overburden, appearance of this phenomenon is very high and occurrence of squeezing in Met-Sch formations are expectable. Although the risk index of encountering squeezing ground along Golab tunnel alignment by shielded TBMs is medium, a double shield TBM because of its high excavation rate in comparison with a single shield one is preferable in such conditions. The double shielded TBM proved however to be able to cope with the rapid convergences of the tunnel walls without any problem and without having to use the full overboring capability of the machine, thanks to the particular shield design of this type of TBM. On the other hand it is expected that using the preventive measures as presented in Table 2 such as over cutting, prevention of machine break downs and use of lubricator such as bentonite cause machine pass through this hazard without getting stuck.

4 CONCLUSION

According to geological and geotechnical conditions along Golab tunnel alignment, the ideal TBM to be selected must have some main characteristics including excavation of a wide range of rock mass quality from very weak to very strong, possibility of precast concrete segments installation and achievement high advance rates and working in difficult ground conditions such as tunnel walls and face instabilities. Due to the high occurrence likehood of water inflow the use of shielded TBMs are rational. The results of tunnel face stability analyses have indicated that application of an open TBM is limited. The double shielded TBM advanced in schist formations when a significant overbreak was detected. The overbreak evolves to important rock falls and squeezing of the fine material. The cutterhead became trapped and the advance was no longer possible

However, according to limits of construction duration, a double shield TBM because of its continuous operation and more flexibility when encountering difficult ground conditions was proposed. Generally, double shield TBMs have high preference based on geotechnical risk assessment.

REFERENCES

AITES-ITA Working Group No. 14, 2000. Recommendations and Guidelines for Tunnel Boring Machines (TBMs). www.ita-aites.org.

António Campos e Matos, Luís Ribeiro e Sousa, Johannes Kleberger, Paulo Lopes Pinto, 2006, *Geotechnical Risk in Rock Tunnels*, Taylor & Francis Group plc, London, UK.

Barla, G., Pelizza, S. 2000. TBM tunneling in difficult ground conditions. In: Geoeng, Melbourne, Australia.

Barton, N., 2000. *TBM Tunneling in Jointed and Faulted Rock*. Balkema, Rotterdam.

Bernhard Maidl, Leonhard Schmid, Willy Ritz, Martin Herrenknecht., 2008, *Hardrock Tunnel Boring Machines, Ernst & Sohn Verlag für Architektur und technische Wissenschaften* GmbH und Co.KG, Berlin.

Imensazan Consulting Eng. 2008. Golab tunnel construction method. Report No. 039-01.

Khademi, J., Shahriar, K., Sharifzadeh, M. 2006. A methodology for rock TBM selection based on geotechnical hazards mitigation. In: *8th Regional Rock Mechanics Symposium*, Turkey.

Shahriar, K., Sharifzadeh, M., Khademi, J., 2008. Geotechnical risk assessment based approach for rock TBM selection in difficult ground conditions. *Tunnelling and Underground Space Technology* 23, pp. 318–325.

Shahriar, K., Sharifzadeh, M., Khademi, J., Haddadi, M.R., 2006. Selection of rock TBM based on geotechnical hazards mitigation. In: *7th Iranian Tunneling Conference*, Tehran, Iran, pp.1059–1070.

Sharghi, A., Shakour, I., Habibagahi, M.A., Pelasi, M., 2004. Using open TBM in caving zones and it's controlling in Gavoshan tunnel. In: *6th Iranian Tunneling Conference*, Tehran, Iran.

Sharifzadeh, M., Hemmati Shaabani, A., 2006. TBM tunneling in adverse rock mass with emphasis on TBM jamming accident in Ghomrud water transfer tunnel. In: Van Cotthem, A., Charlier, R., Thimus, J.F., Tshibangu, J.P. (Eds.), *Processing of Eurock2006*, May 9–12, Liege, Belgium. Taylor & Francis Publication, pp. 643–647.

Application of Modified Kuz-Ram Fragmentation Model by Gheibie et al. at the Sungun Copper Mine

Sohrab Gheibie, Sebnem Duzgun
Mining Engineering dept., Middle East Technical University, Ankara, Turkey

ABSTRACT Kuz-Ram model is used as a common model for estimation of rock fragmentation distribution in mining industry. However, researches have demonstrated that Kuz-Ram model doesn't give reliable outcomes in certain cases; therefore, researchers have proposed different models to have a better estimation of fragmentation. Recently Gheibie et al. has developed a new version of Modified Kuz-Ram fragmentation model in which a factor of 0.073 is included in the formula for prediction of X_m. In the model, a Blastability Index (BI) has been used to correct the calculation of the Uniformity Index of Cunningham.

In this paper, Kuz-Ram modified and Kuz-Ram modified model by Gheibie et al. were applied for five blast sites of Sungun Copper Mine, Iran to estimate the run of mine size distribution. Results show that new version of Kuz-Ram model gives more reliable estimation of size distribution comparing to the Modified Kuz-Ram model at Sungun Copper Mine.

1 INTRODUCTION

Kuz-Ram model which was proposed by Cunningham has been used as a common model in mining industry for the prediction of rock fragmentation size distribution by blasting (Cunningham 1983 and 1987). Although it has been used extensively in practice, it has certain shortcomings like timing effect and lack of prediction of fines.

There are some models which are proposed to improve these shortcomings. CZM (Kanchibotla et al. 1999) and TCM (Djordjevic 1999) models are two examples of extended Kuz-Ram models to improve the prediction of fines which are known as JKMRC models.

In CZM model, size distribution of rock fragments is divided into coarse and fines parts. According to the CZM, two different mechanisms control the rock fragments produced by blasting; coarse part is produced by tensile fracturing in which Kuz-ram model is used to predict this part of size distribution. However, fines part is produced by compressive fracturing in crushed zone, which Rosin-Rammler function gets a different value of n and X_C. In the TCM model, two Rosin-Rammler functions are used for ROM size distribution. TCM is a five-parameter model in which two of the parameters are related to coarse, one for fines fraction and the other two are related to fines part of the distribution.

In addition, by replacing the original Rosin-Rammler equation with Swebrec function, KCO model is arrived to predict the ROM size distribution (Ouchterlony 2005). Like Rosin-Rammler, it uses the median or 50% passing value X_m as the central parameter but it also introduces an upper limit to fragment size X_{max}. The third parameter, b, is a curve-undulation parameter. The Swebrec function removes two of Kuz-Ram's drawbacks the poor predictive ability in fines range and the upper limit cut-off of block size.

Also, Spathis suggested that the X_m should have the prefactor $(Ln2)^{\frac{1}{n}} / \Gamma\left(1+\frac{1}{n}\right)$ claiming that the correction indicates that the original implementation of Kuz-Ram overestimates the size of the rock fragments leading to the original Kuz-Ram to underestimate the fines faction when the uniformity index is 0.8 to 2.2 (Spathis 2004).

Recently, Gheibie et al. (2009) has proposed a new version of Kuz-Ram Model for getting better results in rock fragmentation of size distribution by blasting (Gheibie et al. 2009, 2010).

In this paper the new version of modified Kuz-Ram model developed by Gheibie et al. (2009) was used to predict size distribution of rock fragmentation at Sungun Copper Mine, Iran. The model has also been applied in Kirka borax mine in Turkey (Kilic et al. 2009).

2 RESEARCH METHOD

2.1 Modified Kuz-Ram Model

An empirical equation of the relationship between the mean fragment size and applied blast energy per unit volume of rock (powder factor) has been developed by Kuznetsov (1973) as a function of rock type. The model predicts fragmentation from blasting in terms of mass percentage passing through versus fragment size. Kuznetsov's equation is given below:

$$X_m = 0.073BI\left(\frac{V_0}{Q_e}\right)^{0.8} Qe^{1/6}\left(\frac{S_{anfo}}{115}\right)^{+19/30} \quad (1)$$

Where X_m is the Mean fragment size (cm), A is the rock factor, V_0 is the rock volume broken per blast hole (m^3), Q_e is the mass of explosive being used (kg), S_{anfo} is the relative weight strength of the explosive to ANFO (ANFO =100).

The Blastability Index, which was first proposed by Lilly (1986), has been adapted for Kuznetsov's model, in an attempt to better quantify the selection of rock factor A (Cunningham 1983 and 1987). Cunningham stated that the evaluation of rock factors for blasting should at least take into account the density, mechanical strength, elastic properties and structure. The equation is given below:

$$A = 0.06*(RMD + JF + RDI + HF) \quad (2)$$

A useful indirect check on the index of uniformity has been performed by Cunningham (1987). In the study of Cunningham the prediction of fragmentation is based on the Kuznetsov equation and the relationship between fragmentation and drilling pattern is used to calculate the blasting parameter of the Rosin-Rammler formula. The blasting parameter, n, is estimated by

$$n = \left(2.2 - 14\frac{B}{D}\right)\left(1 - \frac{W}{B}\right)\sqrt{\left(\frac{1+\frac{S}{B}}{2}\right)} \left(0.1 + abs\left(\frac{BCL - CCL}{L}\right)\right)^{0.1}\left(\frac{L}{H}\right) \quad (3)$$

Where B is the Burden (m), S is the Spacing (m), D is the Borehole diameter (mm), W is the Standard deviation of drilling accuracy (m), L is the Total charge length (m), BCL is the bottom charge length (m), CCL is the column charge length (m) and H is the Bench height (m). Using a staggered pattern, it should be multiplied by 1.1.

The value of n determines the shape of the Rosin-Rammler curve; high values indicate uniform sizing and low values on the other hand suggest a wide range of sizes including both oversize and fines. Combination of the Kuznetsov and Rosin-Rammler (1933) equation results in what has been called the Kuz-Ram Fragmentation Model. The Rosin-Rammler formula is used to predict the fragment size distribution. It has been generally recognized as giving a reasonable description of fragmentation in blasted rock, which is given by:

$$R_m = 1 - e^{-0.693\left(\frac{X}{X_m}\right)^n} \quad (4)$$

Where R_m is the proportion of material passing the screen, X is the screen size (cm); X_m is the mean fragment size (cm), n is the index of uniformity.

2.2 Modified Kuz-Ram Model by Gheibie et al.

According to Gheibie et al. (2009) the modified Kuz-Ram Model has some lacks in predicting of the ROM size distribution, therefore, they have proposed a new form of the Kuz-Ram with some corrections in which a factor of 0.073 is included in the formula for prediction of X_m. In the model, a Blastability Index (BI) has been used to correct the calculation of the Uniformity Index of Cunningham. The new model has a two parameter fragmentation size distribution that can be easily determined in the field. The Rosin-Rammler function is used as the size distribution with X_m as central parameter and n, as the uniformity index for:

$$X_m = 0.073BI\left(\frac{V_o}{Q_e}\right)^{0.8} Qe^{1/6}\left(\frac{S_{anfo}}{115}\right)^{-19/30} \quad (5)$$

$$n' = 1.88 * n * BI^{-0.12} \quad (6)$$

All parameters in equations (5 and 6) are similar to those described in equations (1 and 3). Where n' is the Modified Uniformity Index, n is the Uniformity Index (Cunningham) and BI is the Blastability Index.

2.3 Prediction of ROM size distribution

Based on a modified Blastability Index, the geomechanical properties of five blast sites were collected prior to blasting. Several laboratory tests were carried out according to ISRM standards to determine the mechanical and physical parameters such as Young's modulus, Density and Uniaxial Compressive Strength. Then for both of the original and new Kuz-Ram models, the rock fragmentation size distribution has been estimated (Table 1).

2.4 Fragmentation assessment

After estimating the ROM size distribution for each case of blasting at the Sungun mine, image processing studies were carried out for five blasted sites muck piles. All blasts results were analyzed after conducting blasting operation in three positions of muck pile (soon after blasting, after loading around half of muck pile and end of muck pile) (Figure 1). For image processing, 15 digital photographs were taken from each muck pile position and then processed by the Gold size program. The analyzed photo's results were merged to get a better analysis of the photo analyses.

Since there are some fine particles that are hidden, the results obtained by image analysis are always different from those of by sieving. Fines correction usually is the common deal to overcome this problem in practice. Some methods that can be used to correct fines have been discussed in the literature (Cho et al. 2003, Maerz and Zhou 2000, Chung and Katsabanis 2000). In this paper, for correcting the fines Cho et al. (2003) method was adopted which uses a Gaudin- Schuhman distribution (Cho et al. 2003). The final distribution obtained from image processing can be seen in Table (1).

3 DISCUSSION

In this article, five different sites were selected to investigate the applicability of the two fragmentation models in the Sungun Mine. Comparing the results derived from Modified Kuz-Ram, the new Modified Kuz-Ram and image analysis demonstrates that the new version of Kuz-Ram model gives more reliable results comparing to the original Kuz-Ram model (Table 1).

Rock masses are an anisotropic and inhomogeneous media, with different physical and mechanical behaviors in different directions and there are many parameters used in the technical description of rock masses, which Blastability Index

(BI) uses some of these parameters such as Rock Mass Description, joint Spacing, Joint Plane Angle, etc.

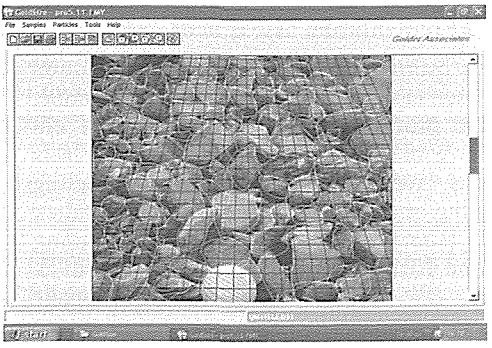

Figure (1) - A sample of analyzed muckpile by the software

Table 1- Predicted and actual size distribution for each blast site

Blast site	Models	X_{30} (cm)	X_m (cm)	X_{80} (cm)
DI-1	Kuz-Ram	11.8	20	39.3
	Image Proc.	16.7	26.5	48
	New Model	16.1	25.8	47
DI-2	Kuz-Ram	12.9	22	43.2
	Image Proc.	17	27	49.2
	New Model	17.38	27.3	48.4
DI-3	Kuz-Ram	13.5	23	45
	Image Proc.	18.8	28.5	51.7
	New Model	17.7	28	50.9
DI-4	Kuz-Ram	14	24	47
	Image Proc.	18	29	53
	New Model	18.3	29.5	53.8
DI-5	Kuz-Ram	15.3	26	51
	Image Proc.	19.8	32	58.7
	New Model	19.7	31.7	58.1

Therefore, geomechanical properties as the most important parameters in rock blasting are not considered explicitly (Gheibie et al. 2007 and Momivand 2005) Thus, Kuznetsov's equation, theoretically and practically will not predict the mean fragment size desirably.

In addition, Gheibie el al. (2009) showed that uniformity index depends on rock mass properties since, explosive type used in mines is usually ANFO, which has high gas energy (EB) and produces high gas pressures and the gas particles passing the joints activate the elder joints and then liberate the insitu blocks. Through decreasing the joint spacing, the size of insitu blocks becomes more uniform and by releasing adequate gas particles, the blocks will liberate. Boulder formation is common in widely spaced jointed rock mass blasting (Chung and Katsabanis 2000). Bhandari (1997) also concluded that blasts in rock masses with parallel or perpendicular joints to bench face, leads to a uniform fragmentation.

According to the above mentioned ideas it can be understand that the new version of Kuz-Ram model will predict the rock fragmentation size distribution more reliable than original Kuz-Ram which the table shows the reliability of application of new modified Kuz-Ram model at the Sungun Mine.

4 CONCLUSION

Obtaining the rock fragmentation size distribution has always been a challenging matter in rock blasting, for this the researchers have developed a list of empirical models to estimate it. However, selecting a proper model for a blasting site is also main point in the field. In this paper, the original and the new version of Kuz-Ram model modified by Gheibie et al. have been selected to compare their application reliability at the Sungun Mine.

According to the theoretical discussion it is more reliable to use the new version of Kuz-Ram developed by Gheibie et al. at the Sungun, since, it also considers the impact of factors that are not considered in Kuz-Ram model. As an example, the Kuznetsov model does not include the influence of joint's aperture which is believed as an important parameter in retention of explosives energy in rock mass, also it does not other rock mass parameters such as joint infillings, etc. However, in the new version of Kuz-Ram, Gheibie et al. have considered the cumulative influences of those parameters as

the coefficient factor. According to the pervious findings, the distribution uniformity is related to rock mass properties; however, Cunningham has not included any parameter related to rock mass to consider its effects. Gheibie et al. have experimented that the rock mass parameters influence the distribution uniformity of rock fragmentation by blasting. They have included BI (Blastability Index) as the rock mass representative in the uniformity index. Therefore, it can be predicted that the new version will estimated the rock fragmentation size distribution by blasting more precise than original Kuz-Ram.

Also from the practical aspects, this study showed that the new version of Kuz-Ram estimates the ROM size distribution more reliable; therefore, it is suggested to apply the new version of Kuz-Ram model at the Sungun Copper Mine, Iran. It should also be noted that the new version itself is lacking of some key factors like timing effects. At the end, it is suggested that a more reliable model to be developed that does not have those lacks which uses a most prefect rock mass classification system other than BI.

REFERENCES

Cunningham C.V.B. 1983, *The Kuz-Ram model for prediction of fragmentation from blasting*, in: Proceeding of the 1st Int. Rock Fragmen by Blasting Symposium. Lulea, Sweden, P.439 –454.

Cunningham C.V.B. Fragmentation estimations and the Kuz-Ram model. In: Proceedings of the Second International Symposium on Rock Fragmentation by Blasting, Keystone, Colorado, USA, 1987. Pp.475 – 487.

Kanchibotla S. S., Valery W., Morell S. 1999, *Modeling fines in blast fragmentation and its impact on crushing and grinding*. In: Proc. Explo Conf., Carlton, VIC, AusIMM, P.137–144.

Djordjevic N. 1999, *Two-component model of the blast fragmentation.* In: Proceeding 6th Int Symp on Rock Fragment by blast. Johannesburg, South Africa, Pp. 213-219.

Ouchterlony F. 2005, *The Swebrec© function: linking fragmentation by blasting and crushing*. Mining Technology: IMM Transaction section A, 2005; Vol. 114, No.1. Pp. 29-44.

Spathis A.T. 2004, *A correction relating to the analysis of the original Kuz-Ram model.* Fragblast- Int J for Blast and Fragment. 8. Pp. 201 – 205.

Gheibie S, Aghababaei H, Hoseinie SH, Pourrahimian Y 2009a, *Modified Kuz-Ram Fragmentation Model and its Use at the Sungun Copper Mine*, Int. J. Rock Mech. Min. Sci. 66: Pp. 967-973.

Gheibie S., H. Aghababaei, S.H. Hoseinie and Y. Pourrahimian, Sanchidrián (ed), 2010, *Kuznetsov model's efficiency in estimation of mean fragment size at the Sungun copper mine,* Rock Fragmentation by Blasting, ©Taylor & Francis Group, London, ISBN 978-0-415-48296-7

A. M. Kiliç, E. Yaşar, Y. Erdoğan and P. G. Ranjith, 2009, *Influence of rock mass properties on blasting efficiency*, Scientific Research and Essay Vol.4 (11), Pp. 1213-1224, Available online at http://www.academicjournals.org/SRE

Kuznetsov V.M. 1973, *the mean diameter of fragments formed by blasting rock*, Soviet Mining Science; 9. Pp.144 –148.

Lilly P.A. 1986, *An empirical method of assessing rock mass blastability*. In: Proceedings of Large Open pit Planning Conference. The Aus IMM, Parkville, Victoria, October, Pp. 89 –92.

Rosin, R., and Rammler, E. 1933, *Laws governing the fineness of coal.* J. Inst of Fuels, 7.Pp. 29 –36.

Cho SH, Nishi M, Kaneko K. 2003, *Fragment size distribution in blasting*. Mater Trans, 44:Pp.1–6.

Maerz NH, Zhou W., 2000, *Calibration of optical digital fragmentation measuring systems*. Int J Blast Fragment (Fragblast), 4(2):Pp.126–38.

Chung SH, Katsabanis PD., 2000, *Fragmentation prediction using improved engineering formula.* Int J Blast Fragment (Fragblast), 4:Pp.198–207.

Gheibie S., Hoseinie S.H. and Pourrahimian Y. 2007, *Prediction of blasting fragmentation distribution in Sungun copper mine using rock mass geomechanical properties.* In: 3rd Iranian Rock Mech. Conference. Tehran, Iran, Pp. 751-756

Moomivand H. 2005, *Development of a method for Blasthole Pattern Design in Surface Mines*. In: 2nd Iranian Open Pit Mines Conference. Kerman, Pp. 159-168

Bhandari. S. 1997, *Engineering Rock Blasting Operations*. Rotterdam, A. A. Balkema.

Comparison of RMR and SRC systems for determination of support requirements

Ali Entezari[1], Ali Farhadian[2], Hossein Mirzaei[3]

1- M.Sc. student of mining engineering. Shahrood University of Technology, Shahrood, Iran
2- Haraz Rah consulting engineers group.
3- Department of mining, petroleum and geophysics, Shahrood University of Technology, Iran

ABSTRACT The rock mass classification methods such as RMR and Q system are widely used in analysis of structure stability and support requirements of underground excavations. In dealing with high tectonized regimes, the RMR system, predicts a lighter support in comparison with those actually installed. To overcome this problem, the SRC system was developed by considering some extra parameters related to geological conditions. In this study, the SRC system employed to evaluate the stability and design of support system for Qazvin–Rasht railway tunnel which is situated in weak rock masses under high tectonic stresses. The results obtained from 20 sections of tunnel, showed that supports proposed by SRC were much closer to the reality than those proposed by RMR.

1 INTRODUCTION

Rock mass classification systems are very useful tools to investigate the stability of underground openings and designing support systems. Various rock mass classification systems such as RMR, Q, RMi and GSI had successful applications in the preliminary design stage of different projects (Bieniawski 1989, Barton et al. 1974, Hoek et al. 1995, Palmström 2000).

Despite the widespread application of the mentioned empirical methods, they cannot adequately calculate stress distributions, support performance and deformations around the tunnels. Therefore it is necessary to evaluate their results in comparison with the results monitored in practice. The RMR system is used broadly in many rocks engineering projects and showed acceptable results (Palmström 2009, Singh, B. & Goel, R.K. 1999). The predictions of this classification system (preliminary support design) in dealing with weak rocks under high tectonic conditions are not agreed with the actually installed support, (Gonzalez de Vallejo 2003).

The Qazvin-Rasht Lot 2 railway project is consisted of 14 tunnels. The seventh tunnel of this project is now excavating. In this tunnel, in some sections, the installed support based on the estimations of RMR system, were not stable and large scale collapses were occurred, as an example one of these collapses is shown in Figure 1. It seems that the underestimation of RMR in this tunnel is related to the high tectonic condition and thin overburden. Surface Rock Classification (SRC) is a new rock mass classification system (Gonzalez de Vallejo 1983, 1985), developed from the RMR to take into account in-situ stress, data from outcrops and tunnel construction conditions such as excavation method and distance to adjacent excavation.

Figure 1. Collapse of tunnel roof in Qazvin-Rasht seventh tunnel.

Application of SRC system is for situations with high horizontal tectonics stresses, low rock strength, thin overburden and highly anisotropic rock behavior show successful results, (Gonzalez de Vallejo 2003).

Therefore, in this paper, the SRC system will be employed to determine rating of rock masses in different sections of tunnel and designation of required support system. Then obtained results will be compared with RMR results.

2 QAZVIN-RASHT RAILWAY TUNNEL

The Qazvin-Rasht Lot 2 railway project is located in the Qazvin province as showed in Figure 2. This project contains 14 tunnels. In this study the seventh tunnel with the length of 594.8 m is considered. Tunnel has a semi-circular (horseshoe) shape and its cross section area is approximately 104 m^2 (for two rail lines), with dimensions of 12.5 m width and 9.4 m height as shown Figure 3.

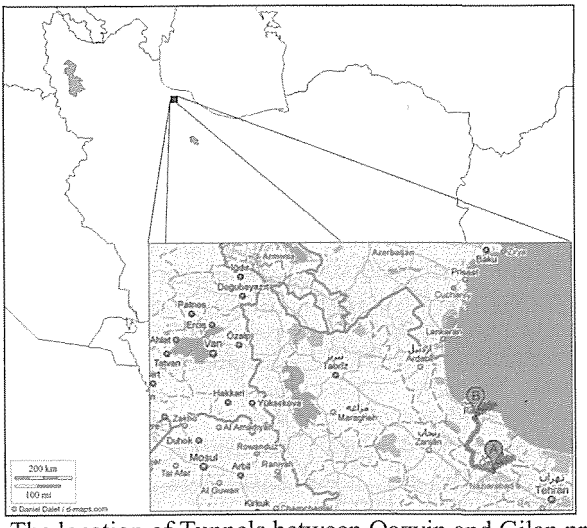

Figure 2. The location of Tunnels between Qazvin and Gilan provinces.

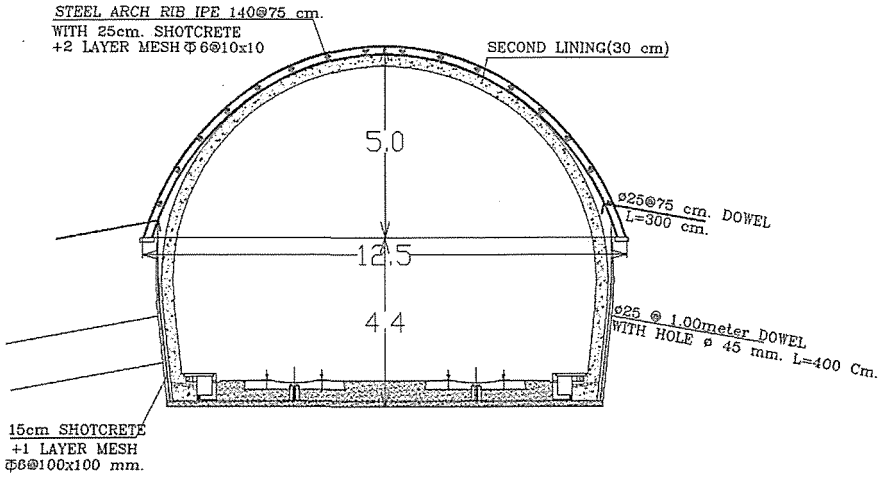

Figure 3. The shape of tunnel cross section and its dimensions.

2.1 Geology

The tunnel site is located in western Alborz orogeny. The type of rock masses is mainly of andesite and also in some parts of basalt. The tunnel portal is consisted of Eocene andesite rocks with two major and two minor joint set. Geological profile of the tunnel is given in Figure 4.

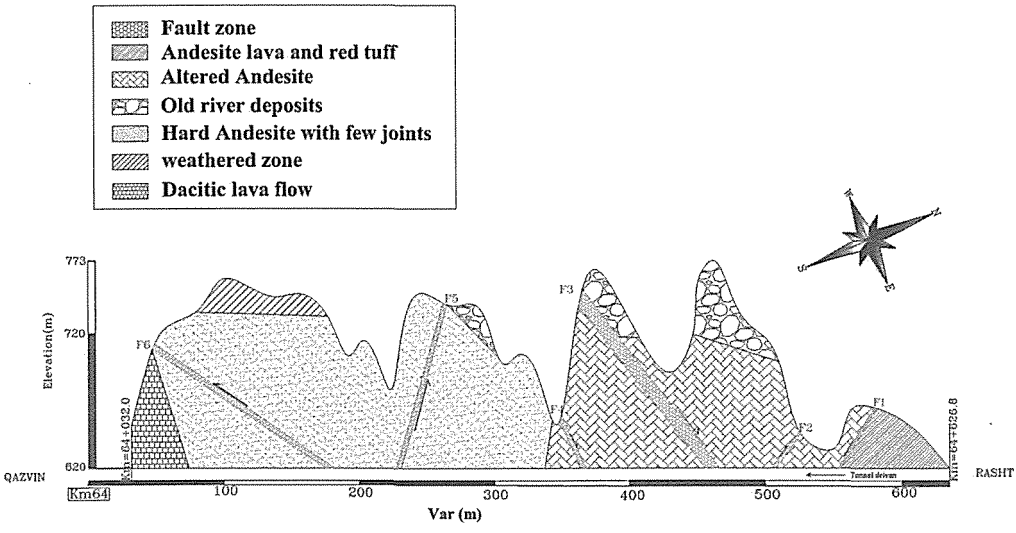

Figure 4. Geological profile of Qazvin-Rasht seventh Tunnel.

2.2 Engineering Geology

The tunnel starts from 64+0.32 to 64+626.8 and the azimuth of its axe varies from 349 to 357. The strike of major joint sets is in eastern north to western south, and western north to eastern south, which are perpendicular to each other. Joints with N30E direction are the most frequent joints

in the site. The average dip of these joints is almost 90°. A stereographic representation of major joint sets is shown in figure 5. These joints are the major joints for about 20 m of tunnel length, 64+ (473-493).

The other major joint sets have a N40W strike and are of complete different geometry. Part of them with a dip of 40-50° and dip direction toward east north; while the other part has a low dip of approximately 10-30°and dip direction toward west south. The minor joint sets are not of noticeable importance. Rocks which are located in middle part of tunnel are highly tectonized.

In parts near the portal outlet, some faults are cutting the trough tunnel direction and had a great effect on stability of tunnel as they caused a great collapse in this region. Clay infilling and infiltration of water into the joints are of other bad parameters that affect the stability and made many problems during the excavation.

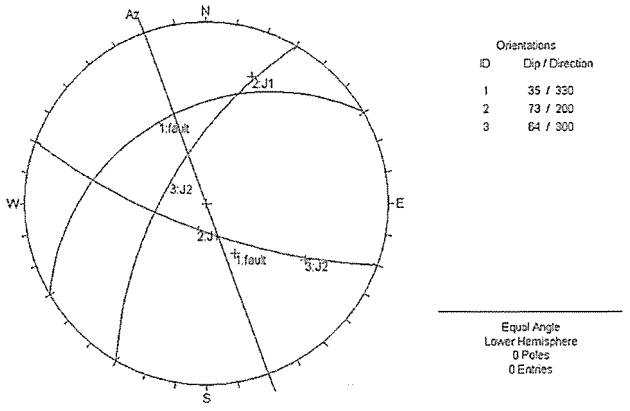

Figure 5. Stereographic representation of major joint sets in a cross section of tunnel.

2.3 Excavation method

As the tunnel has a cross section area of approximately 104 m^2 (for two rail lines), it is classified as large scale excavation. The method used for this tunnel is NATM with two phases of heading and benching. The cutting height is 9.4 m of which 5 m excavate during the heading and the left 4.4 m in benching phase. The excavation method in both phases is drilling and blasting and also in some sections road header is used. Drilling performed by the use of jumbo drill machines and the drill pattern had 80 boreholes with 3 m length.

3 ROCK MASS CLASSIFICATION SYSTEMS

In this paper SRC classification system is employed and rock mass rate is evaluated and compared with the results of RMR system. The RMR system is considers 6 parameters (Uniaxial compressive strength, RQD, Spacing of discontinuities, Condition of discontinuities, Groundwater conditions, Orientation of discontinuities) to determine rock mass rating. The RMR system is well defined in literature and we focus on SRC methodology.

3.1 SRC Method

The surface rock classification (SRC) system (Gonzalez de Vallejo 1983, 1985) was developed from the RMR index to take into account in-situ stress, data from outcrops and tunnel construction conditions.

The SRC is well introduced in Gonzalez de Vallejo's paper, and here only the main table which gives the base SRC ratings is presented, and a brief overview is made up to clear the minds about this issue.

Five parameters are included in SRC system (Tab. 1). In the case of using the data obtained from outcrops, the correction factors must be employed and there is also some correction factors related to construction process that can be found in Gonzalez de Vallejo's paper on SRC. By applying these correction factors, the SRC value will differ significantly, that says the construction method has changed rock mass conditions.

Table 1 - Geomechanics rock mass classification SRC, (Gonzalez de Vallejo 2003).

Rock Quality Indices		Range of values						
1.Intact Rock Strength	Point-Load test (MPa)	>8	8-4	4-2	2-1	Not applicable		
	Uniaxial compressive strength (MPa)	>250	250-100	100-50	50-25	25-5	5-1	<1
	Rating	20	15	7	4	2	1	0
2.Spacing or RQD	Spacing (m)	>2	2-0.6	0.6-0.2	0.2-0.06	<0.06		
	RQD (%)	100-90	90-75	75-50	50-25	<25		
	Rating	25	20	15	8	5		
3.Condithion of Discontinuities	Roughness Continuous Separation Filling	Very rough surfaces. Not continuous joints. No separation. Hard joint wall.	Slightly rough surfaces. Not continuous joints. Separation >1mm. Hard joint wall.	Slightly rough surfaces. Not continuous joints. Separation 1mm. Soft or weathered joint walls.	Slicken-sided surfaces. Continuous joints. Joints open 1-5mm. Gouge materials.	Slicken-sided surfaces. Continuous joints. Joints open <5mm. Gouge materials.		
	Rating	30	25	20	10	0		
4.Groundwater	Inflow per 10 m tunnel length(l/min)	None	<10	10-25	25-125	>125		
	General conditions	Dry	Slightly moist	Occasional seepage	Frequent seepage	Abundant seepage		
	Rating	15	10	7	4	0		
5.State of Stresses	Competence factor	>10	10-5	5-3	<3	-		
	Rating	10	5	-5	-10	-		
	Tectonic structures	Zones near thrusts/faults of regional importance		Compression	Tension			
	Rating	-5		-2	0			
	Stress relief factor[2]	>200	200-80	80-10	<10	Slopes		
						200-80	79-10	<10
	Rating	0	-5	-8	-10	-10	-13	-15
	Neotectonic activity	None or unknown		Low	High			
	Rating	0		-5	-10			

Gonzalez de Vallejo, during comparative analysis between different types of supports used in tunneling and the recommendations obtained from rock mass classifications as RMR and Q, suggests that:

-for good and fair quality rocks, either the RMR or Q systems can be used.

-in week rocks under significant in-situ stress, the SRC classification can predict the rock behavior during excavation better than the RMR.

-use of a particular classification system should consider both the rock mass type and the parameters involved in the classification because different classifications are not

equivalent. Therefore correlations between rock mass classifications are not recommended for poor and very poor quality rocks. SRC is based on the parameters as listed below: Intact rock strength, spacing of the discontinuities or RQD, condition of discontinuity, groundwater inflow, and state of stress.

The last parameter is made up of the following parameters:
Competence factor, Fc, is defined as ratio between uniaxial intact rock strength and vertical stress.

Tectonic structures: considered when significant faults or tectonic structures are present in the area.

Stress relief factor: age of the main tectonic orogeny (in years $\times 10^3$) that has affected the region (Alpine or Hercynian orogeny), divided by maximum thickness of the overburden during its geological history (in meter). This factor is estimated from regional geological data, (Gonzalez de Vallejo 2008).

Seismic activity: considered if the area has a history of significant seismic activity.

In SRC method similar to RMR method, rock mass rated from 0 - 100 and then rock mass class and suggested support system is selected with the use of Guidelines for excavation and support of 10 m span rock tunnels according to the RMR System, which is introduced by Bieniawski in 1989.

Table 2 – SRC Class number selection, (Gonzalez de Vallejo 2003).

Class number	I	II	III	IV	V
Rock quality	Very good	Good	Fair	Poor	Very poor
Rating	100-81	80-61	60-41	40-21	≤20

4 COMPARISION OF RMR AND SRC SYSTEMS

In this study, 40 sections of the tunnel with the length of approximately 558 m from excavated part of the project were considered. The ratings of surrounding rock mass in different sections were determined using RMR and the mentioned SRC classification methods. Then the class of rock mass in each section was recognized according to its rating value for both methods and the required support system was designed by the results of the RMR and SRC methods and compared with the actually installed support systems.

4.1 RATING OF ROCK MASSES

In SRC method, the score of each parameter was determined with the use of Table 1 and the rating of rock mass was calculated from all of affecting parameters. Then the base SRC rating was adjusted by considering the other rock engineering factors according to the correction factors, which are provided in Gonzalez de Vallejo's paper on SRC.

The results of rating of rock mass for both classification methods for different sections are listed in Table 3.

4.2 SUPPORT DESIGN AND COMPARISION OF THE RESULTS

For different sections, the classes of surrounding rock mass and suggested support systems for both systems were selected from Table 2, which is based on RMR's class selection, due to their corresponding rating values and listed in Table 3. Then to evaluate the accuracy of these classification methods, their recommended support systems were compared with actually installed support systems.

According to the results of RMR and SRC, in sections with thin overburden and high tectonic conditions, RMR suggested lighter support systems in comparison to SRC.

In table 3, abbreviations L, M, H and VH stands for Light, Medium, Heavy and Very Heavy steel sets. Very Heavy is inserted for rating lower than 10, Heavy for lower than 20, medium for lower than 30 and light for lower than 40, except for support in practice

column, which shows the real support type installed in tunnel.

Table 3 - Comparison of RMR and SRC results.

Section No.	SRC			RMR			Support in practice
	Class	Value	Support	Class	Value	Support	
1	IV	24	Steel Ribs (M)	IV	40	Steel Ribs (L)	Steel Ribs (H)
2	IV	27	Steel Ribs (M)	III	51	Mesh +10cm shotcrete	Steel Ribs (M)
3	IV	32	Steel Ribs (L)	III	54	Mesh +10cm shotcrete	Steel Ribs (L)
4	IV	32	Steel Ribs (L)	III	54	Mesh +10cm shotcrete	Steel Ribs (L)
5	IV	32	Steel Ribs (L)	III	58	Mesh +10cm shotcrete	Steel Ribs (L)
6	IV	27	Steel Ribs (M)	III	58	Mesh +10cm shotcrete	Steel Ribs (L)
7	V	18	Steel Ribs (H)	III	44	Mesh +10cm shotcrete	Steel Ribs (M)
8	V	18	Steel Ribs (H)	III	44	Mesh +10cm shotcrete	Steel Ribs (M)
9	V	14	Steel Ribs (H)	IV	35	Steel Ribs (L)	Steel Ribs (H)
10	V	4	Steel Ribs (VH)	IV	35	Steel Ribs (L)	Steel Ribs (VH)
11	V	9	Steel Ribs (VH)	IV	33	Steel Ribs (L)	Steel Ribs (VH)
12	V	9	Steel Ribs (VH)	IV	33	Steel Ribs (L)	Steel Ribs (VH)
13	V	11	Steel Ribs (H)	IV	38	Steel Ribs (L)	Steel Ribs (H)
14	III	42	Mesh +10cm shotcrete	III	50	Mesh +10cm shotcrete	Steel Ribs (L)
15	III	50	Mesh +10cm shotcrete	III	50	Mesh +10cm shotcrete	Mesh +10cm shotcrete
16	III	60	Mesh +10cm shotcrete	III	60	Mesh +10cm shotcrete	Mesh +10cm shotcrete
17	III	50	Mesh +10cm shotcrete	III	60	Mesh +10cm shotcrete	Steel Ribs (L)
18	III	50	Mesh +10cm shotcrete	III	60	Mesh +10cm shotcrete	Steel Ribs (L)
19	III	60	Mesh +10cm shotcrete	III	60	Mesh +10cm shotcrete	Steel Ribs (L)
20	IV	32	Steel Ribs (L)	III	50	Mesh +10cm shotcrete	Steel Ribs (L)

5 DISCUSSION AND CONCLUTIONS

In this study, approximately 558 m of excavated part of the Qazvin-Rasht tunnel was considered and the results of the widely used rock mass classification method, RMR and new developed rock mass classification system, SRC were evaluated and the required support system for tunnel were predicted by both of systems and compared with the actually installed support system. The SRC system was developed on the basis of RMR with some additional parameters. The main difference between these two classification methods is that SRC brings together the RQD and Spacing parameters as one parameter and it adds Stress State to the classification. The "State of Stress" parameter includes: competence factor, tectonic structures, stress relief factor and neotectonic activity. So it is expected that in underground structures under high tectonic and high in-situ stress conditions, the SRC shows proper results. Comparison of the results of the mentioned two classification

method for the Qazvin-Rasht tunnel shows that:

- In the sections of tunnel in which the tectonic structures affect the behavior of surrounding rock mass, the rating of SRC is smaller than RMR. So SRC propose a heavy support system with respect to RMR that is more proper than RMR designation in comparison to actually installed support systems.
- In some sections of tunnel in which the overburden thickness is low the prediction of SRC method is near to actually installed supports.
- In the parts of tunnel in which tectonic conditions don't affect the stability, the ratings of RMR and SRC are nearly similar to each other.

REFERENCES

Barton, N.R., Lien, R., Lunde, J., 1974. *Engineering classification of rockmasses for the design of tunnel support*. RockMech. 4, 189–239.

Bieniawski, Z.T., 1989. *Engineering Rock Mass Classifications*. Wiley, New York.

Gonzalez de Vallejo, L.I., 2003, SRC rock mass classification of tunnels under high tectonic stress excavated in weak rocks, *Engineering Geology*, 69, pp. 273–285.

Gonzalez de Vallejo, L.I., and Hijazo, T., 2008. A new method of estimating the ratio between in situ rock stresses and tectonics based on empirical and probabilistic analyses, *Engineering Geology*, 101, pp. 185–194.

Hoek, E., Kaiser, P.K., Bawden, W.F., 1995. *Support of Underground Excavations in Hard Rock*. Balkema, Rotterdam. Pp. 215.

Singh, B. and Goel, R.K., 1999, *Rock Mass Classification, A Practical Approach in Civil Engineering*, Elsevier, pp 34-46.

Palmström, A., 2000. Recent developments in rock support estimates by the RMi. *Journal of Rock Mechanics and Tunnelling Technology*. 6 (1), 1–19.

Palmström, A., 2009. Combining the RMR, Q, and RMi ' classification systems, *Tunnelling and Underground Space Technology*, Volume 24, Issue 4, pp. 491-492.

The Introduction of UK Rock Bolting Technology into Coal Mines around the World

Dr.Graham Daws
Graham Daws Associates Ltd, England

Andrew Oxley
Minova Weldgrip UK Ltd, England

N. Woodward
Rockbolting Technology Ltd

ABSTRACT Many mines around the world have been seeking ways to achieve sustainable developments and reduce operating costs. Rockbolting is a technology that needs to be considered as it provides a means of reducing operating costs and improving safety whilst allowing improved production to be achieved. The problem is how to introduce this technology in the knowledge that a successful outcome will be achieved. The authors have considerable experience in the introduction of UK rock bolting technology in many large underground coal mines around the world. Rockbolting is a complete package and not only includes the consumable materials but also initial design, training, production of Codes of Practice, monitoring schemes and long term management of the systems. All of these aspects are considered in this paper. The role of long tendon reinforcement is discussed as part of the initial design and also as a response to monitoring information. This paper explains the methods that have been applied for the successful introduction of rockbolting technology and discusses several case studies. It is intended to allow decision makers to gain a basic understanding of the method used to successfully introduce current state of the art rockbolting technology to a mine.

1 INTRODUCTION

Rock bolting as sole roof support in coal mines in the UK was introduced in the late 1980's by the British Coal Corporation, mainly as there was a need to improve productivity to match coal prices on the world market, whilst maintaining or improving safety standards.

British Coal delegations visited several coal producing countries and noted the rapid adoption of rockbolting techniques, particularly in the US and Australia. As Australian conditions were more similar to UK conditions than the generally favourable US conditions, progress in Australia was monitored closely. It was apparent that rockbolting consumables used in Australia had been formulated to cater for the demands of sole support

In 1987, it was decided to commence with a full scale trial of rockbolting with the objective of progressing onto sole support of a roadway by rockbolts. Previous to this rockbolts had been trialled in low risk, non strategically important sites such as new face lines in conjunction with steel standing supports and face salvages.

Wistow Mine in the Selby Complex was chosen as the trial site. In order to ensure compatibility with Australian techniques, all required consumables were imported from Australia for this trial. Experience in Australia had shown that the following

parameters were essential to the success of rockbolting in coal mines.

- An understanding of the in situ stress regime, particularly the influence of horizontal stress
- Detailed information on immediate roof strata properties
- Information on the bond strength between the resin and rock
- The use of sophisticated monitoring methods to measure rockbolt performance and ground behaviour

These techniques were also adopted as part of the trial at Wistow Mine.
Following the successful trial, consumables, equipment and design techniques were further developed in the UK and the technology has been developed over the last 20 years to the current situation where this technology is now exported overseas.

Three companies in combination have joined together to form a partnership known as Rockbolting International where all aspects of this work are covered from concept, through design, training and installation to ongoing maintenance of all the systems to allow rock bolting technology to be applied safely and long term. The companies and their expertise are as follows;

Minova Weldgrip UK:
- Materials and equipment supply
- Training
- Compilation of documentation

Graham Daws Associates Ltd:
- Design of systems and analysis of monitoring results
- Classroom training and presentation of courses
- Compilation of documentation
- Implementation of the systems

Rockbolting Technology Ltd:
- Classroom and underground training
- Implementation of the systems
- Installation of monitoring equipment

The use of partnerships removes compatibility and responsibility issues with multiple suppliers and representatives. The projects are usually led by a small, very experienced team of 3 people.

2 METHODOLOGY

The introduction of rock bolting is carried out in three phases;

- Phase 1 Rock bolting assessment
- Phase 2 Trials
- Phase 3 Sole support

2.1 Phase 1: Rock bolting assessment

This commences with an underground site visit and discussion with the mine management. It will also consider during this time, the types of existing support systems in use and their effectiveness, the geological environment and rock properties, particularly near seam, the stress regime and its effects on roof and ribs, roadway size, use and life span.

The discussions would be extended if the prospects look favourable to include local and possibly national unions, mines inspectors and relevant senior company staff, to ensure they understand the process and the approach to the introduction of rock bolting and answer any questions. The financial implications would be discussed which generally offer significant cost and operational benefits.
From this assessment a report would be finalised giving recommendations normally to proceed to the trial phase.

2.2 Phase 2: Trials

If the assessment recommends trials can be carried out and is agreed by all parties then suitable equipment and consumables are purchased for the trials. Rock bolting machinery, drilling consumables and rock bolts and associated consumables are purchased. Following this, underground trials are carried out to prove rock bolts can be installed successfully, different drill bits are trialled, the most effective bit type is then used for short encapsulation pull tests to prove adequate bond stress can be generated with the chosen system of drill

machine, drill rod, drill bit, rock bolt and resin. The compatibility of all these components is critical to the success of the trials, with all the support consumables being covered by a British Standard 7861 part 1 [1] . This ensures minimum standards for all components and ensures lesser alternatives are not purchased which can prejudice trials and ongoing support performance underground. Roof cores will also be taken at this stage and these will be logged and tested to establish lithology; fracture frequency, type and condition; RQD; UCS and modulus of each rock unit; Rock Mass Rating (RMR) and Coal Mine Roof Rating (CMRR) of the immediate roof. This information will be used to confirm that the structure is adequate for sole support by rock bolts and used to design initial rockbolt patterns.

This information along with all aspects that may affect a sole supported roadway are considered and compiled in a geotechnical appraisal and design document. This confirms the suitability of the site and factors taken into consideration include other potential influences such as environmental factors and roadway use. The design document will detail a rock bolt pattern for the roof and ribs which is then drawn up into a ground control rule, which details how the bolts are to be installed safely and the pattern and spacing to be used.

Ongoing consultation with unions, mines inspectors, workmen, line managers and senior management is critical to ensure opposition to rock bolting is kept to a minimum. A transparent monitoring system and educational training system is offered to all levels within the organisation to ensure all staff develop their knowledge base at the same time and to a minimum level.

For training a simple format is used;

- Surface familiarisation with equipment and consumables
- Surface training on theory and best practise
- Underground rock bolt installation training
- Underground rock bolt monitoring tell tale installation training
- Underground site supervision for setting the full support cycle stage 1 – free standing steel supports with supplementary rockbolts
- Underground site supervision for setting the full support cycle stage 2 – Sole support by rock bolts followed by the setting of free standing steel supports immediately behind the rock bolts
- Underground site supervision for setting the full support cycle stage 3 – Sole support by rock bolts

Training is carried out by a small team of experienced miners who carry out shift coverage on site. These people have international experience on the introduction of rockbolting to coal mines and will train the mine staff in all aspects of rock bolt installation and problem solving.

It will be necessary to set action levels before a trial is commenced in order to give guidelines for the possible onset of roof dilation leading to eventual failure. These action levels may be conservative in the early stages of a trial and will be refined as more data is gathered which will allow a "footprint" to be determined regarding strata movement and the action of the rockbolts in achieving stability.

At the same time underground trials are being carried out it is normal practice to appoint an individual from senior management from the mine to oversee rock bolting. This function is called a rock bolting co-ordinator, with specific duties within the mine structure.

During the trial phase sophisticated monitoring devices comprising sonic extensometers and strain gauged rock bolts will be installed to show the roof movement and bolt loadings around the excavation. The results are analysed and used to verify the support design pattern.

This process is both time and distance dependant, with sufficient time and distance required to establish stable trends on the monitoring systems. Tell tales are installed at regular intervals of maximum 20m. These

are simple, easy to read devices which indicate roof movement and its location either below or above the rock bolted height. From these results the rock bolt pattern and spacing can be modified to account for excessive or biased loading on the bolts and roof dilation. An example of three different scenarios of roof dilation is given in Fig. 1 and show distance into roof versus displacement plots for three scenarios involving a roadway initially supported by the use of 2.4m long roofbolts. All three scenarios are described below. When deciding upon remedial actions, the distance into roof versus strain graph and the time dependant plots should also be consulted.

2.2.1 Scenario A: Typical normal roof displacement

Figure 1 shows total roof displacement over the 7 m monitored height of 10mm of which 2mm is above the bolted height and 8mm within the bolted height. A vertical line, shown dotted on Fig. 1 is drawn from the point where the extensometer graph intersects the horizontal line representing the bolted height in order to determine the above values.

In this case, the rockbolts are controlling roof movement and no further action is required.

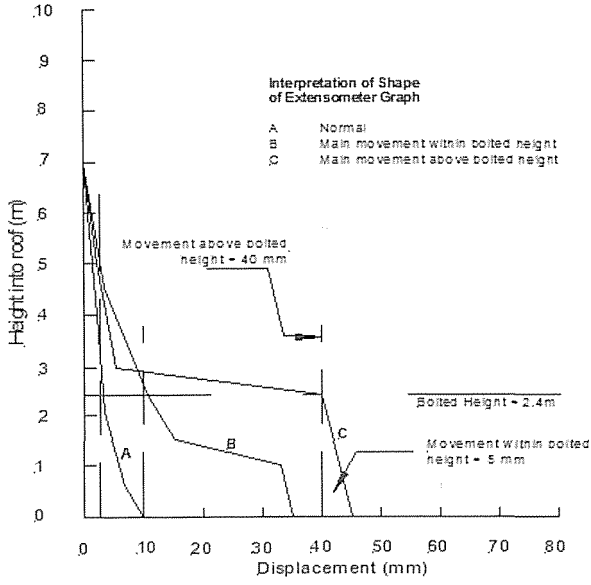

Figure 1. Total roof displacement

2.2.2 Scenario B: Movement within the bolted height

Figure 1 shows total roof displacement over the 7m monitored height of 35mm of which 10mm is above the bolted height and 25mm within the bolted height.

In this case, the bolting pattern is insufficient to control dilation within the bolted roof beam and additional spot bolts are required.

2.2.3 Scenario C: Movement above the bolted height

This graph shows total roof displacement over the 7m monitored height of 45mm of which 40mm is above the bolted height and 5mm within the bolted height.

In this case, there is very little dilation within the bolted roof beam but the whole beam is detaching from a parting plane / clay band / zone of weakness located, in this example at about 3m into the roof. Long tendon reinforcement is required in order to anchor the roof beam into the more competent, non dilating strata above.

2.3 Phase 3: Sole support

After a brief period the system used is assessed and the monitoring results, along with underground observations, rock bolt installation standards and the attitudes of both the workmen, management and unions are all considered and a final recommendation is given on the ability of the mine to proceed to sole support.

Once sole support is established then the ongoing maintenance of the support system requires regular monitoring readings, regular inspections and this gives a progressive knowledge base for all mine staff. Normal practice is to utilise rock bolts initially in face access gate roads, over time this then normally expands to face junctions, face lines, lateral roadways and lateral junctions. As the knowledge at each mine increases the application of rock bolting techniques and ground control improves.

3 COLLATION OF EXPERIENCE AND APPLICATION IN FUTURE DEVELOPMENTS

In some mines the geotechnical environment does not remain constant and various features may influence the stability of rockbolted roadways. Examples include:

- Interaction effects from previous workings in other seams (i.e. crossing pillar edges)
- Intrusions of weak roof rocks which may converge or lift away from existing good roadway roofs
- Seam splits

In such cases available information should be collated and used in future designs at the mine. For example, in the UK weak areas of highly listricated Mudstones are sometimes present in the roof of certain seams and as these lift away from or converge onto roadway roofs, high levels of movement are experienced. In order to ensure good conditions and minimise or reduce time consuming remedial works, long tendon reinforcement, particularly Flexibolts, are installed at the head end as part of the normal bolting cycle. Length and density are determined by analysis of monitoring results where these conditions have been experienced in the past.

Similarly, it is common practice to increase bolt density on either side of pillar edges in longwall gate roadways. Although good conditions are sometimes experienced on drivage under or above such pillar edges, the increased stress regime created on retreat often gives rise to poor conditions in such areas. Consequently, the small additional time required to install an increased bolt density on drivage is often preferable to the need to install long tendon reinforcement on retreat after movement has started.

4 CASE STUDIES

- Phalen mine Nova Scotia Canada
- Sulcis mine Sardinia Italy
- Tabas mine Iran
- Aberpergwm mine South Wales UK

In all cases a similar approach is taken and this comprises the following:

i. Initial assessment
ii. UG cores / drill bit trials short encapsulation pull tests
iii. Geotechnical assessment /design document
iv. Purchase drilling equipment and consumables
v. Surface training of workforce, including theory of rockbolting
vi. Underground training of workforce
vii. Rockbolting trials & monitoring
viii. Sole support

4.1 Phalen colliery

Phalen Colliery was located on the North East coast of Nova Scotia, Canada and

mined coal from the Phalen Seam which dipped gently out below the Atlantic Ocean. The seam was 2.5m to 3m thick with no known faulting and dipped at about 1 in 8 to 1 in 10. Consequently, the gate roadways were driven on strike and the longwall face retreated at a slight angle to the gates in order to lessen dip along the face line. There were overlying workings in the Harbour Seam located about 140m away and worked by the neighbouring Lingan Colliery.

Increase in working depth undersea (+550m) and increase in single entry drivage length i.e. Main and Tail Gates of up to 3.5km prompted interest in roofbolts as prime means of support. The existing supports of steel squarework were suffering considerable deformation on longwall retreat necessitating expensive and time consuming repair work.

The Colliery organised some initial trials in house and used US rock bolt consumables in association with the steel squarework. Initial trials were not promising and movement could not be controlled. The steel rockbolts were changed to a stronger design but movements still could not be controlled.

Graham Daws Associates Ltd (GDA) were invited to examine the problems as they were working on the rockbolting design for the undersea Point Aconi cooling water intake tunnel nearby.

Limited monitoring had been installed and consequently some results were available. It was found that the roof of the Phalen Seam was very similar to UK conditions and unlike those in the US, i.e. there was no immediate Sandstone bridging beam and consequently stiff resins were needed in order to give good load transfer characteristics and allow the rockbolts to provide confinement to the roof.

US resins were not stiff and the manufacturer was unconvinced that this was the problem, citing good pull out test results. They did not appreciate that in addition to a good bond strength a stiff resin was required in order to transfer load to and from the rockbolt. Consequently, UK specification AT resin was imported and with reduction in drill hole diameter to 27mm, the use of Wombats and a reduction in roadway width from 5.5m to 4.8m, a phased trial commenced.

The phased trial was conducted in 5 East Bottom Drivage (5's East Main Gate) and used rockbolts and steel sets initially, then open out spacing of steel before progressing to sole support. Sophisticated monitoring was used to provide detailed information on rockbolt performance.

Detailed training courses for both management and workforce were carried out and a manual was produced explaining how rockbolts work in coal mine situations.

There was much resistance from Unions initially with sabotage of tell tales being encountered to give the impression of large roof movements. They hadn't reckoned with sonic extensometers and so the true movements were known and found to be within the limits proscribed.

Roofbolting proved to be a great success and was adopted in all main and tail gate drivages and face salvages and was critical to mining at greater depths. Also cable bolts were introduced to support large span excavations and junctions.

The systematic phased approach combined with extensive detailed monitoring allowed for the success of the programme.

The mine experienced the condition known as back swamp facies in some areas where weak listricated Mudstones were converging on or moving away from the roadway roof. Cable bolting was used to control such situations.

4.2 Sulcis mine

Sulcis Mine is located in the South West corner of Sardinia and mining has taken place in the region since 1885. The present mine was developed in the early 1940's with shaft systems at Seruci and Nuraxi Figus and developments have continued.

The Sulcis coal basin represents the only sub bituminous coal deposits in Italy. The nearest condition that existed at the time of

deposition resembled those of the Florida Everglades. The coal seam or Produttivo is up to 30m thick within the take of the mine and comprises of 10 separate seams separated by Limestone bands. Consequently, the geology is very changeable. The main seam worked at the mine is the upper seam known as Seam 10.

The high cost of supports and slow drivage rates prompted consideration of roofbolting. However, there was concern over hard roof conditions with some Limestone having a UCS of up to 200 MPa. Drillability was considered a major issue and some previous trials had been unsuccessful.

The first step was to carry out drilling trials and these proved to be successful using modern lightweight pneumatic rotary roofbolting machines.

A staged approach to the introduction of roofbolting was planned using UK advanced technology rockbolting consumables.

The initial trial was planned for E1 GdT but a 4m upthrow fault was encountered on the day the trial commenced. However, tens of metres of bolting was installed in conjunction with flat top TH supports. This proved to be a good training ground as the workforce could see the effectiveness of bolts in heavy conditions

A new trial site in W2's GdT was selected and a phased approach was adopted in conjunction with extensive classroom training. This consisted of 2 full weeks on two separate shifts in the year 2000, the longest and most comprehensive course presented at that time. Experienced underground trainers were used to impart knowledge and confidence to the workforce.

Very accurate monitoring was used to assess the performance of the rockbolts. The Rockbolts were installed in conjunction with TH flat top arches at 1m spacing. Initially movement was experienced along clay rich parting planes. Bolt patterns were modified in response to the monitoring. Design techniques using Rock Mass Classification systems were developed and refined to meet changing conditions at the mine.

Following favourable monitoring results the roadway progressed to the next stage where steel supports were set at 2m intervals. Further monitoring showed that the bolts were performing a sole support function and so the roadway progressed to sole support by roofbolts.

The mine has now used bolts extensively for the past 9 years, including main drivages and junctions. Monitoring is still the key to success as the geology constantly changes.

4.3 Tabas coal mine

This new coal mine was developed in the Eastern part of Iran in the desert area about 70 kilometres from the oasis town of Tabas, It was the first mechanised longwall mine in Iran and was planned by UK based consultants. The consultants also provided the project management and the training required to develop the mine.

There was history of small, hand worked, mines in the area generally mining at quite shallow depths. The major deposit dipped down from outcrop in the desert at about 1 in 4.

The main declines from the surface were supported by steel arches as the area is seismically active. However, roofbolting of gates was planned from the outset, but sparse geological/geotechnical information existed. Due to the strata gradient, the Main and Tail Gates were driven on strike.

The design methods developed in Sardinia and refined in UK were used. The geological information from surface boreholes suggested weak roof conditions and this information was used for design purposes. From the outset it was planned to use UK advanced technology rockbolting consumables and the complete package was imported into Iran.

Once the declines had reached the horizon of the first Tail Gate, this roadway was commenced. After a suitable distance supported by flat top steel supports to move away from the stress effects of the decline, a roofbolting trial commenced.

A phased approach was adopted for the introduction of the roofbolting and

classroom training for the management and workforce was carried out. Experienced underground trainers from the UK were used to impart knowledge and confidence to the workforce.

Very accurate monitoring was used to assess the performance of bolts. The bolts were initially installed with TH flat top arches at 1m spacing. Very little movement was experienced as underground conditions were better than the surface boreholes suggested.

The project progressed rapidly to the next stage where steel supports were set at 2m intervals with the same bolting pattern as previously used. Further monitoring showed the bolts were performing a sole support function and consequently the roadway progressed to sole support by roofbolts. Some unanticipated faulting was experienced in the gate but this was dealt with by increasing bolt density and proved to be a good training exercise.

The mine has used bolts extensively for the past 5 years and now sources some consumables, notably mesh locally. This initially gave some problems as the Iranian management were unaware of the high tech specification required and did not realise that bolting consumables have been developed over many years and perfected to the current state where the whole package is compatible yet easy to use.

4.4 Aberpergwm colliery

Aberpergwm Colliery is located in the Neath Valley in South Wales, UK. It was developed by the National Coal Board in the 1960's as a drift mine to extract the valuable anthracite coal. The mine closed during the general run down of the coal industry in the early 1980's.

Following privatisation of the UK coal industry, the mine was re opened in 1998 and a new seam of coal, the Eighteen Feet Seam, was entered in 2008. It was considered by the mine management that this seam had a good potential for support by rockbolts but this technology had not previously been introduced into South Wales in gate roadways.

After discussions with the workforce and unions it was decided to initiate a rockbolting trial. Consequently, at the end of June 2009 a trial was commenced in S2's Gate whereby rockbolts were installed in addition to the steel standing supports with the aim of introducing rockbolts as the sole means of support should the trial prove to be satisfactory.

Comprehensive monitoring comprising sonic roof and rib extensometers and strain gauged rockbolts were used to assess the role of the rockbolts in providing support and confinement to the strata.

Instrumentation indicated stabilising trends very quickly. Strata movement was low with a maximum of 3mm being recorded in the roof. It was anticipated that rib movement may have been a problem but the rib bolts contained the ribs very well with a maximum of 90mm being recorded and remained stable

Based on the instrumentation results it was planned to progress to sole support by rockbolts but unfortunately a fault / disturbance was encountered moving across the roadway from the left hand side. Consequently it was decided to pull back from the head end and drive a cross gate in order to mine areas away from this disturbance.

The results from the trial showed that the Eighteen Feet Seam had a good potential for rockbolting to succeed and consequently another trial site was scheduled.

S3's Return was chosen as the new trial site and from the outset it had been proposed to use a Beretta track mounted drilling machine to install the rockbolts rather than the gopher leg mounted roof bolting machine and turmag hand held rib bolting machines used in S2's Gate. This had the advantage of enabling longer, 2.1m rib bolts to be installed in the new trial site as part of the bolting pattern.

Rockbolting was introduced into S3's Return in a phased manner, initially in conjunction with flat top steel standing supports. Comprehensive monitoring

comprising sonic roof and rib extensometers plus strain gauged roof bolts were installed to verify the performance of the rockbolts. As in S2's a stabilising trend was established very rapidly with a maximum roof movement of 1.5mm and consequently S3's Return progressed onto sole support by rockbolts.

This trial was significant as it proved to management and the workforce that rockbolts could be successfully employed in the South Wales coalfield.

Aberpergwm continues to use roofbolting and in March 2011 started their first room and pillar section completely supported by rockbolts.

5 CONCLUSIONS AND RECOMMENDATIONS

If a mine is considering introducing roofbolting for the first time, the authors consider that the following issues are important.

i. Open and truthful discussions between the mine personnel and consultants regarding the aspirations of the mine and the standard and adaptability of the workforce.

ii. Classroom training so that all personnel gain an understanding of rockbolting technology and how it can be implemented

iii. The employment of experienced trainers who can work alongside the workforce and impart knowledge and confidence.

iv. The employment of experienced engineers who have worldwide experience in roofbolting systems in a variety of geological settings to establish and oversee the project.

v. A phased approach to the introduction of roofbolting, with the use of sophisticated monitoring for design verification

vi. Continued monitoring to verify the performance of the rockbolting system

REFERENCES

Strata Reinforcement Support System Components used in Coal Mines – Part 1 Specification for Rockbolting British Standard, 2007. BS 7861- 1

Development of Cuttability Abacuses in Diamond Wire Cutting Method on Limestone Sample

Bir Kireçtaşı Numunesi için Elmas Tel Kesme Yönteminde Kesilebilirlik Abağının Geliştirilmesi

Y. Özçelik
Hacettepe Üniversitesi, Maden Mühendisliği Bölümü, Ankara

E. S. Kanbir
Ahi Evran Üniversitesi, Kaman Meslek Yüksekokulu, Doğal Yapı Taşları Teknolojisi Programı, Kırşehir

ABSTRACT The purpose of this study is to develop cuttability abacuses in diamond wire cutting method with single bead test machine on limestone sample. Therefore, single bead test machine that can best reflect the field conditions was developed in Hacettepe University Department of Mining Engineering and studies were made by using this machine. Cuttings on exclusively designed 300 diameter samples taken by using core drill were performed at four different peripheral and hoop rotation speeds. A cuttability abacuses in diamond wire cutting method taking into consideration the cutting rate with diamond wire and unit wear on diamond bead was developed with Design Expert 7.0 software for Sivrihisar Beige limestone sample by using the results obtained.

ÖZET Bu çalışmanın amacı, bir kireçtaşı numunesi üzerinde tek boncuk test cihazı ile kesimler yaparak, elmas tel kesme yönteminde kesilebilirlik abağının geliştirilmesidir. Bu amaçla kesimlerde Hacettepe Üniversitesi Maden Mühendisliği Bölümü'nde geliştirilen ve arazi şartlarını en iyi şekilde yansıtabileceği düşünülen tek boncuk test cihazı kullanılmıştır. Özel olarak hazırlanmış 300 mm çaplı karotiyer kullanılarak alınan numuneler üzerinde dört farklı çevresel hız ve dört farklı kasnak devir hızında kesimler yapılmıştır. Elde edilen sonuçlar kullanarak Design Expert 7.0 paket programı ile Sivrihisar Bej kireçtaşı numunesi için elmas telle kesme hızı ve elmas boncuktaki birim aşınmayı göz önüne alan kesilebilirlik abağı geliştirilmiştir.

1 INTRODUCTION

Today, diamond wire cutting method is widely used in marble quarries. In this method, regular geometric shape blocks are taken out from a rock mass using diamond bead on the wire.

Despite its short history, diamond wire cutting machine has gained a strong place in operation in several sectors thanks to the advantages it brings. Particularly, such advantages as speed, security, easy access to the final product, not requiring an operator during manufacturing, which are not offered by its alternatives, have increased the demand for the machine (Hanecioglu 2006).

Machines used in diamond wire cutting method are fixed investments for a marble quarry business. The variable costs in this method are the diamond beads. The wear control on diamond beads helps decrease costs in a business. Besides, the most essential issues in diamond wire cutting method are determining the economy of a marble business and the amount of wearing on the beads, which mostly affects business economics, before performing cutting, detecting whether the diamond bead to be

used is suitable to the rock and arranging the conditions accordingly (Ozcelik 1999).

Some studies are made for the purpose of controlling the wearing on diamond beads, which makes up the variable costs in diamond wire cutting method. However, since these studies are made under quarry conditions, several problems emerge during the process. Foremost among them are working difficulties due to environmental conditions, working costs and waste of time. Considering these difficulties, Single Bead Test Machine was developed in Hacettepe University Mining Engineering Department and thus cutting works can be performed under laboratory conditions (Ozcelik 2008).

In order for the natural stone manufacturers to make the suitable diamond bead selection, it is necessary to determine the properties of the rock to be cut, the cutting conditions and the relationship between these and the diamond bead parameters to be used. It is a fact that the physical, mechanical, mineralogical and petrographical properties of the rocks and cutting conditions are effective on the wearing occurred on diamond beads and cutting rate. Therefore, it is an essential issue that the effects of physical, mechanical, mineralogical and petrographic properties of the rocks to be cut and cutting conditions on the wearing of diamond beads and their relationships with diamond bead parameters be known. By means of this information it can be maintained that the cutting parameters are adjusted and optimum cutting conditions are determined. The parameters generally affecting the cutting parameters in diamond wire cutting method are shown in Table 1 (Ozcelik 1999). Therefore, it is aimed to determine the optimum machine working conditions (peripheral speed and hoop rotation speed) and also to develop cuttability abacuses for the diamond wire cutting in terms of considering unit wear and cutting rate by using a special statistical program (Design Expert 7.0) in this study.

Table 1. The parameters affecting cutting performance in diamond wire cutting method

Fixed Parameters Non-controlled parameters	**Partially-controlled or controlled parameters**	
	Properties of cutting tools and equipment	**Environmental and working conditions**
• Rock hardness • Rock strength • Water content • Degree of alteration • Discontinuities • Mineralogical properties and textural characteristics	• Machine power • Structure of diamond wire and bead structure • Dimensions of block • Cutting geometry of the wire during cutting duration • Machine vibration • Water consumption • Hoop diameter • Number of beads per meter	• Qualified personnel • Technique used

2 WORKING METHODOLOGY

The method used within the scope of experimental studies made by using Single Bead Test Machine is shown in Figure 1.

In the studies conducted with single bead test machine, two different parameters were used as the bead motor rotation speed that moves the diamond bead and the motor rotation speed of the marble sample on which the rock to be cut is attached. Bead motor rotation speed were chosen at the values of 1600, 1800, 2000 and 2200 rpm, marble sample motor was chosen at the values of 200, 240, 270 and 300 rpm. While choosing these parameters, machine working parameters implemented on the field with the diamond wire cutting machine were considered. The peripheral speed and the hoop rotation speed on the diamond wire cutting machine correspond to bead motor

rotation and sample motor rotation on the single bead test machine. The equivalents of these on fields were put forth by Kanbir (2007) and shown in Table 2.

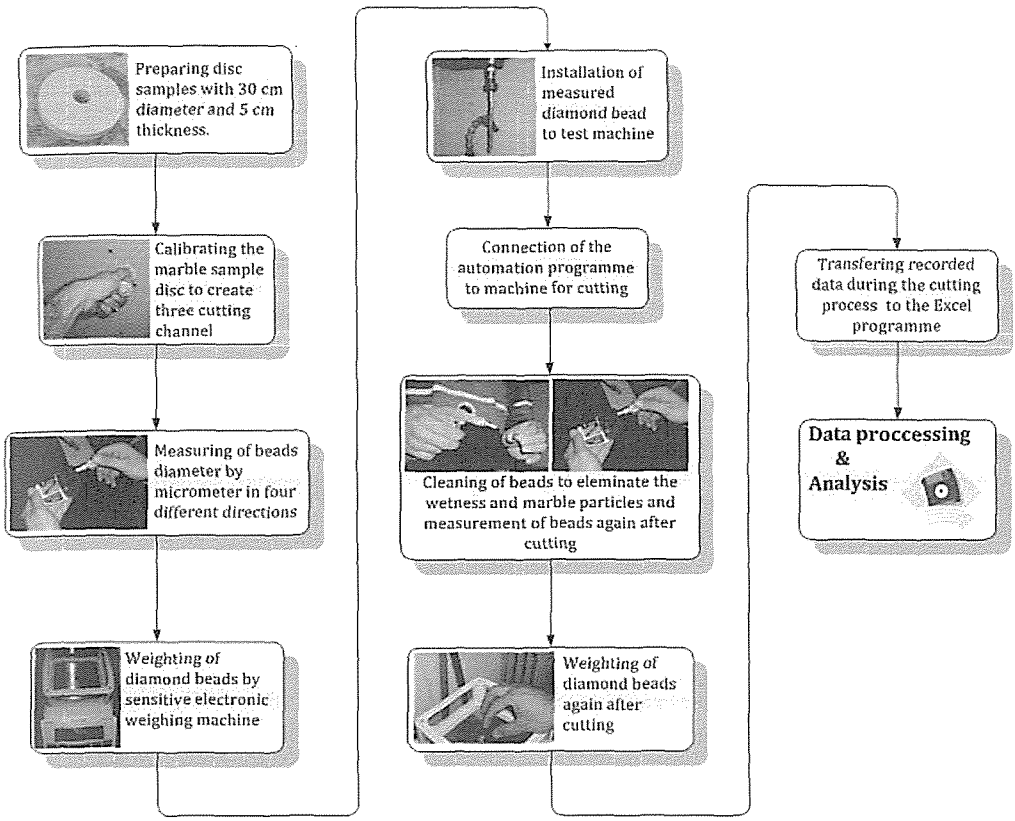

Figure 1. The methodology of the study (Kanbir 2007)

Table 2. Motor rotation speed of the bead and marble sample calculated depending on hoop diameter and rotation speed

HOOP ROTATION (RPM)	BDH (rpm)	*Hoop diameter (cm)*			
		50	**60**	**70**	**80**
900	1620	173	207	242	276
1000	1800	198	239	268	306
1100	1980	211	253	296	337
1200	2160	230	276	323	369
		SRS (rpm)			

2.1 Introducing Single Bead Test Machine

Performing the cutting operation suitable to the rock to be cut is possible by detecting the variable parameters correctly. The single bead test machine designed and used for this study was developed in Hacettepe University Department of Mining Engineering (Fig. 2)

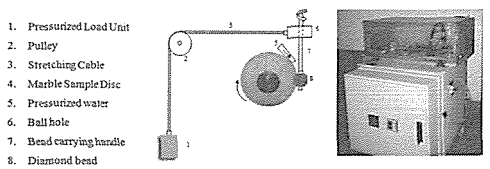

Figure 2. The general and schematic view of single bead test machine used in the study

This machine (Fig. 2) is a cutting machine where the machine parameters effective during cutting (vibration, energy used etc.) can be determined and cutting conditions (bead rotation speed, sample rotation speed, cutting rate etc.) can be controlled sensitively.

As it can be seen in Figure 2, test machine has two motors one of which rotates the marble sample (4), the other rotates the diamond bead (8) and a movable mechanism that approaches the diamond bead to the sample to be cut and puts pressure on it (1,2 and 3). While cuttings are performed, both motors are in motion and it is ensured that the diamond bead puts pressure on marble sample by implementing a determined load value. A specifically designed automation program was used in the system in order to control the experimental mechanism and provide the data record during the experiment.

2.2 Workpiece characteristics

Natural stone samples commercially named as Sivrihisar Beige was selected for the cutting experiments. The stone samples were prepared as square samples in sizes of 35 cm x 35 cm with a 5 cm thickness and then they were made as samples suitable for the single bead test machine by using specially designed core drill with an inner diameter of 60 mm and an outer diameter of 300 mm. Some physical and mechanical properties of the tested limestone are given in Table 3. The physical and mechanical tests were performed according to the procedures suggested by ISRM (1981).

2.3 Statistical Analysis

Within the scope of this study, Design Expert 7.0, which is a special statistical program, was used for data analysis and for determining the optimum points of sample rotation speed and bead motor rotation speed for Sivrihisar Beige limestone sample.

2.3.1 Design Expert 7.0 Statistical Software

Design Expert 7.0 is a widely used program which was developed for the experimental optimization process and which can effectively design the experiments in the most suitable way according to different methods. After making the experiments based on the design selected and entering the results obtained in the program, it derives the most suitable equations for dependent variables (response) and can realize the determination process of the optimum points by means of the derived equations. Imaging the optimum working points and the estimated results obtained as a result of the experiments made on these points is possible with this program.

Table 3. Some physical and mechanical properties of the tested marble (Sivrihisar Beige)

Tested Rock	*UVW (gr/cm^3)*	*WA (W/W) (%)*	*Porosity (%)*	*Shore Hardness*	*UCS (MPa)*	*TS (MPa)*
Sivrihisar Beige	2,70	0,12	0,22	62	70,00	7,05

2.3.2 Design Summary

Before initializing the statistical analysis, information that reflects the properties of each variable regarding the factors and response was analyzed. This information is composed of the data such as mean and standard deviation for describing the frequencies about the variables and also definitions of the methods and models to be used in modeling studies. The design properties used in this study are demonstrated in Table 4 and the descriptive statistical data regarding factors and response are shown in Table 5 and 6, respectively.

However, the relationship between unit wear and cutting rate and sample rotation speed were examined at various bead rotation speed values and the results are shown in Figure 3 and 4, respectively.

The complexity of most scientific mechanisms is such that in order to be able to predict an important response, a well-known multiple regression model is needed. The model formed for regression analysis is a model which involves dependent and independent variables. In such a model, the change in dependent variable is tried to be explained with independent variables. The first phase in forming simple or multiple regression models is determining the coefficients that form the model and then the statistical test of the validity of the model with variance analysis. The figures demonstrating the results obtained from here are called ANOVA (Analysis of Variance) figures. F value obtained from the figures is the value to be tested for the validity of the general model. F value and the results of ANOVA in regression analysis and in other models show the validity of the model formed, in other words, the representativeness of the system.

Table 4. Statistical design properties used in the study

Study Type	Factorial	**Runs**	16
Initial Design	D-optimal, Point Exchange	**Blocks**	No Blocks
Design Model	2FI		

Table 5. Descriptive statistical data of the factors

Factor Name	Units	Type	Low Actual	High Actual	Mean	Std. Dev.
Sample Rotation Speed (SRS)	rpm	Numeric	200.00	300.00	252.50	36.99
Bead Rotation Speed (BRS)	rpm	Numeric	1600.00	2200.00	1900.00	223.61

Table 6. Descriptive statistical data of the response

Response Name	Units	Obs	Analysis	Min.	Max.	Mean	Std. Dev.	Model
Unit Wear	μ / m^2	16	Polynomial	0.095	0.37	0.23	0.079	Linear
Cutting Rate	m^2/h	16	Polynomial	0.055	0.13	0.092	0.025	Linear

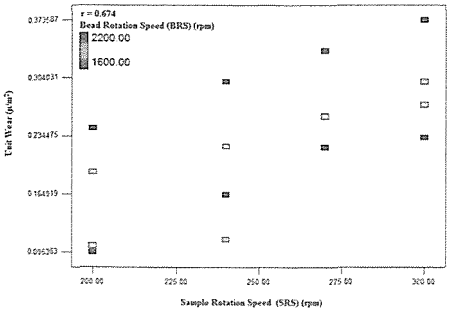

Figure 3. The relationships between unit wear and sample rotation speed at various bead rotation speeds for Sivrihisar Beige

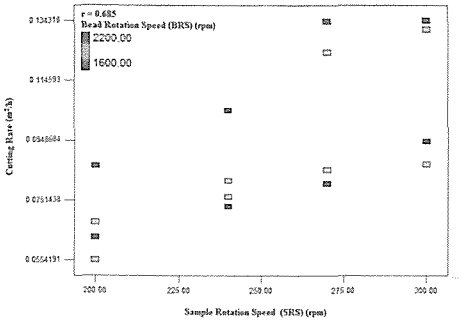

Figure 4. The relationships between cutting rate and sample rotation speed at various bead rotation speeds for Sivrihisar Beige

2.3.3 Statistical assessment related to unit wear

Multiple regression analysis were made for the purpose of estimating unit wear by using sample rotation speed and bead rotation speed and the unit wear model equation was obtained. The linear model for Sivrihisar Beige which were found to be statistically the most significant in the analysis, were chosen as the most suitable model for unit wear estimation (Table 7). The validity of the models (linear and cubic) established were tested with variance analysis. The results obtained were presented in Table 8 and 9, respectively. The model based on the regression coefficients given in Table 8 is statistically significant at 99% (α=0.01) confidence level (*P=0.0001<α=0.01). The estimation graph of the developed model is given in Figure 5.

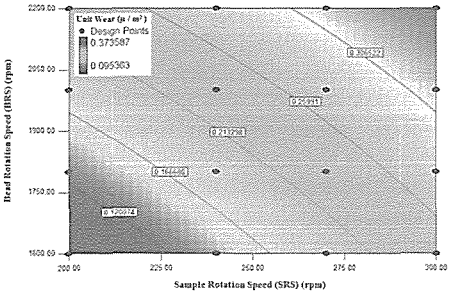

Figure 5. The estimation graph of the developed model for unit wear

The equation of the linear model established according to Table 7 is as follows:

Unit Wear=0.23+0.072*SRS+0.067*BRS

It is possible to test whether a regression model is statistically significant or not by means of variance analysis method. As well as this, there are different approaches serving for the same purpose. One of them is to examine the scattering graph between the measurement results obtained from the experimental studies and the results obtained from the model. The graph obtained for the unit wear for this purpose is shown in Figure 6. When Figure 6 is examined, it is seen that the results obtained from the model reflect the results of the measurement quite well.

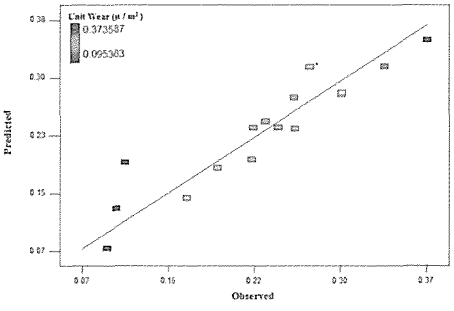

Figure 6. The relationships between predicted-observed values for unit wear

Table 7. The results of statistical analysis for unit wear

Source	R^2	Adjusted R^2	Predicted R^2	
Linear	0.8577	0.8358	0.8063	Suggested
2FI	0.8662	0.8327	0.7901	
Quadratic	0.9064	0.8597	0.7873	
Cubic	0.9228	0.8070	0.2595	

Table 8. The results of the multiple regression analysis for unit wear

Factor	Coefficient Estimate	Degree of freedom	Standard Error
Intercept	0.23	1	8.277E-003
Sample Rotation Speed (SRS)	0.072	1	0.011
Bead Rotation Speed (BRS)	0.067	1	0.011

Table 9. The ANOVA of the regression model for unit wear

Source	Sum of Squares	df	Mean Square	F Value	p-value Prob > F	
Model	0.086	2	0.043	39.19	< 0.0001	significant
(SRS)	0.045	1	0.045	41.54	< 0.0001	
(BRS)	0.040	1	0.040	36.84	< 0.0001	
Residual	0.014	13	1.091E-003			
Cor Total	0.100	15				

2.3.4 Statistical assessment related to cutting rate

In the analysis made for the purpose of estimating the cutting rate by using sample rotation speed and bead rotation speed, the linear model for Sivrihisar Beige was found to have the most significance (Table 10). By using these models, cutting rate model equation was obtained. The validity of the models (linear) developed was tested with variance analysis. Results of the multiple regression analysis are given in Table 11 and the results of the variance analysis are given in Table 12. The model based on the regression coefficients given in Table 11 is statistically significant at 99% (α=0,01) confidence level (*P=0,0028<α=0.01). The estimation graph of the developed model is given in Figure 7.

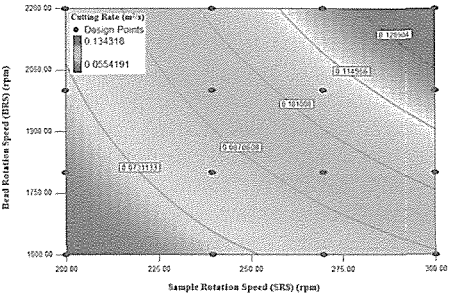

Figure 7. The estimation graph of the developed model for cutting rate

The equation of the linear model established based on Table 10 is as follows:

Cutting Rate =0.091(0.023*SRS–0.019*BRS

Besides this, the scattering graph between the results of the unit wear measurement obtained from experimental studies and results estimated from the model is shown in Figure 8.

Table 10. Model Summary Statistics

Source	R^2	Adjusted R^2	Predicted R^2	
Linear	0.7950	0.7634	0.6996	Suggested
2FI	0.8409	0.8012	0.7115	
Quadratic	0.8669	0.8004	0.6518	
Cubic	0.8929	0.7321	-0.1962	

Table 11. The results of multiple regression analysis for cutting rate

Factor	Coefficient Estimate	df	Standard Error
Intercept	0.091	1	3.150E-003
Sample Rotation Speed (SRS)	0.023	1	4.247E-003
Bead Rotation Speed (BRS)	0.019	1	4.216E-003

Table 12. The ANOVA of the regression model for cutting rate

Source	Sum of Squares	df	Mean Square	F Value	p-value Prob > F	
Model	7.966E-003	2	3.983E-003	25.20	< 0.0001	significant
(SRS)	4.703E-003	1	4.703E-003	29.76	0.0001	
(BRS)	3.263E-003	1	3.263E-003	20.65	0.0006	
Residual	2.054E-003	13	1.580E-004			
Cor Total	0.010	15				

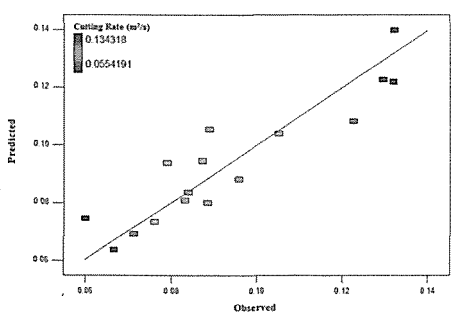

Figure 8. The relationships between predicted-observed values for cutting rate for Sivrihisar Beige

When Figure 8 is examined, it is seen that the results obtained from the model reflect the results of the measurement quite well.

2.3.5 Optimization

The main purpose of this study is to determine the optimum bead rotation and sample rotation speed values that would maximize the cutting rate values and minimize the unit wear values in cutting Sivrihisar Beige natural stone sample with diamond wire and also to develop cuttability abacuses for diamond wire on limestone sample. For this purpose, the aforesaid Design Expert 7.0 program was used. Here, firstly design limitations were defined. The design limitations used in determining the optimum points for Sivrihisar Beige natural stone sample are shown in Table 13.

The optimum points were found out by using Design Expert 7.0 program for Sivrihisar Beige natural stone samples considering the design limitations indicated in Table 14.

By using the model equations obtained as a result of the statistical analyses, the cuttability abacuses were developed separately according to unit wear and cutting rate. The estimated unit wear and cutting rate values to occur under optimum cutting condition were demonstrated on these abacuses. The cuttability abacus according to unit wear is shown in Figure 9 and the cuttability abacus according to cutting rate is shown in Figure 10.

Table 13. Design limitations used in determining the optimum points for tested sample

Name	Goal	Lower Limit	Upper Limit	Importance
SRS	in range	200	300	3
BRS	in range	1600	2200	3
Unit Wear	minimum	0.095363	0.373587	5
Cutting Rate	maximum	0.0554191	0.134318	5

Table 14. Optimum working conditions for tested sample

Sample Rotation Speed (SRS)	300.00
Bead Rotation Speed (BRS)	1605.34
Unit Wear (μ / m^2)	0.23233
Cutting Rate (m^2/h)	0.09563
Desirability Level	0.509

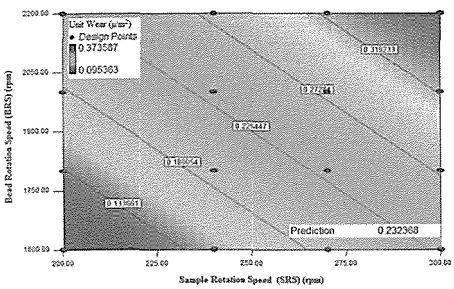

Figure 9. The cuttability abacus including the optimum conditions according to unit wear

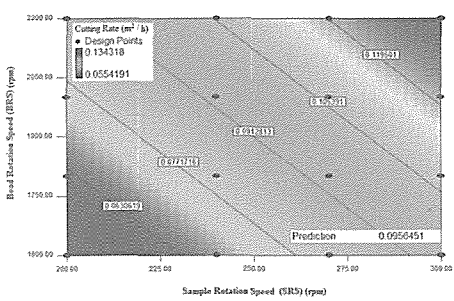

Figure 10. The cuttability abacus including the optimum conditions according to cutting rate

3 CONCLUSION AND SUGGESTIONS

It is an important issue that resources in natural stone sector, which is the leading sector in mining in Turkey, are used efficiently in terms of both country's economy and not wasting natural resources. Therefore, efficient usage of methods and machines during natural stone production is essential. Diamond wire cutting machines are widely used in natural stone sector. In this study, cutting optimization studies were made for maintaining a more efficient usage of these machines intensely in the sector and it was aimed that a new expansion was provided to the sector with the obtained results. In this study, the optimum points of bead and sample rotation speed for Sivrihisar Beige natural stone samples were determined by using a specifically designed statistical program (Design Expert 7.0), considering unit wear occurred on diamond bead and cutting rate. As a result, it was determined that for Sivrihisar Beige limestone sample, 300.00 rpm sample rotation speed and 1605.34 rpm bead rotation speed points were found as the optimum cutting conditions. The field equivalents of these optimum points were determined as 950 rpm of hoop rotation with 80cm of hoop diameter.

As a result of this study, unit wear and cutting rate values that can be come across at the cuttings performed at different sample and bead rotation speeds by using the estimation graph and cuttability abacuses developed for unit wear and cutting rate were determined. By developing them, unit wear and cutting rate values that may be come across at the marble quarries using diamond wire cutting machine could be estimated in advance. Thus, this will provide an opportunity for detecting the cutting costs in advance. Additionally, unit wear values

determined beforehand will ensure that diamond bead life is determined at the cutting condition implemented. By this way, quarry owners will be able to estimate how much cutting diamond beads can do for their rapid manufacturing.

ACKNOWLEDGEMENTS

This study is supported by TUBITAK project numbered 109M106 and named "Development of Cuttability Abacuses on Diamond Wire Cutting Method and Numerical Modeling of Cutting Mechanism of Diamond Bead". Therefore, we would like to thank to TUBITAK-MAG group and also Hacettepe University Department of Mining Engineering for their contributions.

REFERENCES

Hanecioglu, B, 2006. *Constitution of model diamond wire cutting machine and investigation of the effective parameters in cutting*, MSc Thesis, Hacettepe University (in Turkish)

Kanbir, ES, 2007. *Investigation of efficient parameters on cutting in single bead test machine*, MSc Thesis, Hacettepe University (in Turkish)

Ozcelik, Y, 1999. *Investigation of the working conditions of diamond wire cutting machines in marble industry*, PhD Thesis, Hacettepe University (in Turkish)

Ozcelik, Y, 2008. Development of a single diamond bead test machine for marble cutting, *Industrial Diamond Review*, Vol. 68. pp. 56-62.

MINING METHODS

Use of Pyrotechnical Method in the Bench Planes Recultivation at The Limestone Open Pit "Krivelj"

Ruzica Lekovski, Miomir Mikic,
Mining and Metallurgy Institute Bor, Bor, Srbija

Radoje Pantovic
Technical Faculty Bor,Bor, Srbija

ABSTRACT :This paper gives the use of pyrotechnical method with material rejection from blast hole and formation of a pit for seedling at the bench planes of the limestone open pit Krivelj near Bor-Serbia, in a shape of funnel, that is filled with humus in planting, is safer and more secure method of reclamation the bench planes with rocky ground than the method with a protective stone wall and filling of waste material.

The blasting works around the pit (funnel), 40 cm diameter and 40 cm depth, form the cracks that spread in the depth of 1,5-2,0 m and width of 2-3 m, which allows the proper formation of seedling root system. Breaking and fissuration of stone foundation by the use of explosive around the seedling pit improves the water-air regime and water infiltration to the seedling, which provides better reception and development of seedlings.

1 INTRODUCTION

The ore body Kriveljski Kamen is set aside in the central part of deposit and from all sides has no natural boundaries (Figure 1). The deposit is built of the Cretaceous sediments: limestone, marble and andesite (II phase) and the Paleogene marble and breakthrough of quartz diorite porphyrite, out of which the limestone and marble have the largest distribution. Limestones are characterized by the weak compactness, belonging to the fractured-cavernous type with tectonic fracturing along fault. Along the cavities and fault lines that are usually filled with the decomposition products of the original core mass, the water penetration is also possible into deeper parts of deposit. Marbles are more compact and also fractured along the fracture surfaces. The greatest impact, in the grouping of rocks and classification into appropriate category, had cracks of rock masses, the type of porosity and their evaluation as the abundance of spring.

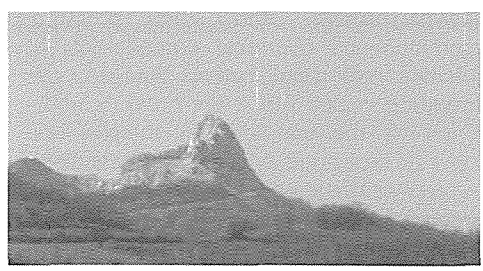

Figure 1. The Kriveljski Kamen deposit.

The Upper Cretaceous hornblende biotite dacite pyroclastic, hornblende and hornblende - biotite andesite, are located in the roof of separated ore body, which also made the floor. The andesite pyroclastic rocks are located and with limited propagation Parties of tuffs, tuffites and marls and marly limestone are located in the

andesitic pyroclastic rocks with limited outspreading.

The boundaries between these carbonate rocks and their varieties are not regular. They are irregular, especially between the marble and limestone and marble and dolomite. Limestone and marble are usually massive, rarely emphasized thick-bedded structure.

Limestones, the Lower Cretaceous age, are the most common rocks in the deposit, and they are important and most common within the carbonaceous materials, belonging to the nonclastic rocks that were formed in the aqueous phase.

The mentioned limestone resulted as the chemical formation and by deposition - accumulation of organic matter, followed by recrystallization process and diagenesis.

Limestones are sedimentary marine-type deposit. They are monomineral rocks in composition and composed of calcite.

Marbles were formed under the influence of penetration the quartz diorite porphyrite. In the Laramian - Pyrenean phase - the Alpine Orogeny and magmatic rocks of diorite and quartz diorite broke their underlying structure, the Upper Cretaceous magmates and instilled in the Lower Cretaceous limestones of this deposit. Depending on the depth, where the injection was performed, and the pressure, temperature and chemical composition of magmatic melt had also changed the surrounding rocks. Thus, the breakthroughs had led to the contact and metasomatic changes of limestone. Marbles were made by the precrystallization of calcite in the limestones. Marbles, as opposed to the transitional varieties to the limestones, are more distributed and physically cover the central part of ore body.

Dolomitic carbonate rocks in this deposit are rarely reported and they are of small thickness. These are dolomitic limestones, the Lower Cretaceous and dolomitic marbles, which can be separated as the rocks of Palaeogene age.

2 OPEN PIT

Open pit is a hilly type and elongated shape in the north – south direction. Longer axis of the open pit is 530 m and the shorter axis is 250 m. The lowest bench (bottom of theopen pit) was designed at K +510 m. The average width of the open pit bottom is about 85 m and it was left to the possibility of"descent" at K +500 m. The highest elevation of the mine is +660 K m (ridge). And maximum designed bench at the open pit is K +640 m. The designed depth of the open pit is 130 m.

The construction of the final slope of the open pit was made depending on the physical -mechanical properties of limestone. On the east side, due to the fault, the slope of the final open pit slopes was designed with an angle of 45° and minimum width of the final bench plane width of 8.23 m. The final slopes on the west side of the open pit were designed with the angle of 50° and minimum width of the final bench plane of 6.63 m, while on the northern side of the open pit, the of final slopes is slopes 55° , and minimum final width of bench plane of 5.24 m. The final slopes on the south side of the open pit were designed with the angle of 55°, but due to the roads, this slope is alleviated, and it is 51°.

The roads at the open pit were designed on the south and west side of the open pit with the rise and fall of 7.5%. Two-way road width is 15 m, and one-way road width is 7.5 m.

3 SELECTION OF RECULTIVATION AT THE OPEN PIT BENCH PLANES

On the termination of limestone exploitation, the degraded areas in the form of bench planes and bench slopes have remained at the open pit. For the aim of bringing the degraded areas to the useful purpose, the excavated area of the open pit after the exploitation of limestone should be recultivated. Black ash, hornbeam and lilac are planted at the bench planes of open pit. Slopes of the open pit will not be recultivated due to the slope. The bottom of the open pit at +510 K m is the flat surface in limestone and during the end of

exploitation at the open pit, this area can be designated for the construction of prefabricated buildings for tourism or other purposes. To protect buildings from landslides of stones from the open pit slopes on the bottom, a trapezoidal protective dam is built. The holes are dug manually on the dam crown to raise the green belt.

Pyrotechnic method will be used for digging the holes for planting the trees at the open pit bench planes.

4 SELECTION OF PYROTECHNIC METHOD

Three types of **pyrotechnic method**, ways of explosion action in blasting, are used in the world for re-cultivation (digging the pits for seedlings). The methods depend on a depth of setting the explosive charge and the amount of explosives, as well as:

a) **Camouflet method**, where the radius of action - **r is less** than the line of the lowest resistance - W, (r <W), Figure 2,

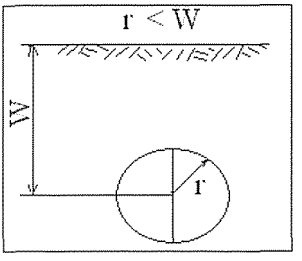

Figure 2. Camouflet.

b) **Disintegration method,** where the radius of action - **r is equal** to the line of the lowest resistance -W, (r = W), Figure 3,

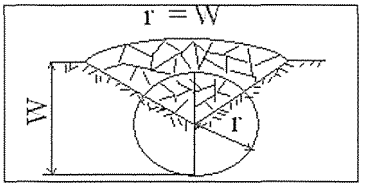

Figure 3 Disintegrated crater.

c) **Method of effect the material rejection,** where the radius of action - **r is greater** than the line of the lowest resistance -W, (r>W). Figure 4.

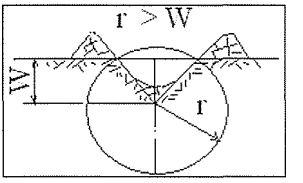

Figure 4 Crater of rejection.

The third method with material rejection from funnel was selected for reclamation the bench planes at the open pit Smiljkova glava.

4.1.1Drilling the blast holes

Drilling the blast holes will be done by the hand pneumatic drill ATLAS COPCO RH572E. For drilling the blast holes for the aim of reclamation, the vertical borehole, 32 mm diameter and 50 cm depth, are used. Distance of blast holes is 2.24 m; depth is 0.5 m, Figure 5. Development of one blast hole is 2 minutes. Pits for seedlings at the bench planes have funeral form, 40 cm diameter and 40 cm depth, as shown in Figure 6, obtained by the pyrotechnical method.

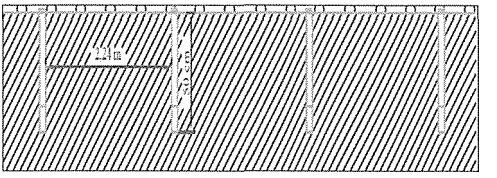

Figure 5. Arrangement of blast holes.

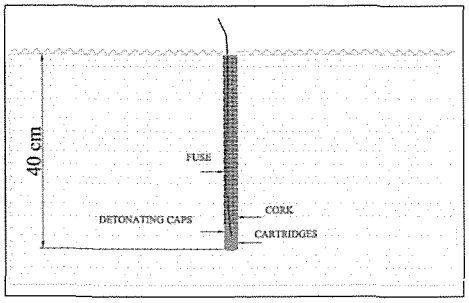

Figure 6. View of the blast hole.

The required time for drilling mine drills: $t = N_b \cdot T_b + N_b \cdot t_m$, where N_b - total number of pits for seedlings at the benches (6 076), T_b – required time for drilling one pit for seedling (2 min) and t_m – time of operator maneuvers on each pit (0.5 min), t = 12 816 min = 253.1 h. Price of engagement the hammer drill is 30 € / h. Costs of drilling are: $T_b = t \cdot C_b$, where : C_b – price of engagement the hammer drill (30 € / h). Drilling costs amount 7 595 €.

As it was predicted that the technical and biological reclamation successively follow the agro-technical re-cultivation, it is required to carry out immediately, after drilling the blast holes at the bench plane of open pit, blasting and then planting the seedlings

The third method of blasting the blast holes - pyrotechnical method of reforestation is the best choice in a case of the Smiljkova glava- the effect of rejection, that is rejection of disintegrated material out of the funnel by the action of explosion. Since it is a skeletal material and as such is not returned in planting the seedlings, but a stone wall is made of it as a protection of humus in the pit on torrent.

5 BLASTING

Blasting the first series is determined by the quality of drilled pits - funnels and adjustment of blast hole depth is possible in order to obtain the necessary volume of pit for planting the seedlings using the pyrotechnical method in the next blasting. The high strength explosives are the most suitable for blasting the pits for seedlings. The cartridge explosives are used for ease manipulation. The adopted cartridge explosive is AMONEX-1. Cartridge diameter is 28 mm, length from 15 to 16 cm, until cartridge weight is 100 g. The blast hole, Figure 5, will be filled with a cartridge of 100 g, an electric detonator is installed as well as the slow-burning fuse. The rest of blast hole is filled with the surrounding material or clay material that forms so called plug of the blast hole. After blasting, the pit for seedlings is obtained in the shape of a funnel as shown in Figure 4.

Using the pyrotechnical method around the pit, the longitudinal cracks are formed in the rocky ground. Braking and phissurization the ground by the explosives around the pit improve the water-air mode what provides better reception, development and survival of the seedlings on a very unfavorable ground.

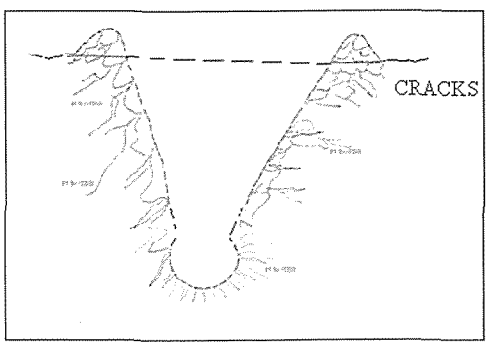

Figure 7. Pit shape, at the bench planes of the open pit, dug by the pyrotechnical method .

Blasting costs are: $T_m = N_b \cdot Q_{ex} \cdot C_{ex}$, where : Q_{ex}- quantity of explosive per blast hole (0.1 kg), N_b – total number of pits for planting at the benches (6 076), C_{ex} – price of explosive (1.5€/kg).

6 RECLAMATION OF DEGRADED AREAS

Series of complex works, aimed to bring degraded areas to the useful purpose, is

called reclamation. For the greening of the bench planes at the open pit, the optimum reclamation (eurecultivation) will be used. Works on the optimum reclamation will be carried out in the following order:

- Agrotechnical phase of eurecultivation,
- Technical phase of eurecultivation,
- Biological phase of eurecultivation.

Works of agrotechnical and technical reclamation technical reclamation cannot be clearly delimited as a part of works of agrotechnical reclamation precede the technical reclamation and a part of works are carried out technical reclamation.

- Agrotechnical phase of reclamation is the phase in which the preparatory works are conducted that enable realization of technical and biological reclamation and include construction of the access roads and preparation of bench for drilling the blast holes, setting the explosives and blasting.
- Technical phase of eurecultivation includes the following measures: digging the humus, loading, transport of humus to the site, cleaning the blasted material and making the drywall around the pit (hole) for seedlings.
- Biological phase of eurecultivation includes the complex of biotechnical and phytomelioration measures for growing the forest plantations on the prepared final open pit benches and protective dam for the aim of restoring the ecosystem.

6.1.1Selection of plant species for afforestation

For selection of forest species, it was taken into account their adaptation to the conditions of substrate, climate, great reception when planting and resistance to the action of the basic natural factors.

The biological phase of reclamation of degraded surfaces of the open pit after the application of technical phase of reclamation, it was concluded that the best use is the species that grow in natural conditions in limestone terrain of the eastern Serbia, and these are:

- lilac (Syringa vulgaris),
- hornbeam (Carpinus orientalis),
- ash tree (Fraxinus ornus).

These species in nature are mixed together in the stands. Because of the adverse primary substrate and possibility of admission, the number of seedlings of 2500 units/ha is adopted. Classic seedlings are selected for afforestation. The age of seedlings should be 2 +0.

Selection of grass and leguminous mixture for reclamation of protective dam on the bottom of open pit primarily depends on the altitude and quality of substrate. For the area grassing on the protective dam at the bottom of open pit, the following was adopted:

meadow grass.....8kg.....14,8%
tall fescue.....20 kg.....37,0%
red fescue.....20 kg.....37,0%
white clover.....6 kg.....11,2%
∑.....54 kg.....100,0%

In this case, a mixture of grasses was selected with the capacity of substrate binding and its protection from water and wind erosion. Also, the attention was paid to the following features:

- resistance to the specific environmental conditions,
- tolerance to the climatic conditions,
- distribution,
- ground covering, and
- ability of substrate binding, etc.

7 TECNOLOGY OF THE AFFORESTATION WORK OF THE OPEN PIT BENCH PLANES

At the final open pit bench planes, after the technical phase of reclamation, the afforestation will be done into dug holes using the **pyrotechnical method** for seedlings with diameter of 40cm and depth of 50 cm as well as 2500 holes/ha according to the schemes in Figure 8.

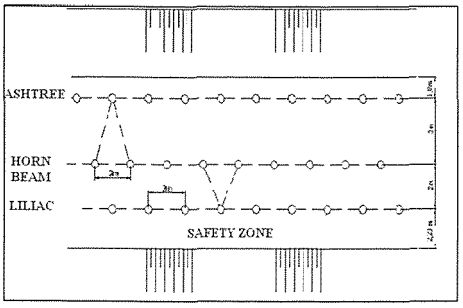

Figure 8. Scheme of afforestation the bench planes in the eastern and southern rim of the open pit.

Planting is done in three rows. In the first row towards the outer slope, the lilac is planted, then in the second row, the hornbeam is planted and, in the third row, up to the inner slope, the ash tree is planted, according to the given the schemes in Figures 8,9 and 10.

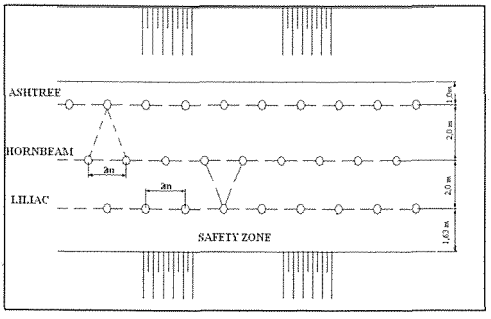

Figure 9. Scheme of afforestation the bench planes in the western rim of the open pit.

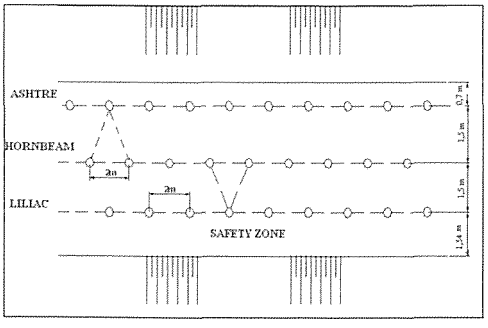

Figure 10. Scheme of afforestation the bench planes in the northern rim of the open pit.

7.1 Protective dam on the bottom of the open pit

Development of protective dam on the bottom of open pit is intended to protect the flat surface - the bottom of open pit from the filling with stones that due to the effects of natural factors slide from the higher benches. Protective dam is made of the waste material (dirty grit, stone chippings, clay and terra rossa) that remains on the bottom of open pit in obtaining the limestone. Its formation requires the work of bulldozers and loaders. Crown of the dam is planned using the bulldozer along which the tractor with humus and seedlings will move Dimensions of the protective dam are given in Figure 11.

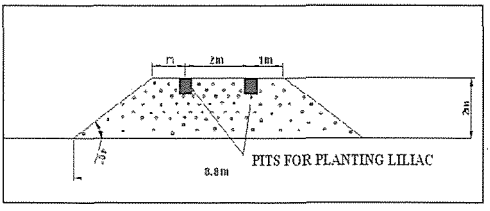

Figure 11. Protective dam on the bottom of open pit.

Protection zone on the crown of dam is formed by planting of lilacs in two rows, according to the scheme given in Figure 12.Technology of planting is the same as at the open pit bench planes.

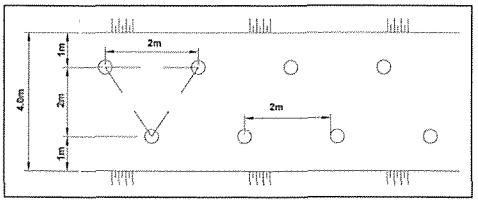

Figure 12. Protective dam and planting of lilacs and grass cover.

On the outer slope of protective dam, the humus layer is applied with height of 10 cm. Humus is transported by tractor and poured on the crown of dam and it is used for filling the pits for seedlings and filling the outer slope. Filling or spreading of humus is

carried out manually by rakes. In preparing the slope of protection dam for sowing with grass legume mixture, the humus is mixed with waste (small stones). Actually, it is an objective because the homogenization of waste material and humus contributes to the stabilization deposited humus on the slope and in that way the washing of humus is stopped. Emergence of grass on the slope of protection dam is achieved by binding of humus. Protective dam with protective belt of lilac has a protective role against filling of the bottom with stones from the higher benches as well as a nice aesthetic appearance, grassing of the slopes of protection dam is aimed at stabilizing the buried humus

Works on grassing consist of:
- manual cross sowing of grass mixture in a given relationship. Sowing depth ranges between 1 - 1.5 cm,
- rolling with roller of sown areas,
- fertilizing the planted areas with NPK (15:15:15) fertilizer, and
- dewing (watering) the planted areas to the grass cropping and after it depending on weather conditions.

The planned appearance planted open pit is shown in a cross section in Figure 13.

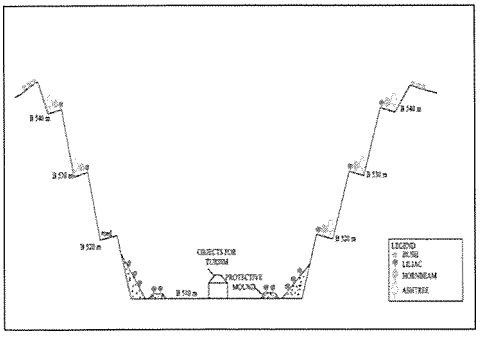

Figure 13. Cross section of the open pit Kriveljski Kamen with the types of plants.

8 CONCLUSION

Reclamation of degraded areas the open pit Kriveljski Kamen, in order to preserve the environment and using the provided technical and biological measures, can expect good results despite very unfavorable base. In this case, a profit is not expected from forests but only protection of degraded grounds from erosion and improvement the micro climate of the town in immediate environment as well as the conservation of plant species such as lilac. In addition, the root system of plants and leaves that fall and rot on degraded soil surfaces will launch the pedological processes towards the creation of humus and development of ground flora.

The recultivated protective dam has a protective and decorative role on the bottom of open pit and built facilities for tourism purposes.

REFERENCES

Mining and Metallurgy Institute Bor, 2011. *Project of recultivation the final bences at the open pit kriveljski kamen, 105 p.*

Influencing the Energy Efficiency in Clay Mineral Open Pit Mines by Corrections in Current Technology Processes

Slobodan Vujic[1], Karolj Kasas[2], Igor Miljanovic[1], Aleksandar Petrovski[1], Zolt Kermeci[3], Katica Popov[4], Aleksandar Milutinovic[1], Milena J. Pejovic[1]

[1]*Faculty of Mining and Geology, University of Belgrade, Serbia*
Tel. +381 11 3238564, Fax. +381 11 3347934, e-mail: vujic@rgf.bg.ac.rs
[2]*Faculty of Technology, University of Novi Sad, Subotica, Serbia*
[3]*Potisje Kanjiza, Kanjiza, Serbia,* [4]*IGK Polet, Novi Becej, Serbia*

ABSTRACT The paper presents a part of the results and findings discovered in the framework of researching possibilities for improvements of energy and ecological efficiency at open pit mines of the non-metallic mineral-raw materials by adapting the existing technological processes without any additional investments.

1 INTRODUCTION

More than 100 types of non-metallic mineral resources are mined today. In a business, economy and general development significance, non-metallic mineral-raw materials are a strategic foundation on which the development of the construction, agriculture, extractive, food, chemical, pharmaceutical, electronics and electro industry relies. They have demographic and social significance, positively influencing external market balances, and business and economy flows of every country.

In an overall world production of non-metallic mineral-raw materials, more than 60 % accounts for mineral-raw materials intended for the production of construction material, bricks, tiles and ceramics.

Proportional to the size of territory and its population, Serbia holds important potentials of the clay mineral raw-materials, with different genesis, mineral and petrographic composition that have a great economic significance to the country. The largest share of brick, tiles and ceramics production is traditionally related to the north of Serbia, the area of Vojvodina. Number of companies is approximately 70, and the annual production is over 100 million of brick and ceramic units. At the moment, Serbia produces more than 3.5 million of tons of clay mineral-raw materials, with market value of 400 million euros, expressed via final products.

The general feature of clay mineral-raw materials mining in Serbia is that it is being accomplished with opencast mining, predominantly the discontinual technology. The majority of open pit mines have problems with underground waters, influencing the increase in excavated material moisture. In order to lower the moisture of mineral-raw materials to the level necessary for the production of brick, tiles and ceramics, the energy is spent, and the time of production cycle is prolonged, resulting in the increase of production costs. A logical question imposes whether changes and adaptations of technological processes with existing machinery at the open pit mines, without additional investments, can influence the moisture of mineral-raw materials to decrease before they enter the processing plants for bricks, tiles and ceramics production? This question started the Project of research of adaptability of the process of clay mineral-raw material mining at open pit mines in order to improve energy and production efficiency. The two-year research, realized during the last two years,

was conducted by the Department of Applied Computing and System Engineering of the Faculty of Mining and Geology of the University of Belgrade, with financial support of the Ministry of science and technology development of the Republic of Serbia. The logistics support to the experimental field research was provided by the three distinguished companies: "Potisje" from Kanjiza, "Polet" from Novi Becej and "Strazilovo" from Sremski Karlovci. The paper presents a part of results and findings discovered by these researches, confirming the justification of an idea of improving the energy efficiency in the course of production of clay mineral-raw materials by an adaptation of existing technological processes at open pit mines without the additional investments.

2 IDENTIFICATION OF ADAPTIVE POSITIONS IN TECHNOLOGICAL PROCESS

The general characterization of open pit mining of the clay mineral-raw material, regardless of process being discontinual or continual, the production technological flow consists sequentially of the following activities: excavation, load, transport and mineral-raw material deposition. By using this generalization as a starting point, the analysis of the flow shows that every technological phase can influence the drop of moisture content in the mineral-raw material to a greater or a lesser extent.

Excavation: The drop of moisture content in the mineral-raw material during the excavation is largely influenced by the: advancing speed of the excavator machine – the excavator during the excavation, the thickness of the cut, i.e. the depth of excavation and the excavator capacity. Time of excavator advance depends on the length of the excavation front and intensity of its work. The longer excavation front and lower excavation intensity enables for a longer exposure of the workplace surfaces to the sun and wind, and their drying.

Since the raw-mineral material for the brick industry are clays that quickly absorb and slowly release the water for the purpose of excavation of this material with the aim of moisture decrease, only the surface layer of the clay, that has been dried, should be selectively excavated. For this sort of operation, small capacity bucket-conveyor excavators are the most suitable, having the small thickness of the cut.

Excavation machines and complete technological system reserves have a very important role in decreasing the moisture, since they enable campaign forcing of the production during the dry periods, and the decrease or a full stop of the production in the periods of increased clay moisture due to atmospheric precipitation.

Load: The loading as an interphase activity between the excavation and the transport of clay can influence the decrease of its moisture up to a certain point. What effect will be achieved depends on the way the loading is performed. In general, there are several alternative solutions, and we will discuss here the two most commonly present in practice.

For an alternative when the excavation and load are performed as united technological operations of the hydraulic bucket excavator, findings show that effects of clay drying are negligible.

With continual technological systems, where the loading is performed by dropping the excavated material from the excavator belt to the conveyor belt, the drying effect is expressive, in particular when aided by a suitable atmospheric conditions (sun, wind, slight humidity of the air).

Transport: It is certain that the way of transport influences the drop of moisture in the mineral-raw material. With the truck transport, the drop of moisture depends on the levee of material to the truck trunk and the length of the transport road. Findings show that the effect of drying up the material is not excessive in this form of transport. With the transport of the material by belt conveyor, the drying effect can be

prominent, and it depends on: levee of the material on the belt, number of loading locations, and the overall length of the transporter. The lower material of the levee, the larger number of the loading locations and the longer length of the transporter, alongside with favourable atmospheric conditions, influence the drop of material moisture positively.

Deposition of the material: The deposition and standing time of the excavated clay before it is used for the production of bricks, tiles and ceramics is applied for two reasons. The one is the necessary reserves of the excavated material for the purpose of production reliability, and the second is of technological nature, and it is a consequence of the need of stabilizing the oxidation processes of the organic material in the mineral-raw material.

The effect of drying the material at the disposal location depends on the way of deposition, the geometry of the disposed mass body, time of standing, and the way of taking the material from the location.

Findings show that the clay disposal locations, formed by dropping the material from the truck, and levelling the disposed mass by a bulldozer, have weaker drying than the drying at the disposal locations created by the belt conveyor spreaders.

The elements of this short analysis shows that by managing the technological processes at the open pit mines of clay mineral-raw material, the drop of moisture in the mineral-raw material can be influenced, and thus accomplish the savings in energy resources and improve energy efficiency.

3 EXPERIMENTAL MEASUREMENTS

With the aim of verifying the assumptions laid out, and the proofs of possible improvements of the energy efficiency of the brick and tile mineral-raw materials by the adaptation of technological processes, the experimental measurements were performed on three clay open pit mines. Due to reasons of rationality, the paper presents only a part of measurements from the two open pit mines: "Majdan III" of the "Potisje" company from Kanjiza, and "Garajevac Istok" of the "Polet" company from Novi Becej. The data from the third open pit mine of the "Strazilovo" company from Sremski Karlovci were not presented, since they are equivalent to data obtained at the open pit mine in Novi Becej, which is rational, since the similar exploitation technology was employed at both open pit mines.

Open pit mine "Majdan III": The open pit mine excavates mineral raw-material for the production of tiles and bricks, with an annual production level of 400,000 t. The continual technology of operations at the open pit mine with two benches is applied. At the lower bench, 800 m long, the higher quality blue clay is excavated, and at the higher bench, 1000 m long, the lower quality yellow clay is excavated. The mineral-raw material is excavated by four bucket-conveyor excavator, two of them for each bench. The transport of the material is accomplished by six rubber belt conveyors, 800 mm wide. The overall length of the transporter is approximately 3,000 m. Selective deposition of the mineral-raw material is performed by a spreader at the open disposal location, 600 by 70 m. Time of material deposition at the disposal location is approximately 3 months. Figure 1 shows the principle technological circuit of the production system of the "Potisje" company, i.e. "Majdan III" open pit mine as a part of it. The specific feature of this technological complex is dry processing of the clay, i.e. the micron grinding of the clay for the purpose of limestone granule removal, and the improvement of brick quality. This detail is particularly important from the aspect of the topic of this paper. The clay from the disposal location, with the moisture content of 20 % on an average, is dried to the moisture content of 7 %, and then ground. For the purpose of drying, as an energy resource, a gas was used. 1 kg of evaporated water from the clay spends approximately 4,110 kJ, with gas consumption at approximately 21 m^3 per ton

of material processed, and the consumption of electric power approximately 25 kWh.

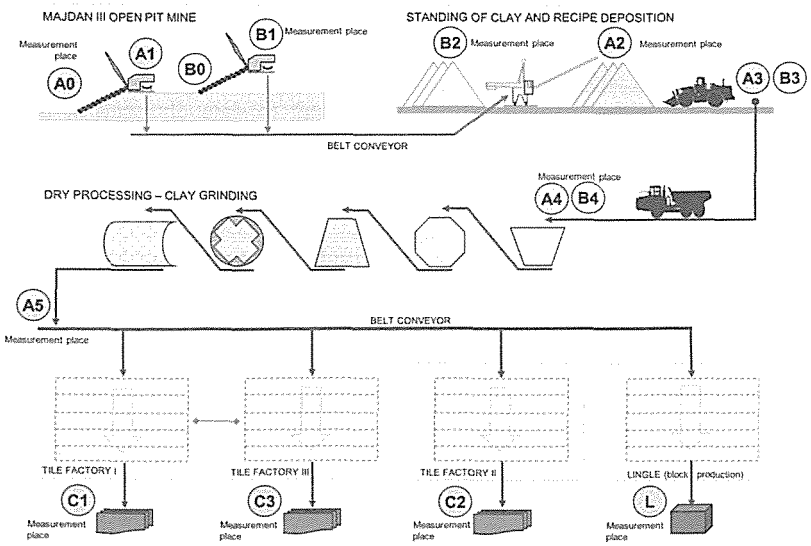

Figure 1. General technological circuit of the "Potisje" company production system.

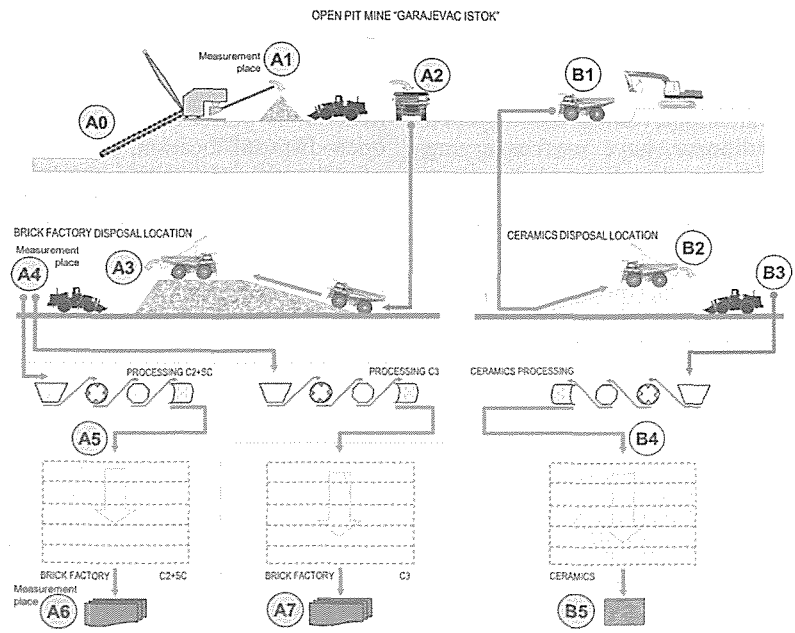

Figure 2. Principle technological circuit of the "Polet" company production system.

Open pit mine "Garajevac Istok": At the open pit mine, mineral-raw materials for the production of tiles, bricks and ceramics are excavated, with the annual production of

250,000 tones. The discontinual technology of operation at two benches is applied. At the lower bench, 700 m long, the mineral-raw material for the production of tiles and bricks is being excavated. At the higher bench, the material with increased contents of sand is excavated, and used for the production of ceramic tiles. The material at the lower bench is excavated by two bucket-conveyor excavators, and the loader is loading the material to the trucks. The raw material at the higher bench is excavated and loaded into the trucks by the hydraulic excavator. The length of the truck transport route is 2,000 m. Selective deposition of mineral raw-materials is accomplished by transferring the material from trucks to two disposal locations. The surface of the tile raw material disposal location is 200 by 50 m, and the ceramics material disposal location is 30 by 60 m. Time of material lay-off at the disposal locations is approximately 3 months. Figure 2 shows the principle technological circuit of the production system of the "Polet" company, owning the open pit mine "Garajevac Istok".

Results of the two-year research and experimental measurements, confirms that it is possible to influence the decrease in moisture content in the mineral-raw material by managing the processes in all phases: from excavation, loading, transport to the deposition of raw materials, without additional investments and the additional energy consumption. The analysis of the results of the measurements performed at the "Majdan III" and "Garajevac Istok" open pit mine points out the following conclusions:

- By performing the exploitation operations at the open pit mine, control and management over the speed of excavation and the control of the thickness of the cut, i.e. the excavation depth, it is possible to lower the contents of the clay moisture up to 40 %, which is an equivalent to the energy saving of 360 kJ per kg of clay with 22 % of natural moisture;
- In the loading phase with the continual exploitation systems, clay moisture drops by 1.5% on average, which is an equivalent of the energy saving of 14 kJ per kg of clay. With discontinual systems using the hydraulic excavators at the excavation and load, a drop of mineral-raw material moisture was not registered in this technological phases of operation;
- During the truck transport, the drop in clay moisture is up to 1 %, which is an equivalent of the energy saving of 9.33 kJ per kg of clay. In belt conveyor clay transport, an average drop of moisture by 3.37 % is registered, which is an equivalent of 31.45 kJ per kg of clay. Figures 3 and 4 shows graphical representations of the changes in moisture content for the blue and yellow clay at the "Majdan III" open pit mine;
- At the clay disposal location, created by the belt conveyor spreader, a drop of moisture by 8.9 % is registered, which is an equivalent of 80.5 kJ by a kg of clay. At the disposal location created by dropping the material from the truck, the drop of moisture is 2.5 %, which is an equivalent of the energy saving of 23.32 kJ per kg of clay.

Based on these facts, it is clear that effects of moisture decrease in mineral-raw materials by an adaptive management of the technological process can save significant amounts to the companies, influence the improvement of their business, market competitiveness and improvement of their ecological rating. Based on the example of the "Potisje" company, and the open pit mine "Majdan III" as one of its segments, this is clear to see. The procedure of dry grinding of "Potisje" spends approximately 8,400,000 m^3 of gas and 10,000,000 kWh of electric power. The decrease of moisture in the mineral-raw material reflects directly to the decrease of energy resources consumption in a way that a total amount of 84,000 m^3 of gas and 100,000 kWh of electric power is spent less annually for every percentage of moisture drop.

Based on the experimental measurements (figures 3 and 4), at the "Majdan III" open pit mine, it is realistic to expect that during the course of technology process between the excavation and clay takeover, blue clay

moisture decrease by 2.76 %, which would result in gas savings by 231,840 m^3, and electric power by 276,000 kWh.

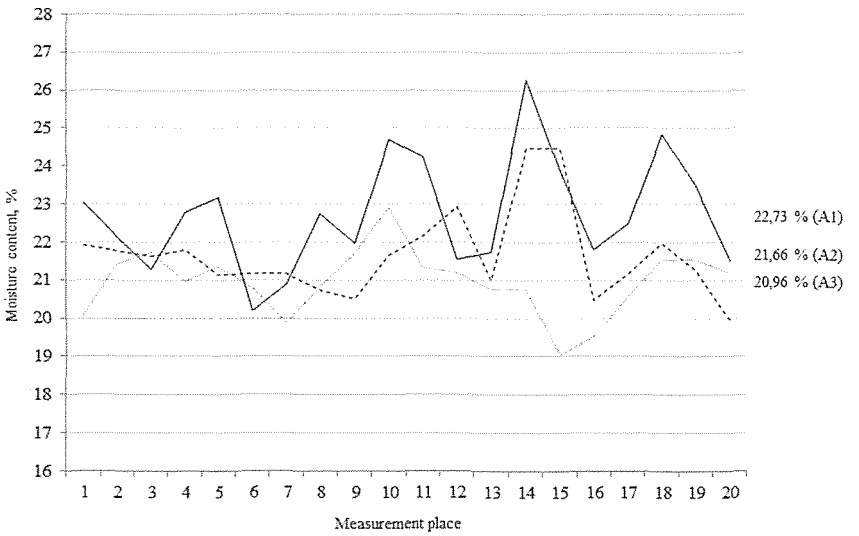

Figure 3. Graphical representation of the moisture content variation for the blue clay at the "Majdan III" open pit mine.

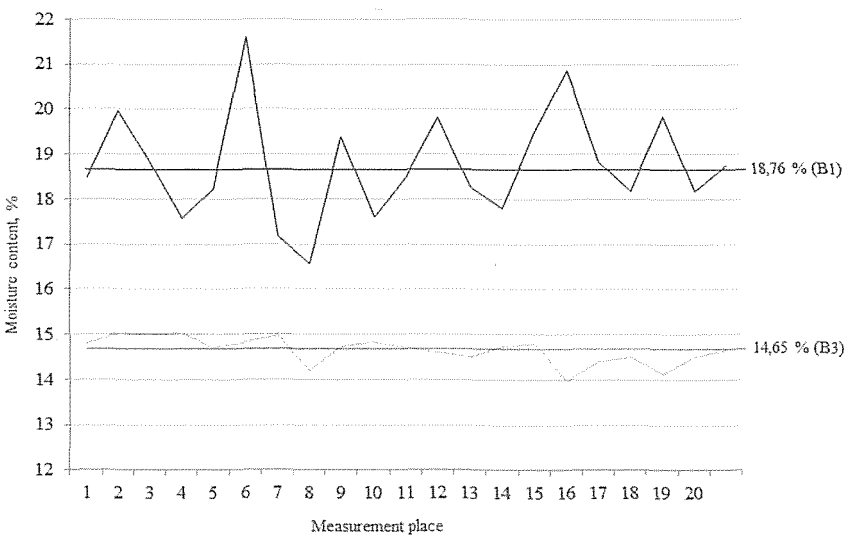

Figure 4. Graphical representation of the moisture content variation for the yellow clay at the "Majdan III" open pit mine.

CONCLUSION

Research results allow for the generalization of an assessment that by an adaptive management and directing of every phase of an exploitation process at the open pit mines of brick and ceramics mineral-raw materials, the decrease of energy consumption and an improvement of energy and ecological efficiency can be influenced.

The real benefits and effects will differ between the open pit mines, depending on their natural, technical-technological, financial, organizational and other particularities.

REFERENCES

Vujic S., et al., 2003, *A study research on the energy and ecological efficiency of the ECS complex of "Majdan III",* Faculty of Mining and Geology, Belgrade, NP EE 301-96A, Belgrade, 2003. (in Serbian).

Vujic S., et al., 2006, *Selective excavation and overburden deposition with the aim of land reclamation of coal open pit mines,* Faculty of Mining and Geology, Belgrade, Electric Power Industry of Serbia and the Academy of Engineering Sciences of Serbia, Belgrade, 232 p., (in Serbian).

Vujic S., et al., 2006, *Mineral-raw material complex of Serbia today: challenges and crossroads,* Academy of Engineering Sciences of Serbia, Faculty of Mining and Geology, Belgrade, Chamber of Commerce of Serbia, Belgrade, 482 p., (in Serbian).

Vujic S., et al., 2010, *Study research of adaptability of the process of clay mineral-raw material mining at open pit mines in order to improve energy and production efficiency and ecological safety of production systems,* Faculty of Mining and Geology, Belgrade, 2009-2010., (in Serbian).

Vujic S., et al., Improving the energy efficiency in production of non-metallic mineral-raw materials by adaptations of technological processes, *All-Russian scientific-technical Conference dedicated to the 50 years of the Mining Institute of Kola Scientific Centre of the Russian Academy of Sciences "Problems and tendencies of the rational and safe exploitation of georesources",* Russian Academy of Sciences, Apatiti, 2010., (in Russian).

Ground Surface Deformation as Effect of Longwall Mining of the Coal Seam No. 3 of the Livezeni Mine

Prof. Eugen Cozma, *Min.Eng.Ph.D*
Prof. Ilie Onica, *Min.Eng.Ph.D.*
Ph.D. Student Dacian Marian, *Min.Eng.*
University of Petroşani (Romania)

ABSTRACT The Livezeni Mine is situated in eastern part of the Jiu Valley coal basin (Romania) and produces about 0.5 million tons of hard coal (presently, in totality from coal seams no.3). In the case of this thick and gentle coal seam, the mining methods are by use of the longwall mining technologies with roof control by rocks caving. In this paper, it is presented the analysis of the complex deformations of ground surface, as a consequence of superposed effect of three mining panels. Also, it is analysed the ground surface subsidence phenomenon using the 2D finite element method. The modelling is made in the elasticity and the elasto-plasticity behaviour hypothesis. The obtained results are compared with the in situ measurements data basis.

1 GENERALITIES

The Petroşani Hard Coal Basin, under the management of the Hard Coal Company of Petroşani, contains the most important hard coal deposit of Romania, with a balance reserve about on billion tons of coal. This coal deposit was known and mined since the year 1788, as far back as the Austro-Hungarian Empire (Almăşan 1984). But, the intensive coal mining of this deposit began in the same time with the Romania's industrialisation, after the Second World War, reaching after 1980 the over 9-10 millions tons of coal per year (Almăşan 1984).

Due to Romanian industry reorganisation, after the year 1990, in conformity with the new demands of the market economy, the coal production of this basin was reduced to about 3.5 millions of tons per year, from which 0.5 million are obtained from the Livezeni mining field. From the beginning this coal deposit was split into 16 mining fields, from which following several successive reorganisation and closing stages, only 7 mining fields are left in activity.

The complicated deposit tectonics determines the delimitation in geological blocks of reduced extent (most of them varying between 200 and 300 m) and an equally technical difficulty in mining. Moreover, there occurs a methane gas emission (of over 10 to 15 methane m^3/coal ton) and there is a marked tendency of coal self-ignition (Almăşan 1984, Petrescu 1987).

In this mining perimeter, through the geological research works, there was identified a number of 18 coal seams, of which the most economical importance having the coal seam no.3 (48%) and coal seam no.5 (12%). The sedimentary rocks complex, in which these coal seams are present, consists in rocks deposits which belong to Superior Cretaceous, Neocene and the Quaternary (Petrescu 1987).

The subject of this study consists in the underground mining influence analysis on the ground surface of three adjacent mining panels (panel (3-4), panel 5 and panel 6), situated on the coal seam no.3, block VI A. Coal seam no.3, for these panels, was mined in inclined slices (about 2.5m thickness) with the longwall mining system, complexly-mechanized (powered support SMA-P2H, shearer 2K52-MY and armoured conveyer TR-7) and roof control by caving (Covaci 1983). The underground excavations sizes results from the coal mining corresponding of these panels are presented into Table 1.

Table 1. The average sizes of the mining panel of the coal seam no.3, block VI A

Panel	Slices number	Total thickness of mined seam (m)	Longwall face length (m)	Panel extent (m)
Panel (3-4)	4	10	119	346
Panel 5	5	12.5	87	440
Panel 6	1	2.5	137	362

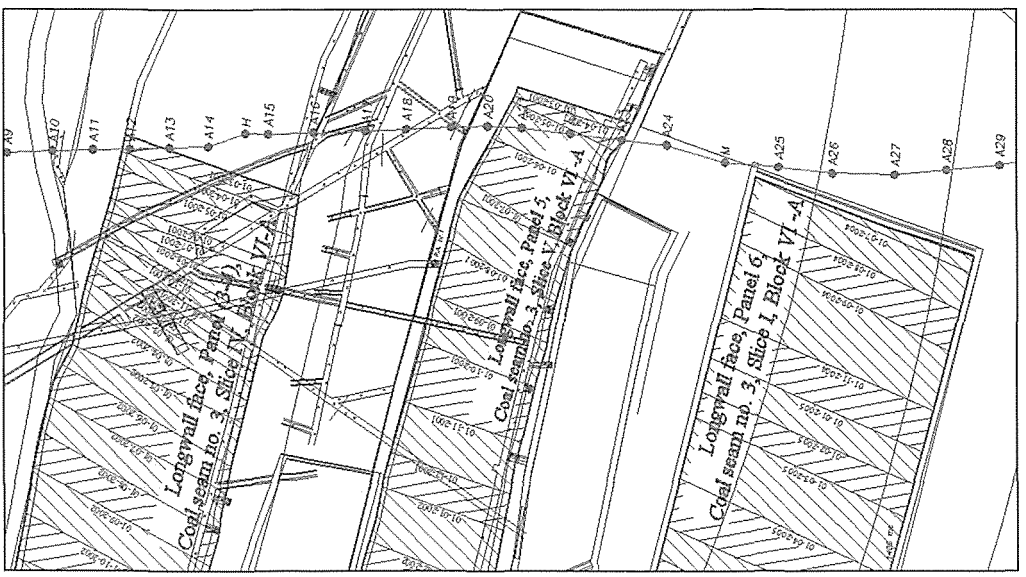

Figure 1. The monitoring station of ground displacement and deformation of Livezeni Mine

2 GEO-MECHANICAL CHARACTERISATION

As the deposit genesis is sedimentary, the most frequent rocks in the basin are: limestones, marls, argillaceous or marly sandstones, conglomerates, etc., their strength ranging between 15–16 MPa up 50–60 MPa, sometimes even more. Mainly, they are rocks of relatively low stability (Onica & Cozma 2008).

The main factors that contribute at the definition of the stress and strain state surrounding the excavations generated by the coal seams mining with the roof rocks caving, in the Jiu Valley coal basin, are the following: the excavation sizes, the seam dip, the coal and surrounding geo-mechanics characteristics, the mining depth, the face supports characteristics, the face advancement speed, the distance from the adjacent panels, the distance from nearby coal seams, etc (Oncioiu & Onica 1999, Onica & Cozma 2008).

The average values of the main mechanical and elastic characteristics of the rocks used in the ground surface deformation analysis, in the Livezeni Mine conditions, are shown in the Table 2 (Hirean 1981, Todorescu 1984).

As a result of the measurement analysis made on the ground surface under the underground mining influence, so as to find the optimum design parameters of the main safety pillars, the limit angles of subsidence have been set for the different coal mining fields of the Jiu Valley coal basin (Ortelecan 1997).

Table 2. The average values of the geo-mechanical characteristics of the roof and floor rocks of the coal seam no.3 (Hirean 1981 şi Todorescu 1984).

Rock characteristic	UM	Rock		Coal seam
		roof	floor	no.3
Apparent specific weight, γ_a	kN/m^3	26.63	27.01	14.5
Young modulus of elasticity, E	kN/m^2	5 035 000	5 268 000	1 035 000
Poisson ratio, ν	-	0,19	0,20	0,13
Compressive strength, σ_c	kN/m^2	43 500	46 000	12 500
Tensile strength, σ_t	kN/m^2	4 600	4 950	1 000
Cohesion , C	kN/m^2	6 130	6 630	1 300
Internal friction angle, φ	°	55	56	50

3 GROUND SURFACE DEFORMATION MONITORING

Now, the monitoring of the ground surface deformation parameters under the underground mining influence at the Livezeni Mine is made using a monitoring (surveying) station that consists in 50 benchmarks. The benchmarks' emplacement is along the access road toward the Parâng Mountains tourist area (Ortelecan & Pop 2005). The topographical measurements were made every three months, beginning with the year 2001. This monitoring station provides data concerning the ground subsidence area affected by the mining of the coal seam no.3, block IV A, panel (3-4), 5 and 6. Taking into account the values of the measured parameters, with the aid of the known calculus relations, there were determined the main parameters of the subsidence basin, namely: subsidence or vertical displacement, horizontal displacement, horizontal strain and the slope (Onica 2001b, Onica e.a. 2006).

The subsidence basin from the Figure 2 is a composed basin, resulted from the superposition influence of the three panels. This subsidence basin has an irregular shape due the fact that the three individual basin are intersected, and also because the monitoring station is situated toward the mining boundaries of the panels (Fig.1), area where the transversal deviations are maximum.

In this case, the accuracy of the values that characterise the obtained subsidence basin is lower because the fact that, it is not only the result of the ground subsidence but also the result of the displacement of it, and the deviations were corrected in conformity with the following methodology. Even if the transversal deviations that act on this subsidence profile are approximately equal in all the points situated inside the goaf, the difference level between every point benchmark at the base measurement and the their level at the final measurement is not the same, because the ground surface elevation mark is different (Fig. 3).

In these conditions, we are considering the points A and B that belong to a displacement and subsidence monitoring profile and the following parameters are defined:
D_{AB} –distance between the points A and B; ΔD_X – displacement following the X axis (horizontal displacement); ΔD_Y – displacement following the Y axis (transversal deviation); S_A – displacement following the Z axis (real subsidence of the point A);
$S_{A`m}$ – the measured subsidence in the point A`. $S_{A``m}$ – the measured subsidence in the point A`` ; $S_{A```m}$ – the measured subsidence in the point A```;$\Delta H_{AA``}$ - initial level difference between the point A and the point A``; $\Delta H_{AA```}$ - initial level difference between the point A and the point A```.

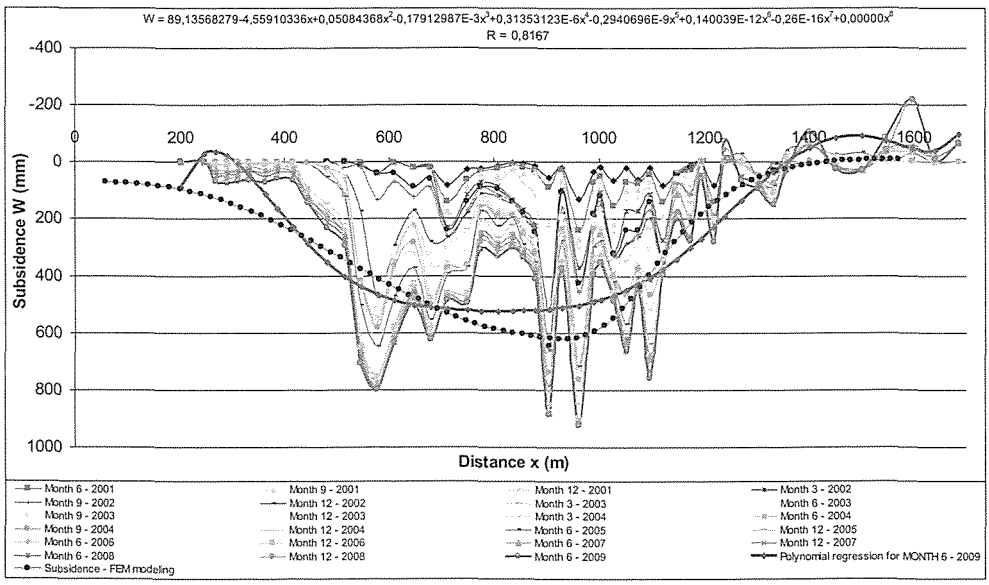

Figure 2. The subsidence profiles at the Livezeni Mine

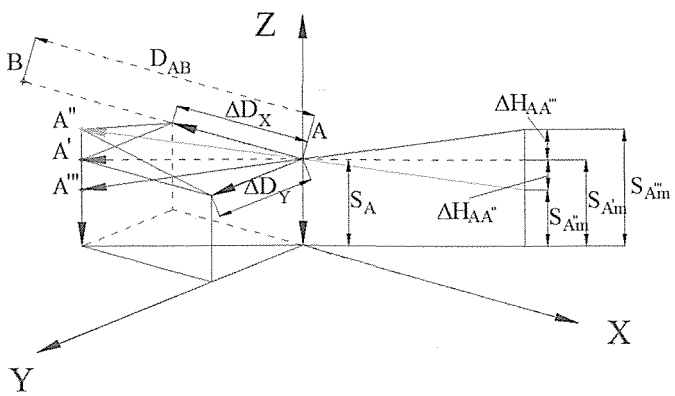

Figure 3. The displacement and the subsidence of a point A

Because the displacement is under few meters we can consider that the subsidence in the point A is equal to the subsidence in the point where that was displaced (the points A`,A``,A```), that is $S_A=S_{A`}=S_{A``}=S_{A```}$.

The subsidence and the vertical displacements, previous mentioned, are calculated with the relation: $W_i = H^*_i - H_i$ (mm) (where: H^*_i is the level of the point "i" at the zero measurement; H_i – the level of the point "i" measured at a given moment).

Analysing the in situ measurements situation, we can conclude that, taking into account the ground surface subsidence and displacements there are three cases of the correction determination of the measured values, namely:

1) Case when the point A, with the level H_A, is displaced in the point A`, having the initial level equal to the level of the point A. In this case, there is no correction because the ground slope is zero, and by consequence,

the measured subsidence is equal to the real subsidence ($S_A = S_{A`m}$);

2) When the point A, having the level H_A, is displaced in the point A``, having the level $H_{A``}>H_A$. In this case the measured subsidence is less then the real subsidence ($S_{A``m} < S_A$) and, as a consequence, must be applied a correction equal to the initial difference level between the point A and the point A`` ($\Delta H_{AA``}$): $S_A = S_{A``m} + \Delta H_{AA``}$;

3) When the point A, having the level H_A, is displaced in the point A```, having the level $H_{A```} < H_A$, the measured subsidence is greater than the real subsidence ($S_{A```m} > S_A$) and, as a consequence, must be applied a correction equal to the initial difference level between the point A and the point A``` ($\Delta H_{AA```}$), namely: $S_A = S_{A```m} - \Delta H_{AA```}$.

These adjustments of the measured values are necessary only in the case when the horizontal displacement and (or) the transversal deviation are significant and when the ground surface is inclined.

In the case of this monitoring (surveying) station, the maximum measured subsidence is of W_{max} = 924mm and the horizontal displacement ranges between the value of U = + 3712mm and U= - 3625mm. The average of maximum subsidence is W_{max} = 524mm (the reference value in the case of numerical modelling).

4 NUMERICAL MODELLING OF THE SUBSIDENCE PHENOMENON

4.1 Model description

To build the 2D finite element calculus models the CESAR-LCPC finite element code was used. The CESAR software, development of which began in 1981, is the successor of the ROSALIE system developed by the Central Laboratory of Bridges and Roads of Paris, between 1963 and 1983. CESAR is a computational general code, based on the finite element method, addressed to the following areas: structures; soils and rocks mechanics; thermo-mechanics; hydrogeology. The CESAR-LCPC code, version 4, which involves the Cleo2D processor, completed with the C0 option (linear and non-linear static mechanics & diffusion) was used in this work, to perform the following models.

To determine the displacement and the ground surface deformation in the case of Livezeni Mine, where the ground is affected by the three panels, there were made two different models, in the plane strain hypothesis, namely: 1) the model "with mining voids" resulted as a consequence of underground coal mining; 2) the model "with caved zones" (on a height equal to eight times the mined height), due the roof rocks caving in the goaf (Fig. 4).

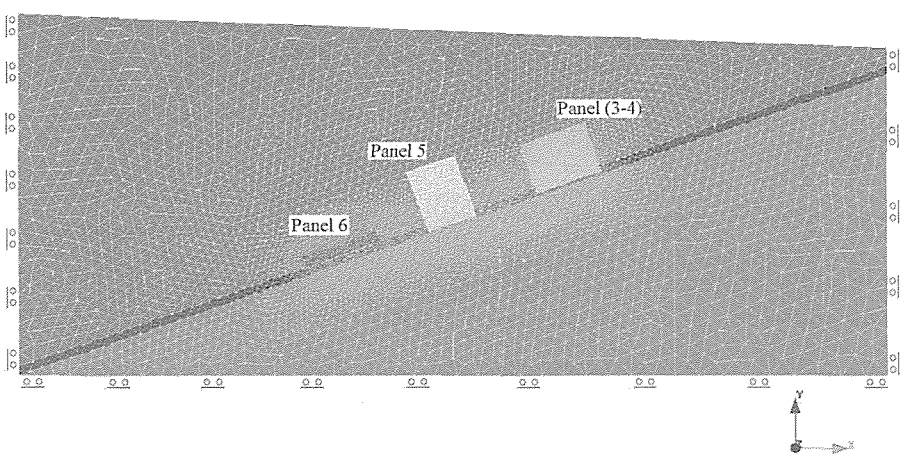

Figure 4. The finite element model "with caved zones"

The calculus for these two models was performed in two hypotheses: a) in the elastic behaviour of the rock massive and b) in the Mohr –Coulomb elasto – plastic without hardening behaviour.

In view of finding the influence degree of every panel on the entire subsidence basin, generated by mining all of these three panels, maintaining the geo-mechanical conditions constant, there were made certain models where the coal seam mining was simulated with every independent panel.

In all of the modelling cases, both rocks and coal seam no.3 were supposed to be continuous, homogenous and isotropic and the geo-mechanical characteristics taken into the calculus having the average values (Tab.2).

The natural state of stresses was estimated being geostatic, characterized by the vertical stress $\sigma_v = \gamma \cdot H$ and horizontal stress $\sigma_h = \frac{\nu}{1-\nu} \cdot \sigma_v$ (because of the lack of the real values in situ measured).

To fit on the models in function of the measured values of the maximum vertical displacements and to correct the rocks and coal characteristics in laboratory obtained (Tab. 2) toward the in situ values, the calculus of the models was made successively using the values reduced by 0%, 30%, 50% and 70% (respectively multiplied with a reducing coefficient K = 1; 0,7; 0,5; 0,3 .- structural weakness coefficient). Because the numerical models were significantly sensitive only to the modulus of elasticity variation, only the reduction of this parameter was taken into analysis.

4.2 Modelling achievement

2D modelling achievement, in the plane strain hypothesis, for every previous defined model the following steps were necessary: a) establishment of boundaries, interest zones and meshing of the model; b) determination of zones (regions) and computational hypothesis and the geo-mechanical characteristics input; c) boundaries conditions establishment; d) initial conditions and loading conditions establishment; e) achievement of calculus and stoking of results (Onica, 2001a).

4.2.1 Establishment of boundaries, interest zones and meshing of the model

For a better precision of the calculus, the models were performed with sizes X=1500m and Y = 690m. Also, the sizes of the interest zone around underground excavations were established so as to involve the model surface where the stress and strain variation is maximum. Model meshing, respectively of every region, was made by triangle finite elements with quadratic interpolation. Respectively, the model meshing was performed with a total number of nodes of 23 448 and surface elements of 11 661.

4.2.2 Determination of regions and computational hypothesis and the geo-mechanical characteristics input

In order to make a qualitative description of the models, there were taken into consideration 3 regions with various geo-mechanical characteristics, in the case of the models "with mining voids", respectively 4 regions in the case of the models "with caved zones", adequate at the roof and floor rocks, coal seam and the caved rocks of the goaf.

The rocks characteristics, considered to be homogenous and isotropic, are presented in Table 2, and taken in the calculus in the elastic behavior hypothesis, respectively elasto- plastically without hardening behavior Mohr-Coulomb hypothesis, were reduced successively, taking into account the structural weakness coefficient.

The caved rocks of the goaf was considered being a very compressible elastic body, characterized by the elasticity modulus of 5000kN/m^2, Poisson ratio of 0.4 and specific density of 1800kg/m^3.

4.2.3 Boundaries conditions establishment

The superior side of the model is considered free and the lateral sides, blocked (for the inferior side the vertical displacements v = 0

and the horizontals $u \neq 0$ and for the lateral sides $v \neq 0$ şi $u = 0$).

4.2.4 Initial conditions and loading conditions establishment

Initial loading conditions of the model were considered as geostatic $[\sigma_o]$, corresponding to an average mining depth of H=337m, namely: the vertical geostatic stresses $\sigma_{oy} = \rho_s \cdot g \cdot H = 87819\,\text{kN/m}^2$=87.8MPa and the horizontal geostatic stresses $\sigma_{ox} = \frac{\nu}{1-\nu} \cdot \sigma_{oy} = k_o \cdot \sigma_{oy} =$ 21076kN/m^2= 21.076MPa (where: $k_o = \frac{\nu}{1-\nu} = 0.24$). The induced stress by the excavation presence was $[\sigma_e]$, respectively the stresses variation represented by the horizontal stress σ_{ex} = -21.076MPa and the vertical stress σ_{ey} =-87.8MPa. Thus, the loading of the model was performed in the total stresses: $[\sigma_T] = [\sigma_o] - [\sigma_e]$ (Onica 2001a).

4.2.5 Achievement of calculus and stoking of results

The calculus was made taking 60 iterations per increment and a tolerance of 1% of the results, using for the resolution the initial stress method with non-linear behaviour of geo-mechanical problem. The calculus results were stocked in the graphical form on the model surface (isovalue, vector and tensor representation) and in the predefined sections following the ground surface. The results obtained are corresponding to the subsidence W (mm) and horizontal displacement U (mm).

4.3 Analysis of the numerical modeling results

Analyzing the obtained results from the numerical modeling it is observed that the surface basin has a simple shape, different by report to the real basin, because of their emplacement toward the goaf boundaries. In contrary, in the case of FEM modeling, the profile is situated in the middle part of the subsidence basin.

The maximum subsidence and displacements values obtained from the numerical modeling, in elasticity and elasto-plasticity, previous presented, are shown in Table 3.

Table 3. Maximum subsidence and displacements obtained from the numerical modelling for individual mining panel and for grouped mining panels

ELASTICITY - Models "with mining voids"												
	Panel 6			Panel 5			Panel (3-4)			Panel (3-4) +5+6		
Coef.	W	U		W	U		W	U		W	U	
	Max.	Max.	Min.	Max.	Max.	Min.	Max.	Max.	Min.	Max.	Max.	Min.
	mm	mm	mm	mm	mm	mm	mm	mm	mm	mm	mm	mm
K=1	-155	46	-46	-66	24	-19	-74	28	-19	-237	78	-71
K=0,7	-221	65	-66	-95	34	-27	-106	40	-27	-339	111	-101
K=0,5	-310	92	-92	-133	48	-37	-148	55	-37	-474	156	-142
K=0,3	-516	153	-153	-222	80	-62	-247	92	-62	-790	260	-237
ELASTO - PLASTICITY - Models "with mining voids"												
	Panel 6			Panel 5			Panel (3-4)			Panel (3-4) +5+6		
Coef.	W	U		W	U		W	U		W	U	
	Max.	Max.	Min.	Max.	Max.	Min.	Max.	Max.	Min.	Max.	Max.	Min.
	mm	mm	mm	mm	mm	mm	mm	mm	mm	mm	mm	mm
K=1	-158	47	-47	-68	24	-19	-74	28	-19	-241	79	-72
K=0,7	-226	67	-67	-97	35	-27	-107	40	-27	-344	113	-103
K=0,5	-317	94	-94	-135	48	-38	-149	55	-37	-482	158	-144
K=0,3	-528	157	-156	-225	81	-63	-248	92	-62	-803	264	-240

ELASTICITY - Models "with caved zones"												
	Panel 6			Panel 5			Panel (3-4)			Panel (3-4) +5+6		
Coef.	*W*	*U*		*W*	*U*		*W*	*U*		*W*	*U*	
	Max.	Max.	Min.	Max.	Max.	Min.	Max.	Max.	Min.	Max.	Max.	Min.
	mm	mm	mm	mm	mm	mm	mm	mm	mm	mm	mm	mm
K=1	-160	47	-49	-104	25	-41	-87	25	-28	-309	68	-121
K=0,7	-229	67	-69	-148	36	-58	-125	36	-40	-442	97	-173
K=0,5	320	93	-97	-208	50	-82	-175	51	-56	-619	136	-242
K=0,3	-534	156	-162	-346	84	-136	-291	84	-94	-1032	226	-404
ELASTO - PLASTICITY - Models "with caved zones"												
	Panel 6			Panel 5			Panel (3-4)			Panel (3-4) +5+6		
Coef.	*W*	*U*		*W*	*U*		*W*	*U*		*W*	*U*	
	Max.	Max.	Min.	Max.	Max.	Min.	Max.	Max.	Min.	Max.	Max.	Min.
	mm	mm	mm	mm	mm	mm	mm	mm	mm	mm	mm	mm
K=1	-156	46	-47	-104	25	-41	-87	25	-28	-310	68	-122
K=0,7	-218	64	-65	-148	36	-58	-125	36	-40	-444	98	-174
K=0,5	-312	92	-94	-208	50	-82	-175	51	-56	-621	137	-243
K=0,3	-521	153	-156	-346	84	-136	-291	84	-94	-1035	228	-405

From the previous table it could be observed that, there are very small differences between the models computed in elasticity and the same ones in elasto-plasticity behaviour (the rocks having behaviour to the limits between these). The results more appropriate to the in situ measurement are for the "caved zones" models, in elasto-plasticity behaviour, for a structural weakness coefficient of *K*=0.5.

In the Figure 5 are represented the subsidence basins obtained for the models "with caved zones", in elasto-plasticity (for *K*=0.5), as result of three panels mining, as well as the subsidence basin generated by the every singular panel and various combinations between them, and the horizontal displacements curves are shown in Figure 6.

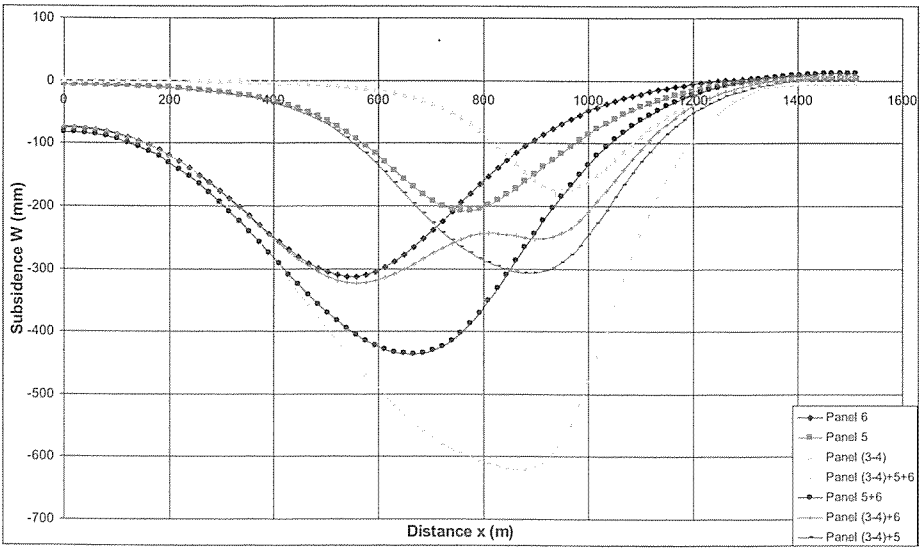

Figure 5. The subsidence basins obtained from the numerical modelling

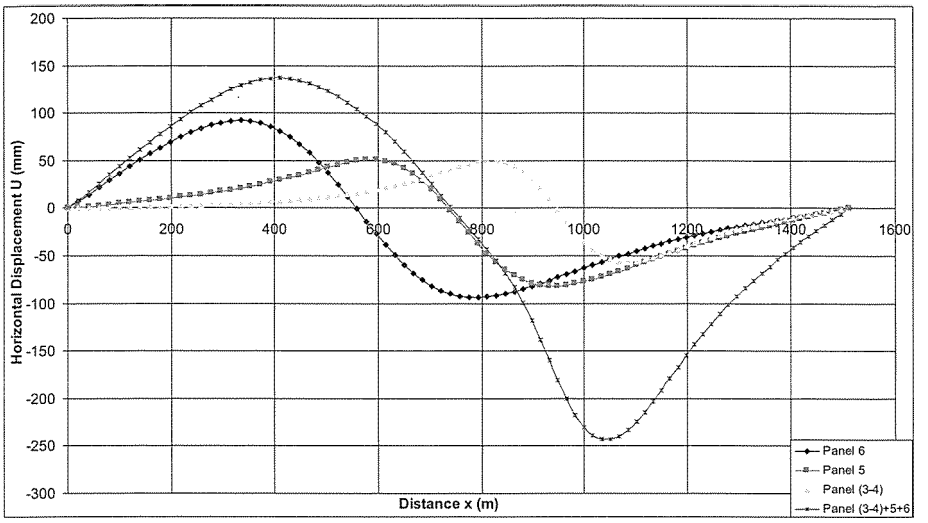

Figure 6. The horizontal displacement graphics obtained from the numerical modelling

The subsidence basins obtained from the numerical (FEM) modelling on the model "with mining voids" and on the model "with caving zones", for all that three mining panels, in elasticity and elasto-plasticity, for an structural weakness coefficient of K=0.5 are presented in the Figure 7 and the horizontal displacement curves in the Figure 8.

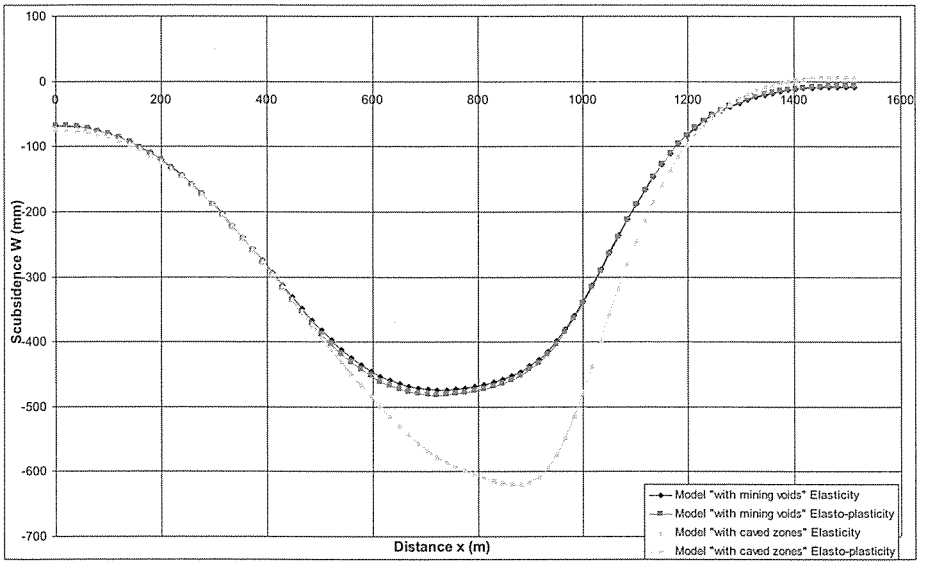

Figure 7. The subsidence basins obtained from numerical modelling in elasticity and elasto-plasticity rocks behaviour

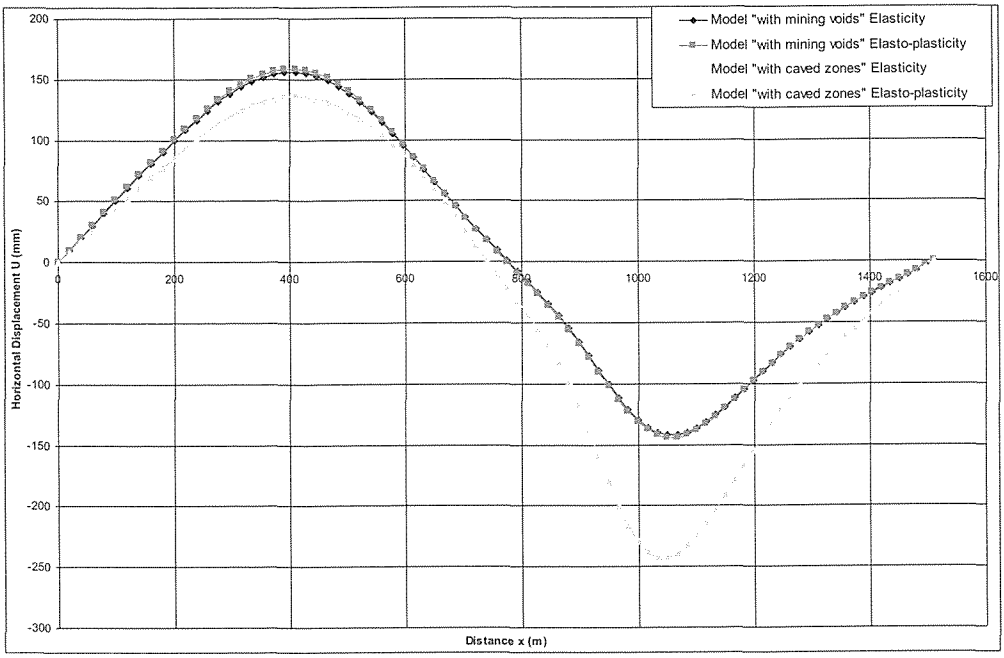

Figure 8. The horizontal displacement graphics obtained from numerical modelling

From the Figure 7 can be concluded the fact that between the model "with mining voids" and the model "with caved zones" there is a small difference, about of 200mm. Also, between the same type models, computed in elasticity and elasto-plasticity, the difference is very small (negligible).

5 CONCLUSIONS

The subsidence and displacement monitoring (surveying) station, in the case of Livezeni Hard Coal Mine, that consists of 50 benchmarks, where there are measured the ground surface subsidence and displacement every three months. This ground surface is affected by the coal underground mining of three panels, mined with longwall faces and roof control by total caving. Thus were determined the main parameters of the subsidence basin (subsidence or vertical displacement, horizontal displacement, horizontal strain, slope and the curvature).

The subsidence basin has a very complicated shape, being the result of coal seam no.3 mining with three neighbouring panels, and the monitoring (surveying) station is situated towards the boundaries of these three mining panels (where the deviations are considerable).

In this case, for a better understanding of the subsidence phenomenon, the 2D modelling with finite element method was used. Thus, with the aid of CESAR-LCPC code was generated two models groups, namely: "with mining voids" and "with caved zones". The calculus was performed in the elasticity rock behaviour and in the elasto-plasticity behaviour Mohr-Coulomb hypothesis.

After the analysis of the obtained results we can conclude the fact that the model with the more appropriate values by the in situ reality is the one "with caved zones", computed in the elasto-plasticity Mohr-Coulomb hypothesis, for a structural weakness coefficient K=0.5 (the maximum obtained subsidence is of W_{max} = -621mm and the horizontal displacements ranging between of U = + 137 and of U=- 243mm).

REFERENCES

Almăşan,B. (1984) *The Mining of Romanian Mineral Resources Deposits, Tom I* (in Romanian), Technical Publishing House, Bucharest, pp. 70-291.

Covaci,St. (1983) *Underground Mining, Tom I* (in Romanian), Didactical and Pedagogical Publishing House, Bucharest, 424 p.

Hirean,C. (1981) *Rocks Mechanics* (in Romanian), Didactical and Pedagogical Publishing House, Bucharest, 322 p.

Oncioiu,G., Onica,I., (1999) *Ground Deformation in the Case of Underground Mining of Thick and Dip Coal Seams in Jiu Valley Basin (Romania)*, Proceedings of 18th International Conference on Ground Control in Mining, 3-5 August, 1999, Morgantown, WV, USA, pp.330-336.

Onica,I. (2001a), *Introduction in the Numerical Methods Used in the Mining Excavations Stability Analysis* (in Romanian), Universitas Publishing House, Petroşani, 156 p.

Onica,I. (2001b) *Environmental Mining Impact* (in Romanian), Universitas Publishing House, Petroşani, pp.173-198.

Onica,I., Cozma,E., Goldan,T. (2006) *Land Degradation Under the Underground Mining Influence* (in Romanian), AGIR Revue, year XI, no.3, pp.14-27.

Onica,I., Cozma,E. (2008) *Stress and Strain State Developed Around the Longwall Faces in the Jiu Valley Coal Basin*, Proceedings of the 21 World Mining Congress & Expo –Session 6: Coal Mining – Chances and Challenges, Krakow, pp.153-163.

Ortelecan,M. (1997) *The Study of Ground Surface Displacement Under the Underground Mining of Jiu Valley Coal Deposits – Eastern Zone* (in Romanian), Ph.D. Thesis, University of Petroşani, 195p.

Ortelecan,M., Pop,N. (2005) *Topographical Methods for Buildings and the Ground Surfaces Behaviour Surveying* (in Romanian) AcademicPres Publishing House, Cluj-Napoca, 256p.

Todorescu,A. (1984) *Rocks Properties* (in Romanian), Technical Publishing House, Bucharest,676 p.

Petrescu,I. e.a. (1987) *The Coal Deposits Geology, Tom 2* (in Romanian), Technical Publishing House, Bucharest, pp.81-106.

Development of an Underground Coal Mine Project in Turkey Using a 3D-Modelling Program

Ina Förster
Bucyrus Europe GmbH, Saarbrücken, Germany

ABSTRACT Bucyrus is one of the world leaders in the design and manufacture of high productivity mining equipment for underground and surface mining.

In addition to machine manufacturing, Bucyrus provides support services for its equipment including mine modeling, mine planning and engineering services for its customers.

Using the concrete and actual example of a Turkish deposit, the presentation describes the different steps from the initial geological studies of the deposit up to the recommendation for suitable mining method and the related underground mining equipment based on an example of a Turkish deposit.

A new underground mining project starts normally with a scoping study including the development of a 3D-model of the deposit. A lot of geological data and information have to be reviewed and processed. After having all relevant parameters and information about the deposit and its seams an exact assessment and estimation of the deposit will follow and the geological coal resources can be calculated.

Subsequently a first mine layout proposal will be developed. The mine layout is most important for the next step, the definition of specifications for suitable underground mining equipment. Therefore several alternatives will be investigated.

After definition of suitable underground mining equipment specification guaranteeing economic viability of the project the mineable coal reserves will be calculated.

1 OVERVIEW BUCYRUS

Bucyrus is a world leader in the design and manufacture of high productivity mining equipment for surface and underground mining. Bucyrus draglines, rope shovels, hydraulic excavators, drills and trucks are used for mining coal, copper, iron ore, oil sands and other minerals in surface mining applications. Bucyrus automated longwall and room & pillar equipment are primarily used for mining coal in underground mining applications, while the Bucyrus highwall mining system links surface and underground coal mining operations. Bucyrus belt system solutions are used in both surface and underground mining applications for all bulk material handling requirements.

2 OVERVIEW ABOUT THE DEPARTMENT

The Bucyrus Application Engineering & Consulting Team is located in Saarbruecken, SW of Germany. This team of 35 employees consists of international experienced mining engineers/project engineers, mechanical engineers, electrical engineers, mine surveyor and commercial people.

2.1 Scope of services and supply

Our main target is to solve the client's problems and to offer them the required services for the development of green field projects as well as for the improvement of existing mining operations. To achieve this we use a phased approach:

- Analyze the client's problems/requirements
- Develop and offer suitable solutions
- Guide the client to the milestones
- Supply the client the right products and services

Our services include:

- System Engineering
- Mine Engineering / Modeling
- Technical Planning / Commercial Planning
- Supervision of the supply of complete systems and / or system components
- Supervision of system integration
- Service contracts for operation and maintenance
- Overall project Management

3 EVALUATION OF A DEPOSIT BASED ON AN EXAMPLE OF A TURKISH UNDERGROUND COAL MINE PROJECT

3.1 Overview

In March 2008 Bucyrus was assigned by Adularya Energy Electricity Generation and Mining Co. to visit their coalfield located approximately 150 km west of Ankara.

The project started with preparation of an initial study called "Geological Review & Global Strategy" on the Koyunagili coalfield project.

With this report recommendations were made for further drill program to proof uncertain areas in the existing model. Related to the progress of the drill program a monthly report with an update of the 3D-model was prepared. Based on this a draft layout was developed and suggestions made aiming on the most economic suitable mining method and the equipment package.

Finally a contract between Adularya Energy Electricity and Mining Co. and Bucyrus Europe GmbH was signed in December 2009 about the supply of underground mining equipment and operational services on-site.

3.2 The modeling software

For the 3d-modelling of the deposit and the calculation of the coal reserves the DUDE software was applied.

DUDE (Digital Underground and Deposit) is the standard modeling software of the German underground hard coal industry (RAG). The main purpose of DUDE is the designing of 3D-models of seam deposits including the calculation and determination of all important data for the development of the mine.

DUDE is available in English language and in case of existing software on client's side all necessary interfaces can be provided.

3.3 Data collection

In order to start the 3D-modelling with the software DUDE it is very important to collect all available data that could be provided. That means general data, deposit data and geological data. For the modeling you need information about:

- Drill holes / Drill cores

(Drill logs, coordinates, drilling density, core dip, etc.)

- Faults

(Dip, throw, classification of assumed or explored faults, disturbed areas, etc.)

- Seams

(Dip, thickness, qualities, overburden, distances between seams, etc.)

- License area

(Coordinates, surface situation of mining areas under consideration)

- Information received during the exploration, drifting & exploitation

(Seamroof (20m), seamfloor (5m), parameters & characteristics about the seams)

- Information provided by the mine surveyor or geologist

(Reports and studies of former explorations or geologic surveys, plans & maps about surface, seams & drilling density, sections, lines of intersection, maps regarding existing mining activities and abandoned mining areas)

After modeling the deposit and calculating the geological coal reserves the mine

engineering and the technical & commercial planning will be the next steps. To consider all facts and aspects about the surroundings of the mine it is also necessary to get the following information:

- What is the target production (per day and per year)?
- Clients / Market demands for coal parameters (Is a preparation plant necessary?)
- Is there any infrastructure in the mining area under consideration (roadways, power supply, voltage, ventilation)?
- What about the investment budget?

After collection of all available data the next steps for the modeling and the calculations are always the same. Figure 1 shows the typical step on the development of a project up to the successfully end with the supply of equipment and operational and maintenance assistance.

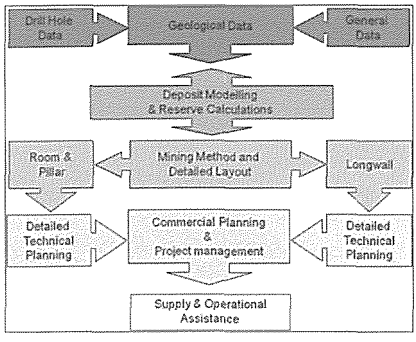

Figure 1. Typical Procedure

3.4 3D-modelling & reserve calculations

After all available data has been sorted, controlled and discussed within the joint (with client) project team, the following information is usually provided to the client.

- Contour maps of Floor conditions, dips & thicknesses of the seams
- Geological reserves
- Mineable reserves based on the proposed mining method and equipment
- Mineable reserves panelwise (ROM, clean coal, percentage of rock)
- Quality aspects like calorific values, ash content, etc.

3.4.1 Evaluation of drill holes

The first important act is to inspect and to classify the drill hole information. That signifies to define the coal layers, the intermediate layers, the seamfloor height (of the geological coal) and to determine the coordinates of the drill holes.

If all data are checked and seems to be reliable the information will be imported into the DUDE program.

Figure 2 represents the drill hole information (seamfloor elevation and the geological thickness) after loading into the modeling program.

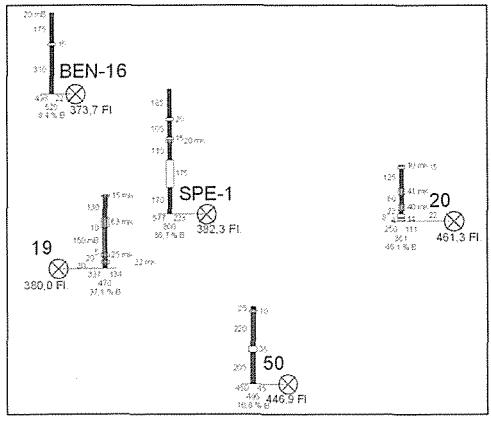

Figure 2. Koyunagili coalfield; Drill holes

3.4.2 Seamfloor

Afterwards the seamfloor heights of the geological log will be evaluated and interpolated and the seamfloor layer could be generated. A typical result is shown in Figure 3.

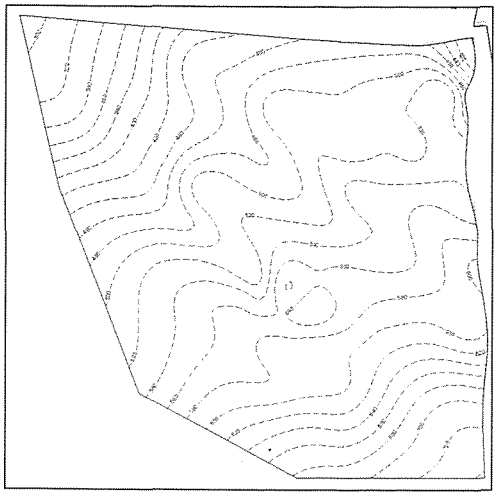

Figure 3. Koyunagili coalfield; Seamfloor layer

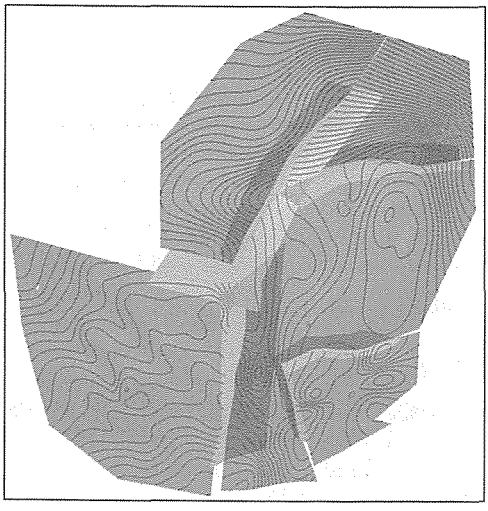

Figure 4. Koyunagili coalfield; Major Faults

3.4.3 Faults

The calculation and the modeling of faults is one of the most difficult parts during the modeling of a deposit. The geological information about faults is often insufficient and needs additional interpretation by personal experiences, assessments, estimations and evaluations. Figure 4 represents geological faults that are explored and mapped. The throw and the dip are known.

Beside these major faults there are often additional smaller faults which can be assumed and indicated by irregularities in the seamfloor contours. In order to find out either there are real small-scaled faults or other unknown irregularities inside the seamfloor there is often only the possibility to develop these disturbed areas by driving of roadways. The undulation of the seamfloor and the real seamfloor heights will be an important support during the development of all roadways.

3.4.4 Qualities

For the customer one of the most important parameter is the calorific value. It is a major criterion for the achievable sales price and possibly the related necessity of a washing plant.

It will be also possible to calculate and modulate the distribution of other criteria like ash content, volatile matters, etc.

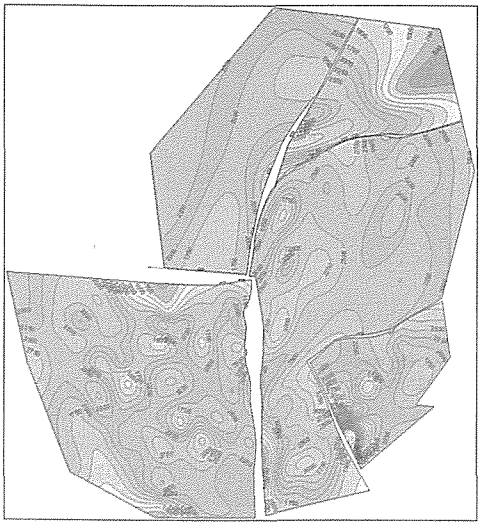

Figure 5. Koyunagili coalfield; Distribution of calorific values

3.5 Mining method and mining layout

When the evaluation of the deposit is finished the model can be used for the next steps. The deposit will be interpreted by the mine surveyor and the mining engineers and the general mining method and the mining layout can be developed.

Both, mining method and layout, depend on several factors:

- o Coal reserves and depth of the seam
- o Dips of the seams
- o Roof & floor conditions
- o Number of faults & general UG conditions

The general mining method will be recommended such as:

Longwall Technology

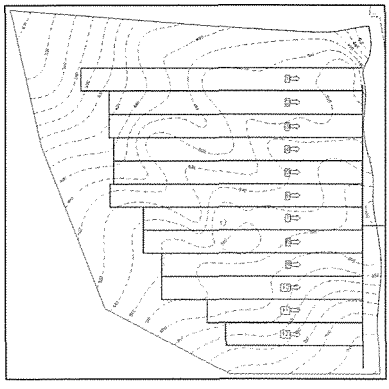

Figure 6. Longwall Technology

or

Room & Pillar Technology

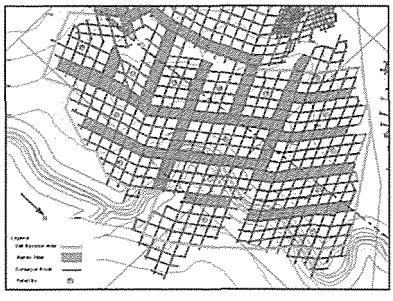

Figure 7. Room & Pillar Technology

In the present example of the Koyunagili coalfield project, the proposal by the engineering experts was to mine the coal with longwall technology.

The first block that used to be mined has suitable conditions and parameters for applying longwall technology.

Contrary to surface mining or Room & Pillar operations, there is no standard mining equipment for Longwalls and any underground longwall mining equipment needs to be customized for the present conditions on the clients deposit.

In case of the Koyunagili coal deposit the seam structures are so variable that the optimized "workable thickness" has to be defined. In order to supply the most economic underground mining equipment different working ranges were considered and consequently calculations made for different working thicknesses.

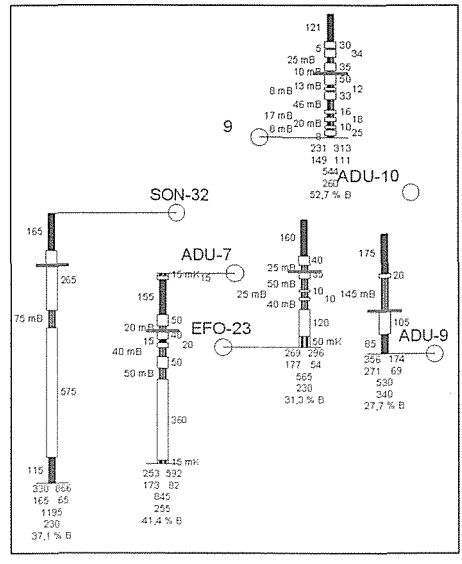

Figure 8. Koyunagili coalfield; Definition of workable thickness

After defining the underground mining equipment the definition of the mining layout could start.

The layout depends, among others, also on:

- o Dip / Strike of the seamfloor

○ Thickness of the coal seam
○ Annual production rate
The following two figures (figure 9 and 10) show exemplary the longwall mining layout for the Koyunagili coalfield project.

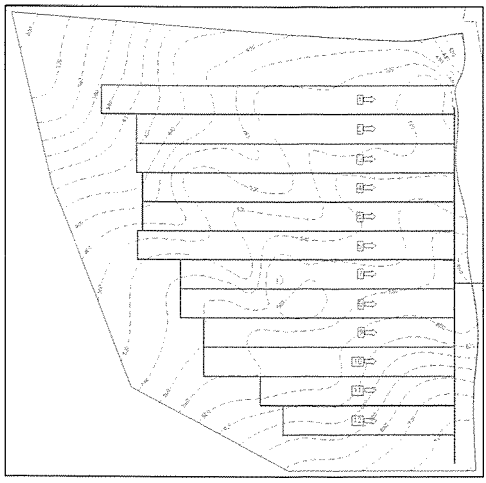

Figure 9. Koyunagili coalfield; Mining Layout

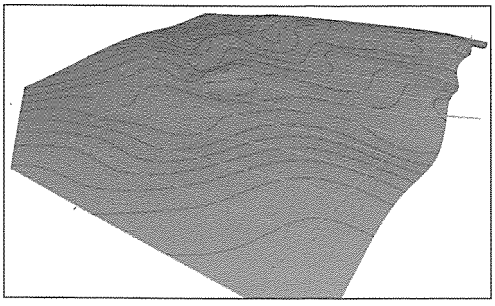

Figure 10. Koyunagili coalfield; Mining Layout (3d-picture)

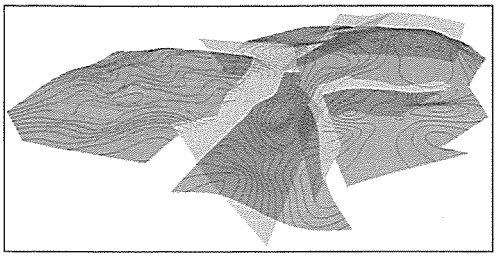

Figure 11. Koyunagili coalfield; Overview about the deposit (3D-model)

Figure 11 represents the whole deposit of the Koyunagili coalfield project. The first block is being estimated and evaluated. The mining layout is made and the underground mining equipment is determined.

This step is a so called "milestone" for the development of underground mining project. Based on the provided information
○ Reserves (geological, mineable)
○ Rough investment cost estimates
○ Rough operating cost estimates
○ Actual market prices for the mineable mineral

The client can decide whether the project can be economical feasible or not. Depending on this investigation it will be decided to go ahead with the project and the further engineering steps or not.

3.6 Detailed technical planning

After the decision to proceed with the development of the project, the detailed engineering can start.
Depending on the clients demands the detailed engineering can include all relevant aspects like:
○ Detailed technical specification of the mining equipment (in cooperation with design and engineering departments)
○ Detailed technical specification of "Third party equipment"
○ Electrical mine planning
○ Ventilation planning
○ Coal transport
○ General infrastructure (i. e. fresh and waste water handling, material transport)
The following figures indicate several parts of the technical planning.

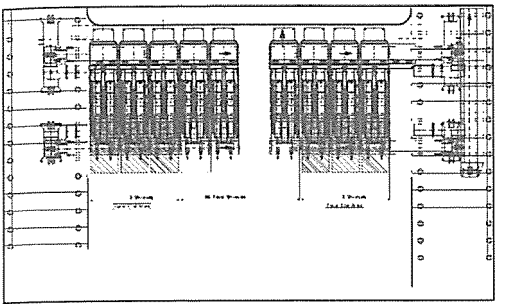

Figure 12. Technical face layout

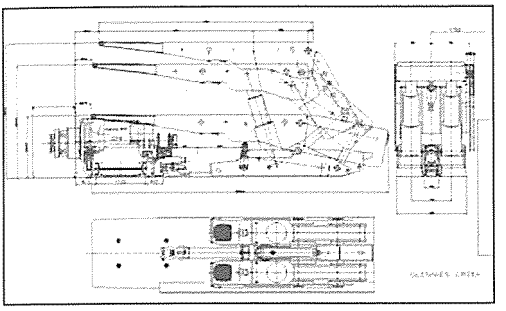

Figure 13. Face cross section

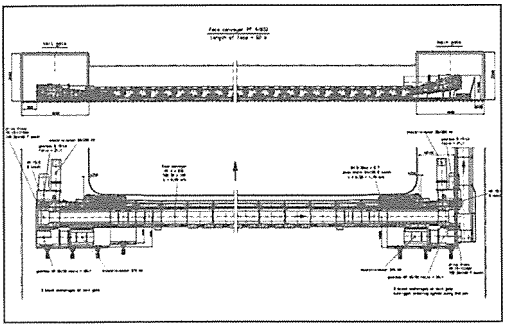

Figure 14. Face end solution

3.7 Further Activities - Supply & Project Management

Beginning with the date of placing the order until the start of production, the cooperation with the client should include the project management for:

- Supervision of manufacturing schedules
- Interface treatment to "Third party products"
- Transport of the equipment packages
- Supervision of implementation schedules
- Supervision of training schedules

3.9 Service contracts

After start of production the client will be supported by some on-site assistance until the end of the performance test. Also afterwards up to the complete lifetime of the project, the success of the project often depends on extended services to be provided by the supplier and long term partner to the client:

Operational Services:

This will require a mobile team of experienced experts familiar with the operation of the specific mining equipment available with the supplier.

Maintenance Service:

The maintenance service contracts will cover the provision of service people on-site for the supervision of maintenance as well as the complete spare part management for the state of the art equipment.

4 SUMMARY

The above described evaluation and modulation of the Koyunagili coalfield project is one of the main tasks of the department "Application Engineering & Mining Consulting" in Bucyrus, located in Saarbruecken.

Figure 1 gives a good overview about all main steps.

The first and most important part before starting a calculation / modulation of a deposit is the collection of data. This information should include data about the drill holes, seams, faults, surface, purposes of the client, etc.

Afterwards the deposit modeling and the reserve calculations need to be done. The evaluation of the 3D-model is the most time-consuming part of such a study.

Subsequently the mining method and the mining layout have to be investigated and determined.

These steps of the Koyunagili coalfield project are finished now. The mining activities are still in progress and the following tasks will be determined.

Formation of geoinformation system of the coal mine with underground coal exploitation

Aleksandar Milutinovic[1], Igor Miljanovic[1], Aleksandar Petrovski[1], Milena J. Pejovic[1], Cedomir Beljic[1], Grozdana Gajic[2], Vladimir Cebasek[1], Branko Gluscevic[1]

[1]*Faculty of Mining and Geology, University of Belgrade, Serbia*
Tel. +38111 3238564, Fax. +381 11 3347934, e-mail: vujic@rgf.bg.ac.rs
[2]*Faculty of Forrestry, University of Belgrade, Serbia*

ABSTRACT Mining is a complex technical-technological activity, specific by its permanent changes of condition in space, different occurrences, large number of different objects, both by type and purpose, and by its size, i.e. dimensions. Having in mind the uniqueness inherited in mining, the formation of the geoinformation system (GIS) is completely justified and necessary. If the underground exploitation is analysed as a part of mining, as a way for mineral resource exploitation, often the only way, GIS bears an important function in all the phases of mining production. Underground exploitation of coal from the point of view of a spatial position and the geometry of underground rooms, machinery and equipment contained within, is a complex activity, also from the point of view of occurrences in spaces making the mining operation environment difficult (rock pressure, coal dust presence, underground water, swelling, creation of fissures, attrition and collapse of the rock massif, etc.). The specific properties mentioned are separating the coal exploitation from the exploitation of other mineral resources, both in a technical-technological sense of the exploitation method solution, and securing the safe operating conditions, and in a need to constantly monitor and record the condition and spatial changes of condition. The paper presents the formation of GIS of capital mining areas: main transport dip heading (GTN-1, GTN-2), main ventilation dip heading (GVN-1), pit bottom (N) at the level of H=+170.00(m) and haulage shaft (O).

1 CONTENTS OF THE GIS OF AN UNDERGROUND MINE

GIS contains large number of different data, that can be adequately input, processes, archived and presented, depending on objects or occurrences they describe and define. An adequate way is the one that would ensure needs for a unique, easy and prompt presentation, and, in general, work with the data in all the stages of design, management and utilization of GIS. The data collected are aimed to fulfil the demand in question, but they are divided by its form and purpose to:

- Alphanumeric data (attributes);
- Graphical data (spatial data)

All data in GIS (alphanumeric and graphical) that determine the spatial data of an underground room, the position of the objects and locations of different occurrences, have x, y, z coordinates determined within the georeferenced coordinate system.

All the spatial information is related to the underground room, regardless of the aspect of collection, process and utilization of that information (geometry, objects, and occurrences). The underground room is a subject (entity) for which all of the spatial information are defined, created, developed and related, in the process of creating the information system as well as its creation, input and updating the data, utilization, search according to various criteria, publishing reports on alphanumeric and

graphical form, etc. For this reason, in defining the contents of spatial information on underground rooms, it is necessary for GIS to contain the records on the underground rooms, for a single mine shaft, with an overview and a division of rooms according to certain criteria with the aim of obtaining the information on type, number and the purpose of rooms for which the data on geometry and thematic contents are recorded.

Spatial information on underground mining rooms is presenting the basis for formation of the spatial information system, both alphanumeric and graphical database within the GIS. Regarding the need that an underground room exists in the records, to hold a certain position within the space, and to hold certain dimensions that are reserving the space, but also the objects located in the room, those certain occurrences are an inevitable part of the underground exploitation, the contents of the spatial information is divided into three groups of information:

- Underground rooms records;
- Geometry of the underground room;
- Thematic content of the underground room.

This division is accomplished with the aim of easier definition and readability of the GIS contents, its formation, utilization and spatial information management. Large quantity of data within each of the three groups of information, made inevitable the division inside one of the information group. Information on the evidence of underground rooms is divided into two groups of data:

- Type of room according to the spatial position (corridors, dip headings, rise headings, shafts);
- Room purpose (haulage, transport, ventilation, excavation, etc.).

Information on the geometry of the underground room is divided into:

- Geometry elements of the spatial position of the room (spatial coordinates of the main axis, descent-ascent, curve elements, etc.);
- Geometry elements of the underground room (width, height, length, light profile area, etc.).

Information on the thematic contents of the underground room is divided, similar to the previous cases, into two data sets:

- Objects in an underground room (transport, haulage and excavation systems, machinery and equipment);
- Underground room occurrences (rock pressure, coal dust presence, gas presence, underground water presence, etc.).

2 COLLECTING THE DATA FOR GIS FORMATION

Data necessary for formation of GIS according to the listed content were collected on the basis of technical documentation of the mine, and immediate geodesic measures in excavations (Figure 1), by using the appropriate geodesic equipment.

Geodesic measurements provided the data on the spatial position and the geometry of rooms and equipment within. The activities aiming to obtain the data on geometry consist of:

- Analysis of the room and determination of typical lateral profiles and dots within the room;
- Determination of instruments, equipment and methods of measurements;
- Determination of points of the survey base (polygonal and levelling georeferenced point),
- Geodesic measurements.

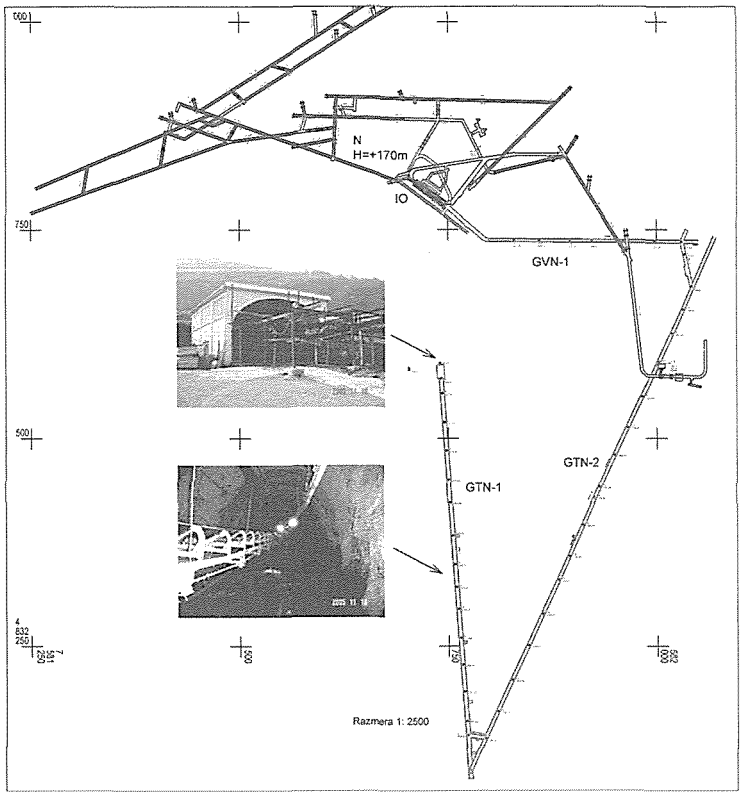

Figure 1. Situation plan of the "Soko" coal mine in Sokobanja

3 FORMATION OF ALPHANUMERIC AND GRAPHICAL DATABASE

After the collection and processing of data, the following phase in GIS design is a development of alphanumeric and graphical database. The alphanumeric database is created by manual formation of all the necessary elements (Blank Database), by using the Microsoft Access software (Figure 2, 3). The database consists of tables with following titles and contents:

- Underground rooms records;
- Geometry elements of the spatial position;
- Communication with other rooms;
- Lateral profile data;
- Longitudinal profile data;
- Curve room;
- Machinery, devices and equipment;
- Support unit;
- Occurrences;
- Polygon and levelling points.

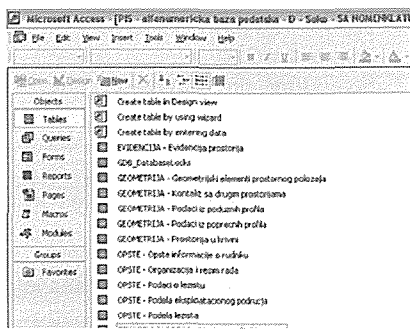

Figure 2. Alphanumeric database

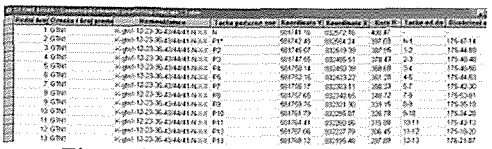

Figure 3. Table with attribute data

For the needs of GIS, all the graphical reviews (plans, profiles, sections, 3D models, etc.) were developed digitally, after which the graphical database was formed, using the AutoCAD map application, contained in the AutoCAD Land Development Desktop software package. After naming the project (mine title), graphical data were imported in the workspace (*Project Workspace*) (figure 4.).

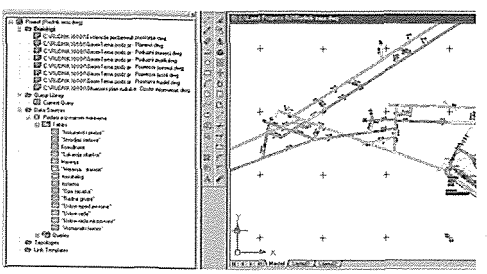

Figure 4. Graphical database

4 INTEGRATION AND CONNECTING THE ALPHANUMERIC AND GRAPHICAL DATABASE IN ARCGIS

Activities conducted in GIS creation (integration of alphanumeric and graphical database) and their uses in ArcGIS are:

1. Formation and review of the database in the ArcGIS;
2. Searching the database, queries and analyses;
3. Database updating;
4. Data transfer;
5. Printing of data;
6. Archiving of data.

Formation and review of the database in the ArcGIS is made of following activities:

- Data input from the alphanumeric and graphical database into the ArcCatalog module, creation of database and database review;
- Input data from the alphanumeric and graphical database into the ArcMap module, creation of layers, linking the alphanumeric data with the graphical entities and a review of database;
- Data input from alphanumeric and graphical database (spatial models) into ArcScene module, creation of layers, linking the alphanumeric data with graphical entities and database review.

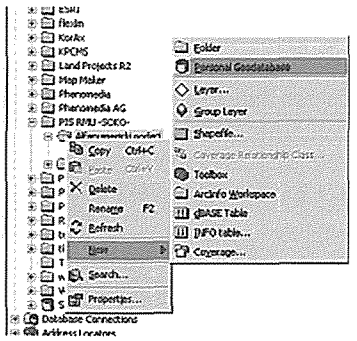

Figure 5. Formation of alphanumeric data database

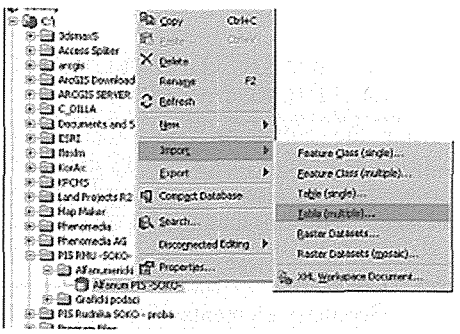

Figure 6. Importing the tables from the alphanumeric database (Microsoft Access) to the GIS database

Input of data into the ArcCatalog is accomplished after the creation of the folder (for the purpose of this example, named PIS RMU –SOKO-) and subfolders alphanumeric data and Graphical data. After the folder is formed, an empty file (Personal Geodatabase in the example entitled

Alphanum PIS –SOKO-) (Figure 5) is created and tables from the Microsoft Access database were imported (Figure 6). After this procedure, a review of data by tables is accomplished, aiming to control the correct transfer of data from one database into the other. The data in the created database can be searched according to a given criteria, exported into some other type of database, geocoded, etc.

The procedures with graphical data input are the same as with input of alphanumeric data. The difference exists with creation of blank – empty files. Figure 7 shows data files according to different types of graphic representation, or by a created graphical database into the AutoCAD Land Development. For each imported drawing, ArcCatalog is creating five layers, without participation from the operator (user). Each layer contains a certain type of entity (dots, lines, polygons, attributes).

After the creation of database in the ArcCatalog module, the next activity in ArcGIS is to create a database in the ArcMap module, where it is possible to link the alphanumeric data with graphical entities, repeating the different queries, updating the data, geocoding, analyses, data conversion, printing, etc. Listed activities within ArcMap are just a small portion of possibilities of ArcMap, as a consequence of a large number of tools in ArcToolbox. In the ArcMap module, the data are imported from ArcCatalog, where the data files with titles according to the titles provided when creating the database in ArcCatalog are located.

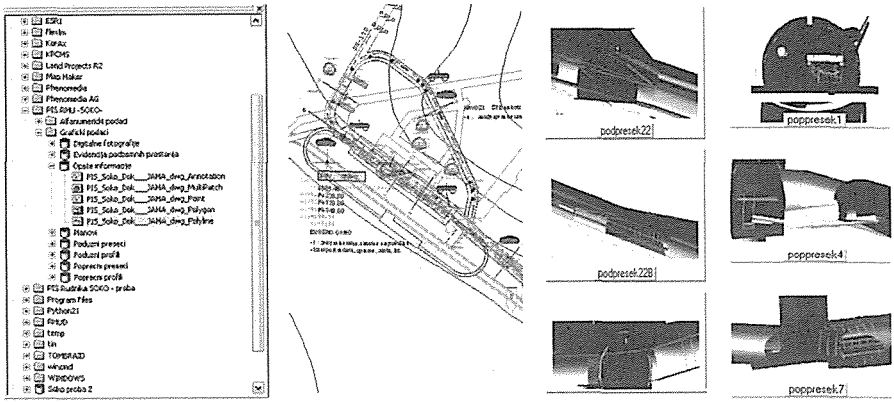

Figure 7. Graphical database of data in GIS application

During the input of graphic reviews into ArcMap, alphanumeric attributes are added to each graphic entity: ID number, type of graphic entity (line, polyline, circle, polygon, etc.), corresponding layer, entity colour mark, peak elevation of the entity and the textual description (if it exists for a certain entity), Figure 8.

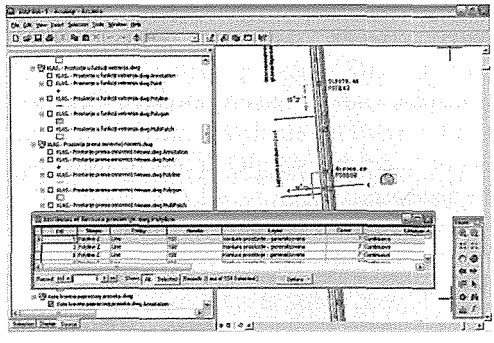

Figure 8. Graphical entities attributes in ArcMap

The procedure of linking the spatial and attribute data in creating the GIS is accomplished upon input of all graphical and alphanumeric data into ArcMap. By using the existing commands of ArcMap (Join, Join Data), a selection of an alphanumeric table and the graphical entity to be joined is accomplished.

The database created in ArcScene provides an ultimate form and shape of the GIS of underground rooms. It is a last activity in a whole line of activities for achieving the spatial information system. In ArcScene, the geometry, objects and occurrences in the underground exploitation are presented spatially, and connected with the alphanumeric data that describes the space beneath the Earth's surface additionally. The virtual presentation, enriched by the data from the alphanumeric database, and whole line of tools from the ArcScene used for spatial navigation (Navigate, Pan, Fly, etc.) ensures the quality interpretation of space with the aim of correct decisions and conclusions (Figure 9.).

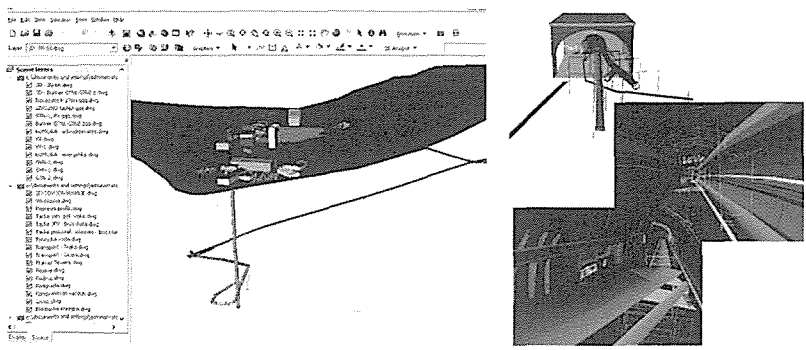

Figure 9. Visualisation of mine in ArcScene

5. SEARCHING THE DATABASE, QUERIES AND ANALYSES

Tools of software packages, such as ArcGIS, enables different queries, conditions and criteria in searching the database, i.e. in setting the different demands for obtaining the certain data. More often, in creating the queries, with obeying certain procedural principles and the exactly expected answer, it is desirable to employ creativity with the aim of easier and simpler access in searching the database.

Figure 10 shows an example of determining the quantity of waste (limestone) in m^3, in developing the underground room GTN-1.

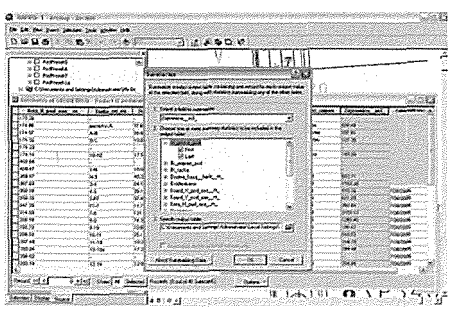

Figure 10. Determining the volume of GTN-1 by creating a certain query

CONCLUSION

By using the approach presented here in the development of GIS, the defined methodology and phases of operation in its creation, and in defining its content in particular, a background for GIS application

in coal underground mines was created. From the practical point of view, the application of GIS in mines is expected to improve the operation effects of the geodesic, design and technical services, reflecting further to the quality and production effects, thus influencing the profitability, humanization of work, etc. Therefore, GIS finds its application in mines from the following points of view:

- Design foundation for mining operations;
- Monitoring the spatial condition for different purposes and demands;
- Resolving potentially damaging situations and saving the miners;
- Process of closing the mines or revitalization;
- Developing the design on using the mine for other purposes and intents;
- One of the influential elements of the economic effects of exploitation and support for other analysis on production.

Aiming to successful application of GIS from the points of view listed above, it is necessary to accomplish the following:

- A connection between the graphical entities and the alphanumeric database according to its organization and technological membership;
- A simple and fast search and access to data by different spatial, thematic and temporal criteria, by opening the database with a visual query to the graphical entity;
- A possibility of separate reviews and reports by certain organizational entities and topics;
- An automatic and timely updating the condition changes in space with the minimal piling the data of same type;
- Prompt preparation of the report and presentation as a foundation for decision making and planning of activities in an underground room;
- Compatibility and standardization of information on space with project and technical documentation at the mine level.

REFERENCES

Milutinović A., Dimitrijević S., 2005, A proposition of the contents of GIS for underground rooms in mining, *Underground operations,* No. 14, Faculty of Mining and Geology, Belgrade, (7-12) (in Serbian).

McCoy J., 2004, *Geoprocessing in ArcGIS*, ESRI, Wilson, North Carolina.

Pasternack S., Kirkbride R., 2003, GIS applications in the GeoSciences, *OTEC - Ohio Transportation Engineering Conference*, 2003.

Burrough P. A., McDonnell R. A., 2006, *Principles of Geographical Information Systems*, Oxford University Press, 2nd edition.

Perencsik A., Woo S., Booth B., 2004, *Building a Geodatabase*, ESRI, Wilson, North Carolina.

Price, M., 1999. Terrain modelling with ArcView 3D Analyst, *ESRI ArcUser Magazine,* Jan-March,1999.

Torries F. T., Kern J., 1999, *Using GIS to Identify High Value Areas in Large Coal Resources*, Society for Mining, Metallurgy, and Exploration, Denver, CO, February.

Vujic S., Ognjanović J., GIS philosophy – a foundation of development of a hypertext interface for the information-management systems in mining, *First Yugoslav scientific meeting on GIS technologies,* SANU, 1996., Belgrade, (273-280) (in Serbian).

Vujić S., et al., An intelligent system for visual monitoring of the ecs complex of the „Majdan III" open pit mine, Potisje Kanjiza, *Application of Computers and Operations Research in the Minerals Industries*, The South African Institute of Mining and Metallurgy, (Series S31), Cape Town, 2003., (73-780).

Vujić S., Miljanović I., Petrovski A., GPS supported systems for surveillance and monitoring of energetic and technological parameters at open pit mines, M*odern techniques and technologies in mining,* Faculty of mining and geology, University "St. Cyril and Methodius" Skopje, 2006, (1-10).

Vujic S., et al. A concept of information support for land reclamation and spatial arrangement of the open pit mines of electric power industry of Serbia, *2nd Balkan Mining Congress*, 2007, (361-369).

Vujic S., et al., *Study research on the justification of selective excavation of overburden – Phase 2: Information logistics of land reclamation, revitalization, and spatial arrangement of the exploitation fields of the EPIS coal mines;* Electric Power Industry of Serbia, 2006.

Vujić S., et al., A concept of the establishing the computer supported information-management system at the „Drmno" open pit mine, Coal Basin Kostolac, *Journal of Mining Science* , Springer New York, Vo. 44, No. 3, 2008, (312-319).

MINERAL PROCESSING

Investigation of Lead Extraction Process from Galena Concentrates by Full Factorial Design

Nuran Ay*, Golibsho Nasymov*,+
*Anadolu University, Material Science and Eng. Dept., Eskisehir,TURKEY
+Tajik Technical University, Inorganic Materials Dept., Dushanbe,TAJIKISTAN

ABSTRACT Nowadays the use of environment-friendly processes is gaining an increasing importance in metallurgy. Environmental regulations are continuously making it difficult to produce lead from galena concentrates by pyrometallurgical means. In this work, the hydrometallurgical extraction process of lead from galena concentrates supplied from Balya-Turkey and Koni Mansur-Tajikistan deposits in nitric acid solutions is studied. The chemical analyses were conducted with XRF and EDX while mineralogical analysis was carried out with XRD. The galena concentrate was ground and sieved till the -63 μm particle size and used for further extraction processes. The extraction experiments were conducted using Full Factorial experimental design technique. Temperature, acid solution concentration and particle size were the operating parameters. Stirring speed was kept constant during the tests. After the extraction processes solid-liquid separation was carried out and the amount of lead in solution was determined using FAAS. The results were analyzed using MINITAB 15.0 statistical software program.

1 INTRODUCTION

Being widely spread in nature, lead ores are mainly composed of galena (PbS) and its oxidized forms, such as anglesite ($PbSO_4$) and cerussite ($PbCO_3$). Along with these, it usually occurs with other sulphide minerals such as sphalerite (ZnS), pyrite (FeS_2) and chalcopyrite ($CuFeS_2$) (Abel et al., 1973). Flotation concentrates in general are treated by pyrometallurgical processes resulting in release of metallic dusts and vast amount of SO_2 gas, consequently presenting substantial environmental problems. Yet another drawback for conventional smelting processes is their incompatibility for treating complex and low grade ores as well (Chen, 1992; Burkin, 1966). Hence, application of hydrometallurgical methods for the purpose is considered adequate in the light of recent developments in this field (Habashi, 2007).

Several hydrometallurgical systems are proposed for the oxidation of sulphide minerals; dissolution in solutions of nitric, sulphuric or hydrochloric acids and dissolution in concentrated solutions of multivalent transition metals (mainly Fe III) and alkaline or alkaline earth metals facilitating lead salts solubility (Strunnikov and Koz'min, 2005; Raghavan et al., 2000; Farahmand et al., 2009; Pashkov, et al., 2002; Chenglong et al., 2008). Some other studies have been made on dissolution of galena in wide range of oxidative media such as fluotitanate (Duyvesteyn, 2002), fluosilicate (Chen, 1992), bioleaching (Pacholewska, 2004) and acidic oxygen saturated solutions (De Giudici and Zuddas, 2001). However, it has been mentioned that each system has its own drawbacks depending on different characteristic properties of selected methods. Chloride

hydrometallurgical systems are based either on the temperature dependence of lead chloride solubility or on ability of oxidized lead compounds to dissolve, forming soluble complex structures in concentrated chloride solutions. Several experimental small-scale industrial productions have been established on this scheme (Andersen et al., 1980). In spite of the fact that this method provides sufficient degree of extraction and contributes lead refining process, it is associated with uneconomical energy consumption and the necessity of handling large volumes of solution.

Sulphate hydrometallurgical schemes mainly involve sulphuric acid as leaching reagent and have been studied thoroughly in comparison to other systems due to reagent availability. Though this system gives a better process selectivity due to low solubility of lead sulphate, the same factor makes it hard to separate lead sulphate during further procedure. A series of additional processes involving the use of organic complex-forming compounds have been applied to this scheme to assist lead sulphate extraction. Overall, both chloride and sulphate systems were not acceptable to industry mostly because of the low lead sulphate and chloride solubility in water and the complexity of reagent regeneration processes (Strunnikov and Koz'min, 2005).

Nitric acid is a good sulphide mineral oxidizing agent considering high solubility of lead nitrate. A series of studies have been conducted on nitric acid leaching with or without additives. Though there are many studies on the dissolution of galena in nitric acid solutions still there some aspects remain to be investigated regarding oxidizing reagents, oxidation products and impact of factors on the process (Aydoğan et al., 2007; Halikia et al., 2002; Fuerstenau et al., 1987; Adebayo et al., 2006; Mikhlin et al., 2004).
For evaluation of the effect of various parameters on dissolution process of sulphide minerals, statistical techniques have been used to determine the degree and extent of factors and factor interactions impact on the process. Farahmand et al. (2009) applied orthogonal array design for optimization of lead and zinc recovery from plant residues in consequent sulphuric acid and brine solutions.

The scope of this study is to analyze the galena concentrate dissolution in nitric acid by use of full factorial design with MINITAB 15.0 statistical software program. The effects of main factors (temperature, concentration and time) and the effects of interactions between these parameters are studied by application of variance technique (ANOVA technique). The response is the percentage of lead extraction from galena concentrate.

2 EXPERIMENTAL

Galena concentrates supplied from Koni Mansur/Tajikistan and Balya/Turkey were used for the leaching experiments in nitric acid solutions. The chemical compositions of galena concentrates from Koni Mansur (KM) and Balya (BA) are given in Table 1. A general level $5^2 8^1$ full factorial design with two replications was applied for analysis. The factors (temperature, concentration and time) and their interactions are given in the Table 2.

Table 1. Chemical compositions of Koni Mansur and Balya galena concentrates.

	KM	BA
Element	wt.%	wt.%
Pb	46,569	50,613
S	21,886	16,426
Zn	4,016	16,233
Fe	20,693	4,849
Cu	2,037	2,687
Si	3,887	8,170
Al	1,297	0,866
K	0,907	-
Ca	-	0,703

Experiments were performed with -63 μm particle size and at constant stirring speed of 400 rpm. Distilled water and Merck grade reagents were used to prepare solutions. Dissolution of samples was conducted in a closed, thermostatted 1 L stirred glass reactor. 500 mL of nitric acid solution with predefined concentration was added into the

reactor and after reaching the desired temperature 1 g of sample was introduced into solution. At determined time intervals sample solutions were taken out from reactor up to 90 min and diluted with distilled water for determination of lead concentration using flame atomic absorption spectrometer. Each experiment was performed twice and arithmetic mean of the obtained values was used for evaluation of the experimental results.

Table 2. Main factors and their interactions.

Main factors	Two factor interactions	Three factor interactions
Temperature	Temperature x Concentration	Temperature x Concentration x Time
Concentration	Temperature x Time	
Time	Concentration x Time	

The chemical analysis of samples was carried out with XRF (Rigaku-ZSX Primus), the elemental and structural analyses with SEM-EDX (ZEISS Supra 50 VP), phase analysis with XRD (Rigaku Rint RAD 2000). The response values i.e. concentrations of lead in leach solution were measured with Spectra AA model Flame Atomic Absorption Spectrometer. Measured response values were analyzed with MINITAB 15.0 statistical software program.

3 RESULTS AND DISCUSSION

In order to examine the main factors and their interactions for the galena concentrates supplied from Koni Mansur/Tajikistan and Balya/Turkey a general $5^2 8^1$ full factorial design was used. Experimental design involved two variables with five levels and one variable with eight levels. Thus total number of experiments became 200 for each galena sample with two replicates. The main parameters, their levels and corresponding codes are given in Table 3. Analysis of parameters and interactions was conducted with ANOVA for all response values. An abbreviated list of the mean values of two replicates for the lead yields obtained from both concentrates under study, Koni Mansur (KM) and Balya (BA) with coded factors and their levels are given in Table 4.

ANOVA table is used to test the equality of several means. **Source** of variations denotes factors and their interactions, ***DF*** defines degrees of freedom, ***Seq SS*** stands for the sum of squares and ***MS*** for the mean square (***AdjSS*** and ***Adj MS*** denote adjusted values of ***SS*** and ***MS***, respectively). ***F*** distribution is used for the inference about differences between factor variance. Thus, the effectiveness or ineffectiveness of a factor can be determined with ***F*** values in ANOVA table. The ***P*** value represents the probability the test statistics will take on and is useful for decision making. The error includes ineffective parameters and their interactions (Montgomery 2001).

Table 3. Factors and their levels (with codes).

Factors		Levels							
	Codes	1	2	3	4	5	6	7	8
Temperature,°C	x_1	25	35	45	55	65	-	-	-
Concentration,M	x_2	0.5	1.0	1.5	2.0	3.0	-	-	-
Time, min	x_3	5	10	15	20	30	50	70	90

Table 4. Means of two replications for lead yield values obtained from Koni Mansur (KM) and Balya (BA) galena concentrates.

		KM	BA
Runs	Codes	Pb yield, %	Pb yield, %
1	111	12.43	4.75
2	112	12.60	6.82
3	113	11.90	9.38
4	114	12.70	11.50
5	115	13.02	12.25
6	116	13.68	12.87
-	-	-	-
-	-	-	-
197	555	86.44	93.46
198	556	90.63	99.35
199	557	95.46	100.00
200	558	100.00	100.00
201	111	11.90	4.11
202	112	12.32	4.46
203	113	12.85	8.32
204	114	12.18	11.09
-	-	-	-
-	-	-	-
395	553	80.64	82.35
396	554	85.51	88.24
397	555	87.19	94.12
398	556	89.13	99.35
399	557	94.19	100.00
400	558	99.98	100.00

The ANOVA table that covers meaningful effective main factors and their interactions for Pb yield values of Koni Mansur (KM) galena concentrate is shown in Table 5. The results observed in this table demonstrate that in addition to the main factors, their interactions (Temperature x Concentration, Temperature x Time, Concentration x Time and Temperature x Concentration x Time) were effective within 95% confidence interval. Though the effectiveness of factor interactions on the process remain within a limited range and they are not great in value as are the main factors. This is shown on the pie chart depicting the effective main factors and interactions between them, Figure 1. As it is seen from pie chart the three largest factors on Pb yield values are temperature, concentration and time in decreasing order (42.8%, 31.9% and 15.5% respectively).

The error value is 0.5% which support the correctness of the analysis. The regression analysis was conducted and it gave the regression equation that represents the process for 90.4% within 95% confidence interval. The equation derived is as follows (Equation 1):

$$\text{Pb Yield} = -33,9 + 0,877\,x_1 + 12,5\,x_2 - 0,378\,x_3 + 0,146\,x_1 * x_2 + 0,0177\,x_1 * x_3 + 0,359\,x_2 * x_3 - 0,00873\,x_1 * x_2 * x_3 \quad [1]$$

Where x_1, x_2, x_3 are temperature (°C), concentration (M) and time (min.) respectively.

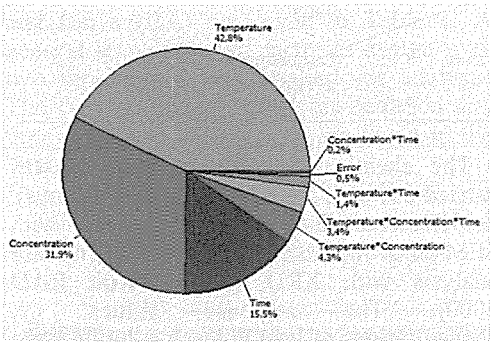

Figure 1. Pie chart of Pb yield values for Koni Mansur (KM) galena concentrate.

In the Figure 2 the plots for the main factors are given where effectiveness of each factor is shown. The mutual interactions between factors are given in the Figure 3 showing the relationship of a single factor to other ones. All factors have nearly linear effect on the leach process, with relatively close intensities. But still some slight deviations can be observed, defining the optimal point for the effect of a factor in a particular interval. Similarly, the aforementioned statistical analysis was applied to the response values obtained from Balya galena concentrate.

Table 5. ANOVA table of Pb yield values for effective factors for Koni Mansur (KM) galena concentrate.

Source	*DF*	*Seq SS*	*Adj SS*	*Adj MS*	*F*	*P*
Temp	4	127429,5	127429,5	31857,4	4563,27	0,000
Conc	4	95075,4	95075,4	23768,9	3404,66	0,000
Time	7	46301,3	46301,3	6614,5	947,46	0,000
Temp*Conc	16	12933,8	12933,8	808,4	115,79	0,000
Temp*Time	28	4144,3	4144,3	148,0	21,20	0,000
Conc*Time	28	617,3	617,3	22,0	3,16	0,000
Temp*Conc*Time	112	10022,8	10022,8	89,5	12,82	0,000
Error	200	1396,3	1396,3	7,0		
Total	399	297920,6				

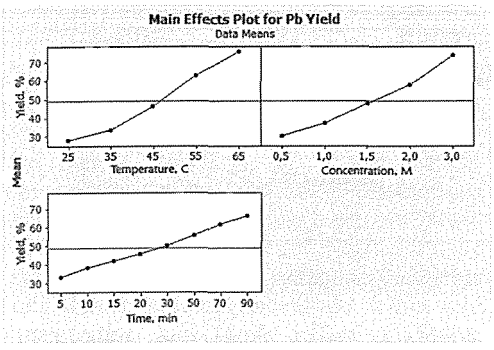

Figure 2. Main effects plot of Pb yield values for Koni Mansur (KM) galena concentrate.

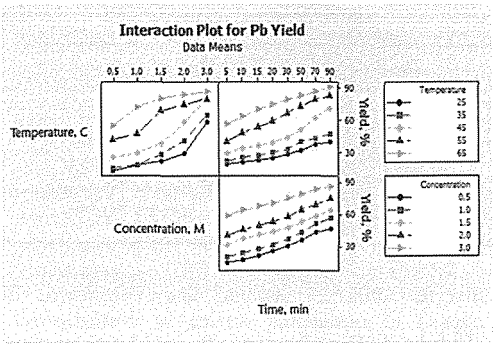

Figure 3. Factor interactions plot of Pb yield values for Koni Mansur (KM) galena concentrate.

Table 6. ANOVA table of Pb yield values for effective factors for Balya (BA) galena concentrate.

Source	*DF*	*Seq SS*	*Adj SS*	*Adj MS*	*F*	*P*
Temp	4	92985,2	92985,2	23246,3	5992,15	0,000
Conc	4	131075,1	131075,1	32768,8	8446,74	0,000
Time	7	85618,9	85618,9	12231,3	3152,83	0,000
Temp*Conc	16	8454,1	8454,1	528,4	136,20	0,000
Temp*Time	28	5263,9	5263,9	188,0	48,46	0,000
Conc*Time	28	3061,4	3061,4	109,3	28,18	0,000
Temp*Conc*Time	112	5780,0	5780,0	51,6	13,30	0,000
Error	200	775,9	775,9	3,9		
Total	399	333014,5				

The ANOVA table for Balya (BA) concentrate analysis is given in the Table 6. Resulting data and patterns demonstrated not too much difference with respect to effectiveness of parameters and their interactions. However, as it can be seen from Figure 4, interactions such as temperature*concentration and temperature*concentration *time had less but the main factor time had larger impact on the dissolution of Balya concentrate. Besides, in contrary to Koni Mansur concentrate the most effective factor is the acid concentration factor for the Balya concentrate.

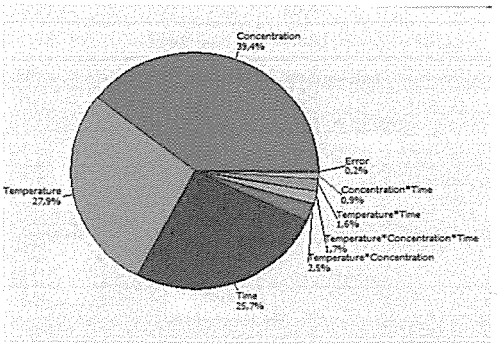

Figure 4. Pie chart of Pb yield values for Balya (BA) galena concentrate.

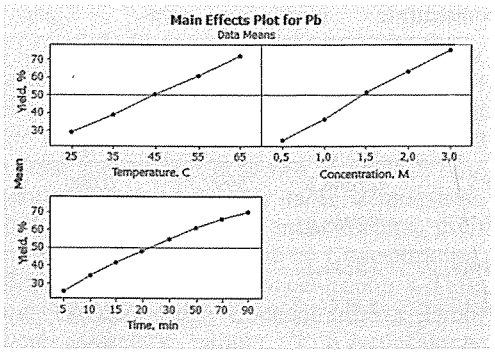

Figure 5. Main effects plot of Pb yield values for Balya (BA) galena concentrate.

The statements made above are supported by main effects plot given in the Figure 5 and factor interactions plot given in the Figure 6. The effect and intensities of the main factors and their interactions show some differences in smaller intervals, which is considered to be caused by the differences in chemical compositions of the concentrates. But in general it is observed that all main factors have intense and linear effects on the dissolution process for both concentrates. Finally, a regression analysis based on the data in ANOVA table of Pb yield values from Balya concentrate was conducted.

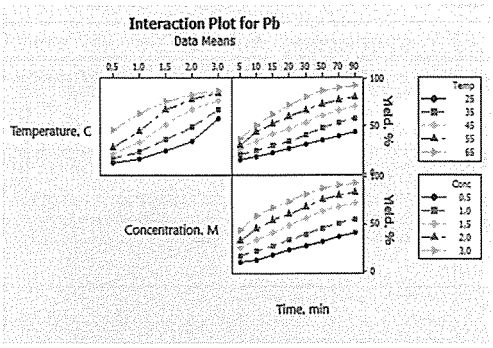

Figure 6. Factor interactions plot of Pb yield values for Balya (BA) galena concentrate.

The regression equation (Equation 2) representing the process for 89.2% within 95% confidence interval is given below:

$$PbYield = -20,7 + 0,528\,x_1 + 9,03\,x_2 - 0,384\,x_3 + 0,217\,x_1 * x_2 + 0,0171\,x_1 * x_3 + 0,375\,x_2 * x_3 - 0,00717\,x_1 * x_2 * x_3 \quad [2]$$

Where x_1, x_2, x_3 are temperature (°C), acid concentration (M) and time (min.) respectively.

Aydogan et al., (2007) state that dissolution process of galena accelerates with increase of nitric acid concentration up to 0.75 M in presence of hydrogen peroxide. Kholmogorov et al., (2003) reached the completeness of dissolution at higher

temperatures (80-85 °C) and 1,5 M acid concentration. In this work, the dissolution process of Koni Mansur galena speeded up the most after 2.0 M acid concentration at temperature intervals 25-45 °C and dissolution process completes at 65 °C, whereas dissolution rate of Balya galena showed a slight but almost linear increase for all acid concentrations and dissolution ends in 3.0 M at 55 °C. As it was mentioned by Mikhlin et al., (2004) the reason for decrease in dissolution rate is the passivation of galena surface. Most effective factor for Balya galena is acid concentration due to its surface passivation caused by the difference in its mineralogical composition.

4 CONCLUSION

In this study, Koni Mansur and Balya galena concentrates leaching in nitric acid is investigated by the use of full factorial design. The study showed that, the parameters such as temperature, concentration, time and their interactions have different effect on two separate galena concentrates.

Temperature was most effective factor for Koni Mansur galena concentrate, while acid concentration had larger effect on Balya galena concentrate. The parameter interactions had less effect in comparison to main factors and had relatively similar impact on the extraction process for both galena concentrates.

Mathematical models obtained by regression analysis and their corresponding equations (Eq.1 and Eq.2) represent the dissolution processes of Koni Mansur and Balya galena concentrates 90.4% and 89.2%, respectively.

These results demonstrate the suitability of application of statistical techniques on determination of optimal leaching conditions for galena extraction from concentrates.

REFERENCES

Abel, E.W., (Bailar J.C., Emeleus H.J., Nyholm R. and Trotman-Dickenson A.F. eds.), 1973. *Comprehensive inorganic chemistry*, Pergamon Press, New York, 458 p.

Adebayo, A.O., Ipinmoroti, K.O. and Ajayi, O.O., 2006. Leaching of sphalerite with hydrogen peroxide and nitric acid solutions. *Journal of Minerals and Materials Characterization and Engineering*, 5(2), pp.167-177.

Andersen, T., Boe Y.H., Danielssen, T., Finne, P.M., 1980. Production of base metals from complex concentrates by ferric chloride route in a small, continuous pied plant, *Complex Sulfide Ores*, Rap. Conf., Rome–London, pp. 186–192.

Aydoğan, S., Erdemoğlu, M., Uçar, G. and Aras, A., 2007. Kinetics of Galena Dissolution in Nitric Acid Solutions with Hydrogen Peroxide, *Hydrometallurgy*, 88, pp.52-57.

Burkin, A.R., 1966. *The Chemistry of Hydrometallurgical Processes*, E and FN Spon Ltd., London, p. 168.

Chen, A.A., 1992. Kinetics of leaching galena concentrates with ferric fluosilicate solution, *Master Thesis*, University of British Columbia, The Faculty of Graduate Studies, 127 p.

Chenglong, Z., Youchai, Z., Cuixiang, G., Xi H. and Hongjiang, L., 2008. Leaching of zinc sulfide in alkaline solution via chemical conversion with lead carbonate, *Hydrometallurgy*, 90, pp.19-25.

De Giudici, G. and Zuddas, P., 2001. In situ investigation of galena dissolution in oxygen saturated solution: Evolution of surface features and kinetic rate, *Geochimica et Cosmochimica Acta*, 65(9), pp. 1381–1389.

Duyvesteyn, W.P.C., 2002. Hydrometallurgical processing of lead materials using fluotitanate. *US Patent*, No: 6340423 B1.

Farahmand, F., Moradkhani, D., Safarzadeh, M.S., and Rashchi, F., 2009. Brine leaching of lead-bearing zinc plant residues: Process optimization using orthogonal array design methodology. *Hydromettalurgy*, 95, pp. 316-324.

Fuerstenau, M.C., Nebo, C.O., Elango, B.V. and Han, K.N., 1987. The kinetics of leaching of galena with ferric nitrate. *Metallurgical Transactions. B, Process Metallurgy* 18, pp.25–30.

Habashi, F., 2007. New Frontiers in Extractive Metallurgy, *Acta Metallurgica Slovaca*, 13, 3, pp.420-433.

Halikia, I., Zoumpoulakis, L., Christodoulou, E., 2002. Lead sulphide leaching kinetics in nitric acid solutions. *Erzmetall*, 55 (3), pp.166-175.

Kholmogorov, A.G., Pashkov, G.L., Mikhlina, E.V., Shashina, L.V., Zhizhaev, A.M., 2003. Activation of hydrometallurgical treatment of PbS in nitric

solutions. *Chemistry for Sustainable Development*, 11, pp.879–881.
Mikhlin, Yu., Kuklinskiy, A., Mikhlina, E., Kargin, V. and Asanov, I., 2004. Electrochemical behavior of galena (PbS) in aqueous nitric acid and perchloric acid solutions. *Journal of Applied Electrochemistry*, 34, pp. 37-46.
Montgomery, D.C., 2001. *Design and analysis of experiments*, John Wiley and Sons, New York, 684 p.
Pacholewska, M.,2004. Bioleaching of galena flotation concentrate. *Physicochemical Problems of Mineral Processing*, 38, pp.281-290.
Pashkov, G.L., Mikhlina, E.V., Kholmogorov, A.G. and Mikhlin, Y.L., 2002. Effect of potential and ferric ions on lead sulfide dissolution in nitric acid. *Hydrometallurgy* 63, pp.171–179.
Raghavan, R., Mohanan, P.K., Swarnkar, S.R., 2000. Hydrometallurgical processing of lead-bearing materials for the recovery of lead and silver as lead concentrate and lead metal. *Hydrometallurgy*, 58, pp.103-116.
Strunnikov, S.G. and Koz'min, Yu. A., 2005. Hydrometallurgical Schemes of Lead Concentrate Processing", *Chemistry for Sustainable Development,* 13, pp.483-490.

Ultra Fine Grinding of Calcite Powder in a Stirred Media Mill: The Effect of Some Parameters on Product Size Distribution

Kalsit Tozunun Karıştırmalı Bilyalı Değirmende Çok İnce Öğütülmesi: Bazı Parametrelerin Tane Boyut Dağılımına Etkisi

O.Y.TORAMAN
Nigde University, Mining Engineering Department, 51245, Nigde, Turkey

ABSTRACT Experimental investigations on the wet ultra fine grinding of calcite ($CaCO_3$) powder in stirred bead mill are presented. The net volume of the milling chamber is 0.75 liters. The grinding chamber is made of ceramic to reduce the wear on the materials of the mill. For cooling purposes, the grinding chamber is also equipped with a water jacket for cooling. The grinding media selected for the tests are 1 mm diameter zirconia beads. The influence of some operating parameters such as solids concentration (%), grinding time (min.), stirrer speed (rpm) and bead filling ratio (% of net mill volume) on the size distribution of ground product is discussed. The effect of grinding time on the particle size distribution and fineness is highly significant and positive. The variables stirrer speed and bead load have also positive effects on the grinding.

1 INTRODUCTION

The grinding equipment used for production of micron and submicron particles are mainly stirred media mills. These mills provide an effective size reduction in the product. The reductions are mainly due to the use of small grinding media with high stress intensities in the mills (Becker et al., 2001). These mills are very effective in the production of micronized material due to their easy processing, simple construction, high size reduction rate and less wear contamination, stirred bead mills have received more and more attention in recent years. Therefore, it has been started extensively to be used in the recent decade in many industries especially such as mineral, coal, ceramic, metallurgy, paint, chemical, agriculture, food, medicine and energy (Mankosa et al., 1986; Wang and Forssberg, 2000; Kwade and Schwedes, 2002). Two grinding modes including dry and wet modes are applied in the grinding processes such as ceramic, pharmaceutical, paint, mechanical activation of material and/or minerals, mechano-chemistry and many other industries. The comparison of the wet and dry grinding effects on the structural changes usually was made at the same grinding mill. For example, the effect of dry and wet milling in a vibratory mill for carbonates and quartz in air and aqueous environments was investigated by Tkáčová and Stevulová (1987). It was indicated that the use of an aqueous environment resulted only in enlarged specific surface area of the ground products. Baláž (2000) concluded that during wet milling in either an attritor or a vibration mill yield the least structural changes compared with their dry milling modes. According to Tkáčová (1989), wet grinding

proceeds with the preferential formation of new surfaces and little bulk deformation in the particles. Since the contribution of the non-equilibrium defects to the integral excess enthalpy content is considerably higher than the contribution resulting from the surface energy, the expected magnitude of excess enthalpy in wet grinding is lower than that one in dry grinding (Pourghahramani et al., 2008).

The objective of this study was to investigate the effects of operating parameters on ultra fine grinding of calcite powder. Batch grinding tests were conducted in a laboratory stirred mill.

2 EXPERIMENTAL

2.1 Material

The high purity calcite (99.5% $CaCO_3$ content) used in this study was from Nigde, Turkey. Chemical analyses and physical properties of the sample are shown in Table 1 and Table 2, respectively. Typical size distributions of the feed sample are shown in Fig. 1. The grinding media selected for the stirred mill tests was 1 mm diameter zirconia beads (Table 3).

Table 1. The chemical composition of the calcite (%)

$CaCO_3$	$MgCO_3$	Fe_2O_3	SiO_2	Al_2O_3
99.5	0.2	0.01	0.01	0.02

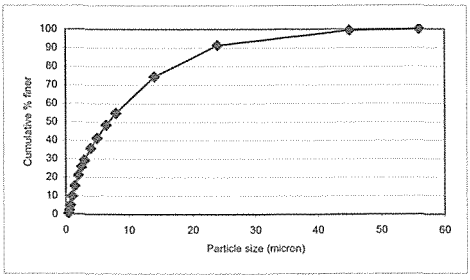

Fig.1. Particle size distribution in the feed material

Table 2. The physical characteristics of the calcite

True density (kg/m^3)	Mohs hardness	d_{50} (μm)	d_{98} (μm)	Specific surface area (m^2/g)
2700	3	6.88	36.22	2.07

Table 3. The physical properties of the grinding media

Composition	Specific density (g/cm^3)	Bulk density (g/cm^3)	Hardness
$ZrSiO_4$	>4.00	>2.60	>900 Hv

2.2 Method

The grinding tests were performed in a stirred mill Standard-01 Model manufactured by Union Process (U.S.A.). The dimensions and shapes of the grinding mill pot of the experimental stirred mill are schematically illustrated in Fig. 2. The net volume of the milling chamber is 0.75 liters. The grinding chamber is made of ceramic (Al_2O_3) to reduce the wear on the materials of the mill. For cooling purposes, the grinding chamber is also equipped with a water jacket for cooling. Table 4 shows a summary of the experimental conditions. The grinding experiment was carried out as a batch process in which samples were taken from the pot at a determined grinding time interval. After each test, all of the media and ground samples were removed from the mill, and the media were separated from the products by sieving. In order to investigate the effect of experimental parameters such as solids concentration, grinding time, stirrer speed and ball filling ratio on the particle size distribution of the products, a series of experiments were carried out. The particle size distribution of the feed and ground products were analyzed by wet laser diffraction using a Malvern Mastersizer 2000 apparatus.

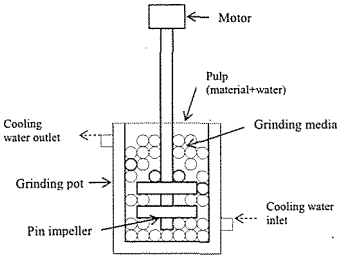

Fig.2. Schematic diagram of the experimental stirred mill

Table 4. Summary of the experimental conditions

Item	Experimental conditions
Solid concentration, wt%	10-50
Grinding time, min.	20-60
Rotation speed, rpm	300-500
Bead filling ratio, % of mill volume	45-70
Bead size, mm	1.0
Temperature	Room temperature
Material of media	Zirconia

3 RESULTS AND DISCUSSION

3.1 Effect of the Solids Concentration

The solids concentration is usually considered as an important parameter. An increase in the slurry concentration leads to an increase in the number of particles and hence the stress number, i.e. increase in the probability of a particle to be in the stressing zone. However, the more concentrated the suspension, the more viscous is the slurry and the lesser the probability of contact between particle and bead. The effect of the solids concentration on the grinding result depends mainly on the material and other operating conditions (Fadhel and Frances, 2001). The effect of per cent solids on the product size distribution is shown in Fig. 3. The results obtained for solids concentration of 10%, 20%, 30%, 40% and 50%. It could be concluded that a decrease in slurry density will increase the product particle size distribution curve shifts to be a finer size, resulting in a reduction of the mean size. For example, a slurry concentration of 50% produced a mean size of 2.86 μm, while 10% a mean size of 1.99 μm was obtained.

3.2 Effect of the Grinding Time

The effect of grinding time on the product size distribution, specially the d_{50} value was studied by conducting a series of grinding tests. The results obtained for grinding time of 20, 30, 40, 50 and 60 min. are shown in Fig. 4.

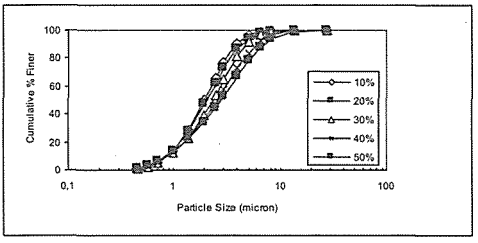

Fig. 3. The effect of solid concentration on the product size distribution for the attrition milling of calcite powder (grinding time: 30 min., stirrer speed: 350 rpm, ball filling ratio: 50%, ball size: 1 mm)

A finer product was obtained increasing the duration of attrition from 20 to 50 min. For example, a grinding time of 20 min. produced a mean size of 2.42 μm, while 50 min. a mean size of 1.77 μm was obtained. Fig.5 shows the relation between the median product size (d_{50}) and the grinding time.

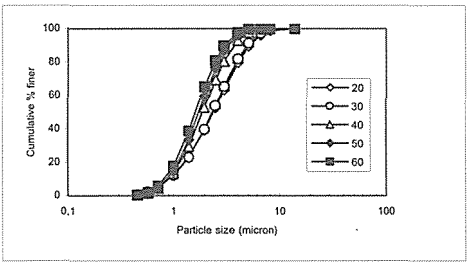

Fig.4. The effect of grinding time on the product size distribution for the attrition milling of calcite powder (slurry concentration: 30%, stirrer speed: 350 rpm, ball filling ratio: 50%, ball size: 1 mm)

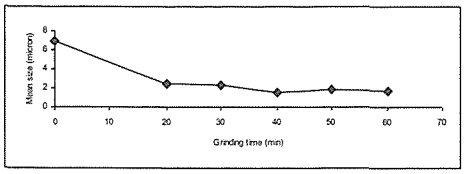

Fig.5. The relation between the mean product size and the grinding time

3.3 Effect of the Stirrer Speed

The stirrer speed is one of the most important parameters since it acts on the number of contacts between beads and the intensity of collision (Fadhel and Frances, 2001). The effect of stirring speed on the product size distribution was studied by conducting a series of grinding tests. The results obtained for stirring speed of 300, 350, 400, 450 and 500 rpm are shown in Fig. 6. It has shown that as stirring speed is increased the product particle size distribution curve shifts to be a finer size, resulting in a reduction of the mean size. For example, a stirring speed of 500 rpm produced a mean size of 1.72 μm, while 300 rpm a mean size of 2.1 μm was obtained.

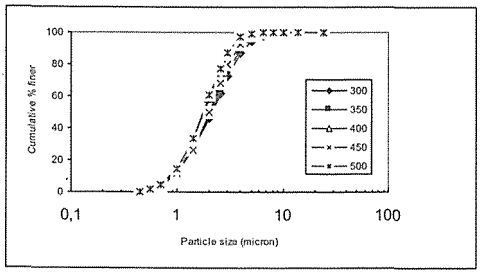

Fig.6. The effect of stirrer speed on the product size distribution for the attrition milling of calcite powder (slurry concentration: 30%, grinding time: 50 min., ball filling ratio: 50%, ball size: 1 mm)

3.4 Effect of the Bead Filling Ratio

The filling volume of grinding media also affects the product size distribution and fineness. The effect of bead filling ratio on the product size distribution for the milling of calcite powder has been reported on Fig.7. The results obtained for filling ratio of 45%, 50%, 60% and 70%. According to these results it seems that better fineness was achieved at the higher filling volume.

Fig. 8 shows the particle size distributions of the feed and best product.

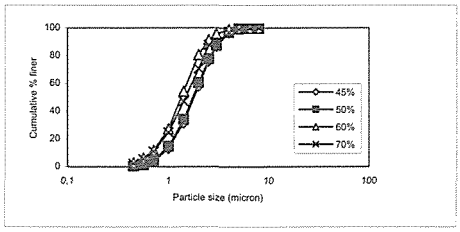

Fig.7. The effect of bead filling ratio on the product size distribution for the attrition milling of calcite powder (slurry concentration: 30%, grinding time: 50 min., stirrer speed: 500 rpm, ball size: 1 mm)

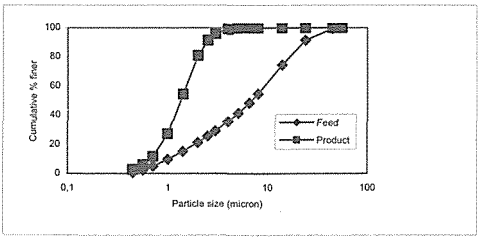

Fig. 8. Particle size distributions of the feed and best product (slurry concentration: 30%, grinding time: 50 min., stirrer speed: 500 rpm, ball filling ratio: 60%, ball size: 1 mm)

4 CONCLUSIONS

This paper presents the results of an investigation into the influence of various process parameters such as solids concentration, grinding time, stirrer speed and bead load (% of net mill volume) on the particle size and size distribution of the final ground calcite powders. Laboratory tests were conducted using a laboratory stirred bead mill. The effect of grinding time on the particle size distribution and fineness is highly significant and positive. The variables stirrer speed and bead load have also positive effects on the grinding. On the other

hand, a decrease in slurry density shifts the product particle size distribution curve to be a finer size, resulting in a reduction of the mean size.

5 ACKNOWLEDGEMENTS

Financial support from The Scientific and Technological Research Council of Turkey (TÜBİTAK)(Project No:108M623) for this project is acknowledged

REFERENCES

Baláž, P., 2000. Extractive Metallurgy of Activated Minerals, Elsevier, Amsterdam.

Becker, M., Kwade, A., Schwedes, J., 2001. Stress intensity in stirred media mills and its effect on specific energy requirement, Int.J.Min.Process., 61 (3), pp.189-208.

Fadhel, H. B. Frances, C., 2001. Wet batch grinding of alumina hydrate in a stirred bead mill, Powder Technology, 119, pp.257-268.

Kwade, A., Schwedes, J., 2002. Breaking characteristics of different materials and their effect on stress intensity and stress number in stirred media mills, Powder Technology, 122, pp.109-121.

Mankosa, M.J., Adel, G.T., Yoon, R.H., 1986. Effect of media size in stirred ball mill grinding of coal, Powder Technology, 49, pp.75– 82.

Pourghahramani, P., Altin, E, Mallembakam, M. R., Peukert, W., Forssberg, E., 2008. Microstructural characterization of hematite during wet and dry millings using Rietveld and XRD line profile analyses, Powder Technology, 186, pp.9-21.

Tkáčová, K., Stevulová, N., 1987. Change in structure and enthalpy of carbonates and quartz accompanying grinding in air and aqueous environments, Powder Technology, 52 (2), pp.161-166.

Tkáčová, K., 1989. Mechanical activation of minerals, in: D.W. Fuerstenau (Ed.), Developments in Mineral Processing, 11, pp.93-105.

Wang, Y., Forssberg, E., 2000. Product size distribution in stirred media mills, Minerals Engineering, 13 (4), pp.459-465.

The Effects of Ball Filling and Ball Diameter on Breakage Kinetics of Barite Mineral

Vedat Deniz
Hitit University, Department of Chemical Engineering, Çorum, Turkey

ABSTRACT Barite is an industrial material that is used in many applications such as a filler in paint, paper and plastic, etc. In these industries, ultrafine grinding of barite mineral is generally needed. The absolute fineness of the ball diameter and the ball charge grading are important factors for the optimal operation of a ball mill. Therefore, the effects on breakage kinetics of the ball diameter and the fractional ball filling were investigated on the barite at batch grinding conditions based on a kinetic model. For this purpose, firstly, nine different mono-size fractions were carried out between 2.8 mm and 0.106 mm formed by a $\sqrt{2}$ sieve series. Then, S_i and $B_{i,j}$ equations were determined from the size distributions at different grinding times, and the model parameters were compared for three different ball filling (25%, 35% and 45%) and three different ball diameter (15 mm, 25.4 mm and 40 mm). Finally, model parameters were discussion for every test.

The result of tests, the effect of ball filling and ball diameter on the grinding was found more different in terms of some results than other investigators.

1 INTRODUCTION

For all dry grinding applications, chemical industries, mineral industries and cement production are certainly the most important. Energy necessity is very high in grinding processes. There are many grinder manufactures and many varieties of machines made for grinding minerals. The correct selection between all alternative is a difficult problem (Deniz, 2011a; Deniz, 2011b).

Barite is being produced in various region of Turkey, mainly in Adana, Konya, and Isparta that is widely used as painting sector, paper and plastic sector, etc. In these industries, ultra fine grinding of barite mineral is needed.

The analysis of size reduction in tumbling ball mills using the concepts of specific rate of breakage and primary daughter fragment distributions has received considerable attention in recent years. Austin (1972) reviewed the advantages of this approach, and the scale-up of laboratory data to full-scale mills has also been discussed in a number of papers, summarized by Austin, Klimpel and Luckie in 1984.

Various laboratory studies, pilot plant works and full size plant observations showed that, ball diameter which is operating variables can affect grinding efficiency at a given output fineness.

Studies for selection of optimum ball size are reported in the literature (Bond, 1958; Shoji et al., 1982; Deniz, 2003; Schnatz, 2004). There is also no agreement on the effect of ball size to grinding kinetic. Despite its importance, most of the data published in the literature have been obtained from small diameter laboratory mills (McIvor, 1997).

Austin et al. (1984) showed that, typical variation of the specific rate of breakage versus particle size for various ball diameters in a tumbling mill as fallow Figure

1. Figure 1 shows that coefficient α, specific breakage parameter, is unchanged ball with diameter increasing.

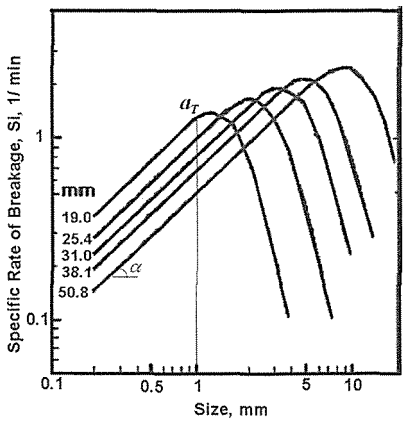

Figure 1. Variation of specific rate of breakage versus particle size for ball diameters (Austin et al., 1984)

Additional, considering a representative unit volume of mill, the rate of ball-on-ball contacts per unit time will increase as ball diameter decrease because the number of balls in the mill increases as $1/d^3$. Thus the rates of breakage of smaller sizes are higher for smaller ball diameters. The effect of ball diameter in a 0.6 m diameter mill, which gives the relation S_i and $a_T \alpha\ 1/d$, was shown in Figure 2 (Austin et al., 1984).

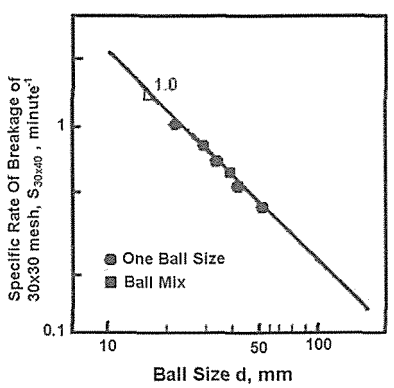

Figure 2. Variation of specific rate of breakage with ball diameter (Austin et al, 1984).

B values from batch grinding quartz with a mixture of ball size, a compared to values for grinding with 25 mm (1″) or 50 mm (2″) diameter balls were shown in Figure 3.

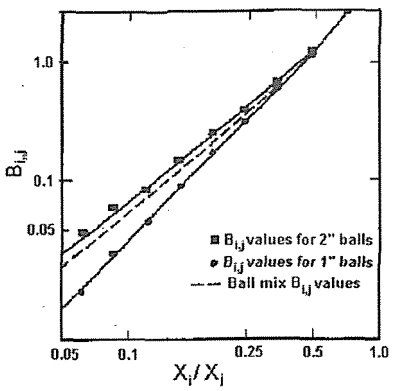

Figure 3. Experimental B values with ball diameter (Austin et al., 1984)

The best current estimates of the variation of *B* parameters for quartz were given in Table 1. It appears that the greater impact force of collision involving a larger ball give a somewhat bigger proportion of fines, that is, γ is lower, ϕ_j is higher. Thus, the lower specific rate of breakage due to larger balls is partially compensated by the production of a bigger proportion of fine fragments (Austin et al., 1984).

Table 1. B parameters as a function of ball size (Austin et al, 1984)

Ball Size, mm	γ	ϕ_j
19	1.10	0.51
22	1.09	0.58
25	1.08	0.63
32	1.05	0.68
38	1.00	0.69
44	0.95	0.70
51	0.88	0.70
64	0.78	0.70

The tumbling action and the rates of breakage will clearly depend on how much of the mill volume is filled with balls. A high filling of ball obviously gives a small rate of breakage. As the amount of ball is

decreased, higher rates of breakage are obtained. When all the effective space in which collisions between tumbling balls are occurring is filled with powder, the rates of breakage reach a maximum. Further reduce of ball increases the mill hold-up but does not give increased breakage because the collision zones are already saturated. Eventually, underfilling leads to deadening of the collions by powder cushioning, the ball-powder bed expands to give poor ball-ball powder nipping collions, and the breakage rates decrease (Austin et al., 1984).

The values of the coefficient ϕ_j are related to the coarse end of the breakage distribution function and show the rapidity with which fractions close to the feed size pass to the smaller size interval. Higher values of ϕ_j for increase in ball filling show the rapid grinding of gypsum especially at sizes close to feed size (Deniz, 2011b).

The ball charge filling ratio and ball diameters are influencing the specific power consumption and the throughput simultaneously. Furthermore, the absolute fineness of the ball charge and the ball charge grading are important factors for the optimal operation of a ball mill (Schnatz, 2004).

This paper will present some results on the effect of ball diameter (d) and ball filling (J) on breakage parameters for a laboratory ball mill, with a constant powder filling (f_c=4.7%) and rotational speed of mill (ϕ_c=0.75).

2 THEORY

Population balance modeling is a widely used tool for the quantitative analysis of comminution processes at the process length scale. The traditional size-discrete form of the population balance equation for batch comminution is linear and assumes first-order breakage kinetics (Austin, 1972).

$$\frac{dw_i(t)}{d_t} = -S_i W_i(t) + \sum_{j=1}^{i-1} b_{ij} S_j W_j(t), \qquad (1)$$

Thus, the breakage rate of material that is in the top size interval can be expressed as:

$$\frac{-dw_1}{dt} = S_1 w_1(t) \qquad (2)$$

Assuming that S_1 does not change with time (that is, a first-order breakage process), this equation integrates to

$$\log(w_1(t)) - \log(w_1(0)) = \frac{-S_1 t}{2.3} \qquad (3)$$

where $w_1(t)$ and is the weight fraction of the mill hold-up that is of size 1 at time t and S_1 is the specific rate of breakage. The formula proposed by Austin et al. (1984) for the variation of the specific rate of breakage S_i with particle size is

$$S_i = a_T X_i^{\alpha} \qquad (4)$$

where X_i is the upper limits of the size interval indexed by i, mm, and a_T and α are model parameters that depend on the properties of the material and the grinding conditions.

On breakage, particles of given size produce a set of primary daughter fragments, which are mixed into the bulk of the powder and then in turn have a probability of being refractured. The set of primary daughter fragments from breakage of size j can be represented by $b_{i,j}$, where $b_{i,j}$ is the fraction of size j material, which appears in size i on primary fracture, $n \geq i > j$. It is convenient to represent these values in cumulative form.

$$B_{i,j} = \sum_{k=n}^{i} b_{k,j} \qquad (5)$$

where $B_{i,j}$ is the sum fraction of material less than the upper size of size interval i resulting from primary breakage of size j material: $b_{i,j} = B_{i,j} - B_{i+1,j}$. Austin et al. (1981) have shown that the values of $B_{i,j}$ can be estimated from a size analysis of the product from short time grinding of a starting mill charge predominantly in size j (the one-size fraction *BII* method). The equation used is,

$$B_{i,j} = \frac{\log[(1-P_i(0))]/\log[(1-P_i(t))]}{\log[(1-P_{j+1}(0))]/\log[(1-P_{j+1}(t))]}, \quad n \geq i \geq j+1 \quad (6)$$

where $P_i(t)$ is the fraction by weight in the mill charge less than size X_i at time t. $B_{i,j}$ can be fitted to an empirical function (Austin and Luckie, 1972).

$$B_{i,j} = \phi_j [X_{i-1}/X_j]^{\gamma} + (1-\phi_j)[X_{i-1}/X_j]^{\beta} \quad n \geq i) j \quad (7)$$

$$\phi_j = \phi_1 [X_i / X_1]^{-\delta} \quad (8)$$

where δ, ϕ_j, γ, and β are model parameters that depend on the properties of the material. If $B_{i,j}$ values are independent of the initial size, i.e. dimensionally normalizable, then δ is zero (Austin et al., 1984).

3 EXPERIMENTAL STUDIES

3.1 Material

Barite samples taken from Başer Mining Co. in Isparta (Turkey), were used as the experimental materials. The characterization of the raw material included chemical analysed with the XRF spectrometer to determine its chemical composition. Chemical properties of barite sample using experimentally were presented in Table 2.

Table 2. Chemical composites of barite sample using in experiments

Oxides	(%)
SO_3	40.90
CaO	0.43
MgO	0.37
SiO_2	0.50
Fe_2O_3	0.07
Na_2O	0.02
K_2O	0.02
Al_2O_3	0.01
$BaSO_4$	98.44
Loss on ignition	21.91

Mineralogical investigations were conducted using X-ray diffraction. Results indicate that samples prove to be mixtures of barite ($BaSO_4$) and quartz (SiO_2). The sample had a barite content of about 98%, attributed to the presence of quartz with very low quantities of clay minerals (Figure 4).

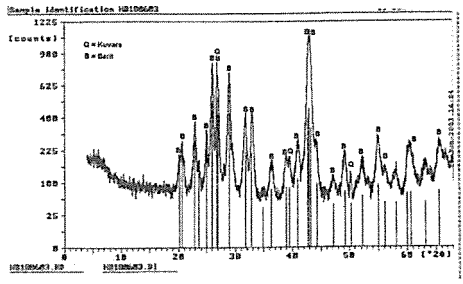

Figure 4. Characteristic X–ray diffractogram of barite sample

3.2 Grinding Tests

Firstly, Standard Bond Work index test was made for barite sample. Result of test, Bond Work index value of sample was appeared 7.25 kWh/t.

The standard set of grinding conditions used was shown in Table 3. Nine mono-size fractions (-2.8+1.7, -1.7+1.18, -1.18+0.850, -0.850+0.600, -0.600+ 0.425, -0.425+0.300, -0.300+0.212, -0.212+0.150, -0.150+0.106 mm) were prepared and ground batch wise in a laboratory-scale ball mill for determination of the breakage functions. Samples were taken out of the mill and dry sieved product size analysis.

4. RESULT AND DISCUSSION

4.1 Determination of S Functions

The first-order plots for various feed sizes of barite samples were illustrated in Figures 5-10. The results indicated that grinding of all size fractions, samples could be described by the first-order law. In additional, parameters of specific rate of breakage to supply by first-order plots were present in Tables 4-5. The specific rates of breakage of each mono-

size fraction that exhibited first-order grinding kinetic behaviuor were determined from the slope of straight-line of first-order plots. Additional, Figures 11-12 show the values of S_i for grinding of the three ball filling and the three- ball diameter studied as a function of size, respectively.

4.2. Determination of B functions

By definition, the values of B were determined from the size distributions at short grinding times. The parameters were determined according to the *BII* method (Austin et al, 1984), and show the graphical representation on Figures 13-14. Barite samples show a typical normalised behaviour, and the progeny distribution does not depend on the particle size, and it followed that the parameter δ was zero. Model parameters supply by cumulative distribution and these parameters were presented in Tables 4-5.

The slope of the lower portion of the $B_{i,j}$ curve can be denoted by γ with smaller values of γ and indicating that once particles of a certain size break, they produce many much smaller progeny fragments (Deniz, 2011a). With respect to ball size, Kelsall et al.(1967/68) reported no effect on $B_{i,j}$; but later work by Austin et al. (1982) demonstrated for quartz that $B_{i,j}$ altered in a systematic manner expressed in terms of γ and ϕ_j, with β remaining unchanged. These trends are in keeping with the concept of the greater impact force of a collision involving a larger ball producing a somewhat larger proportion of fines than with a smaller ball, i.e. reduced of γ and increased of ϕ_j.

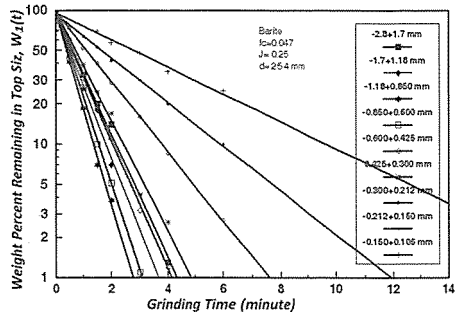

Figure 5. First-order plots for J=0.25

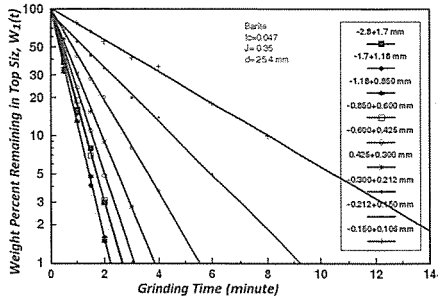

Figure 6. First-order plots for J=0.35

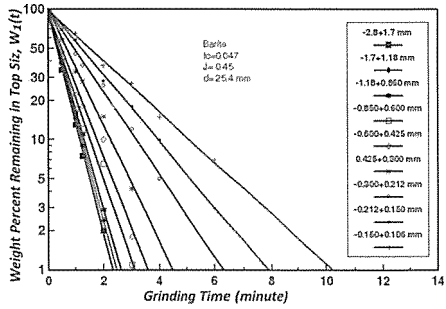

Figure 7. First-order plots for J=0.45

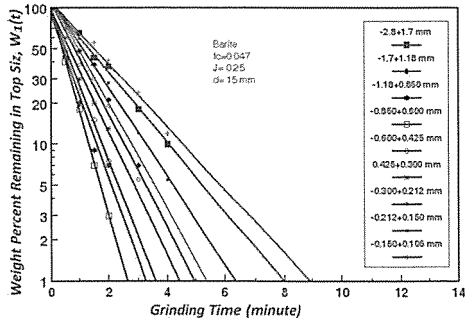

Figure 8. First-order plots for d=15 mm

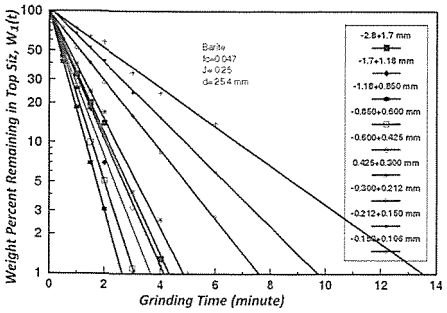

Figure 9. First-order plots for d= 25.4 mm

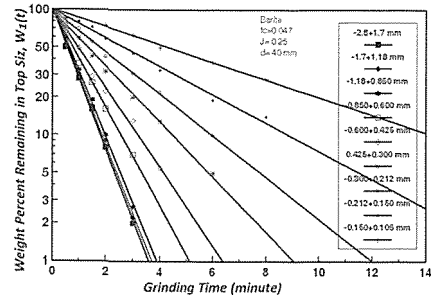

Figure 10. First-order plots for d= 40 mm

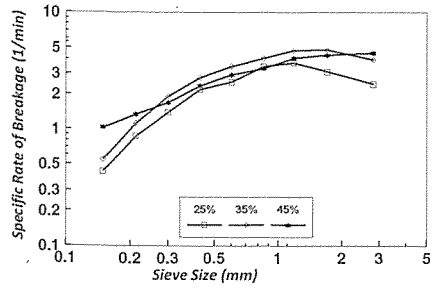

Figure 11. Specific rates of breakage for different ball filling

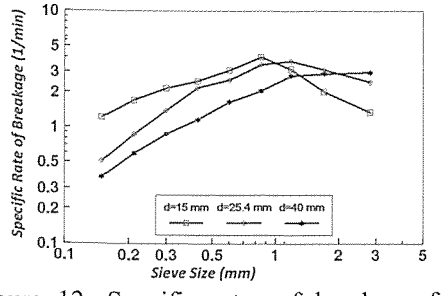

Figure 12. Specific rates of breakage for different ball diameter

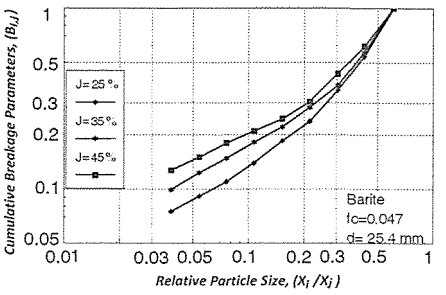

Figure 13. Cumulative breakage distribution functions for different ball filling

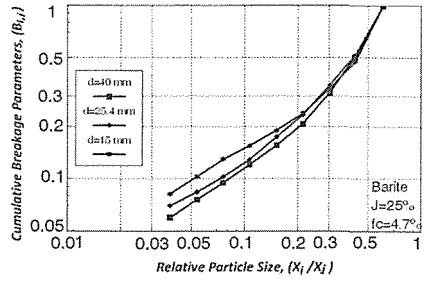

Figure 14. Cumulative breakage distribution functions for different ball diameter

4.3. Variation of specific rate of breakage with ball diameter and ball filling

As the amount of ball from $J = 0.25$ to 0.35 increased, the collision spaces between the balls were filled and higher rates of breakage were obtained. When all the effective space in which collisions between balls were filled with powder, the rates of breakage reached a maximum value ($J = 0.35$). Further addition of ball ($J > 0.35$) increased the mill hold-up but did not give increased in the rates of breakage because the collisions zones were already saturated. Underfilling ($J < 0.25$) leaded to deadening of the collisions by powder cushioning, the ball–powder bed expanded to give poor ball–ball powder nipping collisions and the breakage rates decreased. This study shown that $J = 0.35$ was the optimum filling condition for the maximum breakage rates.

Austin et al. (1984) demonstrated that, the specific rates of smaller sizes are higher for smaller ball diameters. The specific breakage

parameter, coefficient α, was unchanged with ball diameter increasing, was shown in Figure 1. The effect of ball diameter, given the relation $S_i \propto 1/d$, was shown in Figure 2.

For this same purposes, variation of specific rate of breakage with ball diameter for barite sample was investigated, and the graphical represent was shown in Figure 15. The result of graphical representation, it was found same results with Austin et al. (1984). However, a graphical represent of the variation of specific breakage parameter α with d for barite sample was shown in Figure 12. It was shown different results than Austin et al. (1984).

Austin et al. (1984) demonstrated a larger ball give a somewhat bigger proportion of fines, that is, γ is lower, ϕ_j is higher. The best current estimates of variation of B parameters (γ, ϕ_j) for quartz were given in Table 1. For this same purpose, variation of breakage parameters with ball diameter for barite samples was calculated, and the result of calculated breakage parameter values were shown in Table 4. The result of variation of breakage parameters with ball diameters, it was found different results than Austin et al. (1984), this study demonstrates that, γ values of barite sample have not increase with respect to increasing ball size. Larger ball diameters (40 mm) are not affected on the fine particle size, that is, very fine particles are lost among larger balls.

The values of the coefficient ϕ_j is related to coarse end of the breakage distribution function and show how fast fractions close to the feed size passes to smaller size interval. The ϕ_j values of barite sample have decreased with respect to increasing ball size as different from Austin et al (1982).

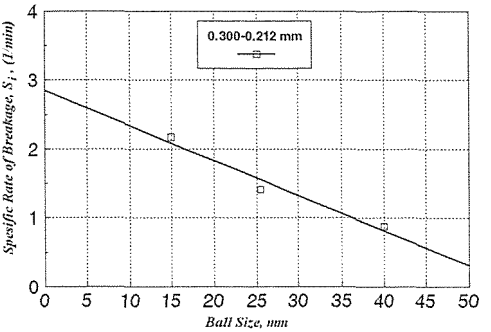

Figure 15. Variation of ball diameter with first order breakage constant

5. CONCLUSIONS

Dry grinding of size intervals of barite samples showed that the ball filling and ball diameter followed the first-order breakage law with constant normalised primary breakage distributions. In additional, these samples do not depend on the particle size from cumulative breakage distribution function.

As the amount of S_i and a_T values (shown in Table 4) increased, expressed more effective breakage and broke as very fast in the undersize of original particle size. Additional, it is given effective breakage for d=15 mm for ball diameter. From S_i values experimentally obtained, grinding is faster grinding for J=0.35 as suitable value of ball filling for barite sample (Table 5).

Austin et al (1982), the relation between ball diameter d and S_i has been shown to be: $S_i \propto 1/d$. In this study, as same results with Austin et al. (1984), this reduction of with an increase in d was seen as Figure 15. However, the relation between ball diameter d and α has been shown to be different results from Austin et al. (1984).

The slope of the lower portion of the $B_{i,j}$ curve can be denoted by γ with smaller values of γ indicating that once particles of a certain size break, they produce many much smaller progeny fragments. Thus γ values tend to decrease with the increase in the ball diameter, which emphases that the grinding produces finer material. More different than other researches, this study demonstrates that

the grinding produces finer materials for d= 25.4 mm as suitable value of ball diameter for barite sample.

The values of the coefficient ϕ_j is related to coarse end of the breakage distribution function and show how fast fractions close to the feed size passes to smaller size interval. Higher value of ϕ_j for increase ball diameter shows the rapid grinding of barite especially at sizes close to feed size; it is found different results from Austin et al (1984).

Proportion of fines increase, that is, ball filling volume fraction (J= 0.25) is low and very fine particles are lost among larger balls. However, ball filling volume fraction (J=0.45) is high and underfill the mill with powder. At low underfill much of the energy of the tumbling balls is taken up in the stell-to-stell contact giving low values of γ. It tend to increase up to J =35% of ball filling and than start to show a decreasing trend after J=35%. Therefore, the maximum of γ was found about 35% of ball filling, it was found same results with Deniz (2011b).

This study showed that grinding kinetic parameters could be different for different ball filling and ball diameter. Therefore, it has appeared that the grinding kinetics for each material must be evaluated in order to lower the energy costs in grinding process.

Table 3. The standard set of grinding conditions

Mill	Diameter, mm		200	
	Length, mm		200	
	Volume, cm^3		6280	
Mill speed	Critical (N_c) [a] , rpm		101	
	Operational (ϕ_c= 75%) , rpm		76	
Balls	Diameter range, mm	15	25.4	40
	Specific gravity,		7.8	
	Quality		Alloy Steel	
	Assumed bed porosity		40%	
	Ball filling volume,(J%) [b]	25	35	45
Material	Formal bulk density,g/cm^3		3.676	
	Powder filling volume (f_c%)[c]		4.7	
	Interstitial filling (U%)[d] (J=0.25)		47.00	
	(J=0.35)		33.57	
	(J=0.45)		26.11	

[a] *Calculated from* $N_c = 42.3/\sqrt{D-d}$ (D, d *in metres*)

[b] *Calculated from* $J = \left(\frac{mass\ of\ balls\ /\ specific\ gravity\ of\ balls}{mill\ \ volume} \right) \times \frac{1.0}{0.6}$

[c] *Calculated from* $f_c = \left(\frac{mass\ \ of\ \ powder\ /\ formal\ \ bulk\ \ density}{mill\ \ volume} \right)$

[d] *Calculated from* $U = \frac{f_c}{0.4J}$

Table 4. Model parameter values for different ball diameter

d mm	-0.300+0.212 mm S_i (1/min)	α	a_T	γ	ϕ_j
15	2.172	1.094	3.65	0.644	0.509
25.4	1.412	1.454	3.58	0.574	0.468
40	0.878	1.239	2.42	0.669	0.442

Table 5. Model parameter values for different ball filling

J %	-0.300+0.212 mm S_i (1/min)	α	a_T	γ	ϕ_j
25	1.412	1.693	3.89	0.569	0.425
35	1.911	1.805	4.72	0.580	0.435
45	1.671	0.783	3.94	0.486	0.395

REFERENCES

Austin, L.G. 1972. A review introduction to the description of grinding as a rate process. *Powder Technol.* 5: 1-7.

Austin, L.G. & P.T. Luckie, 1972. Methods for determination of breakage distribution parameters. *Powder Technol.* 5: 215-222.

Austin, L.G., R. Bagga & M. Çelik. 1981. Breakage properties of some materials in a laboratory ball mill. *Powder Technol.* 28: 235-241.

Austin, L.G., R.R. Klimpel, P.T. Luckie & R.S.C. Rogers. 1982. Simulation of grinding circuits for design. *Design and Installation of Comminution Circuits.* A.I.M.E.,S.M.E., NewYork, USA, 301-324.

Austin, L.G., R.R. Klimpel & P.T. Luckie. 1984. *Process Engineering of Size Reduction: Ball Milling*, A.I.M.E., S.M.E., NewYork, USA.

Bond, F.C., 1958. Grinding ball size selection. *Mining Eng.* 10 (5), 592–595.

Deniz, V., 2003. A study on the specific rate of breakage of cement materials in a laboratory ball mill. *Cem. Concr. Res.* 33: 439–445.

Deniz, V. 2011a. Comparison with some porous materials and the effects of powder filling on breakage parameters of diatomite in dry ball milling. *Particulate Sci.& Technol.* (doi: 10.1080/02726351.2010.509855) (in Press).

Deniz, V. 2011b. Influence of interstitial filling on breakage kinetics of gypsum in ball mill. *Adv. Powder Technol.* (doi:10.1016/j.apt.2010.07.004) (in Press).

Kelsall, D.F., K.J. Reid & C.J. Restarick 1967/68. Continuous grinding in a small wet ball mill: Part I. A study of ball diameter. *Powder Technol.* 1: 291-300.

McIvor, R.E., 1997. The effect of media sizing on ball milling efficiency. (Ed.: Komar Kawatra, S.), *Comminution Practices*. SME, AIMM., Colorado, pp. 279–292.

Schnatz, R. 2004. Optimization of continuous ball mills used for finish-grinding of cement by varying the L/D ratio, ball charge filling ratio, ball size and residence time. *Int. J. Miner. Process.* 74S: 55-63.

Shoji, K., Austin, L.G., Smaila, F., Brame, K., Luckie, P.T., 1982. Further studies of ball and powder filling effects in ball milling. Powder Technol. 31, 121–126.

The Enrichment Possibility of Çorum-Alaca Chromites by Magnetic Separation

İ. Bentli, Ç. Yıldırım
Dumlupınar University, Mining Engineering Department, Main Campus, Kütahya-Turkey

ABSTRACT Chromites used in industries change with regard to its grade and property. Accordingly, the chromite content must comply its consumption area, such as refractory, metallurgy and chemical industry. The result of chemical analysis for the Çorum-Alaca chromite samples contain 26.81% Cr_2O_3, 11.82% Fe_2O_3, 10.93% Al_2O_3, 16.22% SiO_2, 25.59% MgO, 1.16% CaO, 0.21% MnO with 6.50% loss on ignition. According to these results, it is not suitable for the market as the run-of-mine ore. Therefore, it is compulsory to increase its chromite content by mineral processing methods. The mineralogical analysis of the chromite ores revealed serpentine and magnesite as gangue minerals. The limiting liberation size of the chromite samples was measured with microscopy as -0.300 mm and at this size the degree of liberation is 92.4%. In this study, dry (Permroll) and wet magnetic separators (Master Magnet) were used for the beneficiation of Çorum-Alaca chromites ores. A concentrate with 41.75% Cr_2O_3 was produced at a recovery rate of 86.22%. Although chromite recovery rate for combinations of magnetic separation is high, this concentrate cannot be saleable to market.

1 INTRODUCTION

Chromites, which are used in metallurgical industry, ratios of 46-48% Cr_2O_3, 2-3/1 Cr/Fe, maximum 8% SiO_2 and minimum 25% Al_2O_3+MgO are desired (Çilingir, 1990). Metallurgical industry is the branch of industry, in which the substantial quantity of chromites ores is consumed. Even though hard and partial ores are preferred in terms of physical characteristics, concentrated chromium may also be used (Önal and Güney, 1990; Gül et.al., 1995). The highest quality metallurgical ores are located in Turkey, Iran and Rhodesia (Tahtakıran, 2008).

Chromites exhibit weak magnetic properties. It is preferred for separators with high magnetic field. Dry and wet magnetic separators with high magnetic field are used for enrichment of chromites (Yamık and Çilingir, 1990). As the ore is to be ground as fine particles (-0.1 mm), wet magnetic separators with high magnetic field are preferred (Yüce et.al., 2005). In order to have a high efficiency in relation to magnetic separation, it is necessary to classify materials in similar sizes and to have a moisture-free environment if dry magnetic separation is applied. In the event that gravimetric methods cannot be used, the chromite ores are liberated in very fine size (-0.2 mm) and there is a substantial quantity of gangue mineral olivine or gangue mineral which has a similar intensity level with that of chromites, magnetic separation methods are used (Wills, 1988).

2 MATERIALS AND METHODS

2.1 Materials

Chromite mineralization, which forms the basis of these tests, is the chromite field of Alaca Madencilik, which is located in Çorum Province, Alaca District, İsmailli Village. Chromite mineralization in the field has an apparent length of 200 m, a width of 125 m and a thickness of 0.5 m. Mineralization emerges in the podiform (Alpine) type and it is a northern dipping zone in east-west direction (Yıldırım, 2009a). The sample used in the experimental work, was retrieved as nearly 10 tons through excavators during production in an open quarry and blended by coarse crushing. The sample, which was reduced down to 350 kg through coning-quartering method, was brought to the laboratories.

Large particles of the raw material with a particle size of 300 mm were crushed with a hammer and fed to jaw crusher and cone crusher, successively. The entire sample was reduced to 20 mm by jaw and below 5 mm by cone crushers. After the crushed ore was reduced through Jones Riffle sample divider, it was stored in packages of 750 g. Some samples were separated from the crushed raw sample in order to perform size analysis, to determine its liberation size and perform chemical and mineralogical analysis. The crushed ore was ground below -0.425 mm in a ball mill to obtain the liberation size. Grinding process was performed in dry type ceramic ball with a mill length of 350 mm and diameter of 180 mm by feeding a sample of 1000 g at 50% ball charge. The mill was operated for 30 minutes at 60% of the critical speed. The sample, which was extracted from the mill, was manually sieved, separated into various size fractions of -0.425 +0.300 mm, -0.300 +0.212 mm, -0.212 +0.150 mm, -0.150 +0.106 mm, -0.106 +0.045 mm and -0.045 mm stored for the subsequent tests.

Chemical analysis of the chromite ore was performed through a Spectro X-LAB 2000 XRF. The same sample was also tested with wet analysis method in order to confirm its accuracy. The chemical analysis of the Alaca chromite ore is given Table 1 (Yıldırım, 2009b).

Table 1. Chemical analysis of Çorum-Alaca chromites.

Content	%
Cr_2O_3	26.81
Fe_2O_3	11.82
Al_2O_3	10.93
SiO_2	16.22
MgO	25.59
CaO	1.16
MnO	0.21
LOI	6.50

According to these results, it is not possible to market the run-of-mine Çorum-Alaca chromite and it is necessary to increase its chromite grade by processing. Existence of 25.59% MgO grade in the ore shows that the ore consisted of a high quantity of Mg containing minerals. Cr/Fe ratio is 2.3. Therefore, this ore could be used in metallurgical industry after it is processed (Çilingir, 1990).

2.2 Mineralogical Analysis

Mineralogical analysis of the ore was performed through peaks obtained from RIGUKA XRD. The evidence of XRD peaks shows that chrome mineral is of chromite (FeO Cr_2O_3), magnesium chromite (Mg, Fe Cr_2O_3) and silicious chromite (Cr_2O_3 SiO_2) while gangue minerals are of serpentine ($Mg_6Si_4O_{10}(OH)_2$) and magnesite ($MgCO_3$) minerals in Çorum-Alaca chromites (Figure 1). According to these results, it is understood that high level of %MgO as specified in the chemical analysis originates from serpentine, magnesite and chromite. The LOI value of 6.5 % is normal considering that the loss of CO_2 upon firing

of magnesite detected in the mineralogical studies will lead to such result.

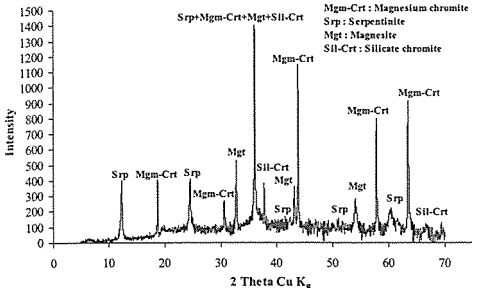

Figure 1. XRD patterns of the Çorum-Alaca chromites.

2.3 Sieve Analysis and Liberation

Dry sieving was performed in order to determine the particle size of the chromite, which was crushed down to the size of 0.425 mm in ball mills depending on the liberation size. Sieve analysis results and Cr_2O_3 distributions of the sample are given in Figure 2. As seen in the Figure 2, 80.4% of the crushed sample is below 0.3 mm. Cr_2O_3 grade increases up to -0.212 +0.150 mm and then decreases. Depending on the particle size fraction, both size and Cr_2O_3 efficiency have nearly equal distribution except for -0.045 mm, which is the smallest size (Figure 2).

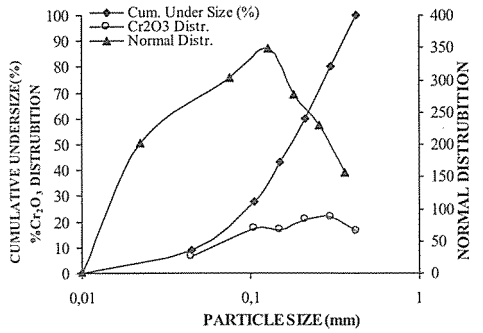

Figure 2. The sieve analysis results and Cr_2O_3% distributions.

For success of magnetic separation, it is of great importance to ensure that particles become liberated. Hence, it is compulsory to determine the liberation size prior to enrichment for shedding light to the method and performing an efficient process. The liberation size is primarily determined by means of two experimental methods. The process method, which is the first of these methods, gives the liberation size while the particle counting method ensures that the grade of liberation size is determined. Both methods were used in our studies in order to determine the liberation size with regard to the chromite sample. The liberation grade was given Table 2 through the microscopic method (Önal, 1980; Ergin et.al., 1998).

Table 2. The liberation grade depending on particle size.

Particle Size (mm)	Liberation (%)
-0.425 +0.300	66.57
-0.300 +0.150	92.42
0.150 +0.106	96.16

2.4 Method Selection

The aim of the chromite process is to obtain a chromite concentrate with as high grade as possible. To this end, the most economic and modern methods were selected in the experimental studies (Agacayak et al., 2007; Özkan and İpekoğlu, 2001; Gence and Özdağ, 1986). The size groups -0.425 +0.300 mm, -0.300 +0.212 mm, -0.212 +0.150 mm dry magnetic and -0.212 +0.150 mm, -0.150 +0.106 mm, -0.106 +0.045 mm, -0,045 mm wet magnetic separation were processed.

3 MAGNETIC SEPARATION

Chromites and gangue minerals (olivine, serpentine etc.) with different magnetic sensitivity levels are enriched through magnetic separation depending on combined effects of various forces, in particular, magnetic force within a proper magnetic field (Wills, 1988). In general practice, dry

magnetic separators are used for large sizes while wet magnetic separators are used for fine particles. Magnetic field strength of chromites is in the range of 1.0-1.6 Tesla. Magnetic sensitivity of chromites varies between $3000x10^{-6}$ – $7500x10^{-6}$ while their specific magnetic sensitivity varies between $650x10^{-6}$ – $2000x10^{-6}$ cm^3/gr. For this reason, chromites can be magnetized in magnetic fields with 6000-20000 Gauss depending on their structural states (Atalay et.al, 1984).

3.1 Dry Magnetic Separation

PERMROLL laboratory type dry magnetic separator with high magnetic field was used for enrichment tests. Dry magnetic separation tests with high magnetic field were conducted through a sample quantity of 2000 gr, a drum rotation speed of 300 rev/min, a magnetic field strength of 25 000 Gauss and particle sizes of -0.425+0.300 mm, -0.300+0.212 and -0.212+0.150 mm. Results of dry magnetic separation tests are shown in Figure 3 (Yıldırım, 2009b).

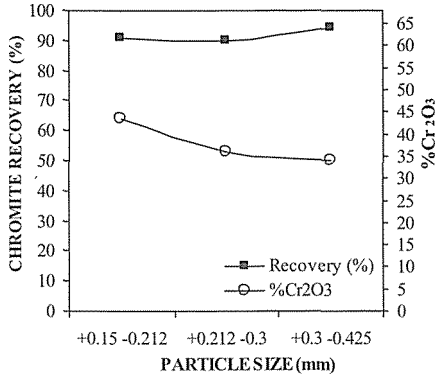

Figure 3. Effect of particle size on grade and recovery in terms of Dry Magnetic Separator

As shown in Figure 3, as the particle size increases in dry magnetic separators with high magnetic field, recovery increases, but Cr_2O_3 grade decreases. Given the liberation size, it is natural to face such a situation. While Cr_2O_3 grade increases on the liberation size, there is a relative decline in efficiency and this complies with the literature (Wills, 1988, Atalay et.al, 1984).

A concentrate with 43.33% Cr_2O_3 is recovered with an efficiency of 90.9% in the -0.212+0.150 mm. As a result of tests conducted through dry magnetic separators with high magnetic field, a saleable Cr_2O_3 concentrate could not be obtained. Therefore, it was envisaged that these concentrates would be taken as pre-concentrates, pre-concentrates should be fed into shaking tables and final product would be obtained in this way (Bentli et.al, 2010). Appearance of concentrates and tailing obtained through dry magnetic separation is given in Figure 4.

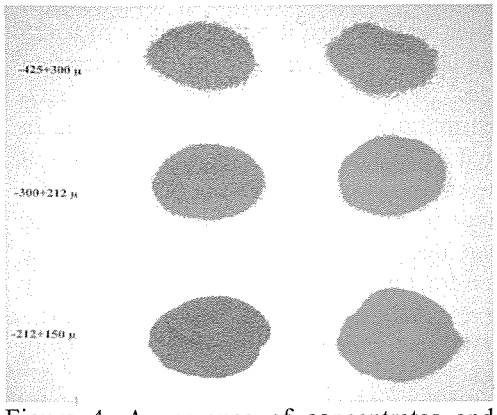

Figure 4. Appearance of concentrates and tailing obtained through dry magnetic separation.

3.2 Wet Magnetic Separation

Master Magnet M5695 laboratory type wet magnetic separator with high magnetic field were used for enrichment tests. Wet magnetic separation tests were conducted through a sample quantity of 1000 gr, an electric field intensity of 170 V and a current intensity of 30 Amperes and particle sizes of -0.212+0.150 mm, -0.150+0.106 and -0.045 mm. Results of wet magnetic separation tests are shown in Figure 5 (Yıldırım, 2009b).

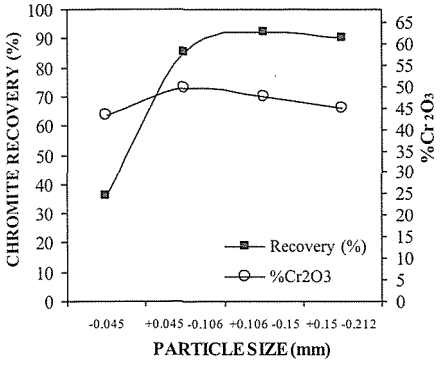

Figure 5. Effect of particle size on grade and recovery in terms of Wet Magnetic Separator

As shown in Figure 5, the highest efficiency was obtained with a particle size of -0.150+0.106 mm while the highest Cr_2O_3 grade was obtained with a particle size of -0.106+0.045 mm. A concentrate with 49,5% Cr_2O_3 grade was obtained with an efficiency level of 85,36% in a particle size of -0.106+0.045 mm while a concentrate with 47,61% Cr_2O_3 grade was obtained with an efficiency level of 91,96% in a particle size of -0.150+0.106 mm. The concentrate within these ranges is a marketable product. A concentrate with 43,26% Cr_2O_3 grade was obtained with an efficiency level of 36,07% in a particle size of -0.045 mm and a concentrate with 44,9% Cr_2O_3 grade was obtained with an efficiency level of 90,08% in a particle size of -0.212+0.150 mm, but these concentrates are not saleable. Appearance of concentrates and tailing obtained through wet magnetic separation is given in Figure 6.

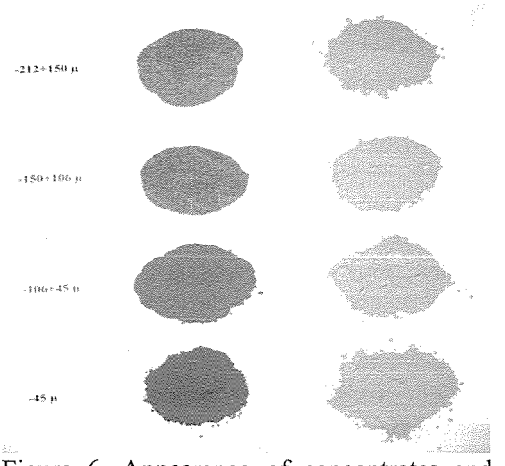

Figure 6. Appearance of concentrates and tailing obtained through wet magnetic separation.

4 CONCLUSIONS AND SUGGESTIONS

Dry and wet magnetic separation tests with high magnetic field were conducted with a chromite ore with an average grade of 26,81% Cr_2O_3, which was liberated in fine particles from Çorum-Alaca region to Alaca Madencilik.

Cr/Fe ratio of Çorum-Alaca chromites used in the experimental studies is 2,3. This ration is suitable use in the metallurgical industry. Çorum-Alaca chromites are sufficiently liberated below 0.300 mm.

Mineralogical analysis of the ore through XRD peaks identified that the ore consisted of chromites and gangue minerals such as serpentine and magnesite.

A concentrate with 43,33% Cr_2O_3 and 90.90% recovery in the particle size range of -0.212+0.150 mm, 35,94% Cr_2O_3 and 90.06% recovery in the size range of -0.300+0.212 mm, 34.03% Cr_2O_3 and 94.15% recovery in the size fraction of -0.425+0.300 mm through dry magnetic separator, was obtained respectively. In all fractions, very low quality concentrates could be obtained with dry magnetic separator.

In wet magnetic separation studies 43.26% Cr_2O_3 and 36.07% recovery in -0.045 mm size range, 49.50% Cr_2O_3 and 85.36% recovery in -0.106+0.045 mm size range, 47.61% Cr_2O_3 and 91.96% recovery in -0.150+0.106 mm size range, 44.90% Cr_2O_3 and 90.08% recovery in -0.212+0.150 mm size range, respectively.

When results of wet magnetic separation and dry magnetic separation are combined, a concentrate with 41,7% Cr_2O_3 grade is obtained with an efficiency level of 86,22% depending on the feed. It seems possible to obtain the ore through the magnetic separation with a low grade and high efficiency in a facility to be established. It is not sufficient simply to apply magnetic separation on all-in ore.

KAYNAKLAR

Agacayak, T., Zedef, V., and Aydoğan, S., 2007. Beneficiation of low-grade chromite ores of abandoned mine at Topraktepe-Beyşehir, Acta *Montanistica Slovaca*, 12, pp 323-327.

Bentli, İ., Yıldırım Ç., and Çınar, M., 2010. Beneficiation of Çorum-Alaca chromite ores by gravity separation, *Proceedings of the 12th International Mineral Processing Symposium*, Nevşehir, pp 201-207.

Çilingir, Y., 1990. *Metalik cevherler ve zenginleştirme yöntemleri-I*, Dokuz Eylül University, Eng. Faculty Publish, Chrome section: 3, İzmir, 20 p.

Atalay, Ü., Doğan, Z., Özbayoğlu, G., Hiçyılmaz, C. and Bilgen, S., 1984. Concentration of Etibank Üçköprü chromite gravity tailing, *4th Balkan Mineral Processing Congress*, İstanbul, Turkey, pp 460-469.

Ergin, Z., Semerkant, O. and Cöcen, İ., 1998. *Cevher hazırlama-I laboratuvar ders notları ve deney özetleri*, Dokuz Eylül University, Eng. Faculty Publish No:191, İzmir, 139 p.

Gül, A., Yüce, A.E., Güney, A., Gürkan, V., Arslan, F., and Önal, G., 1995. Adana-Karsantı bölgesi düşük tenörlü kromit cevherinin değerlendirilmesi, *14th Mining Congress of Turkey*, pp 419-424.

Önal, G., 1980, *Cevher hazırlamada flotasyon dışındaki zenginleştirme yöntemleri*, İstanbul Technical University, Publish No:1156, İstanbul, 232 p.

Önal, G., Gürkan V. and Acarkan, N., 1979. Krom zenginleştirme tesisleri artıklarının yüksek alan şiddetli yaşmanyetik ayırmayla değerlendirilmesi, *Türkiye Madencilik ve Teknik 6.Kongresi*, Ankara, pp 13/1-13/22.

Önal, G., and Güney, A., 1990. Türkiye'de krom madenciliği, *J Isparta Eng. Faculty, Akdeniz University*, Mining, 5, Isparta, pp 183-192.

Tahtakıran, E., 2008. Krom cevher standartları ve pazarlanması, *Madencilik Bülteni*, Ocak-Mart, 55-58.

Özkan, Ş. and İpekoğlu, B., 2001. Concentration studies on chromite tailings by multi gravity separator, *17th Mining Congress and Exhibition of Turkey*, pp 765-768.

Gence, N., and Özdağ, H., 1986. Elazığ-Kefdağı kromitlerinin zenginleştirilmesi, *J Eng. and Arch. Faculty*, Anadolu University, Vol.3, No.1, pp 121-133.

Yamık, A., and Çilingir, Y., 1990. Fethiye yöresinden alınan örnek kromit cevherinin sallantılı masa ve manyetik seperatörle laboratuvar çapta zenginleştirilmesi, *J Isparta Eng. Faculty*, Akdeniz University, Mining, 5, Isparta, pp 79-94.

Yıldırım, Ç., 2009a. *20061626 Numaralı İşletme Projesi*, MİGEM, Ankara.

Yıldırım, Ç., 2009b. Çorum yöresi düşük tenörlü krom cevherlerinin zenginleştirilmesi, *MSc Thesis*, Dumlupınar University, Kütahya, 71 p.

Yüce, A.E., Güney, A. and Önal, G., 2005, Üçköprü krom artıklarından geri kazanım ve atık alanının rehabilitasyonu, *Madencilik ve Çevre Sempozyumu*, Ankara, pp 109-115.

Wills, B.A., 1988. *Mineral Processing Technology*, Pergamon Press, New York, 584 p.

The Effect of Heap Height and Particle Size on the Copper Recovery and Acid Consumption

Mohsen Hashemzadeh
Iran Mineral Processing Research Center (IMPRC), Karaj, Iran.

ABSTRACT Nowadays heap leaching has become established as the technology for treatment of some low grad copper, gold and zinc minerals, as well as its extension to the treatment of other types of minerals such as saltpeter and mine tailings. The present study makes an analysis to determine the effects of height of the heap and particle size on copper recovery and acid consumption. Heap heights of 2, 4 and 6 meters and particle size of less than 1 and 2 inch were selected as variables in experiments. The results of the study showed the inverse relation between heap height and copper recovery as well as the acid consumption.

1 INTRODUCTION

Heap leaching is a widely used extraction method for low-grade minerals, including those of copper, gold, silver, and uranium. This method has new applications including nonmetallic minerals such as saltpeter Valencia et al. (2008) and soil remediation Hanson et al. (1993). Although a number of experimental studies have been carried out Wu et al. (2007), Yorio et al. (2006) as well as modeling Petersen and Dixon (2007), Leahy et al. (2007) which have allowed better understanding of the phenomenon and its operation, few studies have been carried out with the objective of optimizing the process. Most of the studies either experimentally or through the use of models, have done from the technical perspective, for example, Pennstrom and Arnold (1999) studied the management of leaching solutions around the leaching heap as a way of optimizing recovery. Bartlett (1997) analyzed the effect of other operations, such as agglomeration, on the optimization of recovery, Mason et al. (1997) made an experimental study of the optimization of recovery of uranium using sodium bicarbonate and sodium peroxide, and some studies have done from the economical perspective such as Luis A. Cisternas (2008) who studied the economical aspects of heap height. Objective of this present study was to investigate the effect of heap height and particle size on recovery and acid consumption. Future studies can use presented data to investigate other aspects of optimization such as economical aspects.

2 EXPERIMENTAL

The copper ore originated from an Iranian mine. The as-received ore was crushed by jaw crusher to less than 2 and 1 inch in order to use for column leaching tests. After blending, samples were collected for

chemical analysis, size distribution and mineralogical characterization.
Screen analysis was performed by mechanically shaken Tyler sieves. The results of size distribution are given in Figure 1.

The chemical determination of elements was carried out by ICP-emission spectrophotometry. Table 1 shows the main elemental composition and mineralogical species of the ore. The X-ray diffraction analysis (Figure 2) of the ore revealed the presence of the mineralogical species.

Table 1. Mineralogical species and Chemical composition of the ore

Mineral	%	Elements	%
$NaAlSi_3O_8$	36.5	Cu	1
SiO_2	32	Fe	3.7
$KAlSi_3O_8$	13	Si	28.74
$CaCo_3$	5	Al	7.4
Fe_2O_3- FeOOH	6	Ca	2
$K_2Al_4(Si_6Al_2O_{20})(OH,F)_4$	3	K	3.05
$(Mg,Al,Fe)[(Si,Al)_8O_{20}](OH)_{16}$	2.3	Mg	1.1
$Cu_2CO_3(OH)_2$	2	Na	2.65
CuS	0.2	S	0.05

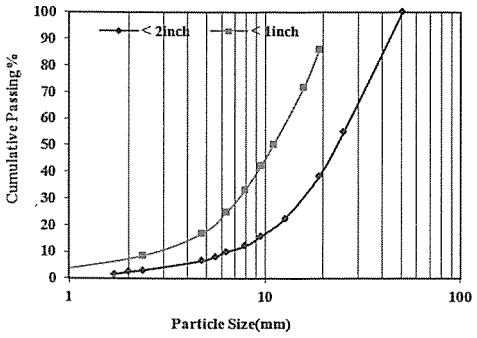

Figure 1. Size distribution of crushed ore

Crushed samples were agglomerated with 30 percent of their maximum acid sulfuric consumption (30 kg /Ton) and then charged within the columns. All factors were studied in 6 columns and all columns were operated with conditions shown in Table 2 for 78 days.

Acid sulfuric leaching solutions were papered as needed, every three or four days. Leaching solutions were fed by peristaltic pumps. Every other days of leaching, a given amount of PLS solution sample was given and quantitatively analysed for copper and free sulfuric acid. Copper was extracted from PLS solutions by solvent extraction method using LIX984N and Raffinate solutions were circulated after adjusting its acid concentration. Recovery of copper in 2-meter columns were completed within the 78 days and in 4 and 6 meter columns, copper extraction was modeled for the rest of completing time.

When leaching was completed, the columns were washed with distilled water and the residue solids were dried for few days. These residue solids were then analyzed for copper element.

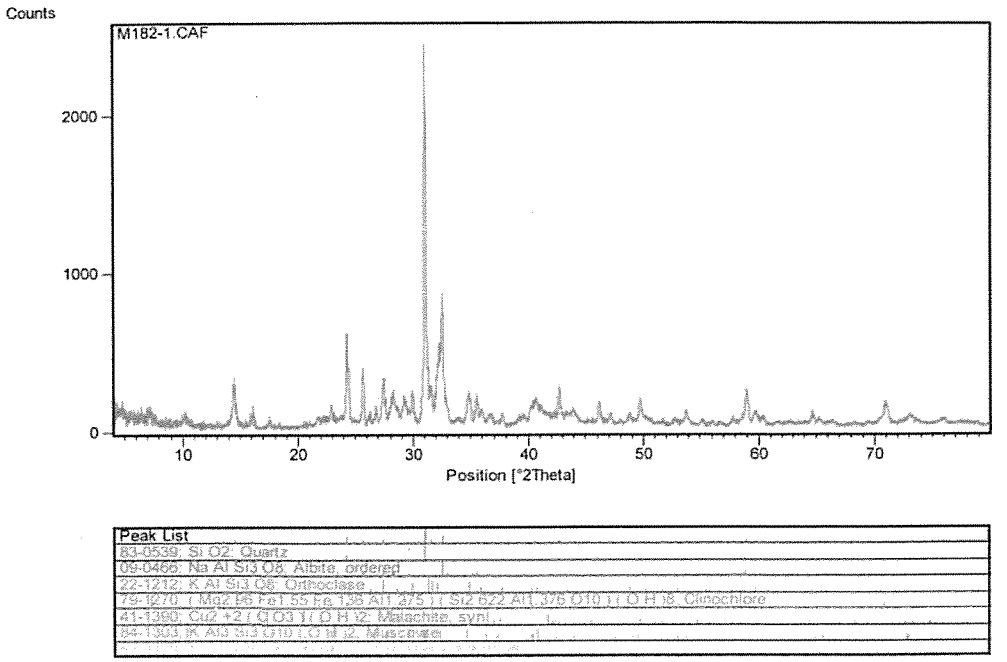

Figure 2. X-ray diffraction analysis of the ore

Table 2. Column leaching test conditions

Columns	Diameter(cm)	Height(m)	Particle size (inch)	Flow rate(l/m^2/h)	Acid concentration(g/l)
Column 1	20	2	1	10	20
Column 2	20	2	2	10	20
Column 3	50	4	1	10	20
Column 4	50	4	2	10	20
Column 5	50	6	1	10	20
Column 6	50	6	2	10	20

2.1 Modeling

The modeling of the system is carried out under the following assumptions: (1) There is a single heap with a known mineral feed. (2) After the mineral has completed its leaching, it is discarded carrying with it a volume of static solution (impregnation moisture). (3) The mass of the discarded mineral is the same as the mass of feed mineral. (4) Each heap behaves as a simple reactor, that is, based on input conditions the output conditions are determined, without any internal profiles or residence time distributions. (5) The following empirical model is considered for the extraction of copper Eq. (1):

$$R = R\infty\left(1 - e^{-k(t-\theta)^n}\right) \quad (1)$$

where n is an adjustable parameter, R is the percentage of extraction of copper from the mineral, R∞ is the maximum extraction of copper from the mineral, k is the kinetic constant of extraction, t is the leaching time, and Θ is a parameter which represents the delay in the percolation of the irrigating solution on the heap. This model take into account a global behavior for the extraction/time curve, neglecting the effects of each controlling step in the leaching processes. (6) A model analogous to the extraction of copper Eq. (2) is used for determining the acid consumption.

$$C_H = H\infty(1 - e^{-k_H(t-\theta_H)^{n_H}}) \quad (2)$$

Where C_H represents the acid consumption [Kg H_2SO_4/Ton mineral], H_∞ is the maximum acid consumption, and k_H, Θ_H and n_H have the same physical meaning than Eq. (2). Experimental data were used for determining the parameters indicated in the models mentioned, obtaining the values presented in Table 3. The values determined are applicable to heaps measuring 4, and 6m in height, with an irrigation rate of 10 l/h/m^2, and mineral with a grade value of 1 % agglomerated with 30 Kg H^+/Ton, using an acid concentration in the leaching solution of 20 gpl.

The model consists basically of the mass balances of each one of the units, that is, the balances in the stages of leaching, enriched solution pool, extraction step by solvent extraction–electrowinning, and the irrigation solution pool. For all these cases it was considered that the system was in steady-state, and thus the mass accumulation rate within each unit was nil. From the component perspective, we consider the balances of water, sulfuric acid, and copper regarding the solutions, and the copper and gangue in the case of solids flows.
The mass balances derived are simple, and thus are not shown in detail in the present study.

3 RESULTS

The effects of heap height and particle size on recovery and acid consumption have been investigated in this study. Many of the commercial simulation models (Quast, 2000, Bartlett, 1992) of heap leaching consider the restriction of the SX-EW stage equivalent to a grade value of 8 gpl copper in the PLS solution, which is important due to the order of magnitude of capital investments. However, it has not been considered in this study because of not considering economical aspects.

Table 3. Parameters of fit for the recovery of copper and acid consumption

Particle size (inch)	Height (m)	R ∞ (%)	K	Θ (days)	n	H ∞ (kg/ ton)	K_{H^+}	Θ_{H^+}(Days)	n_{H^+}
1	4	80	0.01	5	1.09	70	0.01	5	1.18
	6	69.9	0.04	12.96	0.7	59.95	0.04	4.96	0.73
2	4	30	0.02	8	0.91	39.99	0.05	5.73	0.64
	6	25.58	0.01	11.59	1	30	0.06	5.9	0.59

3.1 Effect of Heap Height

The effect of heap height of 2, 4 and 6 meters on copper recovery and acid consumption is now presented.

3.1.1 Effect of heap height on recovery

The effect of heap height on copper recovery from ore crushed to less than 1 and 2 inch has been shown in Figures 3 and 4 respectively. An inverse relation exists between the height of the heap in the percentage of extraction, confirming the observation of Lizama et al. (2005) about the inverse relationship between recovery and heap height.

Copper recovery decreases sharply when the heap height increases from 2 meter to 6 meter in both particle sizes.

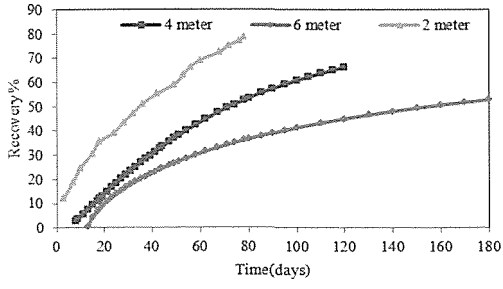

Figure 3. Copper recovery of ore crushed to minus 1 inch in different heap height

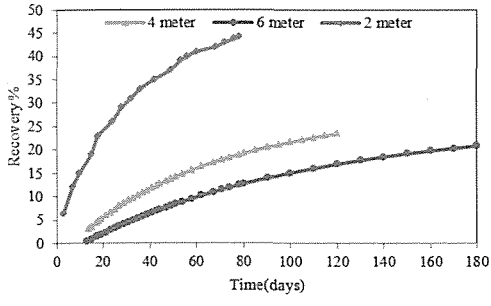

Figure 4. Copper recovery of ore crushed to minus 2 inch in different heap height

3.1.2 Effect of heap height on acid consumption

The height of the heap has an effect on the acid consumption the same as on the copper recovery. This effect is shown for samples crushed to minus 1 and 2 inch in Figures 5 and 6 respectively. The acid consumption is enhanced by decreasing the height of the heap due to increasing of the copper recovery.

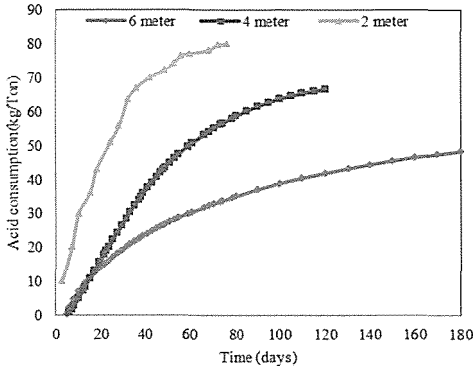

Figure 5. Acid consumption in different height of the heap for samples crushed to minus 1 inch

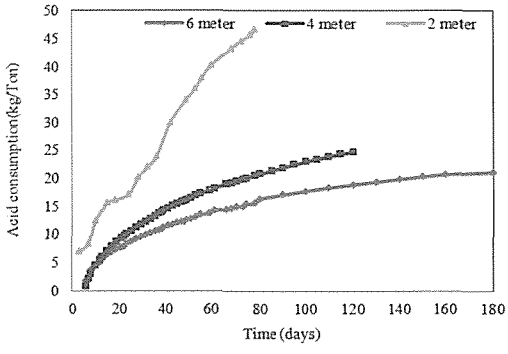

Figure 6. Acid consumption in different height of the heap for samples crushed to minus 2 inch

3.2 Effect of Particle Size

The influence of particle size on copper recovery and acid consumption at different heap heights were investigated in this study. The effects of particle size of less than 1 and 2 inch on copper recovery and acid consumption are shown in Figures 7 and 8 respectively. In all different heights of the heap, the copper recoveries in samples crushed to minus 1 inch are more than 2 inch. It shows that the ore should be crushed to minus 1 inch to achieve a good recovery.

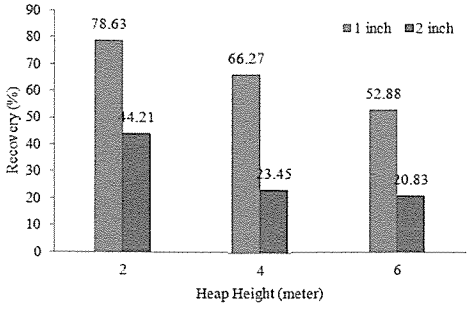

Figure 7. Comparison between copper recovery in 1 inch and 2 inch crushed ore

Figure 8 shows the acid consumption for 1 inch and 2 inch crushed ores. It can be clearly seen that 1 inch crushed ore consumes more sulfuric acid than 2 inch crushed ore. This fact is the same for different heights of the heap. When the ore crushed to minus 1 inch, more minerals are liberated and sulfuric acid can leach more copper. Therefore, both copper recovery and acid consumption increase.

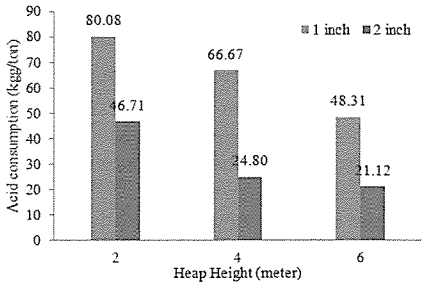

Figure 8. Comparison between acid consumption for 1 inch and 2 inch crushed ores

4 CONCLUSIONS

The results suggested the particle size and height of the heap have the significant influence on copper recovery and acid consumption. The considerable difference between copper recoveries in 1 inch and 2 inch crushed ores force to use 1 inch crushed ore for heap leaching but the only heap height cannot be a good factor to make a decision. There are other factors such as capital investment, annual production and copper concentration in PLS that affect on the decision.

REFERENCES

Bartlett, R.W., 1992. Simulation of ore heap leaching using deterministic models, Hydrometallurgy, 29, 1–3, pp.231–260.

Bartlett, R.W., 1997. Metal extraction from ores by heap leaching. Metallurgical and Materials Transactions B-Process Metallurgy and Materials Processing Science, 28, 4, pp.529–545.

Cisternas, L. A., Padilla G. A., Cueto J. Y., 2008. On the optimization of heap leaching. Minerals Engineering, 21, pp.673-678.

Hanson, A.T., Dwyer, B., Samani, Z.A., York, D., 1993. Remediation of chromium - containing soils by heap leaching: column study. Journal of Environment Engineering, 199, 5, pp.825–841.

Leahy, M.J., Davidson, M.R., Schwarz, M.P., 2007. A model for heap bioleaching of chalcocite with heat balance: mesophiles and moderate thermophiles. Hydrometallurgy, 85, 1, pp.24–41.

Lizama, H.M., Harlamovs, J.R., McKay, D.J., Dai, Z., 2005. Heap leaching kinetics are proportional to the irrigation rate divided by heap height. Minerals Engineering, 18, 6, pp.623–630.

Mason, C.F.V., Turney, W.R.J.R., Thomson, B.M., Lu, N., Longmire, P.A., ChisholmBrause, C.J., 1997. Carbonate leaching of uranium from contaminated soils. Environmental Science and Technology, 31, 10, pp.2707–2711.

Pennstrom, W.J., Arnold, J.R., 1999. Optimizing heap leach solution balances for enhanced performance. Minerals and Metallurgical Processing, 16, 1, pp.12–17.

Petersen, J., Dixon, D.G., 2007. Modelling zinc heap bioleaching. Hydrometallurgy, 85, 2–4, pp.127–143.

Quast, K.B., 2000. Leaching of atacamite (Cu2 (OH) 3Cl) using dilute sulfuric acid. Minerals Engineering, 13, 14–15, pp.1647–1652.

Valencia J.A., Mendez, D.A., Cueto J.Y., Cisternas L.A., 2008. Saltpeter extraction and modelling of caliche mineral heap leaching. Hydrometallurgy, 90, pp.103-114.

Wu, A.X., Yin, S.H., Yang, B.H., Wang, J., Qiu, G.Z., 2007. Study on preferential flow in dump leaching of low-grade ores. Hydrometallurgy, 87, 3–4, pp.124–132.

Yorio, C., Betancourt, E., Vivas, R., Rus, J., 2006. Ni, Co recovery study and Fe by acid leaching in columns. Revista de Metalurgia, 42, 1, pp.41–48.

Back-calculation of mechanical parameters of shell and balls materials from DEM simulations

Bahareh Arabzadeh[a], Akbar Farzanegan[a] and Vahid Hasanzadeh[a]

[a]*School of Mining, University College of Engineering, University of Tehran, Tehran, Iran, P.O. Box: 11155-4563*

ABSTRACT

Discrete Element Method (DEM) is appropriate for mathematical modeling and simulation of behavior of discrete discs (2D) or spheres (3D). Prediction of particles flow regime and power draw for a laboratory or an industrial mill is possible by DEM. In this article, a new approach was used to assess the main parameters of a transparent ball mill constructed in laboratory of University of Tehran. The mill shell and crushing balls are made of Plexiglas and compressed glass, respectively. The mechanical parameters of Plexiglas and compressed glass materials which are necessary for performing DEM modeling were unknown. The authors back-calculated the best values of mechanical properties of materials based on a large number of DEM simulations. Back-calculation procedure was mainly based on the comparison between electrical power draw measured in real mill and mechanical power draw calculated by DEM while trying to accurately simulate particle flow regime inside the real mill.

1 INTRODUCTION

In mineral processing plants, tumbling mills of any kind are used for size reduction. This process consumes energy in high levels (Mishra, 2003). For economical matters, experts in the field focus more on modeling of tumbling mills in a short period of time and approaching to most optimized mill with extensive level of utilization. For this reason, almost from twenty years ago, discrete element method (DEM) is used as a practical modeling method of industrial equipment. DEM models the behavior of assemblies of disks and balls realistically (Cundall and Strack, 1979).

For the first time, two dimensional numerical methods were used for improving the deficiency of ball mills during 1990's (Mishra and Rajamani, 1992). After that, discrete element method was used extensively in modeling of ball and AG/SAG mills. Also, this method was used adequately in prediction of charge motion, power draw and segregation in ball mills (Cleary, 1998). Other investigations such as comparison between numerical modeling and experimental measurements in a pilot SAG mill were done (Cleary, Morrison and Morrell 2003).

Optimization of the power draw has a drastic effect on the overall economic performance and environmental effect of a mineral processing plant (Djordjevic, Shi and Morrison, 2004). In recent decades, DEM has been established as a useful tool in simulation and optimization of mills in laboratory or industrial fields (Djordjevic, Shi and Morrison, 2004). Prediction of power draw utilization by DEM as a numerical method has been implemented in many cases. In this research, the authors

have used mill power draw in experimental and numerical study for a new purpose, i.e., back-calculation of materials mechanical properties. The numerical simulations was performed using PFC3D (Particle Flow Code in 3 Dimensions) software.

In geotechnical engineering, researchers for explaining the behavior of materials and having tangible explanations for many different responses of materials against natural effects, they have defined many parameters for various kinds of materials. Values of parameters such as normal stiffness, shear stiffness, cohesion, Young modules, Poisson's ratio, frictional angle and coefficient are necessary for the physical equations that are used in DEM numerical modeling. Therefore, to achieve adequate correspondence between reality and numerical modeling, these parameters should be defined accurately in numerical equations. Therefore, in laboratory or industrial cases that there is no geotechnical laboratory equipments for measuring the amounts of parameters or in the cases that laboratory tests are not either accurate or economical, the approach of comparison between net power draws that is suggested in this paper to assess the best estimates of materials parameters and best flow regime in modeled mills, can be used as a back-calculation method. The details of the back-calculation method are presented in this paper.

A transparent ball mill was built at mineral processing laboratory of University of Tehran which can be used to demonstrate the movement regime of crushing elements inside the mill. The structure of mill cylindrical shell is Plexiglas® with 5 mm thickness and its inner wall is protected by diaphanous plastic liner with 2 mm thickness. Also, the lifters have been made of diaphanous plastic. The mill is filled with balls made of compressed glass as crushing elements. As there was no available information about the values of mechanical parameters for Plexiglas, plastic liner and compressed glass, DEM model calibration was done to obtain the optimal values of the required parameters. This was performed by comparison made between balls movement regime and electrical power draw observed in laboratory experiments and balls movement regime and mechanical power drawn predicted in DEM simulation. The optimal values of parameters will be found when an adequate agreement between experimental observations and numerical predictions is achieved.

2 TRANSPARENT LABORATORY BALL MILL

The main purpose of constructing a transparent ball mill was to make it possible to view the charge motion inside the mill and capturing necessary images by a high-resolution camera. The properties of the transparent mill are as follows in Table 1.

Table 1. Mill specification

Property	Value
Mill diameter (cm)	25
Mill length (cm)	30
Effective mill length (cm)	20
Diameter of small balls (cm)	1.6
Diameter of big balls (cm)	2.5
Number of small balls	500
Number of big balls	90

The properties are also shown in Figure 1. The mill filling is equal to 18% of mill's total volume.

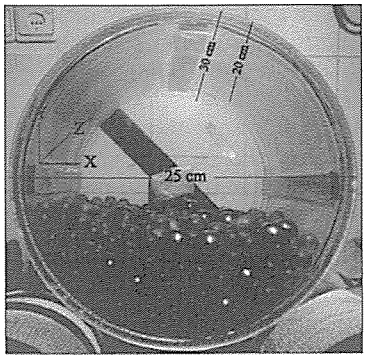

Figure 1. A view of the transparent ball mill with main geometrical dimensions.

There are some unknown mechanical properties such as the normal and shear

stiffness of mill's shell and balls (K_{nwall}, K_{swall} , K_{nball}, K_{sball}) and also the friction coefficient (μ) of shell and balls which are needed in order to do DEM simulations.

This is similar to some real life cases. A good example is a mill abandoned for some years. Engineers need to know the critical parameters, for setting it up again and modeling it for new conditions. In the next part of this article, the approach used by the authors to solve these kinds of problems is presented.

3 DEM MODEL CALIBRATION

In discrete element method, assembly of discs in two dimensional or balls in three dimensional modeling are influenced by stresses. Therefore, displacements and contact forces are found through a series of calculations. These calculations trace the movements of the individual particles (Cundall and Strack, 1979). To perform these calculations, some physical parameters for mill shell and balls are necessary. Normal stiffness (K_n), shear stiffness (K_s) and friction coefficient (μ) for mill shell and balls should be used in numerical modeling. During preliminary laboratory work, the mill was put in rotation with just one ball (big or small).The rotational speed was equal to 71 rpm. All experimental conditions in laboratory; such as mill and its charge specifications and rotational speed, were used to set variables in numerical modeling. In DEM modeling procedure, unknown or erroneous values of mechanical properties are some of the main sources of discrepancies between observed measurements and simulation predictions. To back-calculate the mechanical parameters, the initial values of stiffness and frictional coefficients for Plexiglas and glass were considered the same as the values of these parameters published in rock mechanics literature. In this part, the visual results from numerical modeling are qualitatively compared with images that were taken from the rotating transparent ball mill. By changing mentioned parameters in numerical modeling and simultaneously comparison between experimental and numerical visual results, it was possible to approach to the proper properties. It should be mentioned that only comparison between images is not a suitable approach for achieving to the best parameters for DEM modeling. Comparison between measured power draw in laboratory and numerical modeling helped in approaching to the best values for mechanical properties. Model validation by comparing between electrical and mechanical power draw will be explained in the next part of this paper.

The best approximate values of normal and shear stiffness and frictional coefficient for making proper agreement between experimental and numerical modeling are shown in Table 2.

Comparing measured net power draws (experimental) and predicted net power draw from DEM modeling is elaborated in this part. If an acceptable correlation exists, then a calibration coefficient can be assessed by a linear regression between measured and numerical net power draw.

In laboratory work and DEM modeling, seven mill configurations were considered as basic designs for assessing calibration coefficient. These configurations are presented in Table 3. The net power draw was measured by a Wattmeter that was connected in series with the mill electrical circuit. Therefore, the first row of Table 3 demonstrates electrical net power draws that have measured during laboratory work.

In numerical modeling, mechanical net power draw is calculated and compared with the electrical net power draw. The calculations of net power draw in numerical modeling are as follow:

$$W_{net(new)} = W_{net(old)} - \sum_{N_w} F_i \Delta U_i + M_i \Delta \theta_i \qquad (1)$$

Where N_w is the number of walls, F_i and M_i are the resultant force and moment acting on the wall at the start of the current time step; and ΔU_i and $\Delta \theta_i$ are the applied displacement and rotation occurring during the current time step. Note that this is an approximation in that

Table 2. Adequate amounts for mechanical properties by comparing between figurative results.

	Mechanical Properties		
	K_n (N/m)	K_s (N/m)	*fric*
Wall	400000	400000	0.85
Lids of Mill	400000	400000	0.85
Lifters	1500	1500	0.85
Big ball	600000	8000000	0.25
Small ball	600000	8000000	0.45

Table 3. Seven experimental setup for assessing calibration coefficient

Mills Property	Type of Mills						
	No Lifter-Big Balls	No Lifter-Small Balls	No Lifter-Big & Small Balls	2 Lifters (6 mm)-Big & Small Balls	4 Lifters (6 mm)-Big Balls	4 Lifters (6 mm)-Small Balls	4 Lifters (6 mm)-Big & Small Balls
Measured net power draw, Experimental (W)	5.000	10.000	15.000	17.500	10.000	15.000	25.000
Predicted net power draw, Numerical (W)	4.846	15.446	22.780	39.323	14.198	48.285	53.392

it assumes that F_i and M_i remain constant throughout the time step (Itasca, 1998). W is the total accumulated work done by all walls on the crushing elements; therefore, net power draw will be calculated by Eq. (2):

$$W = \frac{\Delta W}{\Delta t} \qquad (2)$$

The net power draw calculated based on Eqs. 1 and 2 have been shown in second row of Table 3. To fit the mechanical parameters, their values were changed, so that an acceptable agreement between experimental and numerical net power draws is achieved. The final parameters that were considered for DEM modeling are presented in Table 4.

In addition to checking closeness of net power draws, the real power draw measured by Wattmeter in laboratory experiments and predicted power draw calculated by using Eq. 2 (work and torque at a specified Δt) based on presented parameters in Table 4, were compared. The visual validation of DEM modeling has been illustrated in Figure 2.

Table 4. Optimal mechanical parameters obtained for DEM simulations

	Mechanical Properties		
	K_n (N/m)	K_s (N/m)	*fric.*
Wall	4000	4000	0.85
Lids of mill	40000	40000	0.85
Lifters	1500	1500	0.85
Big ball	2000	800000	0.25
Small ball	25000	800000	0.45

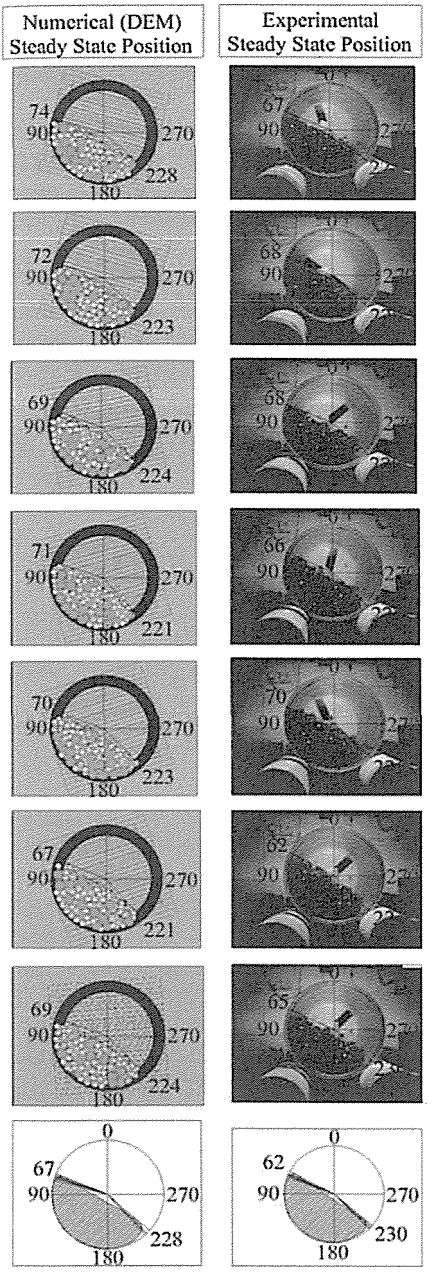

Figure 2. DEM validation for the mill without lifters and 18% mill filling

By comparing (1) between photographs from laboratory rotating mill and prepared snap-shots in DEM simulation; and (2) between net power draws in experimental and numerical modeling that are presented in the Table 3, a calibration diagram to find an acceptable relationship between numerical and experimental results of net power draw has been demonstrated in Figure 3.

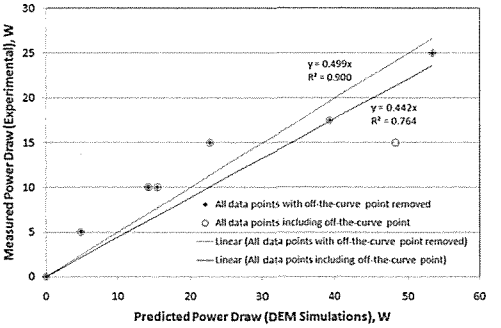

Figure 3. Electrically measured power draws during laboratory experiments vs. numerically predicted power draws during DEM simulations shows an existing correlation with a regression coefficient equal to 0.442.

A correlation was found between measured and predicted power draw of the mill with a linear regression coefficient equal to 0.442 with an R-squared value equal to 0.764. (The linear relationship can be seen in Figure 3 with solid line). It is evident that one data point corresponding to DEM simulation No. 6 is off-the-curve. For this reason, the authors repeated the same simulation with no change in result. Therefore, the data point was included for calibration purpose. However, if this point is removed, while there is a little change in linear regression coefficient, the R-squared value increases to 0.900. The linear regression equation could be used in optimization of mill. It means that through mill optimization there is not any necessity to build all types of mill for optimization procedure in laboratory. Hence, the optimization states could be simulated by relying to DEM simulation.

4 CONCLUSIONS

The following conclusions can be derived from DEM modeling and simulations:

- The unknown mechanical parameters required for DEM-based simulation and optimization can be back-calculated by qualitative comparison between experimental measurements and numerical results.
- To obtain the best estimates of mechanical parameters, values given for the same or similar materials in rock mechanics' tables can be considered as default and initial guesses to start search process. The best estimates of parameters can be found by changing default parameters, until approaching an acceptable agreement between experimental and numerical modeling for both net power draws and balls flow regimes in the mill.
- Determination of calibration coefficient for DEM model can be done by modeling of mill at various configurations using the best estimates of mechanical parameters.

ACKNOWLEDGMENTS

Authors are grateful to the University College of Engineering Schools at University of Tehran for the financial support to construct the transparent laboratory mill.

REFERENCES

Cleary, P. W., 1998. Prediction charge motion, power draw, segregation and wear in ball mills using discrete element methods. Minerals Engineering, 11, 1061-1080.

Cleary, P. W., Morrisson, R., Morrell, S., 2003. Comparison of DEM and experiment for a scale model SAG mill. International Journal of Mineral Processing, 68, 129-165.

Cundall, P. A., Strack, O. D. L., 1979. A discrete numerical model for granular assemblies. Geotechnique, 29, 47-65.

Djordjevic, N., Shi, F. N., Morrison, R., 2004. Determination of lifter design, speed and filling effects in AG mills by 3D DEM. Minerals Engineering, 17, 1135-1142.

Mishra, B. K., 2003. A review of computer simulation of tumbling mills by the discrete element method: Part I contact mechanics. International Journal of Mineral Processing, 71, 73-93.

Mishra, B. K., Rajamani, R. K., 1992. The discrete element method for the simulation of ball mills. Appl. Math. Modelling, 16, 598-604.

PFC3D Particle Flow Code in 3 Dimensions, 1998. Itasca Consulting Group Inc., Minneapolis, MN, USA.

Estimation of Soil Water Characteristic Curve through Weighted Residual Approximations

Kaveh Shakiba Nia
Faculty of Civil Engineering, K. N. Toosi University of Technology, Tehran, Iran;
email: k.nia@live.com

ABSTRACT Hydrologic studies at mine sites usually involve analysis of unsaturated flow for predicting infiltration and seepage. The soil water characteristic curve, "SWCC", plays a significant role in simulation of unsaturated flow and hydrological studies at mine sites. Experimental methods for assessment of the SWCC are often time consuming. Feasibility analysis and studies at mine sites are often subject to deliverable times that might hinder laboratory assessment of the SWCC. Therefore, here to avoid lengthy and expensive laboratory tests, a model based on the Van Genuchten equation; for estimation of the SWCC for cohesive soils is developed. The parameters a, b, and c of the Van Genuchten equation are assumed to be functions of the PI and the percentage passing the No. 200 sieve and are estimated through weighted residual approximations. Verification illustrates that the results from the proposed model are in a relatively good agreement with those from laboratory tests.

1 INTRODUCTION

Hydrologic studies at mine sites usually involve analysis of unsaturated flow for predicting infiltration and seepage. The soil water characteristic curve, "SWCC", plays an important role in simulation of unsaturated flow and hydrological studies at mine sites. It has played a significant role in the study of unsaturated soils [1]. Knowledge of the soil water characteristic curve is fundamental for understanding unsaturated soils [20]. The SWCC illustrates the relationship between soil suction and moisture content. Fredlund and Morgenstern (1977) showed that the shear strength of unsaturated soils can be estimated by any two of three stress variables including soil suction.

The experimental methods of suction evaluation are often time consuming, requiring expensive laboratory tests. Studies show that the SWCC can be estimated using characteristics of soils. The measurement of soil parameters used to describe behaviour of unsaturated soils is expensive, difficult and often impractical to obtain [6].

Figure 1 illustrates several approaches which can be taken to determine unsaturated soil property functions. Measurement of the soil-water characteristic curve for a soil can be used as an indirect laboratory test to compute an unsaturated soil property function [7].

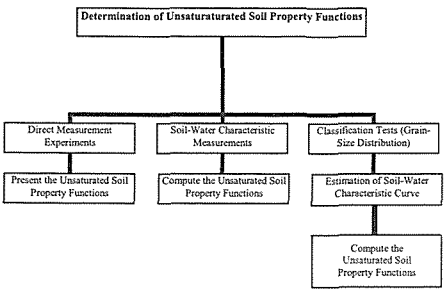

Figure 1: Approaches that can be used in the laboratory to determine the unsaturated soil property functions [7]

The SWCC shows the relationship between soil suction and either the degree of saturation or the volumetric water content. The volumetric water content is the ratio of the water volume to the total volume as follows:

$$\theta = \frac{V_w}{V_t} = \frac{V_w}{V_v} \cdot \frac{V_v}{V_t} = S \cdot n = \frac{S \cdot e}{1+e} \qquad (1)$$

Where θ is the volumetric water content; V_W, volume of the water within the soil; V_t, total volume of the soil; V_V, volume of the pores within the soil; S, degree of saturation; n, porosity ratio; e, void ratio.

Figure 2 describes a typical plot of a soil-water characteristic curve which consists of three stages: capillary saturation, de-saturation and residual saturation. When the suction value exceeds the air-entry value, the degree of saturation decreases rapidly at relatively low suction values and then reduces more gradually when the suction becomes high [7].

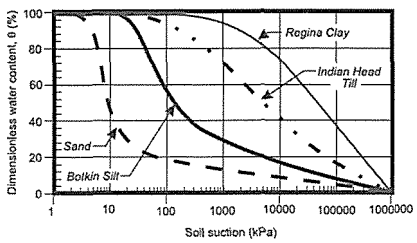

Figure 2: Typical SWCCs [7]

Both empirical and theoretical investigations indicate that the SWCC is an essential element in unsaturated soil modeling and it is hysteretic in nature, owing to the energy dissipation during moving fluids in or out of the soil [15].

Water content and suction affect the permeability, shear strength, volume change and deformability of unsaturated soils [18]. Many characteristics of unsaturated soils such as the coefficient of permeability, shear strength, pore size distribution and water content at any suction, can be obtained from the SWCC. Many researchers have tried to predict the SWCC, Gardner (1956), Brooks and Corey (1964), Brutsaert (1966), van Genuchten (1980), McKee and Bumb (1987), Burdine (1953), Mualem (1976), Kosugi (1994), Fredlund and Xing (1994). However there is still a need for further research on prediction of the SWCC since most of the models can not predict the SWCC accurately. The expressions with three or four parameters seem to be more appropriate to represent the SWCC [14]. Soil suction measurement tests are often categorized as either direct or indirect. Direct methods include pressure membranes, pressure plates and tensiometers while indirect methods include filter paper, porous blocks and hit dissipation sensors. An important reason why functions should be fit to SWCC experimental raw data is that many applications of the SWCC require that

differentiated or integrated and be continuous [22].

Zapata (2000) categorizes the predictive algorithms that can predict the SWCC based on grain size distribution and soil characteristics into three major approaches:

1- The approach which is based on statistical estimation of water contents at selected matric suction values.

2- The approach which includes the methods which correlate, by regression analysis, soil properties with the fitting parameters of an equation which represents the SWCC.

3- The approach which includes the methods that estimate the SWCC using a physics based conceptual model.

Experimental methods for assessment of the SWCC are lengthy and Feasibility analysis and studies at mine sites are usually subject to deliverable times that might hinder laboratory assessment of the SWCC. Here, a model for prediction of the SWCC is introduced which is based on the PI, fine content and the Van Genuchten (1980) equation. The equations are developed through weighted residual approximations and are validated by simulating experimental observations.

2 VAN GENUCHTEN EQUATION

The Van Genuchten equation (1980) is widely used due to its flexibility. It can be written as equation 2. In this equation parameter b corresponds to pore size distribution index. Parameter a does not affect the curve shape, but shifts the curve towards the higher or lower suction regions of the plot, parameter c is related to the asymmetry of the curve; a smaller c corresponds to a moderate slope in low suction range and a steeper slope in high suction range [11]. The equation introduced by Van Genuchten (1980) has been used in this study.

$$S = \frac{1}{\left[1+\left(\frac{\psi}{a}\right)^{b}\right]^{c}} \qquad (2)$$

Where S is the degree of saturation and ψ □is soil suction.

Zapata et al. (2000) suggested that for cohesive soils, the product of the percentage passing the No. 200 sieve, as a decimal, multiplied by the PI as a percentage, can be used to form the weighted PI, "W.PI". The equilibrium soil suction at a given degree of saturation is expected to be proportional to the specific surface area of the soil. The PI is a fair indicator of surface area and the use of PI alone can be considered. However, a soil with a small percentage of highly active clay would have a high PI but only a moderate specific surface area. Therefore, the weighted PI (W.PI) can be considered a better index of soil particle surface area for predicting the Soil-Water Characteristic Curve [23].

The smaller the initial void ratio, "e", the higher the air-entry value, "AEV", and the higher the residual degree of saturation as well [12]. The air-entry value and the residual degree of saturation can be expressed together by void ratio, "e", using empirical relationships. The air-entry value is an important parameter for partially saturated soils since the degree of saturation starts to drop rapidly when the suction exceeds the AEV. The denser the soil, the higher the AEV, which implies that for soils with low void ratio values, small changes in degree of saturation can be assumed at low suctions [11].

3 ESTIMATION OF THE SWCC FOR COHESIVE SOILS USING WEIGHTED RESIDUAL APPROXIATIONS

The following equations have been driven by fitting the Van Genuchten Equation (1980) to

experimental observations through weighted residual approximations.

The parameters a, b, and c, are assumed to be functions of the PI and the percentage passing the No. 200 sieve (see equation 2). A function ϕ(x) can be approximated trough weighted residual approximations as follows:

$$\phi \cong \hat{\phi} = \psi + \sum_{m=1}^{M} a_m \cdot N_m \qquad (3)$$

Where (a_m, m=1, 2, 3, ... m) represents the parameters which should be calculated to in order to fit function $\hat{\phi}$ to the given function ϕ properly. Nm represents shape functions. The value of shape functions should approach zero at boundary conditions. Here shape functions along $1 \le W.PI \le 50$ are considered as follows:

$$N_m = (W.PI - 1)^m .(50 - W.PI) \qquad (4)$$

Where m represents point number along the given curve. ψ is introduced to fulfill boundary conditions. Here they are assumed to be linear. Three functions are driven considering the given curves as follows:

$$\psi a = 4.235.W.PI + 8.236 \qquad (5)$$
$$\psi b = -0.00898.W.PI + 1.81898 \qquad (6)$$
$$\psi c = 0.000031.W.PI + 0.137735 \qquad (7)$$

The following curves are driven through weighted residual approximations. These curves are shown in figures 3 through 5.

$$a = 0.000031.(W.PI)^4 - 0.002341.(W.PI)^3 + 0.099801.(W.PI)^2 + 1.20196.(W.PI) + 11.1716 \qquad (8)$$
$$b = 0.0000000266873.(W.PI)^4 - 0.000007.(W.PI)^3 + 0.000638.(W.PI)^2 - 0.028121.(W.PI) + 1.83749 \qquad (9)$$
$$a = -0.000000108456.(W.PI)^4 + 0.000011.(W.PI)^3 - 0.000321.(W.PI)^2 + 0.003462.(W.PI) + 0.135848 \qquad (10)$$

Where W is the percentage passing the No. 200 sieve; e, initial void ratio; PI, plasticity index as a decimal.

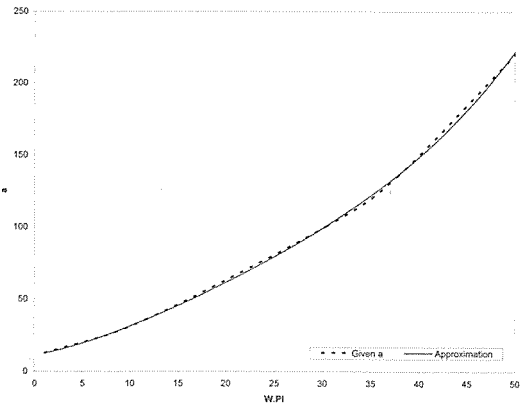

Figure 3: a versus W.PI

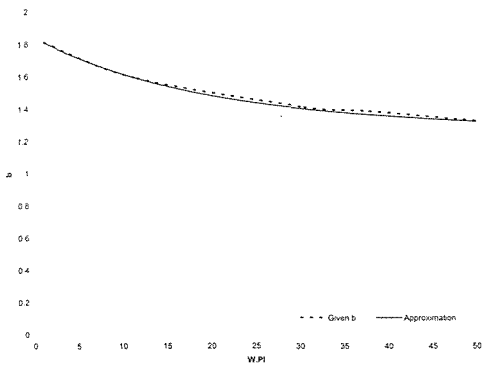

Figure 4: b versus W.PI

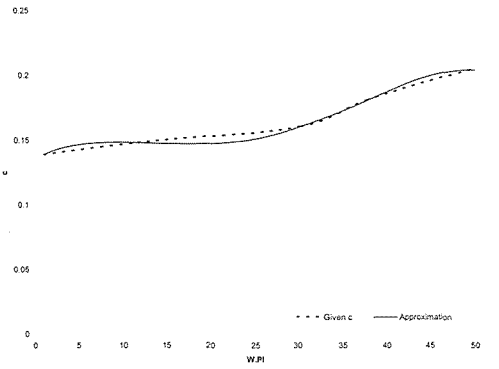

Figure 5: c versus W.PI

Figures 6 through 8 show the SWCCs of three of the samples which have been used to predict the above equations.

Table 1 shows the characteristics of the soils and the parameters of the Van Genuchten equation.

Table 1: The Characteristics of the Soils and the Parameters of the Van Genuchten Equation

Soil	γ_d (gr/cm3)	PI (%)	W	W.PI	Parameters of Equation (2)		
					a	b	c
Red Silty Clay	1.80	14	0.83	0.48	38.25	1.627	0.158
Madrid Clayey Sand	1.91	8	0.13	0.38	41.85	1.756	0.18747
Fountain Hills Clay	1.14	35	0.92	1.386	261.2	1.46	0.158

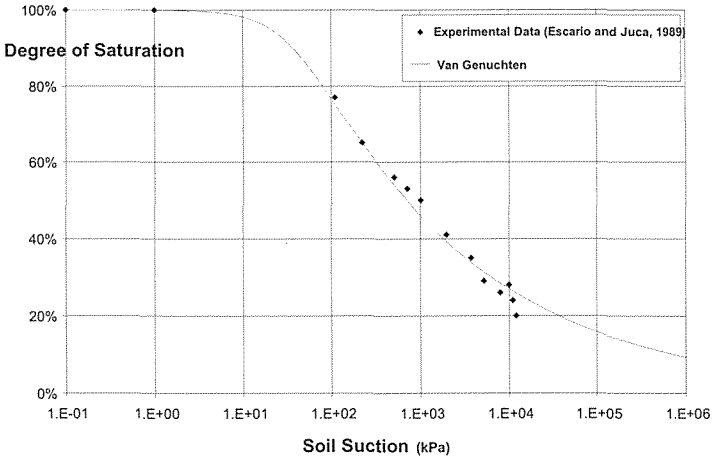

Figure 6: Experimental and Estimated SWCCs (Red Silty Clay)

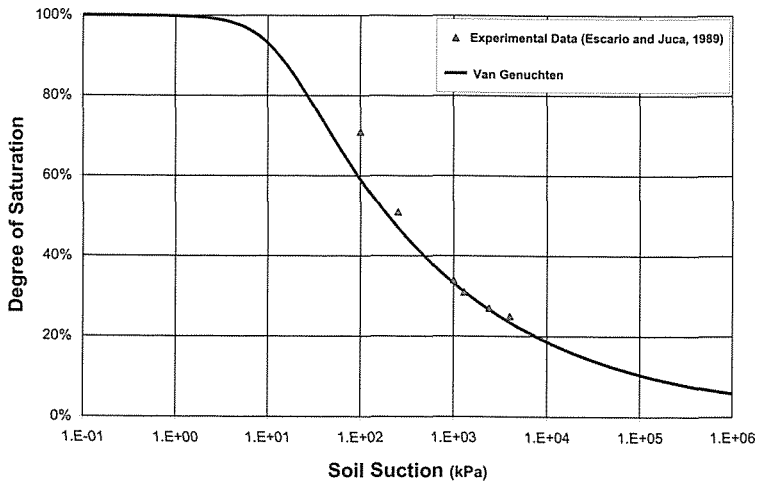

Figure 7: Experimental and Estimated SWCCs (Madrid Clayey Sand)

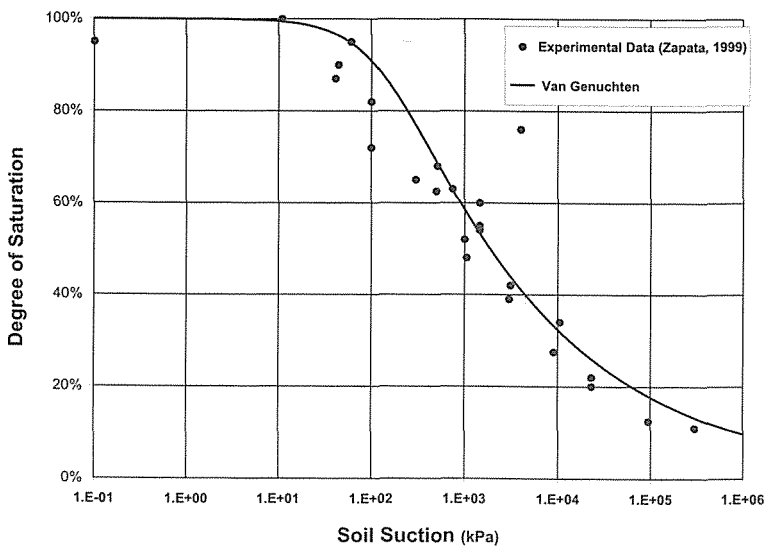

Figure 8: Experimental and Estimated SWCCs (Fountain Hills Clay)

Figure 9 illustrates the predicted SWCCs for different values of W.PI. As the value of W.PI increases, the SWCC often moves to the right.

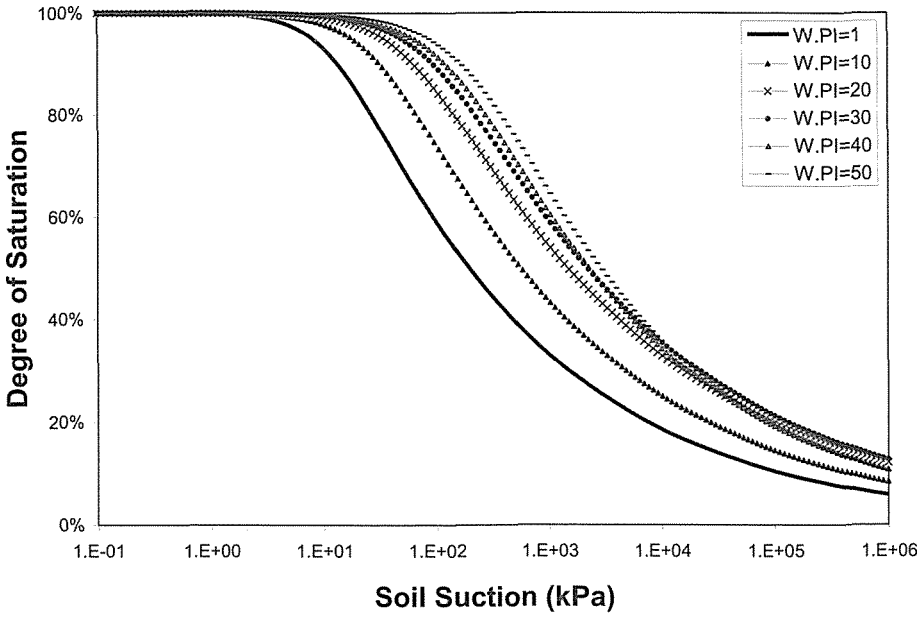

Figure 9: Predicted soil water characteristic curves for different values of W.PI

4 VERIFICATION

In order to validate the proposed equations, the results from this model have been compared to those from experimental observations. It should be noted that these observations have not been used to predict equations 8 through 10 and have only been used for verification. Figure 10 illustrates the grain size distribution curves of three soils whose SWCCs have been used here for verification.

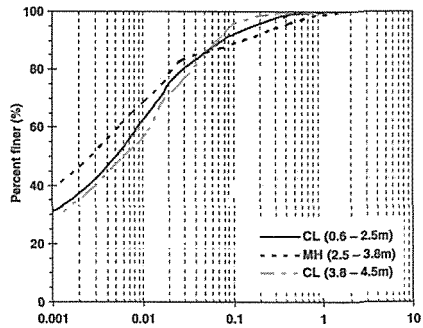

Figure 10: Grain size distribution curves of the soils (Nam et al., 2010)

Table 2 shows the characteristics of the soils and the predicted parameters of the Van Genuchten equation. Soil samples were obtained from riverbank by Nam et al. (2010). A representative soil profile along the river bank consists of silty sand, low plasticity clay, CL (0.6–2.5m), high plasticity silt, MH (2.5–3.8m), and low plasticity clay, CL(3.8-4.5m), (Nam et al., 2010).

Table 2: The Characteristics of the Soils and the Parameters of the Van Genuchten Equation

Soil	PI (%)	W	W.PI	Estimated Parameters of Equation (2) from the proposed model		
				a	b	c
CL (06-2.5m)	[16 20]	0.31	[4.96 6.2]	[19.32 21.95]	[1.686 1.713]	[0.146 0.147]
MH (2.5-3.8m)	[18 24]	0.4	[7.2 9.6]	[24.21 30.1]	[1.62 1.67]	0.148
CL(3.8-4.5m)	[15 20]	0.29	[4.41 5.8]	[18.22 21.08]	[1.72 1.69]	[0.146 0.147]

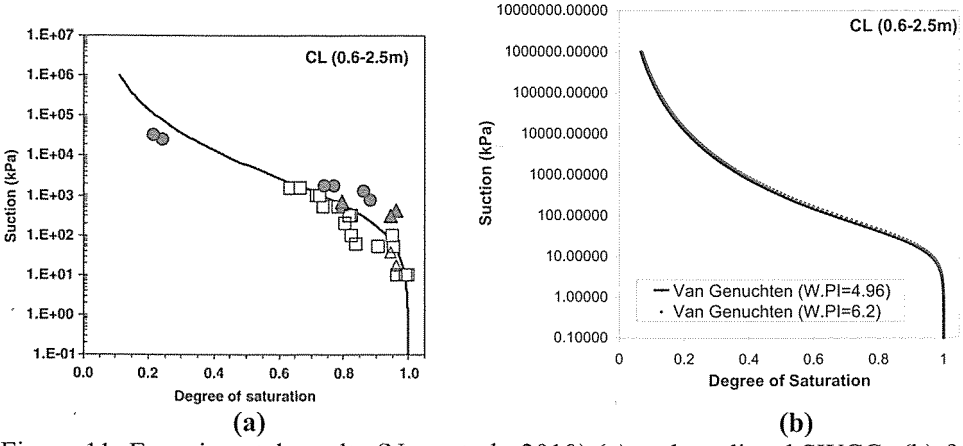

Figure 11: Experimental results (Nam et al., 2010) (a) and predicted SWCCs (b) for CL (0.6-2.5m)

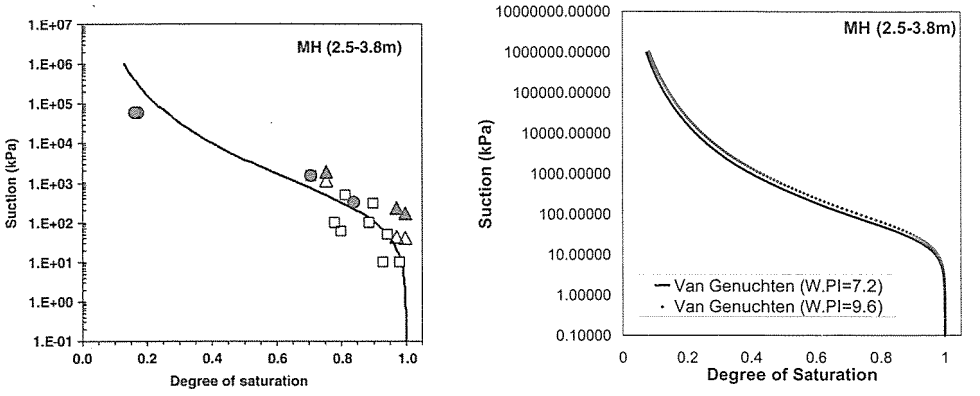

(a) (b)

Figure 12: Experimental results (Nam et al., 2010) (a) and predicted SWCCs (b) for MH (2.5-3.8)

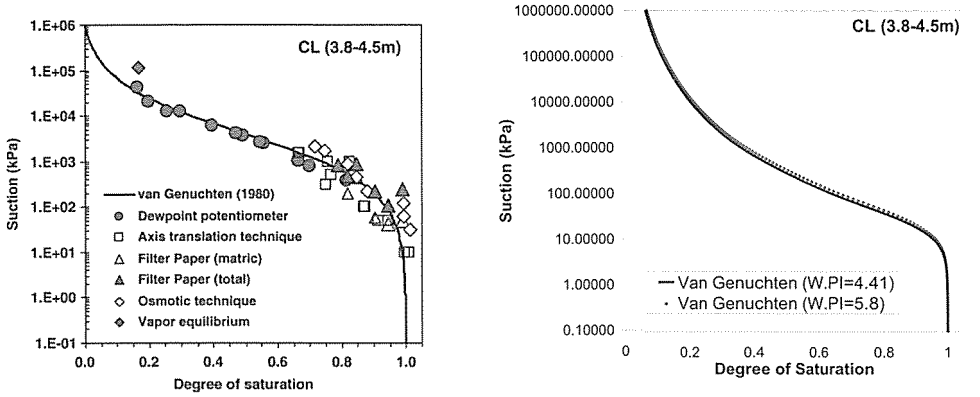

(a) (b)

Figure 13: Experimental results (Nam et al., 2010) (a) and predicted SWCCs (b) for CL (3.8-4.5m)

Figures 11 through 13 illustrate the experimental and predicted SWCCs of the three soils. Results from the proposed model, shown in figures 11(b), 12(b) and 13(b) are in a good agreement with those from experimental methods (see figure 13(b)). The CL soils have higher values of suction than the MH soil. The Comparison of the results supports the validity of the proposed equations.

The observations of Zapata et al. (2000) have also been used for verification. The ranges of Experimental SWCCs of 64 soils with various values of W.PI and the ranges of the predicted SWCCs corresponding to them are shown in figures 15 through 17. The

curves represent the predicted band corresponding to W.PI and the points represent the range of empirical SWCCs.

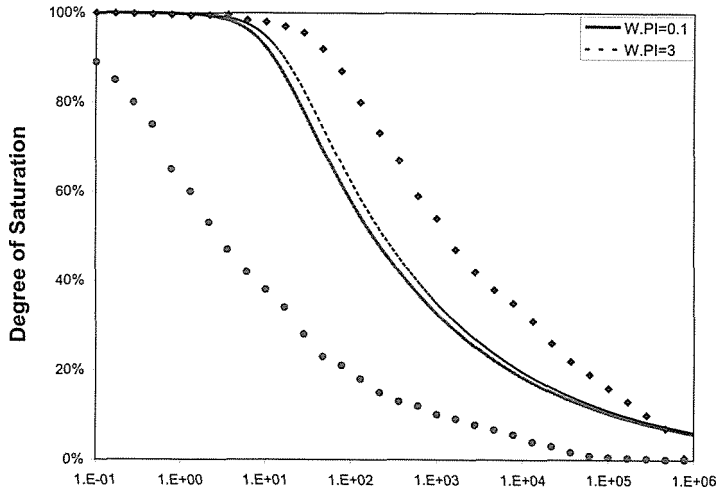

Figure 14: Range of SWCCs for 14 soils (Zapata et al., 2000) and results from proposed model (0.1<W.PI<3)

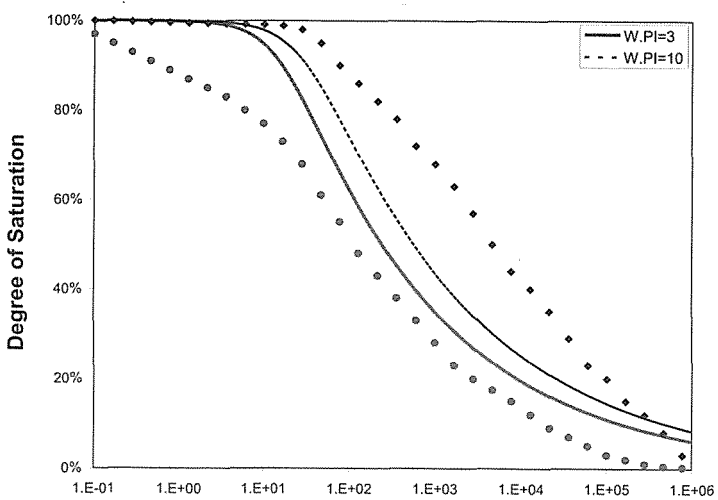

Figure 15: Range of SWCCs for 21 soils (Zapata et al., 2000) and results from proposed model (3<W.PI<10)

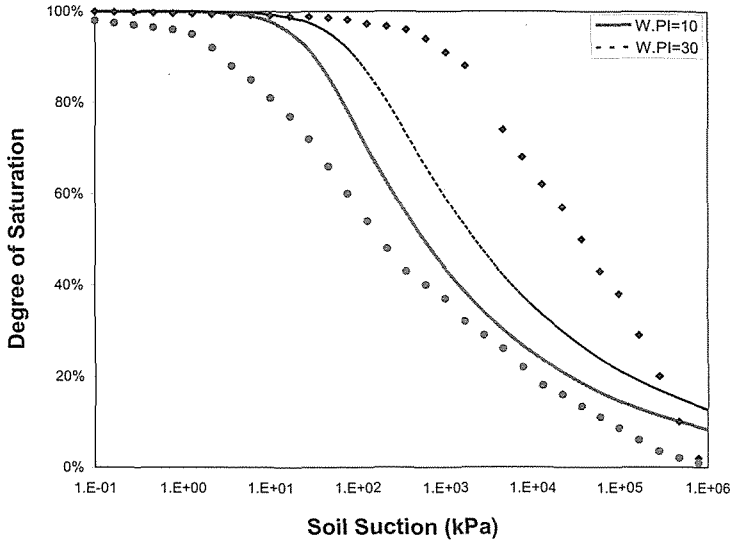

Figure 16: Range of SWCCs for 24 soils (Zapata et al., 2000) and results from proposed model (10<W.PI<30)

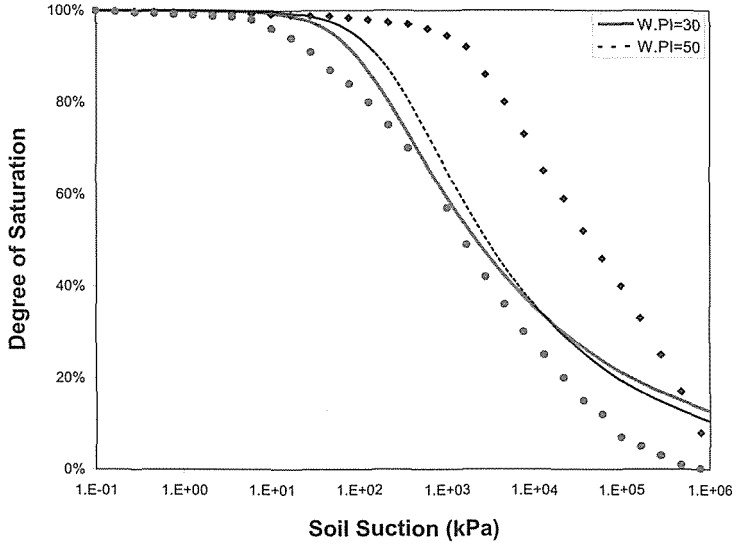

Figure 17: Range of SWCCs for 5 soils (Zapata et al., 2000) and results from proposed model (30<W.PI<50)

The air-entry value increases with increasing of W.PI. As illustrated, the estimated results are in a relatively good agreement with those of experimental observations.

5 CONCLUSIONS

In this paper, a simple model for predicting the SWCC of cohesive soils has been introduced. Three equations have been developed through weighted residual approximations for predicting the parameters of the Van Genuchten equation which are assumed to be functions of the PI and the percentage passing the No. 200 sieve. The comparison of the results from this model to those from laboratory tests demonstrates that it makes relatively acceptable results.

REFERENCES

[1] Barbour, S.L., 1998. "Nineteenth Canadian Geotechnical Colloquium: The soil-water characteristic curve: a historical perspective." Canadian Geotechnical Journal, 35: 873–894.

[2] Brooks, R.H. and Corey, A.T., 1964. "Hydraulic properties of porous media." Hydrology Papers, 3. Fort Collins, Colorado State University.

[3] Brutsaert, W., 1966. "Probability laws for pore size distribution." Soil Science, 101:85-92.

[4] Burdine, N.T., 1953. "Relative permeability calculations from pore size distribution data." Journal of Petroleum Technology, 5:71-78.

[5] Escario, V. and Juca, J.F.T. 1989. "Strength and Deformation of Partly Saturated Soils", Proceedings of the Twelfth International Conference on Soil Mechanics and Foundation Engineering, Vol. 2, pp. 43-46.

[6] Fredlund, D.G. 1995. "The prediction of unsaturated soil property functions using the soil-water characteristic curve." In Proceedings of the Bengt Broms Symposium in Geotechnical Engineering, Singapore, 13–16 Dec., pp. 113–133.

[7] Fredlund, D.G., 2000. "The implementation of Unsaturated Soil mechanics into geotechnical engineering.", Can. Geotech. J., 37:963-986.

[8] Fredlund, D.G., and Morgenstern, N.R. 1977. "Stress state variables for unsaturated soils." Journal of the Geotechnical Engineering Division, ASCE, 103(GT5): 447–466.

[9] Fredlund, D.G., and Xing, A., 1994. "Equations for the Soil-Water Characteristic Curve", Canadian Geotechnical Journal, 31(3): 521-532.

[10] Gardner, W., 1956. "Mathematics of isothermal water condition in unsaturated soils." Highway Research Board Special Report 40 International Symposium on Physico-Chemical Phenomenon in Soils. Washington D.C., p.78-87.

[11] Jian, Z., and Jian-lin, Y., 2005. "Influences affecting the soil-water characteristic curve.", Journal of Zhejiang University SCIENCE, 6A(8):797-804.

[12] Kawai, K., Karube, D., and Kato, S., 2000. "The model of water retention curve considering effects of void ratio." In: Rahardjo, H., Toll, D.G., Leong, E.C.(Eds.), Unsaturated Soils for Asia. Balkema, Rotterdam, p.329-334.

[13] Kosugi, K., 1994. "The parameter lognormal distribution model for soil water retention." Water Resource Research, 30:891-901.

[14] Leong, E.C., and Rahardjo, H. 1996. "A review of soil-water characteristic curve equations." Geotechnical Research report NTU/GT/96-5, Nanyang Technological University, NTU-PWD Geotechnical Research Centre, Singapore.

[15] Li, X., 2005. "Modelling of hysteresis response for arbitrar wetting/drying paths." Computers and Geotechnics, Volume 32, Issue 2, March 2005: 133-137.

[16] McKee, C., Bumb, A., 1987. "Flow-testing coalbed methane production wells in the presence of water and gas. SPE Formation Evaluation, (10):599-608.

[17] Mualem, Y., 1976. "A new model for predicting the hydraulic conductivity of

unsaturated porous media." Water Resources Research, 12:593-622.
[18] Nam, S., Gutierrez, M., Diplas, P., Petrie, J., Wayllace, A., Lu, N., Muñoz, J. J., ."Comparison of testing techniques and models for establishing the SWCC of riverbank soils ." Engineering Geology, Volume 110, Issues 1-2, 2010: 1-10.
[19] Nuth, M. and Laloui, L., 2008. "Advances in modelling hysteretic waterretention curve in deformable soils." Computers and Geotechnics Volume 35, Issue 6, November 2008, 835-844.
[20] Prunity , L. and Bell , J., 2007. "Soil Water Hysteresis at Low Potential." Pedosphere, Volume 17, Issue 4, August 2007, 436-444.
[21] Van Genuchten, M.T., 1980. "A closed-form equation for predicting the hydraulic conductivity of unsaturated soils." Soil Science Society of America Journal, 44:892-898.
[22] Zapata, C.E., 1999. "Uncertainty in soil-water characteristics curve and impact on unsaturated shear strength predictions." Ph.D. Dissertation, Arizona State University, Tempe, United States.
[23] Zapata, C. E., Houston, W.N., Houston, S.L, and Walsh, K.D., 2000. "Soil-water characteristic curve variability." In: Proceedings of Advances in unsaturated geotechnics, Sessions Geo-Denver 2000: 84-124

Treatment of Low-Grade Nickel Ores By Sulfuric Acid Leaching

F.Hassaine-Sadi, Z. Boukhemikhem
Laboratory of Electrochemistry-Corrosion, Metallurgy and Inorganic Chemical Chemistry Faculty. University of Sciences and Technology, Algiers. (Algeria).

ABSTRACT The treatment of low-grade ores and marginal ores (from an economic standpoint) is primarily hydrometallurgical. In the exploitation of minerals, this process is used for the extraction of gold, silver, the treatment of certain pre-focused or concentrated Sn, W, Cu and includes various stages: preparation mechanical, characterization and selective dissolution of the metal followed by a solid-liquid extraction. In the present work, we were interested in the recovery of the metallic ions Nickel from the low-grade charged effluents, we then applied the solid - liquid extraction of nickel ore. We made one leaching conventional by the sulphuric acid of the nickel ore. The returns on extraction of nickel depend on a large number of strongly interdependent variables such as the Solid / Liquid, the acidity, the time of leaching, the speed of leaching and the temperature were examined. If the sulphuric acid were the reagent of predilection, the choice of the parameters of extraction remained to be determined

1 INTRODUCTION

The treatment of marginal ores and the treatment of solid residues containing metals, we can associate the techniques of solid–liquid extraction or leaching is now well known in the processing of small-content ores. The valorization of the dismissals became an important axis these last years, because of the regulations and instructions that get in place in the world for the protection of the environment It could be easily used to abstract the dissolved fraction of the residues and contribute to their inerting. It only remained the setting of systems of treatment of leaching solutions suitable with solid–liquid extraction from the kinetic, technological and economic point of view. The integration of these main preoccupations, drove us to fix like objective the exam of the systems of extraction of the Nickel [1] by sulphuric acid leaching [2, 3]. The leaching is a hydrometallurgical process the purpose of which is to extract by selective dissolution in a liquid (solution of attack) one or more aqueous solutions (mineral species or organics) of a ore. The study of the chemical variable : ratio S/L, acidity, time of stirring , speed of stirring and temperature permitted us to determine optimum outputs, to understand the reactional process.

2 EXPERIMENTAL

The conduct experiments of the acid leaching of nickel ores were performed as follows:

2.1Aqueous phase

The leaching experiments were conducted batchwise at atmospheric pressure. They are

to put ore in contact with the acid leach solution. The conditions were as follows: The leach solutions were prepared with pure water supplied by the laboratory. Reagent leaching sulfuric acid is chosen whose characteristics e.g: purity: 96%. The acid solutions were prepared from concentrated sulfuric acid (37M) to obtain different concentrations.

2.2 Solid phase

The samples subjected to treatment by acid - leaching concern the class size 50 μm <d <80μm.
The effect of pulp density, while the leaching was evaluated by different ratio solid / liquid and this during a time 8 hours. The leaching is performed in a 150 ml beaker, introducing the ore sample studied, dissolved by an acid solution of H_2SO_4. The device used is equipped with a stirrer speed motor adjustable.

2.3 Characterization of the ore

The quantitative analysis was performed by X-ray fluorescence, which aims to quantify the components of the ore studied.
The results of the quantitative composition of nickel ore are summarized in tables 1 and 2.

Major Elem.	Mg	O	Si	Fe	Cr	Ca	Ni
T(%)	40,2	34,2	19,8	4,3	0,5	0,39	0,24

Table 1. Analysis by X-ray fluorescence of major elements of nickel ore.

Minor Elem.	Al	Mn	P	As	S	Co	Zn
T(%)	0,11	0,69	0,07	0,04	0,03	0,01	0,003

Table 2. Analysis by X-ray fluorescence of minor elements of nickel ore.

The analysis by X-ray fluorescence shows that the major metals present in the nickel ore are Fe, Cr and Ni content of 0.245%.

3 RESULTS AND DISCUSSION

Important parameters of the leaching, have been the subject of study:
-The ratio liquid-solid;
-the stirring time;
-the stirring speed;
-the temperature.

The sulphuric acid leaching of nickel ore was carried out batchwise at atmospheric pressure, by mechanical agitation using a stirrer with adjustable speed. We determined the concentrations of nickel (II) in solutions after leaching sulfuric clarified. The experiences were performed by a spectral technique specific metal trace, which is the atomic absorption spectroscopy (AAS) [5]. Measurements were made at wavelengths of absorption of 232 nm for Ni (II).

Calculation of the efficiency

The leaching percentage is determined by the content of the leach solutions and the residual content in the ore after treatment.

$$R(\%) = \frac{Ni\ leached}{Ni\ leached \quad + Ni\ residual} \times 100$$

3.1 Particle Analysis

The results for the nickel ore are shown in Figure 1 below. Particle size analysis [4] ore has noted on the histograms giving the weight yields of dissolution of nickel for

each size class shows that nickel (II) returned an unevenly in the five size fractions.

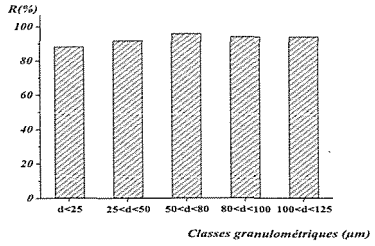

Figure 1. Influence of particle size on the recovery of nickel (II)

We note that the efficiency of dissolution of nickel ore from a peak of around 96% for a grain size between 50 *µm* and 80 *µm*. This class provides a degree of liberalization optimum mineral species containing nickel (II).

3.2 Influence of the ratio liquide-solide

We studied the influence of pulp density on leaching ore nickel (II) by performing a series of experiments where we varied the liquid / solid ratio (volume / mass) for different times of maintaining constant stirring the sulfuric acid concentration 0.5M, the stirring speed is *500 trs/mn.*

Figure 2 below shows the influence of liquid to solid ratio of nickel ore on the leaching percentage

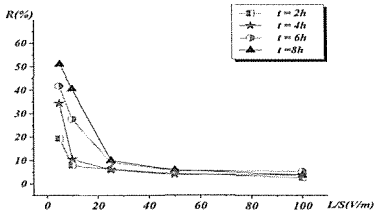

Figure 2. Variation of the leaching percentage of Ni(II) according to the L/S ratio for different leaching time.

50 <d <80 *µm*, $[H_2SO_4]$ = 0.5M, V = *500 trs/mn*, T ambient

Figure 2 shows that the recovery efficiency of nickel (II) increases if the leach solution has a solid mass of larger (L / S ratio decreases) up to a maximum of 51.02% compared to a Liquid-Solid equal to 5 and that for a time of 8 hours. This can be explained by the higher metal loading of the leach solution of Ni (II) for a ratio of 5. It is necessary to maintain the solid content to the maximum possible value allowed for a good stirring and handling of the pulp (suspended solids in the leach solution) [6, 7]. For this, we expressed the amounts of solutions used in the form of the ratio of the amount of solution needed to obtain a given yield to the amount of ore processed: the liquid / solid ratio. This representation has the advantage of allowing access to water consumption, reagents and to establish a material balance.

3.3 Effect of stirring time

We will study the influence of stirring time on the leaching yield of nickel ore, carrying sulfuric leaching both studied minerals whose concentration is fixed at 0.5M H_2SO_4. The stirring speed is kept constant at *500 tr /mn* for a period of 8 hours of leaching.

The result obtained are shown in figure 3 .

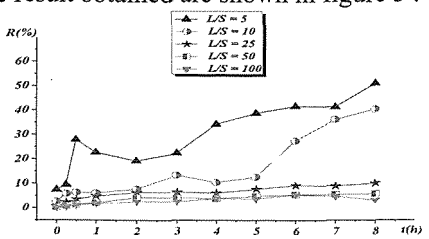

Figure 3. Variation of the recovery efficiency of Ni (II) in function of time for different L/S ratio.
50 < d <80 μm, $[H_2SO_4]$ = *0.5 M*, V= *500 tr /mn,* T ambient.

The figure 3 shows that the recovery efficiency of nickel (II) increases if the leach solution has a greater of the ratio decreases up to a maximum of 51.02% for a liquid/ solid ratio equal to 5 and that during a leaching period of 8 hours.

3.4 Influence of the concentration of sulfuric acid

We conducted the leaching of nickel ore by varying the concentration of sulfuric acid. The liquid-solid ratio is kept constant at 5 with a stirring speed of 500 tr /mn. for a period of 8 hours of leaching. The figure 4 shows the variation of acid concentration on the leaching of nickel ore.

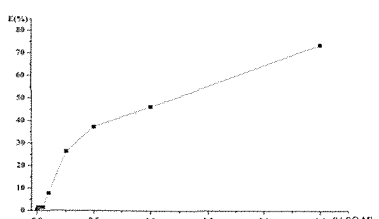

Figure 4. Variation of leaching efficiency of nickel in function of the concentration H_2SO_4.

50 < d <80 μm, L/S =5, Time=8 h, V=500 tr /mn.

We observe that the extraction efficiency of Ni (II) increases when the acid concentration increases. Maximum recovery of nickel (II) is reached or 73% if the leach solution has a sulfuric acid concentration of 2.5 M. This increase is explained by the penetration of protons from acid to the interior of the grains of ore. The leaching efficiency of nickel (II) lower, this can be explained by explained by the microstructure of nickel

3. 5 Influence of the stirring speed

Given the heterogeneous nature of the reaction, the mass transfer (diffusion phenomenon) controls the speed [8]. the leaching process, agitation plays an important role on the reaction rate. For this reason, the leaching of nickel ore (II) is accomplished in beakers equipped with a stirrer with adjustable speed. The figure below shows the influence of stirring speed on the recovery of Ni(II).

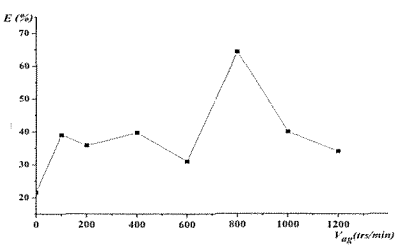

Figure 5. Variation of leaching efficiency of nickel in function of the stirring speed
50< d <80 μm, L/S=5, $[H_2SO_4]$ = *2.5 M,* Time = *8h.*

From figure 5, we note that the leaching behavior of nickel ore is as follows: the recovery percentage of nickel (II) increases when the stirring rate increases. The

extraction of nickel (II) is greater than 65% when performing leaching at a stirring speed equal to 800 tr /mn., this increase is due to acceleration by agitation of the transfer phenomenon of nickel the solid / liquid interface. Beyond this speed the leaching yield of nickel (II) decreases significantly.

3.6.Influence of the temperature

The influence of the temperature [9,10,11] on the leaching of nickel ores was studied. To determine the best performance of the leaching of nickel ore , we varied of the ambient temperature at 80 ° C. The stirring speed is kept constant at *800 trs/mn* for a period of 8 hours of leaching. The result of variation efficiency recovery of nickel in function of leaching temperature is shown in figure 6 below.

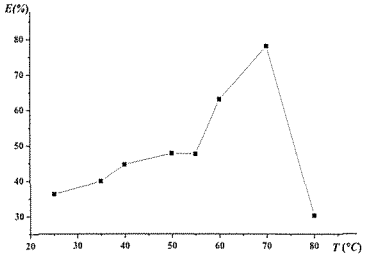

Figure 6. Influence of temperature on the leaching efficiency of nickel (II). 50 <d <80, L / S = 5 , $[H_2SO_4]$ = 2.5M, V= 800 trs/mn, Time = 8h.

We note that the efficiency of nickel ore leaching are low, about 35% to 45% in the temperature range [*35-55°C*]. By increasing the temperature to 70 ° C, the recovery yield of nickel (II) reaches a maximum of about 80%, this result shows the acceleration of the leaching reaction by increasing temperature. Beyond that temperature evaporates the leach solution, which explains the very low efficiency of recovery of Ni (II) in this temperature range.

CONCLUSION

This work is objective was to recover nickel, it has been achieved through the hydrometallurgical treatment. The application of solid-liquid extraction of nickel ore. This technique allows the solution mining of valuable metals contained in ore. Before leaching with sulfuric acid, various steps have been made. First, elemental chemical analysis of nickel ore by X-ray fluorescence shows that the major metals in the ore studied are Fe, Cr and Ni with nickel content of 0.245%. Mechanical preparation was needed before the selective dissolution, particle size and chemical analysis, allowed us to obtain a maximum percentage of 99.89% nickel for a class size 50 μm <d <80 μm this corresponds to the mesh release mineral species containing nickel.
Then, treatment with selective dissolution by sulfuric acid of the two minerals, leaching took place at atmospheric pressure. Determining the parameters of conventional leaching, allowed us to obtain chemical and physical variables giving optimum percentage. We obtain maximum yields for the dissolution of Nickel 51.02% when the liquid / solid ratio equal to 5 for a leaching time of 8 hours.
The recovery of nickel (II) reaches a maximum of 73% when the concentration of sulfuric acid is equal to 2.5 M
The influence of stirring speed was examined, we get a yield of ore leaching of nickel (II), the percentage extraction of nickel (II) is 65%, when performing a leaching a stirring speed equal to 800 trs/mn, this increase is due to acceleration by agitation of the transfer phenomena of the mineral to the solid / liquid interface.

The effect of temperature on the leaching of nickel ore is an important parameter. We obtain leaching yields of 80% for nickel at a temperature of 70 ° C.

The hydrometallurgical treatment presents wide perspectives in the case of the treatments of ores to low content and the recovery of metals from industrial waste. The selective dissolution is a unitarian operation is thus very thrifty in water and in raw materials thanks to the recycling of the reagent.

REFERENCES

[1]: Minister of mining of Cu, Ni, Co and Cr : d'Arak, Tin felki, Tinhihaou and Akofou.Algeria.
[2]: Zhuo Cheng, Guocai Zhu, Yuna Zhao, Hydrometallurgy, 96 (2009) 176–179
[3]: Tao Jiang, Yongbin Yang coll., Hydrometallurgy, 69 (2003) 177–186
[4]: W. MASSA, Crystal structure determination, Springer, Berlin, (2000).
[5]: Atomic Absorption Spectrometry, Technics and instruments in analytical chemistry, Elseviers Scientific publishing company, Amesterdam, Oxford, New York, (1982).
[6]: F.Hassaine-Sadi,Z.Boukhemikhem. Treatment of hydrometallurgical Process. Application of leaching sulphuric manganese ores Minerals to Materials Conference, 15-18, Dec., (2008), Egypt.
[7]: F.Hassaine-Sadi, Z.Boukhemikhem, Desalination 223 (2008) 205-211.
[8]: H.R Bae., R.Barna, J. Mehu , Van der Sloot H., P. Moszkowicz & C. Desnoyers, Proceedings, Houthem St. Gerlach, Netherlands, (1997) 647-660.
[9]: N. Dreulle, journal metallurgy, C.I.T, Aout-Sep, (1982), 701-713.
[10]: E. Büyükakinci, Y.A. Topkaya, Hydrometallurgy 97 (2009) 33–38.
[11]: T.A. Lasheen, M.N. El Hazek, A.S. Helal, Hydrometallurgy, 98 (2009) 314–317.

Copper Cementation with Zinc Powder from Zinc Sulfate Solution

D. Moradkhani
Faculty of Engineering, Zanjan University, Zanjan, Iran.

A. Aghajanloo, B. Sedaghat
R&D Center, Research and Engineering Co. for Non-ferrous Metals (RECo), Zanjan, Iran.

A. Aghajanloo, A.A. Abdollahzadeh
Faculty of Engineering, Kashan University, Kashan, Iran.

ABSTRACT In this research, the cementation of copper from the leaching filtrate of zinc-bearing brass slag has been studied. The influence of several parameters on the course of the reaction such as zinc powder quantity, temperature and reaction time was examined. The optimum copper cementation conditions were found to be zinc powder quantity :30 times of stoichiometric value, time : 45 min, temperature : 60 °C. Using the optimized conditions, the copper removal from zinc sulfate solution was nearly 99%.

1 INTRODUCTION

Cementation is the process of precipitating a metal ion in a solution with a more active metal. This process is widely applied in mineral industry. Generally, iron is used for cementation of copper (Nadkarni and Wadsworth, 1967). Cementation is one of the most effective and economic techniques used for recovering toxic and valuable metals from industrial waste streams (Angelidis et al., 1989; Biswas et al., 1976; Habashi, 1970; Gould et al., 1984; Hendrickson et al., 1984; Zarraa, 1992).cementation is also considered an important reaction in hydrometallurigical processing and in metal winning (Biswas et al., 1976; Habashi, 1970). Dilute copper containing solutions are encountered in chemical industries as waste from pickling and electroplating industries. The rate of cementation reaction of cupric ions in solution with zinc metal has been studied on a number of previous occasions(Zarraa, 1992; Jiang et al., 1986; King et al., 1934; Strickland et al., 1971).

However, during cementation of copper with iron, the recovery of economically valued metals such as zinc from the solution is difficult since the solution contains high iron concentration. Therefore, the recovery of zinc as a side product from zinc rich oxidized copper ores with weak character leaching reactants such as ammonium salts may be important.

Copper cementation has been extensively studied and this subject is still widely investigated (Strickland and Lawson, 1970; MacKinnon and Ingraham, 1970; Rickard and Fuerstenau, 1968; Nadkarni et al., 1967; Stefanowicz et al., 1997; Dönmez et al., 1999; Gamboa et al., 2005; Karavasteva, 2005). Nadkarni et al. (1967) and Nadkarni and Wadsworth (1967) studied the kinetics of copper cementation on iron from cupric sulfate solutions at various concentrations and stirring speeds. The cementation was reported to follow first order kinetics. Depending on the stirring speed precipitated copper formed spongy layer to colloidal mass. The reaction was reported to reach a limiting value and a theoretical model based

on diffusion through a limiting boundary film was proposed.

The aim of this study is to discuss the copper cementation from zinc-bearing brass slag with reference to the effects of variables such as zinc powder quantity, temperature and reaction time from zinc sulfate solution.

2 MATERIALS AND METHODS

2.1 Materials

Brass slag was obtained from Yazd Brass Plant, located at Yazd, Iran. Prior to use in this study, the brass slag sample was dried, ground and homogenized. The chemical analysis was carried out by atomic absorption spectrometer (Perkin-Elmer AA300atomic). The analytic results were given in Table 1. Sulfuric acid was used to adjust the solution pH as required.

Table 1.Chemical analysis of brass slag

Elements	Percent
Zn	66.52
Cu	12.63
Fe	0.09
Pb	0.07
Ca	0.37
Ni	0.0006
Co	0.0003
Mn	0.0006
Cd	0.0012

Cementation of copper was examined encompassing three parameters of zinc powder quantity, Temperature and contact time. For each parameter three levels were chosen as shown in table2.

Table2. Special parameters in cementation of copper

Parameters	Units	Level 1	Level 2	Level 3
Zinc Powder	-	20	25	30
Temperature	°C	30	60	90
Time	min	15	30	45

2.2 Procedure and equipment

Experiments were carried out in a glass beaker of 1 l volume equipped with a mechanical stirrer submerged in a thermostatic bath. Mechanical stirrer (Heidolf RZR 2020) had a controller unit and the bath temperature was controlled using digital controller (within ±0.5 °C). For minimizing aqueous loss when the system is heated, a reflux condenser mounted on top of the cell. After adding 1l of solution to the reaction vessel and setting the temperature at the desired value, a specific weight of zinc powder was added to the reactor for adjusting pH while stirring the content of the reactor at a certain speed. At the end of the reaction period, the contents of the beaker were filtered and the amounts of copper in the filtrate were analyzed.

3 RESULTS AND DISCUSSION

3.1 Leaching of Zinc

Based on the results from leaching experiments in the previous study (Moradkhani et al., 2010), the following optimum leaching conditions were chosen: H2SO4 concentration 200 gr/l , temperature : 25 °C, the liquid to solid ratio (l/s) 10:1, pH=2 and reaction time 15 min. Using the optimized conditions, the zinc recovery was nearly 95%. After completion of the leaching experiment, the leaching filtrate has been studied. The chemical analysis of the achieved filtrate in this stage is shown in Table3.

Table 3. Chemical analysis of the leaching filtrate

Elements					
gr/l	ppm	ppm	ppm	ppm	ppm
Zn	Co	Fe	Ni	Cu	Cd
66.52	0.001	148.2	1.03	158	0.8

3.2 Investigation of effective parameters

Because of present impurity such as copper, the leaching filtrate couldn't send for electrowining. For removing of this impurity, zinc powder was used for cementation of copper.

3.2.1 Effect of Zinc powder

Experiments were carried out to investigate the effect of zinc powder quantity on the cementation of copper. Minimum Cu in solution was 2.25 ppm in Fig.1, in zinc powder of 30 times of stoichiometric value. As can be seen in Fig. 2, maximum copper cementation is in zinc powder of 30 times of stoichiometric value. In this zinc powder quantity, cemented fraction of copper was 98.57%. Therefore, to investigate the other separation parameters, the zinc powder of 30 time of stoichiometric value was chosen for the optimum zinc powder quantity.

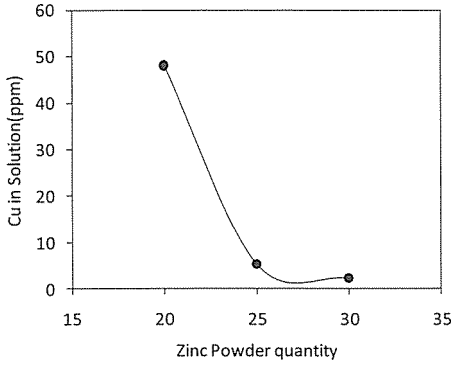

Figure1. Effect of zinc powder quantity on the amount of copper in solution (temperature : 90◦C; time : 15 min; stirrer speed: 250 rpm).

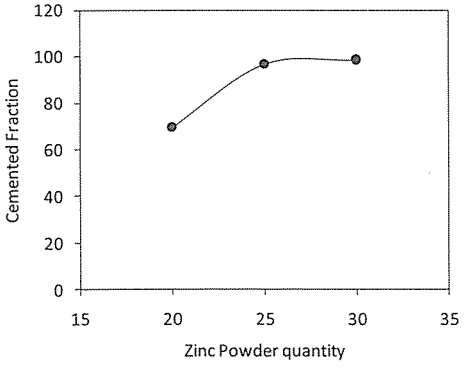

Figure2. Effect of zinc powder quantity on the cementation of copper (temperature : 90°C; time : 15 min; stirrer speed: 250 rpm).

3.2.2 Effect of temperature

Fig.3. shows the effect of temperature on the amount of copper in solution. Minimum amount of copper in solution was achieved at 60 °C that was equal to 1.4 ppm. As seen in Fig.5, increasing the temperature up to 90°C resulted in a decrease in copper cementation. The maximum cementation of Cu was noticed in the temperature of 60 °C that was equal to 99.11%.

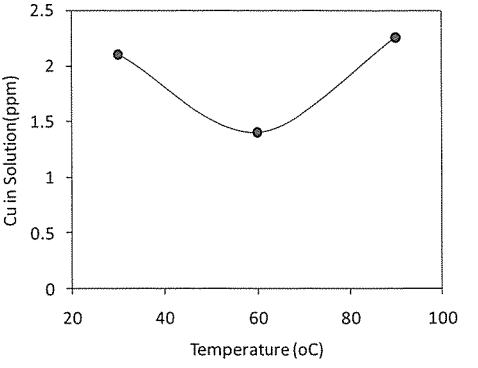

Figure3. Effect of temperature on the amount of copper in solution(Zinc powder quantity: 30 times of stoichiometric value; time : 15 min; stirrer speed: 250 rpm).

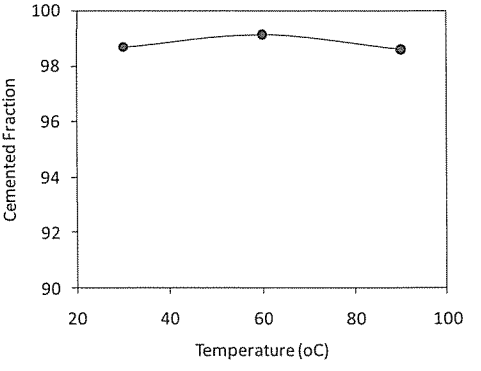

Figure4. Effect of temperature on the cementation of copper(Zinc powder quantity: 30 times of stoichiometric value; time : 15 min; stirrer speed: 250 rpm).

3.2.3 Effect of reaction time

Experiments were carried out to investigate the effect of reaction time on the cementation of copper. Fig.5. shows the minimum amount of copper in solution was achieved at 45 min that was equal to 0 ppm. As can be seen in Fig. 6, the maximum cementation of the copper at reaction time : 45 min was 100%. Therefore, the time : 45 min was chosen for the optimum time.

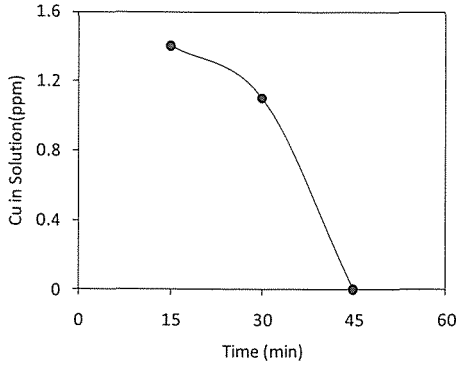

Figure5. Effect of reaction time on the amount of copper in solution(Zinc powder quantity: 30 times of stoichiometric value; temperature : 60°C; stirrer speed: 250 rpm).

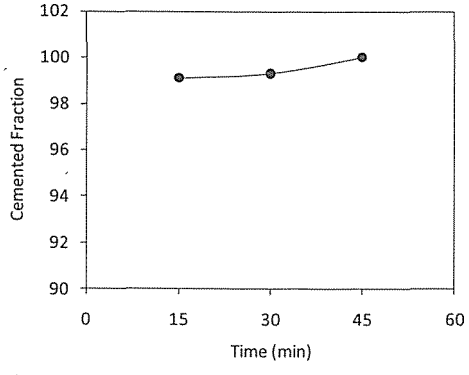

Figure6. Effect of reaction time on the cementation of copper (Zinc powder quantity: 30 times of stoichiometric value; temperature : 60°C; stirrer speed: 250 rpm).

4 CONCLUSION

This study has mainly focused on the cementation of copper from zinc sulfate solution using by zinc powder. The effect of operating conditions such as zinc powder quantity, temperature and time on copper cementation was studied. As a result, the ultimate optimum cementation conditions were found to be t :45 min, T :60 °C, stirring speed=250 rpm and zinc powder quantity: 30 times of stoichiometric value. Under these conditions, cementation of copper was 100%. With remove of copper from leaching solution, this solution is ready for sending to zinc electrowining and production of zinc cathode.

ACKNOWLEDGEMENTS

The authors are thankful to the Research and Engineering Co. for Non-Ferrous Metals for financial and technical support and the permission to publish this paper.

REFERENCES

Angelidis, T., Fytianos, K. and vasilikiotis, G., Resour. Conserv. Recycl., 2(1989) : 131-138.

Biswas, A.K. and davenport, W.G., Extractive Metallurgy of copper. Pergamon, Oxford (1976).

Dönmez, B., Sevim, F., Saraç, H., 1999. A kinetics study of the cementation of copper from sulphate solutions onto rotating aluminumdisc. Hydrometallurgy 53, 145–154.

Gamboa, G.V., Noyola, M.M., Valdivieso, A.L., 2005. The effect of cyanide and lead ions on the cementation rate, stoichiometry and morphology of copper cementation from cyanide solutions with zinc powder. Hydrometallurgy 76, 193–205.

Gould, J.P., Masingale, M.Y. and Miller, B., J. F. and Goebel, L., J. Water Pollut. Control Fed., 3(1984) : 280-286.

Habashi, F., Principles of Extractive Metallurgy. Vol.2, Hydrometallurgy. Gordon and Breach, New York (1970).

Hendrickson, K.J., Benjamin, M.M., Ferguson, J.F. and Goebel,L., J. Water Pollut. Control Fed., 5(1984): 468-473.

Jiang, X. and Ritchie, I.M., A comparative study of different techniques for measuring the rate of the copper(II)/zinc cementation reaction. Hydrometallurgy, 16(1986): 301-314.

Karavasteva, M., 2005. Kinetics and deposit morphology of copper cementation onto zinc, iron and aluminum. Hydrometallurgy 76, 149–152.

King, C.V. and Burger, M.M., J. Electrochem. Soc., 65(1934) : 403-411.

MacKinnon, D.J., Ingraham, T.R., 1970. Kinetics of Cu(II) cementation on a pure aluminum disc in

acidic sulphate solutions. Canadian Metallurgical Quarterly 9, 443–448.

Nadkarni, R.M., Jelden, C.E., Bowles, K.C., Flanders, H.E.,Wadsworth, M.E., 1967. A kinetics study of copper precipitation on iron: part I. Transactions of the Metallurgical Society of AIME 239, 581–585.

Nadkarni, R.M., Wadsworth, M.E., 1967. A kinetics study of copper precipitation on iron: part II. Transactions of the Metallurgical Society of AIME 239, 1066–1074.

Rickard, R.S., Fuerstenau, M.C., 1968. An Electrochemical investigation of copper cementation by iron. Transactions of the Metallurgical Society of AIME 242, 1487–1493.

Stefanowicz, T., Osinska, M., Napieralska-Zagozda, S., 1997. Copper recovery by cementation method. Hydrometallurgy 47, 69–90.

Strickland, P.H. and Lawson, F., Proc. Austral. Min. Metall., 237 (1971): 71-79.

Strickland, P.H., Lawson, F., 1970. Cementation of copper with zinc from dilute aqueous solutions. Proceedings - Australian Institute of Mining Metals 236, 25–33.

Zarraa, M.A., Effect of gas sparginig on the removal of heavy metals ions from industrial wastewater by a cementation technique. Hydrometallurgy, 28 (1992) : 423-433.

Design and Manufacturing of Laboratory Jameson Flotation Cell

D. Moradkhani[1], M. Khoda Karami[1], B. Sedaghat[2,*]

[1] *Faculty of Engineering, Zanjan University, Zanjan, Iran*

[2] *Research and Engineering Company for Non-ferrous Metals (RECo), P.O. Box 45195-1445, Zanjan, Iran*

*(*Corresponding author: beh_sed@yahoo.com)*

ABSTRACT Invention of new developed flotation machines can have some important effects on the mineral processing technology. One of the newest flotation machines is jameson flotation cell, which has different advantages in comparative with other flotation cells such as column cell and mechanical cell. Some of unique features of jameson cell include: higher grade, higher recovery, high production rates in a small space, high availability and low maintenance costs, minimal moving parts, easy and safe maintenance, low operating costs, simple scale up to large machines. Due to the necessity of using this technology in flotation circuits, decided to design and manufacture one laboratory jameson flotation cell adapted with specification of Lead and Zinc flotation and SX-EW application in RECo. The jameson cell height and diameter was estimated to be 25 cm and 16 cm, respectively. The downcomer height and diameter was achieved to be 30 cm and 2.5cm, respectively.

1 INTRODUCTION

1.1 History, advantages and applications

The Jameson Cell combines a novel method for air and slurry contact where a plunging jet naturally entrains air, achieving high voidage, fine bubbles and intimate bubble particle contact. Small bubbles (0.3-0.5 mm) are consistently produced, and intense bubble-particle contact occurs in a short time (6-10 secs) in the downcomer. As a result, the Jameson is a high intensity cell producing fast mineral flotation rates, especially for fines. Since bubble/particle contact occurs in the downcomer, the purpose of the "cell" is simply for bubble-pulp separation, therefore cell volume is very small compared with columns. The high flotation rates resulting from the intense aeration mean a high productivity per surface area, making froth washing attractive to increase concentrate grade. Power consumption is lower than the equivalent mechanical or column flotation cells (the only power is the feed pump, with no blower or compressor) and the orifice and feed pump are the main wearing parts. The fundamentals of Jameson Cell operation have been described by numerous authors, including Clayton, Jameson and Manlapig (1991).

The first production Jameson Cells installed were lead cleaner units at Mt Isa, as described by Jameson and Manlapig (1991). This installation showed a vast difference in flotation kinetic rates between the Jameson Cell, mechanical cells and flotation columns. Additionally the size, footprint and cost of the Jameson Cell installation was much lower

than conventional mechanical cells and flotation columns.

The jameson cell is a high intensity flotation device, which utilizes induced air from atmosphere. It was a joint development between Mount Isa Mine and Prof. Graem Jameson of the University of Newcastle (Jameson 1988). The principle of jameson cell operation have been discussed by numerous authors including Jameson et al (1988), Evans et al (1995), Harbort et al (2002) and Harbort et al (2004). Operation is shown in figure 1. It is proven to generate fine bubbles, in the order of 300 to 500μm, in a high intensity, high shear and compact zone contained in the downcomer. This aerated mixture exits the downcomer into the pulp zone, which is the quiescent mineral and gangue separation zone.

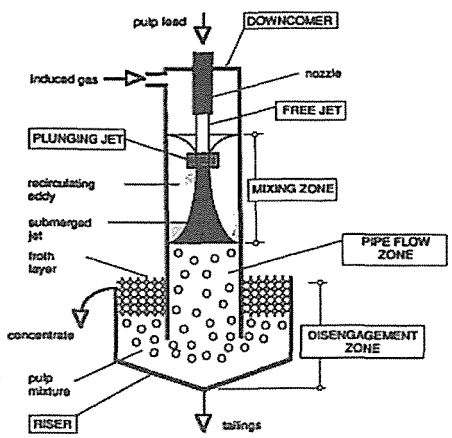

Figure.1. Jameson cell operation

The aim of the present study is to discussed the design and manufacturing of laboratory jameson cell. Two parameters are important in jameson cell that include cell and downcomer. The height and diameter of jameson cell and downcomer were discussed in this article.

2 KEY FACTORS OF JAMESON CELL OPERATION

Key factors of jameson cell operation were included :

- Stability of bubbles in the downcomer
- Separation of bubbles and particles in the cell

Both factors are related to Air to Pulp Ratio (APR) and also shape and form of the tank. Experience in some applications indicated that low APR values would not affect recovery provided the J_g was maintained. Later work at the university of Newcastle by Evans, Atkinson and jameson (1995) subsequently confirmed theoretical aspects. Lower APR values allow tank diameter to be reduced, and also allowed operation with lower frother addition. Reduction of APR from an initial value of 0.3 to 0.2, while maintaining J_g at 1.2 cm/s allowed the diameter required to be reduced from 4.0m to 2.75m. usually low velocity of air and lower air to pulp ratios are ideal and can provide following conditions:

- Generating of fine bubbles
- Lower residence time in downcomer
- More stability of operation
- Maximum contact time between bubbles and particles.

3 IMPORTANT PARTS AND PARAETERS FOR DESIGN OF JAMESON CELL

3.1 Second column of jameson cell

Design of tank of jameson cell is controlled by some parameters like pulp flow rate, superficial gas velocity, air to pulp ratio and particle size of feed. According to size and cross-section, there are three types of jameson cells:

- E series: with rectangular cross-section

- Z series: with circular cross-section
- B series: cells used for flotation of coal.

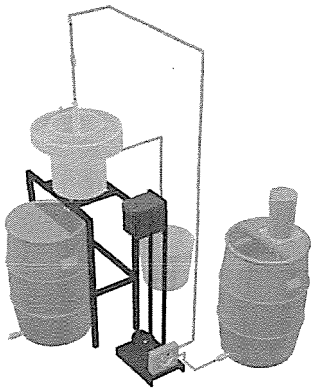

Figure.2. designed jameson cell

For the processing of Angouran Pb/Zn ore deposit and SX-EW circuit in Research & Engineering Co. for Non-ferrous Metals (RECo), Z-cell is selected and designed. One important advantage of Z-cell is the lower dead area inside the jameson tank. In figure.2, designed jameson cell in RECo, is schematically shown.

For designing the second column of jameson cell, effective capacity and height of tank is calculated by using the pulp flow rate and residence time in the tank. To determine the total capacity of tank, volume of froth layer, internal parts of tank and dead area inside the tank should be added to effective volume. Equation 1 is used to calculate the effective volume of second column.

$\tau = V_{eff} / Q_{Pulp}$ equation (1)

V_{eff}: effective volume (m^3)
τ : theoretical residence time (minute)
Q_{Pulp}: pulp flow rate

Different residence times and pulp flow rates have been examined and finally the residence time of 45 seconds and pulp flow rate of 6 liter per minute has been chosen as suitable data. For the residence time of 45 seconds and pulp flow rate of 6 liter per minute, V_{eff} is estimated:

$(45 / 60) = V_{eff} / 6 \rightarrow V_{eff} = 4.5$ liter $= 4500\ cm^3$

If the tank diameter is 16 cm, height of tank would be:

$V = \pi r^2 h \rightarrow 4500 = 3.14 * (8^2) * h \rightarrow h = 22.4$ cm

If the dead area inside the tank is supposed one tenth of effective volume of tank, the final height of the tank will be estimated 24.7 cm (≈25cm). In figure.3, different sections of second column of designed laboratory jameson cell are shown.

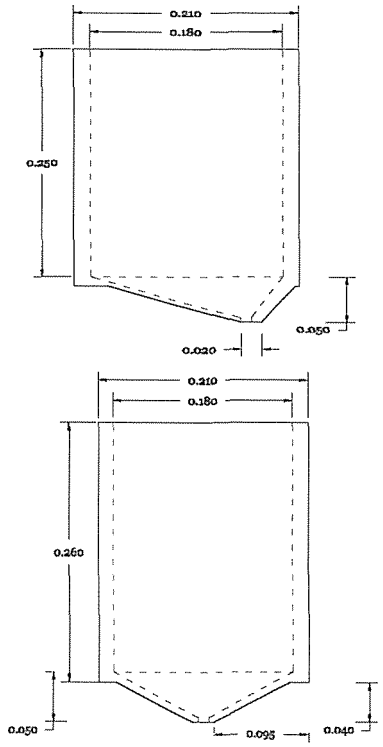

Figure.3. Tank of Jameson cell

3.2 Downcomer of jameson cell

The downcomer is the heart of the jameson cell and its design and operability are keys to the performance of the technology. Although various designs have been used for different applications and improvements introduced, the basic design remained the same for some time. A fresh approach to downcomer design reduces the number of parts by over half and further increases the simplicity of operation of the equipment (Cowburn, J, 2005). This design allows all parts to be located outside the downcomer, with access greately simplified. Additionally, with the location of the slurry lens compared to the orifice plate, the effective length of the downcomer has been increased by 15%, thereby improving residence time in the mixing zone and allowing operation at higher Air-to-Pulp ratios. Laboratory scale test work has shown that the longer length in downcomer allows increased air entrainment for a given vacuum. The interaction of aerated slurry exiting neighbouring downcomers would cause increased pulp phase turbulence that could affect overall cell recovery by causing particles recovered in the downcomer to become detached, so the distance between the downcomers should be designed properly.
The downcomer diameter is considered 0.156 of tank diameter. This number is achieved using standard tank diameters and downcomer sizes.

Downcomer diameter = 0.156*160 = 24.96 mm ≈ 25 mm

Length of the downcomer is designed 30 cm with considering the residence time, amount of mixing zone and length of free jet. In figure.4, dimension of the downcomer of the jameson cell is shown.

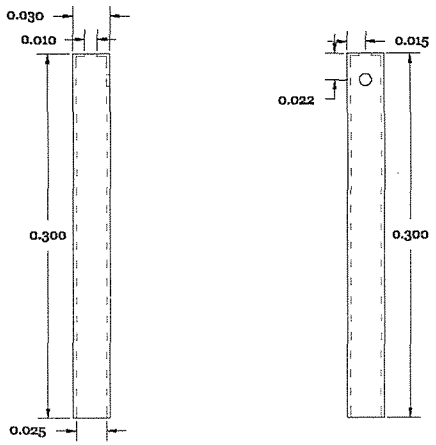

Figure.4. Downcomer of Jameson cell

3.3 Slurry lens

Orifice plate is where the pulp is entered into the downcomer. Additionally it forms the plunging jet and it can control the entraind air. 1999 saw the replacement of the orifice plate with the slurry lens. The key feature of the design is the smooth shallow entry angle (Xstrata Technology). This ensures an optimum flow regime over the ceramic for maximum wear life. The ceramic is backed by polyurethane to cushion the impact of large heavy objects such as bolts. If the ceramic is damaged, the polyurethane serves to keep the ceramic serviceable.

Size of feed particles and blockage of the orifice plate should be considered in design of that. Outlet diameter of slurry lens, used in this design, is considered 3.5 mm. infact the outlet diameter of slurry lens is about 0.14 of downcomer diameter.

Orifice diameter = 25*0.14 = 3.5 mm

Figure.5, shows the designed slurry lens.

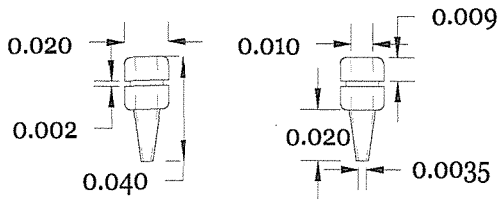

Figure.5. Slurry lens of Jameson cell

3.4 Air to pulp ratio

As mentioned in previous sections, Air-to-Pulp ratio is an important operating parameter which can affect the jameson cell size. Jameson cells generally operate with a volumetric air/feed ratio of 0.3 to 0.9. experiences with large (2-3 diameter) jameson cells indicate that operation at a low air/feed ratio does not appear to detract from metallurgical performance providing the superficial gas velocity J_g is maintained above a certain minimum value. operation at lower air/feed ratios has a stabilizing effect producing a more uniform and finer bubble size. A significant advantage of operation at lower air/feed ratios is that lower concentration of frother are required.

4 CONCLUSION

Due to great success of Jameson cell in flotation and SX-EW circuits, RECo decided to design and manufacture a Jameson cell to be utilized in SX-EW circuit of a zinc plant in Zanjan. Important items for design include: tank, downcomer, slurry lens and pulp flow rate. With the residence time of 45 seconds and pulp flow rate of 6 liter per minute, the diameter of Plexiglas tank is calculated by 160mm. Also a 25 mm outlet diameter Plexiglas downcomer, fitted with a 3.5 mm outlet diameter slurry lens, is designed considering the residence time and air to pulp ratio. Other designed items include: A 45 liter capacity feed sump with stirrer, A 32 liter capacity underflow tank, A 15 liter capacity overflow tank, A variable speed and centrifugal pump, A flow meter measuring the feed stream and An air flow rotameter. It is important to mention that the operational parameters should be optimized considering the tests have been done to achieve an ideal result from jameson cell.

ACKNOWLEDGEMENTS

This research was made possible by funds received from the Research & Engineering Company for Non-ferrous Metals.

REFERENCES

Clayton, R., Jameson, G.J., Manlapig, E.V., 1991, The Development and Application of the Jameson Cell; Minerals Engineering ,July-Nov 1991

Cowburn, J, Stone, R, Bourke, S , Hill, B, 2005. Design Developments Of The Jameson Cell Centenary of flotation 2005 Symposium, Brisbane. June 5-9 2005.

Evans, G, M, Atkinson, B, W, Jameson G, J, 1995. The Jameson cell. Flotation Sci. Eng. (Ed: K A Matis), pp331-363 (Marcel Dekker: New York).

Harbort, G.J., Cowburn, J.A., Manlapig, E.V., 2004. Recovery interactions between the froth zone, pulp zone and downcomer within a Jameson cell. In: Membrey, W. (Ed.), Proc. 10th Australian Coal Preparation Conference, Pokolbin, 17th–21st October 2004. Australian Coal Preparation Society Limited, pp. 91–101.

Harbort, G.J, Manlapig, E.V., DeBono, S.K, 2002. A discussion of particle collection within the Jameson Cell downcomer. Trans IMM (Section C: Mineral Process. Extr. Metall), 111 / Proc. Australas. Inst. Min. Metall., 307, January/April, 2002, ppC1-C10.

Jameson, G.J. and Manlapig, E.V., 1991 - Flotation cell design - experiences with the Jameson Cell, 5th Aus IMM Extractive Metallurgy Conference.

Jameson, G.J, 1988. A new concept in flotation column design. Column "88 proceedings of an International Symposium on Column Flotation, SME, Phoenix Arizona, 1988. Sastry, KV, ed. pp 281-289.

Determination of the Optimum Conditions for the Separation of Co and Mn Using by N-N Reagent

D. Moradkhani
Faculty of Engineering, Zanjan University, Zanjan, Iran.

E. Ataei, B. Sedaghat, D. Behnian
R&D Center, Research and Engineering Co. for Non-ferrous Metals (RECo), Zanjan, Iran.

ABSTRACT The orthogonal array design has been used to determine the optimum conditions for the separation of cobalt and manganese from a leaching of purification filter cake and hence to achieve the highest manganese recovery and the best robustness of the quantitation from the least number of trials in a laboratory scale. separation was performed using by N-N reagent . The orthogonal array L9 (3^4) that comprises four parameters at three levels was chosen. The parameters and their levels were as: N-N quantity : 1, 1.25 and 1.5 times of stoichiometric quantity of cobalt; time : 15, 30 and 45 min; temperature : 40, 60 and 80 °C; and pH: 1, 1.5 and 2. The ultimate optimum extraction conditions were found to be 1.5 time of stoichiometric quantity of cobalt, Temperature :40 °C , time : 30 min and pH=1.5. Under these conditions, recovery for manganese and cobalt were 98.35% and 9.81%, respectively.

1 INTRODUCTION

In metal extraction processes, large amounts of various solid wastes including flotation tailings, slags, slimes and flue dusts etc. are generated. These wastes become activated due to the process applied such as grinding, leaching, roasting, smelting, quenching etc. Exposure of these wastes to atmospheric oxygen and moisture results in solubilization of toxic metals which may seriously affect the water quality and biological life in surface waters. The potential release of toxic heavy metals from such by-products and waste materials to the surface and ground water are of particular concern (Altundogan et al., 1992, Tumen, 1988, Tumen et al., 1991, Tumen et al, 1992).

In the zinc plant located in Zanjan, Iran, a leach-electrolysis process is practiced for zinc production. In this process, number of filter cakes is generated daily as by products. These wastes are stored for valuable elements' recovery in the future and dumped in open stockpiles where they may cause heavy metal pollution problems. In these plants three types of wastes were produced: leaching filter cake, Cobalt purification filter cake and Ni-Cd purification filter cake. All of the filter cakes have high levels of heavy metals. (Hakami, 2005).

The aim of the present study is to determine the optimum working conditions which provided maximum separation for manganese and cobalt from a reduction leaching of purification filter cake with N-N reagent by using the Taguchi method and then adjusting the experimental conditions such as N-N quantity, time, pH and temperature.

2 EXPERIMENTAL

2.1 Materials

Cobalt filter cake for the leaching study was obtained from Sane Rooy Co., Zanjan, Iran.

After drying, the filter cake was ground and homogenized. The chemical analysis was carried out by a Perkin-Elmer AA300 model atomic absorption spectrophotometer. The chemical analysis of the filtercake is given in Table 1.

Table 1. Chemical analysis of the Co purification filtercake

Elements	Wt.%
Co	1.19
Mn	9.10
Zn	14.66
Ni	0.07
Cd	0.35
Ca	6.64

Based on the results from washing experiments in the previous study for zinc removal, the following optimum washing conditions were chosen: H2SO4 concentration 200 gr/l , 25 °C, the liquid to solid ratio (l/s) 8:1, pH=1 and reaction time 120 min(Eivazi et al., 2008). Using the optimized conditions, the zinc recovery was nearly 96%. After completion of the washing experiment, the washing residue was filtered, washed, dried and weighed. Based on the results from leaching experiments in the previous study for leaching of cobalt and manganese, the following optimum leaching conditions were chosen: sulphuric acid concentration: 30 g/L, amount of hydrogen per oxide: 3 (%v/v), pulp density: 100 g/L, leaching time: 45 min and ambient temperature. Base on the optimum conditions, more than 90% of Co, Mn and Zn could be extracted (Eivazi et al., 2009). The analytic results of the achieved filtrate is given in Table 2.

Table 2. Chemical analysis of the filtrate

Content[g/l]			
Co	Mn	Zn	Cd
1.18	8.58	1.45	0.035

2.2 Procedure and equipment

Experiments were carried out in a glass beaker of 2 l volume equipped with a mechanical stirrer submerged in a thermostatic bath. Mechanical stirrer (Heidolf RZR 2020) had a controller unit and the bath temperature was controlled using digital controller (within ±0.5 °C). For minimizing aqueous loss when the system is heated, a reflux condenser mounted on top of the cell. After adding 1l of acid with a known concentration to the reaction vessel and setting the temperature at the desired value, a known weight of sample was added to the reactor while stirring the content of the reactor at a certain speed. At the end of the reaction period, the contents of the beaker were filtered and amounts of manganese and cobalt in the filtrate were analyzed.

2.3 Making of N-N reagent

Three materials include C10H9O, NaNO2 and NaOH were mixed for making of N-N reagent .The ratio of C10H9O, NaNO2 and NaOH in weight has been 1:1:1. The mention material are mixed with cold water and heated to 70°C with agitation for two hours.

2.4 Taguchi Method

The taguchi method, introduced by Dr. Genichi Taguchi, contains system design, parameter design and tolerance design procedure to gain a robust process and result for best product quality. The parameter design of this method applies orthogonal arrays, providing and alternative to standard factorial design, to minimize the time and cost of experiments in analyzing all the factors and uses the signal-to-noise (S/N) ratio to analyze the experimental data and find the optimal parameter combination. In application of taguchi design three steps should be considered:

1. Planning experiment
   a. Set the effective and noise factors
   b. Set the levels of each factors
   c. Choose an adequate orthogonal array
2. Conducting experiments
3. Analyzing the results

In this research to separation of cobalt and manganese, taguchi technique was used. Primitive rough tests indicate that four parameters including: pH, Temperature, N-N quantity and time are effective. Thus, to investigate the effects of above mentioned parameters in separation of cobalt and manganese, three levels of them were selected. Recovery of Co and Mn were selected as responses of this process. Orthogonal array L9, which clarifies 4 parameters at 3 levels, was chosen to carry out the tests. Table 3 shows the experimental procedure.

Table 3. Experimental procedure

No.	pH	Temperature	Time	N-N reagent
1	1	40	30	1
2	1	60	45	1.25
3	1	80	60	1.5
4	1.5	40	45	1.5
5	1.5	60	60	1
6	1.5	80	30	1.25
7	2	40	60	1.25
8	2	60	30	1.5
9	2	80	45	1

3 RESULTS AND DISCUSSION

Finding the optimized conditions for separation of Cobalt and Manganese and determination of effective factors in this process were the intended aims of this research. To gain them, the four level L9 (3^4) orthogonal table used and two responses, included recovery of Mn and Co, applied. The collected data were analyzed by DX7 software to evaluate the influence of each parameter on the process. Effects of each factor on the whole process will be elaborated on the following sections.

3.1 Effect of pH

Figures 1-2, illustrates the effect of pH on the separation of Mn and Co. Three pH of 1, 1.5 and 2 were evaluated. Based on what Figure 2. indicates lower pH have higher effects on the recovery of Mn. But increasing of this parameter from 1 to 2 on the Figure 1, causes such a striking improvement in the cobalt recovery.

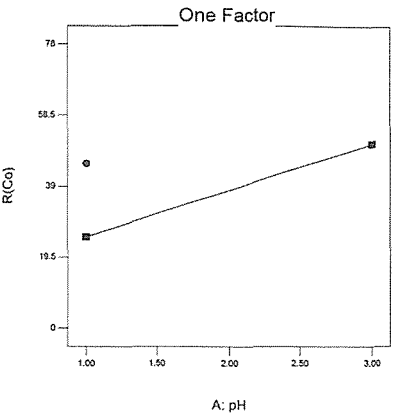

Figure 1. The effect of pH on the recovery of cobalt (time : 45 min, temperature : 60 °C and N-N amount : 1.25 times of stoichiometric quantity of cobalt)

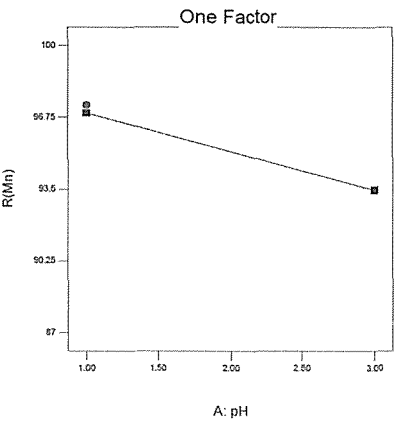

Figure 2. The effect of pH on the recovery of manganese (time : 45 min, temperature : 60 °C and N-N amount : 1.25 times of stoichiometric quantity of cobalt)

3.2 Effect of temperature

In this research 3 levels of temperature were investigated. The temperature effect was examined in the range of 40–80 ◦C. As seen in Figures 3-4, increasing the temperature up to 80°C did not make a significant change in cobalt and manganese recovery. Therefore, this parameter did not have effect in Co and Mn recovery.

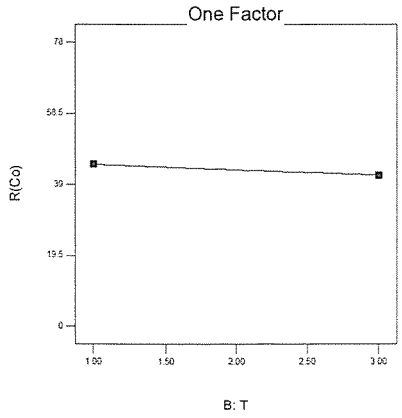

Figure 3. The effect of temperature on the recovery of cobalt (time : 45 min, pH : 1.5 and N-N amount : 1.25 times of stoichiometric quantity of cobalt)

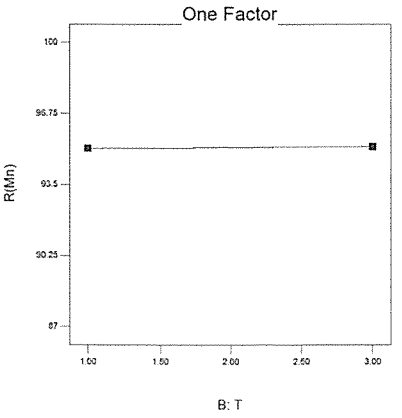

Figure 4. The effect of temperature on the recovery of manganese (time : 45 min, pH : 1.5 °C and N-amount : 1.25 times of stoichiometric quantity of cobalt)

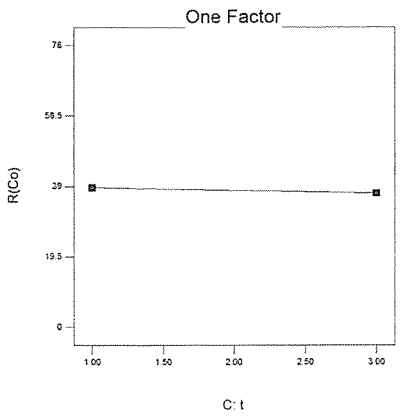

Figure 5. The effect of time on the recovery of cobalt (pH : 1.5, temperature : 60 °C and N-N amount : 1.25 times of stoichiometric quantity of cobalt)

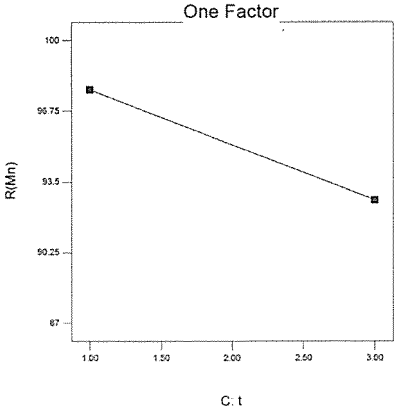

Figure 6. The effect of time on the recovery of manganese (pH : 1.5, temperature : 60 °C and N-N amount : 1.25 times of stoichiometric quantity of cobalt)

3.3 Effect of Time

The main effects of time on the process shows on the Figures 5-6. Increasing of the reaction time from 30 to 60 minutes did not make a change in the recovery of Co. But increase of the time from level 1 to 3 causes a significant decrease on the manganese recovery.

3.4 Effect of N-N reagent

The effect of N-N reagent on the separation of Mn and Co are shown in Figures 7-8. According to experimental results presented in Figure 7, it was found that cobalt recovery decreased from level 1 to 3. As shown in Figure 8, results indicate that the recovery of manganese decrease with increasing N-N

quantity from 1 to 1.5 times of stoichiometric amounts of cobalt.

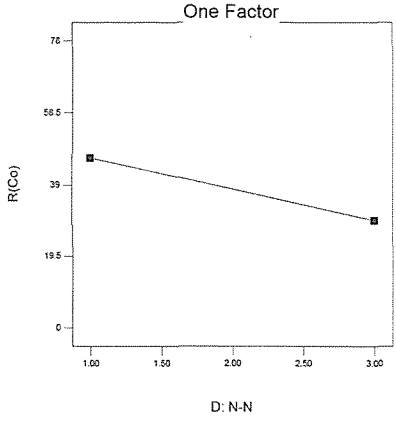

Figure 7. The effect of N-N reagent on the recovery of cobalt (time : 45 min, temperature : 60 °C and pH : 1.5)

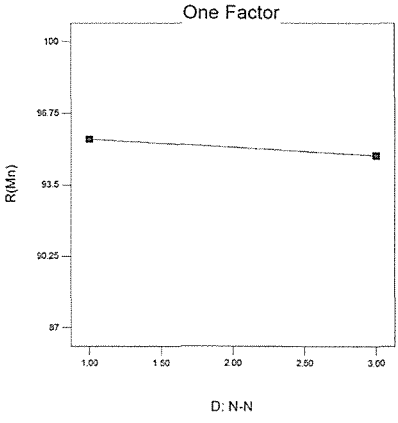

Figure 8. The effect of N-N reagent on the recovery of manganese (time : 45 min, temperature : 60 °C and pH : 1.5)

3.5 Optimum Conditions

Finally, using these findings about influential parameters on the process, optimum working conditions could be predicted. The proposed optimum conditions are: pH on level two (1.5), N-N reagent on level 3 (1.5 times of stoichiometric amounts),temperature on level 1 (40 °C), and time on level one (30 min). The predicted recoveries for Mn and Co are 99.12 and 8.68%, respectively using by DX7. To investigate the accessibility of this result, a test on the optimum conditions was done. The experimental recoveries for Co and Mn are 98.35% and 9.81%, respectively.

4 CONCLUSION

The effect of operating conditions such as N-N quantity, time, pH and temperature on performance of manganese and cobalt separation was studied with the Taguchi method using an L9 (34) orthogonal array. As a result, the ultimate optimum conditions were found to be N-N quantity : 1.5 time of stoichiometric quantity of cobalt, temperature : 40 °C, pH : 1.5 and time : 30 min. Under these conditions, recovery for manganese and cobalt were 9.81% and 98.35%, respectively. The most effective parameter for maximum dissolution of manganese and minimum dissolution of cobalt is found to be pH and N-N quantity.

ACKNOWLEDGEMENTS

The authors are thankful to the Research and Engineering Co. for Non-Ferrous Metals for financial and technical support and the permission to publish this paper.

REFERENCES

Altundogan, H.S., Ozer, A., Tumen, F., 1992, Bakir Curuflarinin Asidik Ortamlardaki Agir Metal Cozunurlukleri, VIII. Kimya ve Kimya Muhendisligi Sempozyumu, 7-11 Eylul 1992. Istanbul, Vol IV, 195-200.

Eivazi, A. R. H., Alamdari, E. K., Moradkhani, D., 2008a, Dissolution kinetics of zinc from zinc plant residue. In: Young, C.A., (Eds.), Hydrometallurgy 2008, Proceedings of the 6th International Symposium. The Minerals, Metals and Materials Society, Vancouver, Canada, pp. 196-200.

Eivazi, A. R. H., Alamdari, E. K., Moradkhani, D., 2008a. Dissolution kinetics of zinc from zinc plant residue. In: Young, C.A., (Eds.), Hydrometallurgy 2008, Proceedings of the 6th International Symposium. The Minerals, Metals and Materials Society, Vancouver, Canada, pp. 196-200.

Hakami, Alireza, 2005, Report of Zinc production in R&D center, IZMDC, Report No.224, 1-10.

Tumen, F., 1988, A Study on the Solubility of Lignite Fly Ash, Doga TU J. Chem, 12(1), 88-96.

Tumen, F., Bildik, M., Boybay, M., Cici, M., Solmaz, B., 1992, Ergani Bakir Isletmesi Kati Atiklarinin Kirlilik Potansiyeli, Doga Tr. J. of Engineering and Environmental Sciences, 16: 43-53.

Tumen, F., Boybay, M., Solmaz, B., Cici, M., Bildik, M., 1991, Elazig Ferrokrom Fabrikasi ve Keban Simli-Kursun Isletmesi Kati Atiklarinin Kirlilik Potansiyeli, Doga Tr. J. of Engineering and Environmental Sciences, 15:464-485, 1991.

Factors Affecting Leaching Behavior of Copper Oxide Ore of Chodarchaei Mine

D. Moradkhani
Faculty of Engineering, Zanjan University, Zanjan, Iran.

B. Sedaghat, A. Rashtchi
R&D Center, Research and Engineering Co. for Non-ferrous Metals (RECo), Zanjan, Iran.

A.Ghaffari
Mineral Processing Research Group, Academic Center for Education, Culture and Research(ACECR) on Tarbiat Modares, Tehran, Iran.

ABSTRACT The determination of the optimum condition of leaching parameters is one of the main concerns in the design of leaching process. In this research, oxide ore samples were obtained from Chodarchaei copper mine. The dissolution of CuO in H2SO4 solutions was investigated in a batch reactor employing parameters expected to affect the dissolution rate of copper such as pH, solid/liquid ratio, temperature and time. It was found that 95.2% of copper was dissolved after 30 min with sulfuric acid concentration of 200 gr/l, temperature : 25 °C and l/s = 8.

1 INTRODUCTION

Copper is used in vast variety of products in domestic and industrial domains as thermal and electrical conductor and as a constituent of various metal alloys. Copper is also used in chemical industry as catalyst in the oxidative conversion of ethyl acetate in water (Armbruster et al., 2001), hydrogen production by partial oxidation of methanol (Wang et al., 2003), liquid-phase oxidation of benzene to phenol (Miyahara et al., 2001), carbon monoxide oxidation (Taylor et al., 1999) and in removal of NOx and SOx from flue gases (Macken et al., 2000). After deactivation, the components of the catalyst can be reused as secondary sources of metals. This is considered as more beneficial from environmental and economical point of views than landfill depositing. Leaching processes of metallic copper or ores containing copper in the divalent state have been the subject of many research works in recent years (Kruesi et al., 1982, Oishi et al., 2007, Forward et al., 1985, Ata et al., 2001).

Copper oxide minerals containing copper in the divalent state, such as azurite [Cu3(OH)2(CO3)2],malachite[Cu2(OH)2CO 3], tenorite (CuO), and chrysocolla (CuSiO3.2H2O), are completely soluble either in acidic or alkaline medium at room temperature (Barlett, 1992 and Ata et al., 2001,Oudenne and Olson, 1983). It has been very well known that sulfuric acid is the most usual leaching agent for oxidized copper ore, and depending on the nature of ore, acid consumption ranges from 0.4 to 0.7 ton H2SO4 per ton of copper recovered. The kinetics and the chemistry of copper oxide ore leaching in sulfuric acid (Habashi, 1970) and extraction of copper through solvent extraction (SX) have been investigated by several researchers such as: Hopkins, 1994, Amores et al., 1997, Navarro and Alguacil, 1999 and Bingöl and Canbazoğlu, 2004.
The determination of the optimum condition of leaching with sulfuric acid parameters is one of the main concerns in the design of leaching process. Parameters such as pH,

acid concentration, solid/liquid ratio, temperature and time have great effect on the leaching process which should be optimized. The above mentioned parameters are dependent on the type of minerals, mineral impurities which can be optimized based on leaching experiment for the specific mine (Wadsworth and Miller , 1979).
The aim of this study is to investigate and discuss the leaching behavior of oxide copper minerals in Chodarchaei copper mine with special attention to the effects of pH, solid/liquid ratio, temperature and time on leachability of copper.

2 MATERIALS AND METHODS

2.1 Materials and Reagents

The copper oxide ore used in this research was collected from the Chodarchaei mine, northeast of Zanjan. The chemical analysis was carried out by AAS (Perkin-Elmer AA300atomic). Table 1 summarizes the chemical composition of the copper ore used in the experiments.

Table 1. Chemical composition of sample used in the experiment (Wt.%)

Component	Wt.(%)
Cu	3.01
Pb	0.25
Fe	2.73
Mn	0.073
Co	0.001
Ni	0.0025
Cd	0.0024
Zn	0.24

Leaching of copper oxide ore were examined in which four parameters of pH, temperature, liquid/solid ratio and contact time were studied. For each parameter fore levels were chosen as shown in Table 2.

Table2. Special parameters in leaching treatment

Parameters	Units	Level 1	Level 2	Level 3	Level 4
pH	-	1	1.5	2	2.5
S/L	-	1/4	1/6	1/8	1/10
Temperature	°C	25	40	60	80
time	min	15	30	45	60

2.2 Experimental Method

Experiments were carried out in a 2 L Pyrex beaker set up in a water bath and equipped with a mechanical stirrer. The bath temperature was digitally controlled within ±0.5 °C. When the solution temperature reached the desired value, the copper ore was added to the solution with an initial volume of 1 L. This was marked as the beginning of the experiment. The copper ore in all cases was constant. After the end of test, the sample was immediately vacuum filtered, then diluted and analyzed for copper. Concentration of copper was calculated with respect to correction of volume (Choo et al., 2006). The H2SO4 concentration in all cases was 200 g/l. Sulfuric acid solution were used to adjust the solution pH. The pH was measured using a WTW portable pH meter with a suitable electrode for aqueous solution with automatic temperature compensation.

3 RESULTS AND DISCUSSION

3.1 Effect of pH

Experiments were carried out to investigate the effect of pH on the copper ore dissolution. As can be seen in Fig. 1, at pH of 2.5, 2, 1.5 and 1 extracted copper after 30 min were 53.71, 65.01, 74.79 and 87.97%, respectively. The lowest copper recovery is in pH of 2.5. Fig. 1 shows that pH has a significant effect on the acceleration of copper dissolution with H2SO4. Therefore, to investigate the other leaching parameters, the pH =1 was chosen for the leaching pH.

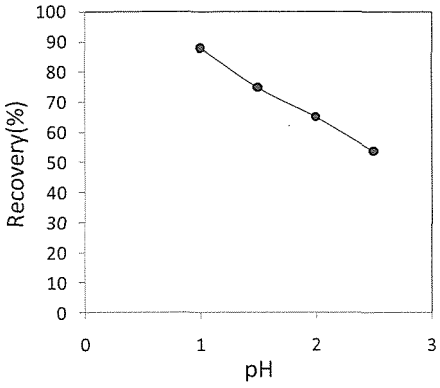

Figure1. Effect of pH on the copper recovery (solid/liquid ratio: 1/6; temperature: 25◦C; time: 30 min; stirrer speed: 400 rpm).

3.2 Effect of solid/liquid ratio

The effect of solid/liquid ratio on the dissolution of copper ore was investigated in the range of 1/4–1/10. The results are presented in Fig. 2. As can be seen in Fig. 2, the copper recovery increased slightly with decrease in the amount of solid after 30 min. The maximum copper recovery at solid/liquid ratios equal to 1/4, 1/6, 1/8 and 1/10 after 30 min were 90.35, 87.97, 95.20 and 95.02%, respectively.

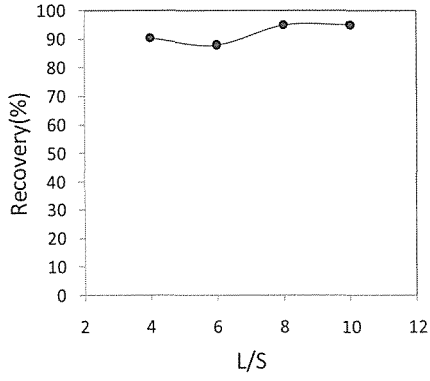

Figure2. Effect of liquid/ solid ratio on the copper recovery(pH:1; temperature: 25◦C; time: 30 min; stirrer speed: 400 rpm).

3.3 Effect of temperature

Experiments were carried out to investigate the effect of temperature on the copper ore dissolution. As can be seen in Fig. 3, increasing the temperature up to 80°C did not make a significant change in copper recovery after 30 min. The maximum copper recovery at temperature equal to 25, 40, 60 and 80 °C after 30 min were 95.20, 91.30, 94.36 and 92.13 %, respectively. Therefore, to investigate the other leaching parameters, the T=25°C was chosen for the leaching temperature.

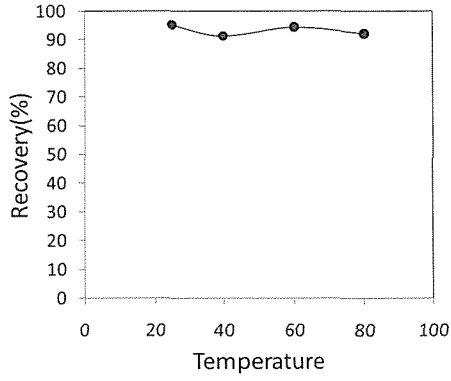

Figure3. Effect of temperature on the recovery of copper (solid/liquid ratio: 1/8;time: 30 min; stirrer speed: 400 rpm; pH: 1).

3.4 Effect of contact time

The effect of contact time on the rate of copper dissolution from CuO when leached in the H2SO4 solution was investigated over a time range of 15-60 min at acid concentration of 200 gr/l, temperature : 25 °C, stirring speed of 400rpm and l/s = 8. As shown in Fig.4, results indicate that the recovery of copper did not make a significant change with increasing leaching time to 60 min. Therefore, the t=30 min was chosen for the best leaching time.

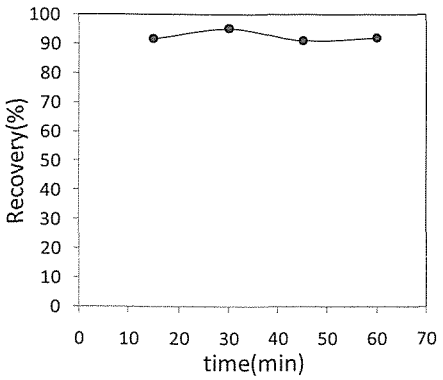

Figure4. Effect of leaching time on the copper recovery (pH:1; temperature: 25°C; solid/liquid ratio: 1/8; stirrer speed: 400 rpm).

4 CONCLUSION

In this research, the copper oxide ore used was obtained from the Chodarchaei mine, Iran. Experiments were carried out to investigate the effects of pH, solid/liquid ratio, temperature and leaching time on copper recovery from copper ore. A maximum recovery of copper was obtained in following condition: pH : 1, solid/liquid ratio : 1/8, temperature : 25°C and leaching time : 30 min.

ACKNOWLEDGEMENTS

The authors are thankful to the Research and Engineering Co. for Non-Ferrous Metals for financial and technical support and the permission to publish this paper.

REFERENCES

Armbruster, U., Martin, A., Krepel, A., Hydrolysis and oxidative decomposition of ethyl acetate in sub and super-critical water, Appl. Catal. B: Environ. 31 (2001) 263–273.

Ata, S. Çolak, Z. and Çopur M., Determination of the optimum conditions for leaching of malachite ore in H2SO4 solutions, Chemical Engineering & Technology 24 (2001) (4), pp. 409–413.

Barlett, R. W., 1992, Solution mining, leaching and fluid recovery of materials vol. 5, Gordon and Breach Science Publishers, Philadelphia (1992), pp. 76–107.

Bingöl and Canbazoğlu, 2004, Dissolution kinetics of malachite in sulphuric acid, Hydrometallurgy 72 (2004), pp. 159–165.

Choo, W.L., M.I. Jeffrey, and S.G. Robertson. Analysis of leaching and cementation reaction kinetics: Correcting for volume changes in laboratory studies, Hydrometallurgy 82 (2006) 110.

Ekmekyapar, A. and Oya, R. 2003 A. Ekmekyapar and R. Oya, Dissolution kinetics of an oxidized copper ore in ammonium chloride solution, Chemical and Biochemical Engineering Quarterly 17 (2003) (4), pp. 261–266

Forward, F.A., Peters, A., Leaching, vol. 2, SME Mineral Processing Handbook, SeeleyW. Mudd Series, New York, 1985, pp. 13.12–13.6.

Habashi F., 1970, Principles of Extractive Metallurgy vol. 1, Gordon and Breach Science Publishers, New York (1970).

Habashi F., 1983 Trends in the hydrometallurgical treatment of copper oxides ores, Arab Mining Journal 4 (1983) (3), pp. 46–52.

Hopkins, W.R., 1994, SX/EW, a mature but expanding technology, Mining Magazine (1994), pp. 256–265.

Kruesi, P.R., Frahm, V.H., Process for the recovery of copper from its ores, US Patent No. 4,324,582 (1982).

Macken, C., Hodnett, B.K., Paparatto, G., Testing of the CuO/Al2O3 Catalyst–Sorbent in extended operation for the simultaneous removal of NOx and SO2 from flue gases, Ind. Eng. Chem. Res. 39 (2000) 3868–3874.

Miyahara, T., Kanzaki, H., Hamadab, R., Kuroiwa, S., Nishiyama, S., Tsuruya, S., Liquid-phase oxidation of benzene to phenol by CuO-Al2O3 catalysts prepared by co-precipitation method, J. Mol. Catal. A: Chem. 176 (2001) 141–150.

Navarro P. and Alguacil F.J., 1999, Extraction of copper from sulphate solutions by LIX 864 in escaid100, technical note, Minerals Engineering 12 (1999) (3), pp. 323–327.

Oishi, T., Koyama, K., Alam, S., Tanaka, M., Lee, J.C., Recovery of high purity copper cathode from printed circuit boards using ammoniacal sulfate or chloride solutions, Hydrometallurgy 89 (2007) 82–88.

Oudenne P.D., and Olson F. A., 1983, Leaching kinetics of malachite in ammonium carbonate solutions, Metallurgical Transactions 14 (1983), pp. 33–40.

Taylor, S.H., Hutchings, G.J., Mirzaei, A.A., Copper zinc oxide catalysts for ambient temperature carbon monoxide oxidation, Chem. Commun. (1999) 1373–1374.

Wadsworth M.E. and Miller J. D., 1979, Rate processes of extractive metallurgy In: H.Y. Sohn and M.E. Wadsworth, Editors,

Hydrometallurgical processes (section 3), Plenum Press, New York (1979), pp. 133–153.

Wang, Z. , Xi, J., Wang, W., Lu, G., Selective production of hydrogen by partial oxidation of methanol over Cu/Cr catalysts, J. Mol. Catal. A: Chem. 191 (2003) 123–134.

Optimization of Lead Flotation of Angouran Low Grade Sample by DX7 Software

D. Moradkhani, M. Rajaie
Faculty of Engineering, Zanjan University, Zanjan, Iran.

B. Sedaghat
R&D Center, Research and Engineering Co. for Non-ferrous Metals (RECo), Zanjan, Iran.

ABSTRACT The aim of this study is to optimize lead recovery and grade response in flotation with special attention to the effects of pH, collector dose rate, activator addition rate and time of concentrate collection. The test was optimized with Design Expert7 software. The orthogonal array L9 (3^4) comprising four parameters at three levels was chosen. The parameters and their levels were as: pH : 8, 9, and 10; collector dose rate : 0.3, 0.6 and 0.9 gram; activator addition rate : 1, 2 and 3 gram and time of concentrate collection : 3, 4 and 5 minutes. The ultimate optimum conditions were found to be pH=10; collector=0.9 gram; activator=1 gram and time=5 minutes. Using the optimized conditions, the lead recovery and grade were nearly 68.13% and 20.73%, respectively at rougher stage. It was observed that the recovery of lead increased with increasing collector addition rate, time and pH and decreasing activator addition rate.

1 INTRODUCTION

Flotation is a process in which valuable minerals are separated from gangue minerals (Leja, 1982). It is a complex combination of various physical principles, such as surface chemistry, colloid chemistry, crystallography and physics. The exact manner in which these interact is still not well understood. Various factors influence the performance of a flotation unit, amongst these are the bubble size (Gorain et al., 1995), the stator and rotor configuration (Forrester et al., 1998), the type and quantity of chemicals added (Evans et al., 1995; Ralston et al., 2001) and residence time(Rubio et al., 2002).

Experimental design methods and factorial methodologies are widely used for modeling process parameters, especially in chemical processes. It has, however, not been widely applied to mineral processing systems. Factorial experimental design and statistical method has been used to investigate the effect of pH, depressant concentration and mineral grade in the feed on the selective floatability of celestite (Martinez et al., 2003).

Common process for the zinc and lead oxide ore flotation is the sulfidization of surface minerals by Na2S reagent and then use of cationic or anionic collectors. In the absence of Na2S, the amine collectors' adsorption density on the hemimorphite mineral surface is low in the aqueous solutions and extremely depends on pH amounts (Salum et al., 1992; Marabini et al., 1984).

In order to determine the optimum flotation variables, many flotation tests must be conducted under various flotation conditions. It is evident that this is practically impossible since the number of sets of flotation conditions is very large. An efficient way to overcome this difficulty is to adopt an efficient modeling method to predict flotation performance. Combining of the factorial method with an experimental

design technique was seen to be suitable for predicting the flotation performance.

The present work is aimed at optimization of four flotation variables (PAX, Na2S, time and pH) of lead flotation which have been predicted to play a very significant role in lead flotation. By using such a procedure, first, main effects of these variables on the flotation performance can be determined and secondly, the optimum flotation variables can also be determined in order to achieve maximum grade or maximum recovery of concentrate.

2 EXPERIMENTAL

2.1 Materials

The low grade lead ore for this study was obtained from Anguran mine, Zanjan, Iran. After drying, the sample was crushed and homogenized, reducing all the mineral to a particle size below 106 μm (80% of all particles being under 106 μm). For identification of sample, the X-ray diffraction analysis was used. For this analysis 100 gram of sample was employed. The XRF analysis of the sample is given in Table 1.

Table 1. XRF analysis of the sample used in the experiment

Component	Wt. (%)
Zn	14.47
Pb	1.88
Fe	4.07
Mn	0.22
Cu	0.01
Ni	0.03
As	0.47
Na	1.39
Mg	0.51
Ca	16.96
Cd	0.12

2.2 Procedure and equipment

The crushed and homogenized sample was mixed with water (2.5 lit) to produce a flotation feed. The sample was transferred to a 3 liters Denver flotation cell and conditioned at different pH, activator (Na2S), collector (potassium amyl xanthate) and then frother (Pine Oil) with each stage having a 2 minutes conditioning period. The concentrate was then collected for different time of flotation by bubbling air through the mineral pulp. Concentrate was analyzed by a Perkin-Elmer AA300 model atomic absorption spectrophotometer for total lead, and the amount of lead determined.

2.3 Taguchi Method

The taguchi method, introduced by Dr. Genichi Taguchi, contains system design, parameter design and tolerance design procedure to gain a robust process and result for best product quality. The parameter design of this method applies orthogonal arrays, providing and alternative to standard factorial design, to minimize the time and cost of experiments in analyzing all the factors and uses the signal-to-noise (S/N) ratio to analyze the experimental data and find the optimal parameter combination. In application of taguchi design three steps should be considered:

1) Planning experiment
   a. Set the effective and noise factors
   b. Set the levels of each factors
   c. Choose an adequate orthogonal array
2) Conducting experiments
3) Analyzing the results

In this research to optimize lead flotation, taguchi technique was used. Primitive rough tests indicate that four parameters including: pH of pulp, collector dose rate, activator addition rate and time of concentrate collection are effective. Thus, to investigate the effects of above mentioned parameters in lead flotation, three levels of them were selected. Grade and recovery of Pb were selected as responses of this process. Orthogonal array L9, which clarifies 4 parameters at 3 levels, was chosen to carry out the tests. Table 2 shows the experimental procedure.

Table 2. Experimental procedure

No.	pH	Collector (gr)	Activator (gr)	Time (min)
1	8	0.3	1	3
2	8	0.6	2	4
3	8	0.9	3	5
4	9	0.3	2	5
5	9	0.6	3	3
6	9	0.9	1	4
7	10	0.3	3	4
8	10	0.6	1	5
9	10	0.9	2	3

3 RESULTS AND DISCUSSION

Finding the optimized conditions for lead flotation and determination of effective factors in this process were the intended aims of this research. To gain them, the four level L9 (3^4) orthogonal table used and two responses, included grade and recovery of Pb, applied. The collected data were analyzed by Design Expert7 software to evaluate the influence of each parameter on the process. Effects of each factor on the whole process will be elaborated on the following sections.

3.1 Effect of pH

Figures 1 and 2 illustrate the effect of pH on the lead flotation. Three pH of 8, 9 and 10 were evaluated. As seen in Figure 1 higher pH have higher effects on the grade of Pb. Based on what Figure 2 indicates, lead recovery was almost insensitive.

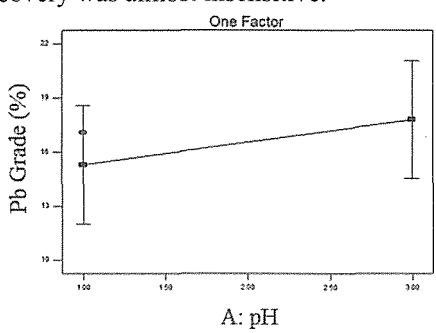

Figure 1. The effect of pH on the Pb grade

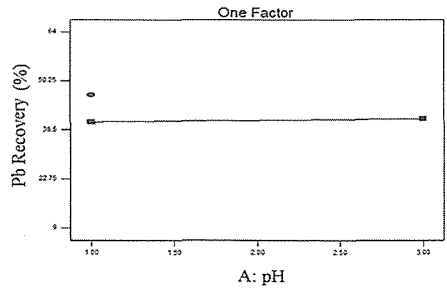

Figure 2. The effect of pH on the Pb recovery

3.2 Effect of Collector Dose Rate

The effect of collector dose rate on lead flotation is illustrated in Figures 3 and 4. According to experimental results presented in Figure 3, the grade of Pb increased as the collector dose rate increased. Based on what Figure 4 indicates, higher doses rate of collector have higher effects on the recovery of Pb.

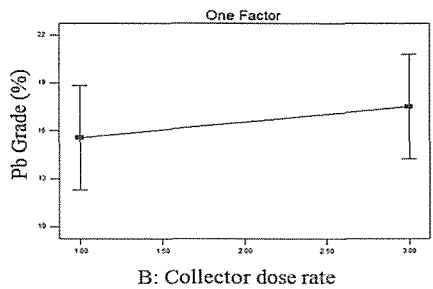

Figure 3. The effect of collector on the Pb grade

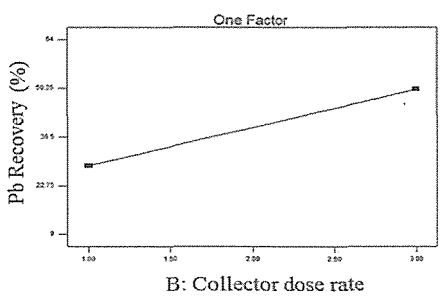

Figure 4. The effect of collector on the Pb recovery

3.3 Effect of Activator Addition Rate

In this research, 3 levels of activator addition rate of 1, 2 and 3 gram were investigated. As seen in Figures 5 and 6, increase of the activator addition rate causes a significant decrease on the recovery and grade of lead. Figure 6 shows that in order to obtain significant lead recovery, it is imperative to decrease the amount of activator.

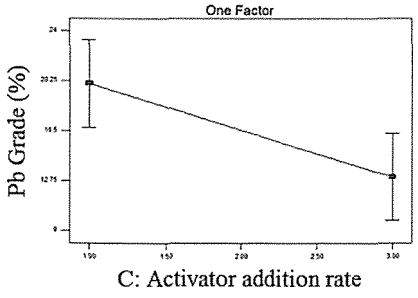

Figure 5. The effect of activator on the Pb grade

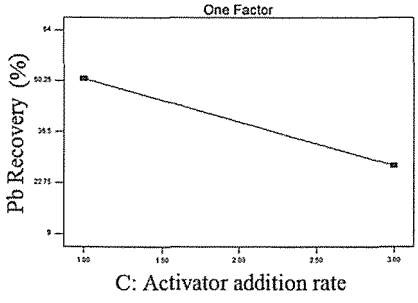

Figure 6. The effect of activator on the Pb recovery

3.4 Effect of Time

The effect of time was examined in three levels of 3, 4 and 5 minutes. The main effect of time on the grade and recovery is shown on the Figures 7 and 8. Grade and recovery of the lead increased as the time of concentrate collection increased.

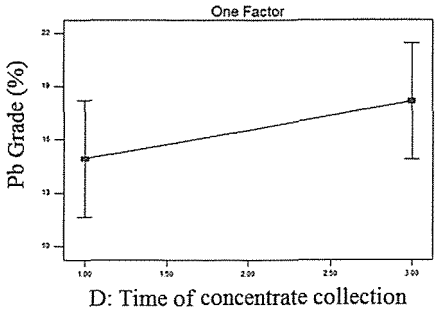

Figure 7. The effect of time on Pb grade

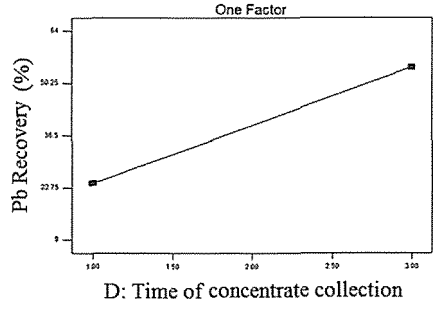

Figure 8. The effect of time on Pb recovery

3.5 Variance Analysis

To determine the most influential factors on each response, Taguchi oriented researchers to use analysis of variance (ANOVA). So the statistical analysis of variance was carried out to see whether the selected parameters are statistically significant. The F-value for each parameter clarifies the effective parameters on the recovery of Pb. Normally, the larger F-value means that this factor has greater influence on the recovery due to the change of the parameters. Besides, P-value is another indicator. Values of less than 0.05 shows the model terms are significant. Optimal combination of the process parameters can be predicted using ANOVA analysis and performance characteristics. According to table 3, F-value for time factor is greater than extracted F-value from the table for 95% confidence level. Therefore variation of this parameter has significant role on the performance of the process. Besides, P-Value confirms this finding, too.

Table 3. Analysis of variance table for recovery of Pb

Source	Sum of Square	DOF	Mean Square	F-Value	P-Value
Model	2921.73	4	730.43	19.60	0.0068
pH	1.33	1	1.33	0.036	0.8591
Collector	696.49	1	696.49	18.69	0.0124
Activator	827.48	1	827.48	22.20	0.0092
Time	1396.43	1	1396.43	37.47	0.0036
Residual	149.06	4	37.47	-	-
Total	3070.79	8	-	-	-

3.6 Optimum Conditions

Finally, using these findings about influential parameters on the process, optimum working conditions could be predicted. The proposed optimum conditions are: pH on level three (10), collector dose rate on level three (0.9 gr), activator addition rate on level one (1 gr), and time should be on level three (5 min). The predicted recovery and grade for Pb are 77% and 18.78%, respectively using by DX7. To investigate the accessibility of this result, a test on the optimum conditions was done. The experimental recovery and grade are 68.13% and 20.73%, respectively at rougher stage. Desirability graph shown in Figure 9, gives the activator addition rate as a function of time. The best desirability is 1. As seen in Figure 9, the maximum desirability was achieved to be activator addition rate on level one and time on level three.

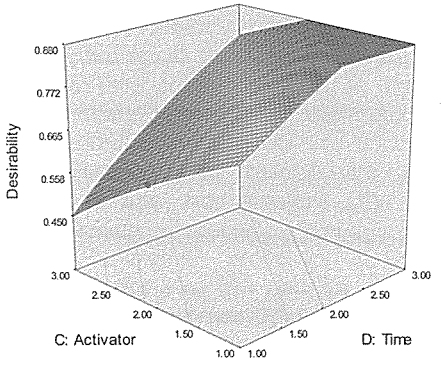

Figure 9. Desirability graph

4 CONCLUSION

In this paper, the effect of operating conditions such as pH, collector dose rate, activator addition rate and time of concentrate collection of lead flotation was studied with the Taguchi method using an L9 (34) orthogonal array. As a result, the ultimate optimum conditions were found to be pH=10; collector=0.9gram; activator=1 gram and time=5 minutes. Under these conditions, recovery and grade for Pb were 68.13% and 20.73%, respectively at rougher stage. The most effective parameter for maximum recovery of lead is found to be time and the most effective parameter for maximum grade of lead is found to be activator addition rate.

ACKNOWLEDGEMENTS

The authors highly extend their gratitude to the Research and Engineering Co. for Non-Ferrous Metals for continuous financial and technical support and the permission to publish this paper. M.R and B.S are thankful to Mr. Hajisoleimani, Miss Taran and Mrs. Asadi for this work.

REFERENCES

Evans, L., Thalody, B.T., Morgan, J.D., Nicol, S.K., Napper, D.H., Warr, G. 1995, Ion flotation using carboxylate soaps: role of surfactant structure and adsorption behavior, Colloids Surf. 102 (pp 81–89).

Forrester, S.E., Rielly, C.D., Carpenter, K.J. 1998, Gas-inducing impeller design and performance

characteristics, Chem. Eng. Sci. 53 (4) (pp 603–615).

Gorain, B.K., Franzidis, J.P., Manlaig, E.V. 1995, Studies on impeller type, impeller speed and air flow rate in an industrial scale flotation cell. Part 1. Effect on bubble size distribution, Miner. Eng. 8 (6) (pp 615–635).

Leja, J. 1982, Surface Chemistry of Froth Flotation, Plenum Press, New York.

Marabini, A.A., Alesse, V., Garbassi, F. 1984, Role of sodium sulphide, xanthate and amine in flotation of lead–zinc oxidized ores. In: Jones, M.J., Oblatt, R. (Eds.), Reagents in the Mineral Industry. The IMM, London, (pp 125–136).

Martinez, A.L., Uribe, A.S., Carrillo, F.R.P., Coreno, J.A., Ortiz, J.C. 2003, Study of celestite flotation efficiency using sodium dodecyl sulfonate collector: factorial experiment and statistical analysis of data, Int. J. Miner. Process. 70 (pp 83–97).

Ralston, J., Fornasiero, D., Mishchuk, N. 2001, The hydrophobic force in flotationa critique, Colloids Surf. A Physicochem. Eng. Aspects 192 (pp 39–52).

Rubio, J., Souza, M.L., Smith, R.W. 2002, Overview of flotation as a wastewater treatment technique, Miner. Eng. 15 (pp 139–155).

Salum, M.J.G., Araujo, A.C., Peres, A.E.C. 1992, The role of sodium sulphide in amine flotation of silicate zinc minerals. Minerals Engineering, 5 (3–5), (pp 411–419).

Zinc Leaching Optimization from Tajkooh Shaking Table Residue

H. Kamran Haghighi, D. Moradkhani
Faculty of Engineering, Zanjan University, Zanjan, Iran.

B. Sedaghat
R&D Center, Research and Engineering Co. for Non-ferrous Metals (RECo), Zanjan, Iran.

ABSTRACT In this study, maximum recovery of zinc and minimum recovery of iron from shaking table residue has been investigated. The residue is discarded as tailing of shaking table Tajkooh processing zinc–lead carbonate ores. The zinc plant residue containing 14.67% Zn, 5.93% Pb, and 10.47% Fe was blended with H2SO4. The orthogonal array L9 (3^4) comprising four parameters at three levels was chosen. The parameters and their levels were as: pH : 1, 1.5 and 2; time : 30, 45 and 60 min; temperature : 40, 60 and 80 °C; and solid/liquid ratio: 1:4, 1:6 and 1:8. The ultimate optimum leaching conditions were found to be Temperature :80 °C , solid/liquid ratio : 1:8, time : 60 min and pH=1. Under these conditions, recovery for zinc and iron was 83.5% and 1.3%, respectively. It was observed that the leaching rate of zinc increased with increasing temperature and time and decreasing pH without influence of S/L.

1 INTRODUCTION

Zinc and lead are the most important non-ferrous metals after copper and aluminum (Gervais, 2000). Zinc is primarily produced from sulphidic ores; however, some zinc is produced from oxide-carbonate ores and different secondary resources such as zinc ash, zinc dross, flue dusts of electric arc furnace, leach residues, etc. Pyrometallurgical and hydrometallurgical routes or their combination can be employed for treating secondary materials. The hydrometallurgical process are regarded as more eco-friendly for treating such materials having a low zinc content (Jha et al., 2001).During recent years, several hydrometallurgical processes have been developed for Co, Mn and Zn from these resources. These processes generally include the following major unit operations:1. roasting (not always), 2. leaching by acids, bases or water, 3. removal of impurities such as iron, 4. separation and recovery processes and 5. refining of recovered metals (Zhang et al, 1998 ; Jandova, et al 2005 ; Arslan, C et al, 2002; Nagib, S et al, 2000 ; Wang, Y et al, 2002 ; Jandova, J et al, 2005 ; Clark, S. J et al, 1996). Many researchers have worked to improve the extraction methods and promote the recovery efficiency of these processes (Jandova, J et al, 2005 ; , Vu, H et al, 2005 ; Pagnanelli, F et al, 2004 ; Kanungo, S et al, 1988; . Agatzini, S et al, 2004; Nathsarma, K et al, 1987; Momade, F et al, 1996; Georgiou, D et al, 1998).

Leaching is the most important starting point of most hydrometallurgical processes. Suitable leaching conditions can be determined for an appropriate design of the leaching system. These parameters consist of leachant concentration, reaction time, size of solid particles, shape of solid particles, solid to liquid ratio and temperature. A leaching process can often be selected for dissolving valuable metals from an ore or a secondary

resource; whilst leaving most of the gangue largely unaffected.

Thermodynamic parameters such as concentration and temperature of the leaching can be used to predict and control the general conditions required for dissolution of secondary resources into water. A large number of studies have been carried out to optimize these processes (Zhang et al, 1998; Arslan, C et al, 2002; Wang, Y et al, 2002 ; Jandova, J et al, 2005 ; Clark, S. J et al, 1996; Nathsarma, K et al, 1987; Momade, F et al, 1996; Georgiou, D et al, 1998).

In this study, zinc recovery from shaking table residue that obtained from Tajkooh plant was investigated. The aim of this study is to discuss the maximum leaching of zinc and minimum leaching of iron with reference to the effects of variables such as pH, time, temperature and solid/liquid ratio. optimum conditions has been determined with Taguchi method by Design Expert software.

2 EXPERIMENTAL

2.1 Materials and methods

Shaking table residue for the leaching study was obtained from Tajkooh plant, Yazd, Iran. After drying, the residue was ground and homogenized. The chemical analysis was carried out by a Perkin-Elmer AA300 model atomic absorption spectrophotometer. The chemical analysis of the shaking table residue is given in Table 1. As can be seen from Table 1, the residue is mostly composed of zinc and iron.

Table 1. Chemical composition of sample used in the experiment (Wt.%)

Component	Zn	Pb	Fe	Mn	Cu	Ni
Wt. (%)	14.67	5.93	10.47	0.052	0.01	0.001

2.2 Procedure and equipment

The leaching reactions were conducted in a glass beaker of 1 L volume equipped with a mechanical stirrer submerged in a thermostatic bath. The mechanical stirrer (Heidolf RZR 2020) had a controller unit and the bath temperature was controlled using digital controller (within ±0.5 °C). Firstly, 500 cc of solution was put into the beaker and when the desired temperature of the beaker content (40, 60 and 80 °C) was reached, a predetermined amount of Tajkooh sample with defined size distribution (-100 μm) was added into the solution while the content of the beaker was being stirred at a rate of 400 rpm. This was marked as the beginning of the experiment. The progress of the leaching reaction was followed by measuring the amounts of zinc in the solution. The samples were immediately filtered using filter paper circles and then diluted and analyzed for zinc and iron. Zinc and iron recovery was calculated according to difference between the initial and final zinc and iron concentrations of the solution.

2.3 Taguchi method

The Taguchi method, introduced by Dr. Genichi Taguchi, contains system design, parameter design and tolerance design procedure to gain a robust process and result for best product quality. The parameter design of this method applies orthogonal arrays, providing and alternative to standard factorial design, to minimize the time and cost of experiments in analyzing all the factors and uses the signal-to-noise (S/N) ratio to analyze the experimental data and find the optimal parameter combination. In application of taguchi design three steps should be considered:

- Planning experiment
  - o Set the effective and noise factors
  - o Set the levels of each factors
  - o Choose an adequate orthogonal array
- Conducting experiments
- Analyzing the results

In this research to leaching of zinc, Taguchi technique was used. Primitive rough tests indicate that four parameters including: pH, solid liquid ratio, temperature and time are effective. Thus, to investigate the effects of above mentioned parameters in leaching of zinc and iron, three levels of them were selected. Recovery of Zn and Fe were

selected as responses of this process. Orthogonal array L9, which clarifies 4 parameters at 3 levels, was chosen to carry out the tests. Table 2 shows the experimental procedure.

Table 2. Experimental procedure

No.	pH	S/L	Temperature (°C)	Time (min)
1	1	1/4	40	30
2	1	1/6	60	45
3	1	1/8	80	60
4	1.5	1/4	60	60
5	1.5	1/6	80	30
6	1.5	1/8	40	45
7	2	1/4	80	45
8	2	1/6	40	60
9	2	1/8	60	30

3 RESULTS AND DISCUSSION

3.1 Effect of pH

The effect of pH on zinc leaching was investigated in pH of 1, 1.5 and 2 at agitation speed of 400 rpm. As seen in Fig. 1 and 2, the dissolution of zinc decreased to pH raise until the pH of 2 and iron recovery was almost insensitive. However, from this point on, a significant decline was observed in the recovery of zinc.

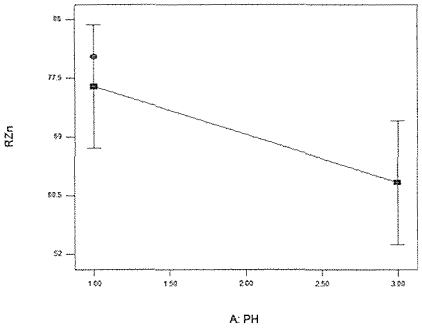

Figure.1. The effect of pH on the zinc recovery

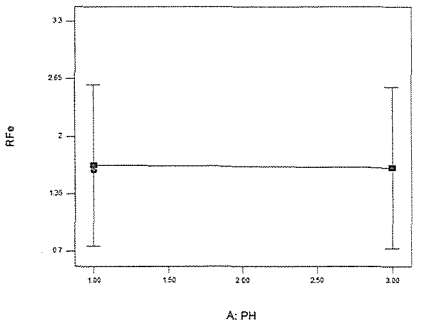

Figure.2. The effect of pH on the iron recovery

3.2 Effect of solid/liquid ratio

Fig.3 and 4 give the recovery as a function of solid to liquid ratio (weight of solid/volume of liquid) at stirring speed of 400 rpm. According to experimental results, zinc recovery increased until the solid/liquid ratio of 1/8, about 72% of zinc and iron recovery decreased until solid/liquid ratio of 1/8, about 1.5% of iron.

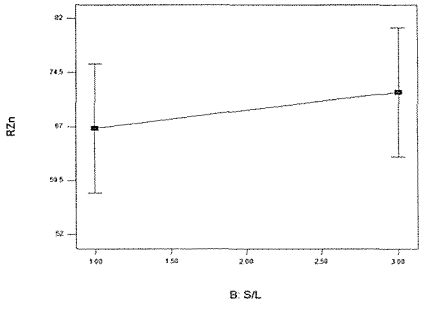

Figure.3. The effect of solid/liquid ratio on the zinc recovery

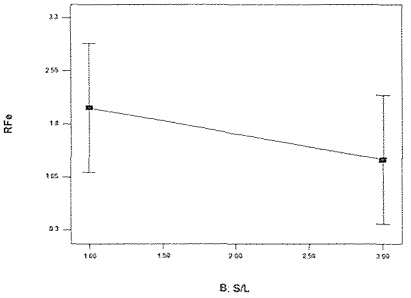

Figure.4. The effect of solid/liquid ratio on the iron recovery

3.3 Effect of temperature

The effect of temperature on zinc and iron leaching is illustrated in Fig.5 and 6. The recovery of Zn and Fe increased as the temperature increased. However, by increasing the temperature from 40°C to 80°C, a fixed slope raise was observed in the recovery of both Zinc and iron.

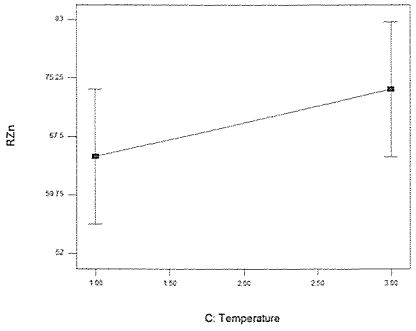

Figure.5. The effect of temperature on the zinc recovery

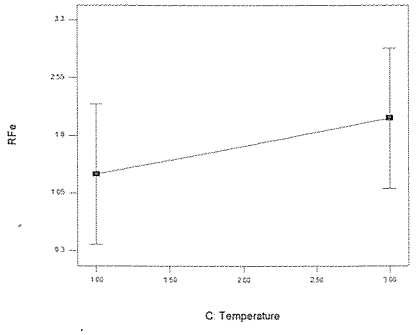

Figure.6. The effect of temperature on the iron recovery

3.4 Effect of time

The effect of time was examined in three level of 30, 45, 60 min at stirring speed of 400 rpm. As seen in Fig.7 and 8, no irregularity was observed in the leaching of Zn and Fe. Zinc recovery increased as the time increased. The recoveries after 60 min reached 72% for zinc and 1.44% for iron, respectively. Zinc leaching in this study was considered to be convincingly completed within 60 min.

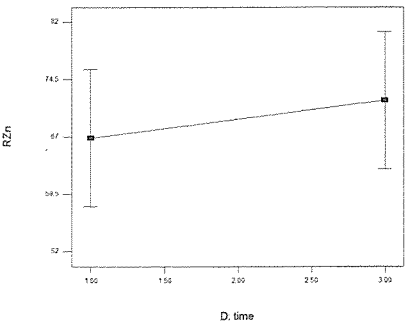

Figure.7. The effect of time on the zinc recovery

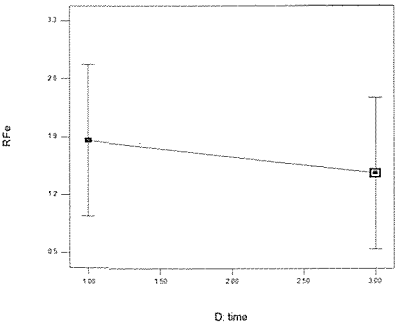

Figure.8. The effect of time on the iron recovery

3.5 Optimum conditions

Finally, using these findings about influential parameters on the process, optimum working conditions could be predicted. The proposed optimum conditions are: pH on level 1 (1), solid / liquid ratio on level 3 (1/8), time on level three (60 min) and temperature was on level three (80 °C). The predicted recoveries for Zn and Fe are 84.5% and 1.15%, respectively. To investigate the accessibility of this result, a test on the optimum conditions was done. The experimental recoveries for Zn and Fe are 83.5% and 1.3%, respectively.

4 CONCLUSION

With the aid of simple leaching, zinc was successfully recovered from zinc shaking table residue as an engaging source of zinc. The process benefited from the advantageous minimum recovery of iron and together with maximum recovery of zinc. Under the optimum leaching conditions (time=60 min, Temperature=80 °C, stirring speed=400 rpm, S/L=1/8 and pH=1), the maximum zinc recoveries was 83.5% for Zn and minimum recovery for iron was 1.3%.

ACKNOWLEDGEMENTS

This research was made possible by funds received from the Research & Engineering Company for Non-ferrous Metals. H.K.H and B.S are thankful to Miss Taran and Mrs. Asadi for this work.

REFERENCES

Agatzini,S. L. and Zafiratos, I. G., "Beneficiation of a Greek serpentinic nickeliferous ore Part II.,Sulfuric acid heap and agitation leaching", Hydrometallurgy, Vol. 74, No. 3-4, (2004), 267-275.

Arslan, C. and Arslan, F., "Recovery of copper, cobalt and zinc from copper smelter and converter slags", Hydrometallurgy, Vol. 67, No. 1-3, (2002),1-7.

Clark, S. J., Donaldson, J. D. and Khan, Z. I., "Heavy metals in the environment. Part VI: Recovery of cobalt values from spent cobalt/manganese bromide oxidation catalysts", Hydrometallurgy, Vol. 40, No. 3, (1996), 381-392.

Georgiou, D. and Papangelakis, V. G., "Sulfuric acid pressure leaching of a limonitic laterite: chemistry and kinetics", Hydrometallurgy, Vol. 49, No. 1-2, (1998), 23-46.

Gervais, E., 2000. Zinc Applications: A World of Performance. In: Dutrizac, J.E., et al. (Ed.), rocedinngs of the Lead-Zinc 2000 Symposium. Pittsburgh, U.S.A. October 22–25.

Jandova, J., Lisa, K., Vu, H. and Vranka, F., "Separation of copper and cobalt-nickel sulfide concentrate during processing of manganese deep ocean nodules", Hydrometallurgy, Vol. 77, No. 1-2, (2005), 75-79.

Jandova, J., Vu, H. and Dvorak, P., "Treatment of sulfate leach liquors to recovery cobalt from waste dusts generated by the glass industry", Hydrometallurgy, Vol. 77, No. 1-2, (2005), 67-73.

Jha, M.K., Kumar, V., Singh, R.J., 2001. Review of hydrometallurgical recovery of zinc from industrial wastes. Resour. Conserv. Recycl. 33, 1–22.

Kanungo, S. B. and Das, R. P., "Extraction of metals from manganese nodules of the Indian Ocean by leaching in aqueous solution of sulfur dioxide", Hydrometallurgy, Vol. 20, Issue, 2, (1988), 135-146.

Momade, F. W. Y., "Sulfuric acid leaching of the Nsuta manganese carbonate ore", Hydrometallurgy, Vol. 40, No. 1-2, (1996), 123-134.

Nagib, S. and Inoue, K., "Recovery of lead and zinc from fly ash generated from municipal incineration plants by means of acid and/or alkaline leaching", Hydrometallurgy, Vol. 56, No. 3, (2000), 269-292.

Nathsarma, K. C. and Bhaskara Sarma, P. V. R., "Separation of iron and manganese from sulfate solutions obtained from Indian ocean nodules", Hydrometallurgy, Vol. 17, No. 2, (1987), 239-249.

Pagnanelli, F., Furlani, G., Valentini, P., Veglio F. and Toro, L., "Leaching of low-grade manganese ores by using nitric acid and glucose: optimization of the operation conditions", Hydrometallurgy, Vol. 75, No. 1-4, (2004), 157-167.

Vu, H., Jandova, J., Lisa, K. and Vranka, F., "Leaching of manganese deep ocean nodules in FeSO4-H2SO4-H2O solutions", Hydrometallurgy, Vol. 77, Issue 1-2, (2005), 147-153.

Wang, Y. and Zhou, C., "Hydrometallurgical process for recovery of cobalt from zinc plant residue", Hydrometallurgy, Vol. 63 No. 3, (2002), 225-234.

Zhang, P., Yokoyama, T., Itabashi, O., Suzuki, T. M. and Inoue, K., "Hydrometallurgical process for recovery of metal values from spent lithium-ion secondary batteries", Hydrometallurgy, Vol. 47, No. 2-3, (1998), 259-271.

Comparison the Performance of Dissolved Nitrogen Predispersed Solvent Extraction and Conventional SX Methods in Synthetic Dilute and Dense Copper Solutions

Seyed Mohammad Javad Koleini, Mohammad Reza Tavakoli Mohammadi, Mahmoud Abdollahy

Mining Engineering Department, Mineral Processing Group, Tarbiat Modares University, Iran

ABSTRACT The difference between Dissolved Nitrogen Predispersed Solvent Extraction (DNPDSE) innovative method and conventional SX method is in aqueous and organic phases mixture mode. In fact, in conventional SX method in laboratory scale a magnetic mixer is used for mixture operation, while this operation in DNPDSE method is achieved using bubbles from organic phase in aqueous phase. This difference in mixture method causes a very large contact area in DNPDSE method for transferring metal ions from aqueous to organic phase as well as its improved extraction process. The obtained results from comparing the performance of this two methods in similar conditions illustrated that the amount of copper recovery, i.e. the amount of copper concentration in organic phase, in DNPDSE method compared with that of conventional SX method, in dilute and dense copper solutions, were increased, respectively to, 22 percents (0.75 gCu/l) and 3 percents (1 gCu/l) on average.

1 INTRODUCTION

Solvent extraction has become one of the most important hydrometallurgical methods due to increased demand for high purity metals, concerns over environmental issues, the need for lower operating costs, and the continuous depletion of high grade ores resulting in the treatment of complex and/or low grade ores (Rydberg & Cox & Musikas & Choppin 2004). This procedure is an effective method for selectivity remove, purification and concentration of certain elements or solution combinations (Gupta 2000).

The suitability of using this method for a separation procedure is determined by thermodynamic and kinetic considerations. The main thermodynamic parameter is the solute distribution ratio, D_M between the organic and the aqueous phases presented as the following equation:

$$D_M = [M]_{T,org} / [M]_{T,aq} \quad (1)$$

where $[M]_T$ is the sum of concentrations of all M-species in a given phase and aq and org subscipts indicate the aqueous and the organic phase, respectively. The magnitude D_M determines the feasibility of the separation and the higher D_M shows the better the solute separation.

Another factor affecting the design of extraction processes is the extraction rate as it determins the residence time of the phases in the contactor and subsequently its size. The extraction rate in a two phase system depends on the rate of interfacial transfer of species M , i.e., the interfacial flux J, and the interfacial area between two liquid phases, Q. These are linked by the following equation:

$$d[M_{t,aq}] / dt = J \cdot Q / V \quad (2)$$

where V is the total volume of the phases, and the subscript t indicates the contact time.

Introducing the definition of specific interfacial area, a_s:

$$a_s = Q / V \quad (3)$$

the equation 2 changes to the following form:

$$d[M_{t,aq}] / dt = J \cdot a_s \quad (4)$$

In each extraction process J will depend on degree of turbulence in the phases and on the concentrations of the reactants. On the other hand, the a_s value depends mainly on the degree of turbulence created by the power input the contactor, and its value increases in higher power inputs due to reduced size of phase droplets (Rydberg et al, 2004). So, degree of turbulence among phases together with reactants concentrations are the most important factors in success of a solvent extraction process.

Considering the above points, the use of solvent extraction for dilute solutions entails some problems. On the one hand, while mass transfer rate between the two phases can be increased with augmented mixture and increased interface area, the amount of power consumed is too high for the resulting concentration amount and vigorous disturbance can cause formation of stable emulsions and a loss in organic phase (Tarkan and Finch, 2005). On the other hand, according to equation 1, processing of dilute solutions using common solvent extraction requires high D_M values, and the volume of necessary organic phase will be disproportionately high in view of safety and environment (Gupta, 2000). In addition, for satisfactory phase disengagement, a short period of time is required to reach equilibrium, increased recovery of metal ion demands maintenance of aqueous/organic ratio equivalent to one (Sebba, 1987). Another reason is decrease in concentration and increase in consumption of organic phase that weakens the effectiveness of this method for dilute solutions.

New solvent extraction technologies in recent years have attempted to display these limitations and overcome them. Froth flotoextraction (Dibrov & Vornin & Kiemyatov 1998), solvent extraction with bottom gas injection without moving parts (Sohn & Doungdeethaveeratana 1998, Doungdeethaveeratana & Sohn 1998), air-assisted solvent extraction (Tarkan & Finch 2005), liquid membranes, nondispersive solvent extraction, microemulsions and reverse micelles (Rydberg & Cox & Musikas & Choppin 2004), Predispersed Solvent Extraction (Tarkan & Finch 2006) and etc are examples of research efforts performed in this field that mainly have not reached industrial scales.

In harmony with development of the technologies for enhancing operation power and improving the performance of solvent extraction equipment, especially for dilute solutions, the new Dissolved Nitrogen Predispersed Solvent Extraction (DNPDSE) method has been developed. What distinguishes this method from conventional SX methods is the approach for mixing aqueous and organic phase. In fact, in conventional SX method in laboratory scale mixture is achieved using a magnetic agitator, while in DNPDSE method it is achieved using bubbles from organic phase (CGAs) in aqueous phase. Such difference in mixture approach gives rise to a very large contact area for transferring metal ions from aqueous to organic phase and resulting in improved extraction process. However, to elucidate the issue and demonstrate the improved performance of DNPDSE method in comparison with conventional SX methods, there is a need for designing proper experiments - based on changing the two important parameters of pH and aqueous/organic ratio - and comparison of the resulted diagrams for two methods in comparable laboratory conditions.

1 EXPERIMENTAL WORK

1.1 DNPDSE principles

Conducting two-phase mixture operations in solvent extraction method through replacement of bubble dispersion of organic phase, i.e. colloid gas aphrons [CGAs],

instead of its droplet dispersion in aqueous phase is the basis of a new innovative method called DNPDSE. This replacement is promising for extraction of valuable elements from high volumes of extremely dilute solutions by providing two important features for organic phase; namely increased contact area, to augment recovery rate and shortening of equilibrium time and increased buoyancy force, to improve phase disengagement.

In this method similar to method proposed by Sebba (PDSE), the solvent phase is changed to a biliquid foam called polyaphron (two-layered bubbles with oil nucleus) with minute dimensions and large contact area and added for mass transfer to pregnant solution. Although these polyaphrons rise to the surface because of being lighter than water (through gravity), this is usually done very slowly because of small polyaphrons size. Sebba used CGAs (two-layered bubbles with μm dimensions stabilized by surfactant) to increase rising speed of liquid colloid aphrons (CLAs) to surface (due to hydrophobic property of soapy shell) to overcome this problem in PDSE method (Save & Pangarkar & Kumar 1994, Sebba 1987). But in DNPDSE method by taking advantage of benefits due to droplet conversion to bubble, this problem is solved by applying the two general changes as follows:

1. Conversion of CGAs in PDSE to ordinary air bubbles by Spurger
2. Conversion of CLAs in PDSE to CGAs by increasing foaminess unit of organic phase (through adding proper surfactant (silicone oil) (Ferris & Rubio 1999) and decreased temperature (Bolles 1967)) and applying Dissolved Air Flotation (DAF) process (by passage of CLAs under pressure from Reynolds tube).

Another important point in this method is the use of nitrogen gas instead of air for saturation process due to the following reasons:

* Neuter nitrogen gas (Poorkani & Banisi 2005) prevents combination of oxygen in air with saturated organic component and precludes explosion.

* Nitrogen gas (unlike oxygen) does not cause chemical destruction of diluent and extractant and also organic phase loss because of solution in water by increased pressure (Young & Dreisinger & Hacki & Dixon 1999).

* Nitrogen does not cause corrosion of tank wall.

* Nitrogen gas provides the possibility of complete tank saturation because of lower solubility than oxygen gas in saturator

Of course due to low volume of nitrogen consumed for producing required pressures (2-3 bar) and also easy availability and production (Poorkani & Banisi 2005), high costs in industrial scale is not expected.

1.2 Reagents and solutions

1.2.1 In conventional SX method

Characteristic of synthetic aqueous solutions (dilute and dense) resulting from reagent grade $CuSo_4.5H_2o$ (MERK (Germany)) have been cited in Table 1.

The used organic phase was a combination of chelating type extractant Lix 984N (with maximum copper loading of more than 5.1 g/L (Cognis 2010)) and kerosene diluent (with 0.78 g/cm^3 density) with 1:9 volumetric ratio. To adjust pH (pH=2.1 for maximum copper extraction and pH=1.2 as the beginning of copper extraction range) of the synthetic solution, a solution containing 500 mg/L sulfuric acid and also a buffer solution containing 0.2 M NaOH, 0.04 M acetic acid, 0.04 M phosphoric acid and 0.04 M boric acid (according to Finch researches (Tarkan & Finch, 2005)) was used.

Table 1. Specifications of synthetic aqueous solutions

Specifications	Dilute	Dense
Concentration (mg $CuSO_4.5H_2O$ /L)	500	7813
Concentration (mg Cu /L)	128	2000
The reason to choose the cited concentrations	Producing a very dilute solution to demonstrate desirable contactor performance	Producing a solution containing minimum permitted copper grade in input feed on circuit of SX (Lazaridis & peleka & Karapantsios & Matis 2004)

1.2.2 In DNPDSE method

Also in this method the same reagents and solutions utilized in conventional SX method were used, except that respectively 0.3 g/l dilute silicone oil (Shin Etsu), 4 g/l sodium dodecylbenzene sulphonate (NaDBS) (Sigma(USA)) and 0.3 g/l dodecytrimethyl ammonium bromide (DTAB) (Aldrich(USA)) was used to produce organic phase polyaphron, aqueous phase polyaphron and aqueous phase of synthetic solution.

1.3 Methods

1.3.1 SX method

In this method, required A/O ratios, given volumes of aqueous solution (dilute or dense) and organic solvent were mixed in a beaker, using a magnetic stirrer (500 rpm). After mixing in period of given time, the contents of beaker were transferred to a separator funnel to separate organic and aqueous phases. The period of time required for complete separation was 20 minutes. After passage of this time, the aqueous phase separated and its equilibrium pH was measured. Finally, copper concentration in aqueous phase was determined using Absorption Spectrometry (AAS); and its concentrations in organic phase were calculated from copper concentration difference in aqueous phase before and after extraction equilibrium (Rao & Devi & Reddy 2000, Navarro & Alguacil 1999).

1.3.2 DNPDSE method

This method consists of the two general steps as follows:

1.3.2.1 Polyaphron preparation

As preparation conditions affect size distribution and stability of CLA phase (He & Wu & Mao 2007, Scarpello & Stuckey 1999), the CLAs were prepared in relatively stable conditions. Toward this end, to produce 220 ml kerosene anionic polyaphron with PVR=10 (volumetric ratio of dispersed organic phase to continuous phase volume), 20 ml water containing 4 g/l anionic surfactant of NaDBS was dispensed in a 500 ml beaker and mixed well using a magnetic stirrer (900 rpm) to obtain gaseous foam (1^{st} step). Next, the resulting gaseous foam was placed in a vessel including water and ice to lower its temperature (2^{nd} step). Then, 20 ml of extraction agent Lix 984N was blended with 0.3 g/l non anionic surfactant of silicone oil and reached 200 ml by adding kerosene as diluents (3^{rd} step). The resulting organic phase was also placed in a vessel containing water and ice to lower its temperature (4^{th} step). After attaining desired temperature, the resulting organic phase was gradually - with a flow rate of 1.5 ml/min - added to foamy aqueous phase by mixing (5^{th} step). At first, solvent dispersion was easily achieved, but after adding two third of solvent, the mixture quickly became viscous, and viscosity was increased up to complete dispersion of volume. Finally, a white creamy dispersion of CLA was obtained (6^{th} step) (Save et al, 1994, Matsashita et al,

1992). The resultant polyaphron was diluted for more contact area in continuous aqueous solution. For this reason, polyaphron was gradually added into distilled water with suitable pH, quadruple volume, regarding dilution constant of 5, and nearly 5 °C temperature accompanied by agitation of distilled water (7th step). After finishing the dilution, proper polyaphron for transfer into the column was reached (8th step).

1.3.2.2 Simultaneous extraction and separation

Simultaneous extraction and separation generally involves in two parts:

- Extraction and separation by making CGAs: in this part, after transfer of produced polyaphron and nitrogen gas for having 2.5-3.5 bar working pressure into tank, and allowing enough opportunity for solution for thirty minutes, the synthetic aqueous solution (1.5 liters) containing 0.3 g/l cationic surfactant DTAB was conveyed into the column. Then, considering the required aqueous/organic ratio, the polyaphron phase was injected into column through Reynolds tube, through counting injection times and measuring height difference of the solution within the column due to CGAs injection. The first sampling from aqueous phase (30 ml) was done from middle part of the column 6.5 minutes after the first injection.
- Extraction and separation by making air bubbles: After 7.5 minutes, by accurate adjustment of flow rate meter (0.1 l/min), required air for producing bubble to carry remaining CGAs to surface and more mixing of the two phases was provided by passing through Spurger. After finishing the operation, 7.5 minutes after second step, the whole remaining aqueous phase was carried to a container through underflow. by separation of the remaining organic phase from it using separator funnel, 30 ml of it was considered as the sample for the second step, to evaluate the effect of produced bubbles on extraction procedure. Total duration of these two steps was 15 minutes.

Finally, copper concentration in aqueous phase of resulting samples was determined by Atomic Absorption Spectrometry (AAS) and its concentration in organic phase was calculated from copper concentration difference in aqueous phase before and after extraction equilibrium (Rao et al, 2000, Navarro and Alguacil, 1999).

2 RESULTS AND DISCUSION

2.1 Evaluation of important copper components in synthetic aqueous solutions

In most of the research experiments conducted to evaluate performance of different equipment, synthetic aqueous solutions have been made to eliminate the effect of unknown factors and chemical compounds resulting from diverse metal and nonmetal components, such as organic compounds. For this reason, to attain results that accurately reflect the extraction performance of the DNPDSE method, we used synthetic solutions instead of real ones. Then, we evaluated the important copper components in these solutions by drawing Eh-pH diagrams (by HSC chemistry 5.11 software). Figure 2 shows thermodynamic copper II distribution in synthetic aqueous solution as a function of Eh-pH. The indicated range in these diagrams - pink line - is the result of connecting points the coordinates of which are Ehs from various pHs of synthetic solutions (Tab. 2-3).

Comparative analysis of the resulting diagrams showed that various salt amounts used to produce dilute and dense solutions, which do not cause considerable difference in the two diagrams, and copper ions in both solutions were in the form of Cu^{2+}, with copper extraction pHs of 1.2-2.4. Furthermore, the results of other investigations in this regard showed no effect of cationic surfactant DTAB added to aqueous solution in DNPDSE method on Eh of the solution and change of associated diagram.

Table 2. Eh values for various pHs of synthetic dilute solution

pH	1.2	1.5	1.8	2.1	2.4	2.7	3	3.3
Eh(mv)	569	545	520	516	506	499	490	483

Table 3. Eh values for various pHs of synthetic dense solution

pH	1.2	1.5	1.8	2.1	2.4	2.7	3	3.3
Eh(mv)	510	506	503	497	495	492	490	488

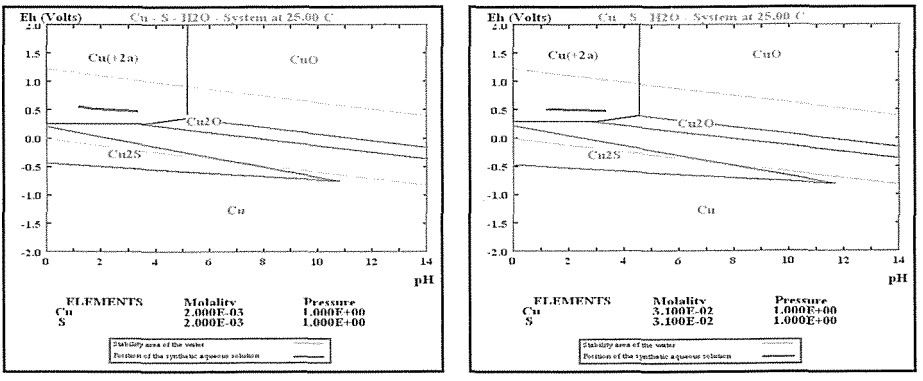

a b

Figure 2. Eh-pH diagrams of synthetic aqueous solutions
(a) dilute solution - (b) dense solution.

2.2 Comparing performance of conventional SX and DNPDSE methods

In DNPDSE method, by injection of organic phase, water released from polyaphron dilution enters to the column and loses its concentration. This reduction for the aqueous phase is not only due to extraction process but the water resulting from dilution. While it is possible to calculate metal concentration in organic phase, it is not possible to draw extraction isotherm and determine distribution coefficient, for lack of concentration of actual remaining metal in aqueous phase resulted from extraction process. It is however possible to determine actual recovery for the DNPDSE method due to probability of calculating initial concentration of pregnant solution after dilution. So, the best way to evaluate the performance of DNPDSE method in comparison with conventional SX method - by designing appropriate experiments based on changing the two major parameters of pH and aqueous/organic ratio - was comparison of concentrations resulting for metal in organic phase and their real recovery in similar laboratory conditions.

2.2.1 pH choice

By performing conventional SX experiments in different pHs and aqueous/organic ratio of 1, for dilute and dense solutions, we chose the proper pH. The diagrams of this survey are presented in Figure 3.

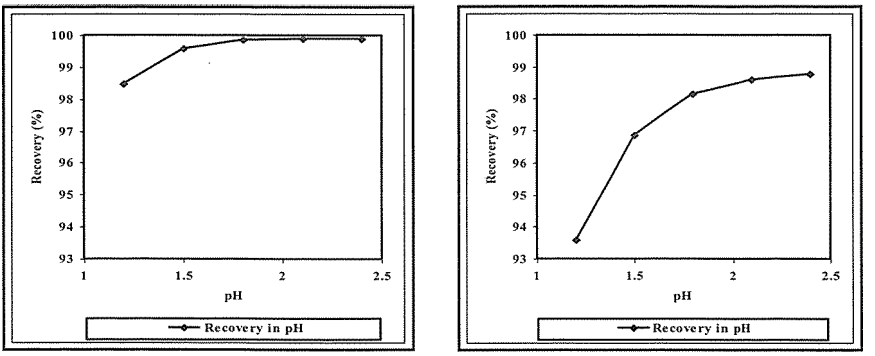

a b

Figure 3. Recovery diagram per pH in a/o = 1/1 (a) dilute solution – (b) dense solution.

According to the above two diagrams in pH=2.1 and values higher than it, there was no considerable change in recovery. Also, based on research performed in pHs higher than 2.1, there was no possibility to survey the selectivity of the two methods - owing to considerable iron precipitation. Hence, we used pH=2.1 to evaluate all the experiments in the same pH and to have the highest recovery for copper. Also, Finch also used this pH for his research activities.

3.2.2 Comparing the results of performance of the two methods in various aqueous/organic ratio and pH=2.1

In DNPDSE method, regarding the volume of foam produced in various aqueous/organic ratios, the conditions are not the same in the second stage of extraction process; so, because of sampling from volume of remnant aqueous solution in the column and errors resultant from analysis, no tendency was observed for increased recovery in the second stage. Then, to provide better conditions for comparison of the performance of the two methods, the results of the first stage of DNPDSE method were used - which were not significantly different with results of the second stage.

3.2.2.1 Comparing metal concentrations in organic phase in various pressure studied in DNPDSE method

The diagrams surveyed for dilute and dense solutions have been presented in Figure 4.

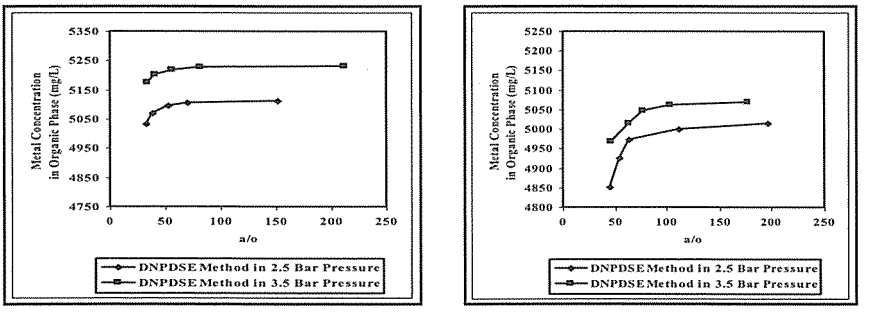

a b

Figure 4. Diagrams of metal concentration in organic phase per a/o ratios in DNPDSE method (two different pressures) (a) dilute solution – (b) dense solution.

The results of analysis for these two diagrams showed that:

- For both solutions, the amount of metal concentration in organic phase, comparable A/O ratios, and 3.5 bar pressure was higher than 2.5 bar indicating better performance of this method in 3.5 bar pressure.
- For both solutions, A/O ratio has a decrease due to increased dilution of initial pregnant solution; also, the metal concentration in organic phase decreased. Because of less metal ions in pregnant solution, decline rate was higher in dilute solutions compared with concentrated solutions.
- For both solutions, downward trend in metal concentration in organic phase was higher in 2.5 bar pressure than that of 3.5 bar, indicating better performance of this method in 3.5 bar pressure because of more contact are provided in 3.5 bar pressure.
- For dense solution, increase in concentration in organic phase was more than dilute solution, because of more metal ions in initial pregnant solution.

3.2.2.2 Comparison of metal concentrations in organic phase in conventional SX and DNPDSE methods for both pressures

The studied diagrams for dilute and dense solutions are given in Figure 5. The resulting diagrams for both solutions indicated significant increase in metal concentration in DNPDSE method at both pressures compared to that of conventional SX method in similar A/O ratios. In addition, because increased organic phase injection, i.e. increased water due to dilution, decreases the initial concentration of pregnant solution in DNPDSE method, then in similar A/O ratios the resulting concentration in organic phase in DNPDSE method is a function of more dilute solutions - compared to conventional SX method. This indicates much better performance of this method compared with conventional SX method.

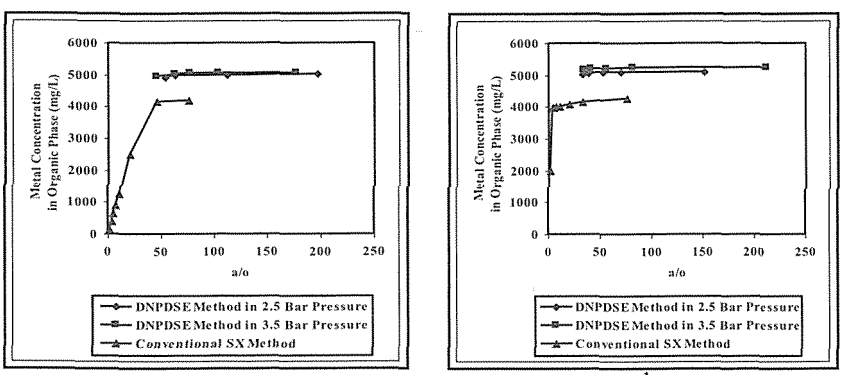

a b

Figure 5. Diagrams of metal concentration in organic phase per a/o ratios in conventional SX and DNPDSE methods (a) dilute solution – (b) dense solution.

3.2.2.3 Comparing recoveries in conventional SX and DNPDSE methods for both pressures

The studied diagrams for dilute and dense solutions are given in Figure 6. The results of analyzing these two diagrams showed that:

- In the DNPDSE method, the concentration amount for organic phase, and therefore recovery rate, was higher in 3.5 bar than that of 2.5 bar pressure; hence the reason for more decline of diagram related to recovery in 3.5 bar pressure compared to 2.5 bar pressure in some points has been lack of accurate implement of A/O ratios.

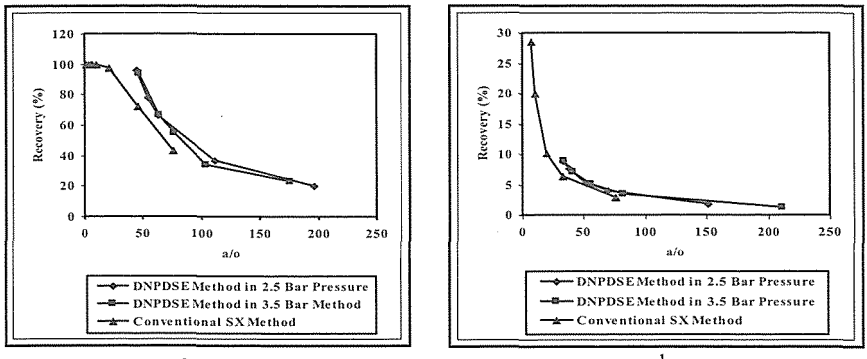

a b

Figure 6. Diagrams of recovery per a/o ratios in conventional SX and DNPDSE methods (a) dilute solution – (b) dense solution.

- Comparing the recovery diagrams for both methods indicated increased recovery rate in DNPDSE method compared with conventional SX method. For instance, increase amount in recovery for the dilute solution in A/O ratio of 45 was averagely 23 percent and for dense solution in A/O ratio of 33 it was 2.5 percent on the average. This numerical comparison shows proper DNPDSE method performance especially for dilute solutions.

- In DNPDSE method, decreased A/O ratio increased dilution amount of aqueous solution; therefore, recovery diagrams in this method were a result of more dilute solutions compared to conventional SX method, indicating better performance of this method in comparison with conventional X method.

- In DNPDSE method through decreased A/O ratio, on one hand - due to upward increase in volume of organic phase - the recovery rate was increased, and on the other hand because of increased dilution the conditions of metal ion recovery became more difficult. So, continuation of recovery diagrams in S method is a function of both above conditions. However, due to produced large contact area, it is expected that increased recovery, due to increase in volume of organic phase, be more than decrease in recovery because of dilution; though, it is predicted that decreased A/O ratio cause downward trend in this increase. Thus, use of lower dilution ratios through improved design of the contactor is especially important in lower A/O ratios.

3.2.3 Comparing the results of performance of the two methods in various pH and same A/O ratios

A/O ratios assigned to dilute and dense solutions was 45 and 33, respectively. While the ratio concerned for dilute solutions is sufficient to completely execute extraction process, but for the concentrated solution it was not possible to apply lower A/O ratios, because of limited column height.

3.2.3.1 Comparison of metal concentrations in organic phase in conventional SX and DNPDSE methods for both pressures

The studied diagrams for dilute and dense solutions are given in Figure 7. Due to lack of accurate implement of A/O ratio in DNPDSE method, comparing the obtained diagrams with regard to A/O ratios showed that:

- For both solutions, increase in concentration in organic phase was higher in 3.5 bar pressure than 2.5 bar.
- While the resulting diagrams for both solutions are not comparable - due to disparity of A/O ratio - but the effect of pH on metal concentration in organic phase (recovery) is more prominent for dense solutions.

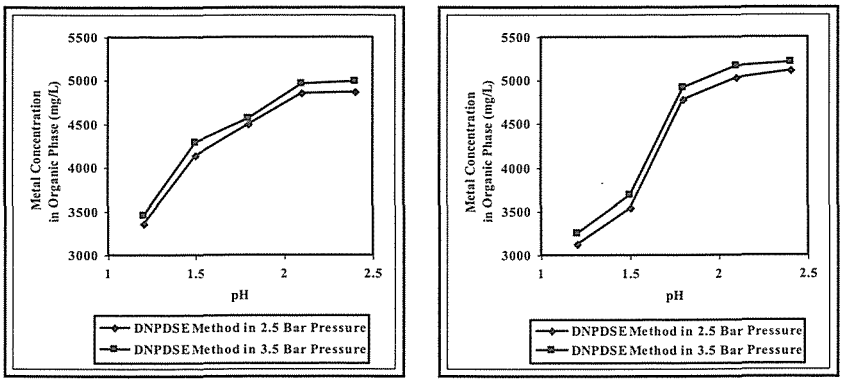

a b

Figure 7. Diagrams of metal concentration in organic phase per pH in DNPDSE method (two different pressures) (a) dilute solution – (b) dense solution.

3.2.3.2 Comparing metal concentrations in organic phase in conventional SX and DNPDSE methods for both pressures

The studied diagrams for dilute and dense solutions are given in Figure 8.

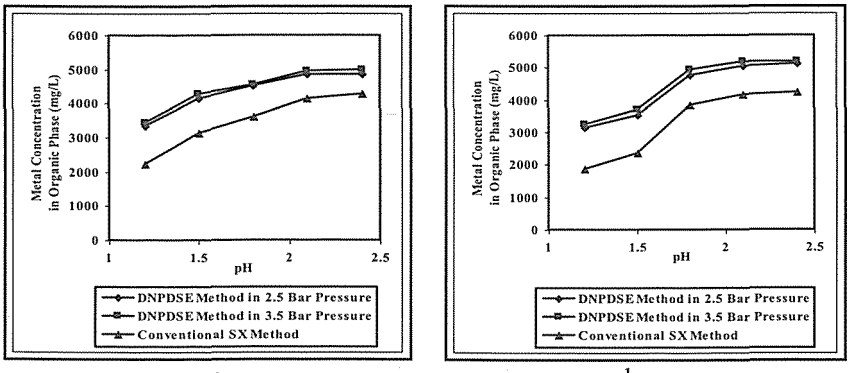

a b

Figure 8. Diagrams of metal concentration in organic phase per pH in conventional SX and DNPDSE methods (a) dilute solution – (b) dense solution.

Evaluation of the resulting diagrams showed that in DNPDSE method, for both pressures, the concentration amount in organic phase is considerably higher than that of conventional SX method - despite having a more dilute solution. In addition, changes amount of metal concentration in organic phase are more pronounced for dense solution in different pHs.

3.2.3.3 Comparing recoveries in conventional SX and DNPDSE methods for both pressures

The studied diagrams for dilute and dense solutions are given in Figure 9. Comparing recovery diagrams for both methods showed an increase in recovery in DNPDSE method, in comparison with conventional SX method. For instance, the amount of increased recovery for dilute and dense solutions in pH=2.4, was 22 and 2.75

percent (in average), respectively. In addition, the resultant recoveries in DNPDSE method were a function of more dilute solutions compared to conventional SX method; indicating proper DNPDSE method performance.

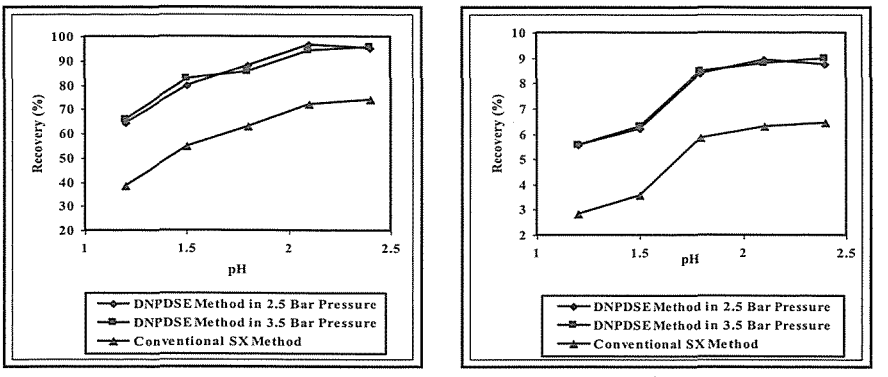

Figure 9. Diagrams of recovery per pH in conventional SX and DNPDSE methods (a) dilute solution – (b) dense solution.

4 CONCLUSION

Comparative analysis of performance of conventional SX and DNPDSE methods, in the same pHs or equal A/O ratios, indicated considerable increase in recovery, especially for dilute solutions, and metal concentration in organic phase, especially for dense solutions in S method. For instance, in studied conditions, the increase in recovery, i.e. metal concentration in organic phase, for dilute and dense solutions was on the average 22 percent (0.75 g/l) and 3 percent (1 g/l), respectively. Also, the results of evaluation of S method in two different pressures (2.5 and 3.5 bar) showed better performance of this method in higher pressures.

ACKNOWLEDGEMENTS

Authors are grateful to Tarbiat Modares University for supporting this research.

REFERENCES

Bolles, W.L., 1967, The Solution Of A Foam Problem, Chem. Eng. Prog., vol. 63, no. 9, p.p. 48-52.

Dibrov, I.A. Vornin, N.N., Kiemyatov, A.A., 1998, Froth Flotoextraction, A New Method Of Metal Separation From Aqueous Solution, International Journal of Mineral Processing, vol. 54, p.p. 45-58.

Doungdeethaveeratana, D., Sohn, H.Y., 1998, The Kinetics Of Extraction In A Novel Solvent Extraction Process With Bottom Gas Injection Without Moving Parts, Hydrometallurgy, vol. 49, p.p. 229-254.

Feris, L.A., Rubio, J., 1999, Dissolved Air Flotation (DAF) Performance At Low Saturation Pressures, Filtration & Separation, vol. 36, no. 9, p.p. 61-65.

Gupta, C.K., Mukherjee, T.K, 2000, Hydrometallurgy In Extraction Processes, vol. 1, CRC Press.

He, Y., Wu, Z., Mao, Z.S., 2007, The Resistance Of Interphase Mass Transfer In Colloidal Liquid Aphron Systems, Chemical Engineering Science, vol. 62, no. 10, p.p. 2803-2812.

Lazaridis, N.K., Peleka, E.N., Karapantsios, Th.D, Matis, K.A., 2004, Copper Removal from Effluent by Various Separation Techniques, Hydrometallurgy, vol. 74, p.p.149-156.

Lix 984N, 2010, Cognis Corporation Mining Chemicals, WWW. Cognis. Com.

Matsushita, K., Mollah, A.H., Stuckey, D.C., 1992, Predispersed Solvent Extraction of Dilute Products Using Colloidal Gas Aphrons and Colloidal Liquid Aphrons: Aphron Preparation, Stability and Size, Colloids and Surfaces, vol. 69, no. 1, p.p. 65-72.

Navarro, P., Alguacil, F.J., 1999, Extraction of Copper from Sulphate Solutions by Lix 864 in Escaid 100, Minerals Engineering, vol. 12, no. 3, p.p. 323-327.

Poorkani, M., Banisi, S., 2005, Industrial Use Of Nitrogen In Flotation Of Molybdenite At The Sarcheshmeh Copper Complex, Minerals Engineering, vol. 18, no. 7, p.p. 735-738.

Rao, K.S., Devi, N.B., Reddy, B.R., 2000, Solvent Extraction of Copper from Sulphate Medium Using MOC 45 as Extractant, Hydrometallurgy, vol. 57, p.p. 269-275.

Rydberg, J., Cox, M., Musikas, C., Choppin, G.R., 2004, Solvent Extraction Principles And Practice, Second Edition, Marcel Dekker, Inc. New York.

Save, S.V., Pangarkar, V.G., Kumar, S.V., 1994, Liquid-Liquid Extraction Using Aphrons, Sep. Technol., vol. 4, no. 2, p.p. 104-111.

Scarpello, J.T., Stuckey, D.C., 1999, The Influence of System Parameters on the Stability of Colloidal Liquid Aphrons, Journal of Chemical Technology and Biotechnology, vol. 74, no. 5, p.p. 409-416.

Sebba. F., 1987, Foams and biliquid foams, aphrons, Wiley, Chichester [West Sussex], New York.

Sohn, H.Y., Doungdeethaveeratana, D., 1998, A Novel Solvent Extraction Process With Bottom Gas Injection Without Moving Parts, Separation and Purification Technology, vol. 13, p.p. 227-235.

Tarkan,H.M., Finch, J.A., 2005, Air - Assisted Solvent Extraction : towards A Novel Extraction Process, Minerals Engineering, vol.18, p.p. 83-88.

Tarkan, H.M., Finch, J.A., 2006, Multi-Bubble Production In The Air - Assisted Solvent Extraction, Proceedings Of XXIII International Mineral Processing Congress, Promed Advertising Agency, Istanbul, p.p. 1340-1345.

Young, S.K., Dreisinger, D.B., Hackl, R.P., Dixon, D.G., 1999, Hydrometallurgy Of Copper, International Conference, Arizona, USA, vol. 4.

Evaluation the Influence of Performance Mode Dissolved Nitrogen Predispersed Solvent Extraction Method on Selectivity of Copper Solvent Extraction

Seyed Mohammad Javad Koleini, Mohammad Reza Tavakoli Mohammadi, Mahmoud Abdollahy

Mining Engineering Department, Mineral Processing Group, Tarbiat Modares University, Tehran, Iran

ABSTRACT Performing two phase mixture operations in solvent extraction method through stitution of bubble dispersion of organic solvent instead of its drop dispersion in aqueous phase is the basis of an innovative method called Dissolved Nitrogen Predispersed Solvent Extraction (DNPDSE).In this method, despite obtained advantages, expect increased extraction percent of interfering elements due to increased contact area, entrainment and precipitation flotation adversely affect selectivity of solvent extraction process.The results of experiments conducted on synthetic dilute and dense copper, zinc and iron solutions, in copper extraction pHs showed lack zinc recovery-no effect on total selectivity-in both methods and increased iron recovery-effect on partial selectivity-in DNPDSE method, compared with conventional SX method. The studies conducted this ascendant increased iron recovery with increased pH, as well as increased contact area, indicated in increased iron precipitation in solution and transfer of resulting precipitates through bubble entrainment and flotation precipitation to surface.

1 INTRODUCTION

Solvent extraction is an extremely useful chemical process in hydrometallurgy with extensive expansion, good acceptance, and a high efficiency for recovery of most elements in periodic table. Selectivity is one of the most important characteristics of this method. This feature effectively enables the concentration procedure (selectivity remove of metal) and purification procedure (selectivity remove of impurity) (Habashi 1999).

Selectivity in copper solvent extraction processes indicates capability of organic phase for selective transfer of copper ions from impure water leach solution to pure copper electrolyte used in electrowinning procedure. This feature can be affected by extraction chemistry, entrainment of aqueous leach solution in charged organic phase, and transfer of impurities in leach solution as cured in charged organic phase and stripping circuit (Merigold 1996).

Dissolved Nitrogen Predispersed Solvent Extraction (DNPDSE) considered as a new innovative method in solvent extraction in which two phases mixture operations is based on replacement of bubble dispersion of organic phase - colloid gas aphrons [CGAs] - instead of its droplet dispersion in aqueous phase. Therefore, due to presence of colloid liquid aphrons (CLAs), CGAs and natural air bubbles in this method and their probable effect on selectivity of the procedure, we compared the selectivity of conventional SX with DNPDSE methods for dilute and dense solutions.

In DNPDSE method decreased concentration of metals for aqueous phase is not just due to extraction procedure and dilution water is also effective in reducing their concentration; hence, it is impossible to

determine distribution coefficient and separation factor to compare selectivity for this method. In addition, reduced concentration of iron in aqueous phase is not merely due to extraction and dilution procedures, and another procedure by the name of precipitation flotation also occurs in pHs in which iron precipitates. So, it is not possible to determine iron concentration in organic phase for these pHs. Therefore, the best way to evaluate the selectivity of conventional SX and DNPDSE methods is comparison of actual recovery diagrams for each ion, resulted from extraction process or extraction process and precipitation flotation, in various pHs.

2 EXPERIMENTAL WORK

2.1 Principles

2.1.1 DNPDSE principles

This method is based on replacement of bubble dispersion of organic phase, i.e. colloid gas aphrons [CGAs], instead of its droplet dispersion in aqueous phase to enhance contact area, which causes increasing recovery rate and shortening equilibrium time, and also increase buoyancy force which leads to improved phase disengagement for organic phase. This method, developed with the goal of overcoming the difficulties associated with the use of solvent extraction method for dilute solutions, has been created by most using patterns of method proposed by Sebba (1987) by the name of Predispersed Solvent Extraction (PDSE).

In the PDSE method, the solvent phase that was changed to a biliquid foam called polyaphron (two-layered bubbles with oily nucleus) with minute dimensions and a large contact area was added to pregnant solution for mass transfer. Though these polyaphrons ascend to the surface because of being lighter than water, affected by gravity, this was usually performed very slowly due to tiny polyaphron size (Sebba, 1987). For this reason, CGAs consisting of aggregates of two-layered micro-sized bubbles stabilized by surfactant) were used to increase rising speed of CLAs to surface (due to hydrophobic property of soapy shell) (Save, et al, 1994).

But in the DNPDSE method the two general changes below were applied to take advantage of droplet to bubble change:

1. Conversion of CGAs in PDSE to ordinary air bubbles (to increase contactor performance speed, lack of dilution of the first solution, etc.) by passage of air produced by compressor through Spurger

2. Conversion of CLAs in PDSE to CGAs (to significantly enhance contact area, increase buoyancy force, etc.) by applying the below two stage procedure:

- Providing optimum conditions for foaminess of organic phase of CLAs (to provide better conditions for nucleation and bubble formation (Feris & Rubio 1999), etc.) through:

a) Choice of appropriate surfactant (silicone oil) for organic phase of polyaphron (Tarkan & Finch 2005).

b) Keeping organic phase and its resulting polyaphron cool until their transfer to tank (to increase foaming of oil products by decreased temperature (Bolles 1967), increased solution through decreased temperature (Feris & Rubio 1999) and augmenting security level).

- Use of DAF process and passage of CLAs under pressure from Reynolds tube.

Nitrogen is used instead of air in saturation process to prevent explosion, lack of chemical combination with organic phase (Poorkani & Banisi 2005), avert corrosion of tank wall, possible for complete tank saturation (Al- Shamrani et al, 2002), etc.

2.1.2 Precipitate flotation principles

In DNPDSE method, always parts of CLAs and CGAs take colloid form and remain suspended in the solution. These suspended particles have mainly negative charge and cause their stability by natural repulsion between colloid particles (due to similar charges). But presence of specific chemicals such as ferric sulfate can cause instability

and deletion of natural repulsion between this particles through coagulation phenomenon and provide their between bond (Sincero and Sincero, 2003, Al- Shamrani et al, 2002). When these coagulant is dissolved in water it is dissociated according to the below reaction:

$$Fe_2(So_4)_3 \longrightarrow 2Fe^{3+} + 3So_4^{2-} \quad (1)$$

After that, as regards the solution conditions (pH amount, etc.), various amounts of solid $Fe(OH)_3$ precipitate and other complexes such as $FeoH^{2+}$, $Fe(OH)_2^+$ and $Fe(OH)_4^+$ are formed (Sincero & Sincero 2003). These complexes combine with charged colloid particles of CLAs and CGAs due to opposing charges and form specific precipitations. Now if a surfactant is used that has a opposite charge to these precipitations, the surfactant is absorbed to the precipitation and all accumulate on the surface of gas bubble and are concentrated with bubble on the surface of solution as foam (Sebba 1987).

2.2 Reagents and solutions

2.2.1 In conventional SX method

Characteristic of synthetic aqueous dilute and dense solutions resulting from reagent grade $CuSO_4.5H_2O$ (MERK (Germany)) and also specifications of synthetic aqueous dilute and dense solutions made from reagents grade $CuSO_4.5H_2O$, $ZnSO_4.7H_2O$ (Fluka (Switzerland)) and $Fe_2(SO_4)_3$. (MERK(Germany)) and purposed selection criteria for their concentration have been cited in Tables 1 and 2.

Table 1. Specifications of synthetic aqueous solutions containing copper

Specifications	Dilute	Dense
Concentration (mg $CuSO_4.5H_2O$ /L)	500	7813
Concentration (mg Cu /L)	128	2000
The reason to choose the cited concentrations	Producing a very dilute solution to demonstrate desirable contactor performance	Producing a solution containing minimum permitted copper grade in input feed on circuit of SX (Lazaridis & peleka & Karapantsios & Matis 2004)

Table 2. Specifications of synthetic aqueous solutions containing copper, zinc and iron

Specifications	Dilute	Dense
Concentration (mg $CuSO_4.5H_2O$ /L)	500	7813
Concentration (mg $ZnSO_4.7H_2O$ /L)	566	8844
Concentration (mg $Fe_2(SO_4)_3.H_2O$ /L)	955	14922
Concentration (mg (Cu, Fe or Zn) /L)	128	2000
The reason to choose the cited concentrations	Making solutions with comparable concentrations of zinc, ferric and copper cations to provide similar conditions in extraction process for these elements and as a result feasibility of correct comparison of selectivity	

The used organic phase was a combination of 10 volumetric percent of chelating type extractant LiX 984N (Cognis) (with maximum loading of 5.1 g/l of copper (Cognis 2010)) and 90 volumetric percent of kerosene diluent (with a density of 0.78 g/ml). Extraction mechanisms of this extraction agent with copper, zinc, and ferric

metal cations which result in formation of insoluble complexes in water in each extraction pH is as follows (cognis 2010, Jha & Kumar & Singh 2001, Aminian & Bazin 2000, Ocana & Alguacil 1998):

$2RH_{(org)} + Cu^{2+}{}_{(aq)} \leftrightarrow R_2Cu_{(org)} + 2H^{+}{}_{(aq)}$ (1)

$2RH_{(org)} + Zn^{2+}{}_{(aq)} \leftrightarrow R_2Zn_{(org)} + 2H^{+}{}_{(aq)}$ (2)

$3RH_{(org)} + Fe^{3+}{}_{(aq)} \leftrightarrow R_3Fe_{(org)} + 3H^{+}{}_{(aq)}$ (3)

To adjust pH of the synthetic solution, a solution containing 500 mg/L sulfuric acid, a buffer solution containing 0.2 M NaOH, 0.04 M acetic acid, 0.04 M phosphoric acid, and 0.04 M boric acid (according to Finch researches (Tarkan & Finch 2005) was used.

2.2.2 In DNPDSE method

Also in this method the same reagents and solutions utilized in conventional SX method were used, except that respectively 0.3 g/l dilute silicone oil (Shin Etsu), 4 g/l sodium dodecylbenzene sulphonate (NaDBS) (Sigma(USA)) and 0.3 g/l dodecytrimethyl ammonium bromide (DTAB) (Aldrich(USA)) was used to produce organic phase polyaphron, aqueous phase polyaphron and aqueous phase of synthetic solution.

2.3 Methods

2.3.1 SX method

In this method, required A/O ratios, given volumes of aqueous solution (dilute or dense) and organic solvent were mixed in a beaker using a magnetic stirrer (500 rpm). After mixing (in period of given time), the contents of beaker were transferred to a separator funnel to separate organic and aqueous phases. The period of time required for complete separation was 20 minutes. After passage of this time, the aqueous phase separated and its equilibrium pH was measured. Finally, copper concentration in aqueous phase was determined using Absorption Spectrometry (AAS), and its concentrations in organic phase were calculated from copper concentration difference in aqueous phase before and after extraction equilibrium (Rao et al, 2000, Navarro and Alguacil, 1999).

2.3.2 DNPDSE method

This method consists of the two general steps as follows:

2.3.2.1 Polyaphron preparation

As preparation conditions affect size distribution and stability of CLA phase (He & Wu & Mao 2007, Scarpello & Stuckey 1999), the CLAs were prepared in relatively stable conditions. To this end, to produce 220 ml kerosene anionic polyaphron with PVR=10 (volumetric ratio of dispersed organic phase to continuous phase volume), 20 ml water containing 4 g/l anionic surfactant of NaDBS was dispensed in a 500 ml beaker and mixed well using a magnetic stirrer (900 rpm) to get gaseous foam (1^{st} step). Then the resulting gaseous foam was placed in a vessel including water and ice to lower its temperature (2^{nd} step). After that 20 ml of extraction agent Lix 984N was blended with 0.3 g/l non anionic surfactant of silicone oil and reached 200 ml by adding kerosene as diluents (3^{rd} step). The resulting organic phase was also placed in a vessel containing water and ice to lower its temperature (4^{th} step). After attaining desired temperature, the resulting organic phase was gradually (with a flow rate of 1.5 ml/min) added to foamy aqueous phase by mixing (5^{th} step). At first, solvent dispersion was easily achieved, but after addition of two third of solvent, the mixture quickly became viscous, and viscosity was increased up to complete dispersion of volume. Finally, a white creamy dispersion of CLA was reached (6^{th} step) (Save & Pangarkar & Kumar 1994, Matsashita & Mollah & Stuckey 1992). The resultant polyaphron was diluted for more contact area in continuous aqueous solution. For this reason, polyaphron was gradually added into distilled water with suitable pH, quadruple volume (regarding dilution constant of 5) and nearly 5 °C temperature accompanied by agitation of distilled water (7^{th} step). After

finishing the dilution, proper polyaphron for transfer into the column was reached (8th step).

2.3.2.2 Simultaneous extraction and separation

Simultaneous extraction and separation generally involves in two parts:

- Extraction and separation by making CGAs: in this part, after transfer of produced polyaphron and nitrogen gas for having 2.5-3.5 bar working pressure into tank, and allowing enough opportunity for solution for thirty minutes, the synthetic aqueous solution (1.5 liters) containing 0.3 g/l cationic surfactant DTAB was conveyed into the column. Then, considering the required aqueous/organic ratio, the polyaphron phase was injected into column through Reynolds tube, through counting injection times and measuring height difference of the solution within the column due to CGAs injection. The first sampling from aqueous phase (30 ml) was done from middle part of the column 6.5 minutes after the first injection.

- Extraction and separation by making air bubbles: After 7.5 minutes, by accurate adjustment of flow rate meter (0.1 l/min), required air for producing bubble to carry remaining CGAs to surface and more mixing of the two phases was provided by passing through Spurger. After finishing the operation, 7.5 minutes after second step, the whole remaining aqueous phase was carried to a container through underflow. by separation of the remaining organic phase from it using separator funnel, 30 ml of it was considered as the sample for the second step, to evaluate the effect of produced bubbles on extraction procedure. Total duration of these two steps was 15 minutes. Finally, copper concentration in aqueous phase of resulting samples was determined by Atomic Absorption Spectrometry (AAS) and its concentration in organic phase was calculated from copper concentration difference in aqueous phase before and after extraction equilibrium (Rao et al, 2000, Navarro and Alguacil, 1999).

3 RESULTS AND DISCUSION

3.1 The reasons to choose zinc and iron elements

Choice of zinc and iron as elements associated with copper was done according to Figure 1.

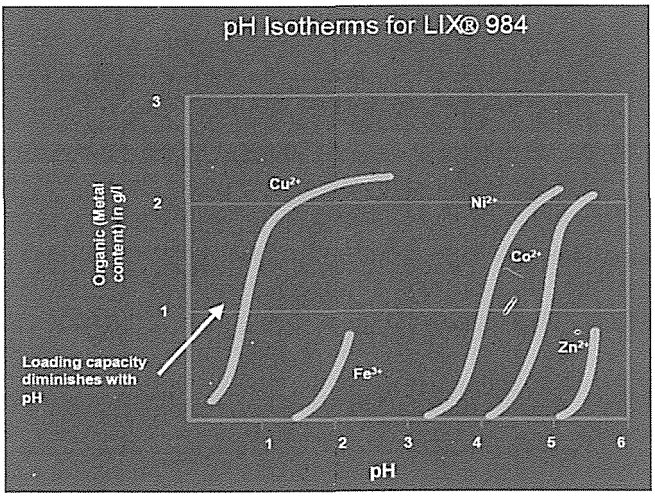

Figure 1. pH isotherms for Lix 984 (Sorensen et al, 2003).

Although in this figure diagrams of various ions concentration in organic phase for different pHs of extractant Lix984 has been plotted, because of higher selective extraction of copper relative to iron by Lix984N for higher extraction rate of type N products (Merigold 1996), it is anticipated that using Lix984N only increase copper ion concentrations in organic phase and decrease ferric ion concentration. According to the figure, appropriate pHs for recovery of ferric and zinc lies in 1.5-2.2 and 5-5.5 ranges, respectively. Therefore, ferric was chosen for survey of total selectivity as the only element with an extraction pH range partly overlaps that of copper. Besides, zinc was selected for survey of partial selectivity as one of the elements with an extraction pH range completely distinctive in relation to copper. In addition, in most of the pregnant solutions resulting from leaching section as input feed of SX circuit, these two elements are present as interfering elements. Hence, the mode of performance of DNPDSE method against these elements in extraction pHs of copper (0.5 to 2.5) is industrially important.

3.2 Evaluation of important copper, zinc, and iron components in synthetic aqueous solutions

Eh-pH diagrams in most of the scientific sources are only practical for a limited value of temperature, concentration, and element combinations. So, we used Eh-pH model of software HSC Chemistry to attain diagrams expressing important components of elements used in selected concentrations and temperatures. This software, while considering concentration of each and every elements in the solution, plots the diagram for all components containing main element, i.e. main element specify by user. Besides, by connecting dots the coordinates of which represent resulting Ehs from various pHs of synthetic solution, it indicates position of the synthetic aqueous solution (Roine 2002). Values in Tables 3 and 4 were used to plot position of synthetic aqueous solutions.

Table 3. Eh values for various pHs of synthetic dilute solution (containing copper, zinc and iron)

pH	1.2	1.5	1.8	2.1
Eh(mv)	760	755	750	741

Table 4. Eh values for various pHs of synthetic dense solution (containing copper, zinc and iron)

pH	1.2	1.5	1.8	2.1
Eh(mv)	778	772	767	760

Figure 2, depicted by considering copper as main element as well as zinc, iron. and sulfur as secondary elements, shows thermodynamic copper II distribution in synthetic aqueous solution as a function of Eh-pH. The important point in these two diagrams is presence of copper as Cu^{2+} in pHs under study for doing conventional SX experiments and DNPDSE.

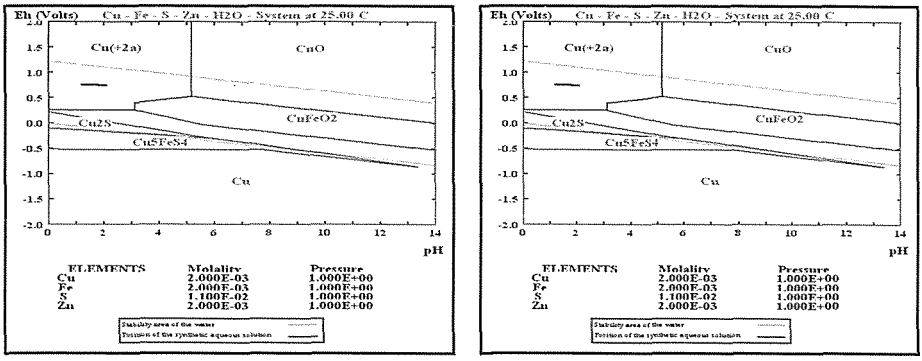

a b

Figure 2. Eh-pH diagrams of synthetic aqueous solutions containing copper, zinc and iron (for copper) (a) dilute solution - (b) dense solution.

Considering zinc as main element and copper, iron, and sulfur as secondary elements, the following two diagrams were plotted for dilute and dense solutions. The specified range in these two diagrams indicates presence of zinc as Zn^{2+} in pHs under study for doing experiments in conventional SX and DNPDSE methods.

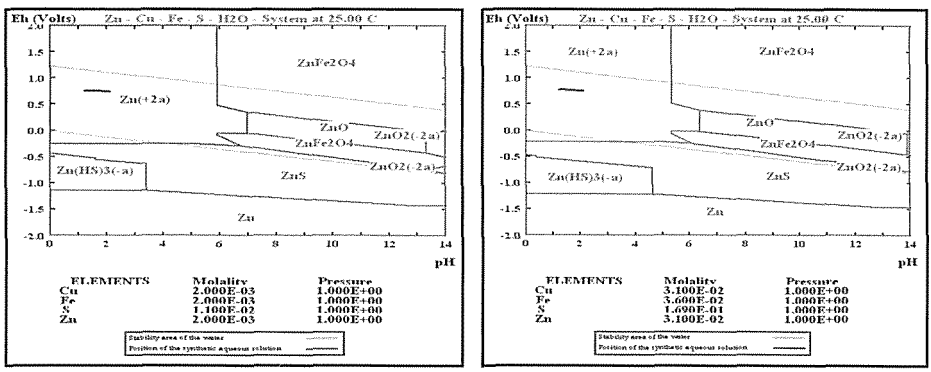

a b

Figure 3. Eh-pH diagrams of synthetic aqueous solutions containing copper, zinc and iron (for zinc) (a) dilute solution - (b) dense solution.

Finally, regarding iron as main element and copper, zinc, and sulfur as secondary elements, the two diagrams below were plotted for solutions under study. The indicated range in these two diagrams signifies presence of iron as precipitate and lack of its dissolving in the solution. This result revealed the most important drawback of HSC Chemistry software in plotting Eh-pH diagrams.

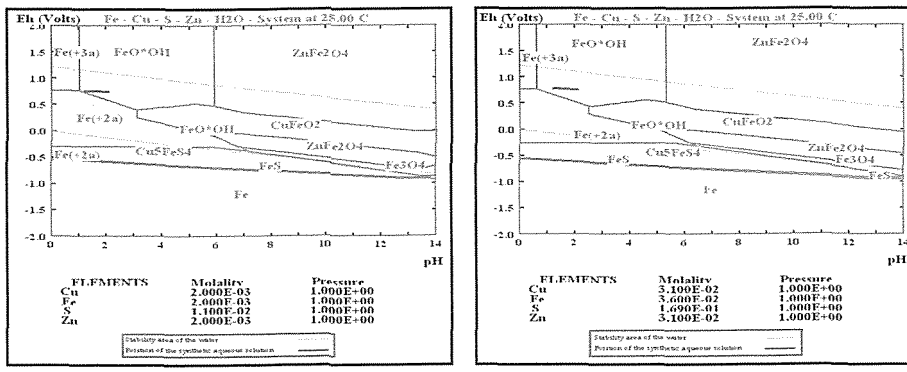

a b

Figure 4. Eh-pH diagrams of synthetic aqueous solutions containing copper, zinc and iron (for iron) (a) dilute solution - (b) dense solution.

Because of ignoring reaction rate (kinetics) in thermodynamic calculations, the HSC Chemistry software makes semi stable diagrams for components with slow reactions, such as dissolving iron sulfate in water, the results of which are partially controversial with practical actions done in the laboratory (Roine 2002). In other words, the range indicated in the two diagrams above showed the solution conditions immediately after pouring iron sulfate in it; while it is anticipated that with passage of time (nearly 20 minutes), the plotted range in the two diagrams move upward and Fe^{3+} stability range shifts to the right due to increased dissolving and enhanced Eh. As a result, the amount of Fe^{3+} in solution increased owing to reduced amount of precipitate. Moreover, it is expected that increased pH in 1.2 to 2.2 range decrease the amount of Fe^{2+} ion in the solution.

Other investigations performed for confirming the above results showed that as the hydroxide of the element precipitates, the following equilibrium is reached between hydroxide precipitate and metal ion that has remained soluble:

$$M(OH)_n \longrightarrow M^{n+} + n(OH^-) \quad (5)$$

And the equilibrium constant will be as follows:

$$K = a_{M^{n+}} \cdot a^n{}_{OH^-} \quad (6)$$

Assuming metallic ion concentration to be equal to its activity, the equation takes the below form:

$$K = [M^{n+}] \cdot a^n{}_{OH^-} \quad (7)$$

If the K value is known, we can calculate the initiation pH of metal hydroxide precipitation for different values of metal ion concentration. The given equations for ferric are as follows:

$$Fe(OH)_3 \longrightarrow Fe^{3+} + 3(OH^-) \quad (8)$$

$$K = [Fe^{3+}] \cdot a^3{}_{OH^-} = 1.58 * 10^{-39} \quad (9)$$

$$a^3{}_{OH^-} = 1.58 * 10^{-39} / [Fe^{3+}] \quad (10)$$

Equation 10 states change of precipitation initiation pH for different values of ferric ion concentration (Monhemius 1977). According to this equation and calculations done for dilute ($[Fe^{3+}] = 2*10^{-3}$ M) and dense ($[Fe^{3+}] = 3.6*10^{-2}$ M) synthetic aqueous solutions, precipitation initiation pH was respectively 1.96 and 1.55, considering negligible effect of these copper and zinc concentrations on precipitation initiation pH of iron.

Anyway, due to lack of effect of cationic and anionic surfactants used in DNPDSE method on Eh-pH diagrams, the solutions utilized for evaluating selectivity in both methods had quite comparable conditions.

3.3 Comparison of selectivity of conventional SX and DNPDSE methods

3.3.1 Evaluation of the general selectivity

To generally evaluate selectivity, zinc was used with an extraction pH quite distinct from copper. The results of conventional SX method indicated no extraction of this element in copper extraction pHs. But, in DNPDSE method, the amount of concentrations for zinc was less than its initial values in pregnant solution. Considering the water added to pregnant solution - resulting from dilution process - and determining its concentration after dilution, it was clear that execution mode of the DNPDSE method did not affect zinc concentration amount in aqueous phase. Therefore, difference in mode of performance for these two methods does not generally change selectivity.

3.3.2 Evaluation of the partial selectivity

Owing to the possibility of iron recovery in copper extraction pHs and its effect on copper recovery, by doing extraction experiments in both methods on dilute and dense synthetic solutions, containing copper and also containing copper, zinc and iron, we evaluated the partial selectivity by comparing recovery diagrams of copper and iron.

Figures 5 and 6 show actual whole recovery diagrams of copper in experiments performed in both methods in dilute and dense synthetic solutions, containing copper and containing copper, zinc and iron, where A/O ratios were 45 and 33, respectively.

The results for analysis of these diagrams showed that, due to high extraction Cu/Fe selectivity of Lix 984N (more than 2000 times) (Cognis 2010), presence of iron had not any considerable effect upon copper recovery rate in DNPDSE method and for both solutions produced comparable variation in values between resulting recoveries in the two methods (no change in proper performance of DNPDSE method in copper recovery).

On the other hand, it was expected that due to the same reason that copper recovery rate increased, i.e. increased contact area, in DNPDSE method, iron recovery rate also increase relative to conventional SX method, especially for more dense solutions and for application of lower A/O ratios. In fact, using this method predicted presence possibility of more iron in organic phase and in feed solution for electrolysis cells. So, to evaluate this issue and clarify the effect of precipitation flotation on iron recovery and reduced selectivity, we compared diagrams resulting from iron recovery (Fig. 7 and 8).

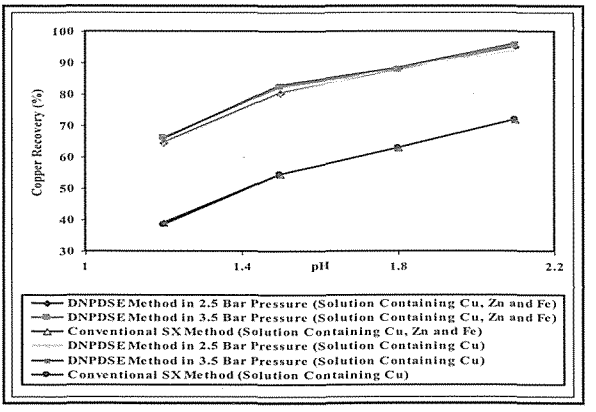

Figure 5. Copper recovery diagrams per pH in conventional SX and DNPDSE methods (dilute solution).

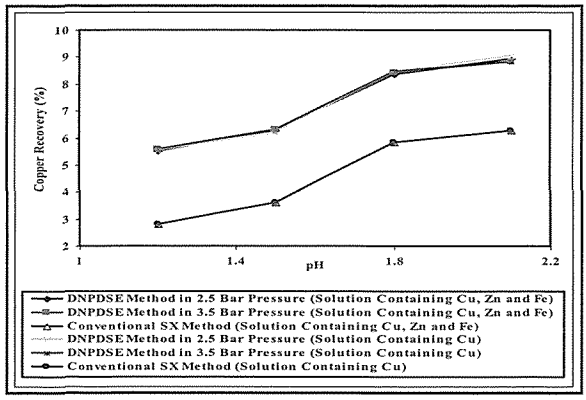

Figure 6. Copper recovery diagrams per pH in conventional SX and DNPDSE methods (dense solution).

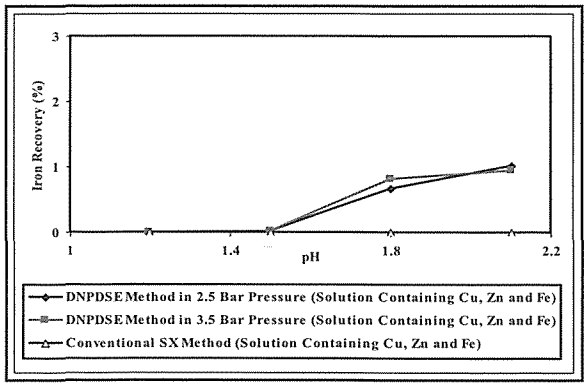

Figure 7. Iron recovery diagrams per pH in conventional SX and DNPDSE methods (dilute solution).

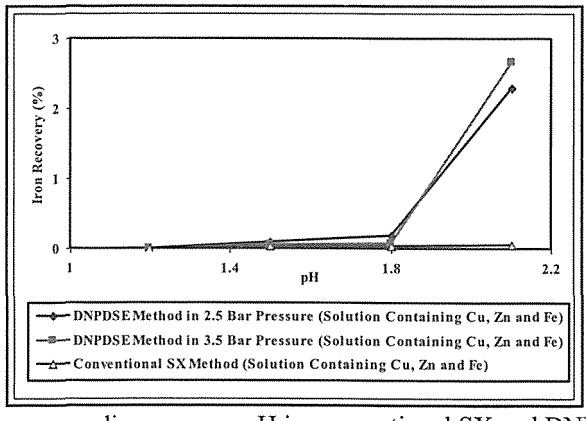

Figure 8. Iron recovery diagrams per pH in conventional SX and DNPDSE methods (dense solution).

Results of comparing the resultant diagrams state increased iron recovery in DNPDSE methods relative to conventional SX method, especially for dense solutions. However, this increased recovery is not just due to difference in execution mode of the two extraction methods, but increased iron precipitation with pH increase and transfer of resultant precipitates to surface, through precipitation flotation with air bubbles and CGAs in DNPDSE method, also decrease iron concentration in organic phase. Hence, part of recovered iron is not transferred into organic phase, and it is possible to eliminate it using simple methods such as washing the organic phase. Thus, considering this fact and also increased copper recovery in DNPDSE method relative to conventional SX method, it is anticipated that higher recovery of iron does not adversely affect proper DNPDSE method execution mode, especially for dilute solutions. Besides, according to other investigations, presence of iron can play an active role in reducing turbidity of remnant aqueous solution, owing to negligible presence of organic phase, in DNPDSE method. Figure 9 shows the orientation mode of organic phase, precipitates of flotation precipitation, and aqueous phase (clarified) on top of DNPDSE cell.

Figure. 9.Orientation mode of organic phase, precipitate and aqueous phase.

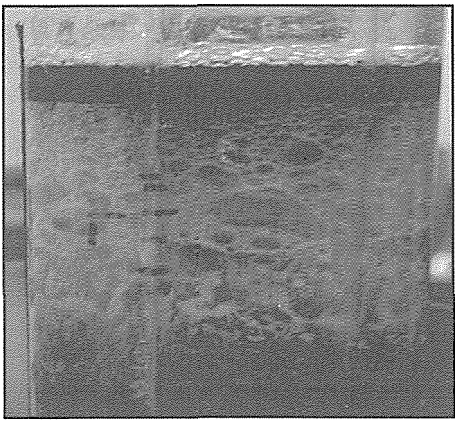

4 CONCLUSIONS

- The results of evaluation of important components of elements present in synthetic dilute and dense solutions, containing copper, zinc and iron, using HSC Chemistry software indicate presence of copper and zinc ions as Cu^{2+} and Zn^{2+} and iron as hydroxide precipitate in pH range 1.2 to 2.1, due to omission of solution kinetics by software. However, in numerical calculations performed the initiation pHs of iron hydroxide precipitation in dilute and dense solutions were 1.96 and 1.55, respectively.

- Lack of zinc recovery in conventional SX and DNPDSE methods showed that difference in execution mode of the two methods did not adversely affect the general selectivity.

- The results of comparing the partial selectivity of both methods showed that increased iron recovery rate in DNPDSE method, due to both extraction process and flotation precipitation, did not considerably affect proper performance of DNPDSE method owing to no transfer of significant amounts of iron in organic phase and concurrent increase of copper recovery rate.

ACKNOWLEDGEMENTS

Authors are grateful to Tarbiat Modares University for supporting this research.

REFERENCES

Al-Shamrani, A.A., James, A., Xiao, H., 2002, Destabilization of oil-water emulsions and separation by dissolved air flotation, Water Research, vol. 36, p.p. 1503-1512.

Al-Shamrani, A.A., James, A., Xiao, H., 2002, Separation of Oil from Water By Dissolved Air Flotation, Colloids and Surfaces A: Physicochemical and Engineering Aspects, vol. 209, no. 1, p.p. 15-26.

Aminian, H., Bazin, Z., 2000, Solvent Extraction Equilibria In Copper (II)-Iron(III)-Lix 984System, Minerals Engineering, vol. 13, no. 6, p.p. 667-672.

Bolles, W.L., 1967, The Solution Of A Foam Problem, Chem. Eng. Prog., vol. 63, no. 9, p.p. 48-52.

Feris, L.A., Rubio, J., 1999, Dissolved Air Flotation (DAF) Performance At Low Saturation Pressures, Filtration & Separation, vol. 36, no. 9, p.p. 61-65.

Habashi, F., 1999, Textbook of Hydrometallurgy, second ed., Metallurgie Extractive Quebec.

He, Y., Wu, Z., Mao, Z.S., 2007, The Resistance Of Interphase Mass Transfer In Colloidal Liquid Aphron Systems, Chemical Engineering Science, vol. 62, no. 10, p.p. 2803-2812.

Jha, M.K., Kumar, V., Singh, R.J., 2001, Review Of Hydrometallurgical Recovery Of Zinc From Industrial Wastes, Resources, Coservation and Recycling, vol. 33, no. 1, p.p. 1-22.

Lazaridis, N.K., Peleka, E.N., Karapantsios, Th.D, Matis, K.A., 2004, Copper Removal from Effluent by Various Separation Techniques, Hydrometallurgy, vol. 74, p.p.149-156.

Lix 984N, 2010, Cognis Corporation Mining Chemicals, WWW. Cognis. Com.

Matsushita, K., Mollah, A.H., Stuckey, D.C., 1992, Predispersed Solvent Extraction of Dilute Products Using Colloidal Gas Aphrons and Colloidal Liquid Aphrons: Aphron Preparation, Stability and Size, Colloids and Surfaces, vol. 69, no. 1, p.p. 65-72.

Merigold, C.R., 1996, Copper extractants: modified and oximes, a comparison, MID, CNNMIEC – Yunnan Company, BGRIMM Annual Technical Seminar, Kunming Yunnan Province, Peoples Republic of China.

Merigold, C.R., 1996, Lix Reagent Solvent Extraction Plant Operating Manual for Small and Medium Size Leach-Solvent Extraction—Electrowinning Copper Recovery Operations, Second Ed., Henkel Corporation, Minerals Industry Division, Tucson, Arizona, U.S.A.

Monhemius, A.J., 1977, Precipitation Diagrams for Metal-Hydroxides, Sulfides, Arsenates and Phosphates, T. I. Min. Metall. C., C202-C206.

Navarro, P., Alguacil, F.J., 1999, Extraction of Copper from Sulphate Solutions by Lix 864 in Escaid 100, Minerals Engineering, vol. 12, no. 3, p.p. 323-327.

Ocana, N., Alguacil, F.J., 1998, Solvent Extraction Of Iron(III) By MOC-55 TD: Experimental Equilibrium Study And Demonstration Of Lack Of Influence On Copper(II) Extraction From Sulphate Solutions, Hydrometallurgy, vol. 48, no. 2, p.p. 239-249.

Poorkani, M., Banisi, S., 2005, Industrial Use Of Nitrogen In Flotation Of Molybdenite At The Sarcheshmeh Copper Complex, Minerals Engineering, vol. 18, no. 7, p.p. 735-738.

Rao, K.S., Devi, N.B., Reddy, B.R., 2000, Solvent Extraction of Copper from Sulphate Medium Using MOC 45 as Extractant, Hydrometallurgy, vol. 57, p.p. 269-275.

Roine, A., 2002, Outokumpu HSC Chemistry for Windows, Chemical Reaction and Equilibrium Software with Extensive Thermochemical Database, Chapter 17: Eh - pH Diagrams (pourbaix-diagrams), Version 5.1., Outokumpu Research Oy, Pori.

Save, S.V., Pangarkar, V.G., Kumar, S.V., 1994, Liquid-Liquid Extraction Using Aphrons, Sep. Technol., vol. 4, no. 2, p.p. 104-111.

Scarpello, J.T., Stuckey, D.C., 1999, The Influence of System Parameters on the Stability of Colloidal Liquid Aphrons, Journal of Chemical Technology and Biotechnology, vol. 74, no. 5, p.p. 409-416.

Sebba. F., 1987, Foams and biliquid foams, aphrons, Wiley, Chichester [West Sussex], New York.

Sincero, A.P., Sincero, G.A., 2003, Physical-Chemical Treatment of Water and Wastewater, IWA Publishing, CRC PRESS, London, p.p. 545-592.

Sorensen, J.L., Milbourne, J., Kennedy, B., 2003, Hydrometallurgy 2003 Short Course, Case Study 1: Leach SX-EW Practices Technology Updates & New Ideas, AMEC E&C-Mining & Metals.

Tarkan,H.M., Finch, J.A., 2005, Air - Assisted Solvent Extraction : towards A Novel Extraction Process, Minerals Engineering, vol.18, p.p. 83-88.

Tarkan, H.M., Finch, J.A., 2005, Foaming Properties of Solvent for Use in Air-Assisted Solvent Extraction, Colloids and Surfaces A: Physicochemical and Engineering Aspects, vol. 264, p.p. 126-132.

Optimization of grinding circuit of Ardabil cement plant by BMCS software

E. Ghasemi Ardi[a,*], A. Farzanegan[b] and A. Valian[c]

[a] School of Mining, University College of Engineering, University of Tehran, Iran, ebrahim.ardi@gmail.com
[b] School of Mining, College of Engineering, University of Tehran, Iran, farzanegan@ut.ac.ir
[c] FARAKAP Consulting Company, Iran, a.valian@farakap.com

ABSTRACT: A multi-compartment tube ball mill in closed circuit with an air separator is very common for grinding of clinker product in most cement plants. Ardabil cement plant in north-west of Iran produces pozzolanic type of cement. To simulate the plant's grinding circuit many samples were collected from around the processing units and inside the tube mill in several stages. Then, particle size distributions of samples were determined with sieve and laser analyses. The raw data were mass balanced before being used in modeling and simulation studies. The tube mill was crash-stopped in order to collect samples from inside, along the mill axis at specified distances. Bond work index and breakage function for each size fraction was determined in laboratory. The industrial-scale selection function was estimated using NGOTC (Numerical Grinding Optimization Tools in C) using the obtained breakage function. After determination of breakage function, selection function, residence time distribution parameters and parameters of Whiten's model for air separator and the diaphragm between the two compartments, performance of the circuit was simulated by BMCS (BMCS-based Modular Comminution Simulator) software for a given throughput and feed particle size distribution. Parameters of Whiten's model were determined by GA (Genetic Algorithm) toolbox of MATLAB. The simulation results were compared with the

1 INTRODUCTION

About 2% of world's energy consumption is absorbed by cement factories, and about a 40% fraction of this amount is consumed for grinding of clinker and a 20% fraction for raw material grinding (Fujimoto 1993). According to such a high energy consumption, efficiency drop in the grinding circuits leads to a considerable increase in production expenses. Vice versa, a significant decrease in production expenses is accessible by a few percents increase in grinding circuit's efficiency. Moreover, optimization of grinding circuits may improve the quality of the product. Therefore, optimization of cement grinding circuits gets a high rate of interest because of its effect on lower energy loss and higher product quality.

Simulation of grinding circuits at steady state which is done based on validated mathematical models is a scientific tool for optimization purposes. Nowadays, it is possible to optimize grinding circuits or prepare an optimum design using process simulation tools. In this article, computer simulation of Ardabil cement grinding circuit is done using BMCS (BMCS-based Modular Comminution Simulator) software.

Ardabil cement plant in north-west of Iran consists of two production lines. This study was implemented on the finish grinding circuit which is located in the second line namely Z2. The Z2 grinding circuit is formed by a two-compartment tube ball mill in closed circuit with an air separator. A schematic flowsheet of Z2 circuit is shown in Figure 1, and design features of Z2 mill are given in Table 1.

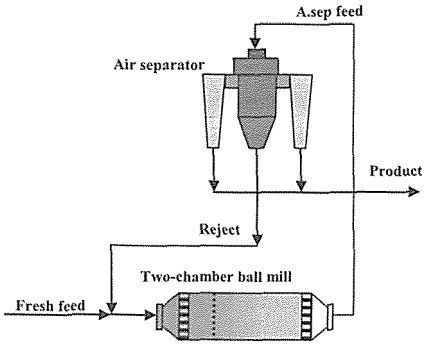

Figure 1. Simplified flowsheet of the Z2 grinding circuit.

Table 1. Design features of Z2 mill.

	First chamber		Intermediate diaphragm width (m)	Second chamber		Mill rotating speed (rpm)
	Inner diameter (m)	Effective length (m)		Inner diameter (m)	Effective length (m)	
Z2	3.75	4.25	0.92	3.9	7.83	15.6

2 ABOUT "BMCS"

BMCS is a recursive abbreviation for "BMCS-Based Modular Comminution Simulator" in which BMCS itself refers to the "Ball Milling Circuits Simulator" the primitive core of the current BMCS (Farzanegan 1998). BMCS version 5 is able to simulate any circuit arrangement consisting ball mills, rod mills, HPGRs, screens, hydrocyclones, efficiency curves, splitting and junction points and convergence of closed circuits. In this article we carry out the simulation using ball mill and efficiency curve modules; the former for simulation of compartments of a multi-chamber ball mill and the latter for simulation of the air separator and the diaphragm between two compartments. BMCS takes the advantage of population balance method and Weller's residence time distribution (RTD) modeling for simulation of ball mills, and Whiten's relationship for simulating efficiency curves.

In Figure 2, the flowchart of BMCS's program is shown. As it seems, structure of the simulator is modular and various units and operations are simulated sequentially based on a nodal representation of the circuit flowsheet. In circuits with no circulating load (recycle streams), sequential processing of nodes is done only in one pass. In case of closed circuits, in order to achieve the steady state, the sequential process is done iteratively until the pre-defined stopping criterion is satisfied.

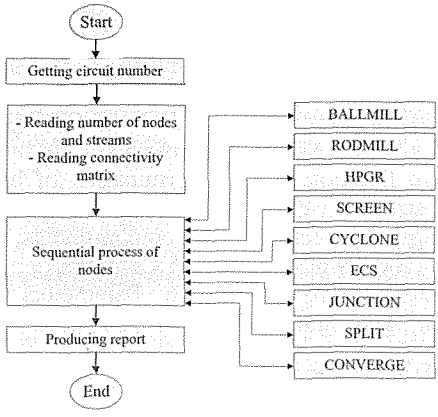

Figure 2. Flowchart of BMCS's program.

3 MODELING OF CEMENT GRINDING CIRCUITS

Modeling of both open or closed circuit of cement grinding is possible using two models: ball mill and efficiency curve.

The approach which is used to model Multi-chamber ball mills is based on mathematical modeling of ball mill. In Fig. 3, a double compartment tube ball mill is

shown which is modeled by a virtual system consisting two sequential simple ball mills in open circuit, one ball mill in closed circuit by a classifier, and another single ball mill at the end (Benzer et al 2001). The mentioned approach has been applied successfully to simulate cement mills in Turkey (Benzer 2001, Özer 2006, Genç et al 2009, Dundar 2010, Aydoğan 2010, Altun 2010) using JKSimMet software.

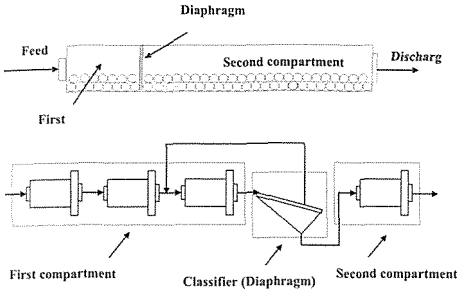

Figure 3. The approach used to model tube mills. Top: A real tube mill. Bottom: The virtual circuit consisting ball mills and a classifier (Benzer et al 2001).

The modeling of tube mills can be done by using ball mill model and a classifier model. The classifier can be modeled by the efficiency curve model. In case of closed circuits, efficiency curve model is also used to model the air separator. Therefore, efficiency curve model is used once to model an open circuit and twice to model a closed circuit.

Population balance method which is used to make the ball mill model is basically a mass balance equation for each size fraction between feed and discharge materials. According to mass balance equations and by considering Weller's model as the residence time pattern, ball mill model can be written as the matrix computations below (Eq. 1). BMCS uses this method for modeling of ball mills.

Equation 1:

$$m_d = T[I + S\tau_s]^{-2}[I + S\tau_l]^{-1} exp[-S\tau_{pf}]T^{-1}m_f \qquad (1)$$

where:

m_d : A column matrix defining the particle size distribution of discharge stream (percent retained)

T : The matrix defined by $T^{-1}[B-I]ST = -S$ equation

B : A lower triangular matrix defining the breakage function

I : Identity matrix

S : A diagonal matrix defining the selection function

τ_s : Mean residence time of small perfect mixer unit in Weller's model

τ_l : Mean residence time of large perfect mixer unit in Weller's model

τ_{pf} : Residence time of plug flow unit in Weller's model

m_f : A column matrix defining the particle size distribution of feed stream (percent retained)

During researches implemented by Lynch et al (2000), and JKMRC (Julius Kruttschnitt Mineral Research Center) institute in Australia Whitten's relationship was found to be valid for modeling of air separators. Also, researchers (Özer 2006, Dundar 2010) have applied Whitten's relationship to model the diaphragm (the virtual classifier which is shown in Fig. 3) between two compartments of tube ball mill. Whitten's relationship (Eq. 2) is written as:

Equation 2:

$$E_{OA} = C\left[\frac{\left(1+\beta.\beta^*.x\right)\left(e^{\alpha}-1\right)}{e^{\left(\alpha.\beta^*.x\right)}+e^{\alpha}-2}\right]$$

where:

E_{OA} : Fraction of feed reported to overflow

C : Fraction of material which is subjected to real classification (fraction of material which circulates the classification is $1-C$)

β : Fish hook parameter of the normalized efficiency curve

β': A parameter used to define d_{50c}

α: Parameter of separation sharpness of normalized efficiency curve ($d = d_{50c}$ when $E = \left(\frac{1}{2}\right)C$)

X: d/d_{50c} ratio

d: Mean size of size class

d_{50c}: Corrected cut size

4 SAMPLING, MASS BALANCE AND CALIBRATION

Model calibration for Z2 grinding circuit was carried out using sampling data. Before sampling, circuit stability was checked and proofed from control room. Then, an extensive sampling campaign was executed on all existing streams. The circuit was then crash stopped in order to go on sampling from inside the mill. In Figure 4, sampling points from inside and outside the mill are shown. This operation was done once again for this circuit (Z2) in different feed rate and particle size distribution of feed material. Consequently, two data sets were obtained. Particle size distribution of collected samples was determined with dry sieving and laser diffraction analyses.

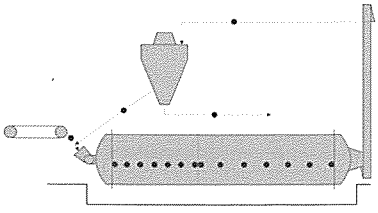

Figure 4. Sampling points inside and outside of a cement grinding mill.

After obtaining particle size distribution (PSD) and flow rate of each sampling point, mass balance was done using NorBal (Noranda Balance) software. This improved the quality of data set and led to a more accurate simulation. The measured size distributions were very close to adjusted values showing that sampling studies were performed successfully. In Figures 5 and 6, particle size distributions along the mill axis are shown for both chambers.

In next step, a representative sample of feed material consist of clinker, pozzolan, and gypsum, were analyzed for bond work index and breakage function. Bond work index was determined equal to 12.2 kWh/st.

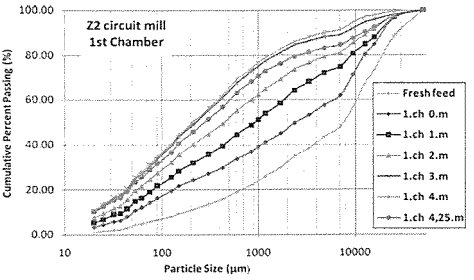

Fig. 5. Particle size distributions in 1st chamber.

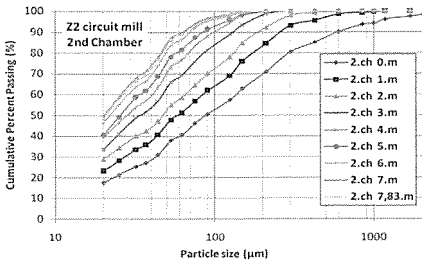

Figure 6. Particle size distributions in 2nd chamber.

To estimate the breakage function values by a laboratory-scale mill a single-sized sample that is a mass of material in one size fraction were prepared for each 22 size fractions, from +25400 µm down to 20 µm. An ideal single-sized sample never exists but a sample with more than 95% in a particular size fraction is an acceptable sample. The sample was ground for a small quantity of time, t. Then, grinding continued to time 2t, 4t, 6t etc until 40% to 60% of primary mass remains on the first sieve. After each grinding period, PSD of material were assessed and then the values of breakage function were calculated using BFDS

(Breakage Function Determination Software), (Yousefi et al 2005).

Calibration of the virtual ball mills that has been shown in Figure 3 was done using the obtained breakage function and sampling data. This consists of estimation of selection function for each virtual ball mill by back calculations using NGOTC (Numerical Grinding Optimization Tools in C) software. In all steps of the modeling and simulation process, Weller's residence time distribution parameters were assumed using the default values (τ_l=0.7, τ_s=τ_{pf}=0.1). Sampling data were also used in calibration of Whitten's model for virtual classifier (intermediate diaphragm). In fact, this classifier should be calibrated in its virtual closed circuit that is shown in Figure 3. To this purpose, the parameters of the virtual closed circuit should vary until obtaining a discharge stream with minimum difference of PSD with beginning point of second chamber. This operation was done using Genetic algorithm (GA) toolbox in MATLAB software. The results of calibration are shown in Figure 7.

The agreement between the measured and fitted size distributions of the fine product (PSD of beginning of 2nd chamber) was found to be perfectly satisfactory. The parameters of Whiten's relationship for classifying behavior of diaphragm are shown in Table 2.

Calibration of Whitten's model was also performed for the air separator. This calibration was easier than previous one because the streams around the air separator are tangible and can be sampled to determine its properties. Model calibration for the air separator was done with GA toolbox of MATLAB software and results are shown in Table 2.

5 VALIDATION OF SIMULATION

At the first step of simulation with BMCS, it is necessary to introduce the virtual circuit to the software. BMCS identifies the circuit arrangement by reading a matrix called connectivity matrix. This matrix should be written and added to library of saved connectivity matrices of the software.

As mentioned earlier, second set of data obtained from sampling was used for validation. Particle size distribution and flow rate of feed stream in this data set with parameters of calibration were introduced to BMCS.

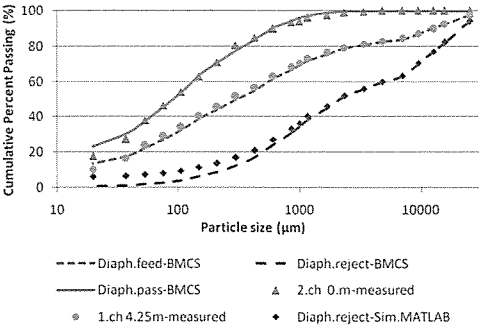

Figure 7. Comparison of measured and fitted size distributions of streams around the virtual classifier (diaphragm) in calibration step.

After running the simulation, predictions of the software were compared with measured data. The chart comparing the PSDs of prediction and measured data is shown in Figure 8. Measured and simulated feed rates are compared in Table 3.

Table 2. Whiten's model parameters for virtual classifier (diaphragm) and air separator

	C	α	β	β^*	d_{50c} (μm)
Diaphragm	1.0	0.366	0.0	1	584
Air separator	0.924	3.074	0.0	0.922	97

6 CONCLUSION

Comparison of predicted and measured size distributions (Fig. 7) showed that the maximum difference between them for mill output (air separator feed), reject from air separator (coarse) and product (fine) streams are in acceptable range. As it seems, simulation error for flow rate of mentioned streams is negligible. Consequently,

simulation operation is evaluated successful and accurate. This shows the high accuracy of sampling and calibration processes, and also validity of BMCS predictions and applied models.

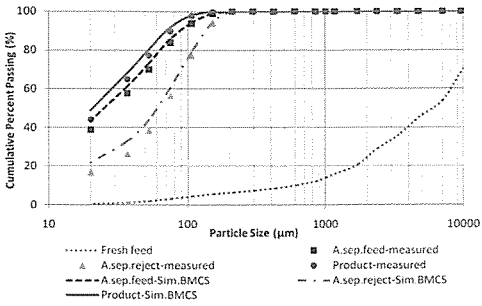

Figure 8. Comparison of measured and simulated size distributions.

Table 3. Comparison of measured and simulated flow rates.

streams	Measured (tph)	Simulated (tph)
Fresh feed	95.0	---
Air separator feed	116.82	118.621
Air separator reject	21.82	23.623
product	95	94.998

As mentioned earlier, simulation is a robust and accurate tool for optimization purposes. After successful simulation of Z2 grinding circuit of Ardabil cement plant, it is possible to run an optimization study on this circuit.

ACKNOWLEDGEMENT

The authors would like to thank all staff of Ardabil cement plant, especially Mr. Azami (managing director of plant), Mr. Geranmaye (plant manager), Mr. Farhadi (quality control manager), and Mr. Mokabber (production manager).

REFERENCES

Altun, O., Benzer, H., Dundar, H. and Aydoğan, N. A., 2010, Comparison of open and closed circuit HPGR application on dry grinding circuit performance. Miner. Eng. (2010), *doi:10.1016/j.mineng.2010.08.024*

Aydoğan, N. A., Benzer, H. 2010, Comparison of the overall circuit performance in the cement industry: High compression milling vs. ball milling technology. Miner. Eng. (2010), *doi:10.1016/j.mineng.2010.08.005*

Benzer, H., Ergun, L., Öner, M., Lynch, A.J, 2001, Simulation of open circuit clinker grinding, *Minerals Eng.* Vol. 14. 2001, No. 7, pp. 701–710.

Dundar, H., Benzer, H., Aydoğan, N. A., Altun, O, Toprak, A. N., Ozcan, A., Eksi, D. and Sargın, A., 2010, Simulation assisted capacity improvement of cement grinding circuit: Case study cement plant. Miner. Eng. (2010), *doi:10.1016/j.mineng.2010.08.003*

Farzanegan, A., 1998, Knowledge-based optimization of mineral grinding circuits, *Ph.D. theses*, Department of Mining and Metallurgical Engineering, McGill University, Montreal, Canada.

Fujimoto, S., 1993. Reducing specific power usage in cement plants. *World Cement* 7, 25–35.

Genç, Ö. and Benzer, A. H., 2009, Horizontal roller mill (Horomill) application versus hybrid HPGR/ball milling in finish grinding of cement, *Minerals Eng.* Vo. 22. pp. 1344-1349.

Lynch, A. J., Öner, M., Benzer, H., 2000, Simulation of a closed cement grinding circuits, *ZKG International* 10, pp. 560–567.

Napier-Munn, T. J., Morrell, S., Morrison, R. D. and Kojovic, T., 1996, Mineral Comminution Circuits; Their Operation and Optimisation, *JKMRC Monograph Series in Mining and Mineral Processing*, No. 2, Jullius Kruttschnitt Mineral Research Center, Australia.

Özer, C. E., Ergün, S. L., Benzer, A. H., 2006, Modeling of the classification behavior of the diaphragms used in multi-chamber cement mills, Int. J. *Miner. Process.* 80, pp. 58–70.

Yousefi, A.-A., Irannajad, M., Farzanegan, A., 2005. Determination of breakage function of ores using BFDS Software. In: *1st Iranian Mining Engineering Conference*, Tehran, pp. 1333–1347.

Flotation of Green Phosphate Sample of Esfordi Phosphate Mine

Mohammad Dehghani, Amin Ostovar, Majid Tatari, Sayed Ziaedin Shafaei
School of Mining Engineering, University of Tehran, Tehran, Iran

ABSTRACT This work is the result of studies on treating green phosphate sample of Esfordi phosphate deposit. Objectives are determining the possibility of processing the sample and reaching to sufficient phosphate grade and recovery and decreasing iron content of the product to acceptable amounts. In order to reach the objectives, primary experiments performed to determine the effective factors in flotation experiments. Pressure of desliming, flotation time, collector type, collector concentration, pH, pulp density, depressant type and its concentration were determined as effective factors and their optimum levels were determined in some experiments. Finally a test in optimum conditions and two stage of cleaning on its product was carried out. The results showed that it's possible to produce a product from this sample with 34.05% Fe_2O_3 content while recovery of the process is 71.38%. So treating the sample separately or with other samples of the mine is possible.

1 INTRODUCTION

Flotation as an effective process has a unique role in treating metallic and industrial ores. Many factors affect on flotation process that can be divided in various categories. In the first category, the factors depend on physicochemical characteristics of minerals exist in the ore. Second category of the factors depends on flotation conditions and methods such as direct flotation, reverse flotation, bulk flotation, sequential flotation and etc. Third category of the factors depends on properties and amounts of various reagents used in selective flotation of the ore such as collectors, depressants, modifiers and etc. in fourth category, factors depend on reaction kinetic, conditioning time and etc. Regarding umpteen effective factors in flotation, optimizing the process in order to producing product with determined properties needs designing and conducting experiments precisely and analyzing the results correctly.

1.1 Flotation of phosphates

Due to their determinant role in production of phosphoric acid and fertilizers, phosphate is in relation with the way of providing food for people of all countries. So it has strategic significance and in all countries there are plans to reach it directly.

Referring to a report from U.S geological survey (USGS) more than 60% of total phosphate are treated by flotation over the entire world in 2007. Concentration of phosphate by flotation is one of the commonest treating methods for phosphate since 1920. During two past decades, because of decrease of high grade phosphate ore supplies and need to produce materials with sufficient grade for phosphoric acid production, good efforts had been carried out in order to increase the recovery of phosphate flotation processes(Zaher & Abouzeid 2000).

Flotation of phosphate ores with silicate gangues is often a successful process

because of differences in surface characteristics between silicates and phosphate minerals. But flotation always meets some difficulties because of similar surface characteristics through treating ores with carbonate gangues (Henchiri 1993).

Igneous phosphates are macro crystalline and concentration them is simpler than sedimentary ores. Sedimentary phosphate minerals are micro crystalline and found in forms of apatite and collophane. Separation of this kind of phosphate from carbonates which accompany them is difficult process due to their similar surface characteristics (Ighal & Anwar 1996).

Regarding degree of liberation of phosphate minerals which is usually below 150 micron, flotation is common method for processing those minerals. Apatite flotation is categorized in low solubility salts flotation. These salts have low solubility in aqueous solutions and their surface decomposition in aqueous solution leads to production of various ions which cause their physico- chemical manner to be complicated and flotation of them to be nonselective. Adsorption density, hydrophobicity and flotation recovery decrease from flourapatite to carbonate apatite, hydroxyl apatite and cholerapatite. It's proved that oleates as the best collectors in phosphate flotation in all cases in presence of alkyl succinates and alkyl sulfonates adsorbs by chemical adsorption mechanism and produces calcium oleate. In flotation of oxide and silicate minerals, tall oils adsorption from anionic collectors category on mineral surface is a paragon for chemical adsorption and alkyl sulfonates adsorption from anionic collectors and amines adsorption from cationic collectors are instances of physical adsorption (Ighal & Anwar 1996).

1.2 Esfordi phosphate plant

In Esfordi phosphate plant ores after exploitation are transferred to crushing unit by dump trucks. The ores with maximum size of 600 mm are feed to a 100t/h jaw crusher through a 60cm*60cm grizzly and a feeder. In this unit, particles below 75mm separated before crusher. The amount of these particles is about 40 t/h. product of the jaw crusher and materials which separated before crushing provides feed for cone crusher with size of 0-175mm. Cone crusher product (0-50mm) sent to a double deck screen with separation size of 22mm, coarse particles return back to the cone crusher in a closed circuit. Materials below 22mm are piled up in feed store of concentration unit with capacity of 4000m^3. This feed then enters a rod mill by a conveyer belt in 57.5 t/h feeding rate. The rod mill product (d_{80}=600 micron) is pumped to a hydro cyclone in pressure of 0.06 bar. Underflow of the cyclone (d_{80}=750 micron) feed to a ball mill which is in closed circuit with the hydro cyclone to reground it and produce particles below 100 micron. Overflow of the cyclone (-150 micron) is pumped to a cluster hydro cyclone for desliming at pressure of 2.4 bar. Overflow of the cluster hydro cyclone (-10 micron) is sent to tailing dam. Underflow of this cyclone enters to conditioning unit as flotation feed (Karimi & Tabatabaei 2003).

In the first conditioner starch is added to depress iron compounds and NaOH is added to set pH at 9.5. In the second conditioner FLO-Ys20 and Lina-Z80 are added as apatite collectors. Overflow of the second conditioner enters rougher flotation cells to recover apatite. Froth produced in rougher cells enters cleaner and re-cleaner cells for more concentration. Re-cleaner cells product as phosphate concentrate which contain 39% P_2O_5 enters a thickener. Underflow of the thickener is dewatered by a drum filter. This filter product is final phosphate concentrate. Flotation tail is sent to low and high field intensity magnetic separator to recover iron. Iron concentrate which contain 64% iron is sent to thickener and filter (Karimi & Tabatabaei 2003).

2 MATERIAL AND METHOD

2.1 Feed

Mineralogical studies on Esfordi phosphate sample was carried out by microscopic

method. These studies showed that about 15% of the particles are iron compounds which 70% of them were magnetite and 30% consist of almost hematite particles. Transparent minerals were apatite, quartz, calcite, amphibole, clay minerals mostly montmorillonite, clyno pyroxene and platy minerals like talk and in very low amounts epidote. In the sample inclusions which contain REE (rare earth elements) can be seen. Chemical analysis carried out on the sample to determine its composition. The results are presented in table 1. Degree of liberation for apatite and magnetite particles determined to be below 100 micron.

Table 1. Chemical analysis results.

CaO	SiO_2	Fe_2O_3	P_2O_5
26.38%	30.52%	16.55%	10.72%

2.2 Flotation experiments

At first some flotation experiments were conducted to distinguish conditions and factors effects on flotation results by using reagents which are used in the plant and some other reagents and in presence of fine particles in the feed. Then other experiments were conducted by removing fine particles from the feed. Conditions and results of these experiments are presented in table 2. By studying these experiments results, effective factors and their levels were half determined. Regarding obtained results some experiments were carried out to determine optimum levels of factors. In this step by varying each parameter in various levels while other factors kept fixed, optimum level of each of them were determined. Finally an experiment was conducted in optimum levels of effective factors to confirm the conclusion.

Table 2. Conditions and results of primary experiment

No.	Collector Conc. (g/t)	Depressant Conc. (g/t)	pH	Desliming Press. (kg/cm^2)	Weight (%)	Grade		Recovery of Flotation (%)	Total Recovery (%)
						P_2O_5	Fe_2O_3		
1	600 FLO-Ys20 80 Lina-Z80	400 Starch	9.5	-	43.77	32.41	12.96	97.87	97.87
2	800 FLO-Ys20 100 Lina-Z80	400 Starch	9.5	-	46.4	30.64	15.84	98.26	98.26
3	400 ALKE 400 Dirol	400 Starch	9.5	-	44.49	29.66	18.92	97.70	97.70
4	500 ALKE 500 Dirol	400 Starch	9.5	-	46.03	28.84	20.76	98.40	98.40
5	600 FLO-Ys20 80 Lina-Z80	800 Starch	9.5	-	42.73	30.95	14.88	98.30	98.30
6	600 FLO-Ys20 80 Lina-Z80	400 Sodium Silicate	9.5	-	47.5	27.78	21.77	98.60	98.60
7	600 FLO-Ys20 80 Lina-Z80	800 Sodium Silicate	9.5	-	42.57	30.92	17.05	95.86	95.86
8	400 ALKE 400 Dirol	400 Sodium Silicate	9.5	-	43.27	30.82	17.25	97.67	97.67
9	600 FLO-Ys20 80 Lina-Z80	400 Starch	10.5	-	46.48	29.94	17.61	98.48	98.48
10	600 FLO-Ys20 80 Lina-Z80	400 Starch	8.5	-	58.67	23.21	36.16	98.07	98.07
11	600 FLO-Ys20 80 Lina-Z80	400 Starch	9.5	0.5	34.89	35.86	8.99	95.10	83.03
12	600 FLO-Ys20 80 Lina-Z80	400 Starch	9.5	0.7	37.15	35.07	11.14	96.33	85.84
13	600 FLO-Ys20 80 Lina-Z80	400 Starch	9.5	1	36.41	34.76	10.42	95.44	87.06
14	400 Oleic acid	400 Starch	9.5	0.5	41.29	31.74	16.98	94.70	82.68

From 14 primary experiments (tab 1) it can be concluded that in experiments without desliming contrary to the conception that apatite flotation is sensitive to fines, recovery was more than 95%. The only minor problem in presence of fines was comparatively long flotation time. Although in these experiments no vast variation were

seen in phosphate grade but using FLO-Ys20 and Lina Z80 led to better results for phosphate and iron grades. The results also showed that starch is better depressant than sodium silicate for this ore. By performing experiments with desliming phosphate grade increased and iron grade decreased. In various desliming pressures 0.5 kg/cm^2 led to better results.

2.3 Optimization

Regarding primary experiments and their results, it concluded that using reagents which are used in Esfordi plant lead to better results than other reagents so optimizing experiments were carried out using these reagents. Results also showed that deslimin led to shorter flotation time and noticeable increase in phosphate grade of concentrate. So in spite of decrease in recovery optimization experiments were carried out with desliming.

2.3.1 Optimizing collector concentration

Five experiments were carried out to optimize collector concentration, conditions and results of these experiments are presented in table 3 and effects of various collector concentrations on recovery are shown in figure 1. By decreasing collector concentration, recovery decreased intensely. By decreasing collector concentration to 500 g/t recovery fell to below 80% and by increasing collector concentration to 700 g/t FLO-Ys20 recovery reached to 95% but P_2O_5 grade of concentrate is low to some extent (25.73%). So 600g/t FLO-Ys20 and 80 g/t Lina-Z80 was chosen as optimum collector concentration. In these conditions a concentrate was produced with 30.63% P_2O_5 grade and recovery of 86.16%.

Table 3. Collector concentration optimization experiments

No.	Collector Conc. (g/t)		Grade (%)		Recovery of Flotation (%)
	FLO-Ys20	Lina-Z80	P_2O_5	Fe_2O_3	
1	700	90	25.7	4.5	95.96
2	600	80	30.6	4.28	86.16
3	550	70	32.1	3.83	78.20
4	400	60	31.5	3.80	70.45
5	350	50	30.6	4.44	32.66

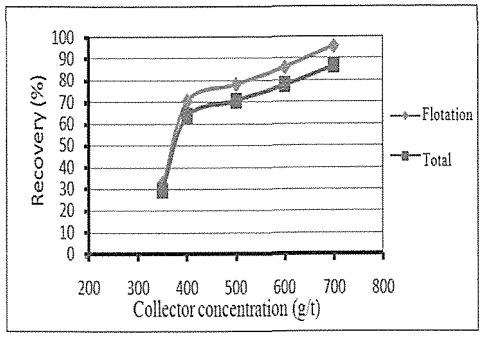

Figure 1. Effect of collector concentration on recovery

2.3.2 pH optimization

Collector and frother concentration fixed during experiments at 600 and 80 g/t for FLO-Ys20 and Lina-Z80 respectively and 400 g/t starch used as depressant. pH varied in three levels 8.5, 9.5 10.5 in three levels. Conditioning time was 7 minutes for depressant and 5 minutes for collector. Desliming was performed under pressure of 0.5 kg/cm^2. Results of these experiments are presented in table 4.

Table 4. pH optimization experiments

No.	pH	Grade (%)		Recovery of Flotation (%)
		P_2O_5	Fe_2O_3	
1	8.5	27.5	3.95	63.66
2	9.5	30.63	4.28	86.16
3	10.5	25.38	5.56	91.08

As it can be seen by increasing pH amount, recovery increased. Increasing in recovery is noticeable when pH varies from 8.5 to 9.5 but by increasing pH from 9.5 to 10.5 recovery varies a little. In pH=9.5 phosphate and iron grades of concentrate are in better state than other pH amounts.

2.3.3 Optimizing depressant concentration

In order to optimize depressant concentration, three experiments were carried out. In these experiments pH and collector concentration set at amounts which determined in previous experiments. Starch used as depressant, variations in its concentration is shown in table 5.

Table 5. depressant concentration optimization experiments

No.	Starch Conc. (g/t)	Grade (%)		Recovery of Flotation (%)
		P_2O_5	Fe_2O_3	
1	8.5	27.5	3.95	63.66
2	9.5	30.63	4.28	86.16
3	10.5	25.38	5.56	91.08

Regarding above table it can be concluded that by increasing starch concentration, Fe_2O_3 grade decreased and P_2O_5 grade increased in concentrate but recovery decreased. So using 400 g/t starch leads to better grades of concentrate and recovery.

2.3.4 Optimized experiment

An experiment was carried out in optimum conditions and to purify the product more, two stages of cleaning performed on the concentrate of rougher. To provide feed for this experiment the sample was milled to size -100 micron and deslimed in pressure of 0.5 kg/cm^2 carried out. Results of this experiment are shown in table 6. As it can be seen by two stages of cleaning a concentrate was produced which containe 34.05% P_2O_5 and 2.11% Fe_2O_3 while recovery of flotation was 71.38% and recovery of the whole process was 64.56%. It should be noted that to determine real amount of recovery tails of second and third stages should also be calculated, because they sent back to the circuit.

Table 6. Optimized experiment

Product	Grade (%)		Recovery of Flotation (%)	Total Recovery (%)
	P_2O_5	Fe_2O_3		
Concentrate	34.05	2.11	71.38	64.56
1st Tail	0.6	20.78	2.59	2.34
2nd Tail	10.25	4.02	14.50	13.11
3rd Tail	1.1	5.07	11.53	10.43

3 CONCLUSION

In this work processing of green phosphate ore of Esfordi deposit which is not treated in the plant yet because of existence of clay minerals is studied. Observed results showed that notwithstanding the problems of existence of fines, processing this ore with acceptable recovery is possible. By performing desliming before flotation P_2O_5 grade increased and Fe_2O_3 grade decreased noticeably in concentrate but recovery decreased too. Experiments showed that using reagents which are used in the plant such as starch, FLO-Ys20 and Lina Z80 lead to better results. Optimization experiments showed that optimum collectors concentration are 600 and 80 g/t for FLO-Ys20 and Lina Z80 respectively. Optimum pH determined to be 9.5 and optimum starch concentration determined to be 400 g/t. Finally an experiment conducted in determined conditions and two stages of cleaning carried out on rougher concentrate. This experiment produced a concentrate which containe 34.05% P_2O_5 and 2.11% Fe_2O_3 while recovery of flotation was 71.38% and recovery of the whole process was 64.56%.

REFERENCES

Henchiri, a., 1993. A contribution to carbonate-phosphate separation by flotation technique, *Beneficiation of Phosphate - Theory and Practice,* 1, 22, pp.225-230.

Ighal, Z., Anwar, M., 1996. Innovation in beneficiation technology for low grade phosphate rocks, *Nutrient Cycling in Agroecosystems,* 1,46, pp.135-151.

Ighal, Z., Anwar, M., 1996. A new route for the beneficiation of low grade calcareous phosphate rocks, *Fertilizer Research*, 1, 44, pp.133-142.

Karimi, G., Tabatabaei, A., 2003. *An investigation on Yazd province mineral processing plants,* Iran mineralogy and exploration institute, Tehran, 209 p.

Zaher, A., Abouzeid, M., 2008. Physical and thermal treatment of phosphate ores - An overview, *International Journal of Mineral Processing*, 1, 85, pp.54-55.

Iron Removal from Mehran Fireclay Sample by Dry Magnetic Separation

Amin Ostovar, Mohammad Dehghani, Mohammad Noaparas, Sayed Ziaedin Shafaei
School of Mining Engineering, University of Tehran, Tehran, Iran

ABSTRACT Mehran fireclay mine is located in Abadeh, north of Fars province, Iran. Commercial ore of this mine contains Pyrophyllitic Hydromica Shale. Materials which exploited from the mine can be transferred for applying in consuming industries directly, if contain low iron content (less than 2%). Materials which contain high iron content, as inferior products have low prices. The sample which prepared for mineral processing experiments contains more than 10% of Fe_2O_3.

Feed size, magnetic field intensity, separator blades angles, feeder speed and drum rotating speed were determined as effective factors. By varying these factors in several levels, best conditions to produce a product with minimum iron grade were determined. To achieve sufficient grade one stage of cleaning carried out on the concentrate and a product with 1.97% Fe_2O_3 was produced while recovery was about 25%. This process produces a middling in a large portion that causes the recovery to be more than this amount.

1 INTRODUCTION

1.1 Fireclay and Mehran mine

Fireclay is applied for clays which contain high amount of alumina (more than 25%) and low amount of impurities (alkalis and iron oxide), its color doesn't go white in high temperatures and its P.C.E (pyrometric cone equivalent) is more than 19 (Ghorbani & Arzani 1994). In other definition any soil which withstands temperatures more than 1500°C and contain considerable amount of Al_2O_3 is called fireclay (Monshi 1996). Existence of impurities such as iron and titanium compounds cause decrease in softening point of the fireclay product (Nourian 1983).

Mehran fireclay mine is located near Abadeh in north of Fars province in Iran. The mine products applied in industries such as glaze, porcelain, ceramics and tail industries. In this ore main gangues are iron minerals. When the exploited materials contain low amount of iron minerals it can be transferred to consuming industries without any treatment for removing iron compounds. But materials which contain high amount of iron compounds need to be treated in order to decrease iron content but no plant is established to process the ore yet and this is because of existence of deposit with low iron content. Now by draining these materials it's seems necessary to process inferior materials. In table 1 specification of the mine products and their prices can be seen. Comparing the prices can help to perceive the necessity of establishing a mineral processing plant.

Table1. Specifications of the mine products

Product	Fe_2O_3 (%)	Al_2O_3 (%)	SiO_2 (%)	Price (Rls/t)
MP100	1.5-2	30	58	500000
MP300	3-4	28	57	250000
MP400	4-5	28	57	150000
MP500	5-8	27	50	70000
MP600	8-12	26	50	50000
MP700	12-16	25	48	40000

1.2 Magnetic separation

Magnetic concentration is achieved by simultaneously applying to all the particles in an ore magnetic force which acts on magnetic particles and a second force or combination of forces which acts in a different direction and affect both magnetic and non magnetic particles. The most commonly applied nonmagnetic forces are gravitational, centrifugal and fluid drag.

Magnetic separators can be classified in four categories depending on the fluid medium used: either air or water, and the strength of the magnetic field, either standard or high intensity. A magnetic separator is generally classified as standard intensity if its maximum field intensity is less than about 0.20 T. High intensity separators generally have field strengths of 1 to 2 T. Standard intensity separators are used to recover ferromagnetic materials, such as iron and magnetite. High intensity separators must be used to treat weakly magnetic minerals, such as hematite.

In high intensity dry magnetic separation the magnetic attraction force is generally opposed by centrifugal and /or gravitational force. The magnetic force can be calculated from equation 1. Since magnetic force is proportional to the volume of the particle, particle size influences the separation only in cases where secondary forces become significant.

$$F = \frac{1}{2}\chi\mu_0 V\nabla(H^2) \qquad (1)$$

In the above equation, F is magnetic force in N, χ is susceptibility which is dimensionless, μ_0 is magnetic permeability in H/m, V is volume of the particle in m^3 and H is magnetizing field in A/m (lawver & Hopstock 1985).

The minerals treated by high intensity magnetic separation are generally so weakly magnetic that magnetic interaction between particles are negligible. However, physical interactions between particles become significant at higher feed rates. On separators in which the magnetic minerals are held onto a magnetic rotor, significant entrainment of nonmagnetics in the magnetic fraction may occur.

The separation efficiency of high intensity dry magnetic separators decrease as the feed size falls below 50μ. Fine particles tend to adhere to each other and to parts of the machine by electrostatic and other adhesive forces. Thus, there is no longer the balance involving only magnetic, centrifugal and gravitational forces which enables one to make a precise separation based only on differences in magnetic susceptibility (Rezaei 1999).

2 MATERIAL AND METHODS

2.1 Feed

A sample was taken from Mehran mine for mineral processing experiments. This sample was studied by microscopic mineralogical investigations and XRD method and impurities grades were determined by chemical analysis. XRD results showed that minerals in different size fractions are: quartz, montmorillonite, feldespar, kaolinite, chlorite, pyrophyllite, halloysite, hematite, goethite, limonite, illite, richterite and nacrite. As it can be seen above iron minerals are the most important impurities in the sample. Microscopic investigations revealed that in the sample limonite predominate over other gangues and more than half of its particles are finer than 20μ. Chemical analysis showed that the sample belongs to MP600 category of the mine products and Contain 10.1% Fe_2O_3.

In order to provide feed for magnetic separation experiments, at first the sample

was crushed in two stages by jaw crusher and one stage by roller crusher to decrease particles size below 2 mm. Then feed of experiments prepared in various sizes from this material

2.2 Experimental

Regarding the mineralogical analysis results, limonite, hematite and goethite (weak magnetic minerals) are iron minerals in the sample so to remove them from the ore by magnetic separation high intensity field is needed. Induced roll dry magnetic separator was applied to carry out the separation experiments. All the experiments were carried out in mineral processing laboratory of university of Tehran.

Feed size, magnetic field intensity, separation blades angles, feeder speed and rotating speed of the roller were determined as most effective factors on results. Some experiments had been carried out to determine feeder speed and roller speed. By studying separation results in various speeds of feeder and roller, their optimum levels were determined and kept fixed through all the experiments. In each step by varying separation blades angle in 4 levels, while feed size and filed intensity were fixed, with respect to the color of the products (darker materials contain more impurities) and weight percentages of them, best conditions for blades were determined in those feed size and field intensity. Products of this experiments were analyzed for determining iron content and if grade and recovery were acceptable one or two stages of cleaning were carried out to get close to the target grade (<2% Fe_2O_3). This trend continued for other feed sizes and field intensities. The blade angels were determined for each size fraction and field intensity separately. Schematic stages of experiments are shown in figure 1 and conditions of experiments and their results are shown in Table 2.

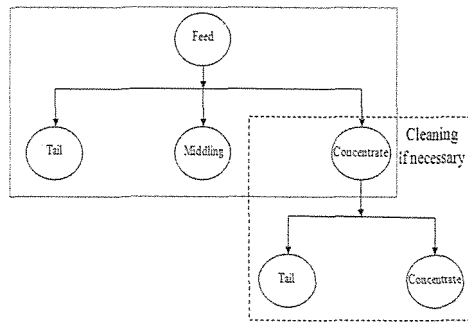

Figure 1. Schematic stages of the process

In each size fraction experiments performed in 3 magnetic field intensities 1.28, 1.35 and 1.40 T. Feed of experiments in first stage was product of crushing that had passed 2 mesh (2362 mm) screen. Regarding the obtained results and reports of similar works, in next experiments particles below 150 micron were removed from the feed. It should be noted that each of the experiments which is shown in table 2 represents the best case between 4 experiments which had been performed with various blades angles in state of iron grade. In other words 15 experiments which are presented in table 2 led to best results among 60 experiments.

3 DISCUSSION

In first 3 experiments in table 2 fine particles (below 150μ) were not removed from the feed. To study the effect of existence of fine particles in feed, 3 experiments were performed in the same conditions but by removing these fine particles by screen from the feed. Results which obtained from these experiments are compared in figure 2. In this figure Fe_2O_3 grades of concentrates are shown in various magnetic field intensities in cases of existence or nonexistence of fines.

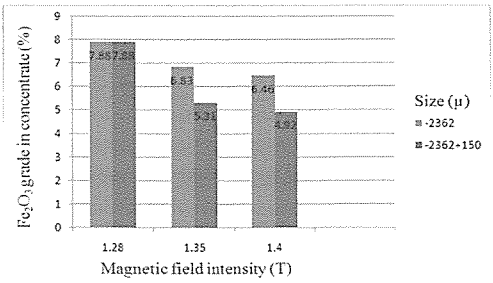

Figure 2. Effect of fines on Fe_2O_3 grade

Regarding observation in the above diagram next experiments carried out after removing fine particles. In this diagram it can be seen that by removing fines from feed iron content of the product decreased. Some experiments conducted in order to observe effects of varying of magnetic field intensity and feed size on concentrate. In experiment 4 to 15 in table 2, results which obtained by varying field intensity in 3 levels (1.28, 1.35 and 1.40 T) and feed size in -2362+150, -1000+150, -560+150 and -300+150 micron are presented. These results are compared in a graph in figure 3.

Table 2. Conditions of experiments and obtained results

No.	Feed size (μ)	Field intensity (T)	Stage	Concentrate Weight Perc.	Fe_2O_3 grade (%)
1	-2362	1.28	Single stage	66	7.88
2	-2362	1.35	Rougher	65	7.08
			Cleaner	91	6.83
3	-2362	1.40	Rougher	66	7.08
			Cleaner	92	6.46
4	-2362+150	1.28	Single stage	78	7.88
5	-2362+150	1.35	Rougher	63	6.31
			Cleaner	90	5.31
6	-2362+150	1.40	Rougher	90	5.51
			Cleaner	87	4.92
7	-1000+150	1.28	Rougher	61	7.08
			Cleaner	91	5.91
8	-1000+150	1.35	Rougher	61	7.08
			Cleaner	88	5.71
9	-1000+150	1.40	Rougher	61	6.29
			Cleaner	85	5.31
10	-560+150	1.28	Single stage	60	8.18
11	-560+150	1.35	Rougher	52	6.26
			Cleaner	84	5.71
12	-560+150	1.40	Rougher	52	6.51
			Cleaner	95	6.31
13	-300+150	1.28	Rougher	50	8.22
			Cleaner	73	5.51
14	-300+150	1.35	Rougher	52	7.39
			Cleaner	72	6.49
15	-300+150	1.40	Single stage	58	8.22

As it can be seen in the graph of figure 3 by decreasing feed size, iron content of concentrate increased. It also can be seen that in all size fractions except -300+150μ by increasing field intensity, iron content of concentrate decreased. This trend is reverse for size fraction -300+150μ. In this fraction increase in field intensity led to increase in iron content of concentrate and this is maybe because of predominance of electrostatic forces over gravitational forces.

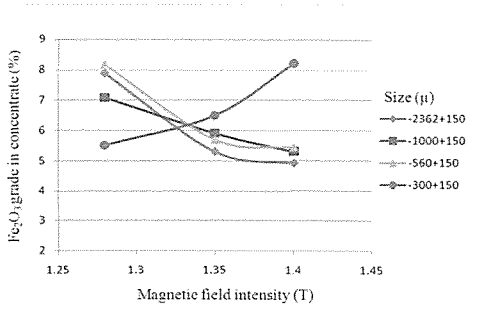

Figure 3. Effect of feed size and field intensity on Fe_2O_3 grade

By investigating Table 2 and Figure 3 it concluded that best concentrate grades obtained in sizes -2362+150 and -100+150 by applying field with intensity of 1.4T. So in next experiments particles with sizes below 300 micron were removed from feed and two experiments were carried out in two feed sizes -2362+300 and -1000+300 and by applying magnetic field with intensity of 1.4T. These two experiments are presented in table 3. If the feed prepare by milling because of low work index of the ore, large portion of -300 micron particles will be produced. So size reduction conducted only by crushing. As the results shows these experiments could reach to an acceptable concentrate grade. Although recovery of these experiments are low to some extent but regarding prices of feed and concentrate (tab. 1) and this fact that the middling that is a large weight portion of the products can be recycled to the circuit, it seems that the process results are acceptable.

Table 3. Experiments conducted in optimum conditions

Feed size (μ)	Field intensity (T)	Stage	Weight Perc.	Fe_2O_3 (%)
-100+300	1.40	Rougher	45	3.93
		Cleaner	65	1.97
-2362+300	1.40	Rougher	47	4.66
		Cleaner	64	2.65

4 CONCLUSION

Regarding large difference between Mehran mine products prices due to their iron content, processing the ore is economically important.

Limonite, hematite and goethite are main gangues in the ore. To separate these weak magnetic minerals from clay, magnetic field with high intensity is needed and with respect to difficulties of processing clays by wet methods and lack of water supplies in the mine site, high intensity dry magnetic separation is one of the most appropriate methods to treat this ore.

Feed size, magnetic field intensity, separation blades angle, feeder speed and rotating speed of the roller were determined as most effective factors on results.

Experiments which were carried out in similar conditions except feed size, showed that by removing fine particles from feed of the experiments Fe_2O_3 grade of concentrate decreased.

By decreasing feed size, iron content of the concentrate increased.

In sizes +300 micron, by increasing magnetic field intensity, produced concentrates contain lower iron content. But this trend is reverse for feed particles finer than 300 micron and removing this fraction from feed led to improvement the separation.

By conducting experiments in sizes -2362+300 and -1000+300, concentrates with Fe_2O_3 grade of 1.97% and 2.65% produced respectively while recovery of the process was about 25% in both cases. Although recovery of these experiments are low to some extent but regarding large difference in

prices of feed and concentrate (tab. 1) and this fact that the middling that is a large weight portion of the products can be recycled to the circuit, it seems that the process results are acceptable

REFERENCES

Ghorbani, M, Arzani, K, 1994. *Mineralogy of Iran (kaolin and firsclays)*, Iran mineralogy and exploration institute, Tehran, 223 p.

Lawver, J.E, Hopstock, D.M, 1985. *Electrostatic and Magnetic Separation,* Society of Mining engineers, New York, 48 p.

Monshi, A, 1996. *Ceramics and refractory materials*, Esfahan academic jahad, Esfahan, 152 p.

Nourian, S.*M, 1983. A brief on Iran fireclay mines,* Iran mineralogy and exploration institute, Tehran, 167 p.

Rezaei, B, 1999, *Mineral processing technology (concentration by magnetic method),* Amir Kabir university of technology, Tehran, 286p.

Ash and Sulphur Rejection from Coal by Using Waste Motor Oil

Atık Motor Yağı Kullanarak Kömürden Kül ve Kükürt Giderimi

M. Yavuz, T.Uslu
Karadeniz Technical University, Mining Engineering Dept., Trabzon, Turkey

ABSTRACT Although oil agglomeration is superior to other fine coal cleaning methods due to its benefits, such as, high recovery, suitability to oxidized coals, simple and cheap dewatering stage, cost of the oil has impeded the commercial application of the process. Use of waste motor oil (WMO) in the agglomeration instead of original oils can be solution to this problem. The aim of the present study is to investigate the potential use of WMO as a bridging liquid in the agglomeration of fine coal.

An oxidized coal with brittle structure was subjected to agglomeration process by using WMO. Experimental variables included coal content, WMO dosage, agitation rate and agglomeration time. 17.94-30.32 % of ash and 4.20-20.55% of pyritic sulphur was removed from the coal with combustible matter recoveries of 69.29-99.65%. Maximum ash separation efficiency index and pyritic sulphur separation efficiency index were achieved to be 27.27% and 16.05%, respectively.

ÖZET Yağ aglomerasyonu yöntemi, yüksek verimi, oksitli kömürlere uygulanabilirliği, basit ve ucuz susuzlandırma işlemi vb. sebeplerle diğer toz kömür temizleme yöntemlerine üstünlük sağlamasına rağmen, yüksek yağ maliyeti bu yöntemin ticari anlamda uygulanmasına engel olmuştur. Orijinal yağ yerine atık motor yağlarının kullanılması bu soruna çözüm olabilir. Bu çalışmanın amacı, toz kömürün aglomerasyonunda atık motor yağının bağlayıcı olarak kullanılabilirliğinin araştırılmasıdır.

Kırılgan yapılı ve oksitli bir kömür örneği, atık motor yağı kullanılarak aglomerasyon işlemine tabi tutulmuştur. Kömür oranı, atık motor yağı dozajı, karıştırma hızı ve aglomerasyon süresi değişken olarak incelenmiştir. Kömürden %17.94-30.32 oranlarında kül ve %4.20-20.55 oranlarında piritik kükürt, %69.29-99.65 organik madde verimleri ile uzaklaştırılmıştır. En fazla elde edilen kül ve piritik kükürt ayırma etkinlik indeksleri sırasıyla %27.27 ve %16.05'dir.

1 INTRODUCTION

Motor oil is used in motor vehicle engines to lubricate engine parts. It reduces friction between moving parts within the interior engine. Large amounts of motor oils are used worldwide (Ssempebwa and Carpenter, 2008). Generally, motor oils comprises hydrocarbon lubricant (80%) and performance enhancing additives (20%) (Lu and Kaplan 2008).

Waste motor oil (WMO) is the oil removed from the engine when the engine is drained during an oil-changing procedure. (Ssempebwa and Carpenter, 2009). WMO is frequently discarded into the environment (Ssempebva et al., 2004). Since it is liquid,

soil (Alugboji and Ogunwole, 2008).Therefore, it affects both marine and human life. Oil in water stops the photosynthesis and prevent oxygen replenishment, thus leading the death of underwater life. In addition, toxic materials in WMO can reach humans through the food chain (Hamad et al., 2003).

Oil agglomeration is a coal cleaning method used for deashing and desulphurization of fine coals. In oil agglomeration, the particles, which are largely organic in nature are agglomerated in preference to those which are largely inorganic. In general, organic components are more hydrophobic and oleophilic than inorganic components. Therefore, when a small amount of oil is introduced into an agitated suspension of coal particles, more hydrophobic coal particles become oil-coated and stick together to form agglomerates while the hydrophilic mineral matter particles remain unaffected. The agglomerated particles can be separated from the other materials by a single screening operation or alternatively by floating and skimming (Şahinoğlu and Uslu, 2008).

Although, oil agglomeration is one of the most promising methods for fine coal cleaning due to a number of benefits including high recovery, suitability to oxidized coals, and to coals with clay slimes, simplicity and cheapness of dewatering stage (Mehrotra et al,1983), it has not been applied commercially due to its high operation cost associated with high oil price and consumption (Yu, 1998; Shen 1999).

Several studies using petroleum originated oils and vegetable oils have been carried out for cleaning fine coal by agglomeration process. However, limited number of studies has been conducted on the use of WMO in oil agglomeration in order to reduce the oil cost. Saripalli et al (1995) conducted agglomeration experiments on thickener underflow and filter cake of coal processing unit by using WMO. Ash rejections from thickener underflow and filter cake were reported as 66.7-90.8% and 24.5-78.4%, respectively. Xu et al.(1991) reduced the ash content of thickener underflow of a plant from 59.4% to 23.1-32.9%. The present study is one of the limited numbers of attempts to investigate the potential use of WMO in agglomeration of coal to increase the competitiveness of this process by reducing the oil cost. Unlike previous studies in which only oil dosage was selected as parameter, this study clarify the effects of coal content, WMO dosage, agitation rate, and agglomeration time on the performance of agglomeration process. In addition to ash rejection and combustible matter recovery, this study is also concentrated on determination of pyritic sulphur rejection which was disregarded in the previous studies using WMO.

2. MATERIAL AND METHOD

2.1. Material

A bituminous coal sample from Muzret mine was used in this study. The chemical and particle size analysis of the sample were illustrated in Table 1 and Table 2. Pyrite is the major mineral matter in the coal. Pyrite occurs in the coal as massive and framboidal forms with particles of 1–500 μm in size. Muzret coal has a brittle character as it is an oxidized coal.

WMO sample is waste of Elf Turbo Diesel 10W-40 motor oil. It was obtained from oil changing station of Renault automobiles and filtered before using in the experiments. The density of the WMO was determined with Alla France type hydrometer. Tanaka AKV-202 viscometer was used to determine the viscosity. The physical properties of WMO are shown in Table 3.

Table 1. Chemical analysis of coal sample

Components	Air Dried	Dried
Moisture (%)	4.30	-
Ash (%)	17.06	17.83
Volatile Matter (%)	21.12	22.07
Fixed Carbon (%)	57.52	60.10
Sulphate Sulphur (%)	1.18	1.23
Pyritic Sulphur (%)	2.72	2.84
Organic Sulphur (%)	3.09	3.23
Total Sulphur (%)	6.99	7.30
CalorificValue (kcal/kg)	5647	5900

Table 2. Particle size analysis of coal sample

Particle Size (mm)	-0.5+0.3	-0.3+0.106	-0.106	Total
Weight (%)	32.03	42.29	25.68	100

Table 3. Properties of WMO sample

Type	Color	Density (g/cm^3)	Viscosity ($40°$)(mm^2/sn)
Waste Motor Oil	Black	(24°C) 0.882	96.57

2.2 Method

Agglomeration tests were carried out in a cylindrical glass vessel (11.7 cm in diameter) with four removable buffles of 1.1 cm in width. The agitation of vessel contents was performed using a IKA RW 20 type overhead stirrer equipped with a 45°-pitched blade turbine (four blade, 50 mm in diameter). Distilled water was used in the tests. Initially, coal–water slurry was conditioned at 1000 rpm for 5 min. in order to achieve complete wetting of coal particles. WMO was then added and coal-water-oil slurry was further agitated over the predetermined agglomeration period to form the agglomerates. After the agglomeration process, the suspension was transferred to a sieve with an aperture of 0.5 mm to separate the agglomerates from water and the tailings. In order to remove mineral matter entrained in the agglomerates, agglomerates were carefully washed with water. The agglomerates removed from the sieve were vacuum-filtered and freed from oil by washing with benzine. (Removal of WMO from the coal is not a required process for industrial applications due to low/no cost of WMO. In this study, oil removing was carried out in order to be able to calculate rejections of ash and pyritic sulphur, and combustible matter recovery. Since feed is oil-free, products should be also oil-free in weighing for analyses.) Oil-free agglomerates were dried at 105±5°C. After drying, agglomerates were weighed and stored for analyses.

The tests were performed at different levels of variables including coal content, WMO dosage, agitation rate, and agglomeration time. Coal content and WMO dosage was based on the mass ratio of the coal to coal-water slurry and mass ratio of the oil to coal, respectively. Experimental details are given in Table 4

Table 4. Test conditions and variables.

Test Conditions	Variables			
	Coal Content (%)	WMO Dosage (%)	Agg. Time (min)	Agitation Rate (rpm)
Coal Content (%)	5-30	10	10	1400
WMO Dosage (%)	10	5-25	10	1400
Agg. Time (min)	10	10	5-25	1400
Agitation Rate (rpm)	10	10	10	1000-1600
Coal Particle Size (mm)	0.5	0.5	0.5	0.5
pH of Pulp	5.68	5.68	5.68	5.68
Washing Water Amount (lt)	1.5	1.5	1.5	1.5
Recovery Screen Size (mm)	0.5	0.5	0.5	0.5

The combustible matter recovery (CMR), ash rejection (AR) and pyritic sulphur rejection (PSR), ash seperation efficiency index (ASE) and pyritic sulphur seperation efficiency index (PSSE) were determined using the following equations:

$$CMR\ (\%) = (W_P/W_F) \times 100 \quad (1)$$
$$AR\ (\%) = [\ (A_F-A_P)/A_F] \times 100 \quad (2)$$
$$PSR\ (\%) = [\ (PS_F-PS_P)/PS_F] \times 100 \quad (3)$$
$$ASE\ (\%) = CMR+AR-100 \quad (4)$$
$$PSSE\ (\%) = CMR+PSR-100 \quad (5)$$

Where, W_P: weight of dry ash and oil-free product (g), W_F: weight of dry ash-free feed (g), A_F: ash in dry feed (wt %), A_P: ash in dry oil-free product (wt %), PS_F: pyritic sulphur in dry feed (wt %), PS_P: pyritic sulphur in dry oil-free product (wt %).

3. RESULTS AND DISCUSSION

Ash and pyritic sulphur contents of Muzret coal were reduced to some extent by oil agglomeration process in which WMO was used. 30.32% of ash and 20.55% of pyritic sulphur could be able to remove from coal. Maximum values of seperation efficiency index for ash and pyritic sulphur was calculated to be 27.27% and 16.05%, respectively. The effects of some variables on the performance agglomeration process were discussed below.

Unsatisfactory results can be attributed to high viscosity of WMO. It was reported that when other parameters such as, pH, washing water amount, size of recovery screen, coal particle size, etc. was included as investigated variable, better results could be obtained (Yavuz, 2011).

3.1. Effect of Coal Content

Theoretically, it was expected that, decrease in combustible matter recovery with increasing coal content would be faced after a threshold value before which CMR would increase with increasing coal content. Because, distance between the particles would be greater at low solid content than that at high solid content. Therefore, the possibility of collisions between oil droplets and coal particles would increase with increasing coal content.

Unlike the expectation, combustible matter recovery decreased generally with increasing coal content as seen from Figure 1. This can be attributed to insufficiency of WMO dosage

.

Increasing the coal content caused little increases in rejections of ash and pyritic sulphur up to coal content of 10%. Further increases in coal content, produced negative impact on ash and pyritic sulphur rejections. This often results from the entrainments of mineral matters into the agglomerates. More mineral matters were entrained into agglomerates with increasing coal content since they fell into a trap in crowded coal particles and could not escape from the medium surrounded by large number of coal particles to water phase.

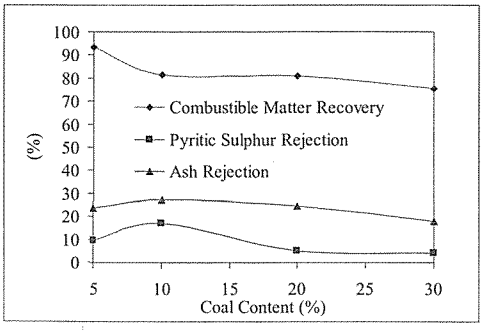

Figure 1. Effect of Coal Content on Combustible Matter Recovery, Ash Rejection and Pyritic Sulphur Rejection

3.2. Effect of WMO dosage

As can be seen from Figure 2, combustible matter recovery increased with increasing oil dosage. Increase in combustible matter recovery with increasing oil concentration could be due to size enlargement of agglomerates caused by the increase in the number of oil droplets available for contact with coal particles to form agglomerates.

Increases in ash and pyritic sulphur rejections were not achieved with increasing oil dosage. As the oil amount increased, less hydrophobic particles and also hydrophilic mineral matters also get agglomerated thus increasing the ash and pyrite content of agglomerates. In other words, selectivity of the agglomeration process decreased with increasing WMO dosage. It can be also resulted from the increased agglomerate size with higher oil dosage such that large agglomerates contained more entrained and entrapped mineral matter.

In previous WMO using agglomeration studies, only WMO dosage was investigated as variable. This study is generally in agreement with previous studies in terms of effect of WMO dosage on ash rejection and combustible matter recovery. Xu et al. (1991) reported that agglomerate ash was insensitive to oil levels. Saripalli et al. (1995) stated that higher ash rejection levels was not achieved with higher oil levels. Positive effect of increasing WMO dosage on combustible matter recovery was reported by Xu et al.(1991). However, Saripalli et al. (1995) mentioned adverse effect after a certain WMO dosage.

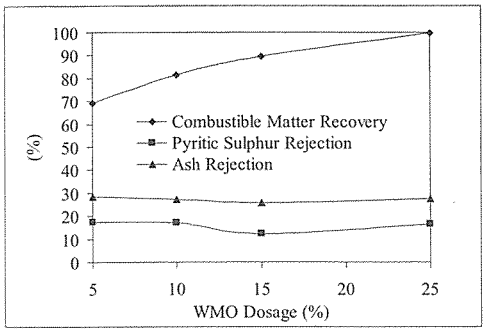

Figure 2. Effect of WMO Dosage on Combustible Matter Recovery, Ash Rejection and Pyritic Sulphur Rejection

3.3. Effect of Agglomeration Time

The combustible matter recovery increased as a function of time in contrast to ash and pyritic sulphur rejections as shown in Figure 3. The improvement in the recovery of combustible matter with time can be due to the increased possibility of the number of the contacts between coal particles and oil droplets, and between coal particles and small agglomerates. Therefore, more strong agglomerates may have been formed. The adverse effect of increasing agglomeration time exceeding 10 min. on ash and pyritic sulphur rejections suggested that more pyrite and other inorganic matters entrained into agglomerates as a result of their increased contact with oil particles over the extended periods. In other words, the possibility of entrapment of mineral matter into the agglomerates increased with time. Another reason for the deterioration in the rejection of ash and pyritic sulphur can be the increase in size of agglomerates.

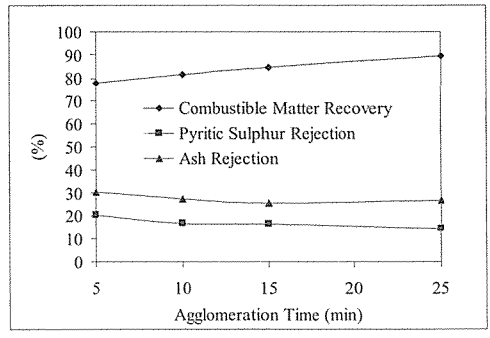

Figure 3. Effect of Agglomeration Time on Combustible Matter Recovery, Ash Rejection and Pyritic Sulphur Rejection

3.4. Effect of Agitation Rate

Figure 4 illustrates that increased agitation rate could not produced considerable effect as much as other parameters on the combustible matter recovery. Agitation rate of 1400 rpm resulted in minimum combustible matter recovery and maximum ash and pyritic

sulphur rejections. Decrease in ash and pyritic sulphur rejections at further and declined agitation rates can be explained by increase in entrainment of mineral matter into agglomerates due to increased turbulence and weak selectivity of oil droplets due to insufficient oil dispersion, respectively.

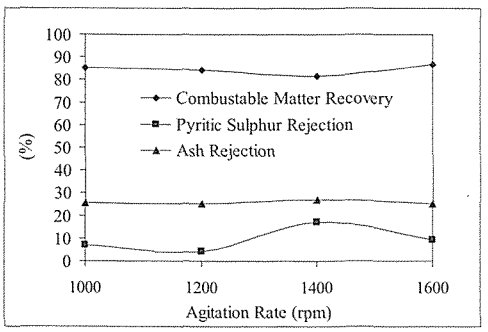

Figure 4. Effect of Agitation Rate on Combustible Matter Recovery, Ash Rejection and Pyritic Sulphur Rejection

4. CONCLUSIONS

Low levels of ash and pyritic sulphur was rejected from the coal sample with the particle size of -500 μ.

Maximum ash rejection, pyritic sulphur rejection and combustible matter recovery were achieved to be 30.32%, 20.55%, and 99.65% respectively.

Maximum ash separation efficiency index and pyritic sulphur separation efficiency index were achieved to be 27.27% and 16.05%, respectively.

Unsatisfactory ash and pyritic sulphur removals results from high viscosity of WMO. Effect of emulsification of WMO prior to agglomeration should be investigated in next studies.

Combustible matter recovery was effected primarily by WMO dosage. However, coal content was determined to be most effective parameter for ash and pyritic sulphur rejections.

REFERENCES

Hamad,B.S., Rteil, A.A., Fadel, M.E., 2003. Effect of used engine oil on properties of fresh and hardened concrete. *Construction and Building Materials*, 17, pp.311-318.

Lu, Shan-Tan, Kaplan, I.R., 2008 Characterization of Motor Lubricating Oils and Their Oil-Water Partition. *Environmental Forensics*, 9, 295-309

Mehrotra V.P, Sastry K.V.S, Morey B.W., 1983. Review of oil agglomeration techniques for processing of fine coals. *Int. J. Miner. Process.*, 11, pp.175-201.

Olugboji, O.A and Ogunwole, O.A., 2008. Use of Spent Engine Oil. *AU J.T.* 12 (1),pp.67-71.

Sahinoglu E, Uslu T., 2008. Amenability of Muzret bituminous coal to oil agglomeration, *Energy Convers Manage.*, 49(12), pp. 3684-90.

Saripalli, G.R, Griffin,R.A, Arnold, D.W, 1995. Fate of Trace Metals During Agglomeration of Blue Creek Coals with Used Motor Oil. *Hazardous Waste & Hazardous Materials*, 12(2), pp.133-148.

Shen, M.,1999. Development and scale-up of particle agglomeration processes for coal beneficiation. *Ph.D. Thesis*, Iowa State University, Iowa

Ssempebwa, J.C, Carpenter, D.O, Yilmaz, B, DeCaprio, A.P, O'Hehir, D.J, Arcaro,K.F., 2004. Waste Crankcase Oil: An Environmental Contaminant with Potential to Modulate Estrogenic Responses. *Journal of Toxicology and Environmental Health, Part A,* 67,pp.1081-1084.

Ssempebwa, J.C, Carpenter,D.O., 2009. The generation, use and disposal of waste crankcase oil in developing countries: A case for Kampala district, Uganda. Journal of Hazardous Materials, 161, pp.835-841.

Xu, W., W. J. Herz., D. W. Arnold and J. K. Alderman., 1991. Oil Agglomeration of Blue Creek Coal. *The Journal of Coal Quality*, 10(2), pp. 61-66

Yavuz, M., 2011. Usability of Waste Motor Oils in Cleaning of Coal by Oil Agglomeration. *Ph D. Thesis,* Karadeniz Technical University, Trabzon, Turkey.

Yu, Z., 1998. Flocculation, hydrophobic agglomeration and filtration of ultra fine coal. *Ph D. Thesis,* University of British Columbia.

Grain Size Distribution Properties of Chromite Particles in Polished Sections of Sieve Fractions

Elek Fraksiyonlarının Parlak Kesitlerinde Kromit Tanelerinin Boyut Dağılım Özellikleri

A. Taşdemir, H. Özdağ
Eskişehir Osmangazi Üniversitesi, Maden Mühendisliği Bölümü, Eskişehir

G. Önal
Yurt Madenciliğini Geliştirme Vakfı, İstanbul

ABSTRACT In this research, particle size measurements determined by sieve analysis and image analysis (*IA*) was compared for a chromite sample. Comminuted chromite sample was subjected to sieve analysis and eleven narrow size fractions were obtained. Polished sections which were prepared from the representative samples of each fraction were examined by *IA* to determine the particle size distributions (*PSD*s) of fractions. Particle area (*A*), particle perimeter (*P*), maximum Feret diameter (length, *L*) and minimum Feret diameter (width, *W*) and three shape factors namely Chunkiness *(Ch)*, Roundness *(R)* and Form Factor *(FF)*, were measured on individual chromite particles. Arithmetic mean of *L* and *W* was chosen as *IA* size definition. Size comparisons were made between geometric means of sieve fractions versus both number and volume (mass)-based *IA* means before and after correction of *IA* diameters with three shape factors. The differences between the two methods were tried to explain by possible effect of particle shape.

ÖZET Bu çalışmada, elek analiz ve görüntü analizi (*GA*) ile belirlenen tane boyut dağılımı ölçümleri bir kromit örneği için karşılaştırılmıştır. Ufalanmış kromit örneği elek analizine tabii tutulmuş ve dar boyutlu on bir elek fraksiyonu elde edilmiştir. Her bir fraksiyonun temsili örneklerinden hazırlanan parlak kesitler, fraksiyonların tane boyut dağılımlarını saptamak için *GA* ile incelenmişlerdir. Bireysel kromit tanelerinin alanı (*A*), tane çevresi (*P*), maksimum Feret çapları (*L*) ve minimum Feret çapları (*W*) ile birlikte tane şekilleri olarak Bodurluk (*Ch*), Yuvarlaklık (*R*) ve Form Faktörü (*FF*) değerleri ölçülmüştür. L ve W'nin aritmetik ortalaması *GA* boyut tanımı olarak seçilmiştir. Elek fraksiyonlarının geometrik ortalamaları ile üç tane şekil faktörü ile düzeltme öncesi ve sonrası hem sayı hem de hacme (kütle) dayalı bulunan *GA* ortalamalarının karşılaştırılması yapılmıştır. İki yöntem arasındaki farklılıklar, olası tane şekil etkisiyle açıklanmaya çalışılmıştır.

1 INTRODUCTION

Knowledge of particle size and particle size distribution (*PSD*) is the most important entity in evaluating particulate materials, since it affects many of their end uses. The determination of particle size on the same sample by various size measurement techniques yield different results for mean size, modal size and quantity distribution by size. There are many size definitions obtained from different size measurement techniques. But none of these methods has been adopted as a comprehensive standard. If the particles under test are spherical, same *PSD*s can be obtained from all different size measurement methods. But in real, particles are not spherical in shape and are irregular having many different shapes.

Various methods can determine particle size distribution of particulate materials (Allen, 1997); sieving is the most common method used. In most methods, size distribution is the only parameter studied and particles are often described as or assumed to be spheres. Particle shape, however, may influence physical behavior during the size measurement in different measuring methods. Thus, the results obtained may differ from each other depending on the different measurement principles and particle shape. Therefore, knowledge of particle shape may be used as a correction factor between different size measurement methods. Image analysis (*IA*) identifies many variables that can be used to describe the powder like size and also particle shape without a priori assumptions (Pabst et al., 2006). Moreover, the method allows direct observation and verification of individual particles.

Comparisons of particle size distribution results for irregular particles by different techniques are often required. Thus, a suitable and simple factor is needed to convert one type of size distribution data obtained to another method. The conversion factor is generally called as apparent shape factor in the literature (Austin, 1998; Ulusoy et al, 2006; Ulusoy et al, 2008). Apparent shape factor is simply calculated from the ratio of the mean particle sizes of different methods. The ratio of calculated means obtained from the two methods may be sufficient to define the relation between them and can be used as a correlation factor but it is necessary to find the possible reasons for the observed differences (Kaye et al., 1997).In this respect, information of detailed particle shape information of particulate materials gets more come into question.

Many researchers from different disciplines have made conversion studies to compare different sizing technologies and to another size distribution being measured by different method in the literature (Petruk, 1978; Kaye, et al, 1997; Austin, 1998; Xu and Di Guida, 2003; Hogg, et al., 2004; Li, et al., 2005; Blott, S. J. and Pye, K., 2006; Ulusoy, et al., 2006; Schneider, at al., 2007; Fernlund, et al., 2007; Ulusoy, et al., 2008;).

Previously, we studied the influence of particle shape on the response of two different sizing techniques for quartz mineral. In these studies, geometric mean of sieve sizes was compared to different *IA* size diameter definitions; the geometric mean of length and width (Taşdemir, et al., 2009), the maximum Feret, length (Taşdemir, et al., 2010) and the mean Feret (Taşdemir, et al., 2011). This paper deals with comparison of *IA* mean sizes of narrow particle size fractions for chromite, with geometric mean sizes of the sieve openings used for generation of a given narrow particle size fraction. It was demonstrated that the mean particle size of a narrow particle size fraction is comparable for both methods provided that the shape factors are taken into account in the *IA* approach.

2 MATERIAL AND METHOD

A chromite sample from Pınarbaşı, Kayseri (Turkey) was chosen and used in the experiments. The sample was subjected to a comminution process by jaw and cone crushing at Mineral Processing Laboratory of Eskişehir Osmangazi University. The material was comminuted to -1 mm. The representative sample of chromite was in a nest of sieves with Retsch sieve series including 1000, 800, 600, 500, 400, 300, 212, 150, 106, 75, 53 and 38 μm sizes. Sieve analysis was initially carried out manually by wet sieving until no particle passage. At the end of sieving, each sieves used was subjected to ultrasonic bath so that cleaning and to prevent the trapped particles between in the sieve apertures, which had difficulty in passing through the sieve. Geometric means of sieve intervals were calculated as;

$$D[S,50]=(D^{i}*D^{i-1})^{0.5} \quad \text{.....(1)}$$

where D^{i} is the upper sieve size through which a particle can pass and D^{i-1} is the retaining sieve size through which the particle did not pass.

The dried powders of each sieve fractions were prepared as polished sections by using

low viscosity epoxy resin which was mixed with appropriate amount of hardener. A grinding and polishing flow sheet was developed and applied successfully for the polished sections of coarse and fine grained powder sieve fractions. The size and shape measurements on polished sections of sieve fractions were performed by automatic image analyzer. Two-dimensional images of fully liberated chromite particles were produced by an Olympus reflected light microscopy associated with the image analyzer. During the *IA*, each particle was allowed to be measured individually.

2.1 Measurements of Particle Sizes and Shape Factors by *IA*

In this research; the measurements such as area (*A*), perimeter (*P*), Feret diameter which is the distance between two parallel lines tangent to the projected cross-section in eight different directions, i.e. at angular resolution of 22.5^0 were performed on the individual chromite particles. The following particle dimensions were derived from these measurements and used as size and shape descriptors in this study:

Length (L): Maximum Feret diameter measured in eight directions.

Width (W): Minimum Feret diameter measured in eight directions.

The *IA* size is defined in this study as the arithmetic mean of *L* and *W* measured for each particle:

$$D = (L+W)/2 \quad \text{.....(2)}$$

The means of each *IA* size descriptors in each sieve intervals were found by dividing the number of particles (*N*) measured. Unlike sieve analysis which is based on mass-based distribution, *IA* generates number-based distributions. Since the number of the particles appears in the equation while finding mean number-based distribution, this is a number mean, more accurately a number length mean. Therefore, following equation equals to mean of number (length)-based distribution:

$$D[\mathrm{L}, 50] = D_1+D_2+..+D_n)/(N) \quad \text{.....(3)}$$

where *N* is the total number of particles measured.

To facilitate comparison with sieve size, it was necessary to convert the results of from number to weight distribution, since the raw data from the IA are reported by number basis. The transformation from a number (length)-based particle size distribution (PSD) to mean of volume (mass)-based PSD for the *IA* measurements has been done by using the following formula;

$$D[\mathrm{V},50] = \Sigma(D_i)^4 / \Sigma(D_i)^3 \quad \text{.....(4)}$$

The advantages with this calculation are that it does not contain the number of observations and that it does not need to be transformed to a 3D measure and that large grains are given a high weight (Engqvist and Uhrenius, 2003).

Individual particle shape information can be extracted from 2D images. Several shape factors may be used to describe the deviation of a non-spherical particle from a sphere. Three shape factors of chromite particles used in this work are chunkiness *(Ch)*, roundness *(R)* and form factor *(FF)* and calculated as the following:

$$\textit{Chunkiness (Ch)} = [W]/[\textit{Feret length perpendicular to } W] \quad \text{.....(5)}$$

$$\textit{Roundness (R)} = (4\pi A)/(P)^2 \quad \text{.....(6)}$$

$$\textit{Form Factor} = (R)^{0.5} \quad \text{.....(7)}$$

3 RESULTS

3.1 Properties of Length and Width of Chromite Particles in Sieved Fractions

Length and width distribution properties of narrowly sized chromite particles were examined by *IA* to facilitate this method for finding the lower and upper size limits of narrowly sieved fractions. An example is given for 1000x800 size fraction in Figure 1.

As seen from this figure, maximum width of the particles within a sieve fraction approximately equals to the diagonal length of the upper sieve. The minimum length of the particles within the sieve interval was

higher than the lower sieve aperture. This result suggests us that even the particles classified to narrow sieve fractions; their size distribution is wider than the limits of sieve fractions. The chromite particles passing through the same screen mesh have the same sieve size, but they have very different axial diameters determined by *IA*. Usually the longest dimension (length) dimension of a particle has little effect on sieve results; the least cross-sectional area is most important (Ferlund, 1998). Our results support these findings since the length of the particles which were higher than the diagonal length of the upper sieve can be found within the narrowly sized fraction with the smaller ones as seen in Figure 1.

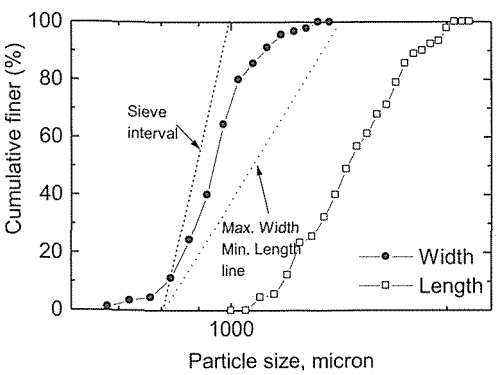

Figure 1. Length and width distribution of 1000x800 sieve interval.

3.1.1 Comparison of Means of Sieve and IA Measurements

The sieving and *IA* measure different properties of a particle, and thus they provide values for diameters representing different kind of averages in sieve intervals. In Table 1, the geometric mean values of sieve intervals and their corresponding number and volume-based mean *IA* diameters and also mean shape factors of sieve fractions obtained by *IA* are given.

As seen from Table 1, the mean sizes of sieve intervals are very different and higher than the means of *IA* sizes obtained by both number and volume-based means. Based on the mean results of sieve fractions Figure 2 describes the number and volume (mass)-based *IA* diameters as a function of the geometric mean diameter of the sieved fractions.

It should be noticed that the slope values on all of the plots in the Fig. 2 and Figs. (3-5) were obtained from the simple linear equations; but the results were presented on log-log graphs in all plots given here to see the differences more clearly for the smaller sieve fractions.

Table 1. Geometric mean sieve sizes, mean IA sizes and mean shape factors of sieve fractions

D[S,50]	*D*[L,50]	*D*[V,50]	*Ch*	*R*	*FF*
894	1238	1273	0.68	0.58	0.76
693	987	1067	0.67	0.54	0.73
548	842	933	0.65	0.55	0.74
447	633	666	0.67	0.54	0.73
346	475	505	0.71	0.56	0.75
252	331	386	0.66	0.63	0.79
178	212	243	0.63	0.64	0.80
126	156	179	0.65	0.59	0.77
89	113	129	0.63	0.58	0.76
63	75	85	0.66	0.75	0.87
45	54	63	0.65	0.67	0.82
		Mean	*0.66*	*0.60*	*0.78*
		1/Mean	*1.51*	*1.66*	*1.29*

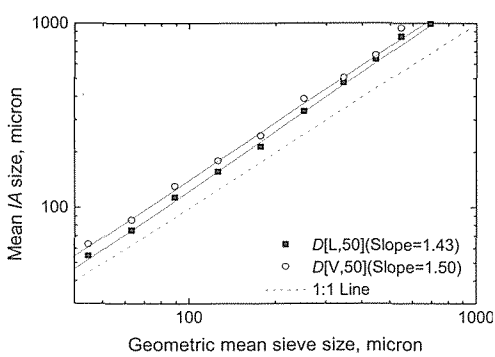

Figure 2. Mean particle sizes based on sieve diameter versus mean grain sizes based on *IA* diameters.

These results indicated that there was a simple correlation between the sieve and *IA* sizes. The following equations, which

describes the relationship between the D[L,50] and D[V,50] and corresponding D[S,50], has coefficients of determinations (R^2) 0.995 and 0.989 respectively:

D[L,50]=1.43*D[S,50]-16.08.....(9)

D[V,50]=1.51*D[S,50]-1.61.....(10)

These basic relations gave the straight lines with slopes. The slopes of the lines may provide a measure of the discrepancy between IA sizes and sieve sizes. The slopes obtained before and after correction were evaluated as the deviations from the ideal 1:1 line. Since the sieve openings can be considered to be uniform, this increasing differences between the two methods can be explained by the irregularities in particle shapes. The values obtained from D[L,50] and D[V,50] calculations were deviated from 1:1 line with slopes of and 1.43 and 1.51 respectively. These values can be used to convert the two methods.

In order to quantify the possible effect of particle shapes on the differences between the two methods, the means after correction by the three shape factors were compared with the D[S,50]. The results are given in Figs. (3-5).

Among the shape factors, the best correlation was obtained with *Ch* to correlate the two methods. The D[V,50] values gave better relationship with D[S,50] than those of D[L,50] values when they were multiplied by their corresponding means of *Ch* values, since most of the points obtained from this process were presented on the 1:1 line and the slope is almost 1 (0.97) (Figure 3). The reverse of the average of mean *Ch* values of all sieve fractions was found as 1.51 which was the same value as the slope calculated before the correction by shape factors for D[S,50] versus D[V,50] plot (1.51) (Figure 2 and Equation 10).

D[L,50] values corrected by the *FF* also gave the good results with D[S,50] (Fig. 4). The slope of this relation is 1.07 but it has higher deviation from 1:1 line than the value obtained after *Ch* correction. Also there is no clear relationship between the mean *FF* values (0.78) or their mean reverse values of sieve fractions (1.29) and slope of Eq. (1) (1.43).

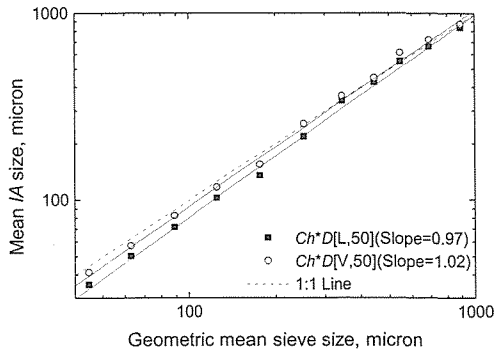

Figure 3. Geometric means of sieve versus mean grain sizes based on *IA* diameters after correction by *Ch*.

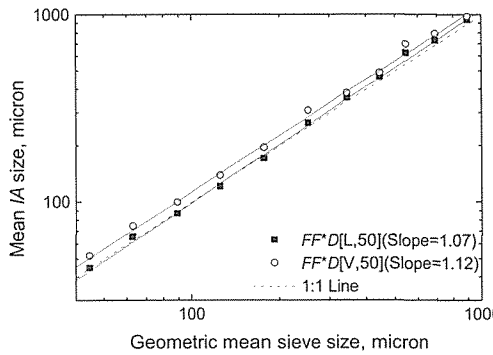

Figure 4. Geometric means of sieve versus mean grain sizes based on *IA* diameters after correction by *FF*.

After correction of the *IA* results by *R* values of particles, the slopes were 0.79 and 0.83 for D[L,50] and D[V,50] means respectively and the deviations were higher than the ones which were obtained by *FF* and *Ch* factors (Fig. 5). Although the relations were also linear when *R* was used as a correction factor, there were no points on the 1:1 line and the points were very far from the 1:1 line in both cases.

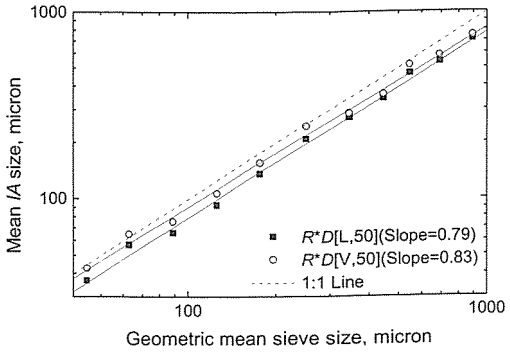

Figure 5. Geometric means of sieve versus mean grain sizes based on *IA* diameters after correction by *R*.

From these results, the differences between between the two methods for chromite sample can be attributed to the effects of particle shape and this relation is related to the mostly *Ch* of particles when arithmetic mean of length and width is used as *IA* size definition.

4 CONCLUSIONS

In this research, a comparative study was carried out to compare the sieve size and *IA* size measured on polished sections of sieve fractions for a chromite ore sample. Three particle shapes were evaluated with number and volume (mass)-based *IA* sizes to compare the results obtained by sieve sizes.

Investigating the effect of particle shape of chromite particles, it was found that the volume (Mass)-based means corrected by Ch gives the closest mean diameters with geometric means of sieve fractions.

This study revealed that the transformation from the number-based means to volume (mass)-based means are necessary for the comparison. Arithmetic mean of length and width values of chromite particles were closely near to the geometric mean of sieve fractions when they were transformed to volume (mass) basis means and then corrected by *Ch* values. The deviation from the ideal 1:1 lines can be explained by the shape of particles. The volume (mass)-based arithmetic means of width and length were the most related *IA* size definitions with particle shape effect on sieving since its slope (1.51) was the same with the reverse of the *Ch* value of all sieve fractions (1.51). On the other hand, number-based means corrected by *FF* were also near to the sieve means but this reason could not be explained by any of the shape factors tested.

KAYNAKLAR

Allen, T, 1997. *Powder Sampling and Particle Size Determination,* in Particle Size Measurement, Volume 1, Scarlet, B. and Jimbo, G. (ed), p. 682.

Austin, L. G., 1998. Conversion Factors to Convert Particle Size Distributions Measured by One Method to Those Measured by Another Method. *Part. Part. Syst. Charact.*, 15, p. 108-111.

Blott, S. J. and Pye, K., 2006, Particle size distribution analysis of sand-sized particles by laser diffraction. An experimental investigation of instrument sensitivity and the effects of particle shape, Sedimentology, 53, 671-685.

Engqvist, H and Uhrenius, B, 2003. Determination of the Average Grain Size of Cemented Carbites, *Int. J. of Refrectory Metals & Hard Materials*, 21, p. 31-35.

Ferlund, J. M. R, 1998. The Effect of Particle Form on Sieve Analysis: A Test by Image Analysis. *Engineering Geology*, 50, p. 111-124.

Fernlund, J. M. R., Zimmerman, R. W. and Kragic, D, 2007. Influence of volume/mass on grain-size curves and conversion of image analysis size to sieve size, Engineering Geology, 90, 124-137.

Hogg, R., Turek, M. L. and Kaya, E., 2004. The role of particle shape in size analysis and the evaluation of comminution processes, *Particulate Science and Technology*, 22, p. 355-366.

Kaye, B. H., Alliet, D., Switzer, L. and Turbitt-Daoust, C., 1997. The effect of shape on intermethod correlation of techniques for characterizing the size distribution of powder. Part 1: Correlating the size distribution measured by sieving, image analysis and diffactometer methods, *Part. Part. Syst. Charact.*, 14, p. 219-224.

Li, M., Wilkinson, D., Patchigolla, K., 2005. Comparison of particle size distributions measured using different techniques. *Particulate Science and Technology*, 23, p. 265-284.

Pabst, W., Berhold, C. and Gregorova, E., 2006. Size and Shape Characterization of Polydisperse Short-Fiber Systems, *Journal of the European Ceramic Society*, 26, p. 1121-1130.

Petruk, W., 1978. Correlation between grain sizes in polished sections with sieving data and

investigation of mineral liberation measurements from polishes sections, *Trans. Institution of Mining and Metallurgy, Trans. C*, 87, p. 272-278.

Schneider, C. L., Neumann, R. and Souza, A. S., 2007. Determination of the distribution of size of irregularly shaped particles from laser diffraction measurements, International Journal of Mineral Processing, 82, 30-40.

Taşdemir, A, Özdağ, H and Önal, G, 2009. Comparison of Geometric Mean Sizes Obtained by Image Analysis and Sieving and Their Correlation, in *4 th Asian Particle Technology Symposium,* p. APT2009.

Taşdemir, A., Özdağ, H. and Önal, G., 2010. Length Measurements of Narrowly Sieved Quartz Particles by Image Analysis and Conversion to Sieve Size, *XII. International Mineral Processing Symposium,* p. 1015-1023.

Taşdemir, A., Özdağ, H. and Önal, G., 2011. Image Analysis of Narrow Size Fractions Obtained by Sieve Analysis - An Evaluation by Log-Normal Distribution and Shape Factors", *Physicochemical Problems of Mineral Processing*, 46, p. 95-106.

Ulusoy, U., Yekeler, M., Biçer, C. and Gülsoy, Z.; 2006, Combination of the Particle Size Distributions of Some Industrial Minerals Measured by Andreasen Pipette and Sieving Techniques, *Part. Part. Syst. Charact.*, 23, p. 448-456.

Ulusoy, U., Gülsoy, O. Y., Aydoğan, N. A. and Yekeler, M.; 2008, Combination of Different Size Distributions for Mineral Particles by Applying Experimentally Determined Apparent Mean Shape Factor. *Particulate Science and Technology*, 26, p. 158-168.

Xu, R. and Di Guida, O. A., 2003. Comparison of sizing small particles using different technologies, *Powder Technology*, 132, p. 145-153.

OCCUPATIONAL HEALTH AND SAFETY

Application of Technical and Economic Analysis on Refuge and Self Breathing Apparatus Design

Amir Taghizadeh Vahed, Nuray Demirel
Middle East Technical University, Ankara, Turkey

Ataallah Bahrami
Hacettepe University, Ankara, Turkey

ABSTRACT Most of the time, accidents happened in mining operations such as drilling, transportation, excavation, and supporting operations. Moreover, underground mining operations have restrictions and hazards. Indeed, lack of oxygen, severe heat, thirst and starvation are some great events when miners trapped in mining accidents. Thus, refuge provides a secure location for workers in accidents, which can solve these problems. These rooms located on specific position and out fitted them with peculiar devices. However, refuges afford enough time for rescue team to save miners who trapped in mining accidents.

This paper presents design of refuges of Hashoni coal mine which is located in Kerman, Iran. Six refuges designed, which provides safe work environments in Hashoni coal mine. Thus, all of refuges layout, sizes, external devices and number of miners which refuge contains them, will be explained. Financial concept of this project shows that initial cost is around 225 to 380 U.S $ for manufacturing of refuges in Hashoni coal mine. Manufacture of refuges will reduce the investment of these tools to 50 percent.

Fire accidents in mines decrease the volume of oxygen, and because of fire some toxic gases are also produced. Thus fresh air must be available. Air provided by air supply respirator, which is called Self Breathing Apparatus contained. Aim of this paper is to promote the safety in mining industry.

1 INTRODUCTION

In 2nd of May 1972, 91 miners of Sunshine mine, which located in Canada had died because of Carbon Monoxide, and 82 miners had been run from that situation. Investigations shows 64 of 91 miners were alive for the first 10 minutes, while 27 miners were alive after 30 minutes. If mine outfitted by self-breathing apparatus, so 64 miners could survive because of enough time which apparatus provides them. Moreover, 27 of miners died, who harbored in a refuges because of lack of oxygen or a machine which provides oxygen to refuge (Cullen, 2002).

In 30th of September 2005, 72 miners in Esterhazy potash mine trapped around 30 hours. However, they were saved by rescue team. Reports present all of miners were safeguarded in 6 refuges. Moreover, every refuge had oxygen provider machines, and every miner had a self-breathing apparatus, too. Esterhazy mine expanded in 30(km) length, and 20(km) width, miners learned to use appropriated refuges, so rescue team searched only location of 6 refuges. Moreover, accidents like this happened every year in mines of Iran, because of lack of knowledge about, how and when miners must use refuges. In this paper, process of refuges planning and other extra devices which should fit out in refuges presents (Contant, 2008).

2 SELF-BREATHING APPARATUS

In firing of a mine, oxygen volume will decrease due to the consumption of oxygen by fire. Indeed, rare combustion, fire produces poisonous gases such as carbon monoxide. Moreover, carbon monoxide tends to mix with oxygen, causing abating the volume of oxygen. Thus, it is necessary to provide fresh oxygen and prevent entering of poisonous and unbreathable gases. Therefore, self-breathing apparatus provides fresh oxygen. Self-breathing apparatus identified as Air Supply Respirator, which is named SCBA (Self Breathing Apparatus Contained). Moreover, self-breathing apparatus are wide range of auxiliary breathing devices, which have masks and refine some gases from breathing gas. However, self-breathing apparatus categorized three parts, i) Self-Rescue Respirator, ii) Air Purifying Respirator, and iii) self-breathing apparatus which includes fresh air (i.e. is named Air Supply Respirator). Air Supply Respirator connects to Air-line Respirator, or Self-Breathing Apparatus.

SCBA has a cylinder, which contains fresh air. Indeed, SCBA are used instead of Air Purifying devices. Application of Air Purifying devices, because of low volume of oxygen in air of mine is forbidden. Moreover, application of SCBA is so popular because of mobility feature of these apparatuses. Utility of SCBA is unique, due to their ability when volume of oxygen is so low or flammable air has higher volume in contraction with oxygen volume. SCBA has high weight and lower life time. SCBA must be controlled every month because of needs for adequate efficiency in operations. Special glasses must apply for SCBA, which is a disadvantage for this apparatus. Moreover, SCBA provides fixed rate of air to a user, so in condition which miners is in running mode it will be made a problem for him (i.e. miners in unusual positions need more air).

3 REFUGE

Obeying the safety regulations and constructing of refuges in coal mine is essential. However, refuge as place which provides a secure location for workers in accidents can solve some problems, such as: place for miners to refuge in it because of underground fires (i.e. places which trapped in fire), missing ventilation system which is not replaceable and repairable, long distance between production faces and a place which provides fresh air, falling in production faces and tunnels, spontaneous combustion, abrupt temperature redaction during drilling progress.

In rescue progress SCBA is not so reliable, because it prevents fast run from galleries. Thus, continuous application of SCBA with entering to refuges and applying SCBAs which exist in refuges will be so suitable. A SCBA has confidence 60 percent of its life time, which carried by miner who has 80 kg weight and 120 heartbeats per minutes. Thus, it is better to use a SCBA for 60 percent of total distance which is evaluated by experts for a SCBA (i.e. this distance blow over by a miner). Moreover, equivalent distance for 60 percent of a SCBA is a distance for arriving to a refuge for replacing cylinder of a SCBA.

Standard refuges categorized two parts on based of mobility properties, i) fixed refuge one, and ii) mobile refuge. Fixed refuges are applied in mines with high concentration of reserve or mines with high rate of production. Indeed, these types of refuges are made of metal or fireproof fiberglass. Moreover, fixed refuges produced in plats mode and assembled in a mine. On the other hand, mobile refuges are used in mines which have high production rate and high advancing or in mines which have vein deposits or mines which extract by continuous miner machines. On base of rules, refuges must locate on place which miners (i.e. that cannot arrive to surface) arrive to them in less than 30 minutes. Indeed, refuge must be made of materials which are fireproof, and have enough capacity for all of miners that work on that confine. A refuge must isolate for toxic gases which exist in air of mine, and it must access to compressed air and water. It must be equipped with enough air or SCBA for

every miner, and a first aid box. A refuge must be far away at least 60 meter from explosives and fuel storages. Moreover, it must be remote from shafts at least 500 meters. Every refuge must have devices which communicate with surface of mine. Indeed, it must have reserved air for 8 hours, and if external air supplier unhanded, inner air provider of refuge must also exist. A refuge should have a eudiometer and monometer.

4 PROVIDING AIR FOR REFUGES

Miners use refuge in polluted air. Therefore, these refuges must have breathable air. One of method is applying SCBA for every of miner in refuges, but these apparatus has time limitation; on the other hand, miners may need more time to spend in refuges. Thus, refuges should be a system of air providers. Variety of methods is used for providing fresh air for a refuge, such as: i) applying compressed air, ii) utility of air provider devices (i.e. Refuge One Air Center), and iii) oxygen cylinders. Moreover, application of compressed air is simple manner, which provides positive pressure in a refuge and this positive pressure prevent external gas come in to the refuge. On the other hand, utility of an air provider device in refuge has been commented by experts. Moreover, compressor must be settled in tidy air and its application is so dangerous, so utility of refuge one air center is better a choice. Moreover, application of refuge one air center needs more number of oxygen cylinders for annihilating carbon monoxide. Indeed, oxygen cylinders based on some chemical processes provide air for the refuge, and diffuse fresh air in which volume of oxygen in the refuge is 19.5 percent. This system can provide fresh air for 15 people (i.e. for 5 hours). This advantage of the system is disability of it in absorbing carbon monoxide. Another system for providing fresh air is application of high pressure of oxygen cylinders. However this method produces carbon monoxide in the refuge. Also, providing fresh air for 20 miners (i.e. for 10 hours) 180 cylinders of 50 cfm oxygen is necessary. Moreover, price of these cylinders are 500-1600 US $ for every cylinder. For providing fresh air in the refuge variety parameters must analyze such as: i) volume of a refuge, ii) maximum number of miners which refuge can included them and iii) evaluating necessary volume for dead air.

5 HASHONI COAL MINE

Hashoni coal mine located in Kerman, Iran, which contains 25 million tone of absolute reserve. The highest level of this mine is 3110 m while lowest level of it is 2400 m. Moreover, coal layer has 6 km length, and 3 km width so its area is 18 km^2. Table 1 shows properties of production faces, advancing breasts in Hashoni coal mine.

Design of self-breathing apparatus (type SCBA) in Hashoni coal mine Major parameters of in selection of self-breathing apparatus consist.

5.1 Life time of oxygen reserve

Hashoni coal mine has short length tunnels, which causes easy achieving to surface or refuges. Thus, SCBAs do not need to have long life time of oxygen. Indeed, capital costs of SCBAs, which have feature of 30 and 60 minutes life time, are roughly same. However variation between these two types is the cost of oxygen cylinders, which is around 300-400 dollar. Thus, application of 60 minutes SCBA has been commented in Hashoni coal mine.

If utility of SCBA is a method for providing air in refuges, so for rescue teams is not necessary to design places for mounting SCBA in these locations for them, in firing situations. On the other hand, if fresh air for refuges which is provided by compressed air, so on based of Hashoni coal mines tunnels, for every 3 km putting SCBA(s) is necessary. Moreover, location of SCBAs is called cabin. Number of SCBA in every cabin is equal with double number of rescue team members in closed circuit type, but for open circuit it can be equal with number of members of rescue team.

Table 1. Properties of Hashoni coal mine

No.	Name of production face	Length of production face (m)	Ave. thickness of coal layer (m)	Ave. slope	High level (m)	Low level (m)	No. of miners in faces	Prod. (t/shift)
1	120	155	2.23	36	2608	2520	20	35
2	622	197	2.08	35	2520	2400	13	15
3	427	170	2.34	47	2545	2400	18	35
4	627	217	2.23	44	2545	2400	22	40
5	521 Adv.	70	1.63	44	Surf.	2545	15	30
6	521 Retr.	210	1.52	42	Surf.	2545	8	15
7	222	156	1.86	30	2480	2400	20	20
8	220	154	1.70	38	2608	2520	–	–
9	127	53	1.17	36	Surf.	2608	22	20

Table 2. Properties of Hashoni coal mine

No.	Name of production face	Type of material	Support type	Section area (m^2)	No. of miner(s) (No./shift)
1	Right hand side of tunnel 7	Rock	Metal support	9/2	15
2	Left hand side tunnel 7	Rock	Metal support	11/2	15
3	Tunnel 1	Rock	Metal support	9/2	10

5.2 Life time of oxygen reserve

Hashoni coal mine has short length tunnels, which causes easy achieving to surface or refuges. Thus, SCBAs do not need to have long life time of oxygen. Indeed, capital costs of SCBAs, which have feature of 30 and 60 minutes life time, are roughly same. However variation between these two types is the cost of oxygen cylinders, which is around 300-400 dollar. Thus, application of 60 minutes SCBA has been commented in Hashoni coal mine.

If utility of SCBA is a method for providing air in refuges, so for rescue teams is not necessary to design places for mounting SCBA in these locations for them, in firing situations. On the other hand, if fresh air for refuges which is provided by compressed air, so on based of Hashoni coal mines tunnels, for every 3 km putting SCBA(s) is necessary. Moreover, location of SCBAs is called cabin. Number of SCBA in every cabin is equal with double number of rescue team members in closed circuit type, but for open circuit it can be equal with number of members of rescue team.

5.3 Weight of SCBA

Improvement of technology in application of light alloy and carbon yarns causes in production of lighter SCBA. Thus, weight of SCBA is not so major parameter in selection of them.

5.4 Cost and grantee of SCBA

Average cost of SCBA, which is mounted on open circuit (life time is 60 minutes), is around 3000-3500 US $. Thus, grantee is so important.

5.5 Design of location and number of SCBA

Design of number and location of SCBA depends on location of refuges and system which provides air to refuges. However, lots of miners work in Hashoni coal mine, so application of SCBA is not good method (i.e. required more number of SCBAs). Thus, after design of refuges and utility of invention systems of providing fresh, number and location of them will be presented.

For rescue team, two SCBA for each member of this team in opened circuit, and one SCBA in closed circuit set in every 3 km. Indeed, number of SCBA in refuges has based on location and required air in a refuge. Thus, financial analyze of providing air by SCBA after design of refuges will be carried out.

Self-respirator has major role in providing security for miners in unexpected situations, and based on low price of them (i.e. 110 US $/per self-rescue respirator), so utility of these apparatuses are suggested for all of miners, that work in tunnels and production faces. Indeed, application of SCBAs which work in opened circuit (i.e. life time is 60 minutes) are recommended.

6 DESIGN OF REFUGES IN HASHONI COAL MINE

Every refuge equipped with devices providing fresh air for refuge and carbon dioxide observer, and a refuge can contain maximum 30 miners. Moreover, if a refuge covers two production faces, so volume of the refuge must be double, or two refuges is necessary (i.e. carbon dioxide observer devices and air providers must be doubled). Major parameter for design of Hashoni coal mines refuges stated as below:

- Maximum distance of refuges from production faces is 1000 m.
- Maximum distance of refuges from advancing breast is 1000 m.
- If a refuge covers two production faces or breasts, volume of it increase (i.e. it has doubled).
- Maximum application time duration for a refuge in bad situation is 8 hours.
- Location of refuge is designed based on miners can achieve surface or shaft after 500 meter.

Refuges must be located in a drivage which have regulators, distance of these regulators are 50 meters, or located them in new underground space (i.e. refuges should not distribute air flow).

Lay out of refuges had been done by GIS (Geographical Information System) program in Hashoni coal mine. Moreover, GIS has an ability, which can input 300 parameters for laying out a refuge. Indeed, GIS on base of all of safety rules and analyzing of network presents best location for lay out.

7 DESIGN AND LOCATION NOMINATION OF REFUGES AND LOCATION NOMINATION OF SCBA OF RESCUE TEAM

Location nomination of refuge and location of SCBA displays on mines operation map. Refuges displayed by RS and SCBA location represented by RC. Moreover, numbers beside RS show miners that exist in refuges. Indeed, location of SCBA represented by RC.

RS_{33} represented refuge in production faces 120, 622.

RS_{28} represented refuge in production face 427, and advancing breast.

RS_{22} represented refuge in production face 627.

RS_{38} represented refuge which refers to advancing breast 521, and retrading breast 521, moreover left hand side production face of tunnel 7.

RS_{20} represented production face 222.

RS_{37} represented production face 127, and right hand side production face of tunnel 7.

8 ANALYZE OF AIR PROVIDER APPARATUS IN A REFUGE

In this section wide parameters of RS_{33} presents, and complete calculation explained. This refuge can provide air for 33 miners.

8.1 Size of refuges

Volume of a refuge is calculated by the formula given below.

Volume of a refuge= length*width*height.

Calculation for RS_{33} is equal with:

$3.65 \times 4.57 \times 9.14 = 152.46\ m^3$.

8.2 Life time of refuges

Life time of a refuge depends on contained air in it. Thus, life time for RS_{33} is eight hours.

8.3 Volume for each miner

Air volume for every miner is calculated by the proportion of total volume of a refuge to maximum number of miners (i.e. that a refuge contained).

$$V = 152.46 / 33 = 4.62\ m^3 \qquad [1]$$

8.4 Proportion of life time and volume per every miner

Proportion of life time to volume for every miner will use in Figure 1 for evaluating oxygen and carbon dioxide.

$$\frac{T}{V} = \frac{8}{163.63} \cong 0.05 \qquad [2]$$

8.5 Evaluation of oxygen and carbon dioxide percentage in a refuge

On based of Figure 1, and above calculations, after 8 hours oxygen volume will be 17.5 percent, and carbon dioxide will be 2.5 percent. Thus, volume of oxygen decreased while Carbon Dioxide increased, so air provider device is necessary.

In table 3, all calculations have been realized for all refuge chambers.

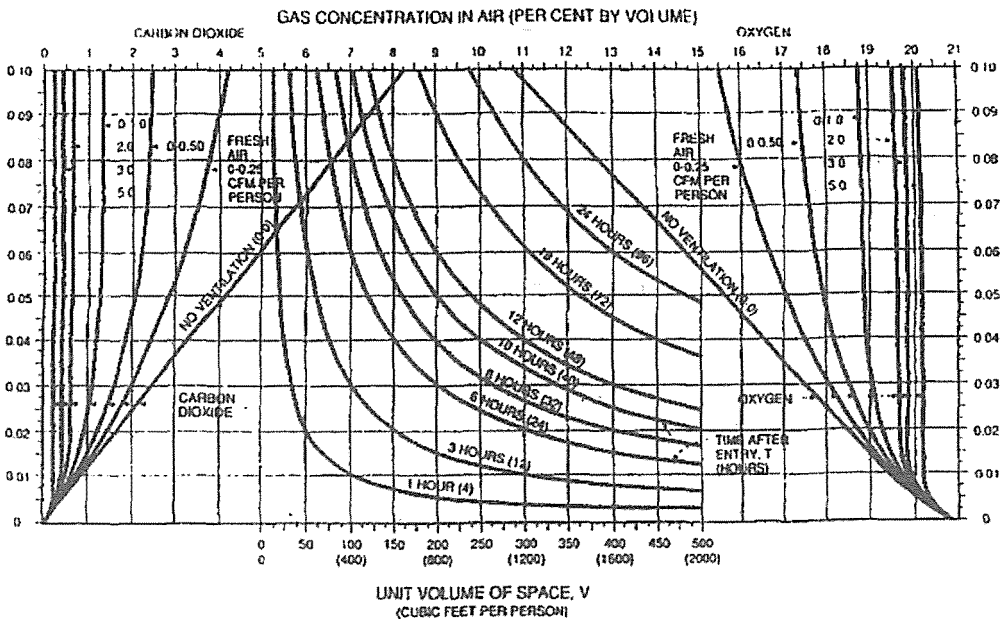

Figure 1. Gas concentration in air of a refuge

Table 3. Calculation of refuges

Refuge name	Prod. face	No. of miner, which consists in accident	Vol refuge (ft^3)	Life time of refuge (hours)	Vol for every miner	Proportional of life time to volume of a miner	O_2 (%)	CO_2 (%)
RS_{33}	622, 120	33	5400	8	163/63	0/05	17/5	2/5
RS_{28}	427	28	5400	8	193/86	0/041	18	2
RS_{22}	627	22	5400	8	245/45	0/032	18/25	1/75
RS_{38}	Adv. 521 Retr. 521	38	5400	8	142/1	0/057	17	3/1
RS_{20}	222 127	20	5400	8	270	0/03	18/4	1/6
RS_{37}	Right hand side tunnel	37	5400	8	145/94	0/054	16	2/75

9 FINANCIAL ANALYZE OF SELF-RESCUE APPARATUS AND EQUIPMENT OF AIR PROVIDER FOR REFUGES

Price of self-rescue with model W65 is 110 US $, and Russian model is 50 US $. Moreover, utility of SCBA in refuges is not suitable from the point of financial aspect. On the other hand, rescue teams needs SCBAs, which for every member of team must be equipped 2 with opened circuits SCBA.

Compressed air in all sections of mine exists, so applications of air provider devices, which work with compressed air, are best choice. Indeed, utility of carbon dioxide sensors are suggested. Manufacturing material of refuges should be fiber glass, which is fire proof. However, abandoned tunnels are appropriate location for placement of refuges that assembled in the mine.

10 EQUIPMENTS COSTS EVALUATION FOR SELF-RESCUE APPARATUS AND REFUGES

Cost of self-rescue device W65 model:
$ 110*178 =19580 US $.

Cost of self-rescue device Russian model:
50*178=8900 US $.

For every member of rescue team 2 SCBAs, which are open circuits (i.e. every rescue team has five members):
$3*5*2*4000= 120000 US$.

10.1 Costs in application of compressed air

Manufacturing cost of a refuge is 3000 US $, utility of carbon monoxide sensor devices cost is 1000 US $, and application of special equipment cost is 1000 US $. Total cost of manufacturing and extra costs of six refuges is equal with:
5000*6= 30000 US $.

Therefore, final cost of outfitted miner and refuges is 170000- 159000 US $, respectively.

10.2 Costs for application of air provider device

Manufacturing cost of a refuge is 3000 US $, special equipment in a refuges 1000 US $, and cost of air provider device is 12000 US $. Thus, total cost of refuges in this method is equal with:

16000*6= 96000 US $.

Therefore, final cost of outfitted miners and refuges is 236000- 225000 US $, respectively.

10.3 Costs in application of prefabricated and mobile refuge

Cost of a prefabricated refuge is 40000 US $. Thus, total cost of refuges in Hashoni coal mine will be

6*40000= 240000 US $.

Therefore, final cost of miner mobilized and refuges is 380000- 369000 US $, respectively.

11 CONCLUSION

In this paper, application of refuge chambers and miners safety equipment in Hashoni coal mine has been presented. Different method of outfitting of mine has been analyzed. Thus, on based of wide range of method, cost ranges from 225000 to 380000 US $.

Indeed, investment on safety is smaller part of cost in comparison of all mining operations. However, utility of air provider devices is best method providing wide secure domain in a mine.

REFERENCES

Cullen, Elaine, 2002. *A New Video Release from NIOSH on the Sunshine Mine Fire,* Retrieved *August*, 2002, from http://www.cdc.gov/niosh/mining/pubs/pdfs/tn497.pdf.

Contant, Jason, 2008, *a Little*, Canadas Occupational Health and Safety Magazine, Retrieved January, 2008, from http://www.ohscanada.com/issues/story.aspx?aid=1000228660&type=Print%20Archives.

Bayat, Mohammadmehdi, 2007, *Ventilation Network Design of Hashoni Coal Mine*, (Dissertation, Tehran University, 2007).

Towards Benchmarking of Safety Performance in the Mining Sector

Bekir Genc and May Hermanus
School of Mining Engineering, University of Witwatersrand, Johannesburg, South Africa

ABSTRACT This paper analyses the safety data in the SHECBenchmarking database for the period 2004 to 2008. A number of mining and minerals processing companies have entered data into this database and the paper illustrates what the SHECBenchmarking project has to offer. The overall safety performance of different companies, and divisions of companies within different industry sectors are compared, and opportunities for benchmarking and identifying potential sources of best practice are identified. The analysis is restricted to injury and fatality data for which the most data are currently available.

1 INTRODUCTION

The mining industry as a whole has a poor public image mostly because of its impacts on health and safety of people, and the environment. A number of initiatives are afoot to minimize these impacts and to align mining activities with imperatives of sustainable development. Examples of initiatives include documenting and sharing best practice, developing guidelines on addressing specific hazards and challenges, pooling resources to investigate and provide solutions for significant health and safety challenges and the SHECBenchmarking project described in this paper. The SHECBenchmarking project is aimed at enabling companies to routinely identify best performers and learn from one another. The acronym "SHEC" refers to safety, health, environment and community and is indicative of the ultimate scope of the indicators to be included in the database. Outstanding performance can be identified at sector level, or linked to the extraction of a specific commodity, a particular operation such as mining, exploration, and minerals processing, or a particular activity. The practices which support good performance can be ascertained thereafter identification, by direct engagement between companies.

2 WHAT IS BENCHMARKING?

Benchmarking is a process of comparing metrics of interest such as performance, output or quality indicators, for a specific purpose. The purpose of benchmarking is varies widely. It could be undertaken to assist consumers in exercising choice, to aid decision-makers and /or to identify potential sources of good practice. Benchmarking can be undertaken by range of means. These include comparing published information, comparing processes and practices through one-to-one interaction between parties, and auditing or review processes in which the relative strengths and weakness of various organization's / or organizational practices are assessed and ranked.

If the purpose of the benchmarking process is to identify good practice, several steps are involved which combine a number of the above activities. For example, first ranking the performance of companies in

terms of appropriate indicators, then identifying those companies which consistently achieve outstanding results or significant improvements over time, and lastly learning through direct interaction with company representatives about how these achievements or improvements have been secured. In the case of safety performance, lagging indicators tracked over time, such as fatality and injury rates usually provide the basis for ranking and identifying performance of interest (Wynn, 2008 and Stephanhurst, 2009).

3 SHECBENCHMARKING DATABASE

The Safety, Health, Environment and Community (SHEC) benchmarking database is a web-based resource. It provides companies with a tool for comparing their SHEC performance indicators to those of their peers, in order to identify the companies or the sites which have implemented or devised best practices and/or which offer opportunities for learning about how to improve health and safety (Benchmarking Database, 2009). At present the database contains only safety and health data. The database is populated progressively depending on the availability and compatibility of the data. At present the availability of the health data is limited.

BHP Billiton, the original developer of the database, transferred the intellectual property pertaining to the database to the Centre for Sustainability in Mining and Industry (CSMI) in March 2004. CSMI approached the International Council on Mining and Metals (ICMM) in May 2004 and proposed a joint venture between CSMI and ICMM for the development of a database. The ICMM agreed to encourage its members to participate in the database in 2005 (CSMI, 2009). The CSMI and the ICMM currently share the intellectual property associated with the project. www.SHECBenchmarking.com includes a facility for standard queries and some tables and graphs herein are the outputs of a standard query (and are indicated as such).

Participating companies must contribute their own data in order to have sight of the data of other companies and to conduct benchmarking queries. In this paper companies names are substituted by a letter of the alphabet in order to respect this agreement. The companies participating to the SHECBenchmarking project are listed on Table 1. All of the figures and tables presented in this paper are based on the the dataset as at 9 October 2009.

Table 1. Participating companies

African Rainbow Minerals
Alcoa Inc.
Anglo American
AngloGold Ashanti
Barrick Gold Corporation
BHP Billiton
Freeport Copper and Gold
Gold Fields
Lihir Gold
Lonmin
Mitsubishi Materials Corporation
Newmont
Nippon Mining and Metals
Rio Tinto
Sumitomo
Teck Cominco
Vale
WMC
Xstrata
Ziniflex

To maintain the integrity of the database, the data of companies are recorded in the database from the date of participation to the date of withdrawal or name change. For this reason the list of participating companies includes companies which have subsequently have merged with, or been sold and incorporated into other companies, for example in the case of Alcoa, WMC and Ziniflex.

4 SCOPE AND LIMITATIONS

There is uncertainty about how many people are employed in the mining and minerals sector world–wide. The ILO estimates that the mining industry alone employs over 30 million people worldwide, excluding the13 million people engaged as an artisan/small scale miners (MMSD, 2002). At the time of writing ICMM member companies account for approximately 750,000 people (CSMI, 2009), a small percentage of those associated with mining and mineral processing.

The data set obtained from the SHECBenchmarking database on the 9th of October, 2009 covers the information from the year 2004 to 2008; this information covers 86-92 per cent of data from participating companies as some companies have either no data or limited data available for this study. Figure 1 shows gaps in the data inputted by participating companies.

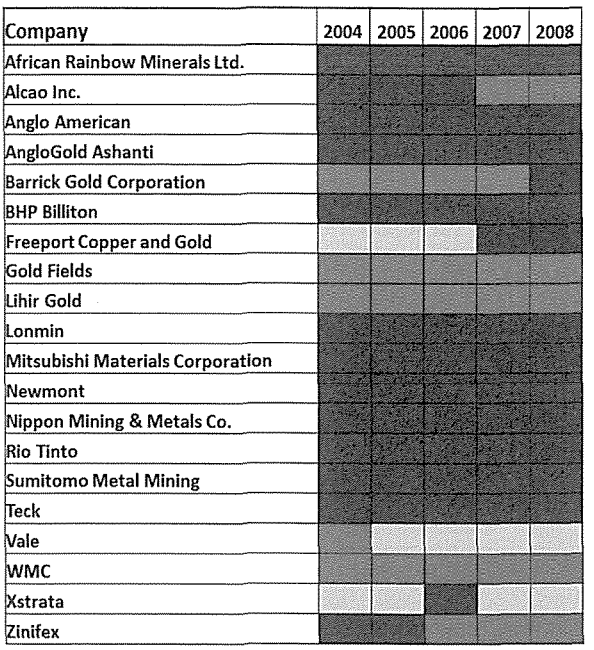

Notes on the Data Completeness Report

1. The basis for comparison is the number of expected operations/divisions (EXPECTED) against the number of reported operations/divisions (ACTUAL) expressed as a percentage.
2. The values displayed on the report are in the format (EXPECTED : ACTUAL : PERCENTAGE)
3. The boxes are color coded according to the PERCENTAGE.
   - 100% - The number of expected operations/divisions are equal to the number of reported operations/divisions
   - Less than 100% - The number of expected operations/divisions are more than the number of reported operations/divisions
   - 0% - No operations/divisions have been reported on for the selected year. Company has ceased to exist
   - Data is not available for the selected reporting year.
4. This report is run on annual data (i.e. totals are calculated for all monthly and quarterly data). Therefore incomplete quarterly or monthly data will not be reflected.

Figure 1. Data gaps by participating companies

Companies report data on the basis of their actual operations and divisions. The operations are categories on the database and the divisions are determined by company structure which is incorporated into the database. This analysis is limited primarily by the above gaps in the dataset which affect ranking and comparison. Of the 20 participating companies, at the time at which this analysis was undertaken, 11 included a complete dataset of injury and fatality data; 7 datasets were are incomplete and 2 had not yet submitted any data. Other limitations of the analysis include:

- The representativeness of the dataset. While the data set is representative of the majority of ICMM members, it is not representative of the mining industry as a whole
- While best performance among the participating companies can be identified, a complete data set would enable better interpretation of the results by giving better insight into the underlying operations.

While the database contains some health data, this is extremely limited and for this reason not included in this study.

Rates are presented as per million hours worked in this paper. The definitions of the indicators used in the SHECBenchmarking database are the outcome of the work of specialist working groups and are as follows:

Fatality - Work-related injury resulting in death of employee or contractor.

Injuries – There are five categories of injuries described as follows.

Lost Time Injuries: A Lost Time Injury (LTI) is a work-related injury resulting in the employee/contractor being unable to attend work on the next calendar day after the day of the injury. If a suitably qualified medical professional advises that the injured person is unable to attend work on the next calendar day after the injury, regardless of the injured person's next rostered shift, a lost time injury is deemed to have occurred.

Restricted Work Injuries: A Restricted Work Injury (RWI) is a work-related injury which results in the employee / contractor being unable to perform one or more of their routine functions for a full working day, from the day after the injury occurred. An RWI should be certified by advice from a suitably qualified health care provider.

Lost Time + Restricted Work Injuries: Some companies do not differentiate between Lost Time and Restricted Work Injuries. For such companies, counts of LTIs reported to the ICMM database include RWIs, and are marked as such in the database. As a result, the main benchmarking injury statistic that should be used is the 'Lost Time + Restricted Work Injury' count (and associated frequency rate). However, the preference is that the ICMM database LTI count excludes RWIs and that RWIs are counted separately.

Medical Treatment Injuries: A Medical Treatment Injury (MTI) is a work-related injury resulting in the management and care of a patient to combat disease or disorder, including any loss of consciousness, which does not result in lost time or restricted work. MTIs include (for example) suturing of any wound, treatment of fractures, treatment of bruises by drainage of blood, treatment of second and third degree burns. MTIs do not include:

- Visits to physicians or other licensed health care professional solely for observation or counseling.
- The conduct of diagnostic procedures, such as X-rays and blood tests, including the administration of prescription medications used solely for diagnostic purposes (e.g. eye drops to dilate pupils etc.).
- Visits to physicians or other licensed health care professionals solely for therapy as a preventative measure (e.g. physiotherapy or massage as preventative therapy, tetanus or flu shots).

First Aid + Medical Treatment Injuries: Some companies do not differentiate between Medical Treatment and First Aid Injuries. For such companies, counts of MTIs reported to the ICMM database include FAIs, and are marked as such in the database. The preference is that the ICMM database MTI count excludes FAIs.

While the data is incomplete, the safety performance of the ICMM as a whole compares well against that of South Africa, Australia and USA. South African underground metal data consist of gold, platinum and chrome only and USA underground metals data is generally based on a small number of events in Figure 2. Figure 2 illustrates ICMM safety performance comparison between these countries. It thus makes sense to search for leading practice amongst ICMM members

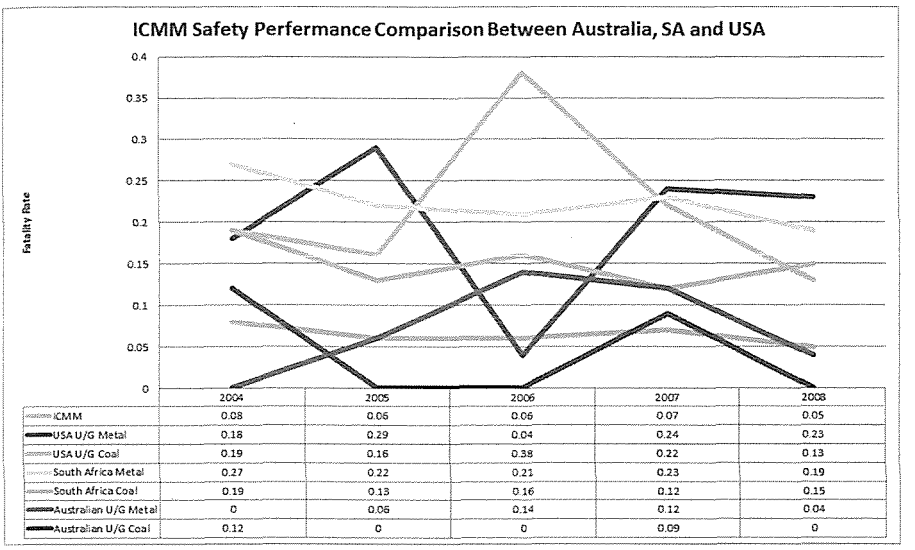

	2004	2005	2006	2007	2008
ICMM	0.08	0.06	0.06	0.07	0.05
USA U/G Metal	0.18	0.29	0.04	0.24	0.23
USA U/G Coal	0.19	0.16	0.38	0.22	0.13
South Africa Metal	0.27	0.22	0.21	0.23	0.19
South Africa Coal	0.19	0.13	0.16	0.12	0.15
Australian U/G Metal	0	0.06	0.14	0.12	0.04
Australian U/G Coal	0.12	0	0	0.09	0

Figure 2. ICMM safety performance comparison between Australia, South Africa and USA (adapted from the reports of the Minerals Council of Australia 2008, the Chamber of Mines of South Africa 2008 and 2009, and NIOSH, 2008).

5 HOW DO COMPANIES PARTICIPATE?

Participating companies assign a Company Administrator, a Data Capturer, and a Data Verifier to upload their data to the database. A Company Administrator is a user that has access in the SHEC Benchmarking system to maintain the Company Structure and Users for a specific company. A Data Capturer is a user that can capture statistics for a specific company for all Open Periods. A Data Verifier is a user that can change statistics for a specific company for all closed periods. The company administrator is the only person allowed to change the company data. The data is usually loaded quarterly by each company administrator.

The SHECBenchmarking system has rules about how data is organized and uses specific health and safety definitions. Injury related definitions were given in section 3 and fatality related definitions are self-explanatory. Table 2 shows safety indicators.

Table 2. Safety indicators

Indicators -- Employees, Contractors or Total Employees & Contractors
Exposure Hours
Fatality – Electrical
Fatality - Explosions & Fires
Fatality - Falls from Heights
Fatality – Geotechnical
Fatality - Hazardous Substances
Fatality - Machinery, equipment and hand tools
Fatality - Mobile Equipment
Fatality – Other
Fatality - Slips, Trips & Falls
Total Fatalities
Injury - Lost Time Case (LTCs)
Injury - Restricted Work Cases (RWCs)
Medical Treatment Injuries
Total Lost Days - Lost Time due to LTCs
Total Lost Days - Lost Days due to RWCs
Total Recordable Injuries (TRIs)

6 METHODOLOGY

The dataset was examined in totality to check data completeness and to assess the value of undertaking various analyses. This examination informed the authors' decision to exclude the health data. Fatality and injury data trends were produced for the ICCM overall, per commodity and per company. Full time employees and contractor outcomes were examined together and separately. Fatality and injury rates for the entire period and for each year were considered.

7 RESULTS

7.1 ICMM Trends in Fatality and Injury Rates (2004 – 2008)

The fatality and injury (lost time + restricted work injuries) rates have improved over the 5 year period, showing an overall downward trend. Figure 3 demonstrates ICMM trends in fatality and injury rates. The reason behind the significant deterioration in the rates in 2007 is not clear.

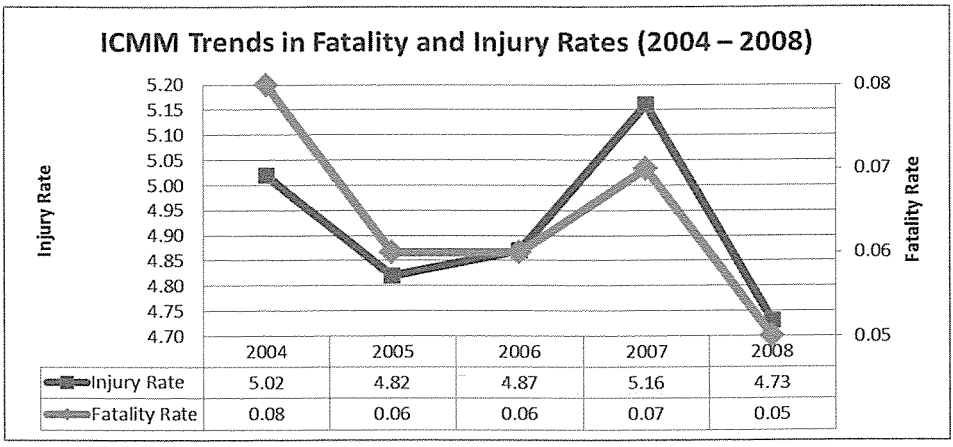

Figure 3. ICMM trends in fatality and injury rates (2004-2008)

Both the fatality and injury rates show a similar trend, with the trend lines almost parallel. This apparent correlation is spurious for the following reasons:

- The correlation is only apparent when the data is aggregated. Since the same trends are not evident at commodity (Figure 12) and company (Figure 9) levels, it cannot be inferred that a consistent relationship exists between the fatality and injury rates (indicated by relatively constant ratio between the rates).
- The aggregated data contains some significant gaps with data for 3 companies not being available for all the years under review. The same "trend" may not be apparent when the full dataset is accounted for.

7.2 Fatality and Injury Rates by Companies

The fatality and injury rate by each participating company has been generated by the following figures (Figure 4, 5, 6, 7, 8, and 9) which show both rates for successive years, 2004-2008. The participant company names have randomly been disguised and renamed by an alphabet.

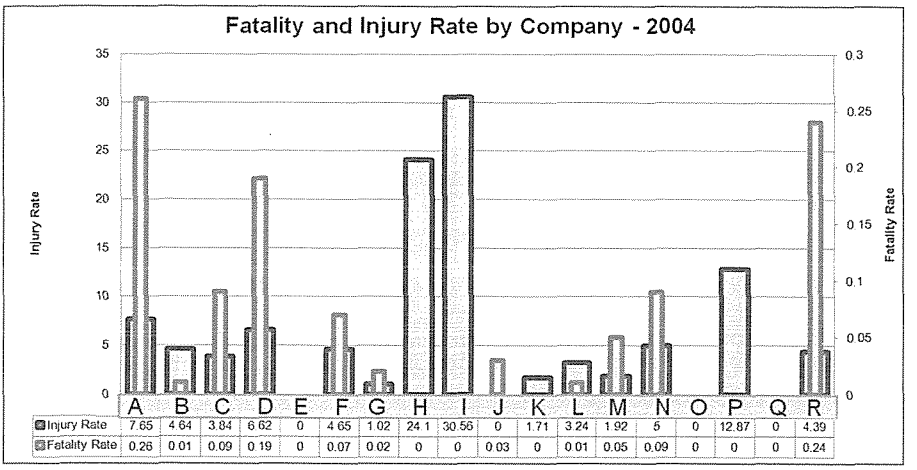

Figure 4. Fatality and injury rate by company – 2004

In 2004 the highest fatality rate was recorded by COMPANY A and the highest injury rate was recorded by COMPANY I (Figure 4).

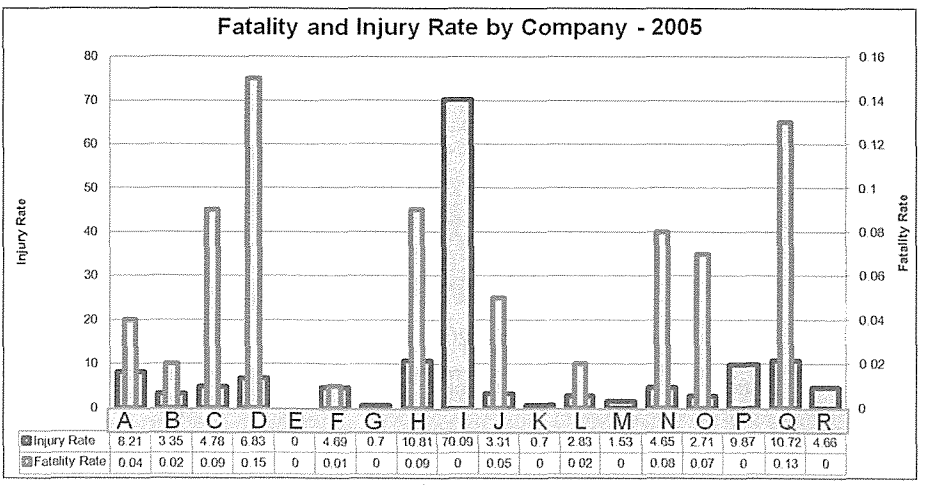

Figure 5. Fatality and injury rate by company – 2005

In 2005 the highest fatality rate was recorded by COMPANY D and the highest injury rate was recorded by COMPANY I (Figure 5).

In 2006 and 2007 the highest fatality rate wasrecorded by COMPANY D and the highest injury rate was recorded by COMPANY H (Figure 6 and 7).

In 2008 the highest fatality rate was recorded by COMPANY A and the highest injury rate was recorded by COMPANY I (Figure 8).

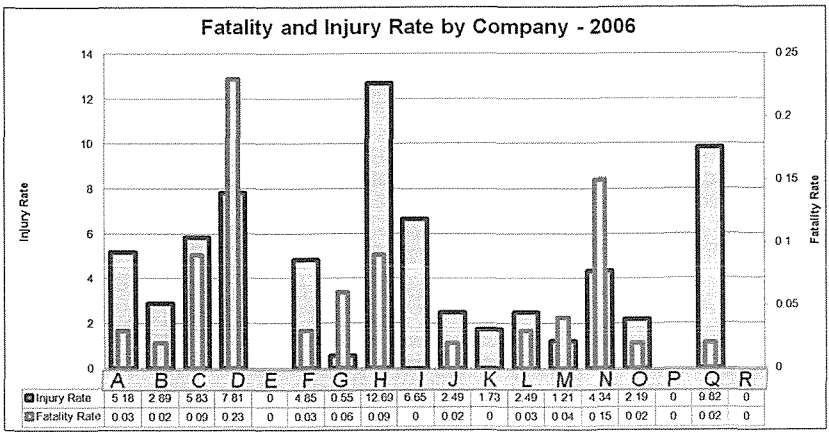

Figure 6. Fatality and injury rate by company – 2006

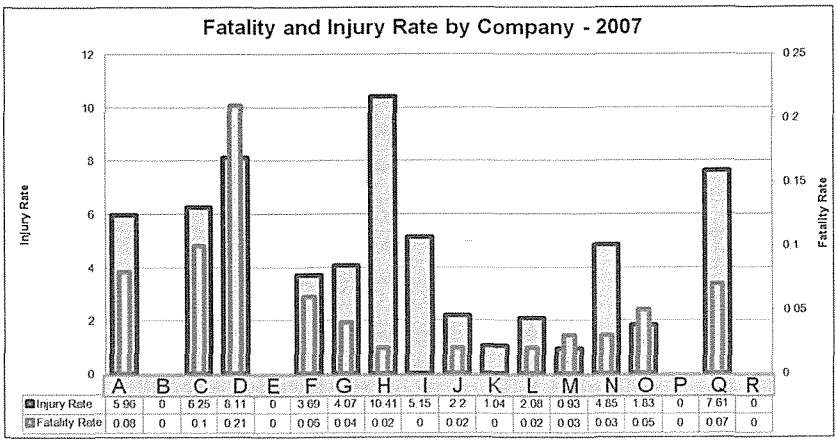

Figure 7. Fatality and injury rate by company – 2007

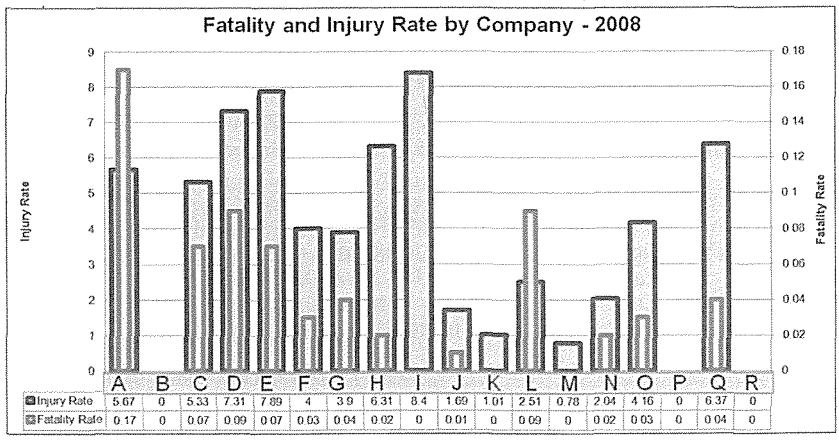

Figure 8. Fatality and injury rate by company – 2008

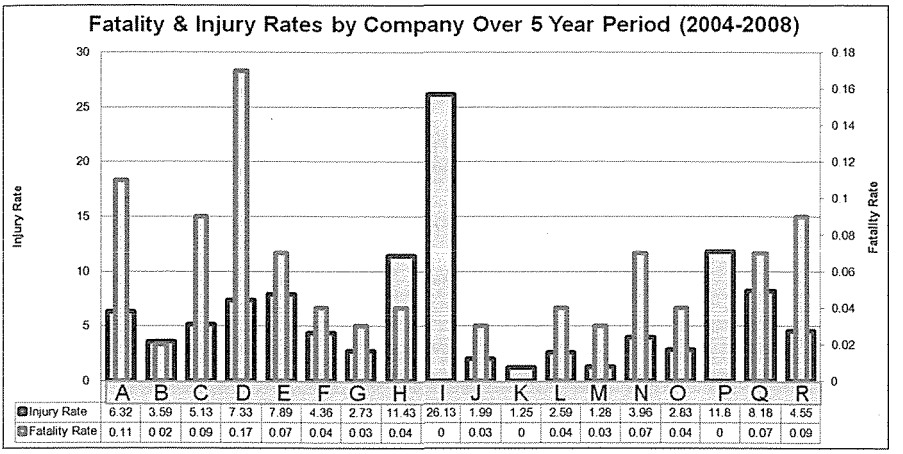

Figure 9. Fatality and injury rate by company – (2004-2008)

The highest fatality rate has been recorded by a gold mining company (COMPANY D) for the 5 year period under review but it was one of the two gold producers which had a full data set available for this exercise and the other participating three gold mining companies' data sets were not complete at the time of the data collection. The lowest fatality rates were most often registered by COMPANY I and COMPANY K over the 5 years reviewed.

The highest injury rate was recorded by a steel producer (COMPANY I) for the 5 year period. Its injury rate is more than 200 per cent higher compared to that of the other participating companies' injury rate. The reason for this anomaly cannot be established by consideration of the injury data alone. COMPANY K achieved the lowest injury rates during the 5 year period. COMPANY K operates in the oil and gas sector.

The *most improved company* in respect of the fatality rate was COMPANY F which is involved in a wide range of activities across a spectrum of commodities. In respect of injury rates, COMPANY H achieved the most significant improvement in the 5 year period. Company H operates in a high energy hazard environment in which personnel could be directly exposed to hazards should controls fail.

The 5-year comparison points to where best practice could be found. The management systems and approach of COMPANIES K, F, I and H could be investigated further through on-site interaction. Issue for investigation could also include specific information on the management of fatal and non-fatal risks, and the nature of the major hazards associated with the operations of these companies. Whether or how COMPANY H has changed its approach to non-fatal risks could be of interest, and the understanding the context and drivers which enable COMPANY K to achieve zero fatalities may be helpful to others wishing to achieve the same.

It is interesting to note that COMPANY A recorded the most variable results in terms of the fatality rate, while Company I recorded the most variable results in the injury rate section. The nature of the hazards associated with these companies' operations and the challenges which they pose may be helpful in designing strategies for improving safety by helping to identify "watch-points. Table 3 summarizes the findings about where to seek best practice.

Table 3. Fatality and injury rate by company

	2004	2005	2006	2007	2008	OVERALL
Fatality Rate - Highest	A	D	D	D	A	D
Fatality Rate - Lowest	H I K	G I K M R	I K	I K	I K M	I K

	2004	2005	2006	2007	2008	OVERALL
Injury Rate - Highest	I	I	H	H	I	I
Injury Rate - Lowest	J	G K	G	M	M	K

7.3 Fatality and Injury Rates by Commodity

The fatality rate for the 5-year period under review was highest in the diamond mining sector (0.26 per million hours worked), followed by the lead mining sector (0.19 per million hours worked) but most fatalities occurred in the gold mining sector (156 deaths), followed by PGMs (94 deaths).

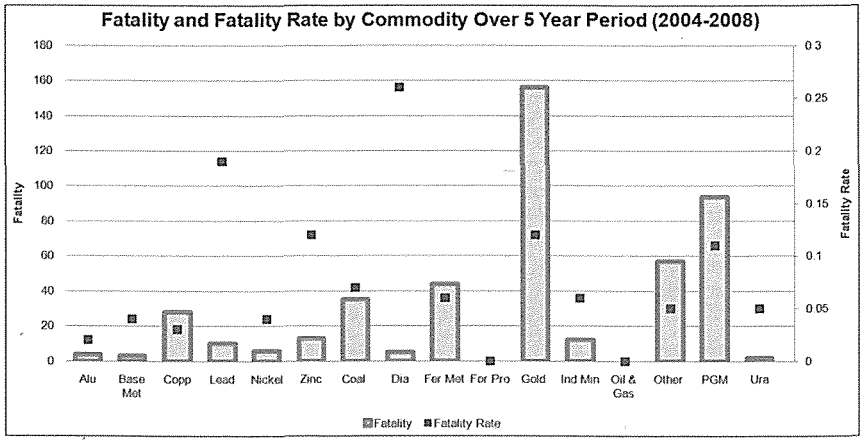

Figure 10. Fatality and fatality rate by commodity – (2004-2008)

Diamond mining is much mechanized, and small numbers of fatalities (5 deaths) translate into large fatality rates. The high fatality rates are due to the low number of people employed and the fact that when an accident occurs they are likely to be serious as large equipment is involved. The high numbers of fatalities in the gold and platinum sector are, in part, due to the labor-intensiveness of mining as well as uncertainties in control of major hazards on these mine sites. In effect, large numbers of people work in areas in which there are major hazards, for which controls are not yet fail safe. Figure 10 shows fatality and fatality rate by commodity between the year 2004 and 2008 while Figure 11 shows the injury and injury rate by commodity for the same time period.

The overall injury rate was highest in Uranium mining sector (9.58 per million hours worked) followed by PGMs (9.55 per million hours worked) but most injuries occurred in PGMs (8306) followed by the gold mining sector (7326) over the 5 year period under review. Again large numbers of people are exposed on the PGM and gold mining sites. Figure 12 illustrates fatality and injury rate by commodity over the 5 year period.

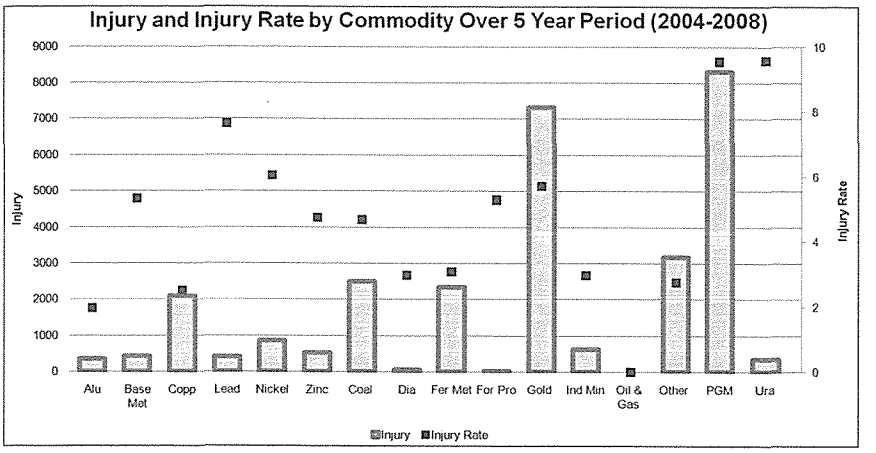

Figure 11. Injury and injury rate by commodity – (2004-2008)

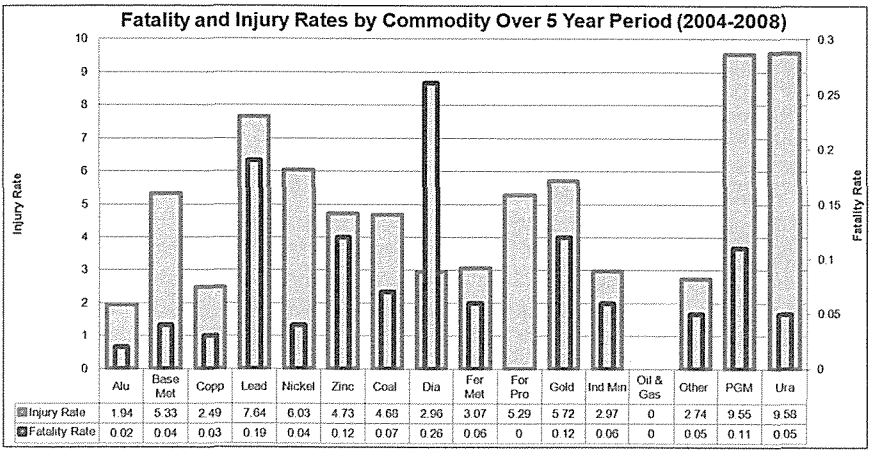

Figure 12. Fatality and injury rate by commodity – (2004-2008)

8 CONCLUSIONS

The data set obtained from the SHECBenchmarking database on the 9th of October, 2009 covers the information from the year 2004 to 2008; this information covers 86-92 per cent of data from participating companies as some companies have either no data or limited data available for this study. Gaps in the dataset affect the ranking and comparison of the company performance. While the data set is representative of the majority of ICMM members, it is not representative of the mining industry as a whole. While the best performance among the participating companies can be identified, a complete dataset would enable a more definitive analysis. Nevertheless this study gives a clear indication about where the best practices amongst the participating companies can be found and where problems can be anticipated. The case of the latter, it is apparent that high levels of injuries – fatal and non-fatal - correspond to situations in which high numbers of people are potentially exposed to major hazards. This implies that attention to both control of major hazards and reduced the numbers of

people potentially exposed would lead to improvements in safety.

REFERENCES

Benchmarking Database, (2009). www.SHECBenchmarking.com, 9 October 2009.

Breaking New Ground – Mining and Sustainable Development. The report of the MMSD Project pp42 and 43. EarthScan Publications Limited. 2002.

Census of Fatal Occupational Injuries, (2009). Hours-based fatality rates by industry, occupation, and selected demographic characteristics, 2008, accessed on 2010/01/19 from http://www.bls.gov/iif/oshwc/cfoi/cfoi_rates_2008hb.pdf

Chamber of Mines, (2007). Facts and Figures, accessed on 2010/01/19 from http://www.bullion.org.za/

Chamber of Mines, (2008). Facts and Figures, accessed on 2010/01/19 from http://www.bullion.org.za/

CSMI calculation based on annual reports and annual reports to society of individual ICCM members, 2009.

ICMM, (2010). Macro Region Comparison Reports, SHEC Database.

Internal Note. Centre for Sustainability in Mining and Industry (CSMI) (2009), www.CSMI.co.za, 29 October 2009.

Minerals Council of Australia, (2007). Safety performance report of the Australian minerals industry 2006 - 2007, Minerals Council of Australia.

Minerals Council of Australia, (2008). Safety and Health Performance Report, accessed on 2010/01/20 from http://www.minerals.org.au/information_centre/s__and__h_performance_report/publications2/

NIOSH, (2007). Mining Occupational Fatalities and Injuries, accessed on 2010/01/19 from http://www.cdc.gov/niosh/mining/statistics/images/pp23.gif

NIOSH, (2007). Mining Occupational Fatalities and Injuries, accessed on 2010/01/19 from http://www.cdc.gov/niosh/mining/statistics/images/pp23.gif

NIOSH, (2007). Number and Rate of Coal Operator Mining Fatalities by Underground and Surface Work Locations by year, 1998-2007, accessed on 2010/01/20 from http://www.cdc.gov/niosh/mining/statistics/images/fusc.gif

NIOSH, (2009). RM Case in SA Mining.

Stapenhurst, T. The Benchmarking Book: A How to Guide to Best Practice for Managers and Practitioners. Elsevier Ltd, 2009. Chapter 2.

Wynn, M L. Highlights of An Industry Benchmarking Study: Health and Safety Excellence Initiatives. Journal of Chemical Health and Safety, May/ June 2008, pp 22-24.

Application of OHSAS 18000 to Bigadiç Boron Work to Improve Existent Working Conditions

OHSAS 18000'in Mevcut Çalışma Koşullarının İyileştirilmesi İçin Bigadiç Bor İşletmesine Uygulanması

S. Gökçek
Orta Doğu Teknik Üniversitesi, Maden Mühendisliği Bölümü, Ankara

T. Güyagüler
Orta Doğu Teknik Üniversitesi, Maden Mühendisliği Bölümü, Ankara

ÖZET OHSAS (İş Sağlığı ve Güvenliği Yönetim Sistemi) 18001 standardı bir yönetim sistemi oluşturarak çalışanlar için daha güvenli, daha huzurlu ve sağlıklı bir çalışma ortamı sağlamayı hedeflemektedir. Madencilik genellikle yüksek risk taşıyan çalışma ortamlarında gerçekleştirildiğinden, OHSAS dünya madenciliğinde gün geçtikçe önem kazanmaktadır. Bu çalışmanın amacı Bigadiç Bor İşletmesindeki mevcut çalışma koşullarını OHSAS 18001:1999 gerekliliklerini uygulayarak iyileştirmektir. Bu çalışmada, işletme için bir risk yönetimi metodu geliştirilmiştir. İşletme genelinde yapılan işlerde bir tutarlılık sağlamak için bir "İş Güvenlik Analizi" formu önerilmiştir. Bu form işletmede bir işi gerçekleştirirken yapılan iş basamaklarını ve mevcut veya olası tehlikeleri tanımlamak, analiz etmek ve kayıt altına almak için kullanılabilir. Risk değerlendirmesinin yardımı ile delme işlemi için "güvenli iş prosedürü" hazırlanmıştır. Buna ek olarak bir acil durum ya da doğal afet durumunda can, mal ve bilgi kayıplarını önlemek ve güvenliği sağlamak için bir "Acil Durum Planı" geliştirilmiştir. Tehlikelerin tanımlanmasında, iş sağlığı ve güvenliğinin geliştirilmesinde ve sistemin mevzuata uygunluğunu kontrol etmede denetimler İSGYS'nin ayrılmaz bir parçasıdırlar. Buradan yola çıkarak, Bigadiç Bor İşletmesi için sistemin sürekli gelişiminde çok önemli bir rol oynayacak olan "İSG Denetleme Aracı" önerilmiştir. Yapılan bu çalışmalar, sistemin uygulanmasında bazı sorunlar meydana çıktığını göstermektedir. En büyük problem veri kaydetme ve saklamadaki yetersizliktir. Çalışanların bilinç düzeyinin azlığı ve sorumluluktan kaçışı da bir diğer önemli sorunu oluşturmaktadır. Bu sorunlar madencilik sektörü içerisinde oldukça yaygın olmasına rağmen, OHSAS 18000'in uygulanması çalışma koşullarının iyileştirilmesinde oldukça önemli bir yer arz etmektedir.

ABSTRACT OHSAS (Occupational Health and Safety Assessment System) 18001 standard aims to provide secure, more tranquil and healthier working space to the employees by means of establishing an assessment system. As mining activities are generally carried out in high risk environments, OHSAS has been increased its importance for mining in the world. The objective of this study is to improve existing working conditions of Bigadiç Boron Work by means of implementing OHSAS 18001: 1999 requirements. In this study, a risk assessment method is developed for enterprise. In order to provide consistency throughout the enterprise a "Job Safety Analysis" form is proposed. It can be used to identify, analyze and record the steps involved in performing a specific task, and the existing or potential safety and health hazards associated with each step. "Safe job procedure" for drilling was also prepared with the help of the risk assessment process. In addition to this, an "Emergency Plan" is developed for enterprise to prevent loss of life, property and information, and provide safety in case of any emergency or natural disaster. Audits are integral part of OHSAS in order to identify hazards, improve health and safety conditions, and check compliance with regulations. From

this point of view an "OHS Audit Instrument" is developed for the Bigadiç Boron Work that will play a key role for continuous improvement of the system. These studies also show that there are some problems in the implementation of the system. The main problem is ineffective data recording and keeping. Lack of consciousness and low commitment of employees constitute another important difficulty. Although these problems are commonly encountered in practice, applying OHSAS 18000 standard is still worthwhile method of improving work environment.

1 INFORMATION ABOUT BIGADIÇ BORON WORK

Bigadiç Boron Works has been established in 1976 and located at 12 Km. North-East of Bigadiç which is a district of Balıkesir. Bigadiç is 36 Km far from the city center and it has population of 15.000. The distribution of personnel in enterprise is given in Table 1. As it can be seen from table, totally 276 workers are employed.

Table 1. Distribution of Personnel in Bigadiç Boron Work

Personnel Type	Number	% Distribution
Contract Personnel	99	25.4
Employee	14	3.6
TOTAL WHITE COLLAR	113	29
Worker	276	71
TOTAL BLUE COLLAR	276	71
GRAND TOTAL	389	100

The enterprise has three open-pit boron mines, one mineral processing plant, and a Crushing & Grinding Plant. 113 white-collar and 223 blue-collar personnel work in Bigadiç Boron Work.

Due to organizational changes and unhealthy record keeping, only the last four years of statistical data is shown at Table 2. As it is shown, the most frequent type of accident is "struck by" accidents. As a result, between 2004 and 2008 there are 52 accidents occurred and caused to 61 injuries, 3 fatalities, and 18671 workday losses.

2 OHSA SYSTEM AND RISK ANALYSIS

OHSA System studies are evaluated and improved continuously in accordance with Application Management method that is shown in Figure 1.

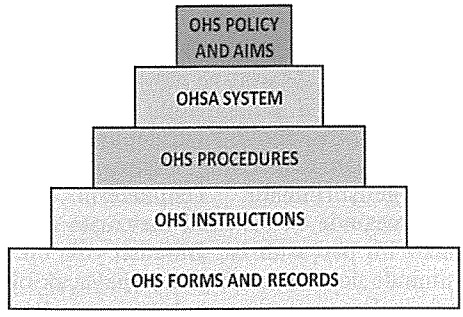

Figure 1. OHSA System Application Management

OHSA System is based upon the OHS Forms and Records. OHS Instruction and Procedures constitute the upper steps. The continuous improvement and updating take place in these steps mainly. The OHS Policy and Aims are standing at the top level of Application Management.

2.1 Establishing the Risk Assessment System

The data collected owing to Hazard Source Inventory and Hazard Identification Checklist documents in which should be prepared according the structure of organization would constitute a helpful feedback for risk evaluation.

Table 2. Accident Statistics by Type

Type of Accident	Number of Accident	Number of Injury	Number of Fatality	Total Number of Victims	Number of Workday Loss
Traffic	2	13	1	14	6132
Struck-by	13	13	0	13	67
Fall-same-	2	2	0	2	55
Fall-to-	3	2	1	3	6117
Caught	5	5	0	5	52
Overexertio	8	8	0	8	63
Cut	6	6	0	6	43
Burn	1	1	0	1	14
Exposure	4	5	1	5	6072
Caught-on	4	2	0	2	21
Struck-	2	2	0	2	21
Caught-in	2	2	0	2	14
TOTAL	52	61	3	63	18671

As long as the data collected from working fields, it would give hints about prominent hazards and form guidance for risk assessment. The Risk Assessment Charts and Risk Evaluation Form are prepared for risk evaluation. The Risk Assessment Form constitutes from several scoring charts that are given in Table 3,4,5 and 6.The risk score of identified hazards is calculated according to these charts. The risk evaluation is based on Kinney Risk Evaluation Method. There are three parameters exist in evaluation of risks. These are the likelihood of risk, frequency of exposure to risk, and consequence of its associated hazard. The Risk Score is calculated from the formulae given below:

$$R = L \times E \times C$$

where;

R: Risk Score
L: Likelihood Score
E: Exposure Score
C: Consequence Score (Taylor and Easter, 2004)

There are three charts used for Risk Assessment. These are the score charts for these three parameters, Likelihood, Exposure, and Consequence. These parameters are shown in Table 3, Table 4, and Table 5 respectively. The risk categorization can be made and the required action is found from the risk score chart which is given in Table 6. The highest risk score that can be attributed is 10000 and the lowest is 0.1. According to risk score a risk categorization is constructed and required action for this categorization is specified. The Risk Evaluation Form is used to detect risks and their corresponding risk scores by means of Risk Evaluation Charts. This is a systematic approach to detect risks and their risk scores. After that the risks are listed from highest score to lowest and the risk reduction action should be naturally started from risk which has the highest risk score. Each hazard should be indicated in Risk Evaluation Form. The "Result" at the top of the form refers to hazard category and "Completion Date" means the required action which has to be taken within the given period of time. The "Present Situation" refers that whether the suggested result (or suggestion) is available in enterprise or not. Finally, the "Responsible people" refers to responsible superior if the hazard is exposed and the person who is responsible to take precautions against the indicated hazards. A sample risk assessment is given in Table 7.

Table 3. Likelihood Score Chart

Likelihood	Score	Qualitative Expression of Likelihood	Quantitative Value of Probability
Highly Unlikely	0.2	Practically Impossible	$P > 10^{-6}$
Unlikely	0.5	Once in fifty years	$10^{-4} > P > 10^{-5}$
Unusual But Possible	1	Once in 3-4 years period	$10^{-3} > P > 10^{-4}$
Possible	3	Tree times or more in a year	$10^{-2} > P > 10^{-3}$
Very Likely	6	Once a month	$10^{-1} > P > 10^{-2}$
Almost Certain	10	Once a week or more	$1 > P > 10^{-1}$

Table 4. Exposure Score Chart

Frequency of Exposure to Risk	Score	Qualitative Expression of Exposure
Very rare	0.5	Once per year or less
Rare	1	A few times per year
Unusual	2	Once per month
Occasional	3	Once per week
Frequent	6	Daily (some hours)
Continuous	10	Constant (during shift)

Table 5. Consequence Score Chart

Consequence Category	Score	Qualitative Expression of Hazard Severity
Noticeable	1	Will not result in injury, no work hour loss
Minor	3	No workday loss but first aid may required
Major	7	Major injury, workday loss
Serious	15	Severe injury or occupational illness, Permanent partial disability, long term treatment
Fatality	40	Fatality
Disaster	100	Number of Fatalities

Table 6. Risk Score Chart

Risk Category	Risk Score	Action
Unimportant Risk	$R < 20$	No attention required. There may be no need for extra risk reduction process but current controls have to be continued and controlled. A long-range study may be initiated.
Low Risk	$20 \leq R < 70$	Attention required. Plan to reduce risk in 30 – 90 days
Moderate Risk	$70 \leq R < 200$	Risk reduction is required. Take precautions within a month
High Risk	$200 \leq R < 400$	Corrective actions required. Stop working and correct within 7 days. Immediate precautions have to be taken
Intolerable Risk	$R \geq 400$	Stop working and correct immediately. If risk reduction is not possible than this operation has to be abandoned.

The performed risk analysis must be repeated whenever the following situations take place:
- Accidents
- Layout plan changes
- New machinery/equipment/construction installation
- Modifications of existent machinery / equipment / construction
- Change of legal requirements

2.2 Application of Risk Assessment System

In order to assess risks, firstly the hazards should be identified. Only the identified hazards can be assessed, and risk assessments will rarely reveal unidentified hazards. Hazard identification includes items that can help about identifying workplace hazards and determining what corrective actions are necessary to control them. These items include jobsite safety inspections, accident investigations, health and safety comities etc. The hazard identification can be carried out by means of the field observations of responsible occupational health and safety staff as well as negotiation with working staff. Before start to risk evaluation, the work fields of Bigadiç Boron Work are identified. The main source of all hazards and their possible effects are indicated.

The opinion of department representatives, operators or workers were considered also and the common ideas has been accepted as hazard and been recorded. The Risk Evaluation Form which has been prepared to record and follow-up the identified risks were sent to all related staff of departments and top management. To contribute risk reduction process the comments, precautions, and suggestions from the department representatives and management are requested.

Application of risk assessment system is based on risk evaluation forms. These forms are prepared with utilization of past accident data, health service records, statistics and experiences. The processes which have high risks are prioritized. In this study, blasting task is examined and the risk evaluation is prepared and given in Table 7. Initially the process, sub-system, activities and staff who may be affected by potential risks are identified. Then L, E, and C scores are assigned according to Risk Evaluation Charts. The risk score is calculated for each activity or hazard, and their expected results and several suggestions are indicated in order to escape from risks by means of these forms.

Table 7. Risk Evaluation Form for Blasting

Date	10/07/2010	**RISK EVALUATION FORM**	**Assessment Number**	3
Dept.	Simav; Tülü & Acep Open-pits Head Eng.		**Prepared by**	
Process	Open-pit Mining		**Approved by**	
Sub-system	Blasting		**Rev. Number &Date**	0&.../.../20...

No	Hazard	Who may be harmed	L	E	C	Risk Score	Result	Completion Date
1	Fall-to-below	Blasting team	0.5	3	40	60	Low	Three months
2	Fall-to-same level	Blasting team	0.5	3	3	4.5	Unimportant	No priority
3	Hit by	Workers	0.5	3	40	60	Low	Three months
4	Traffic accident	Drivers	0.2	3	40	24	Low	Three months
5	Explosion	Workers	0.5	3	100	150	Moderate	A month

No	Consequence	Risk Score	Prevention / Recommendation	Present situation	Responsible people
1	Fatality and/or serious injury	60	Do not close to benches and do not enter cracked and fractured areas. Wear appropriate foot and head protection.	NA	Dept. Head Engineer
2	Injury	4.5	Keep the site clear of obstructions. Wear appropriate foot and head protection.	A	Management
3	Fatality and/or serious injury	60	Overload of drills may cause fly rock. Use proper head protection equipment	NA	Dept. Head Engineer
4	Fatality and/or serious injury	24	All traffic must be stopped before blasting	A	Dept. Head Engineer
5	Many Fatalities and/or serious injuries	150	Always use warning system before blasting and clear the area. Watch the area for trespassing. Close cell phones to avoid unplanned explosion	A	Dept. Head Engineer

L: Likelihood Score E: Exposure Score C: Consequence Score

A: Available NA: Not Available

3 JOB SAFETY ANALYSIS

Job safety analysis (JSA), also known as Safe Work Procedure, is a basic approach to develop improved accident prevention procedures by documenting the firsthand experience of workers and supervisors and at the same time it tends to instill acceptance through worker participation. The five basic steps of JSA are:

1) Select jobs with the highest risk for a workplace injury or illness.

2) Separate the job into its basic steps

3) Identify and record each step necessary to accomplish the task. Use an action verb (i.e. pick up, turn on) to describe each step.

4) Identify all actual or potential safety and health hazards associated with each task.

5) Determine and record the recommended action(s) or procedure(s) for performing each step that will eliminate or reduce the hazard (i.e. engineering changes, Personal Protective Equipments, etc.).

When selecting the job to be analyzed, it should be ranked in the order of greatest accident potential. Jobs with the highest risks should be analyzed fist. In order to rank jobs to be analyzed, the following criteria should be used:

1) Accident frequency

2) Accident Severity

3) Judgment and experience

4) New jobs, non-routine jobs, or job changes (Reese, 2003)

After a job is selected, the JSA can be initiated. A "Job Safety Analysis Form" is introduced for Bigadiç Boron Work. The JSA form lists the basic job steps, the corresponding hazards, and offers notes in order to control each step. The structure of Job Safety Analysis Form can be followed from Table 8. If the sequence of job steps or the deviations from established job steps are critical to the safe performance of a job, this should be noted in JSA. The next step of the JSA is to eliminate or reduce potential accidents or identified hazards. The following points should also be considered for each identified hazard and to them some notes and comments should be indicated for the each job step in the JSA form:

1) Can a less hazardous way to do the job be found?

2) Can an engineering revision take place to make the job or work area safer?

3) Is there a better way to do the job?

4) Are there work-saving tools and equipment available that can make the job safer? (Reese, 2004)

Drilling activity is selected and its job safety analysis is shown in Table 8.. It is important to get involvement of workers in the JSA process. Workers are familiar with the jobs and can combine their experience to develop the JSA. A complete JSA is a continuing effort to analyze one hazardous job after another until all jobs with sequential steps are included in JSA. Once it is established, the standard procedures should be followed by all employees.

4 EMERGENCY PLAN

The actions performed in case of accidents, explosion, fire and natural disasters (flood, earthquake etc.), and any emergency situations should be indicated in an Emergency Plan. The preparation of emergency plan is based on risk evaluation process. An effective emergency plan must include following points:

- Identification of potential emergency situations
- Identification of personnel assigned to work in emergency situations
- Definition of tasks which personnel would perform in case of emergency.
- Definition of mission and authority of teams (fire team, first aid team, rescue team)
- Evacuation procedure, identification of hazardous materials layout
- Communication information about external official authorities and services
- Recovery of crucial information and equipment
- Accessibility of required information

(Reese and Eidson, 2006.)

Table 8. Job Safety Analysis Form for Drilling

JOB SAFETY ANALYSIS FORM				
Date: 02/09/2010 New: ✓ Revised: Form No: 05 Revision No: 0 Revision Date: .../.../20... Page: 1/				
Title of Job/Operation: Drilling			Position/Name of Responsible for the Job: Operator /	
Directorate: Directorate of Production			Analysis Made By (Title/Name): ..... /	
Department: Simav Open-pit Mine Head Eng.			Approved By (Title/Name): Manager of Enterprise /	
No	**Job Steps**	**Potential Accidents**	**Potential Hazards**	**Control Hazards (Notes/Comments)**
1	Drive the drilling machine to the site	Traffic accident	Death and/or serious injury	Plan the move machine before the shift begins
		Hit by vehicle when backing	Death and/or serious injury	Use a ground guide along with a functioning back-up alarm during equipment backing.
		Electrocution	Death and/or serious injury	Inspect for buried and overhead utilities in the vicinity of the drilling location.
3	Drill Rod / Auger / Tool Handling	Struck By	Serious Injury	Drill rods and augers stored and transported in racks shall be blocked to prevent shifting.
		Overexertion while Improper lifting	Joint disconformities	Use proper lifting techniques when manually handling rods, augers and tools.
4	Hoisting Operations	Struck By	Serious Injury	Never engage the rotary clutch until all personnel and equipment are clear.
5	Auger Operations	Struck By	Serious Injury	Use a long handled flat head shovel when removing auger cuttings. Do not wear loose clothing when working.
6	Maintenance	Caught between	Injury	The drilling rig and associated equipment must be maintained in a proper functioning condition.
		Fire	Death and/or serious injury	All motors must be shut off during refueling. Smoking in the vicinity of the drilling rig is not permitted.

Rescue and Save Team, First-aid Team, Fire Team, which consist of minimum seven people, are constructed by the management in Bigadiç Boron Work. These teams perform fire, first-aid, rescue and evacuation drills twice a year. The items of emergency equipment of Bigadiç Boron Work are determined and ensured. The operability of these equipment items should be tested and recorded within a year. All companies may be faced with emergency situations, yet these can show some differences according to company's structure and work.

Identification of risks that may cause to emergency constitutes the basis of Emergency Plan. According to risk evaluation process the "Emergency Plan" of Bigadiç Boron Work is constructed. The full text of Emergency Plan cannot be covered within the context of this study but mainly it consists of evacuation plan, firefighting, first aid and rescue procedures. The emergency teams are established and their missions and responsibilities are defined. The emergency plan introduces how to act in case of emergencies. The preparation of this plan has no importance alone. The important point is that this document must be distributed to all departments and all personnel must be trained.

The proposed emergency plan provides a comprehensive approach to emergency situations. It defines the roles and responsibilities of emergency teams and introduces how the organization and units should act in case of an emergency. The existing incompetent emergency teams were broadened and widened within the organization in this plan.

5 AUDITS

Workplace audits are inspections, which are performed to evaluate certain aspects of the working environment considering occupational health and safety. The use of health and safety audits shows positive effect on companies' loss control initiative. Actually, companies that perform audits have lower accident rate than that of do not perform audits. The audits are not only a part of checking or controlling activity, but also a part of hazard identification and corrective actions. The audits can provide the followings:

1) Identification of the existence hazards
2) Checking compliance with rules and regulations
3) Determination of Health and Safety conditions of workplace
4) Evaluation of supervisors' and workers' health and safety performances
5) Evaluation of progress and effectiveness of health and safety issues.

In Bigadiç Boron Work the daily regular inspections are performed by head engineers or engineers in order to detect hazardous conditions, equipment, material or unsafe working practices. In addition to this, the periodic internal audits are performed by Department of OH&S headed by OHS supervisor. The supervisor, together with health service personnel and management, determines the frequency of audits based on the level and complexity of activities and hazards associated with these activities. The frequency of internal audits is established in the Occupational Health and Safety Manual as at least once a year.

"Health and Safety Audit Instrument" is is a written instrument (consist of 14 pages) that can be applied for internal audits of Bigadiç Boron Work. This audit instrument asks several questions about workplace. These are yes or no questions. For further detailed inspections, audit reports may also be prepared by inspectors.

The self-auditing tool is a very powerful "early warning system" to help management spot the health and safety threats. It gives the management the chance to address and resolve them before they occur, rather than after. This gives management objective data upon which to base decisions. The audits and management reviews are the main revision tools and they must not be delayed or discarded.

6 RESULTS AND DISCUSSION

It is obvious that safety regulations can be ineffective or insufficient if they are not understood or complied with properly. In addition, occupational health and safety in all work environments are always dynamic and changing. It is impossible to get an absolute and perfect health and safety program since the requirements will change as the company evolves. However, the aim of the company should be, "all accidents and incidents are preventable and all levels of management are responsible for health and safety".

Mitigation and elimination of hazards and risks by means of the proposed risk assessment system was set out for Bigadiç Boron Work. The system definition is given in "Risk Assessment Charts". Some existent risks and their potential hazards can be studied with the prepared "Risk Evaluation Form" according to this assessment system. The risk evaluation forms were prepared for blasting activity. The activity was observed and all possible hazards were listed. Their likelihood, exposure and consequence scores were assigned with the help of risk assessment charts. The risk score defines the level of urgency of risks and the preventive actions.

The proposed JSA form can be used to identify, analyze and record the steps involved in performing a specific task, and the existing or potential safety and health hazards associated with each step. Several safe job procedures can also be prepared with the help of the risk assessment process. The selected example is drilling. As JSA requires, all activities and related tasks were listed carefully and the job steps were clearly indicated in imperative form.

As a result of this study, a contribution for consistency of organization was provided by the proposed standardized documents, procedures and forms. The opinions of field workers and foremen were taken. This also improved participation and motivation. The proposed OHSA System forms and risk assessment system lessens dependency on key individuals. It distributes responsibility and accountability across the work force. The application process initializes the awareness of importance of Personal Protective Equipments. During this study some cold facts were observed. The most important matter was deficient and chaotic data recoding. The enterprise had no adequate data recording system and existing statistical data was insufficient and did not cover all workplaces.

It is well known that "safety begins at the top". The management of an organization should control the whole process and combine the maximum production methods with the minimum cost. This process should be conveyed with regard to occupational health and safety because it should be kept in mind that safety is not an extra expenditure. On the contrary, it is a money saving process. The general improvement of occupational health and safety constitutes well-being and motivation of workers as well. The consciousness of occupational health and safety provides a better way of life for both individuals and society. Health, safety, and the comfort of workers are a prerequisite for quality and efficiency. These primary matters are very important for socio-economic, egalitarian, and sustainable development.

REFERENCES

Reese, C.D., 2003. Occupational Health and Safety Management: A Practical Approach, Lewis Publishers, London, 98.

Reese, C.D., 2004, Office Building Safety and Health, CRC Press, USA, 36.

Reese C.D., and Eidson J. V., (2nd ed.), 2006. Handbook of OSHA Construction Safety and Health, New York, 289.

Taylor, G., and Easter, K., Hegney, R., 2004. Enhancing Occupational Safety and Health, 2004, 163-167.

MINING AND ENVIRONMENT

Comparison of CO_2 Emission related to Off-highway Trucks and Belt Conveyors in an Open Pit Coal Mine

M.Erkayaoğlu, N.Demirel
Middle East Technical University, Mining Engineering Department, Ankara, Turkey

ABSTRACT Environmental impacts of extraction and utilization of finite resources are crucial more than ever. In recent years, mining industry has been faced with increasing constraints and forced to manage and mitigate the environmental impacts associated with mining. Mining professionals and practitioners have become obliged to make decisions in accordance with certain systematic standards like Life Cycle Assessment (LCA). This study presents the use of LCA in material handling system selection between off-highway trucks and belt conveyors. The main objective of the study is to provide an aid in comparison of these two material handling systems from the environmental perspective. The research study involves i) the conceptual modeling of LCA framework for both trucks and belt conveyors, ii) implementation of LCA stages, iii) simulations of the developed model. The result showed that LCA provides an important aid in making decisions for mining machinery which may have a substantial contribution to atmospheric emissions.

1 INTRODUCTION

Life cycle assessment (LCA) is used to quantify environmental impact of systems or products in a standardized manner to point out hotspots where improvement is possible. In case of mining, LCA can be utilized as a decision support tool in order to implement environmental evaluation besides economical and technical aspects. Although environmental aspects are not the only criteria in comparison of technically equivalent equipment, global trend and regulations about climate change enforce usage of methodologies such as LCA more commonly. Modelling and interpretation of products or systems by LCA software are keys to achieve environmentally evaluated comparisons in industry.

Comparison of material handling equipment is essentially based on technical competency and economic considerations. Applications in various industrial fields indicate the interdisciplinary characteristics of LCA. For instance, mining is an equipment intensive industry where selection of machinery has a crucial role. Recent improvements in environmental concerns revealed possible future costs related to emissions, especially CO_2. Discussions about a possible carbon tax or penalty for an excessive amount of carbon content have gained itself a place. Therefore, industries such as mining will be obligatory to quantify their CO_2 emissions to sustain their operations in the most efficient way. Possible increase in operation cost caused by regulations about the environment can be diverted to investments for emission reduction. In order to quantify these figures, LCA is used to quantitatively assess environmental effects for equipment, product or operations. Besides applications in other industries there have been several studies in LCA for mining industry.

Landfield and Karra (2000) covered LCA as a relatively new environmental tool and evaluated a crusher in terms of energy consumption, environmental impacts over the life cycle of this equipment. There are also some studies carried out in Europe such as Góralczyk and Kulczycka (2004) studied the financial aspects of LCA in Polish mining industry. Babbitt and Lindner (2005) considered coal for electricity production in Florida and studied the inventory mainly in three stages coal mining, coal combustion, treatment of coal combustion products. Durucan et al., (2006) which developed a mining life cycle model stated that data availability is a major concern in LCA as it might be highly confidential for mining companies. Representing mining operations at a high level of detail causes problems as there are sub-activities occurring at the same time with insufficient data for inputs and environmental burden. Environmental management and life cycle approach in the Mexican mining industry was studied by Suppen et al., (2006) indicating the role of this approach by stating the systematic observation of processes for potential impacts, reduce in operating cost and improvement in efficiency. Stewart and Petrie (2006) dealt with South African and Australian mineral industries in a comparative manner to point out importance of life cycle inventories. Again they confronted certain difficulties in data availability and concluded that change oriented LCA is more valuable for decision making. Demirel and Düzgün (2007) implemented a LCA comparison of mechanical and electrical drive trucks to identify stressor categories and air emissions of mine trucks in a medium scale mine in terms of global warming potentials and acid rain precursors. They also applied multi criteria decision analysis techniques to develop a decision support tool for mine managers, mine owners and environmental policy makers. Use of LCA in the mining industry and research challenges was studied by Lesage et al. (2008) pointing out the two-fold relevance. Authors stated that mining industry has a role providing the LCA community with primary environmental impacts of materials such as metals. On the other hand, mining industry can use LCA in order to evaluate environmental impacts of its activities and identify their hotspots. . Barkhuizen and Pretorius (2008) conducted a survey on mining industry about the maintenance periods and the concept of predictive maintenance where parts are changed prior to fail. Reid et al. (2009) used LCA for comparison of two possible scenarios: sending tailings to the disposal area where they are submerged or partly using them as backfilling material. Yellishetty et al. (2009) summarized major events in LCA history and stated a recent discussion in mining industry. Norgate and Haque (2010) carried out LCA studies for mining and mineral processing of iron ore, bauxite and copper concentrate. Eckelman (2010) considered greenhouse gas life cycle assessment of the global nickel industry.

This paper presents the comparison of off-highway trucks and belt conveyors in an open pit coal mine by means of CO_2 emissions using LCA. Firstly, LCA framework both for off-highway trucks and belt conveyors is conceptually modeled. Secondly, LCA stages are implemented for both material haulage systems. Lastly, developed models are simulated by using SimaPro software.

2 LIFE CYCLE ASSESSMENT

Life Cycle Assessment (LCA) of a product comprises the evaluation of the environmental effects produced during its entire life-cycle, from its origin as a raw material until its end, usually as a waste as defined by Sonnemann et al. (2004).

LCA has a unique multidisciplinary character that covers technical and social aspects. Environmental mechanisms indicating the effect of an emission are inevitably hard to analyze as it is challenging to simulate a condition that has a relatively long time extension such as climate change. LCA studies can also be considered to collaborate with social sciences as subjective choices have to be made such as weighting.

LCA is based on the International Standard EN ISO 14040, documentation and technical guidelines. According to ISO 14040, LCA consist of 4 main stages as seen in Figure 1.

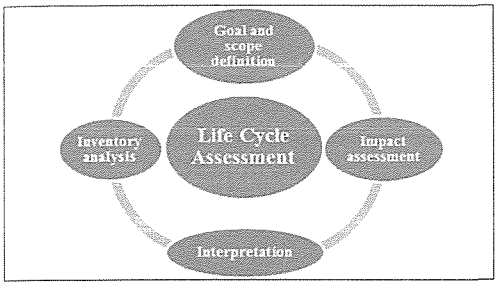

Figure 1. Main stages of LCA

2.1 Goal and Scope Definition

The goal and scope definition part defines the required specifications and identifies the problem to be handled in detail. Subject of the study, functional unit, is defined in detail as it is a quantitative reference.

Another important aspect is to draw the line between this functional unit and environment, pointing out the limits of the system under consideration. In order to make preliminary assumptions for input and output to the environment, a flowchart indicating all unit processes should be prepared. Environmental burden caused by these unit processes is obtained from certain data collected or gathered from databases so that required details have to be clarified in goal and scope definition.

2.2 Inventory Analysis

Within LCA, Life Cycle Inventory (LCI) is considered the step in which all the environmental loads or environmental effects generated by a product or activity during its life-cycle are identified and evaluated. Inventory analysis can be defined as the stage during which all the data of the unit processes within the scope of the study is collected and related to the functional unit. Although recently used databases are sufficient to cover many of the industrial processes, there are always cases that are not readily available or found data is not representative as it is common in the mining industry. This missing data to be collected is classified according to its propriety to the case so that studies in mining industries require foreground data.

2.3 Impact Assessment

The impact assessment phase aims at making the results from the inventory analysis more understandable and more manageable in relation to human health, the availability of resources, and the natural environment. There are certain impact categories that are commonly used according to the subject of the study. Each category has a relevant common unit that has to be applied to the results to obtain the environmental profile of the subject.

2.4 Interpretation

The interpretation phase aims to evaluate the results from the inventory analysis or impact assessment and compare them with the goal of the study defined in the first phase. Important results should be identified and outcomes should be evaluated by sensitivity analysis or consistency checks. Recommendation and critical review of the subject should be included in the final report of the results.

3 METHODOLOGY

3.1 Conceptual Modelling

In order to compare off-highway trucks and belt conveyors on a technically comparative basis, a conceptual production amount is estimated from several open pit operation's average as 20,000 tons/day. 20 tons of lignite has an approximate bulk volume of 30.8 m^3 according to material properties given in the handbook of mining engineering published by Society of Mining Engineers (Gentry and Hustrulid, 1992).

3.1.1 Off-highway truck

It is assumed that 80 tons of coal with bulk density of 0.89 t/m^3 is loaded with a 15 m^3 capacity shovel with a fill factor of 0.8 on a heavy duty truck. Haulage will be performed on a 10 km long, well maintained road. Road and operating conditions for haulage are assumed and based on other open pit coal mines in Turkey.

CAT 772 off-highway truck was initially selected regarding to its capacity and bulk density of the material. Properties of this truck can be seen in Table 1.

Table 1. CAT 772 (Medium Impact steel flat floor) properties

Target Payload	Struck Capacity	Heap Capacity
46,236 kg	23.3 m^3	31.3 m^3

Another important aspect in estimating total required number of trucks in an operation is the cycle time consisting of truck load time, spot time at shovel, haulage time, maneuvering - dumping time and return time. After calculating availability and utilization of the truck, it is found that 23 trucks are required for material haulage.

3.1.2 Belt Conveyor

The belt conveyor to be used in the comparison study is selected by following the handbook published by the Conveyor Equipment Manufacturers (CEMA, 1997). Bulk density is the only key property of the material in truck selection, however, the other characteristics have to be known for belt conveyor design. Material properties for lignite are determined using the handbook published by the Society of Mining Engineers (Gentry and Hustrulid, 1992).

Belt width is selected as 40 in. and belt speed is estimated as 3.56 m/h. As a result, a total of 8 belt conveyor systems are required for the average production capacity of 20,000 tons/day. As a conclusion, total power required to convey material from 5 km long haulage path is calculated as 1320 horse power for the whole belt conveyor system.

3.2 Modelling with SimaPro

Material handling equipment to be compared is initially discussed as unit processes in order to determine inputs and outputs to be considered within the system boundary. Although common practice is to use a methodology based on technical or economical concepts, data availability is also a major criteria in system boundary selection.

A certain cut-off grade is applied to modelled network structures for off-highway truck and belt conveyor in SimaPro software as displaying all input/output creates complex representations difficult to interpret. In the scope of this study, only CO_2 emissions will be considered. As it is seen in Figure 2, belt conveyor is mainly modelled into 5 assemblies.

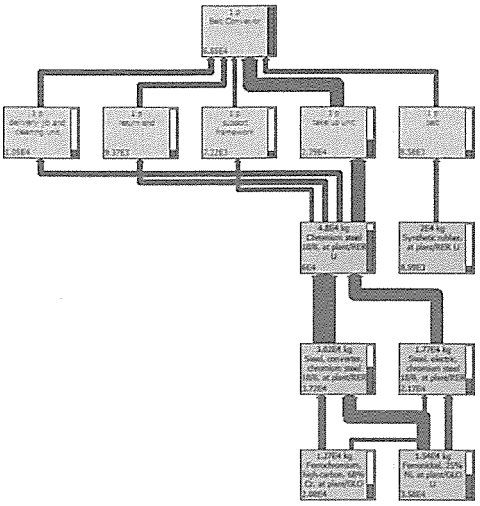

Figure 3. Belt conveyor model in SimaPro

Besides framework and other parts manufactured by steel, synthetic rubber is assigned to be raw material for belt part. Weighted arrows illustrate the major emission sources and indicate hot spots proportionally.

Similarly, off-highway truck is modelled in SimaPro software by dividing it into 3 main parts. As it is seen in Figure 4, steel parts are main contributors of emission compared to tires and other plastic parts of the truck.

Both systems also include the usage phase in their life cycle such as electricity usage for belt conveyor and diesel usage for off-highway truck. All data used in these models are selected from Ecoinvent database embedded in the software.

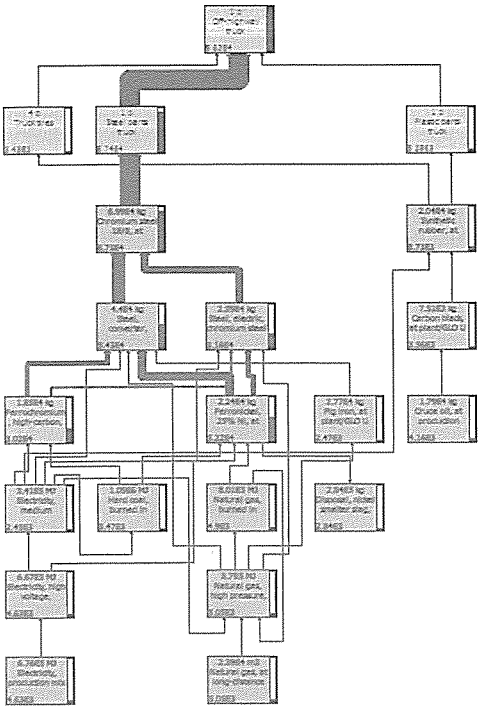

Figure 4. Off-highway truck model in SimaPro

3.3 Comparison of CO_2 emissions

There are many impact categories used in LCA such as global warming potential, eutrophication, depletion of abiotic resources, etc. In the scope of this study, only carbon dioxide emissions of belt conveyors and off-highway trucks are compared as an indicator of global warming potential. Common practice is to use representative scores derived by allocation of emissions, weighting, and in some cases normalization which is an optional step of the LCA methodology.

As it is stated before in order to compare both material handling systems on a technically equivalent basis, 23 off-highway trucks and eight belt conveyor systems are modelled and evaluated in SimaPro software.

As a result of the analysis, CO_2 emitted from off-highway truck and belt conveyor as a life cycle is presented in Figure 5.

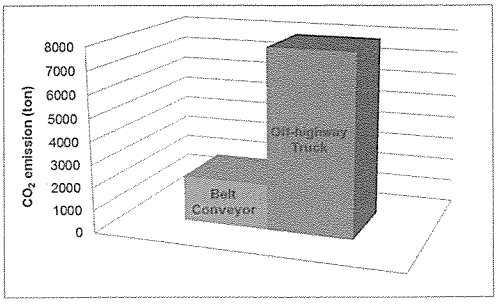

Figure 5. Life cycle CO_2 comparison of belt conveyor and off-highway truck

There is a noticeable difference between belt conveyor and off-highway truck by means of CO_2. Manufacturing stages of off-highway trucks and belt conveyors are major emission sources when compared to the usage phase. Use phase covers diesel consumption for trucks and electricity for belt conveyor.

CO_2 emission can be considered as an indicator for global warming potential although this measure is determined in a long time range such 100 or 200 years.

4 RESULTS AND DISCUSSIONS

As environmental concerns and social responsibility are becoming more active in regulations for mining industry, methodologies like LCA can be considered as a potential tool for estimating hotspots by means of emissions.

Total CO_2 emission estimated for the off-highway trucks is found as 7918,7 kton

whereas approximately 90% is originated from the steel part. Material selected from the Ecoinvent database is classified as chromium steel so it includes downstream processes when defined. Belt conveyors have a total of 2002,8 kton CO_2 emission assigned that is originated mainly from manufacturing process.

Use phases of both material handling systems have similar emission amounts compared to their manufacturing phases. As off-highway trucks have rather high diesel consumption figures, CO_2 emission originated from this phase can be considered as critical for this system. Although electricity utilized for belt conveyor systems is selected to be produced from coal power plants, estimated emission is still lower than CO_2 emitted by fuel combustion.

5 CONCLUSION

CO_2 emission is very important, because it is stated to be responsible for about 60% of the "Greenhouse Effect" (Can, 2004). Earth's temperature is strongly influenced by the density and composition of the atmosphere. Emitted greenhouse gases have adverse effects on the radiative balance of the atmosphere. The earth's surface temperature has a potential to rise by some trapped portion of outgoing energy. Combustion of fossil fuels is responsible for majority of CO_2 emissions being used in various industries.

This study is a step of comparing these material equipment systems using LCA. However, data availability and quality can be considered as an important bottleneck even at this stage of the research. CO_2 emissions are a crucial indicator of global warming potential. Although this impact is commonly evaluated for long time ranges such as 25, 50 or 100 years as stated by Intergovernmental Panel on Climate Change (Eggleston et.al., 2006), this study is a pioneering effort in the mining industry to determine environmental profiles of different operations.

REFERENCES

Landfield, A., Karra, V. (2000), Life Cycle assessment of a rock crusher. Resources, Conservation and Recycling, Vol. 28, pp. 207-217.

Goralczyk, M., Kulczycka, J. (2004), The Financial aspects of LCA in Polish mining industry. The International Conference of Sustainable Post-Industrial Land Management.

Babbitt, C.W., Lindner, A.S. (2005), A life cycle inventory of coal used for electricity production in Florida, Journal of Cleaner Production Vol.13, pp. 903-912.

Durucan, S., Korre, A., Melendez, G. (2006), Mining life cycle modeling: a cradle-to-gate approach to environmental management in the minerals industry. Journal of Cleaner Production Vol.14, pp. 1057-1070.

Suppen, N., Carranza, M., Huerta, M., Hernández, M. (2006), Environmental Management and life cycle approach in the Mexican mining industry. Journal of Cleaner Production, Vol. 14, pp. 1101-1115.

Stewart, M., Petrie, J. (2006), A process systems approach to life cycle inventories for minerals: South African and Australian case studies. Journal of Cleaner Production, Vol. 14, pp. 1042-1056.

Demirel, N., Düzgün, Ş. (2007), Comparison of Mechanical vs. Electric Drive Mine Trucks based on Life Cycle Assessment. Proceedings of MANTEMIN, pp. 133-142.

Lesage, P., Reid, C., Margni, M., Aubertin, M., Deschenes, L. (2008), Use of LCA in Mining Industry and Research Challenges. Symposium sur l'environment et les mines.

Barkhuizen, W.F., Pretorius, L. (2008), Life Cycle Management for Mining Machinery. University of Johannesburg.

Reid, C., Becaert, V., Aubertin, M., Rosenbaum, R.K., Deschenes, L. (2009), Life Cycle Assessment of mine tailings management in Canada. Journal of Cleaner Production Vol.17, pp. 471-479.

Yellishetty, M., Ranjith, P.G., Tharumarajah, A., Bhosale, S. (2009), Life cycle assessment in the minerals and metals sector: a critical review of selected issues and challenges. International Journal of Life Cycle Assessment, Vol.14, pp. 257-267.

Norgate, T., Haque, N. (2010), Energy and greenhouse gas impacts of mining and mineral processing operations. Journal of Cleaner Production, Vol.18, pp. 286-274.

Eckelman, M.J. (2010), Faciliy-level energy and greenhouse gas life-cycle assessment of the global nickel industry. Resources, Conservation and Recycling, Vol.54, pp. 256-266.

Sonneman, G., Castells, F., Schuhmacher, M. (2004). Integrated Life-Cycle and Risk Assessment for industrial Processes. Florida: Lewis Publishers.

Gentry, D.W., Hustrulid, W., (eds), 1992. *SME Mining Engineering Handbook*. Society for Mining, Metallurgy and Exploration, Colorado. 1314 p.

Belt Conveyors for Bulk Materials. Conveyor Equipment Manufacturer's Association. 1997. USA. pp. 30-144.

Can, A. (2004). Investigation Of Turkey's Carbon Dioxide Problem By Numerical Modeling, Ph.D. Thesis, METU, p.263. Ankara

Eggleston, S., Buendia, L., Miwa, K., Ngara, T., Tanabe, K.(eds.) 2006. *IPCC Guidelines for National Greenhouse Gas Inventories*. Institute for Global Environmental Strategies, Japan. pp. 165-190.

Potential of CO_2 Sequestration in Abandoned Coal Mines in Australia

Paria Jalili, Luke Patrick Jordan, Serkan Saydam
The School of Mining Engineering, University of New South Wales, Sydney, NSW, Australia

Yildiray Cinar
The School of Petroleum Engineering, University of New South Wales, Sydney, NSW, Australia

ABSTRACT Deep abandoned mines offer substantial space for CO_2 storage. From a very limited study presented in the literature, the most important criteria set for CO_2 storage in underground mines include that the highest level of the mine be at least 500m deep and the storage pressure not exceed 130% of the hydrostatic pressure. Although these criteria are crucial for the amount to be sequestered, there are also other secondary factors which can affect the process such as total coal reserves, ground water level, tectonic stability and ambient temperature.

Before any large-scale trial of CO_2 storage in underground mines, mines need to be assessed and ranked for their suitability for CO_2 storage. For this purpose, a number of intrinsic and extrinsic criteria varying from geology to economics were developed. During this assessment, each criterion is assigned with the lowest and highest numerical values that correspond to the least and most favorable cases, respectively. The relative importance of each criterion is taken into account through the use of a weighting function that is multiplied by the assigned numerical value to produce a dimensionless parameter that allows inter-criterion comparisons. Finally, the summation of these individual score provides a total that may be used to rank the various mines for feasibility.

Australia presents a significant opportunity for implementation, due to the vast numbers of coal operations and proven tectonic stability. Australia has been selected as the source of data due to the large sequestration potential held by the continent. Subsequently, the mine suitability assessment has provided a set of viable options for CO_2 storage, among which Metropolitan, Appin and Westcliff Collieries in New South Wales were ranked the highest. Each of these collieries presents a significant opportunity to implement CO_2 sequestration as an alternative to mine rehabilitation.

1 INTRODUCTION

A shift to greener sources of power and heavy investment in the development of energy efficient systems has been employed to combat green house gases. However, these technologies alone are not sufficient to bridge the technological gap between current emissions and atmospheric stabilisation. As a result, significant advancement in the development and implementation of alternatives is required. One such alternative is the sequestration of CO_2 in subsurface geological structures.

Coal industry in Australia is one of the responsible industries for CO_2 emission, which will produce 37% of Australia's total emission (New GEN Coal, 2010).

Australia ranks first, among developed countries, with CO_2 emissions of 20.6 tonnes per year, before the United States, which is producing 19.8 tonnes per year (Maplecroft,

2009 and International Energy Agency - IEA, 2005).

This paper analyses the potential for CO_2 sequestration in Australian Coal Mines as a means of mitigating CO_2 emissions and also provides information for eventual site deployment at the prospective storage reservoirs.

2 GEOLOGICAL OPTIONS FOR CO_2 STORAGE

In the last 5 years, many analysts and policymakers have moved towards the notion of another option deemed an "end-of-pipe" solution that would allow the continued usage of fossil fuels, in energy generation, whilst dramatically reducing CO_2 emissions (Bachu, 2003). This is called Carbon Capture and Storage (CCS) technology. CCS has become globally accepted as vital technology for meeting reduction in CO_2 emissions targets. It is estimated that CCS technology would reduce the amount of CO_2 emitted into the atmosphere by a modern conventional power plant by 80-90% (U.S Department of Energy, 2006). Conventional CCS also known as geosequestration involves the long-term underground storage of CO_2 in deep geological formations. The process of geosequestration involves capturing, purifying, compressing and transporting CO_2 from large stationary sources (such as power plants) to a suitable storage site where it is injected before it has the chance to be emitted into the atmosphere (Bachu, 2003). Another option for geosequestration is sequestration of the gas in to the abandoned coal mines, which would be discussed in details followed.

3 CO_2 SEQUESTRATIONS IN ABANDONED COAL MINES

Abandoned coal mines have been considered of large surface area of the unmined coal, large areas of free space and mine water. CO_2 can be stored in an abandoned coal mine through three physical mechanisms: by adsorption on the remaining coal, by solution in the mine water and by compression in the empty space of the mine. The adsorption of CO_2 on coal depends on the type of coal and also the amount of coal available for adsorption. Calculating the amount of coal available for adsorption is very important, as most of the CO_2 would be adsorbed through this mechanism. Part of the CO_2 would be stored in the free space which is the mine out volume after collapsed and subsidence.

CO_2 is also expected to dissolve in ground water which has the less contribution amount compared to the other modes of storage (in most cases, less than 10% of the total sequestration amount) (Jalili et al, 2011). Many factors have to be considered before geosequestration like, storage capacity, water influx, reservoir pressure, and type of cap rock, infrastructures leakage.

There are three completed projects around the world for gas storage into the abandoned coal mines. The first one is Leyden Coal Mine near Denver, Colorado, USA. It was in operation from 1903 till 1950. The other two projects are located in Belgium (Peronnes and Anderlus Abandoned Coal Mines). Anderlus Mine was operated between 1857 and 1969, and Peronnes was in operation from 1860 until 1969.

The sequestration of CO_2 in abandoned coal mines is the result of the achievements of the abovementioned projects and has been considered as an option recently.

Piessens and Dusar (2003) introduced a software package for simulation of CO_2 sequestration, named CO_2-VR, which is the combination of Micro-Excel and Visual Basic. CO_2-VR is capable of calculating the reservoir pressure and the gas density at each depth. Using this software, simulation for CO_2 sequestration has been started. Piessens and Dusar (2004) simulated the Campine Basin in the northern part of Belgium which contains of seven mines for CO_2 sequestration.

Lutyński (2010) is also simulated a typical mine from Upper Silesian Coal Basin in Poland. The case study for these two basins shows that sequestration is a viable option. The results show that, at a reservoir pressure

of 5.43MPa, 3.5 M tonnes of CO_2 can be stored in the empty space as compressed gas and in mine water as dissolved. Almost a similar amount (3.53 M tonnes) of CO_2 can be stored in the remaining coal as adsorbed at the given pressure (Lutyński, 2010).

4 RANKING AND SCREENING OF THE AUSTRALIAN MINES

To find out the most suitable mines the following studies should be done on the geoscience criteria:

- a basin and regional scale suitability assessment.
- the selection characterization and inventory of the proposed storage site.
- an assessment of the safety and long term fate of the sequestered CO_2.
- determination of the storage capacity.

The suitability of coal mine needs to consider geological, geothermal, hydrodynamic, hydrocarbon potential, maturity, economic, political and societal criteria. The geological, geothermal and hydrodynamic criteria are considered hard criteria, as their regimes will not change when based on a human time scale. However, political, economic and societal criteria are regarded as soft, as they may change over very short time scales. The fourth and fifth criteria lie in the middle as hydrocarbon potential and size will change as new data is collected (Bachu, 2000). The next step is to establish site-specific immediate and ultimate safety studies and protocols. The potential for the upward migration and escape of CO_2 into surrounding strata directly after injection is referred to as immediate safety. This generally occurs through open faults and natural or manmade fractures irrespective of the means of sequestration. The ultimate safety of the site is made in reference to the lateral migration of CO_2 in aquifers as part of cross-formational flow or in short residence flow systems (Bachu 2000).

New South Wales (NSW) and Queensland states have two major sources of coal in Australia which contains most of the coal reserves in Australia. Figure 1 compares the New South Wales and Queensland Mines by total coal reserve versus depth (Jalili et al, 2011). The results indicate that, although Queensland's abandoned coal mines have higher coal reserves compared to the New South Wales's coal mines, they do not have sufficient depth for CO_2 sequestration. Similarly, a few mines in NSW are deep enough but their reserves are not as large as Queensland's Coal Mines (Jalili et al, 2011).

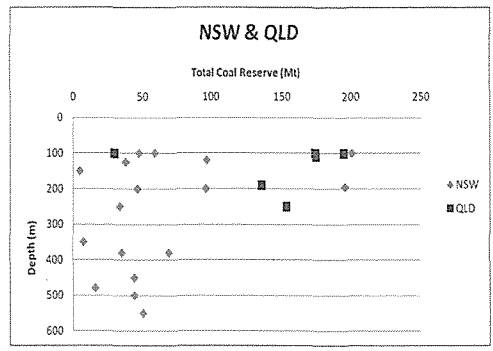

Figure 1. Total coal reserve versus depth data for the abandoned coal mines in New South Wales and Queensland (Jalili et al, 2011) (Updated using International Longwall News, 2010; Geoscience Australia, 2010; Bureau of Meteorology, 2010).

As initial criteria, Piessens and Dusar (2004) suggested the depth of the mine should be at least 500m. So the mines with overburden depth greater than 450m are considered to have met the initial criteria.

It is clear that more investigation needs to be done as the depth and coal reserve are not the only parameters given that many other factors like sealing, mine condition, mine water, existent faults may potentially affect the capacity; (Jalili et al, 2011). Table 1 shows the screening criteria for assessing underground mines for CO_2 sequestration (modified after Golab, 2010; Gibson-Poole et al 2006; Bachu, 2003).

The criteria in Table 1, presents a set of 15 criteria that correspond to either storage capacity, containment security or allow for the consideration of the economic and technological feasibility of implementation.

The least favorable class for each criterion is on the left and the classes become progressively more favorable as you move to the right. It must be noted that the geothermal regime surrounding the mine site has a critical effect on the capacity and security of CO_2 sequestration and storage operations. Thus, the introduction of climatic conditions i.e. surface temperature, geothermal conditions and depth are considered imperative in the ranking and selection of potential underground mines. Climatic conditions are also indirectly representative of the difficulties or lack thereof in installing the necessary infrastructure for CO_2 capture, transportation and injection (Bachu, 2003). Depth range is also important, as CO_2 sequestration at shallow depths is inefficient due to low CO_2 density and/or unsafe due to high CO_2 buoyancy. On the other hand, due to the leveling off of CO_2, increasing depth means a greater operational cost without a corresponding increase in storage capacity. In order to evaluate better, the feasibility of CO_2 sequestration in abandoned coal mines, the Sydney Basin must be broken down further into basin subdivisions. The main basins of interest are the Hunter Valley Domes (HVD), containing Integra and Austar Mines, and the Southern Plateau (SPL), containing Metropolitan, Tahmoor, Westcliff and Appin. There is concern about the location of Metropolitan Coal Mine within the subdivisions and as such, where relevant, data from the Woronora plateau (the southernmost section of the Central Onshore Basin) will also be considered. Additionally due to the lack of data on the Woronora plateau some assumptions may have to be drawn from the closest wells located in the SPL. The criterion of table 1 has been discussed for Australian underground mines for CO_2 Sequestration:

Table 1. Screening criteria for assessing underground mines for CO_2 sequestration (modified after Golab, 2010; Gibson-Poole et al 2006; Bachu, 2003)

		Classes					Weight
i	Criterion	1	2	3	4	5	
1	Tectonic setting	Very Unstable	Unstable	Intermediate	Mostly stable	Stable	0.07
2	Size (km^2)	Very Small (<30)	Small (30-50)	Medium (50-80)	Large (80-120)	Very Large (>120)	0.06
3	Depth (m)	Very Shallow (<250)	Shallow (250-450)	Very Deep (>3,500)	Deep (800-3500)	Intermediate (450-800)	0.07
4	Porosity/permeability	Very poor	Poor	Intermediate	Good	Excellent	0.08
5	Reservoir/seal pair	Very poor	Poor	Intermediate	Good	Excellent	0.07
6	Faulting intensity	Extensive		Moderate		Limited	0.08
7	Geothermal (°C/km)	Warm basin (>40)		Moderate (30-40)		Cold basin (<30)	0.1
8	Hydrocarbon potential	None	Small	Medium	Large	Giant	0.06
9	Hydrocarbon industry maturity	Unexplored	Exploration	Developing	Mature	Over Mature	0.08
10	Coal depth	No coal	Very Shallow (<300)		Deep (>800)	Shallow (300-800)	0.04
11	Coal rank	Anthracite	Lignite		Sub-bituminous	Bituminous	0.04
12	Ambient temperature (°C)	Freezing (<0)	Hot (>35)	Cold (0-15)	Warm (25-35)	Cool (15-25)	0.08
13	Infrastructure	None	Minor		Moderate	Extensive	0.05
14	Accessibility	Inaccessible	Difficult	Acceptable	Easy		0.03
15	CO_2 sources	None	Few	Moderate	Major		0.09

- NSW shows varying degrees of porosity and permeability but the two areas of concern are the HVD and SPL basin subdivisions. Sydney basin is considered to have in general an intermediate likelihood of reservoir seal pairs. For a more conclusive analysis further pressure testing must be conducted on case by case basis for each mine. Metropolitan Mine lies within the Southern Coal Fields, however in terms of its structural domains, it is contained within the Woronora plateau and as such the permeability and porosity of the colliery is difficult to assess. However, the available data shows that Metropolitan Mine has high porosity. The permeability and porosity of Tahmoor, Appin, Westcliff and Metropolitan Collieries are characterised by good porosity and permeability levels at 450-600m depth of cover.
- In terms of faulting intensity and geological structures the mines located in the Illawarra Plateau, namely Tahmoor, Westcliff and Appin are surrounded by an extensive number of faults and folds including the Lapstone Monocline. Integra Mine is located in the HVD and is also surrounded by extensive geological structures. However, Austar Mine is located closer to Newcastle and as such is subject to a limited number of geological structures. There are also, limited major faults and folds in the Woronora plateau and thus Metropolitan Mine can also be classified as having limited geological structures.
- In Sydney Basin, Hunter Valley Region contains a geothermal anomaly that causes the basin temperatures to rise to geothermal gradients over 50°C/km. This is unfavourable for the mines being considered in this region, as the optimal depth of injection will increase beyond that of the mine depths. On the other hand, the mines residing within the southern part of NSWs exist within a cold basin reducing the optimal depth (Jaworska, 2007).
- In terms of industry maturity, there are 8 gas projects in operation in NSW as of 21/10/2009 (Golab, 2010).
- In terms of ranking, bituminous coals are regarded as the best option for CO_2 sequestration. Regarding the Australia Department of Primary Industries, 2005a the Southern Coalfield has the lowest moisture content of any the NSW coalfields.
- Due to the operational nature and location of all seven coal mines within the Sydney Basin access to the site would be considered easy as roads and rail links are already in place in these areas.

Figure 2, highlights the amount of CO_2 produced and their proximity to feasible CO_2 sinks. The blue circles represent the CO_2 emission sources whilst the red circles represent the location of feasible sequestration sites and the numbers contained within the circles are representative of either the storage capacity or emission levels in mega-tonnes per annum. The justification for this study lies in the idea that NSW possesses the largest CO_2 emission sources in Australia, but currently contains no storage sites.

5 RESULTS

For each criterion outlined previously, in Table 1, a *monotonically increasing* numerical function F_i is assigned, which may be continuous or discrete, to illustrate a value placed on a particular class j for that criterion. The lowest and highest values of this function correspond to the least and most favorable classes, within the criterion, respectively. The numerical values assigned to the various classes are evident by the number displayed at the top of each class column, in Table 2, with scores ranging from one (1) to five (5).

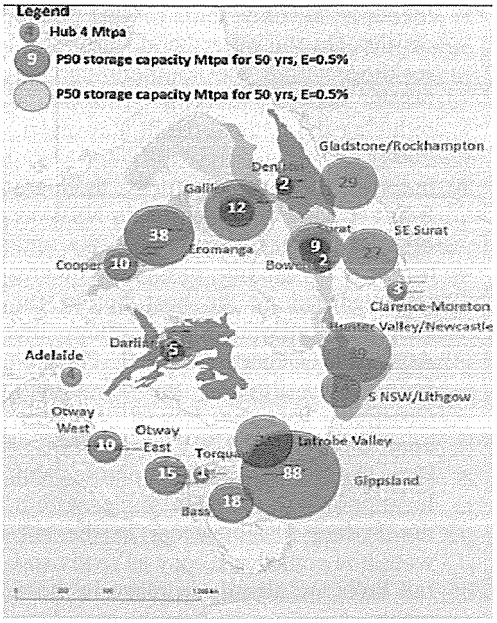

Figure 2. CO_2 emission levels and feasible CO_2 sink capacities (Carbon Storage Taskforce, 2009)

Through the use of parameterization the various characteristics of reservoir suitability with differing meanings are effectively transformed into dimensionless variables (Bachu, 2003). Subsequently, these variables may be added together to produce a total score, R^k, that is used to rank the underground coal mines, which is found using:

$$R^k = \sum_{1}^{15} w_i F_i \qquad (1)$$

Where, w_i are weighting functions that are bound by the condition that:

$$\sum_{1}^{15} w_i = 1 \qquad (2)$$

The values assigned to each of the weights, w_i, has also been outlined in Table 1. This method may be adapted and changed according to varying conditions and priorities. The process was adapted to select underground longwall mines in New South Wales, Australia and the results are outlined in Table 2. The score column shows the raw score achieved by using Equation 1 and the class values given to the fifteen criteria on each mine, where a perfect score for an ideal sequestration site is 4.88. The suitability column represents the fraction of a perfect score or the geological, economic and technical appropriateness of each site. Based on this ranking, Metropolitan Mine would be the ideal site to commit to further investigation into the feasibility of CO_2 sequestration in abandoned coal mines in NSW.

Table 2. Sequestration suitability and mine ranking for New South Wales, Australia

Mine	Score	Suitability	Rank
Metropolitan	4.12	84.4%	1
Appin	3.92	80.3%	2
Westcliff	3.86	79.1%	3
Austar	3.77	77.3%	4
Tahmoor	3.65	74.8%	5
Integra	2.92	59.8%	6

Such results have exciting prospects for the sequestration industry as all first three mines exist within relative proximity to each other and could potentially be linked to become a giant storage reservoir or a series of interconnected reservoirs.

6 ACKNOWLEDGEMENTS

The authors would like to thank Mr W. Green from Peabody Energy Australia for his recommendations and continuous support during the study.

7 REFERENCES

Bachu, S, 2003. Screening and ranking sedimentary basins for sequestration of CO_2 in geological media in response to climate change, Environmental Geology 44:277-289.

Bureau of Meteorology, Australian Government, 2010. Climate data online [online]. Available from: < http://www.bom.gov.au/climate/data/> [Accessed on 01/09/2010].

Carbon Storage Taskforce, 2009. National carbon mapping and infrastructure plan – Australia, Department of Resources Energy and Tourism, Canberra, pp 11-20.

Department of Climate Change, 2007. State and territory greenhouse gas inventories 2007, Australian Government Department of Climate change, pp 1-24.

Department of Primary Industries, 2005a. Typical specifications for NSW coal [online]. Available from: < http://www.dpi.nsw.gov.au/minerals/resources/coal/coal-specifications> [Accessed on: 23/08/10].

Geoscience Australia, 2010. The Australian atlas of mineral resources, mines, and processing centres [online]. Available from: < http://www.australianminesatlas.gov.au/> [Accessed on: 22/07/2010]

Gibson-Poole, C,M, Edwards, S,Langford, R, P and Vakerelov, B, 2006. Review of geological storage opportunities for carbon capture and storage (CCS) in Victoria. The Cooperative Research Centre for Greenhouse Gas Technologies (CO_2CRC), pp 14-65. (Australian School of Petroleum, ICTPL Consultancy Report Number ICTPL-RPT06-0506).

Golab, A, 2010. CSC Atlas of New South Wales, Centre for Greenhouse Gas Technologies (CO_2CRC) 66 p.

International Longwall News, 2010. Australian longwall mines 2009-2010 review [online]. Available from: <http://www.longwalls.com/storyview.asp?storyid=1139886&sectionsource=s50> [Accessed on: 12/07/2010].

International Energy Agency 2005, Investment in Coal Supply and Use - An Industry Perspective on the IEA World Energy Investment Outlook CIAB Collection. Available from: http://www.iea.org/textbase/nppdf/free/2005/ciab_invest.pdf

Jalili, P., Saydam, S. and Cinar, Y., 2011. CO_2 Storage in abandoned coal mines. Underground Coal Operators' Conference, University of Wollongong, Australia, 355 p.

Jaworska, J, 2007. Sydney basin GIS based geothermal studies, NSW Department of Primary Industries, 18 p.

Lutyński, M., 2010, A concept of Enhanced Methane Recovery by high pressure CO_2 storage in abandoned coal mine. Gospodarka surowcami mineralnymi, yr:2010 vol:26 iss:1 pg:93 -104

Maplecroft, 2009, Maplecroft Climate Change Risk Report 2009/2010. [online]. Available from:http://maplecroft.com/Climate-Change_clientrelease2.pdf

New Gen Coal, 2010. Coal in Australia [online]. Available from: <http://www.newgencoal.com.au/coal-in-australia.aspx> [Accessed on: 20/05/2010]

Piessens, K. and Dusar, M., 2003. The Vertical Reservoir Simulator CO_2-VR. Proceedings of the 2003 International Coalbed Methane Symposium, Tuscaloosa, paper 0347, 14 p.

Piessens, K. and Dusar, M., 2004. Feasibility of CO_2 sequestration in abandoned coal mines in Belgium. Geologica Belgica 7/3-4: 165-180.

Schultz, K. 1998. Gas storage at the abandoned Leyden coal mine near Denver, Colorado. EPA report, contract 68-W5-oo18, prepared by Raven Ridge Resources Inc., 12 p.

Modern possibilities for observing land surfaces and constructions in order to reduce subsidence damages

Prof. Ph. D. Eng. Herbei Octavian

University of Petroşani – Faculty of Mine, Petroşani, Romania

Ph. D. Eng. Herbei Mihai Valentin

U.S.A.M.V.B. Timisoara, Romania

ABSTRACT Monitoring the areas due to an underground mining exploitation of useful mineral substances constitutes the main objective of the research in mining industry due to the necessity to conserve the integrity of area surface and existent construction.

The researches made by present lead for establishing some links between the causes and effects of the displacement and deformation phenomenon establishing some prognosis of evolution on long and short term.

The aspects linked to the earth movement intervene from designing phases of future precincts and also from closing and conserving the mines that involve a difficult efficient calculation for establishing the parameters that describe the evolution of this phenomenon in time.

The areas affected by the mining exploitations are mainly mono industrial areas and any potential developments are closely connected to the influence of these exploitations over the environment.

1. FRAME OF MANIFESTATION OF THE PROCESS OF MOVING THE ROCKS AFTER AN UNDERGROUND EXPLOITATION

The practices proved that under exploiting a mineral in some limits of time there is a phenomenon of displacement, flowing, creeping the rocks from the roof to the exploited area. This rocks movement is due to the modification of first state of tension from the massive due to the artificial whole. Mathematically speaking we can separate the causes and follow their evolution in order to establish the effect that can be described by the sinking curve (W):

CAUSES	law	EFECT
(Variables)	function	W(x)

Due to the number of causes recorded as variables for the monitoring the phenomenon they can be numbered after their balance of their cause in effect measure as follows:

- **The depth (H)** - small depth lead to big sinking.
- **The exploited volume (V)** : great volumes lead to big sinking.
- **Rocks feature (strength f):** - for great f we have small sinking or no sinking.
- **System of flaws – fracture (n)** - for a degraded massive the phenomenon is more eloquent than for a less fissured massive.
- **Time (t)** – for a small time the phenomenon cannot appear to the ground.
- **Rock declination (α)**

Theoretically we can express this phenomenon as follows:

$$W(mm) = f(H, V, f, n, t, \alpha) \quad (1)$$

Practically the shape of this function is difficult to be established, studies showed many methods of determining it.

2 DESCRIPTION OF THE PROCESS FOR ROCK MOVEMENT

The rock displacement constitutes a complex process that appears in phases depending on the depth as follows:

- Areas of breaking and caving of the roof under the excessive pressure action;
- Areas of caving under the rocks weight and great pressures;
- Areas of subsidence and inflexion under the pressure from the column.

These areas have a dynamical evolution following the dynamics of face coal fronts.

3 PARAMETERS OF SUBSIDENCE PHENOMENON

The parameters of this phenomenon in order to monitor in time are obtained by using the surveying measurements. These parameters are presented into the following picture (Fig. 1):

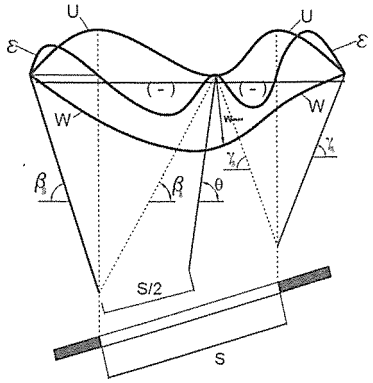

Fig.1 The shape of displacement and deformation curves of field area for the layers with average and great declination

In the fig. 1 we have:
W–sinking bed;
U – curve of horizontal displacements;
ε – curve of specific horizontal deformation

These parameters are (fig. 1):

o ***Sinking curve*** (vertical displacement, W)

$$W_i = (W_i - W_0) \quad (\text{mm}) \quad (2)$$

where: Wi – height of measured point;
W0 – initial height of the point.

o ***Surface declination*** (I_i)

It represents the declination of an area – part between two surveying points – from the surface over the initial position. It is determined with the report between the differences of the sinking of two consecutive marks of observations and the horizontal distance between them as follows:

$$I_i = \frac{S_{i+1} - S_i}{d_{i,i+1}} [\text{mm/m}] \quad (3)$$

where: S_i = sinking of current mark; S_{i+1} = sinking of next mark; $d_{i,i+1}$ = horizontal distance between the two marks.

o ***Curve of horizontal displacements*** (D)

It represents the horizontal component of the displacement vectors of the points. It is the displacement in horizontal plan of a point situated into an area under exploitation influence. It is determined with the difference between the current distance and the same distance measured initially as follows:

$$\mathbf{D}^*_i = \mathbf{D}_{i,i+1} - \mathbf{D}_{0i,i+1} \quad (4)$$

where: $D_{i,i+1}$ = horizontal distance between the two marks at current measurement $D_{0i,i+1}$= horizontal distance between the same marks at zero measurement.

o ***Curve of horizontal deformation*** (ε_i)

It is defined as longing (+) or shorting/compression (-) of a distance between two observation marks when the deformation is positive or negative. There are in fact the longings and compressions along the observation part and they are calculated as follows:

$$\varepsilon_i = \frac{D^*_i}{D_0} (\text{mm/m}) \quad (5)$$

o ***Surface curve and curve ray***

The curving ray (R) is determined by the succession in time of the deformations:

$$R_i = \frac{d_{(i,i+2)}}{I_{i+1} - I_i}(\text{km}) \quad (6)$$

where: Ii+1 - declination of sinking curve in point i+1; Ii - declination of sinking curve in point i;

The surface curve is inverse over the curving ray and it is defined as a limit of the report between the convergence angle of the tangents into in neighborhood points and the distance between them.

$$(K_i)C_i = \frac{1}{R_i}(\text{km}^{-1}) \quad (7)$$

$$d_{(i,i+2)} = \frac{d_{(i,i+1)} + d_{(i+1,i+2)}}{2}$$

- ***Declination of sinking curve I***

$$I_i = \frac{W_i - W_{i+1}}{d_{(i,i+1)}}(\text{mm/m}) \quad (8)$$

where: Wi – current sinking for point i; Wi+1 - current sinking for point i+1; d(i, i+1) – distance between the points i and i+1 for a current measurement.

- ***Limit angles***
- *Angles of displacements* (β, β1, γ, δ)

$$\varepsilon = 2 \ mm/m$$

It is considered: $I = 4 \ mm/m$ (9)

$$k = 0.2 \ km^{-1}$$

- *Breaking angles* ($\beta'', \beta_1'', \gamma'', \delta''$)
- *Angles of total or complete displacements*

4 MATHEMATICAL EXPRESSION OF THE DISPLACEMENTS AND DEFORMING CURVES OF THE SURFACE

To monitor the areas affected by the underground exploitations is made by using topographic observations and following stations which determine the parameters to define its phenomenon and prognosis on short and long term.

Calculation of sinking bed

$$W_{(x)} = W_{max} \cdot \varphi_{(x)} \quad (10)$$

where: Wmax - bed maxim sinking; φ(x) - function of influence;

$$W_{max} = a \cdot g \quad (11)$$

where: g – rock thickness; a – parameter of pressure expression;

It is noticed that

$$T_{(x)} = \frac{dW}{dx} \quad (12)$$

$$k_{(x)} = \frac{d^2W}{dx^2} \quad (13)$$

$$\varepsilon_{(x)} = \frac{dU}{dx} \quad (14)$$

$$U_{(x)} = B_{(y)} \cdot T_{(x)} \quad (15)$$

Due to the fact that U(x) and T(x) have the same shape, where B(y) is a parameter depending on the rock features and depth.

$$\varepsilon_{(x)} = \frac{dU}{dx} = B_{(y)} \cdot \frac{dT_{(x)}}{dx} = B_{(y)} \cdot \frac{d^2W_{(x)}}{dx^2} \quad (16)$$

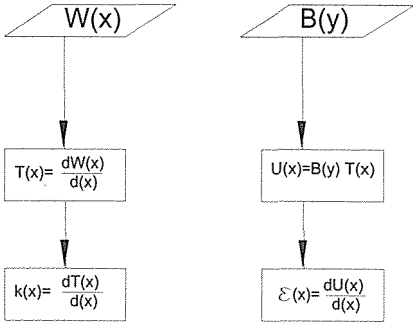

Fig. 2

In order to know the stages of development of the sinking beds we can start from the report between the size of front area and declination of a safety pillar H whose basis could be even the exploited field area.

If: $\frac{H}{A} < 1$ we have sub-critic bed $L < 2Hctg\gamma_S$

If: $\frac{H}{A} = 1$ we have critic bed $L = 2Hctg\gamma_S$

If: $\frac{H}{A} > 1$ we have supra-critic bed $L > 2Hctg\gamma_S$

If we have the functions φ(x) and Wmax and B(y) we can determine the other parameters T, k, ε , U.

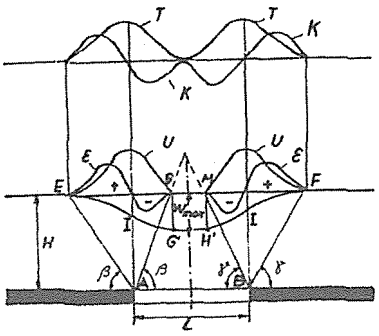

Fig. 3 Supra-critic bed

5 ADJUSTING THE EXPERIMENTAL DATA BY USING THE REGRESSION AND CORRELATION ANALYZE

For a certain point P(x, y, z) from the surface of a sinking area there are known the stages of this points as follows:

1.***Incipient Stage*** – where from the repaus the point will entering movement till it has the speed v_1;

2.***Active Stage*** – where the sinking area may cross through all stages (sub critic - supercritical) and where we can anticipate a variation of the sinking speed around an average value;

3.***Final Stage*** – where the sinking speed decreases continuously till stabilizing the terrain.

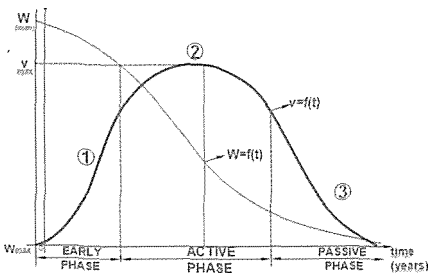

Fig. 4 Evolution of W parameter and of sinking speed V

In correspondence with these stages of the point from the ground it will exist a topic behavior of the sinking parameter W. As a value, from 0 – moment when the effect is not come yet, toll Wmax we can observe a continuously behavior even if the fluctuations of speed are discontinuously from a year to another.

In order to obtain a good prognosis we must chose regression functions of the three areas of development. These functions must have different behaviors during the extrapolation period.

So, we looked for functions **W(t)=f(t)** that must have different behavior at extrapolating the values.

- For the (1) are the tendency of decreasing the speeds to zero:

$W(t)=a_1\exp(-b_1 t)$ - **exponent**

where: a_1, b_1- coefficients determined by regression; t – time in months from the first measurements; W(t) – depended variable (sinking), [m].

- For the (2) are the constant tendency of the speeds around an average value:

$W(t)=a_2\exp(-b_2 t^2)$ - **squared exponent**

where: a2, b2 – numeric coefficients; t – time (months); W(t) – sinking, [m].

- For the (3) area the increasing tendency of the speeds to a maximum value:

$W(t)=a_3 t^3+b_3 t^2+c_3 t+d_3$ - **polynomial type**

where: a_3, b_3, c_3, d_3 – numeric coefficients.

6 METHODS FOR APPROXIMATING THE SINKING BED CURVES AND MAKING SOME PROGNOSIS BY USING THE LESS SQUARE METHOD

The curves resulted after the sinking phenomenon can be mathematically approximated by using some functions.

We start with the sinking function expressed by an exponential one as follows:

$$W_{(x)} = W_0(t)\cdot e^{-bx^2} \qquad (17)$$

where: $W_0(t) = W_0 \cdot e^{-\frac{a}{t}}$ (18)

We have: $W(x,t) = W_0 \cdot e^{-\frac{a}{t}} \cdot e^{-bx^2}$ (19)

The sinking function W(x,t) will depend on the numerical parameters a and b which will be calculated for each profile according to the rocks features.

In general we have: *Calculated value - measured value =correction*

This method can be applied when the volumes are low and when the breaking doesn't reach the surface. Its disadvantage is that the curve of dependence of maxim time sinking is not always respected

Its advantages are that the prognosis of maximum sinking W_{max} we can appreciate that C represents the report between the flexibility and sickness of the rock.

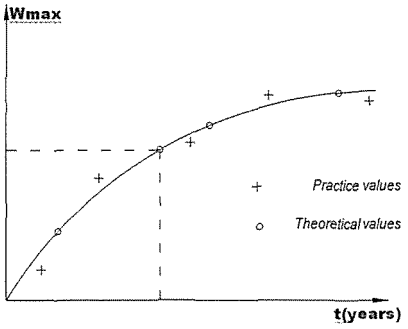

Fig. 5

7 QUALITATIVE ANALYZE DEPENDING ON THE EXPLOITATION DEEPNESS

So we could represent in a spatial shape the dependence of the sinking of I point (maximum point) of exploitation deepness (H).

In Fig. 6 we have as follows:

- Ot – time axis (years);
- OW-axis of sinking speeds (cm./year)
- OH – axis of exploitation deepness (m)

CURVE (1) – represents the function that adjusts the sinking speed of the central mark **I** depending on the time and for an exploitation deep of **H=100 m**. We can notice that for this deep, at the volume of considered gap (v) it is provoked the phenomenon of landfall till the surface into R point from where it is formed the sinking bell.

CURVE (2) - represents the function that adjusts the sinking speed of the central mark **I** depending on the time and for an exploitation deep of **H=200m** at the same volume of considered gap.

In this case the landfall phenomenon does not appear by obtaining a value T_1 for the time in years for which the phenomenon is ended. Correspondent to it we have the value of W_{max1} for the maximum sinking of the mark I.

CURVE (3) – same function but for **H=300m** and same gap volume (v).

Analogy with the curves 1, 2, 3 there will be obtained the curves 4 and 5. Finally it will be obtained the following relations:

$W_{max1} >>> W_{max2} > W_{max3} > W_{max2} > W_{max1}$ - relation between sinking

$T_5 < T_4 > T_3 > T_2 >>> T_1$ - relation between periods (2)

$H_5 < H_4 < H_3 < H_2 < H_1$ - relation between deepness

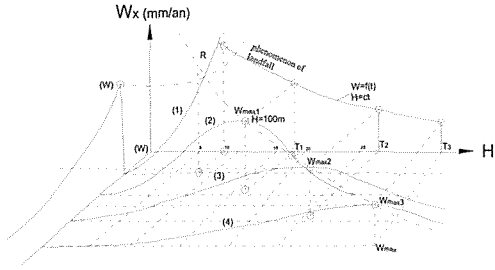

Fig. 6 Dependence W=f(V, H, T)

By excepting the relation between the deepness which had been imposed by the chosen model as being linear, the relations between the maximum sinking ($W_{max}(1)$) and periods of phenomena T(i) are non-linear and cannot be established only based on the real measurements.

The conclusion that comes from this simulation mentioned above is that the maximum sinking of the central mark I for a volume of imposed gap to be constant (v) is decreased non-linear with increasing the deep, the time of developing the phenomenon is decreased non-linear with

increasing the deep and the time is increased with increasing the deep. These curves are presented in the fig. 7.

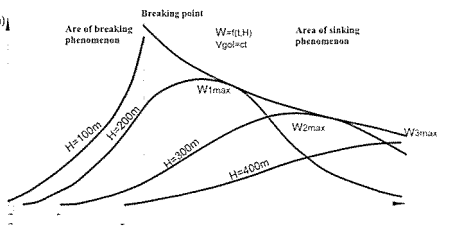

Fig. 7

8 SURVEYING THE STABILITY OF THE TERRAINS AND CONSTRUCTIONS FROM THE SURFACE

After the underground mining exploitation, at the surface it may appear some types of degradations of the terrains and constructions:

- Degradation of the pavages and constructions base
- Horizontal and vertical displacements in report with construction terrain;
- Breakings into the terrain;
- Breakings into construction faces;
- Breakings into portant and non-portant walls.

In order to consolidate the constructions there may be applied different solutions that can be made individuals and in group depending on the degree of construction degradation.

In order to be able to protect the objectives from the surface and also a series of mining workings situated into the covering rocks it is necessary to leave parts of unexploited rock under these called safety pillars.

To protect the exploited area with safety pillars (temporarily or definitively) represents one of the ways for directing the mining pressure.

As definitively safety pillars there are also the pillars necessary for protecting the mine wells or other mining works and also the industrial, social and natural objectives over the mining perimeters (buildings, roads, railways, etc.).

The temporarily safety pillars called also floor pillars are let on, under or around the main preparation workings in order to support the face coal workings and also the preparation ones.

The most used criteria for protecting the safety pillars is the *critic angle criteria* based on the relation between the declination angle of the pillar β and the specific admitted deformation ε_a.If the deformation is greater than 12 mm/m, the buildings cannot be used anymore because they have suffered walls breakings and other main destructions.

Table 1 Critic angle criteria for four categories of objectives

Cat.	Admitted deform ε_a, mm/m	Pillar angle β,°	Destruction character	Objective
I	0,01-1,5	54	Invisible breakings	Wells, industrial objectives, roads, railways, bridges, hospitals, rivers, lakes
II	1,5-3,0	58	Visible breakings of 2-5 mm	Oil pipes, blocks with more than 2 floors, transforming stations, high tension lines, industrial structures and for agriculture
III	3,0-6,0	62	Open fractures of 10-20 mm	Secondary roads and railways, underground works, Airports
IV	6,0-12,0	66	Open fractures >10-20 mm	Temporary buildings, agriculture and forest terrains

The technical and mining measures that are imposed in order to protect the buildings foresee especially to be used different methods of exploitation of the useful mineral substance and using the safety pillars for protecting the objective from the surface (fig. 8)

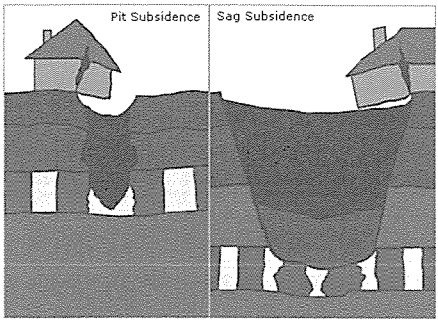

Fig. 8 Examples of degradations

The phenomenon of displacement and deformation of earth surface has a great interest by its implications into the problems of environment protection and the protection of constructions existent at the ground. The researches made by present lead to establishing some links between the causes and effects of the displacement and deformation phenomenon establishing some prognosis of evolution on long and short term.

These prognoses are very important due to the fact that there can be made some future studies for a suitable development of the areas affected by the underground mining exploitations. The methods of approximating the curves that define the deformation and displacement phenomenon of the areas have been made after the observations made in long time in different mining areas.

The monitoring phenomenon of displacing and deforming the areas is made permanently in active areas and also in conserved and closed mining areas because this phenomenon has a time development and the damages that can appear after the development can affect the surrounding environment and the existent constructions or the constructions that will be affected.

If there are some instruments for making the observations by using satellite methods GPS there can be made some monitoring stations that will follow this phenomenon in real time.

9 MONITORING THE SUBSIDENCE PHENOMENON IN JIU VALLEY MINING BASIN

Being situated along the Carpathians Mountains, which are a third of Romania, the Jiu Valley represents the gate to national park Retezat. Situated in the south of Hunedoara County and the south-west of Transylvania, in a depression of Meridional Carpathians, Petrosani depression called Jiu Valley is situated along the two Jiu Rivers (western and eastern Jiu).

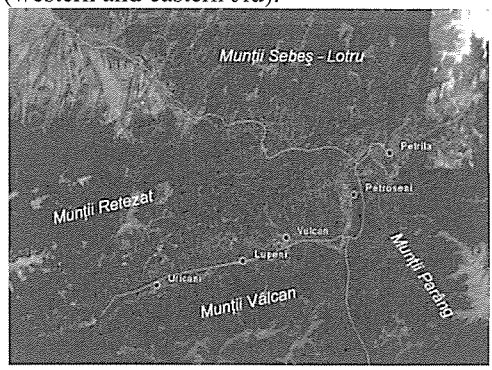

Fig. 9Topography of Jiu Valley mining basin seen from the satellites

9.1 The GPS Network of the Jiu Valley Mining Basin

The network consists of 23 points (Fig. 10), 9 of which are old points and 14 are new points, support network which has been checked and compensated. This network has been executed for the entire Jiu Valley Basin also including the studied area.

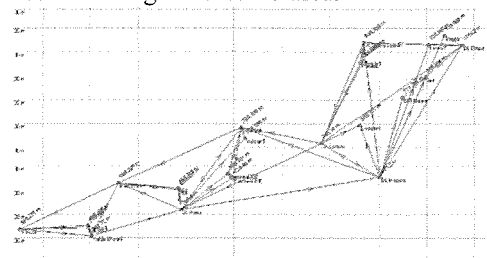

Fig.10 GPS Network of the Jiu Valley Mining Basin

In order to monitor the subsidence phenomenon in Petrosani mining area there was defined the stabile surface and the one subjected to movement. There have been made 2 types of landmarks: one type for the horizontal displacement and another type for vertical displacement. On the stabile surface there have been placed 4 pairs of landmarks (Fig. 11) in order to detect the horizontal and vertical displacements.

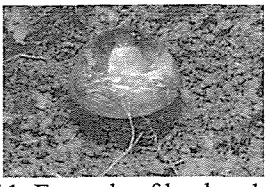

Fig.11. Example of landmarks

9.2 The calculation of parameters of subsidence phenomenon

The protection of the industrial, social and natural objectives from the surface of mining perimeter is made by dimensioning the safety (protection) pillars. In many cases it is put the problem to valor the reserves of useful mineral substance set into these safety pillars so putting into exploitation and introducing them into the economical circuit. In this situation there are made different studies in order to know the displacements and deformations of the terrains under the influence of mining exploitation of a rock situated under certain geological and mining and exploitation conditions.

To determine the values of the displacement and deformation parameters is made by using direct and indirect measurements that are grouped into the following methods:

- o Geodesic measures;
- o Topographical measures;
- o Photogrammetric measures.

To study the displacement phenomenon is made by using the data obtained over the displacement of a group of points from the field that are displaced together with the terrain in movement. The marks that materialize the points in movement are called *working marks* and the stable marks are called *supporting marks*. All the working and supporting marks that are used for supervising the displacement of the ricks constitute a *station for observation the displacements.*

The displacement of the points is observed by topographical periodic measurements for determining their successive positions.

So it was determined the heights of points from the surveying station. Their schedule is as follows:

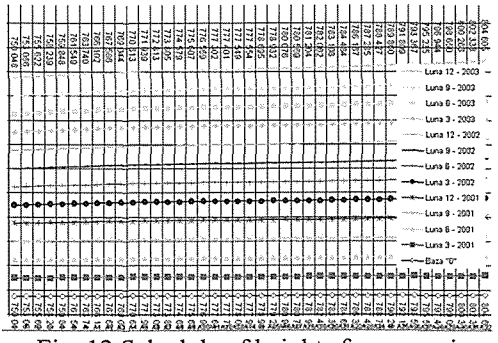

Fig. 12 Schedule of heights for surveying points

The parameters that influence the phenomenon of displacement and deformation were calculated depending on many measurements at different intervals of time, which will be made also in the future.

Table 2 Determination of displacement and deformation parameters

Pct.	S_i [mm]	$S_{i+1}-S_i$ [mm]	I_i [mm/m]	$D_{i+1}-I_i$
A	0	+10	0,373204	-0,517137
1	+10	-3	-,143933	0,585283
2	+7	+9	0,44135	-0,76363
⋮	⋮	⋮	⋮	⋮

$D_{i,i+2}$	R_{i+1} [m/mm]	C_{i+1}	D_i [mm]	ε_i
47,63	-92,118	-,010855	118	+4,4038
41,23	70,453	0,014938	-263	-11,3227

39,20	-51,554	0,01939	-18	-0,8826
:	:	:	:	:

These parameters were represented into the Fig. 13 resulting that the phenomenon of subsidence is active and it need to be monitories in order to be protected the environment.

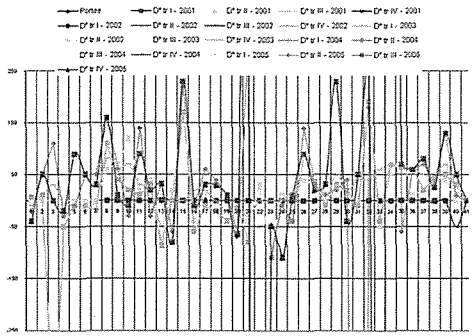

Fig. 13 Schedule of parameters that influence the subsidence phenomenon

9.3 Accomplishing a GIS in Petrosani mining basin

The date acquired from the field togheter with the date acquired from analogical support have been correlated with spatial databases regarding the studied area using ArcGIS software.

When it is put into service the system that contains the geographic data, it was be able to be interrogated by using some simple questions: Who is the owner? What is the distance between 2 points? etc. or there can be used some analytic questions: Where are some proper areas for building a house? Which is the prognosis subsidence area? How many constructions are in subsidence area?

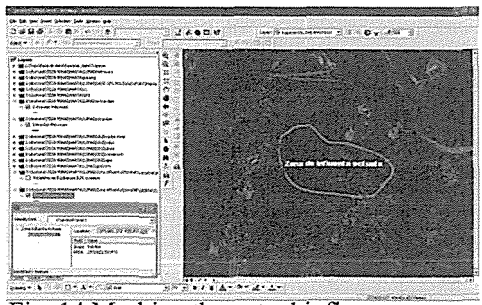

Fig. 14 Marking the actual influence area – Petrosani mining area

To make the calculation for foreseeing the subsidence phenomenon and dimensioning the safety pillars cannot be made without knowing the limit angles of sinking and the angles of maxim sinking.

The size of the surface that is affected by the movement of whole rock over the size of exploited space is limited by planes that together with the horizontal one make some angles called sinking angles (β_s , γ_s , δ_s) breaking angles (β_r , γ_r , δ_r) depending on the height of exploitation, on nature and mechanical features of the rocks into the places where the breaking lines defined by the breaking angles come through the surface appear breaks.

The prognosis of the deformation and displacement phenomenon of the terrestrial surface was based on the values of the sinking angles (Fig. 15) that are between 60-70 grades.

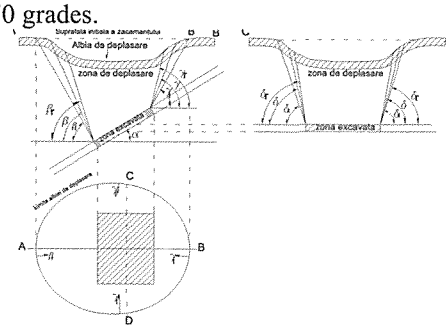

Fig. 15 Sinking angles

From the observations made on the sinking it results that the rock and the

surface suffer displacements and deformations, resulting compression and traction efforts. Among more important factors that influence the displacement and deformation process of the terrain we can mention as follows:

- Physical and mechanical features of covering rocks
- Rock tectonic
- Hydrological and geological conditions
- Declination and measure of exploitation layers
- Exploitation methods
- Method for directing the pressure of surrounding rocks
- Dimensions of exploited space
- Exploitation depth

9.3.1. Examples of query and spatial analysis

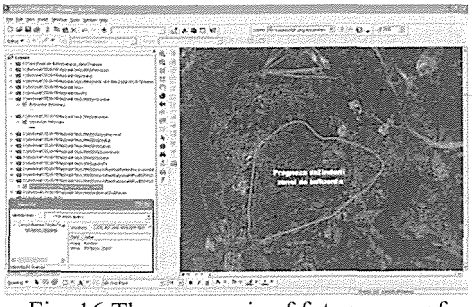

Fig. 16 The prognosis of future area of influence for the next 20 years - Petrosani mining area

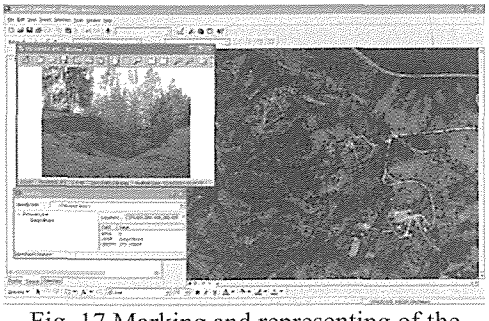

Fig. 17 Marking and representing of the most affected areas - Petrosani mining area

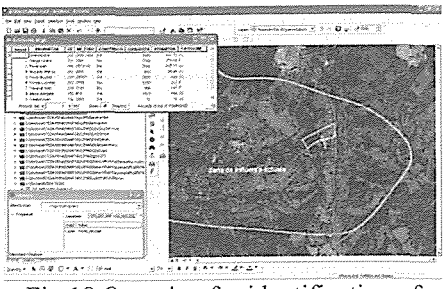

Fig.18 Queering for identification of properties located in - Petrosani mining area

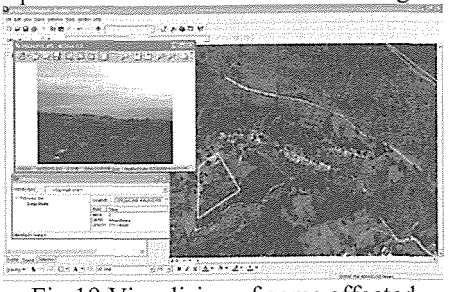

Fig.19 Visualising of some affected properties located in - Petrosani mining area

10 CONCLUSION

The sustainable development of a mining area cannot be made without studying the influence of the underground exploitations over the environment and constructions from outside.

REFERENCES

Herbei O., Herbei M.,2010, *Geographic Information Systems. Theoretical and applications,* Universitas Press, Petroşani, 216p.

Herbei O., Ular R., 2008, Monitoring the displacement and deformation phenomenon of the land surfaces as result of the mining exploitations, *Mining Magazine no.5-6* (ISSN 1220-2053), pp. 50-55.

Dima N., Pădure, I., Herbei, O., 1996, *Mining topography*, Corvin Publishing, Deva, 410p.

Herbei, O., 1995, *Determining the parameters of deforming the terrain surfaces and researching the constructions from the surface under the influence of underground exploitation for the mineral rocks,* Doctorate thesis, University of Petrosani , 220 p.

***, 1985, The manual of the mining engineer *vol II.* Tehnical Publishing, 773 p.

Kratzsch, H., *Bergschdekunde*, Berlin, 1974
Knothe, St., *Observation et interpretation teoretiqe des mauvements de surface*, Revue de l'Industrie Minerale (11), 1969

Use of Remote Sensing in Determining the Environmental Effects of Open Pit Mining and Monitoring the Recultivation Process

Açık Ocak Madenciliğinin Çevresel Etkilerinin Belirlenmesinde ve Rekultivasyon Çalışmalarının Takibinde Uzaktan Algılamanın Kullanımı

Zehra Damla UÇA AVCI
İstanbul Teknik Üniversitesi, Uydu Haberleşmesi ve Uzaktan Algılama Merkezi, İSTANBUL

Muhittin KARAMAN
İstanbul Teknik Üniversitesi, Uydu Haberleşmesi ve Uzaktan Algılama Merkezi, İSTANBUL

Emre ÖZELKAN
İstanbul Teknik Üniversitesi, Uydu Haberleşmesi ve Uzaktan Algılama Merkezi, İSTANBUL

ABSTRACT Remote Sensing is conventionally used for detection of land cover change caused by open-pit mining activities. It also provides an economic, fast and accurate solution for planning and monitoring of rehabilitation processes.

Open pit coal mining has been maintained in Kilyos - Karaburun region (Istanbul) for about 50 years. In this study, a SPOT 5 satellite image acquired on October, 2009 has been used for land cover mapping. First, the natural and the post-formed land cover types (such as vegetation removed surface and artificial pit lakes) were defined as thematic classes. Then, image analyzing methods were applied in two steps as segmentation and classification. The classes were evaluated with respect to their location, area and distribution. Besides, use and advantages of remote sensing for rehabilitation process were also presented.

Classified satellite images can be used as base maps, both for analyzing the environmental effects and spatial planning and management of the region for the future use.

ÖZET Uzaktan algılama, madencilik faaliyetlerinden dolayı oluşan morfoloji değişimlerinin belirlenmesinde kullanılmaktadır. Buna ek olarak, madencilik faaliyetleri sonrası gerçekleştirilmesi gereken ağaçlandırma, yeniden düzenleme ve iyileştirme gibi rehabilitasyon çalışmalarının planlanması ve takibi aşamasında da ekonomik, hızlı ve doğru çözümler sunmaktadır.

Kilyos ve Karaburun (İstanbul) arasındaki bölgede, yaklaşık 50 sene boyunca kömür çıkartma amaçlı açık ocak madenciliği yapılmıştır. Bu çalışmada, Ekim 2009 tarihli SPOT 5 uydu görüntüsü kullanılarak, bölgenin arazi örtüsü haritası çıkartılmıştır. Öncelikle bölgedeki doğal yüzey örtüsü sınıfları ile madencilik çalışmaları sonrasında oluşan yeni yüzey örtüsü sınıfları (bitki örtüsü tahrip edilmiş bölgeler, yapay gölet alanları gibi) belirlenmiş ve daha sonra segmentasyon ve sınıflandırma olmak üzere iki aşamalı görüntü analizi gerçekleştirilmiştir. Elde edilen tematik sınıflar konum, alansal büyüklük ve dağılım açısından değerlendirilmiştir. Ayrıca, uzaktan algılamanın bölgenin rehabilitasyonu sürecinde sağlayacağı faydalar da ortaya konmuştur.

Sınıflandırılmış uydu görüntüleri, bölgedeki kömür madenciliği aktivitelerinin çevresel boyutunu analiz etmenin yanı sıra, ileriye yönelik olarak mekansal planlama için de iyi bir altlık olmaktadır.

1 INTRODUCTION

Mining is the extraction of valuable minerals or other geological materials from the earth, generally with an operation that involves the physical removal of earth surface. Mining activity includes excavations in underground mines, surface excavations in open-pits, and also the mining from the seafloor.

The process of obtaining useful minerals, using the raw material in industry, and furthermore exportation of them, are very important for the development of a country. However, the mining activity has to be organized not only in the aim of extracting the material but also saving the natural surrounding environment. The process has to involve the protection of environment and sustainability principles, which require social, ecological, economic, spatial and cultural dimensions as well.

Environment-friendly mining will save the human-nature balance, meet needs of the day in consideration with the plan for future generations. All these require some operations that have to be done all before the mining activity, during the mining operations and after the mining activities are completed. Respecting it in all process steps is important not to cause permanent harm to the ecology of region.

Generally, the pre-mining activities are categorized as precaution / protection operations, and post-mining activities are categorized as retrieval / recruitment applications, which may be enhanced to reformation, nature restoration and rehabilitation. Post-operations may include the conversion of the mining area to the initial or to a better state; or changing it for a totally different functionality / usage. All these processes including the pre- and post-operations can be defined as recultivation (or reclamation). (Simsir vd., 2007)

The planning, monitoring and controlling of mining and recultivation operations can be done by remote sensing as well as ground surveying. RS technology provides the possibility of collecting data of wide areas in a short time. The data acquired is in a digital form, can be derived and analyzed in various ways and integrated to other information systems.

In this study, satellite data is analyzed to determine the present status of the region and to show the potential of optical data use in mining for monitoring the recultivation process in scope of environmental conscience.

2 STUDY AREA AND DATA USED

One of the important underground resources of Istanbul is the coal mines occurring between Kilyos and Karaburun areas.

Coal formation of Trakya Tersiyer basin is hosted by Danismen Formation of Oligocene age. The Danismen Formation is consisted of grey-colored mica sand; and grey-colored marly, clay stone, silt stone and lignite layers. In Agacli region, where clay-coal layers are observed, the clay seams exist between medium and upper coal seams as 1-1.5 m width. In Bolluca region it occurs as 2.5 m thick layer alternating with upper medium and lower seams. (Koroglu)

The lignite formation is observed in fringe of Istranca massifs. The Agacli lignite basin covers approximately 25 km. squares extending from the Bosphorus entrance at north, to Terkos Lake at west. (Sengüler, 2007) The Ciftalan, Ihsaniye, Bolluca, Akpinar, Yenikoy, Agacli coal basins account for Agacli basin lignites. (Koroglu)

The recent studies show that at the depths of 350-550m and 550-700 m, existing coal seams with thickness between 0.5-4 m have calorific values between 2000-3000kcal/kg. The total reserve was determined as more than 520 million tons. (MTA report, 2005)

As for potential, the sand reserves of the Kilyos region were found to be 55 million tons of quartz in sand dunes of Gumusdere and Agacli, 7 million tons for feldspar and 3.8 million tons for the heavy minerals. (Onal G. 1981)

The coal deposits have been mined out since 1919 using open-pit techniques. All the mining activities have been done by open-pit mining operation.

In this coal basin, the licensees started the production from the coast side through the insides of land and they poured the extracted land\rock into the closest seaside. In some regions, this poured rock has been used for operating the coal veins that lie through the sea bottom.

The land is enlarged and reformed by each filling activity and the coast is shifted through the sea. As confirmed by studies in literature, coastline changes are very important for environment and the living beings of the habitat. This region's coastline has been in change since mining in this region has been started. (Uça, Z. D. et al., 2006)

Pouring land into the sea to form pools and then pumping water out has been applied to reach the coal veins and mine extraction in the sea part. Coast environment has been destroyed by these activities. The land part has also been destroyed by the formation of wide pits which turn into artificial lakes after abandoned by the operators.

In this region many artificial lakes formed after mining activity are observed. (Turnacigil, 2008) In many ways, the lignite coal mining has caused distortions on the morphology of the region.

2.1 Study Area

In this study, to represent the influence area of mining -which is affected in positive or negative ways, before, during or after the operations-, focus area is selected as seen in Figure 1. The region is in Sariyer, Eyup and Arnavutkoy country boundaries.

Gradient of the slopes in the region are between 20-30 %; the highest elevations on the west is about 120 m. and the lowest is beyond negatives by being inside the natural sea level on the north. (Turnacigil, 2008)

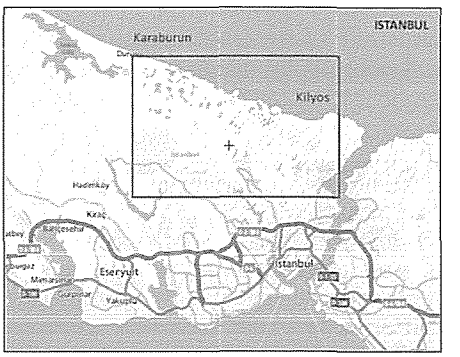

Figure 1. Study Area*

2.2 Data Used

In this study, multispectral SPOT 5 data acquired on October2nd, 2009 was used.

SPOT 5 is an optical satellite that has sensors to detect and record the reflectance of land surfaces on visible and infrared regions of the electromagnetic spectrum. SPOT 5 has multispectral and monospectral data acquisition modes. In this study, multispectral SPOT 5 image was used which has been recorded in four bands. The spectral intervals of SPOT 5 bands are shown in Table 1. The spatial resolution of SPOT 5 images in multispectral mode is 10 m.

Table 1. Spectral Properties of SPOT 5 Data

Band Number	Spectral Region
Band 1	0.50 - 0.58 μm
Band 2	0.81 - 0.88 μm
Band 3	0.78 - 0.89 μm
Band 4	1.58 - 1.75 μm

3 METHOD

The present situation of a mining region and its environment may well be evaluated by using a segmentation and image classification method on satellite data. This kind of situation analysis can also be used as a base and data source for spatial planning process before starting the mining activities.

In addition to the production of a status map, remote sensing may also be used for monitoring the region and quantifying some

of the recultivation activities. Revegetation, which is one of the rehabilitation steps, can be followed up by using satellite data and image analyzing methods. One of the most practical methods, which can be used for identifying the vegetation presence, status and distribution, is using normalized difference vegetation index (NDVI) images.

In this study, as a first step of image processing, segmentation was applied to form image objects. Then image classification was performed to determine the thematic classes. As a second step, the NDVI image was produced to obtain the vegetation status in the region.

3.1 Segmentation

Segmentation process is the division of whole image into separate image parts according to a homogeneity criterion, which is controlled by color, shape, compactness and smoothness parameters. The convenient values for segmentation parameters and the scale parameter, which is also an initial input, were assessed by the analyst.

3.2 Classification

After segmentation process was completed, classification was performed on image objects. Class descriptions were defined and each image object was assigned to a suitable class. In this study, both of the nearest neighbor and condition-based classification algorithms were used.

3.3 NDVI Image

NDVI is a commonly used vegetation index in remote sensing analysis to distinguish the vegetation from non-vegetation features and also identify the vegetation condition.

In an NDVI image, pixels take values between -1 and +1. Higher NDVI values indicate a greater level of photosynthetic activity. (Sellers, 1985; Tucker et al., 1991)

NDVI image is produced with a band math equation as:

$$NDVI = (NIR - R) / (NIR + R)$$

where NIR: Near infrared band, R:Red band.

4 APPLICATION

4.1 Segmentation

Three scale parameters were tested to decide the suitable segmentation layer, which will provide a convenient base for the discrimination of thematic classes.

The resultant segmentation image produced for three different scale parameters (sp) is given in Figure 2.

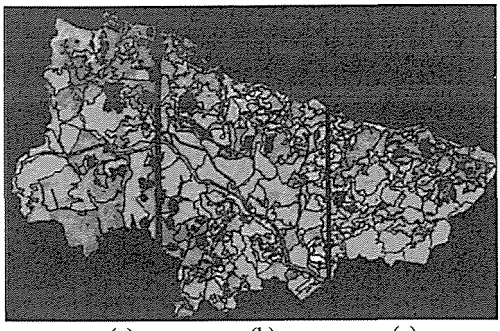

(a) (b) (c)

Figure 2. Segmented Image with sp (a) 200, (b) 100, (c) 50

Sp = 50 was selected as the scale parameter to fit the requirements, by using visual analysis. The other parameters of the segmentation were determined as given in Table 2.

Table 2. Segmentation Parameters Used

Parameter	Value
Color	0.9
Shape	0.1
Compactness	0.5
Smoothness	0.5

4.2 Classification

Thematic classes for this region were determined as: 'Mine Type 1, Mine Type 2, Mine Type 3, Vegetation Type 1, Vegetation Type 2, Vegetation Type 3, Destroyed Land Surface Type 1 (DLS 1), Destroyed Land Surface Type 2 (DLS 2), Destroyed Land Surface Type 3 (DLS 3), Water, Road.

The samples and the related surface views in (RGB: 4,1,2) are given in Table 3.

Table 3. Surface Views of Training Samples

Class Name	Sample Region
Vegetation Type 3	
Vegetation Type 2	
Vegetation Type 1	
DLS Type 3	
DLS Type 2	
DLS Type 1	
Water	
Mine Type 3	
Mine Type 2	
Mine Type 1	

The set of sample objects, which were used as training data, is visualized in Figure 3.

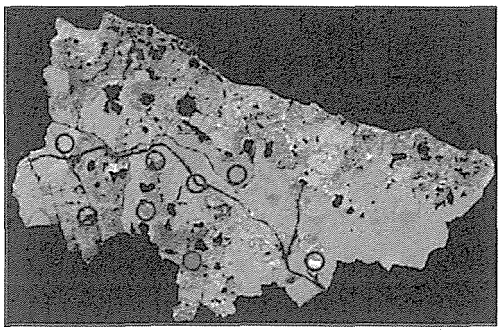

Figure 3. Locations of Training Samples Used

For all of the classes except 'road' class, standard nearest neighbor classifier was used to obtain class distribution functions. For 'road' class, the feature for class description was defined by length/width proportion criterion.

The resultant classification image and the legend of the final classification are given in Figure 4 and 5, respectively.

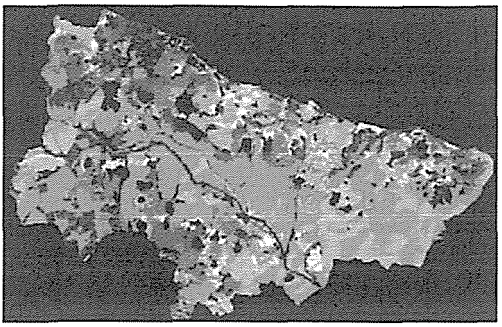

Figure 4. Classification Image

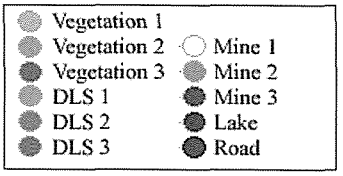

Figure 5. Legend of the Classification Image

After performing classification, the areal percentages of the classes were obtained as given in Table 4.

Table 4. Areal Percentages of the Classes

Class Name	Area %
Vegetation	53
DLS	29
Mine	7
Lake	6
Road	5

The classified image and areal sizes of the classes represent the present situation of the region by the date satellite image was acquired.

4.3 NDVI Image

The NDVI image produced is given in Figure 6.

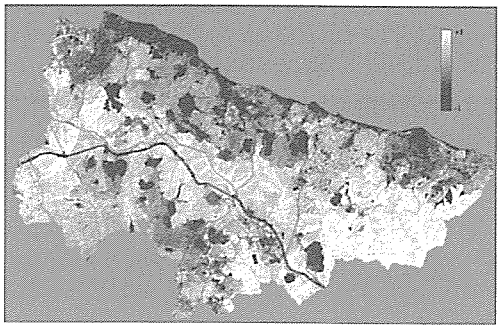

Figure 6. NDVI Image

The NDVI values of pixels were found to be between [-0.63, 0.45] interval. Using the NDVI image, it can be said that the surrounding of the mining areas and especially the coastal region doesn't have dense vegetation when compared to regions relatively far from mining areas. This may probably be an indicator of naturally overrunning weeds, or sodding, whereas high NDVI values may indicate a more dense and/or aged vegetation cover or woodlands (such as in the southeast of the region).

Obtaining satellite images periodically and applying NDVI analysis may be used in recultivation operations to observe the change detection in vegetated areas.

5 RESULTS & CONCLUSION

One of the most common methods of expressing the classification accuracy is using error matrix. Based on error matrix, the overall accuracy of the classification was found to be 83%.

It can be thought that mining activity is relational to 'mine', 'DLS' and 'lake' classes. These classes cover 42 % of the total region, showing that the action has a wide affection area.

Land cover/land use maps derived from satellite data, provide information on both the areal sizes of the thematic classes and spatial distribution of them. This allows the use of results for spatial analysis with RS and/or GIS tools.

In addition to determination of the present situation of the region, the management after completing mining activities and planning the future use of the region may well be organized by using satellite data. Use of satellite data and image analyzing methods may have a significant part on the control mechanism of some recultivation steps.

RS will also be an economic, fast and accurate way of planning and checking on after-use processes. Using satellite data over the region of interest periodically will allow multitemporal processing for change detection analysis.

Sustainable development primarily requires environment-friendly arrangements on the management of sectors which are directly involved with environment. RS can be a useful tool to observe and plan the human activity and its effects on Earth.

Authors would like to thank to Istanbul Technical University - CSCRS, for SPOT 5 data.

REFERENCES

Köroğlu, Ç., 2007. Ağaçlı-Bolluca (İstanbul) Yöresi Seramik Killerinin Malzeme Özelliklerinin Araştırılması, *İTÜ FBE, YL Tezi*, İstanbul.

Önal, G., 1981. Kilyos Bölgesi Kumlarının Değerlendirme Olanaklarının Araştırılması, *Türkiye Madencilik Bilimsel ve Teknik 7. Kongresi*, MMO, Ankara.

Sellers, P.J., 1985. Canopy Reflectance, Photosynthesis and Transpiration, *International Journal of Remote Sensing*, 6:1335-1372.

Şengüler, İ., 2007. Ülkemiz Enerji Bütünlemesinde Marmara ve Trakya Bölgesi Kömürlerinin Yeri, *MTA Genel Müdürlüğü Enerji Dairesi Başkanlığı*, Ankara.

Şimşir, F., Pamukçu, Ç., Özfırat, M. K., 2007. Madencilikte Rekültivasyon ve Doğa Onarımı, *DEÜ Mühendislik Fakültesi, Fen ve Mühendislik Dergisi*, Cilt: 9 Sayı: 2 sh. 39-49.

Turnacigil, A., 2008. Yeniköy Ağaçlı Civarındaki Maden Ocaklarının Rehabilitasyonu, *İTÜ FBE, YL Tezi*, İstanbul.

Tucker, C.J., Dregne H.E., and Newcomb W.W., 1991. Expansion and Contraction of the Sahara Desert from 1980 to 1990, Science, 253:299-301.

Uça, Z. D., Sunar Erbek, F., Kuşak, L., Yaşa, F., and Özden, G., 2006. The Use of Optic and Radar Satellite Data for Coastal Environments, *International Journal of Remote Sensing*, Vol. 27, No. 17.

*Figure 1. was adapted from maps.yahoo.com